Vol. 65 January, 1961 No. 1

D 54 - V

THE JOURNAL OF PHYSICAL CHEMISTRY

CONTENTS

SYMPOSIUM ON COLLOIDAL SILICA AND SILICATES, Cleveland, Ohio, April 13–14, 1960

THE JOURNAL OF PHYSICAL CHEMISTRY

(Registered in U. S. Patent Office)

Published monthly by the American Chemical Society at 20th and Northampton Sts., Easton, Pa.

Second-class mail privileges authorized at Easton, Pa. This publication is authorized to be mailed at the special rates of postage prescribed by Section 131.122.

The *Journal of Physical Chemistry* is devoted to the publication of selected symposia in the broad field of physical chemistry and to other contributed papers.

Manuscripts originating in the British Isles, Europe and Africa should be sent to F. C. Tompkins, The Faraday Society, 6 Gray's Inn Square, London W. C. 1, England.

Manuscripts originating elsewhere should be sent to W. Albert Noyes, Jr., Department of Chemistry, University of Rochester, Rochester 20, N. Y.

Correspondence regarding accepted copy, proofs and reprints should be directed to Assistant Editor, Allen D. Bliss, Department of Chemistry, Simmons College, 300 The Fenway, Boston 15, Mass.

Business Office: Alden H. Emery, Executive Secretary, American Chemical Society, 1155 Sixteenth St., N. W., Washington 6, D. C.

Advertising Office: Reinhold Publishing Corporation, 430 Park Avenue, New York 22, N. Y.

Articles must be submitted in duplicate, typed and double spaced. They should have at the beginning a brief Abstract, in no case exceeding 300 words. Original drawings should accompany the manuscript. Lettering at the sides of graphs (black on white or blue) may be pencilled in and will be typeset. Figures and tables should be held to a minimum consistent with adequate presentation of information. Photographs will not be printed on glossy paper except by special arrangement. All footnotes and references to the literature should be numbered consecutively and placed in the manuscript at the proper places. Initials of authors referred to in citations should be given. Nomenclature should conform to that used in *Chemical Abstracts*, mathematical characters be marked for italic, Greek letters carefully made or annotated, and subscripts and superscripts clearly shown. Articles should be written as briefly as possible consistent with clarity and should avoid historical background unnecessary for specialists.

Remittances and orders for subscriptions and for single copies, notices of changes of address and new professional connections, and claims for missing numbers should be sent to the American Chemical Society, 1155 Sixteenth St., N. W., Washington 6, D. C. Changes of address for the *Journal of Physical Chemistry* must be received on or before the 30th of the preceding month.

Claims for missing numbers will not be allowed (1) if received more than sixty days from date of issue (because of delivery hazards, no claims can be honored from subscribers in Central Europe, Asia, or Pacific Islands other than Hawaii), (2) if loss was due to failure of notice of change of address to be received before the date specified in the preceding paragraph, or (3) if the reason for the claim is "missing from files."

Subscription rates (1961): members of American Chemical Society, $12.00 for 1 year; to non-members, $24.00 for 1 year. Postage to countries in the Pan American Union $0.80; Canada, $0.40; all other countries, $1.20. Single copies, current volume, $2.50; foreign postage, $0.15; Canadian postage $0.10; Pan-American Union, $0.10. Back volumes (Vol. 56–64) $30.00 per volume; foreign postage, per volume $1.20, Canadian, $0.40; Pan-American Union, $0.80. Single copies: back issues, $3.00; for current year, $2.50; postage, single copies: foreign, $0.15; Canadian, $0.10; Pan American Union, $0.10.

The American Chemical Society and the Editors of the *Journal of Physical Chemistry* assume no responsibility for the statements and opinions advanced by contributors to This Journal.

The American Chemical Society also publishes *Journal of the American Chemical Society, Chemical Abstracts, Industrial and Engineering Chemistry*, International Edition of *Industrial and Engineering Chemistry, Chemical and Engineering News, Analytical Chemistry, Journal of Agricultural and Food Chemistry, Journal of Organic Chemistry, Journal of Chemical and Engineering Data, Chemical Reviews, Chemical Titles* and *Journal of Chemical Documentation.* Rates on request.

THE JOURNAL OF
PHYSICAL CHEMISTRY

(Registered in U. S. Patent Office)

VOLUME 65 JANUARY 26, 1961 NUMBER 1

THE REACTION RATES OF POLYSILICIC ACIDS WITH MOLYBDIC ACID

BY T. L. O'CONNOR

Ionics, Incorporated, Cambridge, Massachusetts

Received August 10, 1960

The reaction rates with molybdic acid of polysilicic acids derived from sodium silicate solutions of various mole ratio, concentration and age are reported and approximate kinetic equations derived. In addition, the reactions of polysilicic acid of known chemical composition generated from chlorosiloxanes were studied and the kinetics for the rate of color development with molybdic acid derived. Non-cyclic polysilicic acids develop full color in less than five minutes whereas those derived from silicate anions present in sodium silicate solution require up to several hours.

Introduction

In 1950, Weitz, Franck and Schuchard[1] discovered that the yellow colored silicomolybdate complex utilized in the colorimetric analysis for SiO_2 is formed only from monosilicic acid and that monosilicic acid reacts to give full color development in about 75 seconds. Alexander,[2] Goto,[3] Richardson and Waddams[4] as well as Weitz and co-workers have used the method to estimate the monomer content of various silicate solutions and colloidal suspensions. In this earlier work, it was found that in solutions containing silicate species other than monomer there is a rapid initial color development followed by a relatively slow color development. The slow color development is a result of the rate-limiting step of release of monomer from polymerized species such as colloidal silica or polysilicic acids. The monomer content of the original solution is estimated from the color developed two minutes after mixing or by extrapolation of the slow portion of the color development curve to zero time. Very little work has been reported on the kinetics of the reaction for species other than monosilicic acid. In this regard, Weitz and co-workers[1] as well as Alexander[2] have reported that disilicic acid reacts to give complete color development in about ten minutes.

In the present study the rates of reaction with molybdic acid of silicate anions existing in several types of sodium silicate solutions of different mole ratio (SiO_2:Na_2O) and concentration have been quantitatively measured and analyzed. In addition, simple polysilicic acids prepared from non-cyclic chlorosiloxanes have been studied and the kinetics of depolymerization and reaction to form silicomolybdate complex derived.

Experimental

Materials.—The sodium silicate solutions used in the work were commercial silicates manufactured by the Diamond Alkali Company. Chlorosiloxanes were prepared according to the method of Schumb and Stevens[5] and were purified by fractional distillation. The boiling points were for Si_2OCl_6 137° (760 mm.), $Si_3O_2Cl_8$ 82°(12 mm.), $Si_4O_3Cl_{10}$ 97° (4 mm.), Si_5O_4 Cl_{12} 131° (4 mm.), and $Si_6O_5Cl_{14}$ 154°(3 mm.).

Procedure.—The molybdic acid reagent used in the work was prepared as described by Alexander[2] and produces β-silicomolybdate anions as shown by Strickland.[6] A 10 to 25-microliter sample of silicate solution or chlorosiloxane was added instantaneously to 100 to 300 ml. of a well agitated solution of molybdic acid reagent at 25°. After 30 seconds of mixing, a portion was transferred to a one cm. quartz cell and the rate of color development at 400 mμ recorded with a Beckman Recording Spectrophotometer (DK-2) for a period up to six hours or to full color development. The temperature was maintained at 25 ± 0.5°.

A sample of the β-silicomolybdate formed in each case was placed in a polyethylene bottle and heated for several hours at 90° until complete conversion to α-silicomolybdate had occurred. A total silica analysis then could be obtained from the optical density of the stable α-complex. Both species were shown to obey Beer's law, and the ratio of extinction coefficients was found to be 1.77 with standard samples of SiO_2 prepared by dissolving Mallinckrodt S. L. Silica in dilute caustic.

(1) E. Weitz, H. Franck and M. Schuchard, *Chemiker Ztg.*, **20**, 256 (1950).

(2) G. B. Alexander, *J. Am. Chem. Soc.*, **75**, 5655 (1953).

(3) K. Goto, THIS JOURNAL, **60**, 1007 (1956).

(4) E. Richardson and J. A. Waddams, *Res. Corr. Suppl. to Research (London)*, **7**, 42 (1954).

(5) W. C. Schumb and A. J. Stevens, *J. Am. Chem. Soc.*, **72**, 3178 (1950).

(6) J. D. Strickland, *J. Am. Chem. Soc.*, **74**, 863 (1952).

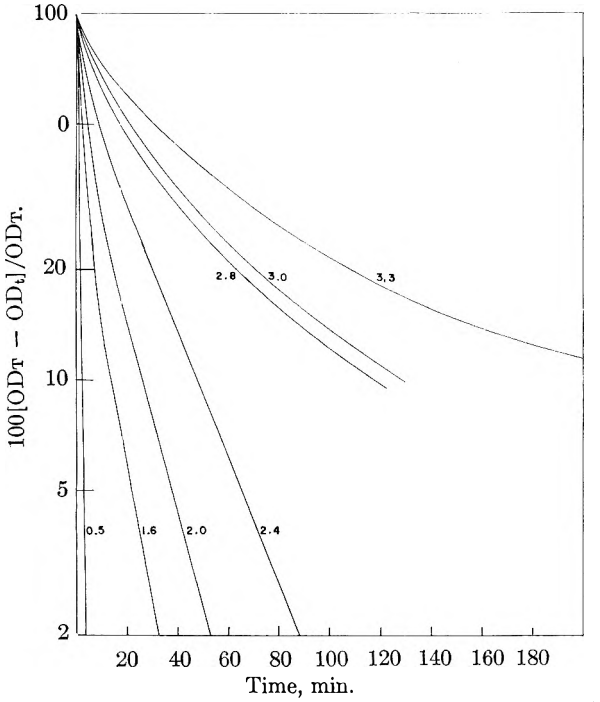

Fig. 1.—Effect of SiO_2:Na_2O mole ratio on the rate of reaction of polysilicic acids from sodium silicate solutions. Numbers on curves are SiO_2:Na_2O ratios.

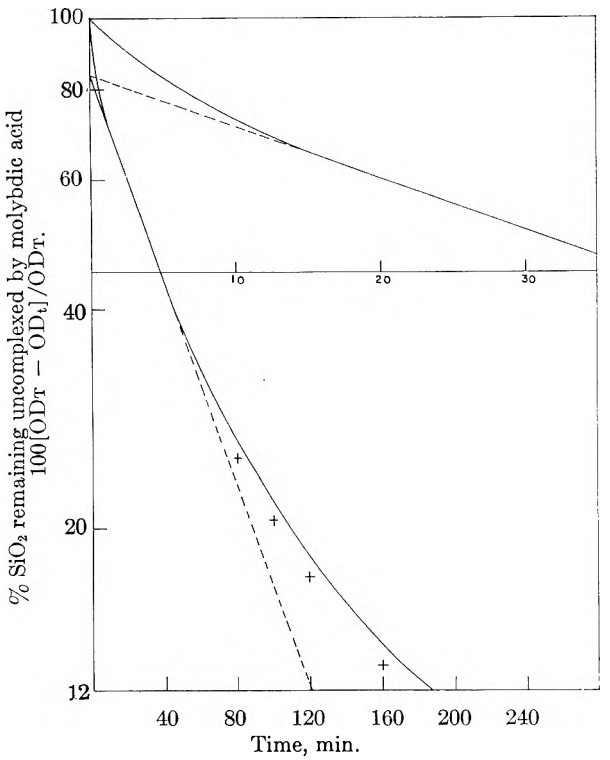

Fig. 2.—Reaction rate of 3.3 ratio sodium silicate with molybdic acid. Solid curve experimental; dashed curve calculated from $p = p_0e^{-k_1t}$; + points from equation 7.

Results

Rate of Reaction of Concentrated Sodium Silicate Solutions as a Function of SiO_2–Na_2O Mole Ratio. —In Fig. 1 the relative rates of reaction of various sodium silicates with molybdic acid are shown as a function of the change in optical density of the solution. The ordinate is a measure of the per cent. SiO_2 remaining uncomplexed by molybdic acid, where OD_T is the total optical density of β-complex corresponding to the total amount of SiO_2 present and OD_t is the instantaneous optical density recorded as a function of time. It is evident that the higher the mole ratio, the slower the rate of color formation. As has been pointed out in numerous investigations, the higher ratio sodium silicate solutions contain increasingly more complex anions which are slow to depolymerize to monosilicic acid necessary for the formation of silicomolybdate complex.

On following the color development for much longer times than shown in Fig. 1, the color is found to reach a maximum and then decrease. This decrease in color is due to transformation of the β-silicomolybdate complex, initially formed, to α-complex which has a lower extinction coefficient. Thus, the curves in Fig. 1 are not a quantitative measure of the amount of SiO_2 remaining uncomplexed because of the continuous conversion of β-complex. Strickland[6] has studied the conversion and reported that the rate of conversion appears to be first order in the amount of β-complex present.

This transformation was quantitatively evaluated in the present study by preparing essentially pure β-complex from a standard solution of monosilicate anions and following the color change over a period up to eight hours at 25°. The concentration of β-complex remaining was calculated from the equation

$$OD_\beta = \frac{1.77(OD_t) - OD_{max}}{0.77} \qquad (1)$$

asssuming the recorded optical density as a function of time (OD_t) is the sum of the optical densities of both species whose extinction coefficients are in the ratio beta:alpha equals 1.77. OD_{max} is the initially attained maximum optical density where all the silica is present as β-complex. The amount of β-complex remaining as a function of time was found to obey first-order kinetics according to the equation

$$\ln OD_t = \ln OD_{max} - k_0t \qquad (2)$$

In Table I, the values of k_0 for various initial amounts of β-complex are given.

Table I

Values of k_0 for the Conversion of β-Silicomolybdate Complex to α-Silicomolybdate at 25°

Mg. SiO_2/100 ml.	OD_{max}	k_0, min.$^{-1}$
0.213	0.078	1.18×10^{-3}
.639	.238	1.15
.852	.311	1.21
1.704	.601	1.13
2.560	.930	1.17
	Av.	1.17

In Fig. 2 the color development curve for a 3.3 ratio sodium silicate is shown on an expanded time scale over the first 35 minutes as well as the complete curve. After the initial rapid color development (10 to 15 min.), $100(OD_T - OD_t)/OD_T$ appears to reach a straight line relationship with time and then continually decrease in slope. Part of the deviation from a straight line relationship in the

later stages of color development certainly is due to disappearance of β-complex. In order to approximate a correction for the decrease in color as a result of complex transformation, the sodium silicate solution is assumed to contain two species, one which depolymerizes rapidly and another more slowly. The species reacting more slowly to produce color is assumed to be polymeric with the rate-limiting step depolymerization to monosilicic acid. The dashed line in Fig. 2 gives the expected color development if no transformation occurred and the depolymerization of polymeric silica is according to

$$P = P_0 e^{-k_1 t} \quad (3)$$

The optical density of the solution (OD_t) is

$$OD_t = \epsilon\beta + 0.565\epsilon\alpha \quad (4)$$

According to the mechanism proposed, the per cent. α-complex is

$$\alpha = 100 - P_0 e^{-k_1 t} - \beta \quad (5)$$

assuming the initial rapid formation of color is instantaneous and therefore β_0 equals $100 - P_0$. The rate of change of β-complex is given by the differential equation

$$d\beta/dt = k_1 p - k_0\beta = k_1 p_0 e^{-k_1 t} - k_0\beta \quad (6)$$

where $k_1 p$ is the rate of formation of β-complex from depolymerizing polysilicate species and $k_0\beta$ is the rate of disappearance of β-complex due to conversion to α-complex. On substituting the equality for α (equation 5) into equation 4 and then for β from the integration of equation 6 the optical density of the solution expressed as a percentage of the total optical density if all the silica were converted to β-complex is

$$\% \text{ color developed} = \left[\frac{0.435k_1}{k_0 - k_1} - 0.565\right] p_0 e^{-k_1 t} + 0.435\left[100 - p_0\left(1 + \frac{k_1}{k_0 - k_1}\right)\right] e^{-k_0 t} + 56.5 \quad (7)$$

The expression $100(OD_T - OD_t)/OD_T$ is derived by subtracting the value obtained in equation 7 from 100. In Fig. 2 equation 7 is shown to fit the experimental data fairly well when k_1 is obtained from the initial staight line portion of the experimental curve and k_0 is 1.17×10^{-3} min.$^{-1}$ for the transformation of β-complex to α.

Rate of Reaction of Simple Polysilicic Acids. —In Fig. 3 is shown the effect of dilution of a sodium silicate on k_1 and P_0 when a 3.3 ratio silicate is diluted from 30 to 2 per cent. SiO_2. Each of the data points is the average of five measurements carried out 2 min., 2 hours, 1 day, and 2 weeks after dilution. k_1 was obtained by graphical solution of equation 7 and P_0 by extrapolation. During the aging period, the samples were kept at 25°. No significant change in k_1, P_0, or pH was observed over this period. The effect of dilution therefore rapidly established a new equilibrium which is stable for at least two weeks.

The per cent. silica remaining uncomplexed by molybdic acid for the reaction with disilicic acid is shown in Fig. 4. Approximately 99% of full color development occurred in five minutes. The shape of the curve is different from those obtained with sodium silicates. A rate curve of this shape is consistent with the assumption of two rate-limiting steps, hydrolysis of the siloxane bond to yield two

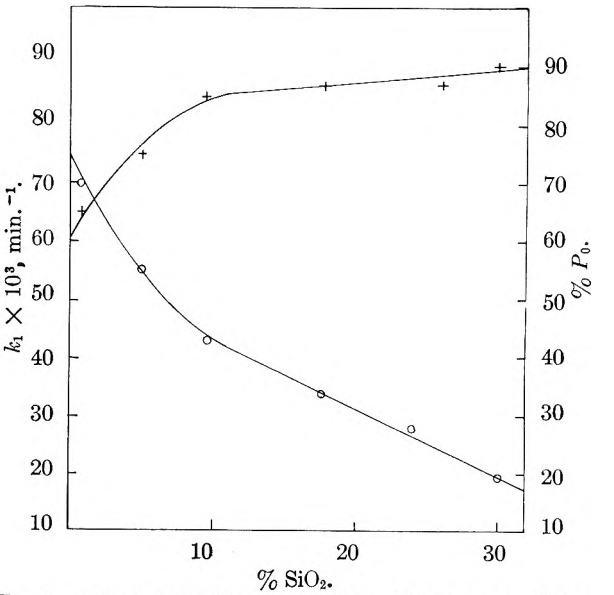

Fig. 3.—Effect of dilution on k_1 and p_0. Upper curve, % P_0; lower curve, k_1.

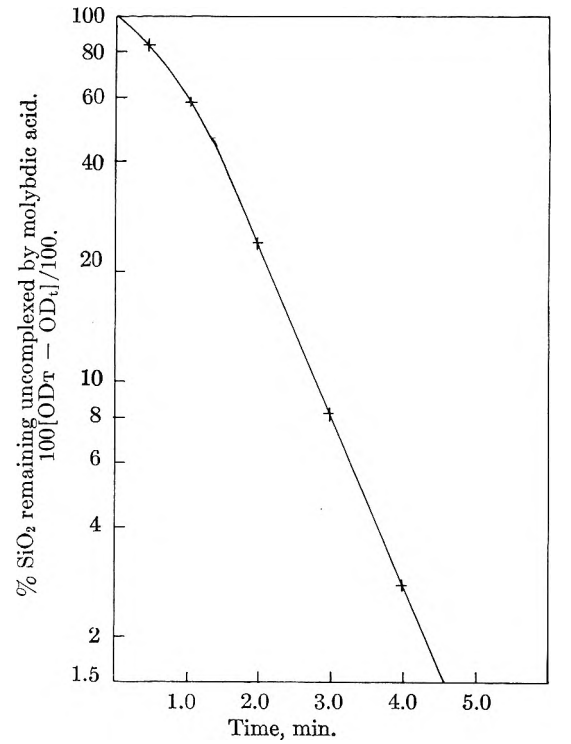

Fig. 4.—Reaction rate of disilicic acid with molybdic acid. Curve experimental; points calculated from equation 11.

monomers and reaction of the monomers with molybdic acid to yield β-complex. In reactions going to completion in five to ten minutes, the β to α conversion is of no concern.

If it is assumed that dimer hydrolyzes to monomer according to the first-order rate law, the concentration of dimer (D) is given by

$$D = D_0 e^{-k_2 t} \quad (8)$$

The rate of change of monomer (M) is

$$\frac{dM}{dt} = 2k_2 D - k_3 M \quad (9)$$

where $2k_2 D$ is the rate of formation of monosilicic

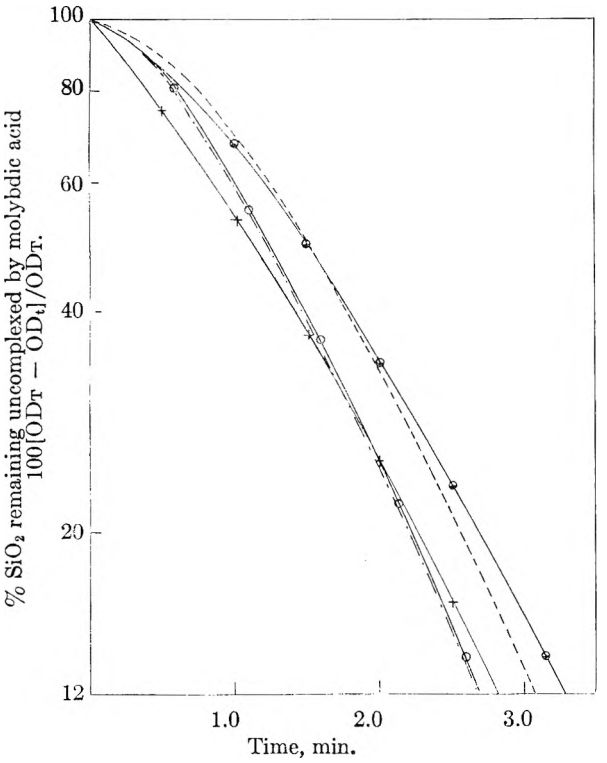

Fig. 5.—Reaction rates of trisilicic acid, +, tetrasilicic acid, ⊙, and pentasilicic acid, ◒, with molybdic acid: ----, curve calculated from equation 12 for pentamer; — · —, calculated for dimer.

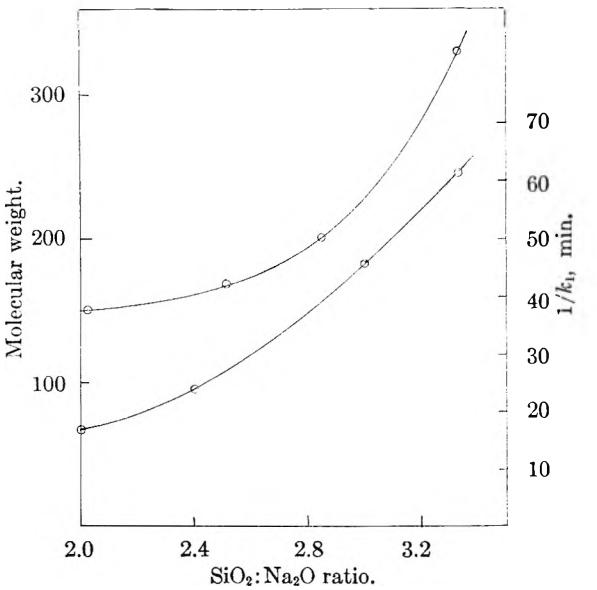

Fig. 6.—Comparison of $1/k_1$ (bottom curve) with molecular weight (upper curve).

acid from disilicic acid and k_3M is the rate of disappearance of monomer through formation of β-silicomolybdate complex. The per cent. of full color development is given by

$$\% \text{ color development} = 100 - 2D - M \quad (10)$$

where D is the per cent. of the total silica present as dimer and M is the per cent. present as monomer when initially 100% of the silica is dimer. Integration of 9 and substitution in 10 gives equation (11) for the per cent. color developed

$$\% \text{ color developed} = 100\left[-e^{-k_2t} - \frac{k_2}{k_3 - k_2}(e^{-k_2t} - e^{-k_3t})\right] \quad (11)$$

The equation was solved graphically for k_2 and k_3 from the experimental data and the points indicated in Fig 4 calculated from the values. The equation describes the experimental data very well with the constant k_2 equal 1.09 min.$^{-1}$ for the hydrolysis of the siloxane bond and k_3 equals 1.87 min.$^{-1}$ for the reaction of the monosilicic acid generated with molybdic acid to form colored complex. The value for k_3 agrees fairly well with that reported by Alexander,[2] 2.3 min.$^{-1}$.

The next four higher polysilicic acids up to hexamer all showed similar color development curves with only slightly longer reaction time. The same mechanism shown to quantitatively describe the rate of color development with disilicic acid applied to the higher polymeric acids gives the general equation

$$\% \text{ color developed} = 100 - \frac{100}{n}\left[(n-2)e^{-2k_2t} + (2n-2)e^{-k_2t} + (2n-2)k_1e^{-k_2t} - \frac{(2n-4)k_2}{k_3 - 2k_2}e^{-2k_2t} + \frac{2k_2(nk_2 - k_3)e^{-k_3t}}{(k_3 - 2k_2)(k_3 - k_2)}\right] \quad (12)$$

where n is the number of SiO_2 units making up the polysilicic acid, k_2 is the rate constant for the hydrolysis of siloxane bonds, and k_3 is the rate constant for reaction of monosilicic acid with molybdic acid. According to these kinetics, the disappearance of a particular silicic acid species is directly proportional to the number of siloxane bonds present. Therefore, trimer disappears from solution at twice the rate of dimer. However, the complete breakdown of trimer to monomer is somewhat slower than dimer because two siloxane bonds must hydrolyze.

The experimentally determined silica remaining uncomplexed as a function of time, $100(OD_T - OD_t)/OD_T$ is given in Fig. 4 for tri, tetra- and pentasilicic acids. A calculated curve for pentamer using equation 12 with the constants k_2 and k_3 fits the experimental data fairly well for this species. Calculated curves for the other polysilicic acids are of the same shape and fall between the dimer and pentamer.

Discussion

The rate of depolymerization of non-cyclic silicic acids in molybdic acid is only slightly affected by increasing complexity up to the hexamer as shown by the rate of reaction of these silicic acids to form the colored silicomolybdate complex. Monosilicic acid (mol. wt., 96) develops 90% of full color in about one min. and pentasilicic (mol. wt. 408) acid in about 3.5 minutes. As has been shown for a number of linear organic polymers,[7] the rate of depolymerization of a particular polysilicic acid is first order in the number of linkages present. The rate of color development is thus a function of two first-order reaction rate constants, one for the hydrolysis of siloxane bands and one for the first-order reaction of monosilicic acid, released by depoly-

(7) H. Marx and M. V. Tobolsky, "Physical Chemistry of High Polymeric Systems," 2nd Edition, Interscience Publishers, Inc., New York, N. Y., 1950, Ch. XIII.

merization with molybdic acid to form colored complex. This also applies to disilicic acid where an earlier investigation by Alexander[2] indicated that color development was first order only in the amount of disilicic acid present. Apparently the disilicic acid prepared by Alexander was contaminated with some monosilicic acid in which case it is difficult to analyze the color development curve. The polysilicic acids prepared in the present work were assumed to be linear and the kinetics derived on this basis. The presence of branched acids would affect the kinetic analysis but to a degree probably not detectable within the experimental accuracy.

The results found with the polysilicic acids show in regard to the nature of concentrated sodium silicate solutions, above a $SiO_2:Na_2O$ ratio of two, that the bulk of the silicate is present as three dimensional anions. Non-cyclic silicic acids depolymerize rapidly, less than five minutes, whereas the polysilicic acids derived from the polysilicate anions existing in sodium silicate require up to several hours for complete depolymerization.

Assuming the rate of depolymerization is inversely proportional to the molecular weight of the anions present in sodium silicate, $1/k_1$ shows a dependence on $SiO_2:Na_2O$ ratio similar to the estimated molecular weights from light scattering as reported by Nauman and Debye.[8] This comparison is shown in Fig. 6. The present study shows, however, that dilution of a sodium silicate solution results in a very rapid equilibration, indicative of depolymerization, to a state which is stable for at least two weeks. On dilution to below 10% (in the range 10 to 2% SiO_2) for a 3.3 ratio sodium silicate there is an accelerated effect on depolymerization of the polysilicate species. No effect of method of preparation or age could be shown for commercial silicate of 2.4 ratio by reaction kinetics with molybdic acid.

Acknowledgments.—The financial support and contribution of sodium silicate samples by the Diamond Alkali Co. is gratefully acknowledged as well as the work of J. Eisenman of Ionics who prepared the chlorosiloxanes and J. B. Frederickson and D. Kingston who made many of the measurements.

(8) R. V. Nauman and P. Debye, THIS JOURNAL, **55**, 1 (1951).

THE SLOW CHANGE IN TURBIDITY OF SODIUM SILICATE SOLUTIONS[1]

BY P. DEBYE AND ROBERT V. NAUMAN

Department of Chemistry, Cornell University, Ithaca, N. Y. *Department of Chemistry, Louisiana State University, Baton Rouge, La.*

Received September 24, 1960

Concentrated sodium silicate solutions in the 1–4 SiO_2/Na_2O ratio range containing 35% or more silicate have been found to have rather stable turbidities over periods of months to a year. Dilute solutions in the same ratio range have slowly increasing turbidities generally accompanied by a small but significant *p*H increase. The turbidity increases are believed to be real and probably result from a very slow polymerization of silicic acid formed by hydrolysis of the silicate ions with OH^- formation.

Introduction

During our light scattering investigations[2,3,4] of particle size in sodium silicate solutions investigations of the turbidity stability of both the concentrated stock silicate solutions and those solutions used for the molecular weight determinations were necessary. No significant turbidity changes were found during the few hours to a few days time that was required to perform a series of experiments after solutions were made from the concentrated stock solutions, and thus it was possible to determine molecular weights characteristic of freshly prepared solutions. Fortuitously the turbidities of some solutions were measured after much longer time intervals, and turbidity increases were observed. These observations led to our studying these turbidity changes whenever possible for long periods of time. Recent conversations[5] indicated that these studies are of such interest as to warrant presentation at this time.

(1) This work was supported by the Sodium Silicate Manufacturers' Institute.

(2) P. Debye and R. V. Nauman, *J. Chem. Phys.*, **17**, 664 (1949).

(3) R. V. Nauman and P. Debye, THIS JOURNAL, **55**, 1 (1950).

(4) P. Debye and R. V. Nauman, unpublished reports to the Sodium Silicate Manufacturers' Institute, 1948–1952.

(5) Symposium on Colloidal Silica and Silicates, 137th Meeting American Chemical Society, Cleveland, Ohio, April 13 to 14, 1960.

Experimental

In the main the experimental procedures have been reported previously.[3] The silicate solutions were stored under nitrogen in polyethylene bottles that were coated with Glyptal. All bottles containing solutions that were used for periods longer than a week were stored in large sealed desiccators that were periodically flushed with nitrogen.

Before each turbidity measurement the solution was filtered through platinum by nitrogen pressure. The platinum filters were cleaned by reverse flushing with sodium hydroxide solution and washing with distilled water.

Results and Discussion

Initially the stability of the turbidity of the concentrated stock solutions was assumed because of the reproducibility of the turbidity of solutions freshly prepared from them. Consequently quantitative results are available for only those stock solutions used in the latter stages of our investigations. Table I summarizes the observations. The first observation is that of the day the solution was first used; the age of each solution is unknown but the reported age is based upon time from day of first use. The precision of these measurements is not high because it is difficult to clean solutions of such high concentration and the same portion of the solutions was not used for all observations. The turbidity decreases probably are

Table I

Turbidity Change in Stock Sodium Silicate Solutions (Ages Are in Days)

Ratio →	3.79		3.75		3.36		2.85		2.03	
g./cc. →	0.37		0.40		0.42		0.52		0.54	
Age	$\tau \times 10^4$	Age	$\tau \times 10^4$	Age	$\tau \times 10^4$	Age	$\tau \times 10^4$	Age	$\tau \times 10^4$
0	29.2	0	15.9	0	17.2	0	7.59	0	8.44
1	27.7	1	16.0	4	16.1	3	7.48	6	12.29
12	28.3	266	14.0	24	14.2	24	6.97	12	7.20
273	28.0					33	6.37	21	1.43
						84	6.34	24	1.38

Table II

Turbidity Change in Sodium Silicate Solutions of Different Ratios (Ages Are in Days)

Ratio →	1.095			2.85			3.36			3.36			3.36[a]		
g./cc →	0.00805			0.01059			0.00626			0.0626			0.0626		
Age	$\tau \times 10^4$		pH	Age	$\tau \times 10^4$	pH	Age	$\tau \times 10^4$	pH	Age	$\tau \times 10^4$	pH	Age	$\tau \times 10^4$	pH
0	0.81		12.50	0	0.57		0	1.12	10.85	0	2.40	11.10	0	2.72	11.00
1	0.78		12.54	7	.52		2	2.17		6	2.41	11.15	6	2.59	11.08
5	1.04			8	.39		4	2.56		33	2.59	11.15	33	3.22	11.10
21	0.90		12.55	17	.42		6	2.49		75	2.92	11.15	75	3.31	11.06
60	1.65		12.50				17	3.66		134	3.22		134	3.39	
88	2.46		12.56				29	3.88		334	2.61		355	3.01	
124	3.05		12.56				70	4.03	10.89	481	3.96	11.22	481		11.15
173	3.51		12.41							602	4.36	11.12	602	3.67	11.05

[a] Stock solution was diluted with water saturated with CO_2.

Table III

Turbidity Change of 3.75 Ratio Sodium Silicate Solutions in Polyethylene (Ages Are in Days)

g./cc. →	0.0052			0.0103			0.0200			0.0294			0.0406			0.0566		
Age	$\tau \times 10^4$		pH	Age	$\tau \times 10^4$	pH	Age	$\tau \times 10^4$	pH	Age	$\tau \times 10^4$	pH	Age	$\tau \times 10^4$	pH	Age	$\tau \times 10^4$	pH
0	0.42		10.53	0	0.47	10.84	0	0.81	10.85	0	0.80	10.92	0	0.95	10.97	0	1.61	11.00
1	1.24		10.81	1	2.03	10.90	1	2.32	10.94	2	1.16	10.96	2	1.26	11.01	2	1.85	11.06
4	1.49		10.82	3	2.18	10.90	3	3.80	10.95	7	2.54	10.96	7	1.42	11.04	7	1.71	11.15
18	2.41		10.83	15	3.39	10.98	15	5.47	11.01	14	4.27	10.90	15	1.45	11.00	15	1.56	11.00
47	2.93		10.90	46	4.49	11.00	45	6.70	11.03	44	10.31	11.02	44	1.38	10.97	44	1.81	10.98
89	3.72		10.83	86	5.07	10.97	88	8.06	11.05	87	15.64	11.00	87	2.31	10.95	87	1.87	10.98
169	3.96			166	5.99		166	9.53		165	21.9		165	14.96		165	2.14	
202	4.67			199	6.50		199	10.47		199	23.6		199	26.5		199	2.50	
355	5.43			352	8.16		351	13.00		350	32.2		350	99.4		351	6.44	
458	6.63		10.90	455	10.16	11.01	455	14.43	11.02	454	35.4	11.02	454	138.7	10.95	454	6.80	10.92
537	7.22		10.86	534	11.12	11.12	534	16.90	11.19	533	42.4	11.07	533	160	11.05	533	10.00	11.00
699	7.75			697	13.69		697	18.07		674	56.5	11.03	674	312	10.99	696	11.62	

caused by removal of minute amounts of very large particles; in the case of the 2.03 ratio the filtrations produced a residue that appeared to be undissolved quartz, but none of the other solutions gave any detectable residue. The 2.03 ratio was analyzed after the final low turbidities were obtained and a 1.98 ratio was found; analyses of the other ratios showed no change or an insignificant increase in ratio. A few other isolated experiments were consistent with the conclusion that the stock solutions, once cleaned, have relatively constant turbidities.

Attempts to reproduce turbidities of dilute solutions were uniformly unsuccessful unless freshly diluted solutions were compared. An examination of the irreproducible results indicates an age dependence; as a result a few tests of the aging hypothesis were made, but a complete study was essentially prohibited by the time required for significant observations.

The *p*H measurements indicated that the measures used to prevent carbon dioxide contamination were successful. In addition a solution was purposely contaminated with carbon dioxide. A comparison of results with this solution with those of one identical except for dilution with pure water is shown in Table II. The carbon dioxide has a definite initial effect on both turbidity and *p*H but otherwise their behaviors are similar. It is felt that carbon dioxide contamination could not possibly cause the turbidity increases that are observed in all cases.

Table III summarizes the only systematic study of the gradual turbidity increase; it was made with the 3.75 ratio because the qualitative results indicated that the turbidity increases at a given SiO_2 concentration were greater in the higher ratio solutions. At the time of mixing the turbidities and *p*H's increase with increasing concentration as expected in this concentration range. In all cases there is a marked *p*H increase in the initial stages. The more concentrated solutions show turbidity stability for greater lengths of time, but the turbidity increase once begun results in higher values in the more concentrated solutions. This turbidity stability at higher concentrations is consistent with the observations in the stock solutions.

Table IV gives results obtained from two 3.75 ratio solutions that were sealed permanently under nitrogen in glass scattering cells. After nearly three years the seal of the glass test-tubes was broken, and after cleaning the tubes showed no sign of reaction with the silicate. The results from solutions kept in glass essentially confirm the results obtained from those in polyethylene. The 0.0122 g./cc. solution probably was not well cleaned but otherwise behaved as expected.

TABLE IV

TURBIDITY CHANGES OF 3.75 RATIO SODIUM SILICATE SOLUTIONS IN GLASS (AGES ARE IN DAYS)

0.0122 g./cc.		0.204 g./cc.	
Age	$\tau \times 10^4$	Age	$\tau \times 10^4$
0	1.96	0	0.67
1	3.28	1	1.50
8	4.65	8	4.78
19	4.89	19	5.65
42	5.31	42	6.25
279	7.12	279	12.68
930	7.85	930	13.24

From these results it is concluded that the turbidity changes are real and are the result of a very slow polymerization[6] of silicic acid formed by a more rapid hydrolysis of silicate ions indicated by the *p*H changes. It is highly unlikely that the turbidity increase is caused by reaction with the container, contamination by carbon dioxide or any other interaction with the surroundings. Some of the turbidity increase after very long storage and repeated very brief exposures to the atmosphere may be caused by carbon dioxide contamination as indicated by small *p*H decreases in some cases, but this influence seems to be minor. It should be pointed out that if one observed many of these silicate solutions for only a few days or less, which for many experiments might seem to be a long time, one might conclude easily that a stable turbidity had been obtained from a solution that was changing too slowly for detection during the observation interval.

(6) For a discussion of polymerization in other circumstances see R. K. Iler, "Colloidal Chemistry of Silica and Silicates," Cornell University Press, Ithaca, N. Y., 1955, pp. 36–55.

THE REFRACTIVE INDICES OF SODIUM SILICATE SOLUTIONS[1]

BY P. DEBYE AND ROBERT V. NAUMAN

Department of Chemistry, Cornell University, Ithaca, New York *Department of Chemistry, Louisiana State University, Baton Rouge, La.*

Received August 10, 1960

The refractive indices of sodium silicate solutions of varying SiO_2/Na_2O ratio were measured relative to that of water by means of a differential refractometer. A useful three-constant equation for the concentration dependence of the differential refractive index as a function of SiO_2/Na_2O ratio was derived; two of the constants were determined by putting a least squares curve through the experimental results obtained from solutions of very pure sodium silicates in the 1.0 to 4.0 ratio range; the third constant was evaluated theoretically. The resulting equation is $(\mu - \mu_0)/c = [0.0698(\text{Ratio}) + 0.4421]/[\text{Ratio} + 1.034]$. This equation fits the data better than one in which all three constants were evaluated experimentally and is valid even in the 5.0 to 53.2 ratio range in which no data were used for the evaluation of the constants. By means of this equation the refractive index of any dilute aqueous sodium silicate solution of any ratio can be estimated with good accuracy.

Introduction

During our light scattering investigations[2,3,4] of sodium silicate solutions differential refractive indices were needed repeatedly. Rarely were the same refractive indices needed, and in order to eliminate the need for a multitude of measurements a general study of the refraction of sodium silicate solutions was made so that frequently needed refraction information could be calculated from results obtained from a limited number of measurements.

Experimental

The refraction measurements were made with a differential refractometer described by P. P. Debye[5] modified only by cell simplification. The measurements were made in a room thermostated to 20°.

The sodium silicates were prepared by the member companies of the Sodium Silicate Manufacturers Institute by fusing crystal quartz with C.P. Na_2CO_3 or NaOH. The melts were dissolved in steam under pressure, and the silicates were stored as very concentrated solutions in polyethylene containers under nitrogen. Shortly before or after the refraction measurements the filtered stock solutions were analyzed for SiO_2, Na_2O and CO_2 by conventional procedures. All stock solutions were analyzed spectroscopically for all elements to which the method was applicable. All impurities in all cases totalled less than 0.3% and were usually appreciably less; the major impurity was CO_2.

The solutions used for refraction measurements were made by diluting weighed quantities of analyzed stock solutions of a given ratio to calibrated known large volumes with conductivity water or C.P. HCl solutions of predetermined concentration.

TABLE I

DIFFERENTIAL REFRACTIVE INDICES OF SODIUM CHLORIDE SOLUTIONS

Concentration, c NaCl (g./cc. $\times 10^3$)	$\mu - \mu_0$ $\times 10^4$	$(\mu - \mu_0)/c$
3.749	6.73	0.1795
5.468	9.83	.1798
7.498	13.18	.1758
7.920	14.06	.1775

From these and other data $(\mu - \mu_1)/c = 0.178 \pm 0.002$
μ is refractive index of solution
μ_0 is refractive index of solvent

The refraction of the high ratio silicates prepared from the stock solutions and HCl was determined by difference; the differential refractive index of the solution compared with water was measured and the contribution of NaCl was subtracted. This contribution was calculated from equation 1 which was obtained from data of the kind

$$\mu - \mu_0 = 0.01043\ M \quad (M = \text{molarity of NaCl}) \quad (1)$$

shown in Table I. The concentration of NaCl in a high ratio silicate was calculated from the known analyses of the stock silicate and the HCl and the dilution data.

The refraction of at least four or five solutions of different concentrations was measured for each ratio silicate used in the determination of the constants of equation 6. The slope of the best line through the points of a $\mu - \mu_0$ *vs.* c plot was taken for the $(\mu - \mu_0)/c$ value. Concentrations, c, are given in g./cc.

Development of the Equation

Additivity of the refractions of atoms having common surroundings has been assumed. In the dilute solutions considered here experimental error makes a more rigorous assumption unnecessary. A sodium silicate that contains by analysis $p SiO_2$ molecules for $q Na_2O$ molecules (ratio p/q) will contain atoms in the proportion pSi atoms, $2q$Na atoms, and $(2p + q)$O atoms. All of the O atoms do not have the same surrounding electron distribution; consequently the polarizabilities, α_0, of all the O atoms will not be the same. Two qO atoms will be essentially in the form of O^- ions in order to compensate for the $2qNa^+$ ions. In these dilute aqueous solutions the silicates can be considered to be essentially dissociated because, even if the anions are aggregated and attract a surrounding cloud of Na^+ ions, the charged oxygen atoms will not be bound to a specific Na^+ and as a first approximation all the charged O atoms can be considered to have the same polarizability. The rest of the oxygen atoms, $(2p - q)$ in number, are -O- atoms which link Si atoms.

It is assumed that a solution contains per cc. a number n of hypothetical $(Na_2O)_q(SiO_2)_p$ molecules. As a first approximation reaction fields may be ignored, and the differential refractive index can be represented by

$$\mu - \mu_0 = n\alpha \quad (2)$$

in which α is the polarizability of the molecule. This equation[6] is strictly applicable only for dilute gases, but the manner in which it is used hereafter makes it applicable as a first approximation in dilute solution. Assuming that the polarizability of the molecules in solution can be represented by

(1) This work was supported by the Sodium Silicate Manufacturers Institute.

(2) P. Debye and R. V. Nauman, *J. Chem. Phys.*, **17**, 664 (1949).

(3) R. V. Nauman and P. Debye, THIS JOURNAL, **55**, 1 (1951).

(4) P. Debye and R. V. Nauman, unpublished.

(5) P. P. Debye, *J. Applied Phys.*, **17**, 392 (1946).

(6) P. Debye, "Polar Molecules," Dover Publications, New York, N. Y., pp. 11-20, gives an equation which reduces to $\mu - \mu_0 = \mu - 1 = 2\pi n\alpha$ for dilute gases. The method of use shows that the adaptation used here is acceptable.

the polarizabilities of the different kinds of atoms in the solution one obtains

$$\mu - \mu_0 = np\alpha_{Si} + 2nq\alpha_{Na^+} + 2nq\alpha_{O^-} + (2p - q)n\alpha_{-O-} \quad (3)$$

The concentration c in g./cc. can be represented by

$$c = npm_{Si} + 2nqm_{Na} + n(2p + q)m_O \quad (4)$$

in which m_{Si}, m_{Na}, and m_O are the masses of Si, Na, and O atoms, respectively. Combination of equations 3 and 4 gives

$$\frac{\mu - \mu_0}{c} = \frac{p[\alpha_{Si} + 2\alpha_{-O-}] + q[2\alpha_{Na^+} + 2\alpha_{O^-} - \alpha_{-O-}]}{p[m_{Si} + 2m_O] + q[2m_{Na} + m_O]} \quad (5)$$

After rearrangement equation 5 can be represented by

$$\frac{\mu - \mu_0}{c} = \frac{Ap/q + B}{p/q + C} + \frac{A(\text{Ratio}) + B}{\text{Ratio} + C} \quad (6)$$

A and B are constants which contain the unknown polarizabilities and the masses of the atoms and cannot be evaluated theoretically. C is $(2m_{Na} + m_O)/(m_{Si} + 2m_O)$ and from the known atomic masses is calculated to be 1.034.

Results and Discussion

The experimental refraction results are summarized in Table II. Only the results in the 1 to 4 ratio range were used in the determination of the constants A and B of equation 6. The results at higher ratios were not obtained from pure sodium silicates because solutions of these ratios are not stable; our measurements were made on solutions that contained NaCl, and because the results are obtained as small differences between two experimental results they are consequently not as reliable as those from solutions of the lower ratios. The 0.478 ratio results were not used because the assumption of $(2p - q)$-O-atoms is not valid below ratio 0.5, and in addition there was considerable doubt about the analyses of this ratio. A least squares treatment of the results in the 1 to 4 ratio range gave $A = 0.0698$ and $B = 0.4421$; equation 6 becomes

$$\frac{\mu - \mu_0}{c} = \frac{0.0698\text{Ratio} + 0.4421}{\text{Ratio} + 1.034} \quad (7)$$

Refraction results calculated from equation 7 at selected ratios also are given in Table II. The calculated and measured results agree very well even at high ratios in which range no experimental results were used for the evaluation of the constants. The indicated errors in Table II are most probable values calculated by a statistical analysis of error from all sources.

TABLE II

Ratio	Measured $(\mu - \mu_0)/c$	Calculated $(\mu - \mu_0)/c$
0.478 ± 0.005	0.285 ± 0.03	
0.50		0.311
1.00		2.48
1.10 ± .005[a]	.242 ± .006	
1.50		.216
1.98 ± .02[a]	.190 ± .004	
2.00		.192
2.50		.175
2.51 ± .01[a]	.176 ± .004	
2.85 ± .01[a]	.164 ± .003	
3.00		.162
3.32 ± .01[a]	.156 ± .002	
3.36 ± .01[a]	.157 ± .003	
3.50		.152
3.64 ± .3	.144 ± .002	
3.75 ± .01[a]	.144 ± .002	
3.79 ± .2	.144 ± .002	
3.80 ± .01[a]	.144 ± .001	
4.00		.143
4.5 ± .3[a]	.126 ± .007	
4.50		.137
4.82 ± .15[b]	.123 ± .006	
4.94 ± .3[b]	.127 ± .007	
5.00		.131
9.5 ± .9[b]	.098 ± .01	
10.0		.103
20.0		.087
29 ± 10[b]	.076 ± .008	
34.2 ± 1.5[b]	.076 ± .009	
35.0		.080
40.9 ± 2.4[b]	.074 ± .01	
50.0		.077
53.2 ± 9.0[b]	.072 ± .01	
100.0		.073

[a] Results used to calculate constants A and B in equation 6. [b] Measured solutions contained NaCl; equation 1 used to correct measured $\mu - \mu_0$ for $\mu - \mu_0$ of NaCl.

Attempts to calculate all three constants of equation 6 from experimental results did not give as satisfactory a fit in all regions as did the adopted procedure. Equation 7 has been used repeatedly with good success to calculate refraction information needed in light scattering studies. It is felt that for most uses the equation will give generally satisfactory results for all ratios above 1; it should not be used at ratios much lower than ratio 1.

A LIGHT SCATTERING STUDY OF THE AGGREGATION OF ACIDIFIED SODIUM SILICATE SOLUTIONS[1]

BY P. DEBYE AND ROBERT V. NAUMAN

Department of Chemistry, Cornell University, Ithaca, N. Y. *Department of Chemistry, Louisiana State University, Baton Rouge, Louisiana*

Received August 10, 1960

An empirical study of the particle growth as indicated by turbidity changes of sodium silicate solutions to which hydrochloric acid was added has been made. Relatively stable solutions containing large particles can sometimes be obtained. The aggregation and the stability of the large particles was found to be dependent upon salt concentration; consequently the SiO_2/Na_2O ratio of the original silicate influenced the stability of the final product. *p*H increases accompany the aggregation. Dilution of the more stable solutions resulted in even greater turbidity stability. The aggregation can be rapidly reversed by sodium hydroxide addition; this result and the low particle density indicated by viscosity measurements indicate that the particles are loose permeable aggregates.

Introduction

Many studies[2] of the aggregation of sodium silicates to gels have been made by classical techniques. Greenberg and Sinclair have made light scattering studies[3] of the polymerization of 1:1 ratio silicate upon the addition of ammonium acetate. The studies described here include work done with the 1:1 ratio silicate as well as some higher ratio silicates, but in this work aggregation was stimulated by addition of hydrochloric acid. The term aggregation is used instead of polymerization because the low particle density found from viscosity measurements and the very rapid decrease of the greater part of the turbidity increase upon addition of sodium hydroxide indicate a much looser accessible structure for the aggregates than that which would be expected to exist if polymerization by formation of Si–O–Si bonds occurred. A slower polymerization probably also occurs to a minor extent. Gels rarely were formed in this work. A few exploratory experiments during our previous work[4,5] indicated that there can be produced large particles nearly as stable as those in the low ratio range.[6] This work was undertaken primarily to study the conditions of stability of large particles in high ratio (>4) sodium silicate systems.

Experimental

The experimental techniques in the main have been described previously.[5,6] A sleeve type calomel electrode was used in the Beckmann Model G *p*H meter in order to prevent clogging of the capillary by large particles. The type E electrode was used above *p*H 8 and the regular electrode below *p*H 8; the electrodes were stored in water, dried with absorbent cloth briefly, and placed immediately with brief swirling in the solution to be measured. Measurement was begun immediately and was continued for a few minutes until no observable change in repetitive measurements occurred. The normal procedure led to erratic results; the adopted procedure gave reproducible results and accurate results for buffer solutions.

The solutions were stored under nitrogen in Glyptal coated polyethylene bottles that were kept in nitrogen-filled desiccators. The platinum filters prior to being rinsed with distilled water were cleaned by reverse flushing with NaOH or HCl depending upon the *p*H of the solution to be filtered; failure to consider the previous history of the filter led to large unreproducible turbidity effects for solutions in the 7–8 *p*H range.

The reported turbidities are uncorrected for dissymmetry.

Results and Discussion

The initial experiments were performed with rather concentrated (0.798 *M* SiO_2) solutions prepared from the 3.37 ratio solution by addition of HCl. Relatively low ratio (<5) silicates resulted, but at the high concentration continuously rising turbidities were observed. Some of these results are shown in Fig. 1A. These results are typical of systems in which no stability results and are characterized by an increasing rate of turbidity increase. Most of these systems eventually gave precipitates. The *p*H's of all these systems were essentially constant throughout the long periods of observation. These results led to the study of more dilute systems.

A multitude of experiments were performed using the 1.095 ratio as a source of silicate. Many concentrations were studied, but only a few results, those most closely comparable with results to be given later, are given in Fig. 1B. The *p*H range from 2.3 to 12.5 was studied in detail for solutions that were 0.07 *M* with respect to SiO_2. The results in acid solution are typical of those for which no stability is found; they show the increasing rate of aggregation. The rate of aggregation decreases as the *p*H decreases in acid solution. In basic solution the rate of turbidity increase is greatest initially giving a hint of the quasi-stability to be found later. At high *p*H the rate of aggregation is lower than the lower *p*H basic solutions. The maximum initial rate of aggregation seems to be at *p*H 7.6, but it is not known accurately because the turbidity-time curve undergoes an abrupt change from one of small initial slope to one of large initial slope in this region.

In both acid and basic solutions prepared from what is essentially the 1:1 ratio silicate the *p*H increases as the turbidity increases. The *p*H's of the five solutions shown in Fig. 1B increase from 3.30 to 3.55, from 9.32 to 9.76, from 2.32 to 2.98, from 9.89 to 10.28, and from 10.21 to 10.52. The three basic solutions show later *p*H decreases coincident with the increasing τ-t slope; these

(1) This work was supported by the Sodium Silicate Manufacturers' Institute.

(2) For reviews see R. K. Iler, "Colloidal Chemistry of Silica and the Silicates," Cornell University Press, Ithaca, N. Y., 1955; W. Eitel, "The Physical Chemistry of the Silicate Systems," University of Chicago Press, Chicago, Ill., 1954; J. G. Vail, "Soluble Silicates," Reinhold Publ. Corp., New York, N. Y., 1952.

(3) S. A. Greenberg and D. Sinclair, THIS JOURNAL, **59**, 435 (1955)

(4) P. Debye and R. V. Nauman, *J. Chem. Phys.*, **17**, 664 (1949).

(5) R. V. Nauman and P. Debye, THIS JOURNAL, **55**, 1 (1951).

(6) P. Debye and R. V. Nauman, *ibid.*, **65**, 5 (1961).

probably result from slight carbon dioxide contamination during filtration.

No solutions prepared from the 1:1 ratio silicate gave any evidence for large particle stability. These solutions usually eventually gave gelatinous precipitates but not rigid gels.

An attempt was made to study the effect of SiO_2 concentration at a fixed ratio on the rate of aggregation. The ratio 5, higher than the commerical range but relatively low where rates would be reasonable, was chosen. Some of the results are shown in Fig. 1C. No concentration gave stable turbidities. The rate of aggregation was greater in more concentrated solutions but the results are complicated by the presence of different amounts of NaCl because all solutions were prepared from the 3.41 ratio and HCl. In all these cases the *p*H increased with aggregation.

The evidence indicated that the initial charge on the aggregating particles has a big influence on the rate of aggregation and of course should influence the stability. A neutral salt should therefore eliminate some of the repulsive charge effects and lead to an increased rate of aggregation. The effect of added NaCl was studied and some results with the 3.79 rate are shown in Fig. 1D. The normal slow turbidity increase[6] is accelerated by the presence of NaCl; thus it is evident that for a valid comparison of the effect of SiO_2 concentration on the aggregation rate, all solutions should contain the same amount of salt.

Evaluation of the many experiments in basic solution indicated that turbidity stability nearly as good as that in the commercial ratio range could be obtained in the higher ratio ranges if SiO_2 concentration and NaCl concentration were properly adjusted. Although a theory[7] of this stability has been developed, it has not been properly tested and quantitative prediction of stability conditions cannot yet be made; however, there is experimental evidence for the stability. Figure 2A shows the results of a solution prepared from the 3.41 ratio. After a rapid initial turbidity increase, the turbidity changed only 5% in 34 days. At that time the viscosity and the angular scattering pattern were determined, and a series of dilutions were made. Angular scattering patterns and viscosities were determined for the dilutions. From these data an intrinsic viscosity of 20 cc./g. was calculated; from this the Einstein equation gives a 0.125 g./cc. density. This compares with 0.64 cc./g. for the metasilicate and 0.43 for the 3.75 ratio[5] and indicates a rather loosely packed particle. The dissymmetry data can be fit well by a spherical particle distribution made up of 99.92% of the molecules with a 330 Å. radius and 0.08% with a 960 Å. radius. Crude electron micrographs indicated essentially a monodisperse system of spheres with a diameter of the order of 300 Å.; however the calibration[8] could have been wrong by a factor of 2 or 3. The molecular weight of the aggregate was determined from the turbidity data and the refraction calculated by the derived equation[9] and found to be 5.78×10^6 uncorrected for dissymmetry. From the radius determined

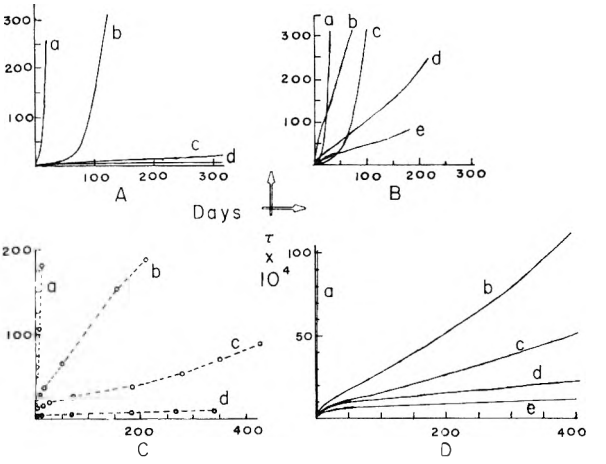

Fig. 1.—Turbidity *vs.* time curves for: A solutions prepared from 3.37 ratio; 0.798 *M* SiO_2; ratios: a, 4.29; b, 4.09; c, 3.89, and d, 3.70. B Solutions prepared from 1.095 ratio: a, 0.0692 *M* SiO_2, 0.0019 *M* HCl, 0.1269 *M* NaCl; b, 0.0698 *M* SiO_2, 0.0066 *M* Na_2O, 0.1257 *M* NaCl, ratio is 10.6; c, 0.0696 *M* SiO_2, 0.0034 *M* HCl, 0.1271 *M* NaCl; d, 0.0693 *M* SiO_2, 0.0067 *M* Na_2O, 0.1132 *M* NaCl, ratio is 10.4; e, 0.0695 *M* SiO_2, 0.0120 *M* Na_2O, 0.1029 *M* NaCl, ratio is 5.78. C 4.99 ratio solutions prepared from 3.41 ratio: a, 0.547 *M* SiO_2, 0.110 *M* Na_2O, 0.102 *M* NaCl; b, 0.383 *M* SiO_2 0.077 *M* Na_2O, 0.071 *M* NaCl; c, 0.274 *M* SiO_2, 0.055 *M* Na_2O, 0.051 *M* NaCl; d, 0.082 *M* SiO_2, 0.016 *M* Na_2O, 0.015 *M* NaCl. D 3.79 ratio solutions containing 0.128 *M* SiO_2: a, 0.253 *M* NaCl; b, 0.127 *M* NaCl; c, 0.101 *M* NaCl; d, 0.0759 *M* NaCl; e, 0.000 *M* NaCl.

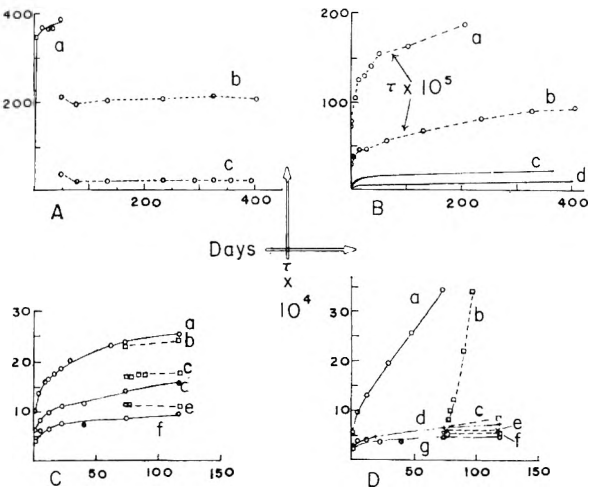

Fig. 2.—Turbidity *vs.* time curves for: A 1.36 ratio solutions prepared from 3.41 ratio: a, 0.0817 *M* SiO_2, 0.0006 *M* Na_2O, 0.0481 *M* NaCl; b, prepared from a by dilution after 49 days, 0.0409 *M* SiO_2; c, prepared from a by dilution after 49 days, 0.0082 *M* SiO_2. B Solutions prepared from 3.41 ratio: a, 59.2 ratio with 0.0817 *M* SiO_2, 0.0014 *M* Na_2O, 0.0452 *M* NaCl; b, 5.01 ratio with 0.0817 *M* SiO_2, 0.0163 *M* Na_2O, 0.0153 *M* NaCl; c, same as a; d, same as b. C 26.8 ratio solutions prepared from 3.44 ratio: a and b, 0.0882 *M* SiO_2, 0.0033 *M* Na_2O, 0.0447 *M* NaCl; c and d, 0.0662 *M* SiO_2, 0.0024 *M* Na_2O, 0.0334 *M* NaCl; e and f, 0.0441 *M* SiO_2, 0.0017 *M* Na_2O, 0.0223 *M* NaCl. D 26.8 ratio solutions prepared from 3.44 ratio containing 0.0221 *M* SiO_2, 0.00083 *M* Na_2O: a and c, 0.1137 *M* NaCl; b, 0.2161 *M* NaCl; d and e, 0.0624 *M* NaCl; f and g, 0.0112 *M* NaCl. In C and D solid lines represent solutions prepared initially and dashed lines represent solutions prepared from 74-day old solution for which data are given in C-b.

(7) P. Debye and R. V. Nauman, unpublished.

(8) The micrographs were made by Stanley Siegelman in the physics department student microscopy laboratory.

(9) P. Debye and R. V. Nauman, THIS JOURNAL, **65**, 8 (1960).

by light scattering and the density estimated from viscosity the molecular weight is calculated to be 11.3×10^6. The check is rather good considering that the first result should be too low and the second too high.

The turbidity and the angular scattering pattern of the dilutions of the sample just discussed remained constant within experimental error throughout the period of observation which was about a year.

Many similar experiments have been run. Figure 2B shows two other solutions that are as stable as low ratio solutions. Figure 2C shows stability produced by dilution of a solution that was not nearly as stable as low ratio solutions. Figures 2C and D shows results from one solution and its dilutions. The results are typical of many others that were obtained. A large quantity of solution was made; one part was sealed for future use and the other was diluted to different silicate concentrations and to different NaCl concentrations at one silicate concentration. After 74 days the sealed portion was opened, measured, and new dilutions exactly like those made the first day were made again. The stored solution gave essentially the same *p*H and turbidity as that which had been opened repeatedly. The new dilutions gave higher *p*H's than the old ones in all cases. The turbidities were higher for the new dilutions except for those which contained added salt. The turbidity increases were in all cases much less rapid for those solutions that were diluted after appreciable aggregation had occurred. The ones lacking excess salt had essentially stable turbidities. In those that contained added salt the decrease in rate of aggregation was remarkable; compare the two solutions that contain 0.1137 *M* NaCl, and observe the one that contains 0.2161 *M* NaCl; its counterpart made on the first day aggregated so rapidly that the data could not be shown on the same scale because it coincided with the ordinate.

Many similar experiments were performed. All showed marked initial *p*H increases which probably result from rapid hydrolysis of the silicate to give some OH^- ion prior to a slower aggregation of the hydrolyzed silicate. Many showed some *p*H decreases at late stages probably due to minor CO_2 contamination during the frequent filterings and transfers. In general the results from similar solutions were the same. Higher ratio starting material gave slightly better turbidity stability for a given SiO_2 concentration.

The addition of NaOH reversed the turbidity change in a time very small compared with that required for the increase. This was true for the very low commercial range ratios as well as the high ratio basic solutions and the acid solutions. The addition of NaOH to the basic solutions frequently briefly caused great turbidity or precipitation, but in all cases within one day the solutions had turbidities characteristic of small particle solutions.

This work has been concerned primarily with aggregation and particle stability. The kinetic data have not been analyzed and particle sizes have not always been determined. It is concluded that the particles are loosely bound aggregates probably held together primarily by van der Waals forces rather than Si–O–Si bonds; it is believed that the density and the NaOH reversal data support this conclusion. In general in basic solution the production of a large particle as stable as the low (0–4) ratio range particles requires that one start with as high a ratio as possible (or perhaps remove as much NaCl as possible) and dilute the solution after the particles have grown appreciably.

REACTION BETWEEN SILICA AND CALCIUM HYDROXIDE SOLUTIONS. I. KINETICS IN THE TEMPERATURE RANGE 30 TO 85°[1]

BY S. A. GREENBERG[2]

Contribution from the Johns-Manville Research Center, Manville, New Jersey

Received August 10, 1960

A study is described of the heterogeneous reaction between silica and calcium hydroxide solutions in the temperature range 30 to 85°. The rates were followed by determining the changes in calcium hydroxide concentrations with time by means of electric resistance measurements. The influences of the amount of silica, the calcium hydroxide concentration, temperature, type of silica, and surface areas of the silica on the rates of reaction were studied. It was concluded that of the more than six processes proceeding in the over-all reaction, the rate determining step was the solution of silica. Since the rate of solution of silica is proportional to the available surface of the silica, the over-all reaction rate is determined by this factor. The influence of aggregation of colloidal silicas on the rate is also discussed.

Introduction

The mechanisms of hydrothermal reactions[3] are of much interest to geochemists, cement chemists, and chemists concerned with inorganic reactions. The hydration of portland cement and the formation of many minerals proceed by hydrothermal mechanisms. In the present study an example of one kind of heterogeneous reaction of this group will be described.

The rates of reaction of several silicas with calcium hydroxide solutions were followed by measuring the conductances of the solutions as a function of time. The influences of the amount of silica, the calcium hydroxide concentration, temperature and type of silica on the rates were examined.

(1) Presented at the Colloid Division Symposium "Colloidal Silica and Silicates," at the 137th Meeting of the American Chemical Society, Cleveland, April, 1960.

(2) Portland Cement Association, Skokie, Illinois.

(3) G. W. Morey and E. Ingerson, *Econ. Geol.*, **32**, 607 (1937).

Theoretical

Morey and Ingerson[3] have proposed that hydrothermal reactions proceed by crystallization from solution. It is apparent from the word hydrothermal that in these reactions water must be present and the rates increase with temperature.

In the present study of the reaction of silica with solutions of calcium hydroxide, it is necessary that the silica dissolves so that the reactions in solutions may proceed. Accordingly, processes 1–6 would be expected.

1. Chemisorption of calcium hydroxide by surface silanol groups. In a previous paper[4] it was shown that the amount of calcium hydroxide chemisorbed could be correlated with the number of silanol groups on the surface.

2. The solution of silica in the aqueous phase. Silica reacts with water to form a saturated solution of monosilicic acid.[5] The solubility of the

$$SiO_2(s) + H_2O(l) = H_4SiO_4(aq) \qquad (1)$$

silica increases with pH because of the formation of $H_3SiO_4^-$ and $H_2SiO_4^{--}$ ions.[6]

Silica has been reported[7] to dissolve in sodium hydroxide solutions (to form a monosilicic acid solution) as a function of the surface area S of the silica

$$dc/dt = k_1S \qquad (2)$$

where c is the concentration of monosilicic acid in moles/l. and k_1 is the rate constant. With the assumption that the silica particles are spherical and monodisperse, the integrated form of Eq. 2 may be derived

$$C_p^{1/3} = C_{p_0}^{1/3} - k_2t \qquad (3)$$

where C_p and C_{p_0} are proportional to the amount of undissolved silica at time t and zero time, respectively, and k_2 is a constant.

3. The reaction of monosilicic acid or its ions in solution with calcium hydroxide in solution

$$H_4SiO_4aq + Ca^{++}aq + 2OH^-aq = n_1CaO\cdot SiO_2\cdot n_2H_2O(s) \qquad (4)$$

4. Formation of nuclei of calcium silicate hydrate.

5. Growth of nuclei.

6. Flocculation and precipitation of crystals.

The velocity of any of these processes might be rate determining. However, the present study demonstrated clearly that step 2, the solution of silica, controlled the kinetics of the over-all reaction

$$SiO_2(s) + Ca^{++}aq + 2OH^-aq = n_1CaO\cdot SiO_2\cdot n_2H_2O(s) \qquad (5)$$

A review of the physicochemical nature of the various hydrated calcium silicates has been presented by Brunauer and Greenberg.[8]

In another paper[9] the activity solubility product for hydrated calcium silicates has been reported

$$K_{sp} = a_{Ca^{++}}a_{H_2SiO_4^{--}} \qquad (6)$$

to be 10^{-7} at 25°. This information is useful for determining the degree of saturation of the solutions with respect to product.

Experimental

Materials.[4]—The various kinds of silica, the sources, per cent. SiO_2 content, "bound" water contents and nitrogen adsorption surface areas are listed in Table I.

TABLE I

NATURE OF THE SILICAS

Silica type	Source	SiO_2, %	"Bound" water, %	Surface areas sq. m./g. SiO_2
Standard luminescent	Mallinckrodt	80.8	7.3	750
Special bulky	Mallinckrodt	84.8	6.0	380
Aerogel	Monsanto	93.5	3.0	250
Ludox (dried)	Du Pont	93.0	2.4	150
Quartz	.....	99.7	..	<1

The difference between 100% and the sum of the silica (SiO_2) and "bound" water contents is the per cent. of water sorbed by the silicas. Solutions of calcium hydroxide were prepared by shaking Baker AR product with distilled water. Then these solutions were passed through Millipore HA filters (Millipore Filter Corp., Bedford, Mass.).

Equipment.—The conductivity apparatus employed in this study consisted of an Industrial Instruments RC1B bridge and dip cells with constants of approximately one $cm.^{-1}$. Reactions were conducted in one-liter flasks inserted into a constant temperature bath maintained at ±0.02°. Surface area measurements were made by the nitrogen adsorption B.E.T. method.[4]

Procedure.—The procedure for studying the reaction of calcium hydroxide and silica was used previously by Cummins and Miller.[10] The method is based on the reduction in electrical conductivity of the solutions as the calcium and hydroxyl ions are removed by reaction with monosilicic acid to form an insoluble precipitate. Essentially the same procedure was followed in this study. A three-necked round bottom flask containing 800 ml. of calcium hydroxide solution was placed in the constant temperature bath. In the center neck a glass stirrer was inserted. The impeller (25 by 10 mm.) was placed at the bottom of the flask. The rod was connected to a motor of variable speed. The conductivity cell was inserted through one side neck and a thermometer through the other. Rubber stoppers sealed the joints. When the solution reached the desired temperature, the silica was added in the opening for the thermometer and stirring was started. Runs were made with a rapid stirring speed to prevent settling except for the experiments performed to determine the effect of stirring speed on rate.

Because reagents and product settled in the cell, stainless steel screens were placed over the openings. However, tests made with and without screens showed the same results.

Although an effort was made to exclude carbon dioxide from the reaction flasks, no effect attributable to carbon dioxide was detected. Experiments performed with carbon dioxide-free air passing through the reaction flask showed no differences in results from those obtained from experiments conducted with the solutions exposed to the atmosphere.

The specific conductance L of a solution is directly proportional to the concentration of calcium hydroxide. Therefore, the rate of disappearance of calcium hydroxide is equal to the rate of change of conductance L times a constant of proportionality C_T, which is temperature dependent. In the present study the rate is referred to as dL/dt or dC/dt. Since the calcium silicate hydrates are very insoluble and silica does not contribute appreciably to the conductance of the solutions, the assumption that

(4) S. A. Greenberg, *J. Phys. Chem.*, **60**, 325 (1956).

(5) G. B. Alexander, W. M. Heston and R. K. Iler, *ibid.*, **58**, 453 (1954).

(6) S. A. Greenberg and E. W. Price, *ibid.*, **61**, 1539 (1957).

(7) T. L. O'Connor and S. A. Greenberg, *ibid.*, **62**, 1195 (1958).

(8) Stephen Brunauer and S. A. Greenberg, "The Hydration of Tricalcium Silicate and Beta Dicalcium Silicate," Fourth International Symposium on the Chemistry of Cement, Washington, D. C., October, 1960.

(9) S. A. Greenberg, T. N. Chang and Elaine Anderson, *J. Phys. Chem.*, **64**, 1151 (1960).

(10) A. B. Cummins and L. B. Miller, *Ind. Eng. Chem.*, **26**, 688 (1934).

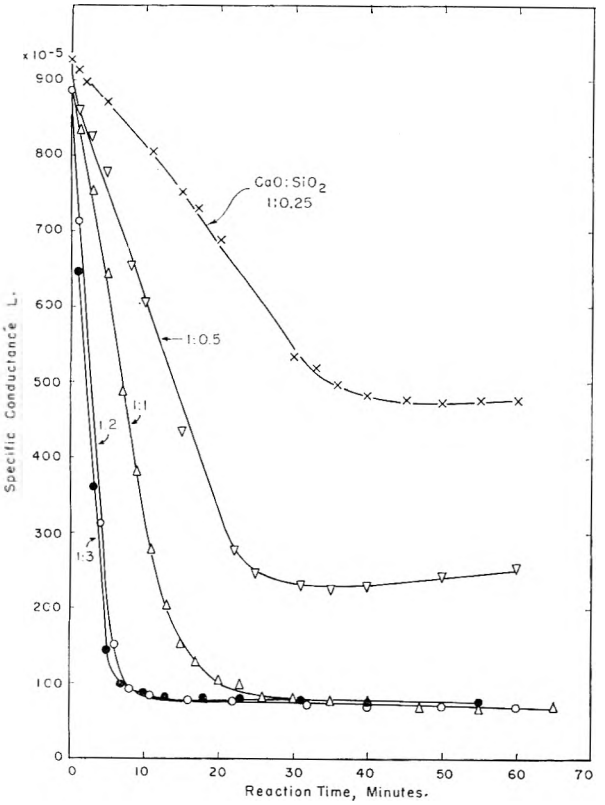

Fig. 1.—Plots of conductance L *vs.* time to show the rate dependence on Ludox silica concentration.

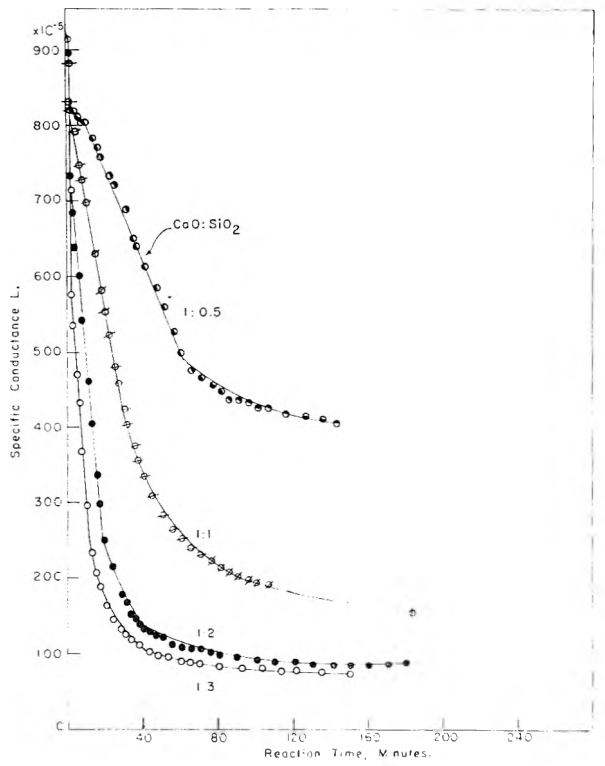

Fig. 2.—Plots of conductance L *vs.* time to show the rate type dependence on special bulky silica concentration.

conductance is directly proportional to the concentration of calcium hydroxide was found to be valid.

The presence of hydrated calcium silicates in these mixtures was demonstrated by differential thermal analysis, thermobalance and X-ray techniques.[11,12]

Results and Discussion

Rate Dependence on the Amount of Silica.—To 800 ml. of calcium hydroxide solution (0.65 g. CaO/l.), Ludox silica was added to make mole ratios of $CaO:SiO_2$ equal to 1:0.25, 1:0.5, 1:1, 1:2 and 1:3. Similarly special bulky silica was added to 800 ml. calcium hydroxide solution (0.65 g. CaO/l.) to make mole ratios of $CaO:SiO_2$ equal to 1:0.5, 1:1, 1:2 and 1:3. In Fig. 1 and 2 the data are presented graphically.

Several things of interest may be noted in the curves. First the intercepts on the ordinate show the initial drop in conductance, which is due to the rapid chemisorption of calcium hydroxide by silica.[4] It is apparent also that the slopes of the curves dL/dt over most of the reaction period is directly proportional to the amount of silica present and, therefore, to the surface area of the silica.

Curves of $L^{1/3}$ plotted as a function of time were made for the Ludox and special bulky silicas. It was noted that the points fall on straight lines for about 90% of the reaction. Also the times for complete reaction, where $L^{1/3}$ is equal to zero, are directly proportional to the amount or surface areas of the silicas. On Table II the rate constants in moles$^{1/3}$ calcium hydroxide per minute per sq. m./g. SiO_2 are listed for Ludox and special bulky silicas as a function of the $CaO:SiO_2$ mole ratios. It may be seen that the rate constants k_2 (eq. 3) are within experimental error 1.0×10^{-4} for Ludox and 0.08×10^{-4} for special bulky silica. The factor for changing the conductance L measurements to concentration of calcium hydroxide is 1.27 at 82°.

TABLE II

RATE CONSTANTS AT 82°

Ludox silica		Special bulky silica	
Mole ratio $CaO:SiO_2$	Rate const. k moles$^{1/3}$/min. sq. m. $\times 10^4$	Mole ratio $CaO:SiO_2$	Rate const. k moles$^{1/3}$/min. sq. m. $\times 10^4$
1:0.25	0.81	1:0.5	0.080
1:0.5	0.98	1:1	.080
1:1	1.00	1:2	.080
1:2	1.04	1:3	.079
1:3	0.89		

Rate Dependence on Calcium Hydroxide Concentrations.—The rates of the reaction were measured while holding the amount of silica constant at 0.093 mole SiO_2, the temperature at 82° and varying the concentration of the 800 ml. calcium hydroxide solutions between 0.0036 and 0.0116 molar. It thus was possible to obtain the rates as a function of calcium hydroxide concentration. The results for Ludox silica are shown graphically in Fig. 3. Similar curves were obtained for the special bulky silica.

It may be noted in Fig. 3 that for concentrations of calcium hydroxide greater than 0.0036 molar, the conductance *vs.* time plots are almost parallel, which indicates that the rate is independent of concentration in this range. Plots of $L^{1/3}$ *vs.* time are linear and parallel except for the curve repre-

(11) S. A. Greenberg, *J. Phys. Chem.*, **61**, 373 (1957).
(12) S. A. Greenberg, *ibid.*, **61**, 960 (1957).

senting the experiment with the 0.0036 molar solution.

Effect of Stirring Speed.—Three runs at 82° were made with three different stirring speeds: (1) 1600, (2) 2400 and (3) 3200 r.p.m. To 800 ml. of 0.0116 molar calcium hydroxide, an equimolar amount of Ludox silica (as SiO_2) was added. No changes in rates of reactions with stirring speed were noted.

King[13] has examined extensively rates of solution of metals in acids. In solution processes in which the rate of solution of the substance is very fast, the rate-controlling step becomes the rate at which the dissolved substance diffuses away from the surface. However, in the case of the solution of silica, the solution reaction involves a slow depolymerization or hydrolysis reaction. Therefore, a diffusion controlled mechanism would not be expected.

Similar experiments with special bulky silica showed a rapid increase in rate when experiments with no stirring are compared to those in which vigorous agitation was applied. It was found that above a certain minimum stirring speed no increase in rate was observed. With very high surface area silicas a certain amount of stirring is necessary to prevent settling. This is especially the case for solution in water[7]; but the effect is not so marked in alkaline solutions. These results are consistent with the experiments and theories concerning the flocculation of silica.[14,15] Khodabov and Plutsis[16] have reported that the rate of solution of quartz is not affected by stirring speed.

James[17] and later King, Wishinsky and Bloodgood[18] reported that stirring speed has little or no effect on the dissolution of magnesium chips in acid solution since the particles swirl freely with the solution. They concluded from these results that the stirring speed is not a test of diffusion control in that case. Therefore, the lack of dependence of rate of reaction on stirring speed above a minimum speed in the present study cannot be considered as *proof* that the rate of reaction is not diffusion controlled.

Dependence of Rate on Nature of Silica.—A comparison was made of the rates of reaction at 82° of calcium hydroxide solutions with alpha quartz, S. L., Sp. B., Aerogel and Ludox silicas. In each case to 800 ml. calcium hydroxide solution (0.65 g. CaO/l.) sufficient silica was added to obtain equimolar quantities of CaO and SiO_2. The results demonstrate that the rates of reaction are not proportional to the surface areas of silicas, in general. Table III compares the surface areas with the dL/dt slopes and the constants k_2. These results are reasonable when the detailed natures of the silicas are considered. Electron micrographs[19] show that some silicas like the S. L. variety are porous. Sp. B. silica is less porous but the fundamental particles are aggregated. On the other hand, quartz and Ludox[20] exhibit discrete separate particles.

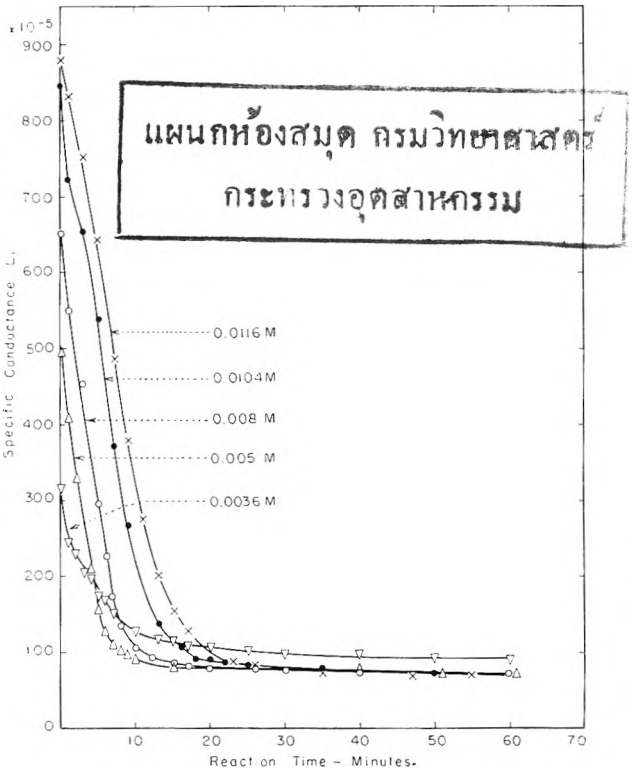

Fig. 3.—Plots of conductance *vs.* time to show dependence of rate of reaction of Ludox silica on calcium hydroxide concentration.

TABLE III

DEPENDENCE OF RATE ON NATURE OF SILICA

Silica	Surface area sq. m./g. SiO_2	$-dL/dt \times 10^6$	$k_2 \times 10^6$ moles$^{1/3}$/min. sq. m.
S.L.	750	110	0.61
Sp. B.	380	145	8.0
Aerogel	250	310	2.4
Ludox	150	380	100
Quartz	<1	0.3	~0

The slow reaction rate of quartz compared to the colloidal silicas may be directly attributed to the low surface area (<1 sq. m./g. SiO_2) and to the low free energy state of the substance.

The results show that S. L. silica reacts rapidly at first, but then the reaction rate slows down markedly. It is reasonable to presume that the pores of S. L. silica are filled very rapidly with silicic acid which reacts immediately with calcium hydroxide. This hydrated calcium silicate product in the pores would retard the further solution of the silica.

The Ludox silica because of a relatively large *available* surface would be expected to react most rapidly and it does show a rate constant of 100 ×

(13) C. V. King, "Transactions of the New York Academy of Sciences," Series II, Vol. 10, No. 7, 262–267, 1948.

(14) H. R. Kruyt, "Colloid Science," Chap. I, Elsevier Publishing Co., New York, N. Y., 1952.

(15) E. S. W. Verwey and J. Th. G. Overbeek, "Theory of the Stability of Lyophobic Colloids," Elsevier Publishing Co. New York, N. Y., 1948.

(16) G. S. Khodabov and E. R. Plutsis, *Dokl. Akad. Nauk, S.S.S.R.*, 845 (1958).

(17) T. H. James, *J. Am. Chem Soc.*, **65**, 39 (1943).

(18) C. V. King, H. Wishinsky and H. Bloodgood, *ibid.*, **68**, 238 1946).

(19) S. A. Greenberg, E. Pressler, L. E. Copeland and Edith G. Schulz, in prepn.

(20) S. A. Greenberg and T. N. Chang, in prepn.

10^{-6} compared to the S. L. silica with a surface area of 750 sq. m./g. SiO_2 which exhibits a rate constant of only 0.61×10^{-6}.

The aerogel and Sp. B. silicas may be seen to react at rates which apparently reflect the amount of porosity or degree of aggregation as well as the surface areas.

Dependence of Rate on Temperature.—The dependence was determined for Sp. B. silica by measuring the rates of reaction at constant concentration of calcium hydroxide (800 ml. 0.65 g. CaO/l.) and silica (0.657 g. Sp. B. silica). Table IV summarizes the results.

Table IV

Dependence of Reaction Rate of Sp. B Silica on Temperature

1 Temp., °C.	2 C_T	3 $dL/dt \times 10^5 \times C_T$	4 $k_2 \times 10^5$ moles$^{1/3}$/min. sq. m.
30	2.3	12	0.81
40	1.90	..	..
50	1.64	38	1.9
60	1.61	60	2.9
68	1.52	73	..
70	1.38	72	3.2
75	1.33	122	..
82	1.27	184	8.0
85 (0.45 g. CaO/l.)	1.35	246	..
85 (0.65 g. CaO/l.)	1.35	150	..

It was noted that at the lower temperatures almost 20 minutes elapsed before the rates became constant. At 82° the rate became nearly constant after 10 minutes. These effects are attributed to the supersaturation initially of the solution with silicic acid with respect to the calcium silicate product and will be discussed separately in connection with a study of the crystallization of the product in solution.[20]

Table IV lists the temperatures of the experiments, the constant C_T which relates the specific conductances L with the concentrations of calcium hydroxide, the third column gives $dL/dt \times C_T$ which is proportional to the rate of removal of calcium hydroxide and the last column lists the constants k_2 at various temperatures. By means of the Arrhenius equation, the activation energy for the reaction of Sp. B. silica was evaluated from the rate constants k_2. Between 30 and 82° the energy of activation is 9.4 kcal.

The two rates observed at 85° (Table IV) were measured on solutions of different concentrations of calcium hydroxide but with equal silica concentrations. The lower rate of 150 (column 3) was found with the higher concentration of calcium hydroxide (0.65 g. CaO/l.). The higher rate, 246, was noted with the lower concentration (0.45 g. CaO/l.) which is the saturation concentration at this temperature. The lower rate with the supersaturated solution may be due to precipitation of calcium hydroxide on the surface of the silica particles. This precipitate may then serve as a barrier to the solution of silica.

In the temperature range 50 to 82° the activation energy for the reaction of Ludox silica is 18.4 kcal.

Acknowledgments.—Thanks are due to Mr. Joseph Pellicane for assistance in making the conductivity measurements. Mr. G. Reimschussel and Miss M. Cronin measured the surface areas of the silicas. Thanks are also due to Mr. C. N. Thompson for his coöperation in checking the purity of the reagents by chemical analyses and to Mr. S. R. Wiley for the spectrographic analyses of the reagents used in the present study.

EFFECTS OF DEHYDRATION AND CHEMISORBED MATERIALS ON THE SURFACE PROPERTIES OF AMORPHOUS SILICA

By W. K. Lowen and E. C. Broge

E. I. du Pont de Nemours & Co., Inc., Industrial and Biochemicals Department, Experimental Station, Wilmington, Delaware

Received March 4, 1960

When the hydroxyl groups on the surface of amorphous silica are removed by heating or replaced by esterification, the properties of the surface are markedly altered. Using high surface area powders with large pores which were obtained from colloidal silica aquasols, semiquantitative studies of these effects have been made. Data are presented which relate the reactivity with trimethylchlorosilane, methyl red adsorption capacity, heat of adsorption of nitrogen, and wetting characteristics of amorphous silica surfaces to the extent of dehydration and/or esterification. Qualitatively, the effects produced by these two types of surface reactions were found to be quite similar. Semiquantitative treatment of the data supports the hypothesis that dehydration of amorphous silica surfaces occurs by random interactions of adjacent hydroxyl groups, and that esterification occurs by random reaction between molecules of alcohol and individual hydroxyl groups. Rehydration of amorphous silica surfaces was found to occur only under relative humidity conditions which favor capillary condensation of liquid water.

Introduction

Each silicon atom on the surface of amorphous silica tends to maintain tetrahedral coördination with oxygen atoms by being covalently bound to an outwardly disposed hydroxyl group.[1] Such hydroxyl groups constitute the "bound water" in silica gels. In humid atmosphere, this layer of silanol groups becomes hydrogen bonded to additional water molecules, so that the surface is covered with physically adsorbed water.

When heated, a particle of amorphous silica loses this physically adsorbed water until at approximately 200°, there remains only the bound water. On this fully hydroxylated surface there are about 8

(1) P. C. Carman, *Trans. Faraday Soc.*, **36**, 964 (1940).

silanol groups per square millimicron of surface, each group occupying an area of approximately 12.5 square Å. Above 200°, additional water is evolved without appreciable sintering or loss of area. Above 600°, the internal structure of the particle becomes more mobile and sintering begins, and the evolution of water continues. Surface silanol groups may also be replaced by chemical reactions. For example, they can be esterified with alcohols, whereupon the surface becomes partially covered with alkoxy groups. They also react with alkylchlorosilanes, splitting out hydrogen chloride.

The paper presents new data on the dehydration of amorphous silica surfaces, and shows the effects of such dehydration on the reactivity and adsorptive characteristics of the silica. The effects of displacing various proportions of the silanol groups by alkoxy groups are described. The close similarity between the effects produced by these two types of surface modification is emphasized, and some insight is provided into the mechanism of these reactions.

Experimental

Sources of Amorphous Silica.—Three amorphous silicas with specific areas of about 100, 180 and 300 m.²/g. were used in this study. In each case, the silicas were prepared in the form of aquasols by methods which have been previously described.[2,3] The silicas were stored in this wet condition to ensure against partial dehydration or other changes. Just prior to use, these sols were deionized with a mixture of anion and cation-exchange resins, and permitted to gel. The silica powders were recovered by filtration, dried at 110°, and dehydrated or esterified immediately after isolation.

Dehydration of Amorphous Silicas.—Portions of these silica powders were heated to constant weight in a stream of air at a series of temperatures to obtain samples which were dehydrated to different degrees. Most of the water came off very quickly, and in all cases no appreciable additional loss of water occurred after heating for 1 hour.

Esterification of Amorphous Silica.—In carrying out the esterification reaction, the silica was suspended in 1-butanol or 1-propanol, free water removed from the system by azeotropic distillation, and the anhydrous slurry was heated at various temperatures to obtain silicas with different degrees of esterification. In certain instances, the final heating was carried out above atmospheric pressure in stainless steel autoclaves. The esterified silica was recovered by filtration and dried *in vacuo*. These procedures have been described in detail by Iler.[4]

Characterization Techniques.—The number of silanol groups on silica surfaces was determined from loss on ignition measurements under reduced pressure at 1100°. The number of alkoxy groups on esterified silica surfaces was determined by removing physically adsorbed organic matter, and analyzing for total carbon. All specific surface area measurements were made according to the manometric technique described by Emmett.[5]

Reactivity of dehydrated silica surfaces was studied by refluxing the material with liquid trimethylchlorosilane until evolution of hydrogen chloride subsided. Excess reagent was displaced by washing repeatedly with absolute ether, the residue was dried *in vacuo* and the number of trimethylsilyl groups attached to the surface was determined by analyzing for total carbon.

Methyl red adsorption capacities were determined by a procedure originally described by Shapiro and Kolthoff,[6] using benzene as a solvent.

The wetting characteristics of silicas were observed qualitatively by shaking small portions of dry powder with distilled water. An equal volume of either butanol, acetal, chloroform or benzene was added, and the contents once again shaken vigorously. After phase separation, the layer containing the siliceous material was determined by inspection.

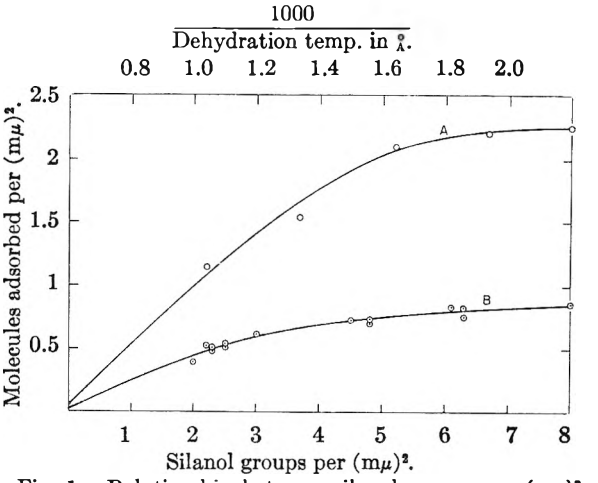

Fig. 1.—Relationship between silanol groups per (mμ)², temperature of dehydration, and adsorption of (A) trimethylsilyl groups, (B) methyl red molecules.

Results and Discussion

Effects of Dehydration.—The state of hydration of silica surfaces after being heated to various temperatures is summarized in Fig. 1. When the number of silanol groups remaining per square millimicron of surface is plotted against the inverse of the absolute dehydration temperature, a linear relationship is obtained

$$\text{Silanol groups per } (\text{m}\mu)^2 = 5200 \times (1/T_A - 1/1600)$$

The significance of this linear relationship is not clear; however, the silanol numbers plotted are characteristic and meaningful in that additional heating at any given temperature causes no further decrease in the silanol number. Furthermore, the same number is obtained regardless of the starting surface area, so long as it was fully hydrated prior to heating. It is interesting that extrapolation of this straight line indicates that temperatures of about 1400° would be required to obtain fully dehydrated amorphous silica by ignition in air.

Both the adsorption capacity of amorphous silica surfaces for polar adsorbates and its chemical reactivity with reagents capable of interacting with the silanol groups on the surface vary with the silanol content. This is shown in Fig. 1 by the plots of the adsorption capacity of the surface for methyl red, and the chemical reactivity with trimethylchlorosilane as a function of the number of silanol groups per (mμ)². When the surface is fully hydrated with 8 silanol groups per (mμ)², the the maximum number of trimethylsilyl groups which becomes attached is about 2.2 per (mμ)². Thus, each trimethylsilyl group covers about 45 Å.². Since only one surface silanol group is required for chemical reaction with a molecule of trimethylchlorosilane, only 2.2 silanol groups per (mμ)²

(2) M. F. Bechtold and O. E. Snyder, U. S. Patent 2,574,902 (E. I. du Pont de Nemours & Co., Inc., 1951).

(3) G. B. Alexander, U. S. Patent 2,750,345 (E. I. du Pont de Nemours & Co., Inc., 1956).

(4) R. K. Iler, U. S. Patent 2,657,149 (E. I. du Pont de Nemours & Co., Inc., 1956).

(5) P. H. Emmett, "Symposium on New Methods for Particle Size Determinations," Philadelphia: American Society for Testing Materials, March 4, 1941, p. 95.

(6) I. Shapiro and I. M. Kolthoff, *J. Am. Chem. Soc.*, **72**, 776 (1950).

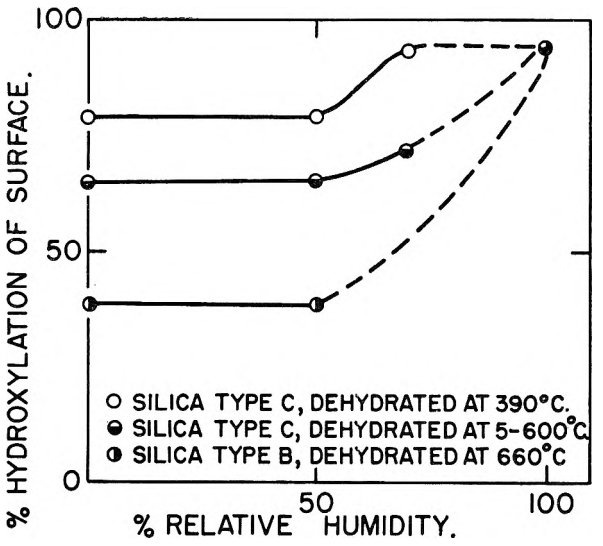

Fig. 2.—Rehydration of dehydrated surface, by exposure to humid atmosphere.

of silica surface should provide enough reactive sites for the attachment of a complete monolayer of trimethylsilyl groups. However, as shown in Fig. 1, the number of trimethylsilyl groups reacted begins to decrease substantially in an approximately linear fashion when the silanol group number drops below 4.

An explanation which is consistent with these observations is that removal of bound water occurs by random interactions of *adjacent* hydroxyl groups from the most water-rich areas. In this manner, silanol-free areas of only 25 Å.^{2} units would be created during the removal of 50% of the hydroxyls by such a mechanism (corresponding to 4 silanol groups per $(m\mu)^2$, and little decrease in the reactivity with trimethylchlorosilane would be expected. However, during the removal of additional silanol groups by interaction of *adjacent* pairs, non-hydroxylated areas greater than 45 Å.^{2} units would be created, and the observed decrease in activity would be predicted. The slope of the curve at the low silanol levels, that is, below 4, also supports this hypothesis.

On the other hand, a random elimination of *isolated* hydroxyl groups from the most water-rich areas would not affect surface reactivity with trimethylchlorosilane until about 75% of the total silanol groups had been removed. This would correspond to a silanol number of about two.

On a fully hydrated silanol surface, 0.86 molecules of methyl red are adsorbed per $(m\mu)^2$, or each molecule covers about 116 sq. Å.^{2}. The adsorption capacity decreases as the silanol groups are removed but in this case the region of maximum sensitivity is not reached until about 5 silanol groups have been removed per $(m\mu)^2$. These observations are consistent with the above hypothesis regarding the mechanism of dehydration, because up to 6 silanol groups could be removed per $(m\mu)^2$ by interaction of adjacent hydroxyl groups before non-hydroxylated areas as large as the covering power of a methyl red molecule are created. Removal of adjacent silanol groups beyond this point by random interaction would create such areas.

It is interesting to note that the adsorption of a non-polar adsorbate is also affected by the silanol content of silica surfaces. The data in Table I show that the heat of adsorption of nitrogen at about −195° decreases as a function of the surface silanol content. These heats of adsorption were calculated from nitrogen adsorption isotherms using the original BET equations.[7]

When dehydrated silica is exposed to moist air, the surface rehydrates. However, as shown in Fig. 2, the extent of rehydration was found to be a function of both the degree to which the surface was originally dehydrated, and the relative humidity under which rehydration was conducted. These observations are consistent with the hypothesis that rehydration of the siloxane surface does not occur unless liquid water is present in the capillaries of the gel. The capillaries in the silica powders used in this study are so large that there is no capillary condensation at 50% relative humidity, and no rehydration occurs under these conditions, even after one month at ordinary temperature. At 75% relative humidity, some of the capillaries are filled with liquid water, and partial rehydration results, while at 100%, the capillaries are completely filled, and complete rehydration occurs. Rehydration was carried out by exposing the dehydrated silicas to controlled humidities from one to four weeks, and the extent of hydration was determined after drying at 100° to remove physically adsorbed water.

TABLE I

HEAT OF ADSORPTION OF NITROGEN ON DEHYDRATED SILICA SURFACES

Dehydration temp., °C.	Specific surface area, m.^{2}/g.	Silanol groups per $(m\mu)^2$	"C"	$E_1 - E_2$ cal./mole	E_1 cal./mole
120	182	10	104	721	2011
620	170	3	53	616	1906
810	141	2	45	591	1881

Effects of Esterification.—When silica reacts with alcohols such as 1-butanol, the hydrogen of silanol groups on the surface is replaced with an alkyl group. As the surface becomes covered with alkyl groups, fewer silanol groups remain exposed on the surface, and the methyl red adsorption capacity of the silica surface decreases (Fig. 3). This effect is similar to that observed during dehydration of silica surfaces, but methyl red adsorption capacity is much more sensitive to low degrees of esterification than it is to low degrees of dehydration. Replacement of only about 1.2 hydroxyl

TABLE II

RELATIONSHIP BETWEEN HEAT OF ADSORPTION OF NITROGEN AND DEGREE OF ESTERIFICATION OF SILICA SURFACES

Sample	Alkoxy groups per $(m\mu)^2$	"C"	$E_1 - E_2$, cal./mole	E_1, cal./mole
Unesterified silica	0	93	712	2002
Esterified with 1-butanol	0.44	81.8	693	1983
Esterified with 1-butanol	1.28	28.3	525	1815
Esterified with 1-butanol	2.52	21.9	485	1775

(7) S. Brunauer, P. H. Emmett and E. Teller, *J. Am. Chem. Soc.*, **60**, 309 (1938).

TABLE III

RELATIONSHIP BETWEEN DEGREE OF ESTERIFICATION OF SILICA SURFACES AND WETTING CHARACTERISTICS

Sample	Degree of esterification, butoxy grps./(mμ)²	Partition data (Phase containing the silica)			
		1-Butanol/Water	Acetal/Water	Chloroform/Water	Benzene/Water
Unesterified silica	0	Water	Water	Water	Water
Partially esterified with 1-butanol	1.16	Organic	Water	Water	Water
Partially exterified with 1-butanol	1.69	Organic	Organic	Emulsion	Water
Completely esterified with 1-butanol	3.11	Organic	Organic	Organic	Organic

groups with butoxy or propoxy groups per $(m\mu)^2$ makes half of the surface inaccessible to methyl red, whereas elimination of 1.2 hydroxyl groups by dehydration had very little effect. Thus, it appears that the polarity of silica surfaces is more markedly altered by esterification than by dehydration. As the population of butoxy groups approaches 2.7 per $(m\mu)^2$ they become so closely packed that no methyl red molecules find access to the surface. Yet even at this point, there is space enough for more butoxy groups, and esterification can continue until there are 3.8 butoxy groups packed onto the surface.[4] Thus, butoxy groups apparently are capable of preventing the access of methyl red to considerably more area than they actually cover. These data are consistent with the hypothesis that reaction between alcohols and silanol groups proceeds quite uniformly throughout the surface, rather than by preferential saturation of isolated areas.

Replacement of hydroxyl groups with butoxy groups also decreases the heat of adsorption of nitrogen on silica surfaces at −195°, as calculated from adsorption isotherms (Table II). This is similar to the effect observed during dehydration, but the heat of adsorption of nitrogen is more sensitive to replacement of hydroxyl groups with butoxy groups than it was to the removal of hydroxyl groups. The heat of adsorption drops from about 2000 to 1775 cal./mole when 2.5 hydroxyl groups are replaced with butoxy groups per $(m\mu)^2$, whereas removal of 6 hydroxy groups per $(m\mu)^2$ by dehydration decreases the heat of adsorption of nitrogen to only 1880 cal./mole.

Based on both methyl red and nitrogen adsorption measurements, it appears that replacement of surface silanol groups with butoxy groups decreases the polarity of the surface substantially. Since hydrolysis of alkoxy groups on the surface of esterified silicas proceeds at a negligible rate at room temperature, it is possible to study the wetting characteristics of esterified silicas without altering their surface. The data in Table III show that as a silica surface is esterified, it becomes preferentially wetted by water-immiscible organic liquids. As the degree of esterification is increased, it becomes less hydrophilic and more organophilic, and silicas

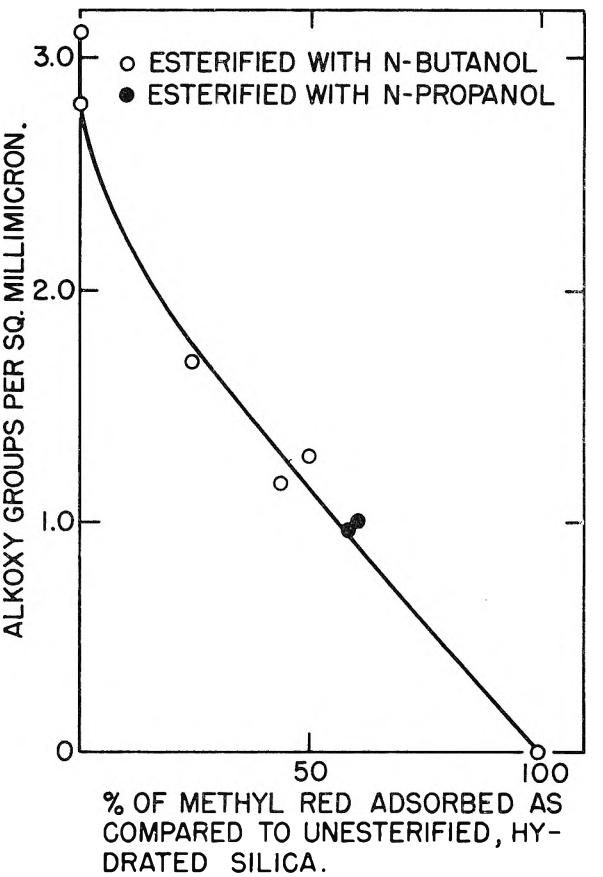

Fig. 3.—Relationship between adsorption of methyl red and degree of esterification of the silica surface.

with highly esterified surfaces are wet by hydrocarbons preferentially to water. More quantitative conclusions regarding surface polarity might be reached by measuring the wetting angle of water on silica surfaces containing varied proportions of alkoxy groups. However, this was not attempted because of the difficulties associated with determining the extent of esterification on the smooth, fused-silica plates of low surface area which would have been required for the measurement of wetting angles.

ESTERIFICATION OF THE SURFACE OF AMORPHOUS SILICA

BY C. C. BALLARD, E. C. BROGE, R. K. ILER, D. S. ST. JOHN AND J. R. MCWHORTER

Contribution from the Industrial and Biochemicals Department, E. I. du Pont de Nemours & Co., Inc., Wilmington, Delaware

Received August 10, 1960

Primary and secondary alcohols react with the silanol groups on the surface of particles of amorphous silica until a monomolecular, oriented layer of chemically-bound organic groups is formed. Numerous types of amorphous silica are shown to take part in this type of topochemical reaction. This chemisorption, with formation of silicic ester groups, proceeds only under essentially anhydrous conditions. The reaction proceeds rapidly to completion only at elevated temperature and pressure. The surface-esterified amorphous silica powders have an organic content which increases with specific surface area and molecular weight of the alcohol used. The products are highly hydrophobic and organophilic in nature. Packing of the alkoxy groups on the silica surface is correlated with molecular size. The equilibrium constant for the reaction $-SiOH + ROH \rightleftarrows SiOR + H_2O$ was measured in the case of *n*-butyl alcohol. The energy of activation for the esterification reaction is 21.9 kcal. per mole of butoxy groups and for hydrolysis is 9.0 kcal. mole^{-1}. The esterification reaction is endothermic and requires 12.1 kcal. mole^{-1}.

Introduction

Although the physical association of alcohols with silica gels and powders has been studied by numerous investigators[1-4] the possibility of a topochemical reaction between alcohol and the surface of amorphous silica has only recently been appreciated. As described by Iler,[5,6] Braendle,[7] and Stevenson,[8] esterification of the surface of finely divided silica renders the powder organophilic and hydrophobic. Recently, Stöber, Bauer and Thomas[9] studied the chemisorption of aliphatic alcohols on the surface of pure fumed silica and showed that the alkyl groups must be oriented normal to the surface and are essentially close-packed. There are about 8 hydroxyl (silanol) groups per square millimicron on the original silica surface.[6] Only about three alkoxy groups such as *n*-butoxy, are required to cover this area, so that two-thirds of the silanol groups are thus covered over and remain inaccessible to further reaction. Esterification of the surface to produce hydrophobic products occurs readily with primary or secondary alcohols containing 2 or more carbon atoms. In the case of methanol,[10] highly anhydrous conditions and elevated temperature and pressure are required. Tertiary alcohols do not react readily and, furthermore, tend to be decomposed by dehydration at elevated temperature. Substituted alcohols will esterify the surface; if the substituent groups are polar, the resulting surface assumes the polar character of the substituent group.[11-16]

The present paper relates primarily to the kinetics of the esterification of the silica surface with some of the lower saturated aliphatic alcohols, principally 1-butanol.

Experimental

Silica Substrates.—Finely divided amorphous silica o different ultimate particle sizes and specific surface areas were prepared from sodium silicate by methods which have been described previously and are categorized as tabulated.

Type of silica	Specific surface, m.^{2}/g.	Method of preparation
A	25–100	Drying sol[17]
B	~100	Sodium silicate and acid[5]
C	180–200	Gelling sol, drying
D	300	Sodium silicate and acid[18]
E	300–800	Special process[19]

Sols were purified by ion exchange; gels were washed with acid and water. Unless noted otherwise, the silica was employed in the wet condition for further reaction with alcohols.

Methods of Esterification.—In preliminary studies, the silica was suspended in alcohol and free water removed from the system, usually by azeotropic distillation. With lower boiling alcohols, the anhydrous mixture was heated either in stainless steel autoclaves or in sealed glass tubes. The alcohol vapor was then either vented from the pressure vessel, leaving a dry product, or the mixture was cooled rapidly and the silica recovered by filtration and dried under vacuum at 100–120°. With high boiling alcohols the mixture was heated at atmospheric pressure, cooled, filtered and the product was washed with a suitable volatile solvent such as acetone, to remove adsorbed alcohol, then dried under vacuum at 100–125°.

The kinetics and equilibria of the surface esterification of silica with 1-butanol were studied by determining the rate of change of carbon content at a series of temperatures ranging from 118 to 320°. Data at 118° were obtained from an extended azeotropic dehydration of silica gel (300 m.^{2}/g. specific surface area) at atmospheric pressure. Samples of slurry (averaging around 8% silica) were removed at intervals and analyzed to determine the water content and the degree of esterification. Data for higher temperatures were obtained by pumping slurry, which had been partially esterified at 118°, through an oil-heated heat exchanger operated under pressures chosen to maintain

(1) D. C. Jones and L. Outridge, *J. Chem. Soc.*, 1574 (1930).

(2) L. Robert, *Compt. Rend.*, **234**, 2066 (1952).

(3) F. E. Bartell and D. J. Donahue, *J. Phys. Chem.*, **56**, 665–670 (1952).

(4) F. E. Bartell and R. M. Suggitt, *ibid.*, **58**, 39 (1954).

(5) R. K. Iler, U. S. Patent 2,657,149 (E. I. du Pont de Nemours & Co., Inc., Oct. 27 (1953).

(6) R. K. Iler, "The Colloid Chemistry of Silica and Silicates," Cornell University Press, Ithaca, N. Y., 1955.

(7) G. C. Meyer and R. O. Braendle, "A New Class of Siliceous Thickening Agents," National Lubricating Grease Institute, San Francisco, Cal., October 25–27, 1954.

(8) A. C. Stevenson, "Effects of Surface Modification on Silica Fillers," Elastomer and Plastics Group, Northeastern Section, Amer. Chem. Soc., Cambridge, Mass., Nov. 16, 1954.

(9) W. Stöber, G. Bauer and K. Thomas, *Ann. Chem.*, **604**, 104–110 (1957).

(10) E. C. Broge, U. S. Patent 2,736,668 (E. I. du Pont de Nemours and Co., Inc., 1956).

(11) R. K. Iler, U. S. Patent 2,739,074 (E. I. du Pont de Nemours & Co., 1956).

(12) R. K. Iler, U. S. Patent 2,739,076 (E. I. du Pont de Nemours & Co., 1956).

(13) E. C. Broge, U. S. Patent 2,739,078 (E. I. du Pont de Nemours & Co., 1956).

(14) M. T. Goebel, U. S. Patent 2,739,077 (E. I. du Pont de Nemours & Co., Inc., 1956).

(15) R. K. Iler, U. S. Patent 2,739,075 (E. I. du Pont de Nemours & Co., 1956).

(16) K. L. Berry, R. M. Joyce and J. E. Kirby, U. S. Patent 2,757,098 (E. I. du Pont de Nemours & Co., Inc., 1956).

(17) G. B. Alexander and R. K. Iler, *J. Phys. Chem.*, **57**, 932 (1953).

(18) See reference 5, Example 2.

(19) G. B. Alexander, E. C. Broge, R. K. Iler, U. S. Patent 2,765,242 (E. I. du Pont de Nemours & Co., Inc., 1956).

TABLE I

DIFFERENT DEGREES OF ESTERIFICATION OF THE SILICA SURFACE WITH 1-BUTANOL

Expt. no.	Type of substrate	Reaction conditions: Temp., °C.	Time, hr.	% H_2O after esterif.	Silica substrate Sp. surf., $m.^2/g.$	Characteristics of Estersil: Specific total area $m.^2/g.$	Specific hydroxylated area $m.^2/g.$	Chem. analysis: SiO_2	% C	% H	Deg. of esterifica.	%[a] Area not esterified
1	D	110	0.1	<0.5	360	356	245	86.6	2.39	1.07	0.84	31.3
2	D	118	3	..	330	317	113	88.8	4.37	1.32	1.72	35.6
3	D	118	8	..	330	304	61	90.0	4.70	1.45	1.94	20.0
4	D	225	2	..	310	269	0	88.2	6.32	1.55	2.95	0
5	D	250	2	..	285	277	4	88.1	6.62	1.42	3.0	1.5
6	D	300	2	..	289	262	0	85.3	8.80	1.86	4.2	0
7	D	200	1	0.4	277	268	22	88.2	5.41	1.34	2.53	8.2
8	D	200	1	1.8	282	270	40	89.8	5.02	1.34	2.33	14.9
9	D	200	1	3.2	284	..	56	90.5	4.21	1.13	1.86	19.7
10	D	200	1	4.7	287	279	..	91.2	2.86	0.90	1.28	...
11	D	Unesterified			298	..	297	94.8	0.2	0.62	0	100

[a] [Total area-hydroxylated area]/[total area].

the slurry density approximately constant. The residence time in the heat exchanger was of the order of 2 minutes at the pumping rates employed; longer times were obtained by returning the cooled slurry to the feed pump for further treatments. Atmospheric pressure dehydration was carried out in a 50 gallon, agitated, steam-jacketed still pot. Fractionation of the azeotrope took place in a 6 inch diameter column, packed with 20 feet of $^3/_8$" porcelain Raschig rings. The condensed distillate was automatically decanted into a butanol-rich layer which was returned as reflux and a water-rich layer which was discarded. The reactor consisted of a 20 gallon slurry feed tank, a piston-type controlled volume feed pump with a hydraulic pulsation dampener and a series of $^3/_{16}$" i.d. tubular heaters surrounded by circulating heat-transfer oil. The heat treated slurry was quenched in a similar water-jacketed cooler and discharged through a pressure-controlled valve into receivers.

Water content of the reaction mixture was determined by titration with Karl Fischer reagent. The free butanol was removed from slurry samples by vacuum drying at 115°, 5 mm. Hg abs., and the esterified powder then characterized.

Characterization and Analysis of Products. Wetting Characteristics.—A simple test was employed to determine whether the product was hydrophobic and organophilic, or merely organophilic without being hydrophobic: The powder was pulverized to pass through a 200 mesh screen and about 0.25 ml. was added to 10 ml. of distilled water in a 6" test tube which was stoppered and given 5 vigorous vertical shakes. The mixture was permitted to stand for 15 minutes, and it was observed whether any of the powder had wetted into the water. Completely hydrophobic silica remains as a dry layer entirely on top of the water. If the silica is hydrophilic, it wets completely into the water. Organophilic silica is defined as one which will preferentially remain suspended in the butanol layer in a butanol–water mixture obtained when 10 ml. of *n*-butyl alcohol is added to 10 ml. of aqueous phase in the test-tube, which is again shaken five times and let stand.

Degree of Esterification.—Samples were analyzed for carbon and hydrogen by conventional combustion methods, and for SiO_2 by ashing at 800–1000°, since no other oxides were present in appreciable amounts. The specific surface area was determined by adsorption of nitrogen by the method described by P. H. Emmett.[20] From these data the degree of esterification or the number of alkoxy groups per square millimicron of surface was calculated by the formula

$$\text{Degree of esterification} = \frac{6.02 \times 10^{23} \times C}{12n \times S_n \times 10^{20}}$$

where C = per cent. by weight of carbon, S_n = specific surface area by nitrogen adsorption, n = number of carbon atoms in the molecule of alcohol employed. In calculating the area, it was assumed that the area occupied by an adsorbed nitrogen molecule was 16.2 Å.^{2}.

Specific Hydroxylated Surface Area.—The specific hydroxylated surface area is defined as that part of the area of silica which is unesterified and thus still presents a silanol (−SiOH) surface. To determine surface, Lowen of our laboratory employed a modification of the method of Shapiro and Kolthoff.[21] The method depends on the fact that methyl red is adsorbed from benzene by a silanol surface, but not by the surface that is covered by alkoxy groups. The method is particularly applicable to less completely esterified surfaces, rather than to completely esterified surfaces which absorb no dye.

Results

Degree of Esterification of the Surface with 1-Butanol.—In Table I it may be seen that the degree of esterification (D.E.) increases with time and temperature of reaction, and decreases with the amount of water in the system at equilibrium. At 118° the specific hydroxylated surface area decreases continuously with time, so that it is probable that eventually it would reach zero. It is possible to calculate the degree of esterification of that part of the surface which is not hydroxylated. Thus, for Experiments 1, 2, 3, 7 and 8 of Table I, the numbers of butoxy groups per square millimicron of esterified area were calculated from the carbon content and the esterified area, which is the difference between the hydroxylated and total surface areas. In this group of experiments the butoxy groups per square millimicron of non-hydroxylated (or esterified) area ranged from 2.53 to 2.88, and averaged 2.7.

It is thus evident that the adsorption of methyl red dye can give a measure of the hydroxylated surface only up to a degree of esterification of around 2.7 butoxy groups per sq. millimicron. Beyond this point the butyl groups are so closely packed that methyl red molecules cannot approach the remaining hydroxyl groups, although butyl alcohol can still penetrate to the surface and reaction can continue until 3.8 groups are attached per sq. millimicron (Expt. 6, Table I).

The packing of butoxy groups at degrees of esterification (D.E.) of 2.7 and 3.8 are represented in Fig. 1. The area covered per butyl group at D.E. of 2.7 is 37 Å.^{2} and at D.E. of 3.8 is 26 Å.^{2} The area covered by a butyl group, in the case of *n*-butylamine adsorbed on silica gel, according to Bartell and Dobay[22,23] is 33 Å.^{2}. It therefore appears that

(20) P. H. Emmett, "Symposium on New Method for Particle Size Determination of the Sub-Sieve Range" Amer. Soc. for Testing Materials, March 4, 1941, p. 95.

(21) I. Shapiro and I. M. Kolthoff, *J. Am. Chem. Soc.*, **72**, 776 (1950).

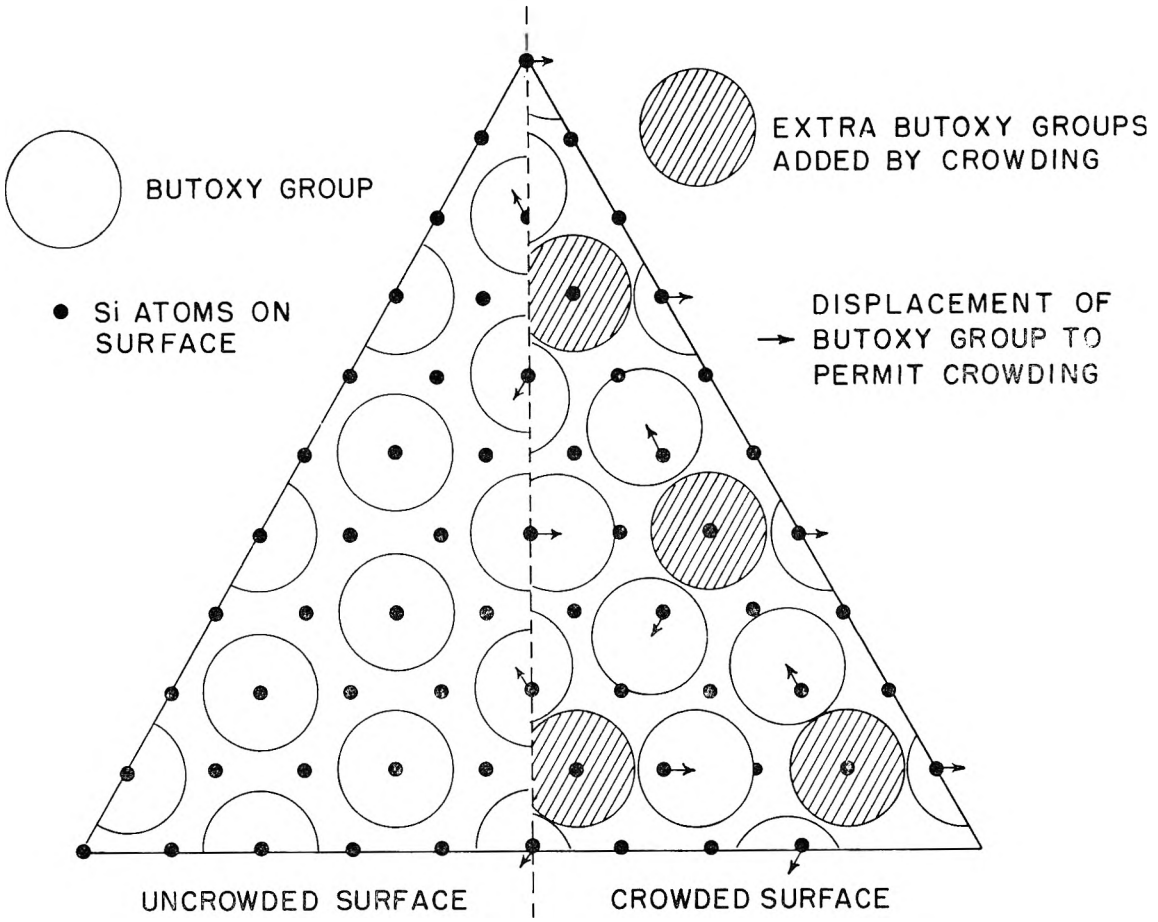

Fig. 1.—Packing of butoxy groups on an idealized uniform surface of amorphous silica: left, 2.7 butoxy groups per square millimicron; right, 3.8 groups per square millimicron.

the butyl groups effectively cover the surface at a D.E. of 2.7. At about this point the surface becomes completely hydrophobic.

Maximum Degree of Esterification with Various Alcohols.—The maximum number of butoxy groups per unit area is determined not only by the cross-sectional area of the butyl group (assumed to be a cylinder of diameter of 4.45 Å.), but also by the fact that each group is attached to an oxygen atom held in the surface by silicon. Thus the butyl groups are not free to move about, but are anchored in fixed positions. As shown in Fig. 1, butoxy groups centered directly over silicon atoms in the surface cannot be packed more densely than one for every three silicon atoms on the surface, the other two being linked to hydroxyls. Since there are, on the average, 7.85 oxygen atoms on each square millimicron of surface,[24] one butyl group for every three oxygen atoms corresponds to 2.62 butoxy groups per square millimicron. This is close to the value of 2.7 found in the above dye-adsorption studies.

However, by straining bond angles and moving three adjacent butyl groups apart as shown in Fig. 1, it is possible to make room for another butyl group and so increase the degree of esterification to 3.8. It requires additional work to attain such close packing, which is not achieved except under conditions of high temperature and pressure. It is evident that such a surface is covered with butyl groups so closely packed that neither nitrogen nor oxygen nor water molecules can penetrate to the underlying silica surface.

Esterification of Different Silica Substrates.—A wide variety of amorphous silica powders has been surface-esterified with 1-butanol, as shown in Table II. The forms of silica include silica-fume formed by combustion of volatile silica compounds, wet and dry silica gels, aerogels and siliceous pseudomorphs obtained by treating certain minerals, such as chrysotile asbestos, with strong acid. Under equivalent reaction conditions, all the forms of amorphous silica having specific surface areas less than 500 square meters per gram are esterified by a given alcohol to roughly the same degree.

Maximum Degree of Esterification with Different Alcohols.—Typical estersils made with different alcohols are shown in Table III. Study of a variety of alcohols has led to these conclusions:

Branched chain alcohols, having a larger cross-sectional molecular area, cover the surface with fewer molecules. For a surface covered by branched chain alkoxy groups, the "degree of esterification," as defined, is thus lower than in the case of straight chain alcohols.

(22) F. E. Bartell and D. G. Dobay, *J. Am. Chem. Soc.*, **72**, 4388 (1950).

(23) See p. 253, ref. 6.

(24) Ref. 6, page 242.

TABLE II

ESTERSILS FROM VARIOUS SILICA SUBSTRATES AND 1-BUTANOL

Substrate type	Spec. surf. m.²/g.	Autoclaving conditions Temp., °C.	Time, hr.	Characterization of Estersils: Specific surface, m.²/g.	Hydroxyl surface, m.²/g.	% SiO_2	% C	Degree of esterification
B	100	195	1	96	...	89.6	2.15	2.8
B	97	190	1	91	4.8	89.44	2.55	3.5
B	~100	200	1	107	0	89.5	2.25	2.6
B	~100	195	1	101	...	89.57	2.15	2.6
B	~150	300	1	150	3.9	88.74	4.15	2.8
Fibrous SiO_2 from asbestos	..	225	2	125	0	85.6	3.58	3.6
Commercial aerogel	137	190	1	127	...	...	3.70	3.0
Fume silica	171	190	1	158			3.70	2.9
Commercial hydrogel (78% H_2O)	..	290	0.5	184	2.0	91.5	5.37	3.6
Commercial pptd. silica	300	285	0.5	234	...	...	6.69	3.5
Commercial pptd. silica	..	285	0.5	240	0	...	5.94	3.1
D	..	~200	1	277	0	87.67	6.56	3.5
D	358	190	1	302	0	...	7.94	3.3
D	370	190	1	312	0	...	8.08	3.2
E	..	~300	1	738	0		18.90	3.2
		Refluxing in anhydrous 1-BuOH						
B	..	118	3	107	24	89.2	1.54	1.8
Commercial aerogel	157	118	3	154	71	93.9	1.88	1.53
C	215	118	3	213	97	90.6	3.46	2.0
"Linde" silica[a]	242	118	3	244	88	92.6	2.80	1.4
D	287	118	3	284	98	89.5	3.26	1.4
Commercial silica gel	..	118	3	356	108	91.4	3.45	1.2
E	571	118	3	567	158	85.2	5.08	1.1 (5)

[a] Linde Air Products Co.—Data Sheet "Silica" (May 19, 1948).

TABLE III

ESTERIFICATION OF SILICA WITH VARIOUS ALCOHOLS (ETHANOL AND HIGHER)

Alcohol	Reaction conditions °C.	Hr.	Substrate Type	Sp. area m.²/g.	Characteristics of Estersil: Sp. area m.²/g.	Hydrox. area m.²/g.	% SiO_2	% C	Degree[a] esterif.
Ethanol	225	1	D	..	287	12	91.3	3.67	3.2
Ethanol	300	1	D	..	303	0	..	5.26	4.3
Ethanol	250	1	B	..	82	0	..	1.10	3.4
Ethylene glycol	190	1	B	200	..	2	92.7	3.29	4.1
1-Propanol	250	1	A	..	82	..	..	1.74	3.5
1-Propanol	..	..	D	..	285			6.42	3.8
1-Propanol	250	0.5	E	..	576	0	79.0	10.30	3.0
2-Propanol	300	1	D	302	302	1	89.0	5.57	3.1
1-Butanol	300	1	D	302	285	0		8.26	3.6
1-Butanol	190	1	B	97	91	5	89.4	2.55	3.5
2-Butanol	300	1	B	..	285	..	..	7.97	3.5
2-Butanol	300	1	B	..	285	..	..	5.88	2.6
2-Butanol	200	0.8	D	..	270	22	..	5.93	2.8
2-Butanol	275	0.8	D	..	355	0	..	6.77	3.2
Methylisobutylcarbinol	250	0.5	D	297	269	22	86.6	7.26	2.7
	225	1	D	..	282	4	89.75	5.05	1.8
Benzyl alcohol	190	3	D	300	261	0	82.2	11.91	3.3
1-Octanol	200	1	D	..	285		80.4	12.05	2.6
1-Octanol	200	1	E	300	521		..	25.11	3.0
2-Octanol	175	1.5	A	133	..	0	91.8	4.34	2.0
1-Dodecanol	200	3	A	..	133		83.6	11.59	3.6
Trimethylhexanol	180	1	A	133	..	0	90.6	5.79	2.4
1-Octadecanol	200	3	A	133	..	0	83.9	12.5	2.6
1-Octadecanol	300	0.5	D	221	183	0	70.9	21.6	3.3
Branched C_{18}[b]	175	1	A	..	220	..	81.4	13.27	1.7

[a] When area of substrate was not available, degree of esterification was calculated from specific surface of the estersil. [b] 5,7,7-Trimethyl-2-(1,3,3-trimethylbutyl)-octanol.

Straight chain hydrocarbon groups, under a given set of reaction conditions, may each cover about 37 Å.². For a hydrocarbon group with one branch, it appears that adjacent groups can orient so that such groups can also pack together so that each group covers about 37 Å.² of surface. The

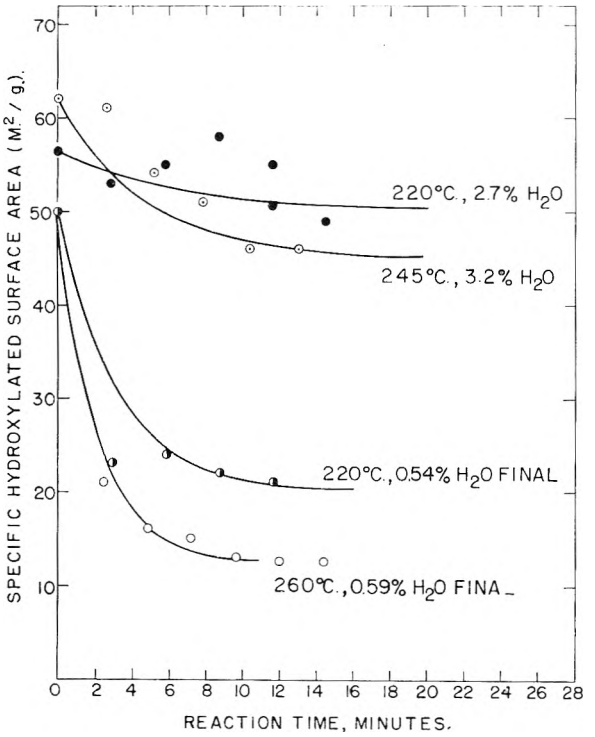

Fig. 2.—Degree of esterification of the silica surface as a function of the reaction time.

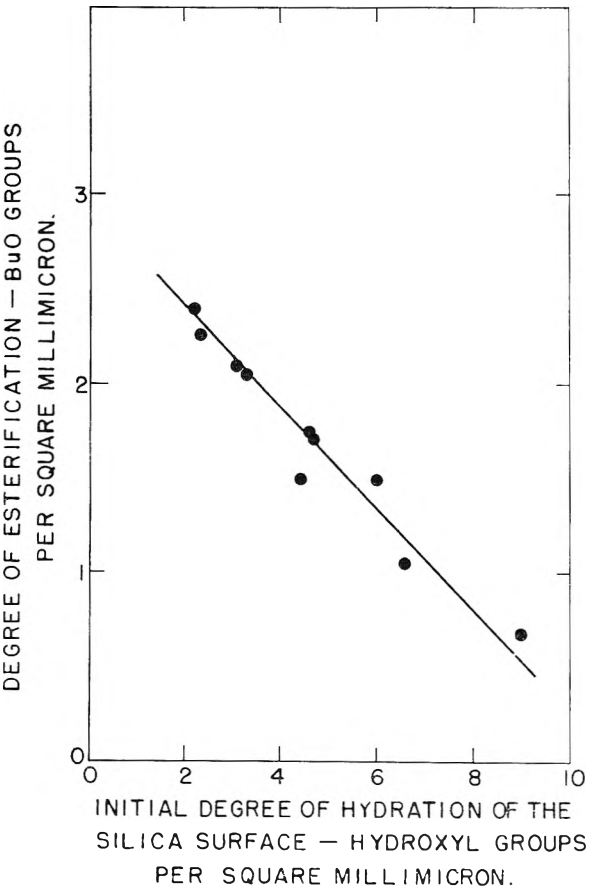

Fig. 3.—Degree of esterification of a silica surface partially dehydrated at elevated temperature before reaction with 1-butanol at 118°.

diameter of a more highly branched hydrocarbon group may be estimated at its widest point in terms of a "branch-number," designated "*n*." Where the branch number is 3 or greater, the cross-sectional area can be estimated as 14 *n* Å.². This assumes that each branch, when closely packed with others, has a cross-sectional area of 14 Å.². This is less than the value of 20 A.² usually given as the cross-sectional area of a straight chain hydrocarbon group in a monomolecular film under compression on water.[25] Thus the ester film must be quite highly compressed or at least oriented so as to permit closest packing. Probably the chains coil or expand to prevent closest packing of the branches.

A series of calculated and observed values for the degree of esterification attainable under conditions where butanol gives a D.E. of 2.7, are listed in Table IV.

The Unusual Behavior of Methanol.—The effective cross-sectional area of the methoxy group is reported to be 18 A.².[26] from measurements of the heat of adsorption of methanol vapor on silica gel. This means that the maximum possible degree of esterification should be about 5.6 for methanol, as contrasted with 3.8 for the higher alcohols. In general, it is not possible to achieve this maximum by merely increasing the temperature and pressure. Thus, increasing the esterification temperature in the autoclave from 225 to 275° increased the D.E. only from 4.4 to 4.6 CH_3O/sq. millimicron. However, it was discovered[27] that if the water formed in the esterification reaction were removed from the system, a close-packed methoxy surface can be achieved. Under anhydrous conditions a maximum of 5.8 CH_3O/sq. millimicron may be attained at 290° and autogenous pressure.

TABLE IV

SURFACE COVERED BY BRANCHED CHAIN ALCOHOLS

Alcohol	*n*	D.E.[a] Observed	D.E.[a] Calculated
1-Butanol	1	2.7	2.7
1-Propanol	1	2.7	2.7
2,3-Hexanediol	2	2.6	2.7
2-Ethylhexanol	2	3.0	2.7
2,2,4-Trimethylhexanol	3	2.4	2.4
Di-isopropylcarbinol	4	1.7	1.8
Octadecyl alcohol[b]	5	1.7	1.4
n-Octadecyl alcohol	1	2.7	2.7

[a] D.E. = degree of esterification, butoxy groups per sq. millimicron. [b] 5,7,7-Trimethyl-2-(1,3,3-trimethylbutyl)-octanol.

Esterification Kinetics and Equilibrium.—The surface reaction is assumed to be

$$\text{-SiOH} + \text{ROH} \rightleftarrows \text{-SiOR} + \text{H}_2\text{O}$$

and the rate equation is formulated as

$$\frac{dA}{dt} = -K_f A(\text{ROH}) + K_r(\text{H}_2\text{O})(A_0 - A)$$

(25) H. B. Weiser, "A Textbook of Colloid Chemistry," 2nd ed., John Wiley & Sons, New York, N. Y., 1950.

(26) N. N. Avgul, *et al.*, *Doklady Akad. Nauk., U.S.S.R.*, **77**, 625 (1951).

(27) E. C. Broge, U. S. Patent 2,736,668 (E. I. du Pont de Nemours & Co., Inc., 1956).

A, the specific hydroxylated surface area (unesterified silanol groups) as measured by the adsorption of methyl red dye from benzene, was taken as a measure of the activity of the surface groups. K_f and K_r are the specific velocity constants for the esterification and hydrolysis reactions, A_0 is the specific silanol surface of unesterified silica and (ROH) and (H_2O) are the activities of butanol and water in the heterogeneous system.

Using a graph (Fig. 2) showing degree of esterification and water concentration as a function of reaction time, a smooth curve was fitted to the data points (see Table V).

The individual values of K_f, K_r and K_e then were correlated by plotting log K *vs.* T^{-1}, and least-squares lines were drawn to fit the data points and serve as best estimates of the kinetics and equilibria of the esterification reaction. Slopes of these lines were used to compute the heats of activation and of reaction.

Correlation of the rate constants by means of a simplified Arrhenius equation gave an energy of activation of 21.9 kcal. per mole of ester groups for the esterification reaction and 9.0 kcal. per mole for the reverse (hydrolysis) reaction. In a similar manner, a simplified van't Hoff isochore equation applied to the equilibrium constants indicated an endothermic heat of reaction of 12.1 kcal. per mole of ester group

Esterification of Thermally Dehydrated Silica.— The silanol groups on the surface of amorphous silica can be partially dehydrated by heating the powder at 150 to 500°.[28] If the silica is thermally dehydrated before reaction with 1-butanol, the esterification reaction proceeds more rapidly.[29] The degree of esterification obtained by refluxing the silica with 1-butanol at 118° depends on the temperature at which the silica previously has been dehydrated. A possible explanation for this effect is that the dehydrated silica surface is much more reactive with alcohol, acting perhaps as an acid anhydride. Although the surface actually cannot be completely dehydrated, extrapolation of the line in Fig. 3 suggests that a completely anhydrous surface, if it could be attained, would become covered with butoxy groups (2.7 per square millimicron). Active Si–O–Si bonds on the silica surface (formed by thermal condensation of adjacent SiOH groups) thus probably react with alcohols as follows, the linkages from silicon to the underlying particle not being shown.

TABLE V

VARIATION IN REACTION RATE AND EQUILIBRIUM CONSTANTS WITH TEMPERATURE

Run	Temp., °C.	K_f (hr.$^{-1}$)	K_r (hr.)$^{-1}$ (wt. % H_2O)$^{-1}$	$K_e = K_f/K_r$ (wt. % H_2O)
1	118	0.012	0.078	0.15
2	160	0.14	0.17	0.82
3	160	0.60	0.22	2.7
4	220	18.4	2.2	8.4
5	220	7.7	0.5	15.4
6	245	11.2	0.6	18.7
7	260	27.9	1.9	14.7
8	320	116	3.6	32

$$\text{Si–O–Si} + \text{ROH} \longrightarrow \text{SiOR} + \text{SiOH}$$

Simultaneously, some of the silanol groups react

$$\text{SiOH} + \text{ROH} \longrightarrow \text{SiOR} + H_2O$$
$$\text{Si–O–Si} + H_2O \longrightarrow 2\text{SiOH}$$

In practice, thermal dehydration of finely divided silica to give fewer surface SiOH groups than about 2.0 per square millimicron is not possible, since temperatures in excess of 650° are required. Sintering, with loss of surface area, occurs above this point. However, by first dehydrating silica at 450–500°, in air, definitely hydrophobic products can be obtained simply by boiling the dehydrated powder in an alcohol such as 1-butanol, and drying.

(28) See p. 234 of ref. 6.

(29) M. T. Goebel, U. S. Patent 2,736,669 (E. I. du Pont de Nemours & Co., Inc., 1956).

FREE ENERGY OF ADSORPTION. I. THE INFLUENCE OF SUBSTRATE STRUCTURE IN THE SiO_2–H_2O, SiO_2–*n*-HEXANE AND SiO_2–CH_3OH SYSTEMS

BY R. L. EVERY, W. H. WADE AND NORMAN HACKERMAN

Department of Chemistry, The University of Texas, Austin, Texas

Received May 2, 1960

The free energies of adsorption for these systems were calculated from adsorption isotherms at 25° using the Gibbs adsorption equation. In particular, the effects of particle size and of outgassing treatments were investigated. Of special interest was the finding of maxima in the free energy of adsorption of all three adsorbates in the middle range of particle sizes studied. Specific surface areas varied from 0.070 to 188 m.^{2}/g.

Introduction

This work is an extension of that reported earlier on the effect of particle size of SiO_2 on calorimetrically determined heats of immersion in water.[1] A review of the literature reveals that although several workers have investigated surface thermodynamics, using a variety of adsorbents, few have tried to correlate adsorption properties to particle size. One group of investigators[2] found that the heat of immersion of silica gels decreased with decrease in particle size and some previous work done in this Laboratory[1,3] indicated a varia-

(1) W. H. Wade, R. L. Every and N. Hackerman, THIS JOURNAL, **64**, 355 (1960).

(2) M. M. Egorov, K. G. Krasil'nikov and E. A. Sysoev, *Doklady Akad. Nauk, S.S.S.R.*, **108**, 103 (1956).

(3) A. C. Makrides and N. Hackerman, THIS JOURNAL, **63**, 594 (1959).

Table Ia

Water

P/P^0	Sample A[a] OG[b] 160° V/P[c]	Sample B OG 160° V/P	Sample C OG 160° & 260° V/P	Sample D OG 115° V/P	Sample D OG 160° V/P	Sample D OG 260° V/P	Sample E OG 160° V/P	Sample F OG 160° V/P	Sample G OG 115° V/P	Sample G OG 260° V/P
0.01	1.299	1.575	3.898	3.642	3.799	3.799	4.390	0.299	0.287	0.228
.025	1.083	1.358	2.677	1.378	2.835	2.835	3.091	.276	.260	.197
.05	0.854	1.126	1.366	1.126	1.693	1.594	1.760	.256	.220	.150
.10	.618	0.783	0.957	0.902	1.146	1.122	1.181	.201	.173	.130
.20	.421	.543	.642	.665	0.728	0.795	0.776	.165	.130	.114
.30	.335	.465	.531	.539	.571	.622	.610	.146	.114	.106
.40	.291	.374	.472	.484	.496	.547	.516	.134	.102	.102
.50	.264	.339	.437	.453	.453	.512	.469	.134	.102	.102
.60	.264	.331	.417	.441	.441	.492	.457	.142	.110	.106
.70	.264	.342	.425	.457	.457	.500	.465	.157	.126	.114
.80	.272	.398	.449	.512	.524	.591	.516	.209	.150	.146
.90	.382	.531	.500	.764	.697	.846	.677	.315	.236	.236
.95	.472	.681	.563	.906	.866	1.035	.866	.374	.307	.307
.98	.571	.815	.614	1.000	1.012	1.181	1.032	.453	.343	.343

[a] See Table II for specific surface area. [b] Outgassing temperature. [c] Units = cc. at S.T.P. per m.^{2} per cm.

Table Ib

Methanol

P/P^0	Sample A OG 160° V/P	Sample B OG 160° V/P	Sample C OG 160° V/P	Sample D OG 160° V/P	Sample D OG 260° V/P	Sample E OG 160° V/P	Sample F OG 160° V/P	Sample G OG 160° V/P
0.01	0.685	0.515	0.860	0.890	0.300	1.100	0.425	0.255
.025	.305	.205	.500	.480	.210	0.825	.305	.180
.05	.172	.255	.297	.286	.156	.470	.186	.122
.10	.100	.158	.172	.151	.103	.204	.109	.077
.20	.055	.091	.098	.089	.056	.117	.061	.045
.30	.040	.065	.070	.065	.041	.085	.042	.035
.40	.033	.054	.054	.054	.035	.067	.036	.029
.50	.029	.046	.047	.046	.032	.058	.032	.025
.60	.027	.043	.044	.043	.030	.053	.030	.023
.70	.025	.040	.043	.043	.030	.050	.030	.022
.80	.025	.042	.044	.045	.035	.050	.032	.024
.90	.029	.049	.049	.055	.045	.056	.038	.031
.95	.032	.059	.053	.064	.053	.065	.045	.041
.98	.035	.067	.056	.072	.060	.075	.057	.050

Table Ic

n-Hexane

P/P^0	Sample A OG 160° V/P	Sample B OG 160° V/P	Sample C OG 160 and 260° V/P	Sample D OG 160° V/P	Sample D OG 260° V/P	Sample E OG 160° V/P	Sample F OG 160° V/P	Sample G OG 160° V/P
0.01	0.0320	0.0360	0.0355	0.0480	0.0480	0.0405	0.0123	0.0123
.025	.0240	.0230	.0301	.0180	.0245	.0305	.0117	.0117
.05	.0173	.0168	.0262	.0153	.0214	.0185	.0110	.0110
.10	.0115	.0142	.0218	.0134	.0180	.0155	.0103	.0103
.20	.0077	.0123	.0179	.0129	.0150	.0138	.0095	.0095
.30	.0065	.0117	.0155	.0128	.0136	.0134	.0095	.0094
.40	.0060	.0115	.0138	.0127	.0131	.0133	.0096	.0094
.50	.0060	.0116	.0130	.0127	.0130	.0135	.0099	.0095
.60	.0060	.0121	.0126	.0127	.0134	.0140	.0105	.0098
.70	.0063	.0132	.0128	.0131	.0140	.0151	.0118	.0105
.80	.0072	.0153	.0142	.0161	.0162	.0170	.0155	.0120
.90	.0097	.0198	.0190	.0216	.0216	.0232	.0257	.0163
.95	.0126	.0260	.0271	.0300	.0300	.0300	.0362	.0200
.98	.0157	.0350	.0356	.0405	.0405	.0375	.0420	.0223

tion of the heats of immersion with specific surface area. Zhdanov[4] noted a change in position of the adsorption isotherms (normalized to unit surface area) of water on quartz of varying specific areas, but made no mention of surface thermodynamics. In another study of the free energy of adsorption on porous solids, no effect due to particle size was found.[5] In the present study, an attempt was made to characterize systematically the adsorbent behavior of seven different, non-porous SiO_2 samples. The adsorbates (water, *n*-hexane and methanol)

(4) S. P. Zhdanov, *Proc. Acad. Sci., USSR*, **120**, 277 (1958).

(5) R. G. Craig, J. J. Van Voorhis and F. E. Bartell, This Journal, **60**, 1225 (1956).

TABLE IIa

Sample	Crystal structure	Surface area m.²/g.[e]	Outgas temp., °C.	π(erg/cm.²) 0–0.9P^0	π(erg/cm.²) 0–1.0P^0	Water ΔH_a, erg/cm.²	Water ΔS_a, erg/cm.²/°C.	Water ω (Å.²)
A[a]	β-Quartz	0.070	160	93.1	105.7	729.1	2.09	20.4
B	β-Quartz	.138	160	118.7	127.8	546.5	1.41	16.8
C	β-Cristobalite	.54	160 & 260	158.8	173.9	531.1	1.20	12.5
D[b]	β-Quartz	.91	115	176.0	199.8	341.5	0.482	12.2
			160	203.5	227.1	388.5	.542	11.0
			260	206.4	233.7	485.8	.845	10.8
E	β-Quartz	8.12	160	191.8	215.1	334.5	.401	11.9
F	Amorphous (?)	162	160	39.5	49.6	−29.2	− .264	36.5
G[c]	Amorphous[d]	188	115	32.8	40.9	43.5	.0087	51.6
			260	25.8	33.9	42.9	.0030	55.5

[a] Supplied by Cleveland Quartz Works, General Electric Company. [b] Supplied by C. A. Wagner, Inc. [c] Supplied by Godfrey L. Cabot, Inc. (Cab-O-Sil). [d] Determined by Godfrey L. Cabot, Inc. [e] Surface areas were measured by Kr adsorption with the exception of samples F and G which were measured by Dr. J. W. Whalen of the Magnolia Petroleum Company Field Research Laboratory using N_2 adsorption.

TABLE IIb

Sample	Surface area, m.²/g.	Outgas temp., °C.	Methanol π(erg/cm.²) 0–0.9P^0	Methanol π(erg/cm.²) 0–1.0P^0	Methanol ω (Å.²)	n-Hexane π(erg/cm.²) 0 – 0.9P^0	n-Hexane π(erg/cm.²) 0 – 1.0P^0	n-Hexane ω (Å.²)
A	0.070	160	75.1	79.7	27.9	12.51	14.62	168.9
B	.138	160	107.3	115.1	19.6	20.47	24.99	70.6
C	.54	160	122.7	129.7	18.6	24.11	28.80	54.8
D	.91	160	121.4	130.3	18.6	21.93	27.61	51.9
		260	54.1	67.8	28.9	23.91	28.53	48.8
E	8.12	160	154.6	163.2	14.1	23.41	28.40	49.8
F	162	160	77.3	83.8	28.4	17.17	23.05	71.4
G	188	160	55.9	61.4	31.9	15.52	18.95	76.2

were chosen to provide a polar compound, a non-polar material, and one which was intermediate in character.

Experimental

Material.—The seven samples of SiO_2 investigated are listed in Table IIa.[3] Samples B and E were obtained from sample A by sedimentation from water. Sample B was drawn off in less than one minute and sample E was that portion which remained in suspension longer than 24 hours. Sample C was prepared from sample D by heating to 1510° followed by a rapid water quench. The resulting material was found by X-ray diffraction to be approximately 90% cristobalite and 10% quartz. Sample F was prepared from sample G by heating for 8 hours at 800° and subsequently exposing it to saturated water vapor for two weeks.

Prior to adsorption measurements, the samples were vacuum outgassed for 36 hours at an elevated temperature. The usual temperature was 160°, selected as the best compromise between the maximum removal of the physically adsorbed water and the minimum loss of surface hydroxyl groups.

The water used was doubly-distilled and after being attached to the vacuum system was repeatedly frozen with Dry Ice and degassed under a vacuum of about 10^{-6} mm. until free of dissolved gases. The *n*-hexane was obtained from Phillips Petroleum Co. and analyzed by them to be 99.98% pure. The methanol was obtained from Baker Chemical Co. and analyzed by them to be 99.9% pure. The *n*-hexane and methanol each were refluxed under vacuum with CaH_2 for a period of two hours to reduce the water content to a minimum. The materials were distilled into receiver bulbs with standard break-off seals and these bulbs were sealed and removed from the condenser while under vacuum. The bulbs then were attached to the adsorption apparatus. They were repeatedly frozen with liquid nitrogen and degassed under a vacuum of about 5×10^{-5} mm. until free of dissolved gases.

Apparatus.—The volumetric adsorption apparatus for water has been described previously.[6] The same general design was used in the construction of two other volumetric adsorption systems for hydrocarbon studies. These were equipped with mercury cutoffs so as to prevent contamination by stopcock lubricant. The sample bulb temperatures were controlled by water-baths to ±0.01°. Room temperature was maintained approximately 2° above sample temperature to avoid spurious condensation. Pressures were read from large bore mercury manometers with traveling telescopes of 0.01 mm. readability.

Calculations.—The free energies of adsorption for the systems indicated were determined from application of the

$$\pi = RT \int_{P=0}^{P=P^0} \Gamma \, d \ln P$$

Gibbs equation to adsorption isotherms measured at 25°.[7-10] Here π is the free energy of adsorption per cm.², R is the gas constant, T is the temperature, Γ denotes the excess surface concentration in moles per cm.², and P is pressure. Assuming ideality in the gas phase, Γ is quite simply related to the volume of gas adsorbed per cm.² at S.T.P., V. π was evaluated graphically from plots of V/P *vs.* P/P^0 to provide the numerical solution to the integral. The isotherms were difficult to reproduce near saturation vapor pressure so that the isotherms and their derived quantities carry some uncertainty in the extrapolation to P^0. However, the isotherms were satisfactory up to about $0.9P^0$ and these values of the integral from zero pressure to 90% saturation were also shown in Table II. The former extrapolation to P^0 realistically limits the accuracy of the π values to ± 5%.

Integrated heats of adsorption ΔH_a for the water–SiO_2 system, as shown in Table II, were calculated from previously published work[3] in which the heats of immersion were reported. The difference between the heat of immersion and the integral heat of adsorption with liquid water as the reference state is just the surface enthalpy of water which is given as 118.5 erg/cm.².[11] From the experimentally determined quantities, π and ΔH_a, the entropies of adsorption (Table II) were calculated for this system using the two dimensional thermodynamic analog

$$\pi = \Delta H_a - T\Delta S_a$$

It should be noted that for a more exact treatment, the entropies of adsorption should be normalized to constant

(6) N. Hackerman and A. C. Hall, THIS JOURNAL, **62**, 1212 (1958).

(7) J. W. Gibbs, "Collected Works," Longmans, Green and Co., New York, N. Y., 1928 p. 315.

(8) L. E. Drain and J. A. Morrison, *Trans. Faraday Soc.*, **48**, 316 (1952).

(9) D. H. Bangham, *ibid.*, **33**, 805 (1937).

(10) D. H. Bangham and R. I. Razouk, *ibid.*, **33**, 1463 (1937).

(11) W. D. Harkins and G. Jura, *J. Am. Chem. Soc.*, **66**, 919 (1944).

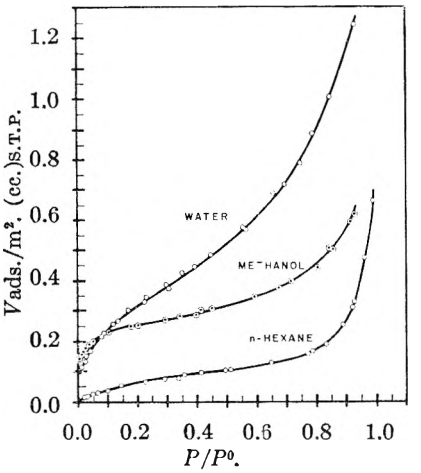

Fig. 1.—Volume adsorbed per m.² *vs.* relative pressure.

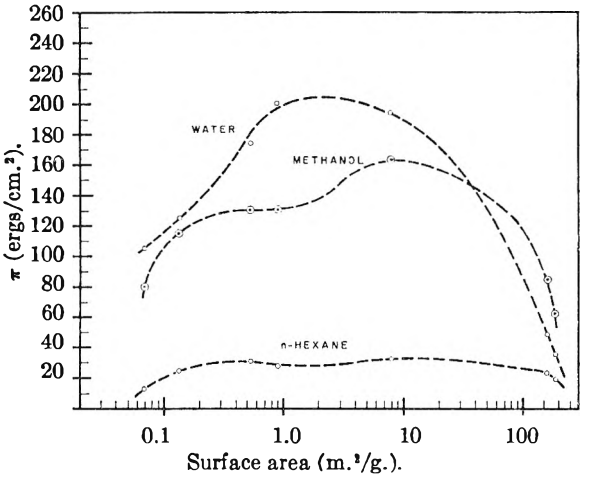

Fig. 2.—Free energy of adsorption *vs.* specific surface area.

surface coverage. The entropies as tabulated were obtained at constant relative pressure and vary from that at constant surface coverage by not more than 15%.

The effective area of the substrate occupied by the various adsorbate molecules, ω (Table II), was calculated using the B.E.T. method. Experimental points used in these calculations were taken in the pressure range $0.05P^0$ to $0.30P^0$.

Results and Discussion

A typical set of adsorption data for the three adsorbates on a particular SiO_2 sample appear in Fig. 2. All graphs used in these calculations were constructed from between twenty and fifty experimental values, with the values having an average deviation of less than 2% from the line as drawn (except as noted in discussion). For the purposes of brevity, only the single set of isotherms is given in Fig. 2, but if one wishes, the remaining isotherms may be reconstructed by reference to Table I. In this table, points at arbitrarily selected intervals of P/P^0 were chosen from the smoothed V/P *vs.* P/P^0 plots.

The non-porous character of the seven adsorbent samples was confirmed by the reversibility of the adsorption isotherms at high relative pressures with all three adsorbates. The hexane, methanol and water desorption branches followed the adsorption branches at all relative pressures, with the exception of the water desorption curves on samples D and E. These two samples showed small hysteresis loops at relative pressures below $0.4P^0$. Most likely, these loops are due to slow hydration–dehydration processes of a small portion of the surface which had been converted to the siloxane surface[12] during the outgassing operation. The hexane adsorption isotherms were difficult to characterize lower than $0.15P^0$, fluctuating about a mean as much as 5%. Since the π-values for hexane (Table II) are only about 0.1 of those for water, these fluctuations may be only a reflection of the weakness of the van der Waals forces involved in hexane adsorption.[13–15]

Effect of Outgassing Temperature.—The effect of outgassing temperature on the adsorption isotherm of water on crystalline SiO_2 was found to differ from that of water on amorphous SiO_2. From Table Ia, it is seen that as the outgassing temperature is increased for the 0.91 m.²/g. quartz, the volume of water adsorbed is increased. This is due no doubt to a progressive removal of physically adsorbed water and surface hydroxyl groups at the highest outgassing temperatures. Since hysteresis was observed, any siloxane bridges formed during outgassing must slowly rehydrate on exposure to water vapor as previously noted. Any methylation of the siloxane groups formed at the higher outgassing temperatures must be a reversible process.[16] This is suggested by absence of hysteresis at low relative pressure and by a decrease in methanol adsorption with increased temperature. The latter behavior, unfortunately, is complicated by the loss of the remnants of physically adsorbed water which might promote methanol adsorption *via* enhanced hydrogen bonding.

In contrast to the water behavior on crystalline SiO_2 an increase in outgassing temperature for the amorphous 188 m.²/g. material results in a decrease of water adsorbed. Apparently the configuration of the amorphous SiO_2 surface is such that the dehydration of silanol groups is completely irreversible. Previous weight loss measurements[1] have set as an upper limit 2OH's/100 Å.² for this material. This increasing hydrophobicity toward polar molecules with increasing outgassing temperature has been noted by others,[17] and would now appear to apply only to amorphous surfaces. Whether adsorption isotherms as a function of outgassing temperature can be used as a criteria for characterizing surfaces as amorphous or crystalline remains to be seen. However, the above noted differences indicate that isotherms could be useful in this respect. Moreover, the increase in the entropies of adsorption with outgassing temperature for samples D and G (Table IIa) would be expected for a progressively dehydrated surface.

Particle Size Effect.—The plot of free energy of adsorption (Fig. 2) for the three adsorbates as a function of specific area of the adsorbents shows a maximum which decreases in prominence in the order: water, methanol and *n*-hexane. If one ex-

(12) R. K. Iler, "The Colloid Chemistry of Silica and Silicate," Cornell University Press, Ithaca, New York, Chapter VIII.

(13) A. V. Kiselev, *Proc. Acad. Sci., USSR*, **100**, 1046 (1956).

(14) A. A. Isirikian and A. V. Kiselev, *ibid.*, **115**, 343 (1957).

(15) L. D. Beliakova and A. V. Kiselev, *ibid.*, **119**, 155 (1958).

(16) A. V. Kiselev, K. G. Krasil'nikov and L. N. Soboleva, *ibid.*, **94**, 85 (1954).

(17) J. H. deBoer, M. E. A. Hermans and J. M. Vleeskens, *Koninkl. Ned. Akad. Wetenschap. Proc. Ser. B*, **60**, 45 (1957).

pected a simple monotonic decrease in π as was observed for the heats of immersion, the results obtained over the particle size range would be quite unexpected. The observed π *vs.* area behavior can be understood only in the light of a previously advanced hypothesis, namely, that the large variation in immersional heats with particle size is due to a direct correlation between crystallinity and particle size. A qualitative explanation based on low specific area samples having crystalline surfaces and high specific area samples having amorphous surfaces has been offered, and in previous work the amorphous character of the SiO_2 surface has been discussed at some length[3]. The entropy data obtained from the present investigation serve to demonstrate the gradual transition from a crystalline to an amorphous surface with decreasing particle size. Unless the adsorbed layer is completely mobile in character, adsorption on a periodic crystalline substrate will produce an entropy change more negative than that for adsorption on an aperiodic amorphous surface. If once again, one assumes a direct proportionality between specific area and crystalline–amorphous character of the surface, then Table IIa provides verification of this in the entropy data for the system SiO_2–water. The comparable magnitudes of the ΔH_a and $T\Delta S_a$ contributions to the free energy explain the existence of the maximum in the water–SiO_2 system. Undoubtedly, the same interpretation should be taken for the methanol–SiO_2 and the *n*-hexane–SiO_2 systems, although there are no experimental enthalpy data available at the present time. One would expect that as bonding forces become progressively weaker in going from water to methanol to *n*-hexane, the free energy would be less dependent on details of the surface structure, and it is noted that the maxima do become less pronounced.

The only data in disagreement with this interpretation are for sample F–water system which gives a negative ΔS_a. Previous anomalous results have been obtained for this sample,[1] but all data taken have been consistently reproducible.

Although the data for the β-cristobalite fit the π *vs.* area curves, this may be fortuitous since the material was converted to β-cristobalite from β-quartz subsequent to any grinding operation. Since bulk recrystallization occurred, it is reasonable that any surface amorphicity was simultaneously removed.

Unfortunately, it was impossible to obtain the entire spectrum of particle sizes studied from a single sample so that the entire mode of surface generation could be laid to a single type of operation, *i.e.*, grinding. The three samples, A, B and E, which were obtained by a single grinding operation, are consistent with the remaining samples. In the actual grinding operation, the largest particles will have had the shortest life. In other words, the smaller the particle, the longer will have been its grinding history. This means that the smallest particles obtained have been subjected to both the highest pressures and highest local grinding temperatures. Here we have two compensating effects: (a) the crushing of the quartz during which the sample is plastically deformed and the Si^{+4} ions are replaced in the surface by the polarizable O^{-2} ions—an amorphous layer being produced[18]—and (b) an annealing process due to the high local temperatures which partially restores the crystal structure.[19] It is impossible from the present data to assign quantitative values for processes (a) and (b). Qualitatively, process (a) seems to overshadow (b) for the samples studied.

It is interesting to note that ω for the adsorbate molecules on the various samples (Table II) parallel the free energies of adsorption, the minimum value of ω occurring in the middle range of particle size studied, coinciding with the maximum value of π. Two independent reasons should be given for the low adsorbate density in the first layer for both the lowest and highest specific area samples. For the crystalline low area samples, the area is governed by periodicities of the lattice substrate, whereas, for the amorphous high area samples, the packing is governed by the concentration of sufficiently high energy adsorption sites.

Acknowledgment.—This work is a contribution from the Department of Chemistry, The University of Texas. The authors wish to take this opportunity to express their appreciation to the American Petroleum Institute (Project 47D) for their continued support and interest in this project.

(18) R. Gomer and C. S. Smith, "Structure and Properties of Solid Surfaces," The Univ. of Chicago Press, Chicago, Ill., 1953, Chap. IV.

(19) D. D'Eustachio and S. Greenwald, *Phys. Rev.*, **69**, 532 (1946).

THE PORE STRUCTURE OF CHRYSOTILE ASBESTOS

BY FRED L. PUNDSACK

Contribution from the Johns-Manville Research Center, Manville, New Jersey

Received August 10, 1960

The pore volume structures of intact bundles of chrysotile asbestos fibers were studied with water vapor adsorption–desorption isotherms. In the three samples examined, the total pore volume ranged from a little less than 4% to a little more than 5% based on the total sample volume. In all the samples more than 80% of the void volume existed in pores less than 60 Å. in diameter. It was concluded from the pore volume distribution that fundamental chrysotile fibrils exist in a cylindrical or near-cylindrical form with an average outer diameter of 200 to 250 Å. and an average effective inner diameter of 20 to 50 Å. The packing space between the fibrils probably is irregular, but it has an effective pore size of the same order of magnitude as the internal pores within the fibrils.

Introduction

The structure of chrysotile asbestos has been the subject of considerable interest and controversy since it was noted about ten years ago that the fibers had the appearance of hollow tubes when viewed with an electron miscroscope.[1] In the case of many natural fibers these "tubes" were reported to have apparent outer diameters in the range of 300 to 400 Å. and inner diameters in the range of 100 to 200 Å. Later, however, it was shown[2,3] that this simple "hollow tube" hypothesis was not in agreement with the small amount of void volume actually observed in naturally occurring bundles of asbestos fibers. Whereas void fractions of 25% or more would be required for bundles of hollow tubes of the dimensions suggested above, the void fractions observed experimentally were of the order of 6%. To account for this discrepancy in void volume, it was suggested then that the fibers might be in the form of distorted laths or ribbons rather than hollow tubes. However, the distorted lath hypothesis is not able to account satisfactorily for the X-ray diffraction data obtained with chrysotile. These data[4–7] appear to indicate that chrysotile does have a cylindrical crystal lattice.

Several hypotheses have been proposed in the past few years which attempt to reconcile the "hollow tube" appearance of chrysotile fibers with the lack of any large amount of void space in macrobundles of the fibers. Whittaker[8] has suggested that the "hollow tubes" are filled with curved laths of the same composition and structure as the tubes themselves. Bates and Comer,[9] on the other hand, have proposed that the tubes contain "amorphous" material of essentially the same composition as chrysotile but with an irregular crystal lattice due to a high degree of strain in the structure. According to Bates the high degree of strain is a result of the physical restriction of the material so that its crystal lattice cannot assume the optimum strain-free radius of curvature which exists in the wall proper of the fiber tube. Some of this "amorphous" material is also said to occupy part of the packing space between the tubular fibers when they exist in the form of bundles. Bates and Comer have presented electron micrographs as evidence of the amorphous material within and around the tubular fibers.

This paper describes pore size distribution studies on intact bundles of natural chrysotile fibers and relates the data to the morphology of the fibers.

Experimental

The determination of pore volume distribution in porous solids with nitrogen gas adsorption–desorption isotherms is a well established procedure.[10] However, the use of nitrogen to obtain adsorption–desorption isotherms with intact bundles of chrysotile presents some difficult experimental problems. These problems arise because the total amount of void volume in the fiber is relatively small—on the order of only 0.02 cc./g. of solid. In addition, the diffusion path of nitrogen into a block of fiber bundles is very long, and it requires many hours, even days, for equilibrium to be established. This is true particularly in the regions where adsorption and desorption change most markedly with variations in the relative pressure of the gas, and it is these regions that are crucial in a pore volume distribution analysis. During the long periods which are required for equilibrium to be established, it is difficult to maintain completely stable conditions in a vacuum apparatus operated at liquid nitrogen temperatures. Therefore, up to this time we have not been able to obtain a satisfactory, reproducible adsorption–desorption isotherm with nitrogen gas on intact blocks of chrysotile fiber bundles.

In view of the unsatisfactory state of the work with nitrogen gas, an effort was made to obtain water vapor adsorption–desorption isotherms at room temperature on relatively large blocks of intact fiber bundles.

Materials.—Sample 1—an intact block of chrysotile fibers about 1.5 cm. long with an average cross-section dimension of 3.1 cm. from the Jeffrey Mine, Asbestos, Quebec. Sample 2—an intact block of chrysotile fibers about 4.0 cm. long with an average cross-section dimension of 1.2 cm. from the Jeffrey Mine, Asbestos, Quebec. Sample 3—an intact block of chrysotile fibers about 5.0 cm. long with an average cross-section of 1.0 cm. from the Cassiar Mine, British Columbia.

Procedure.—The fiber samples were placed in a hygrostat maintained at the desired relative humidity with a suitable saturated salt solution.[11,12] A relative humidity value of 0% (*i.e.*, $p/p_0 = 0$) was assigned to the atmosphere in equilibrium with anhydrous magnesium perchlorate. The temperature range was 25 ± 2° during the course of the sorption experiments.

The fiber samples were removed from the hygrostat from time to time and weighed until constant weight was attained. In the middle range of p/p_0 values it often required a week or more to attain equilibrium. Each sample was run through the entire adsorption–desorption isotherm twice, and the isotherms were found to exhibit very good reproducibility.

(1) T. F. Bates, L. B. Sand and J. F. Mink, *Science*, **111**, 512 (1950).
(2) F. L. Pundsack, THIS JOURNAL, **59**, 892 (1955).
(3) F. L. Pundsack, *ibid.*, **60**, 361 (1956).
(4) E. J. W. Whittaker, *Acta Cryst.*, **7**, 827 (1954).
(5) E. J. W. Whittaker, *ibid.*, **8**, 261, 265, 571 (1955).
(6) H. Jagodzinski and S. N. Bagchi, *Neues Jahrb. Mineral. Monatsh.*, 97 (1953).
(7) H. Jagodzinski and G. Kunze, *ibid.*, 95, 113, 137 (1954).
(8) E. J. W. Whittaker, *Acta Cryst.*, **10**, 149 (1957).
(9) T. F. Bates and J. J. Comer, "Proceedings of the Sixth National Conference on Clays and Clay Minerals," Pergamon Press, New York, N. Y., 1959, pp. 237–248.
(10) E. P. Barrett, L. G. Joyner and P. P. Halenda, *J. Am. Chem. Soc.*, **73**, 373 (1951).
(11) F. E. M. O'Brien, *J. Sci. Instr. and Phys. in Ind.*, **25**, 73 (1948).
(12) A. Wexler and S. Hasegawa, *J. Research, Natl. Bur. Standards*, **53**, 19 (1954).

Results and Discussion

The water vapor adsorption–desorption data for samples 1 and 3 are shown in Fig. 1. The isotherm for sample 2 was similar to that for sample 1. The isotherms can be classified as Type IV in the BET system,[13] and they are characteristic of substances with a limited pore volume. The surface areas of the samples were calculated with the BET equation and are shown in Table I. In making the surface area calculations an area of 10.5 Å.^{2} was assigned to an adsorbed water molecule.

TABLE I

SURFACE AREAS, VOID VOLUMES AND AVERAGE PORE RADII FOR INTACT BUNDLES OF CHRYSOTILE FIBERS

Sample	Surface area, m.^{2}/g.	Void volume, cc./g.	% Void volume[a]	Av. pore radius, Å.
1. Jeffrey	18.9	0.0210	5.1	22.2
2. Jeffrey	16.8	.0218	5.3	26.0
3. Cassiar	21.3	.0158	3.9	14.8

[a] Calculated on the basis that the absolute specific volume of solid chrysotile is 0.391 cc./g.

The total volume of voids per gram of sample is also shown in Table I. This value is based on the assumption that the volume of water adsorbed at $p/p_0 = 1.0$ just fills all the void space in the sample and that to a first approximation this adsorbed water has a density of 1. The volume of voids per gram, V, and the surface area per gram, A, can be related to an average pore radius, $\bar{R}_p$, by the simple relationship shown in equation 1.

$$\bar{R}_p = 2V/A \qquad (1)$$

This expression, which is derived with the assumption that the void space exists in the form of cylindrical pores, has been shown to give fairly reliable estimates of the average pore radii in porous solids.[14] The average pore radii shown in Table I were calculated with equation 1 and they indicate that all the samples have a relatively small average pore size. This verifies the observation[3] that for the most part natural chrysotile fibers do not exist as simple hollow tubes with relatively large pores (*e.g.*, 100 to 200 Å. diameter). However, the pore sizes that are observed are not compatible with a closely-packed ribbon or lath-type of fiber either. On the other hand, the data do fit in a general way the "stuffed-tube" hypotheses which have been advanced recently.[8,9]

Although the use of equation 1 does give an indication of the order of magnitude of the pore size in the samples, a better description of the pore structure can be obtained with a pore volume distribution analysis. In general the condensation of adsorbate vapor in small capillary pores is governed by the Kelvin equation

$$\ln \frac{p}{p_0} = \frac{-2\sigma V \cos \beta}{r_k RT} \qquad (2)$$

where p/p_0 = partial pressure, σ = surface tension of adsorbate, V = molal volume of liquid adsorbate, β = contact angle, r_k = Kelvin radius of the pore, R = gas constant and T = absolute temperature. Several procedures which make use of the Kelvin equation, and in one way or another attempt to correct the Kelvin radius for the physically adsorbed layers which form the boundary of the evaporating pore, have been proposed for the analysis of pore volume distributions. A widely used procedure, particularly with nitrogen sorption data, is one described by Barrett, Joyner and Halenda.[10] A somewhat simpler procedure has been outlined by Oulton,[15] and for relatively fine-pored materials (*i.e.*, pore radius < 50 Å.) it gives results comparable to those of the BJH treatment. Therefore the Oulton approach was used to make the pore volume

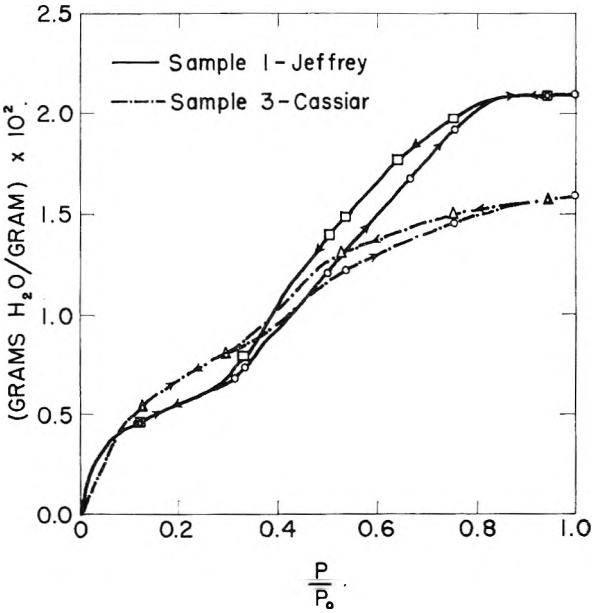

Fig. 1.—Water vapor sorption 25° on chrysotile.

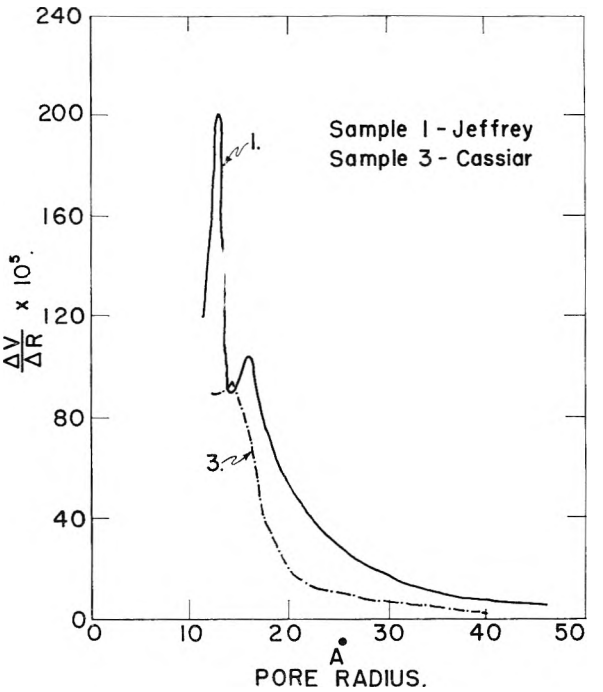

Fig. 2.—Pore volume distribution in chrysotile asbestos.

(13) S. Brunauer, "The Adsorption of Gases and Vapors," Princeton University Press, Princeton, N. J., 1943.

(14) A. Wheeler, "Catalysis," edited by P. H. Emmett, Vol. II, Reinhold Publ. Corp., New York, N. Y., 1955, p. 109.

(15) T. D. Oulton, THIS JOURNAL, **52**, 1296 (1948).

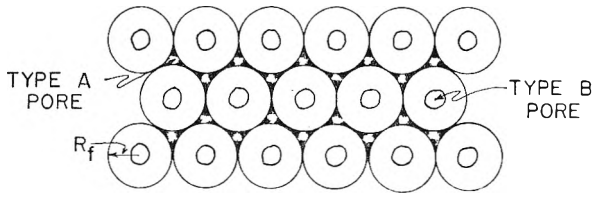

Fig. 3.—"End-on" view of cylindrical fibers in hexagonal close packing.

distribution analyses shown in Fig. 2. The analysis for sample 2 is not shown since it closely resembled the data for sample 1.

The pore volume distribution data leave no doubt but that narrow pores predominate in the three compact bundles of fiber that were examined. In all the samples more than 80% of the void volume exists in pores with radii less than 30 Å. Both Jeffrey samples give evidence of two maxima in their pore size distribution. Sample 1 has maxima at radii of 13 and 16 Å.; sample 2 has maxima at 11 and 15 Å. The Cassiar fiber has a single rather broad maximum around a pore radius of 14 Å. Since these data are based on adsorption–desorption isotherms run at only ten different p/p_0 values, the definition of two maxima in the pore size distribution of the Jeffrey samples must be considered tentative. However, the data do serve as a reliable indication of the general distribution of the pore sizes in the samples.

If a "stuffed-tube" of chrysotile, such as Bates and Comer[9] hypothesize, is considered as a cylindrical tube with a small central opening, then an end-on view of a compact bundle of such fibers in a hexagonal packing arrangement would appear as shown in Fig. 3. The dark areas in the interstices between the fibers represent serpentine-like material which, it is postulated, did not form completely into the cylindrical structure. It can be seen that this idealized structure contains two major systems of pores: the type A pores between the individual fibers, and the type B pores inside the individual fibers. The distribution of pore volume in a system such as this can be expressed in the following way. Let the outer radius of the cylindrical fibrils be R_f. Now consider a 1 cm. cube of these fibrils. From geometrical considerations it can be shown that the number of type B pores is

$$\frac{1}{4R_f^2 \cos 30^\circ} \qquad (3)$$

There are twice as many type A pores as there are type B pores. Therefore, the number of A pores is

$$\frac{1}{2R_f^2 \cos 30^\circ} \qquad (4)$$

If the radius of type A pores is R_a, and the radius of type B pores is R_b, it follows that the total pore volume, V_t, in a 1 cm. cube of the fibrils is

$$V_t = \frac{\pi R_a^2}{2R_f^2 \cos 30^\circ} + \frac{\pi R_b^2}{4R_f^2 \cos 30^\circ} = \frac{0.907\,(2R_a^2 + R_b^2)}{R_f^2} \qquad (5)$$

Now V_t is a value that is available experimentally. For example, sample 1 has $V_t = 0.051$ cc. This sample also has two maxima in the pore size distribution curve; one is at a radius of 13 Å. and the other is at a radius of 16 Å. These maxima may correspond to the average pore size in type A and type B pores. Since the sizes are so close together it does not matter much which one is called type A and which one is type B. For purposes of discussion let $R_a = 13$ and $R_b = 16$ Å. If these values, along with the experimental value for V_t of 0.051 cc., are substituted in equation 5, the value calculated for R_f, the outer radius of an individual fibril, is 103 Å. Interchanging the values of R_a and R_b would increase slightly the value of R_f to 110 Å. These values for the radius of a fibril are reasonable, and they are in fairly good agreement with fibril sizes measured by independent means and reported by other workers. For example, Bates[9] measured the size of 27 fibrils with the electron microscope and reported a mean value of 125 Å. for the outer radius. Fankuchen and Schneider[16] studied the fibril size of chrysotile samples from Canada, the United States and Italy with low angle X-ray scattering techniques and reported radii ranging from 98 to 125 Å. Whittaker[8] has also used X-ray diffraction effects to investigate the fibril size of chrysotile, and he gives a value of 130 Å. for the mean outside radius. Thus, it can be seen that the fibril size calculated from the pore volume data fall within the range of values reported on the basis of X-ray diffraction effects and electron microscope measurements. This is also true of sample 3 which has a single broad pore size maximum around 14 Å. When this pore size value is substituted for R_a and R_b in equation 5 along with the experimental V_t value for this sample of 0.039 cc., the radius of the fibril is found to be 117 Å.

The idealized model in Fig. 3 appears to be in agreement with the pore volume distribution found in bundles of chrysotile and the relatively small amount of total pore volume in the fiber bundles. The model also yields a reasonable size for the fundamental fibrils. However, it does not distinguish between the "stuffed-tube" hypotheses advanced by Whittaker[8] and by Bates and Comer.[9] These hypotheses differ essentially in that the former proposes that almost all the solid material in the fiber bundles is crystalline, and the latter suggests that a considerable amount of amorphous solid is present in the bundles. It may be possible to resolve these differences with more extensive X-ray and electron microscopy work. A technique recently developed by Rice and his co-workers[17] for the preparation of very thin cross-sections of chrysotile fiber bundles for electron microscopy work should be especially valuable in this problem.

It should be noted that the model in Fig. 3 is idealized, and in nature it would be reasonable to expect irregularity in the size of fibrils and in their packing arrangement. This is borne out, of course, by the fact that a range of pore sizes is observed experimentally. It also can be anticipated that fiber from different deposits may show some differences in average pore size and fibril size as a result of differences in the conditions under which the fibrils formed. Nevertheless, the model seems

(16) I. Fankuchen and M. Schneider, *J. Am. Chem. Soc.*, **66**, 500 (1944).

(17) M. Maser, R. V. Rice and H. P. Klug, *Am. Mineralogist*, **45**, 680 (1960).

to be a valid approximation to the morphology of chrysotile asbestos.

Acknowledgment.—Mr. George Reimschussel contributed many valuable discussions to this work, and it is a pleasure to express my appreciation for his assistance.

COMPARISONS OF ELECTROMETRIC MEASUREMENTS IN CLAY SYSTEMS[1]

By K. B. DESHPANDE AND C. E. MARSHALL

Department of Soils, University of Missouri, Columbia, Missouri

Received August 10, 1960

Measurements of salt activity, cation activity and low and high frequency conductance have been made on potassium and calcium montmorillonite (Wyoming bentonite) clay systems, using several additions of halide salts and several degrees of saturation of the clay with the cation. The detailed comparison of results by the three methods indicates, for these dilute (0.39%) clay systems, (1) that cation activity determinations are not measurably affected by potentials at the junction of the KCl bridge and the colloidal clay; (2) that cations in the diffuse part of the double layer have normal mobilities, whereas those in the Stern layer have zero mobility in d. c. conductance and normal mobility at high frequencies. Chemically adsorbed ions showing neither activity nor conductance are also present, both in potassium and calcium systems.

Three types of procedures have been used in this study: (A) Determination of salt activity in clay–water–salt systems by the cell.

Ag. AgX	Clay suspension + alkali halide	Membrane electrode reversible to cation of halide	Std. dil. halide soln.	AgX. Ag

where X = Cl^-, Br^- or I^-

(B) Determination of the cation activity by the cell:

Calomel Satd. KCl	Clay suspension + alkali halide	Membrane reversible to cation of halide	Std. halide soln.	Sat. KCl Calomel

(C) Determination of conductivity over a range of frequencies from low to high, combined in some cases with electrophoretic velocities of clay particles.

Having regard to the extensive discussion from 1951–54[2] upon the validity of Method B as affording a quantitative measure of cationic activities in colloidal systems, it was clear that a thorough comparison of a strictly thermodynamic Method A with the quasi-thermodynamic Method B and non-thermodynamic Method C was desirable.

The liquid junction potential at the tip of the saturated KCl calomel electrode is usually considered negligible for dilute electrolytes but for colloidal suspensions it was conceivable that the charge on the colloidal particles could modify the mobilities of the ions in the liquid junction and the potential might become appreciable.[3]

It appeared even in 1951 that this could not be a very important factor in clay systems because their conductivities could be approximately accounted for by using normal cationic mobilities together with cataphoretic velocities for the clay.[4] Recently, conductivities of clay suspensions have been measured by the authors[5] at various frequencies, and the low frequency values show a good agreement with those calculated from the activity of cations measured by Method B, assuming infinite dilution mobilities of cations and using measured cataphoretic velocities for clay. Also, it has been shown by Bloksma[6] that diffusion rates of cations in montmorillonite clay could best be explained by postulating mean cationic activities which were in good agreement with those obtained in our laboratory by Method B. Davis[7] made salt activity measurements in homoionic clay systems by Method A, but no interpretation in terms of single ion activities was attempted. His results when interpreted through the procedure described below indicate that the clays are only partially dissociated, in agreement with our general results by Method B.

Recently[5] variation in conductivity with frequency was used in order to give a more complete picture of the electrical double layer surrounding clay particles in suspension. Because of the reduction in relaxation effect, more cations can participate in conductance at higher frequency than at low. These additional cations were assigned to the Stern layer of physically adsorbed cations, which lies between the diffuse atmosphere of the Gouy layer and the solid surface with its fixed sites for chemical adsorption. This Stern layer does not contribute significantly to the activity as will be shown later.

In the present series, the first aspect to be considered was whether the thermodynamically sound Method A was affected by such side reactions as

$$\text{K clay} + \text{AgX} \rightleftarrows \text{KX} + \text{Ag clay}$$

in its application to clay systems.

(1) Contribution from the Missouri Agricultural Experiment Station. Journal Series No. 2176. Approved by Director. Presented in the Division of Colloid Chemistry, American Chemical Society Meeting, April, 1960.

(2) C. E. Marshall, *et al.*, *Science*, **112**, 166–67 (1950); **113**, 43 and 418 (1951); **114**, 424 (1951); **115**, 361 (1952); **117**, 686 (1953); **118**, 603 (1953); *Soil Sci. Soc. Amer. Proc.*, **15**, 106, 110 (1951); **17**, 214, 218, 221 (1953).

(3) J. Th. G. Overbeek, *J. Colloid Sci.*, **8**, 593 (1953).

(4) C. E. Marshall, *Natl. Acad. Sci. Natl. Res. Council*, **456**, 288 (1956).

(5) K. B. Deshpande and C. E. Marshall, *J. Phys. Chem.*, **63**, 1659 (1959).

(6) A. H. Blokema, *J. Colloid Sci.* **12**, 40 (1957).

(7) L. E. Davis, *Natl. Acad., Sci. Natl. Res. Council*, **395**, 290 (1955).

TABLE I

COMPARISON OF POTENTIOMETRIC RESULTS FOR ADDITIONS OF 1.30×10^{-4} MOLAR KCl, KBr AND KI, RESPECTIVELY, TO 0.3867% ACID WYOMING BENTONITE SUSPENSION TO WHICH KOH HAD BEEN ADDED.

	Clay concn. 0.3867 g./100 ml. Salt activities ($\times 10^{-4}$) Method A			Halide concn. 1.30×10^{-4} M Cation activities ($\times 10^{-4}$) Method B			
Meq. KOH per g. clay	$A_{\pm KCl}$	$A_{\pm KBr}$	$A_{\pm KI}$	$A_{K(Cl)}$	$A_{K(Br)}$	$A_{K(I)}$	$A_{K(D.Th)}$
0.13	1.90	1.85	1.87	3.33	3.33	3.50	2.78
.26	1.92	1.92	1.92	3.77	3.75	3.88	2.84
.39	2.07	1.98	2.07	4.09	3.89	4.21	3.30
.52	2.24	2.29	2.17	4.93	4.93	4.93	3.86
.65	2.69	2.70	2.69	7.23	7.32	7.27	5.56
.78	3.32	3.32	3.22	10.85	10.94	10.64	8.49

TABLE II

COMPARISON OF KCl ACTIVITIES ($A_{\pm KCl}$), K^+ ACTIVITIES (A_K), AND CALCULATED K^+ ACTIVITIES FROM DONNAN THEORY $A_{K(D.Th)}$, IN 0.3867% WYOMING BENTONITE SYSTEMS TO WHICH VARYING AMOUNTS OF KCl AND OF KOH HAD BEEN ADDED.

Meq. KOH per g. clay	KCl concn. 3.25×10^{-5} M $A_{\pm KCl}$	A_K Activities $\times 10^{-4}$ M	$A_{K(D.Th)}$	KCl concn. 6.50×10^{-5} M $A_{\pm KCl}$	A_K Activities $\times 10^{-4}$ M	$A_{K(D.Th)}$
0.13	1.41	2.74	6.14	1.42	2.87	3.10
.26	1.56	3.02	7.44	1.65	3.20	4.16
.39	1.76	3.42	9.53	1.86	3.73	5.32
.52	2.10	4.32	13.55	2.29	4.86	8.09
.65	2.66	5.68	21.68	2.62	6.96	10.53
.78	3.47	10.98	37.11	3.48	10.90	18.63

For KCl concn. 1.30×10^{-4} M see Table I, Columns 2, 5, and 8

Meq. KOH per g. clay	KCl concn. 1.625×10^{-4} M $A_{\pm KCl}$	A_K	$A_{K(D.Th)}$	KCl concn. 1.95×10^{-4} M $A_{\pm KCl}$	A_K	$A_{K(D.Th)}$
0.14	2.01	2.51	2.49	2.31	2.76	2.74
.27	2.22	2.84	3.04	2.67	3.29	3.67
.39	2.70	4.36	4.39	3.15	4.51	4.50
.54	3.04	4.78	5.67	3.38	5.77	5.79
.68	4.07	7.15	10.18	4.47	8.33	10.16
.84	4.38	11.99	12.00	5.25	12.54	12.50

In order to pass from salt activities to ion activities, non-thermodynamic assumptions must be introduced. Two simple possibilities are:

(1) The anion is negatively adsorbed by the clay and is therefore present in the most dilute parts of the systems. Its activity coefficient therefore can be taken to be nearly the same as corresponds to the concentration of the halide present. Knowing the activity of the halide, that of the cation is readily derived since $A_{Cation} \cdot A_{Halide}$ is constant throughout the system.

(2) The anion is negatively adsorbed by the clay and its activity at different distances from the clay surface can be calculated by using the modified Gouy theory as applied to plate-like particles.

The Clay Systems.—The preparation of the acid montmorillonite clay (electrodialyzed Wyoming bentonite), measurement of its exchange capacity and setting up of the "titration" using potassium hydroxide and potassium chloride, have been described previously.[5] Similar titration series were set up with calcium systems containing the same amount of clay and varying amounts of $Ca(OH)_2$ and $CaCl_2$.

Measurements.—*p*H, A_K, A_{Ca}, $A_{\pm KCl}$ and $A_{\pm CaCl_2}$ were measured in all systems as described previously.[5] The migration velocities of clay particles were measured by Engel and Pauli's method.[5,8] Conductivities were measured at various a.c. frequencies, using a decade bridge (General Radio Co.) and an oscillator (Hewlett Packard), the null point being detected with an oscilloscope.

Discussion of Results

The results obtained are given in Tables I to V. It can be seen from Table I that the measurements with different halide electrodes do not show significant differences and hence reaction of the clay with the silver halide is practically absent.

Application of the first non-thermodynamic assumption corresponds to the use of a simple Donnan system as model. It means that if the square of the mean salt activity (ion pair activity) is divided by the concentration of the halide added, the quotient should be comparable to the cation activity measured by Method B. Tables I, II, and III show that quotient $(A_{KCl})^2 C_{Cl}$ which gives the potassium ion activity through Donnan theory, and is listed as $A_{K(D.Th)}$ differs very widely from the A_{K^+} measured in the systems containing the lowest proportion of KX (3.25×10^{-5} *M*). The difference is less wide with higher halide content until in systems with halide content above 1.3×10^{-4} *M*, there is a close agreement between A_K measured and A_{K^+} thus calculated. This is true for both the K and the Ca systems (Tables IV, V). The cause of this difference lies in the negative adsorption of the chloride ion by the clay. In the systems with the most dilute halide, the negative adsorption makes a substantial change in the general halide concentration away from the surface of the colloid, raising it much above the average value. The denominator in the calculations is thereby underestimated and gives a correspondingly higher quotient for $A_{K(D.Th)}$. This is accentuated in calcium systems by the squaring of the denominator.

(8) W. Pauli and E. Valko, "Elektrochemie der Kolloide," Springer Verlag, Vienna, 1929, p. 165.

TABLE III

ACTIVITY DATA FOR ADDITIONS OF $Ca(OH_2)$ AND $CaCl_2$ TO 0.3867% WYOMING BENTONITE SUSPENSION.

Clay–$CaCl_2$ system: Clay concn. 0.3867% g. per 100 ml. Meq. $Ca(OH)_2$ per g. clay	A_{CaCl_2} × 10^{-5}	$CaCl_2$ concn. 3.25 × 10^{-5} N: A_{Ca} × 10^{-5}	$A_{Ca(D.Th)}$ × 10^{-5}
0.13	10.00	16.21	94.66
.26	8.82	11.37	64.97
.39	5.91	6.58	19.54
.52	8.37	7.01	55.50
.65	8.90	9.66	66.74
.78	11.81	13.41	97.62
$CaCl_2$ concn. 6.5 × 10^{-5} N			
0.13	12.40	16.34	45.12
.26	11.49	12.78	35.90
.39	9.76	8.39	22.00
.52	10.40	8.39	26.62
.65	11.20	10.59	33.25
.78	14.41	14.16	70.69
$CaCl_2$ concn. 1.04 × 10^{-4} N			
0.13	15.17	16.46	32.28
.26	13.95	12.99	31.61
.39	12.43	10.59	17.75
.52	13.10	10.84	20.79
.65	14.41	11.37	27.68
.78	17.20	15.08	63.45
$CaCl_2$ concn. 1.30 × 10^{-4} N			
0.13	17.40	18.81	31.17
.26	16.38	15.35	26.01
.39	13.95	12.35	16.07
.52	15.41	12.80	21.66
.65	15.69	14.25	22.86
.78	17.17	16.51	29.94
$CaCl_2$ concn. 1.625 × 10^{-4} N			
0.13	17.85	20.62	21.52
.26	16.55	17.34	17.17
.39	15.76	14.10	14.83
.52	15.98	14.40	15.45
.65	16.26	16.01	16.26
.78	17.17	18.12	19.16

TABLE IV

COMPARISON OF CONDUCTIVITIES OF CLAY SUSPENSIONS

Clay concn. 0.3867 g. per 100 ml.; KCl concn. 3.25 × 10^{-5} M

Meq. KOH added per g. clay	λ_c Calculated	λ at 60 cycles	λ_m at 10,000 cycles
0.13	3.11 × 10^{-5}	3.20 × 10^{-5}	3.95 × 10^{-5}
.26	3.29	3.34	4.53
.39	3.66	3.71	5.18
.52	4.48	4.50	6.66
.65	5.96	6.01	9.89
.78	11.46	11.51	13.88

In the systems with comparatively higher concentration of halide (1.6 × 10^{-4} molar and higher) negative adsorption does not affect the general concentration of the halide ion significantly and hence the quotient shows good agreement with the A_K measured. As is clear from Table III all these considerations apply equally well to the calcium systems. This difference between the systems with different concentrations of halides is expected since Donnan theory deals with the bulk concentrations of salts on either side of a membrane or "restraint." It does not deal with the details of the layerwise

TABLE V

DATA USED IN CALCULATING MEAN CATIONIC ACTIVITY, n_{av}, FOR COMPARISON WITH EXPERIMENTAL VALUES

A_K (CLAY CONCN. 0.3867 g. PER 100 ml.)

Meq. KOH added g. clay	$(\lambda_m - \lambda_c) = \Delta\lambda$	n_c, molar	ψ_0, volts	ψ_{ave} volts	n_{av} × 10^{-4} molar	A_K × 10^{-4}, molar
KCl concn. 3.25 × 10^{-5} M						
0.13	0.84	0.082	0.163	0.026	3.93	2.74
.26	1.24	.117	.170	.018	3.12	3.02
.39	1.52	.166	.173	.017	3.42	3.42
.52	2.18	.206	.177	.021	4.80	4.32
.65	3.93	.373	.186	.019	5.72	5.68
.78	2.42	.229	.166	.028	10.41	10.98
KCl concn. 6.50 × 10^{-5} M						
0.13	0.95	0.090	0.166	0.018	3.96	2.87
.26	1.23	.117	.169	.017	3.22	3.20
.39	1.41	.133	.169	.018	3.55	3.73
.52	1.63	.154	.167	.019	5.19	4.86
.65	4.02	.384	.187	.025	5.72	6.96
.78	4.80	.454	.185	.029	10.44	10.80
KCl concn. 1.30 × 10^{-4} M						
0.13	1.33	0.126	0.167	0.014	3.42	3.33
.26	1.42	.134	.168	.017	3.80	3.77
.39	1.53	.144	.168	.017	4.14	4.09
.52	1.72	.165	.170	.020	5.06	4.93
.65	2.98	.282	.179	.025	5.94	7.23
.78	4.39	.415	.183	.030	10.29	10.85

ionic distribution, with the effects of which one is faced in the measurement of ionic activities, using potentials developed against standard solutions.

The second non-thermodynamic assumption which can be used to correlate the results of Methods A and B, using Gouy double layer theory, requires the consideration of conductivities of suspensions at low and high frequency a.c. Table IV shows that at low frequencies (10–60 c.p.s.) the conductivity figures agree well with those obtained by adding together the conductivity due to dissociated cations (A_K) with normal mobilities, and that calculated from the electrophoretic velocity of clay particles. This indicates that the cations which are physically or chemically adsorbed by the clay contribute little to the d.c or low frequency conductivity. As has been pointed out,[5] at higher frequencies, because of reduction in relaxation effects (and probably also in electrophoretic retardation), ions from the Stern or physically adsorbed layer contribute to an increasing extent. At a sufficiently high frequency a maximum is reached and conductivity shows no further change with frequency. The concentration of cations in the Stern layer is taken as the equivalent of this maximum increase in conductivity. The number of ions necessary to give this difference in conductivity can be calculated using normal (infinite dilution) ionic mobility. The volume of the Stern layers is estimated from the surface area of the clay and the depth of the Stern layer, which is assumed to be about twice the ionic diameter, *i.e.*, about 5Å.[9] The nature of equation (1) is such that large changes in the depth of the Stern layer make relatively small changes in the calculated potential. Hence n_s, the Stern layer concentration, can be calculated.

Our results, therefore, are interpreted using three groups of cations having these properties: (1) undissociated or chemically held, no contribution to activity or conductance; (2) physically adsorbed,

Stern layer, no contribution to activity or d.c. conductance, fully contributing to conductance at 10,000 cycles; (3) ions of diffuse double layer and true solution, full contribution to activity and d.c. conductance. Using the relation

$$n_s = n_0 e^{-ze\psi/kT} \qquad (1)^{10}$$

the potential at the Stern layer is obtained. Here n_0 is the concentration of cations far away from the clay surface which is given by $A_{\pm KCl}$ measured by Method A.

The activity measured by Method B is calculated from the potential which the system develops against a standard halide solution. This potential is the arithmetic average of the potentials produced by individual concentrations at various distances from the clay particles. These concentrations in turn are related to the respective potentials at various distances from the particles. The potentials measured by Method B, therefore, give an estimate of the geometric average of the various activities, if the liquid junction potentials at saturated KCl tips of the calomel electrodes are shown to be negligible.

Now, if the potential ψ_0 at the Stern layer has been calculated according to (1) the potentials at different distances from the clay surface can be obtained with the relation[11]

$$\kappa_x = \ln \frac{(e^{ze\psi/2kT} + 1)\,(e^{ze\psi_0/2kT} - 1)}{(e^{ze\psi/2kT} - 1)\,(e^{ze\psi_0/2kT} + 1)}$$

$$\kappa^2 = \frac{8\pi n z^2 e^2}{\epsilon kT} \qquad (2)$$

The values of n_0 and ψ_0 for each system were fed into an electronic computer (Burroughs 101) and the values of potentials (ψ) at every 10Å. (x = 10, 20, 30Å., *etc.*) from the Stern layer and their average up to a distance of 50Å. where changes in ψ became very small were obtained from the machine. The concentrations n_{av} corresponding to this average ψ were calculated using the formula (1). The results are given in Table V.

Comparison of the values of n_{av} with the corresponding values of A_{K^+} obtained from Method B, shows that for the systems K clay + KCl, there is a very good agreement between the two, thus justifying the theoretical model. Hence the agreement shown by the results of the first (Donnan) approach for the upper range of halide concentrations and by those of the second assumption for the entire range of halide concentrations, provides proof that the liquid junction potentials present are negligible in these clay systems.

It is also clear from the evidence provided by conductivity determinations that the cations measured potentiometrically have normal mobilities.

It is interesting to compare potassium and calcium systems with respect to relationships between total concentration of cations, measured cationic activities and the concentrations of salt added. The concentration of exchangeable cations is about 3.0×10^{-3} for the completely saturated K systems, and 1.5×10^{-3} for the corresponding Ca systems. The K activities for the lowest and highest salt additions are, respectively, 11 and 12.5×10^{-4}; the corresponding salt additions being 3.25×10^{-5} and 1.95×10^{-4}. In the saturated calcium systems, the calcium activities for the lowest and highest salt additions are, respectively, 1.3 and 1.8×10^{-4}; the corresponding salt additions being 1.6×10^{-5} and 0.8×10^{-4}. The salt added was always a small fraction of the total exchangeable cations and in the case of the potassium systems, which were about 40% dissociated, it was also a small fraction of the mean cationic activity. In the saturated calcium systems which were only about 10% dissociated, the highest salt addition corresponded to about 44% of the total measured activity.

The measured salt activities in the potassium series are, of course, much higher than corresponds to the salt added, and lower than the potassium ion activities. In the calcium series this last relationship does not always obtain.

A remarkable feature of Table III shows itself consistently at each level of salt addition. With increasing degree of saturation with calcium the salt activities and the calcium ion activities both show minima at about 50% saturation. Decreases in divalent cation activity with increasing additions of base have been noted previously here in potentiometric titration curves of clays. The explanation seems to lie in the polyfunctional nature of clays in relation to hydrogen ions and divalent cations. The system adjusts itself to the condition of minimum free energy; this involves not only the formation of water in neutralization, but also the wide range of bonding energies for hydrogen ions as well as for calcium ions.

As regards d.c. conductivity, clearly the reductions in cationic mobility in the diffuse double layer postulated by Overbeek[3] play at most an insignificant role. The increases at moderate to high frequencies are to be expected. They are of a similar order of magnitude to those found for dilute salt solutions in a higher frequency range and it seems reasonable to identify the ions responsible for the increase with the Stern layer.

This investigation has been facilitated by a research grant from the American Petroleum Institute through which a post-doctoral fellowship (K.B.D.) was set up.

(9) E. J. W. Verwey and J. Th. G. Overbeek, "Theory of the Stability of the Lyophobic Colloids," Elsevier Pub. Co., New York, N.Y., 1948, p. 42.

(10) Key to the symbols used in formulae and tables:

A_K	Potassium ion activity (Method B)
A_{Ca}	Calcium ion activity (Method B)
$A_{\pm CaCl_2}$	Mean activity of $CaCl_2$ (Method A)
$A_{\pm KCl}$	Mean activity of KCl (Method A)
n_0	Concentration of cations remote from the clay surface
n_s	Concentration of ions in the Stern layer
ψ_s	Potential at the Stern layer
ψ	Potential at a distance x from the clay surface
z	Valency of the ion
e	Electronic charge or base for natural logarithms where applicable
k	Boltzmann constant
T	Absolute temperature
ϵ	Dielectric constant of the medium
λ_c	Specific conductivity calculated
λ_m	Measured maximum specific conductivity
κ	Reciprocal "thickness of double layer"

(11) H. R. Kruyt, *Colloid Sci.*, Vol. I, Elsevier Publ. Co., New York, N. Y., 1952, p. 130.

THE SORPTION OF WATER VAPOR BY CHARCOAL AS INFLUENCED BY SURFACE OXYGEN COMPLEXES

BY BALWANT RAI PURI, K. MURARI AND D. D. SINGH

Department of Chemistry, Panjab University, Chandigarh, India

Received February 3, 1960

A study of water sorption isotherms on charcoal coated with different amounts of variously disposed chemisorbed oxygen shows that it is the oxygen disposed as CO_2 which enhances the sorption capacity of charcoal and not the rest of the combined oxygen. The area of the hysteresis loop also increases with increase in the amount of this oxygen. An appreciable amount of water, representing about one mole per mole of CO_2, is held so firmly by charcoal that it is not desorbed even on drying to zero humidity. This enhances the hysteresis effect, which, however, persists though to a smaller extent, even on complete elimination of the combined oxygen.

The work of Lawson[1] and King and Lawson[2] shows that the presence of chemisorbed oxygen in charcoal increases the low pressure sorption of water by charcoal and shifts the isotherms to lower pressures than those corresponding to the same amount of sorption in the absence of any such oxygen. Similar results have been reported in more recent papers by Emmett,[3] Dubinin and Zaverina,[4] Healey, *et al.*,[5] Anderson and Emmett[6] and McDermot and Arnell.[7] Smith, *et al.*,[8] are of the view that the increase is due to an extensive reaction of water with oxygen complex producing a new surface complex. McDermot and Arnell[7] believe that the oxygen provides isolated active centers at which the sorption proceeds in the form of "clumps" or "clusters"[9] of water molecules which grow in size by a mechanism of hydrogen bonding until they merge, at a higher relative pressure, to fill the smaller pores. Capillary condensation occurs whenever a cluster reaches sufficient size to bridge the walls of a pore.

It appears that while the influence of chemisorbed oxygen in altering water adsorption isotherms on carbons has received a fair amount of attention, the influence of the various forms in which it is disposed or removed on degassing (*e.g.*, as CO, CO_2 and H_2O) has not been investigated. The present work, therefore, was undertaken.

Experimental

Materials.—Two samples of charcoal were prepared by the carbonization of cane sugar and coconut shells in a limited supply of air at 300° in a Pyrex glass vessel placed in a heat-lagged nichrome coil for uniform electrical heating. The current was controlled with a Variac transformer. The charcoals were transferred to wide trays and allowed to cool in air. Sugar charcoal as prepared was almost free of ash; the other sample was extracted with hydrofluoric acid to lower the ash content to about 0.14%. Several 10-g. portions of the charcoals were evacuated in a resistance tube furnace at 300, 500, 750, 1000 and 1200°. The temperature was allowed to rise gradually and before it was raised another 50° the complete elimination of the gases at the preceding temperature had been ensured. After degassing at each temperature the sample was allowed to remain and cool *in vacuo* and then transferred to a well stoppered bottle.

A few portions of the charcoals were also treated with hydrogen at 400° for different intervals of time in a rotating Pyrex tube of 3/4" bore placed in a tube furnace. Hydrogen was led over the charcoal at the rate of 2 liters per hour. The samples, after the treatment, were allowed to cool in the atmosphere of hydrogen and then transferred to stoppered bottles.

The amount of oxygen retained as well as its disposition in each sample was estimated by evacuating 2-g. portions at 1200°, by gradually raising the temperature in the same manner as described above, collecting water in calcium chloride tubes and analyzing the rest of the gases evolved in an Orsat–Lunge gas analysis apparatus in the usual way. A few of these samples were examined for total oxygen content by ultimate analysis as well. The values tallied very well with those obtained on degassing.

Water Isotherms.—Water sorption isotherms were determined at 25°.[10]

TABLE I

GASES EVOLVED ON EVACUATING AT 1200° THE VARIOUS SAMPLES OF CHARCOAL

Description of sample	Gases evolved on evacuation at 1200° CO_2 (mg./g.)	CO (mg./g.)	H_2O (mg./g.)	H_2 (mg./g.)	Total oxygen evolved (mg./g.)
Sugar charcoal					
Original	155.90	150.63	125.50	13.50	311.01
Evacuated at:					
300°	77.75	147.50	81.62	13.53	213.35
500	47.35	137.88	76.05	13.25	180.78
750	Nil	97.55	61.10	12.12	109.94
1000	Nil	5.85	Nil	1.80	3.34
1200	Nil	Nil	Nil	Nil	Nil
Coconut shell charcoal					
Original	77.18	130.15	80.50	11.15	202.06
Evacuated at:					
300°	55.27	116.51	70.93	11.10	169.79
500	25.32	109.33	59.55	11.15	133.80
750	Nil	73.06	48.52	10.55	84.87
1000	Nil	4.43	Nil	1.10	2.53
1200	Nil	Nil	Nil	Nil	Nil
Sugar charcoal treated with hydrogen at 400°					
Treated for:					
2 hr.	73.75	140.66	116.75	10.85	237.80
4	46.23	118.10	100.50	8.60	190.42
6	32.63	87.85	88.75	7.23	152.82
8	Nil	57.25	77.55	6.34	101.64
12	Nil	30.66	40.66	4.32	53.66

Discussion

It is seen (Table I) that the original samples of sugar charcoal and coconut shell charcoal contain, respectively, about 31 and 20% of combined oxygen

(1) C. G. Lawson, *Trans. Faraday Soc.*, **32**, 473 (1936).
(2) A. King and C. G. Lawson, *ibid.*, **30**, 1094 (1934).
(3) P. H. Emmett, *Chem. Revs.*, **43**, 69 (1948).
(4) M. M. Dubinin and E. D. Zaverina, *J. Phys. Chem.*, (*U.S.S.R.*), **21**, 1373 (1947).
(5) F. H. Healey, Y. F. Yu and J. J. Chessick, THIS JOURNAL, **59**, 399 (1955).
(6) R. B. Anderson and P. H. Emmett, *ibid.*, **56**, 756 (1952).
(7) H. L. McDermot and J. C. Arnell, *ibid.*, **58**, 492 (1954).
(8) R. N. Smith, C. Pierce and C. D. Joei, *ibid.*, **58**, 298 (1954).
(9) C. Pierce and R. N. Smith, *ibid.*, **54**, 784 (1950).
(10) B. R. Puri, S. N. Khanna and Y. P. Myer, *J. Sci. Ind. Res.*, **18B**, 67 (1959).

TABLE II

SORPTION–DESORPTION ISOTHERMS OF WATER VAPOR ON THE VARIOUS SAMPLES OF CHARCOAL

Desorption values are given in parentheses.

Description of sample	Amount sorbed (g./100 g.) at R.V.P. 0.00	0.09	0.18	0.28	0.38	0.48	0.68	0.89	0.996
	2	3	4	5	6	7	8	9	10
Sugar charcoal									
Original	0.00	2.61	3.82	5.26	7.50	9.72	13.21	18.70	27.55
	(6.42)	(7.50)	(10.71)	(14.15)	(14.41)	(17.00)	(17.61)	(21.92)	(27.55)
Evacuated at									
300°	0.00	1.06	2.64	4.01	4.53	6.22	9.94	12.49	19.52
	(3.47)	(4.75)	(7.01)	(10.39)	(12.41)	(13.25)	(14.42)	(15.79)	(19.52)
500	0.00	0.86	1.28	2.11	3.40	5.61	9.76	11.74	16.01
	(1.83)	(2.10)	(3.89)	(4.51)	(8.25)	(10.75)	(12.99)	(14.12)	(16.01)
750	0.00	0.78	1.22	1.81	3.19	5.52	11.00	13.78	18.50
	(0.00)	(0.78)	(1.22)	(3.75)	(7.01)	(11.76)	(15.61)	(16.05)	(18.50)
1000	0.00	0.80	1.22	1.79	2.78	5.78	11.12	13.68	18.97
	(0.00)	(0.80)	(1.22)	(2.65)	(6.50)	(12.75)	(15.35)	(17.51)	(18.97)
1200	0.00	0.81	1.21	1.79	2.90	5.96	11.52	13.70	19.01
	(0.00)	(0.81)	(1.21)	(2.25)	(5.01)	(13.35)	(15.87)	(17.11)	(19.01)
Coconut shell charcoal									
Original	0.00	0.20	4.01	4.70	5.49	6.40	8.51	9.49	12.95
	(3.25)	(4.15)	(5.80)	(7.49)	(8.78)	(9.51)	(10.05)	(10.89)	(12.95)
Evacuated at									
300°	0.00	0.75	2.02	3.21	4.89	6.52	7.74	10.29	12.50
	(1.96)	(2.21)	(2.75)	(4.05)	(5.87)	(8.10)	(11.25)	(12.01)	(12.50)
500	0.00	0.62	1.20	2.01	5.11	6.25	8.24	9.50	11.72
	(1.01)	(1.62)	(1.87)	(3.80)	(6.72)	(8.68)	(10.50)	(11.22)	(11.72)
750	0.00	0.54	1.00	1.49	4.72	7.15	9.00	10.51	12.34
	(0.00)	(0.54)	(1.00)	(5.41)	(7.37)	(8.90)	(10.52)	(11.41)	(12.34)
1000	0.00	0.55	1.01	1.50	4.81	7.20	9.02	10.00	12.10
	(0.00)	(0.55)	(1.01)	(2.75)	(6.75)	(8.78)	(11.50)	(11.92)	(12.10)
1200	0.00	0.55	1.00	1.52	4.78	7.49	9.60	10.61	12.19
	(0.00)	(0.55)	(1.00)	(3.80)	(5.59)	(9.33)	(10.65)	(11.57)	(12.19)
Sugar charcoal treated with hydrogen									
Treated for									
2 hr.	0.00	1.41	3.25	4.49	5.01	5.82	7.31	11.50	17.11
	(2.30)	(2.87)	(4.21)	(5.75)	(7.75)	(9.35)	(11.70)	(14.75)	(17.11)
4	0.00	1.25	2.75	4.15	4.90	5.71	7.10	10.39	14.23
	(1.65)	(2.50)	(5.01)	(6.49)	(7.75)	(8.65)	(10.00)	(12.25)	(14.23)
6	0.00	0.75	2.20	3.51	4.50	5.01	6.11	9.00	13.85
	(1.40)	(2.45)	(3.31)	(4.35)	(5.85)	(6.87)	(8.75)	(11.81)	(13.85)
8	0.00	0.53	1.51	2.85	4.32	4.75	6.00	8.94	12.51
	(0.00)	(0.53)	(1.51)	(2.85)	(4.85)	(6.40)	(8.50)	(10.87)	(12.51)
12	0.00	0.51	1.46	2.76	4.10	4.65	5.51	8.75	12.45
	(0.00)	(0.51)	(1.46)	(2.76)	(4.60)	(5.75)	(7.65)	(11.81)	(12.45)

which is desorbed at or below 1200° as CO, CO_2 and H_2O. When these samples are heated *in vacuo* at increasing temperatures or in hydrogen at 400° for different intervals of time, the amount of the combined oxygen decreases progressively. It is also seen that the samples degassed at 750°, or heated in hydrogen at 400° for 8 hours, retain some oxygen disposed as CO and H_2O but none as CO_2 while those degassed at 1000° retain small amounts of oxygen disposed as CO only. A glance at the table shows that all the 17 samples included therein contain different amounts of the variously disposed oxygen.

As regards water sorption isotherms (Table II) it is seen that degassing at increasing temperatures or heating with hydrogen at 400° for different intervals of time results in lowering the water sorption capacity of charcoal, particularly at lower relative vapor pressures. These alterations cannot be attributed to surface area which, for a given charcoal, has been shown to remain almost the same irrespective of the deoxygenating treatments.[7,11,12] These observations when considered in the light of those recorded in Table I show marked influence of the combined oxygen in altering the isotherms at lower relative pressures. Capillary effects appear to predominate, thereafter, in most cases. These results are in agreement with those reported by

(11) P. H. Emmett and R. B. Anderson, *J. Am. Chem. Soc.*, **67**, 1492 (1945).

(12) B. R. Puri, D. D. Singh and L. R. Sharma, THIS JOURNAL, **62**, 756 (1958).

previous workers.[5-7] But since the sorption values of the samples evacuated at 750° do not materially differ from those of the samples of the same charcoal degassed at higher temperatures and since 750° is the temperature at which the entire CO_2 complex is eliminated, it appears that it is the oxygen disposed as CO_2 and *not* the total oxygen which, apart from capillary effects, influences the water sorption capacity of charcoal. It is significant to note that when degassed at 750° sugar charcoal retains about 11% and coconut shell charcoal about 8.5% oxygen disposed as CO and H_2O yet little or no change in water sorption isotherms takes place when this oxygen is progressively eliminated on degassing at 1000 and 1200°. Similarly, although the samples of sugar charcoal treated with hydrogen for 8 and 12 hours differ appreciably from one another in their oxygen content, disposed as CO and H_2O, yet their water isotherms are almost identical. It appears, therefore, that the view of the previous workers[5-7] that the combined oxygen provides active sites for sorption of water vapor needs modification to the extent that it is the oxygen present as CO_2-complex and not the rest of it which does so.

Hysteresis.—The desorption isotherms of all the samples also were determined. The data are included in Table II. It is seen that in the original as well as in the 300 and 500° degassed samples, all of which contained CO_2-complex, the two branches do not meet even at zero pressure. In other words, the hysteresis loop persists throughout the entire range of vapor pressure. However, in the samples degassed at 750° and at higher temperatures which were completely free of oxygen disposed as CO_2, the two branches of the isotherms are seen to converge at relative vapor pressures well above zero.

Similar conclusion may be drawn from the data for the hydrogen treated samples. The two branches meet only when the CO_2-complex is completely eliminated.

The significance of these observations is that a certain amount of water sorbed by charcoal containing CO_2-complex is not desorbed even when the system is evacuated completely to constant weight at 25°. This water may be regarded as "fixed" at the charcoal surface containing CO_2-complex by some mechanism probably involving hydrogen bonding.

The CO_2-content of each charcoal and the amount of water "fixed" by it are given in Table III. It is evident that the greater the amount of CO_2-complex in a charcoal the greater is the amount of water "fixed" by it. The weights of water "fixed" per mole of CO_2 were also calculated. These values are recorded in column 4. It is interesting to note that these values correspond to the "fixation" of one mole of water per mole of CO_2. This shows that each site containing a "CO_2-complex" can hold almost one mole of water in this intimate manner.

TABLE III

AMOUNT OF WATER "FIXED" BY CHARCOAL AND AREA OF HYSTERESIS LOOP IN RELATION TO THE CO_2-CONTENT OF CHARCOAL

Description of sample	CO_2-content (g./100 g.)	Amt. of water fixed (g./100 g.)	Amt. of water fixed per mole of CO_2 (g.)	Area of hysteresis loop, squares
Sugar charcoal				
Original	15.59	6.42	18.12	1049
Evacuated at:				
300°	7.78	3.47	19.59	901
500	4.74	1.83	17.08	634
750	Nil	..	...	432
1000	Nil	..	...	428
1200	Nil	..	...	425
Coconut shell charcoal				
Original	7.72	3.25	18.37	745
Evacuated at:				
300°	5.53	1.96	15.51	498
500	2.53	1.01	17.56	443
750	Nil	..	...	360
1000	Nil	..	...	358
1200	Nil	..	...	349
Sugar charcoal treated with hydrogen at 400°				
Treated for:				
2 hr.	7.38	2.30	13.80	750
4	4.62	1.65	15.71	596
6	3.26	1.40	18.89	486
8	Nil	..	...	335
12	Nil	..	...	328

It is also seen that the area of the hysteresis loop (col. 5) decreases considerably with decrease in the CO_2-complex and that when this complex is completely desorbed, either on evacuation at 750° or on treatment with hydrogen for 8 hours, the subsequent decrease in the area is quite insignificant. Thus the magnitude of the hysteresis loop also depends much more on oxygen disposed as CO_2 than on the rest of the chemisorbed oxygen.

It may be pointed out that these results are not in accord with the observations of McDermot and Arnell[7] who on the contrary found the hysteresis loop to increase on the elimination of the combined oxygen.

It appears that the "fixation" of water on active sites presented by the CO_2-complex makes a material contribution toward hysteresis in water–carbon systems.

THE DIELECTRIC PROPERTIES OF WATER IN DIOXANE

BY A. R. TOURKY, H. A. RIZK AND Y. M. GIRGIS

The National Research Centre, Cairo, Egypt

Received March 3, 1960

The apparent solution moment of water in dioxane is 1.093 ± 0.03 *D*. The electrical anisotropy of water in dioxane tends to attain that of pure water at concentrations higher than 83 mole % of water. From polarization measurements, the coördination number in liquid water appears to be about 6, which would lead to a value of 1.86 *D* for the calculated vapor moment by Kirkwood's equation. In a mixture containing 83 mole % of water the relaxation time is about double that of pure water, and in 60 mole %, where there are six water molecules for every four dioxane molecules, the enthalpy of activation for viscous flow is nearly equal to that of water in the pure state.

Introduction

Williams[1] determined the dipole moment of water in dioxane as well as in benzene. His values of 1.9 and 1.7 *D*, respectively, were considered nearly identical so that dioxane was assumed to be just as good a solvent as usual non-polar solvents. The values 1.89, 1.90, 1.86 and 1.91 *D* also have been found by other investigators[2-5] as the dipole moment of water in dioxane. On the other hand, Åkerlöf and Short,[6] Wyman (quoted by Scatchard and Benedict[7]), and Hasted, *et al.*,[8] found that the static dielectric constant of water falls linearly and rapidly with the addition of dioxane. This phenomenon in which the molar decrement is about −7.7 at 25°, and also the lengthening of the relaxation time of water in the presence of dioxane were attributed by Hasted, *et al.*,[8] to the formation of a hydration sheath bound by a O-HO hydrogen bond.

The object of this investigation is to study, besides the determination of the dipole moment of water in dioxane, the anisotropic and the association factors, and to evaluate the relaxation time of water and the enthalpy of activation for viscous flow at different concentrations in dioxane.

Experimental

Pure dioxane and conductivity water were prepared according to recommended procedures.[9,10] The measurement of the dielectric constant, density, refractive index, viscosity, and the calculations were made as described previously.[11]

Results and Discussion

The electric moment of water in dioxane, μ_d, calculated from the average or extrapolated value of $P_{2\infty}$ (Table I) is 1.93 ± 0.03 *D*. This value is higher than the value 1.7 *D* obtained by Williams[1] using benzene as inert solvent, and also higher than the true gas moment value, μ_0, 1.84 *D*.[12,13] This indicates that in dioxane there is an additional polarization resulting from the hydrogen bonding action and contributing to the total polarization. The difference of about 0.1 *D* between the apparent solution moment of water in dioxane and the moment in the gaseous state is much smaller than the corresponding difference, 1.09 *D*, in the case of HCl.[2] This small increment in the case of water may be ascribed to its very low acid strength in comparison with that of hydrogen halides, so that its bond moment is only slightly affected by dioxane.

The electrical anisotropy, θ, of water in dioxane as calculated from the Raman-Krishnan equation[4]

TABLE I

THE DIPOLE MOMENT OF WATER IN DIOXANE

w_2	ϵ_{12}	d_{12} (g./cm.³)	n_{12-D}	p_{12} (cm.³)	p_2 (cm.³)	r_{1-D} (cm.³)
Temp. 30°						
0	2.2005	1.02229	1.4179	0.27957		
0.0087291	2.4273	1.02454	1.4174	.31467	4.30057	0.15595
.022298	2.7798	1.02548	1.4163	.36311	4.04437	.17559
.033231	3.0638	1.02553	1.4155	.39742	3.82607	.18566
.056960	3.6803	1.02682	1.4137	.45954	3.43927	.18957
.071679	4.0627	1.02752	1.4127	.49166	3.23837	.19162

$\frac{p_{12} - p_1}{w_2} = A + \gamma w_2 \quad p_{2\infty} = A + p_1$

$A = 4.13485 \quad \gamma = -16.80404$

$p_{2\infty}$ (Graph.) = 4.40 $\quad p_{2\infty}$ (Palit–Banerjee) = 4.41442

$P_{2\infty} = 79.268 \quad P_{2\infty} = 79.530$

$\bar{P}_{2\infty} = 79.399$

$r_{1-D} = \frac{\Sigma r_{1-D}\, w_2}{\Sigma w_2} = 0.18688$, $R_{1-D} = 3.37$, $_EP_2 = R_{2\infty} = 3.27$, $\mu_D = 1.93$ *D*. $\quad _DP_2 = 3.60$

Temp. 40°						
0	2.1835	1.01120	1.4129	0.27977		
0.0087291	2.3996	1.01373	1.4120	.31383	4.18147	0.16597
.022298	2.7353	1.01408	1.4110	.36140	3.94087	.18696
.033231	3.0062	1.01463	1.4102	.39493	3.74507	.19049
.056960	3.5935	1.01624	1.4098	.45627	3.37827	.19545
.071679	3.9578	1.01673	1.4082	.48828	3.18877	.20063

$A = 4.01658$, $\gamma = -15.79754$

$p_{2\infty}$ (Graph.) = 4.25, $\quad p_{2\infty}$ (Palit–Banerjee) = 4.29635

$P_{2\infty} = 76.467 \quad P_{2\infty} = 77.403$

$\bar{P}_{2\infty} = 76.985$

$r_{1-D} = 0.19429$, $R_{1-D} = 3.50$, $_EP_2 = R_{2\infty} = 3.40$, $_DP_2 = 3.74$

$\mu_D = 1.93$ *D*

Temp. 50°						
0	2.1665	1.00009	1.4080	0.27994		
0.0087291	2.3714	1.00163	1.4072	.31322	4.09244	0.14815
.022298	2.6901	1.00218	1.4061	.35957	3.85134	.18651
.033231	2.9469	1.00282	1.4055	.39245	3.66554	.18992
.056960	3.5041	1.00351	1.4052	.45336	3.32464	.19854
.071679	3.8497	1.00492	1.4036	.48478	3.13764	.19847

$A = 3.91661$, $\gamma = -15.09172$

$p_{2\infty}$ (Graph.) = 4.175, $\quad p_{2\infty}$ (Palit–Banerjee) = 4.19655

$P_{2\infty} = 75.218 \quad P_{2\infty} = 75.605$

$\bar{P}_{2\infty} = 75.411$

$r_{1-D} = 0.19347$, $R_{1-D} = 3.48$, $_EP_2 = R_{2\infty} = 3.38$, $_DP_2 = 3.72$

$\mu_D = 1.94$ *D*

(1) J. W. Williams, *J. Am. Chem. Soc.*, **52**, 1838 (1930).

(2) A. J. Weith, M. F. Hobbs and P. M. Gross, *ibid.*, **70**, 805 (1948).

(3) E. P. Linton and O. Maass, *Can. J. Res.*, **7**, 81 (1932).

(4) P. Abadie and G. Champetier, *C. r. acad. Sci.*, **200**, 1590 (1935).

(5) Y. L. Wang, *J. physik. Chem.*, **45B**, 323 (1940).

(6) G. Åkerlöf and O. A. Short, *J. Am. Chem. Soc.*, **58**, 1241 (1936).

(7) G. Scatchard and M. A. Benedict, *ibid.*, **58**, 837 (1936).

(8) J. B. Hasted, G. H. Haggis and P. Hutton, *Trans. Faraday Soc.*, **47**, 577 (1951).

(9) W. Weissberger and R. Proskauer, "Organic Solvents and Methods of Purification," Oxford at the Clarendon Press, 1935, p. 139.

(10) P. Thiessen and K. Hermann, *Z. Elektrochem.*, **43**, 66 (1937).

(11) A. R. Tourky, H. A. Rizk and Y. M. Girgis, THIS JOURNAL, **64**, 565 (1960).

(12) R. Sanger, *Physik. Z.*, **31**, 306 (1930).

(13) J. D. Stranathan, *Phys. Rev.*, **48**, 538 (1935).

(14) C. V. Raman and K. S. Krishnan, *Proc. Roy. Soc.* (*London*) **117A**, 589 (1928).

TABLE II

THE ELECTRICAL ANISOTROPY, θ, AND THE ASSOCIATION RATIO, $P_{p\infty}/P_p$, OF WATER AT DIFFERENT MOLE FRACTIONS IN DIOXANE

f_1	$\epsilon - 1/\epsilon + 2$			$\theta \times 10^{16}$			$P_{p\infty}/P_p$		
	30°	40°	50°	30°	40°	50°	30°	40°	50°
0.041288	0.32239	0.31815	0.31373	4.27	4.29	4.68	1.03	1.03	1.03
.10034	.37237	.36647	.36036	3.70	3.73	4.08	1.10	1.09	1.09
.14391	.40757	.40071	.39356	3.38	3.42	3.73	1.16	1.15	1.14
.22802	.47186	.46368	.45494	2.92	2.95	3.23	1.30	1.28	1.27
.27410	.50519	.49645	.48716	2.73	2.76	3.01	1.38	1.36	1.35
.41869	.65166	.65139	.63532	2.12	2.10	2.30	1.48	1.41	1.41
.59104	.78846	.78007	.76926	1.74	1.75	1.91	1.91	1.85	1.82
.70384	.84989	.84696	.84395	1.62	1.61	1.74	2.42	2.30	2.24
.80985	.90643	.90261	.89742	1.52	1.52	1.63	3.08	2.98	2.90
.83459	.91609	.91178	.90684	1.50	1.50	1.61	3.29	3.19	3.09
1.00000	.96190	.96014	.95830	1.43	1.43	1.53	5.48	5.35	5.19

(Table II) first decreases rapidly with increase of water concentration up till 60 mole %, and then slowly tending to attain the value for pure water at a mole per cent. higher than 83. It may be noted that at 60 mole % of water there are six water molecules for every four dioxane molecules.

The vapor moment, μ_0, in the case of water as calculated by means of the unmodified Onsager equation[15] using Wyman's data[16] of the static dielectric constant of liquid is 3.08 D at 30°, 3.07 D at 40°, and 3.05 D at 50°. Complex formation in liquid water would qualitatively account for the apparent increase in these calculated values of μ_0, as compared with the measured vapor value 1.84,[12,13] or the dilute solution values 1.7–1.9 D.[1-5] According to Kirkwood,[17] each molecule of water is surrounded by a shell of four nearest neighbors beyond which orientational effects do not extend and the H⟨O⟩H bond angle is 105°, so that the correlation parameter accounting for the hindered rotation amounts to 2.482. Hence, the calculated molecular dipole moment in water, μ, from Kirkwood's equation by the temperature-dependence method is equal to 2.66 D, and the calculated vapor moment, μ_0, is 2.12 D. The latter value evidently is nearer to the measured values in vapor or in dilute solutions than the values obtained by Onsager's equation.

As a rough measure of the association of water in dioxane at different mole fractions, Errera's ratio,[17] $P_{p\infty}/P_p$, may be used. It will be seen from Table II that above 60 mole % of water, the increase of this ratio with increase of mole fraction is greater than that at concentrations below, and that the decrease of the ratio with increasing temperature is more pronounced at higher than at lower water concentration. Although the Debye equation is of very dubious significance for a highly polar substance such as water, yet the reduction of the orientation polarization at unit mole fraction to about one-sixth of its value at infinite dilution may be taken as an indication that the hindered rotation in a spherical region surrounding a central molecule in liquid water is due to six neighboring molecules. It may be noted that in order to reconcile the longer distances of O–O and O–H, which are about 3.1 and 2.85 Å., respectively, in liquid water, as compared with the much shorter distances 2.76 and 1.01 Å., respectively, in ice,[19] with the higher density of water, Panthaleon, *et al.*,[20,21] assume that water has a coördination number higher than 4, which was formerly assumed to be present in liquid water. The coördination number pointed out by these authors is 6 with four neighbors at 2.85 Å. joined by hydrogen bonds and two other water molecules at about 3.6 Å. Accordingly, if this value 6 is taken instead of 4 as the number of neighbors which are coördinated around the central molecule in liquid water, a value of 3.223 for the correlation parameter, g, in Kirkwood's equation will be obtained. This in turn will give a value of 2.33 D for the molecular dipole moment, μ, in the liquid, and a value of 1.86 D for the gas or vapor moment, μ_0. This latter value is in satisfactory agreement with the measured vapor value.

Relaxation times calculated by means of Debye's relation[22] using molecular radii and measured viscosities are in most cases not in agreement with those obtained from dielectric loss measurements. For this reason, this equation has been considered as an inadequate representation of the relation between relaxation time, molecular radius and macroscopic viscosity of the medium, and the inadequacy has been attributed either to the departure of the assumed mechanism of orientation from the actual mechanism, or the wrong substitution of the unknown internal friction coefficient by the experimentally measured viscosity. Consequently, in our solutions the relaxation time of water as calculated from this relation, using the measured viscosity coefficients, λ (Table III), and taking the radius of water molecule[19] as 0.782×10^{-8} cm., should be regarded as only approximate. Water in the pure state has a relaxation time calculated in this way equal to 0.807×10^{-11} sec. at 30°, which seems to be in consistency with the measured value 0.83×10^{-11}

(15) L. Onsager, *J. Am. Chem. Soc.*, **58**, 1486 (1936).

(16) J. Wyman, *ibid.*, **58**, 1482 (1936).

(17) J. G. Kirkwood, *J. Chem. Phys.*, **7**, 911 (1939); *Ann. N. Y. Acad. Sci.*, **40**, 315 (1940); *Trans. Faraday Soc.*, **42A**, 7 (1946).

(18) J. Errera, "Leipziger Vorträge," 1929, p. 105.

(19) J. A. A. Ketelaar, "Chemical Constitution," Elsevier Publishing Co., Amsterdam, 1958, p. 420.

(20) V. Panthaleon, H. Mendel and W. Boog, *Disc. Faraday Soc.*, **24**, 200 (1957).

(21) V. Panthaleon, H. Mendel and J. Fahrenfort, *Nature*, **181**, 380 (1958).

(22) P. Debye, *Trans. Faraday Soc.*, **30**, 679 (1934).

sec. at 25° by Collie, *et al.*,[23] and Hasted, *et al.*[8] In any of the mixtures investigated, the relaxation time of water evidently is higher than that in the pure state, and the lengthening in the time of relaxation increases with increase of water concentration till about 80 mole %, above which the relaxation time seems to decrease. In a mixture containing 83 mole % of water (corresponding to 50 weight %) the relaxation time is nearly double that of pure water. The higher values of τ for water in the presence of dioxane relates, as previously suggested by other authors,[8,23] to the hydrogen bonding action, and may also be qualitatively accounted for by assuming that τ is proportional to η/T.

The temperature-dependence of the macroscopic viscosity at each concentration up to 83 mole % of water, is used to calculate the enthalpy of activation for viscous flow, ΔH_v, from the slope of the straight line.[24] From the data obtained (Table III) it will be seen that in a mixture containing 60 mole % of water ΔH_v is nearly equal to that in pure water, below this concentration ΔH_v is lower, and above it ΔH_v is higher than that of water in the pure state.

(23) C. H. Collie, *et al.*, *Proc. Phys. Soc.*, **60**, 145 (1948).

TABLE III

THE RELAXATION TIME, τ, AND ENTHALPY OF ACTIVATION FOR VISCOUS FLOW, ΔH_v, OF WATER AT DIFFERENT MOLE FRACTIONS IN DIOXANE

	$\eta \times 10^5$ (poise)			$\tau \times 10^{11}$ (sec.)			ΔH_v (kcal./
f_2	30°	40°	50°	30°	40°	50°	mole)
0.041288	1083	913	778	1.09	0.89	0.73	3.24
.10034	1104	919	776	1.11	0.90	.73	3.33
.14391	1128	932	812	1.13	0.91	.77	3.35
.22802	1179	975	816	1.19	0.95	.77	3.37
.27410	1215	1055	828	1.22	1.03	.78	3.42
.41869	1261	1069	888	1.27	1.04	.84	3.43
.59104	1543	1269	1063	1.55	1.24	1.01	3.70
.70384	1666	1346	1123	1.68	1.31	1.06	3.82
.80985	1687	1353	1122	1.70	1.32	1.06	3.81
.83459	1601	1278	1038	1.61	1.24	0.98	4.25
1.00000	801	656	549	0.807	0.638	0.516	3.71

(24) S. Glasstone, K. J. Laidler and H. Eyring, "Theory of Rate Processes," McGraw-Hill Book Co., Inc., New York, N. Y., 1941, chap. IX.

NITRIC OXIDE AS A RADICAL SCAVENGER IN THE RADIOLYSIS OF GASEOUS HYDROCARBONS

BY KANG YANG

Radiation Laboratory, Continental Oil Company, Ponca City, Oklahoma

Received March 25, 1960

Nitric oxide reduces energy yields of various products in the radiolysis of gaseous hydrocarbons. These yield reductions can be explained by assuming that nitric oxide scavenged thermalized radicals or that nitric oxide interfered with processes not involving thermalized radicals (such as ionic reactions). Attempts to determine what part of the nitric oxide effect must be attributed to the latter cause have not been successful so far. We have, however, found experimental evidence that as much as 10 mole % nitric oxide has a negligible effect on the product yields of the processes listed which do not involve thermalized radicals: (1) processes yielding hydrogen in the radiolysis of methane, ethylene, propylene and cyclopropane; (2) processes yielding ethylene in the radiolysis of propylene. These results show that, at least in certain situations, nitric oxide can be used to estimate unambiguously the thermalized radical contributions.

Introduction

Scavengers are often used to estimate the contribution of thermalized radical processes in the study of radiolysis mechanisms.[1] For unambiguous conclusions, one must be sure that these two conditions are satisfied: (1) The scavenger reacts with most of the thermalized radicals but has only negligible effects on the product yields of processes that do not involve radicals.[2] (2) Products from the scavenger–radical reactions have only negligible effects on the energy yields of radiolysis products.

Previously, we have used nitric oxide as a radical scavenger in the radiolysis of gaseous hydrocarbons.[1] Extensive work by Hinshelwood and his co-workers established that a sufficient concentration of nitric oxide (10 mole %) almost completely suppresses radical processes in homogeneous gas phase reactions.[3] The use of nitric oxide to elucidate reaction mechanisms in gas phase radiolysis, however, requires careful consideration.

The main difficulty is that a substantial concentration of nitric oxide (several per cent.) must be present at the beginning of an experiment. This is necessary to permit carrying the radiolysis to sufficient conversion to obtain measurable amounts of products while still maintaining a high enough concentration of nitric oxide to scavenge most radicals throughout the experiment.

Recent experimental results seem to indicate that, even with 10 mole % of nitric oxide, conditions 1 and 2 are approximately satisfied. For example, the contributions of radical processes estimated by nitric oxide inhibition data closely agree with the values estimated by isotopic methods where such comparisons are possible.[1,4–6] Another example comes from a study of the ethylene–tritium reaction initiated by β-decay of tritium.[7] There it appeared that only nitric oxide-inhibited

(1) Pertinent literature is cited in K. Yang and P. J. Manno, *J. Am. Chem. Soc.*, **81**, 3507 (1959).

(2) Here, and in what follows, the term "radicals," unmodified, will refer to thermalized free radicals. The processes that do not involve radicals include reactions of ionic and excited neutral species as well as hot atoms and hot radicals.

(3) J. Jach and C. Hinshelwood, *Proc. Roy. Soc. (London)*, **A229**, 143 (1955).

(4) L. M. Dorfman, THIS JOURNAL, **62**, 29 (1958).

(5) L. M. Dorfman, *ibid.*, **60**, 826 (1956).

(6) G. G. Meisels, W. H. Hamill and R. R. Williams, Jr., *ibid.*, **61**, 1456 (1957).

(7) K. Yang and P. L. Gant, *J. Chem. Phys.*, **31**, 1589 (1959).

reactions were affected by temperature. The proposed explanation was that in this system radicals are the only reactive species that participate in reactions involving significant activation energies. The nitric oxide suppresses the radical reactions without measurably affecting the course of reactions that do not involve radicals. Herein we report some further attempts to determine how well nitric oxide fills the requirements for a radical scavenger in the study of gas phase radiolysis mechanisms.

Experimental

Except for dosimetry, the experimental procedures were the same as those described in an earlier paper[1] to which the reader is referred for details. Phillips research grade hydrocarbons, Matheson cyclopropane (99.5%), and nitric oxide (99% min.) were subjected to bulb-to-bulb distillation in a high vacuum line. Varying mole per cent. of scavenger gases were mixed with reactant gases in Pyrex glass vessels (60 cm., 25°, 156 cc.). Gamma sources were four spent fuel elements from the Engineering Test Reactor, Arco, Idaho. Product analyses were made by gas partition chromatography.

Radiation field intensities were measured with an air-gap ionization chamber calibrated against methane radiolysis. Hydrogen in the irradiated methane was analyzed by gas–solid chromatography (silica gel, N_2 carrier, room temperature). Figure 1 shows a plot of hydrogen peak height against mole per cent. of hydrogen in methane. It is a good straight line.

The $G(H_2)$ values in the radiolysis of methane reported by different investigators differ appreciably: 5.5,[8] 5.7,[9] 6.4.[1] We found that methane, after four bulb-to-bulb distillations, each time retaining only the middle third, gave yields of hydrogen with approximately 10% average deviation. It seems likely that the greater part of the deviation comes from the presence of small amounts of impurities which could also account for the differences in the literature values; however the large deviation is not a serious problem in the present work, because all of the conclusions are based on relative yields of the products. In calibrating the ionization chamber we used the value 5.7 molecules/100 e.v. for methane radiolysis.[10]

The calibration factor α for the chamber was 17.1×10^2 e.v./amp. hr. molecule (of methane). The α is the number of electron volts that would be absorbed by one molecule of methane in one hour when the field intensity is such that it gives one amp. of saturation current in the ionization chamber. The α stayed constant within the investigated ranges of experimental variables: methane pressure, (10–90) cm.; energy absorbed, $(1.6\text{–}8.4) \times 10^{-2}$ e.v./molecule; energy input rate, $(1.0\text{–}8.0) \times 10^{-4}$ e.v./molecule hr.; and room temperature.

The energy input rate E to a reactant gas M was calculated as: $\dot{E}$ (e.v./molecule hr.) $= \alpha \dot{X} Z_M/Z_{CH_4}$. Here $\dot{X}$ is the ion chamber current in amp.; and Z_M and Z_{CH_4} are the numbers of electrons in molecules of M and molecules of methane, respectively. Values of $G(A)$, the number of molecules of a product A, formed per 100 e.v. absorbed by the system, then were calculated by dividing the rate of formation of product A in mole per cent. per hour by $\dot{E}$.

Results and Discussion

A. Side Effects from the Products of Nitric Oxide–Radical Reactions.—Experimental testing of condition 2 is relatively simple. It would be expected that, if the products from the reaction of nitric oxide with radicals affected the course of non-radical reactions, the $G(A)$ values in the presence of nitric oxide would change with increasing energy absorption. This has not been observed in any of our experiments.

(8) Result of S. C. Lind and D. C. Bardwell, *J. Am. Chem. Soc.*, **48**, 2335 (1926), calculated by F. W. Lampe (see ref. 9).

(9) F. W. Lampe, *ibid.*, **79**, 1055 (1957).

(10) Lampe's value was chosen because his data seem to show the least scattering compared with other authors.

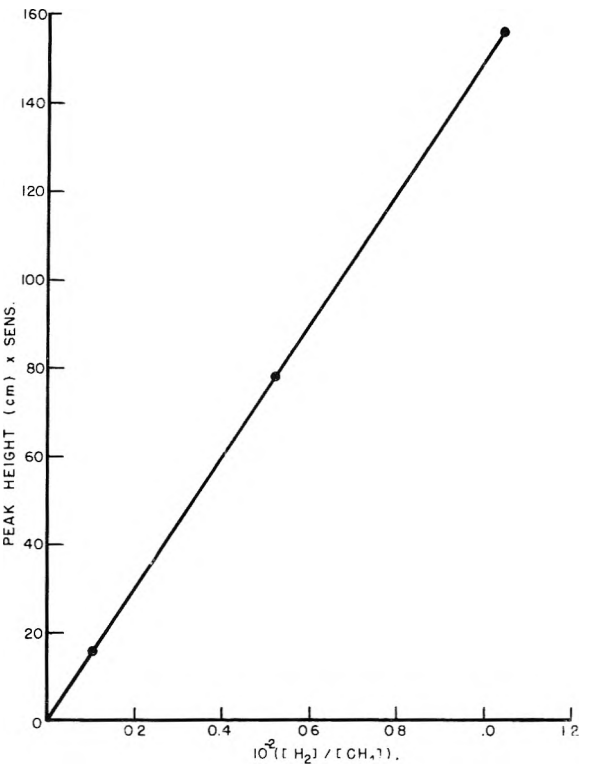

Fig. 1.—Peak height as a function of concentration in the chromatographic determination of hydrogen in methane: silica gel column, N_2 carrier, room temperature.

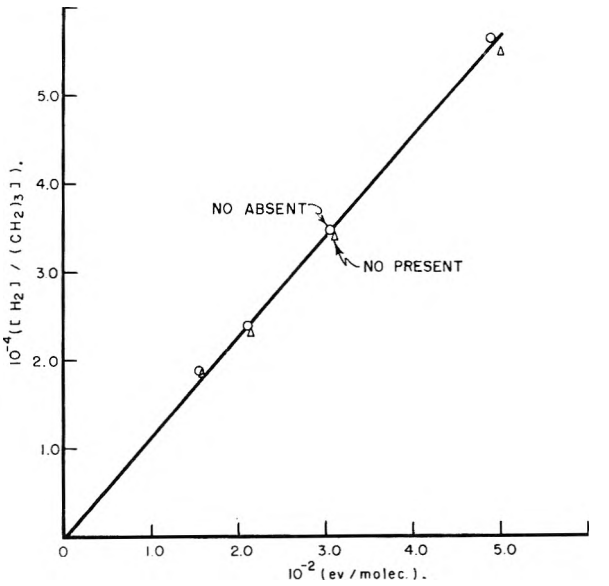

Fig. 2.—Formation of hydrogen in cyclopropane radiolysis in the presence and absence of nitric oxide (10 mole %).

Figure 2 shows the rates of formation of hydrogen in the radiolysis of cyclopropane with 10 mole % nitric oxide and without nitric oxide. The $G(H_2)$ values were 1.12 ± 0.05 and 1.16 ± 0.02, respectively.[11] Within the range of energy absorption

(11) Average deviations are shown to indicate reproducibility in the present experiments. Because of the scattering of $G(H_2)$ values in the methane dosimetry, absolute G-values for the various products could be in error by as much as 10% of the values reported here. In the present paper, the $G(A)$ values are based on the energy absorbed by the hydrocarbons alone; hence it was assumed that energy absorbed by nitric oxide did not contribute to the formation of radiolysis products.

(1.6–5.0) $\times 10^{-2}$ e.v. /molecule, $G(H_2)$ was constant in the presence and in the absence of nitric oxide.

We have also found that various $G(A)$-values in the nitric oxide inhibited radiolysis of methane, ethylene and propylene did not depend on the amount of energy absorption, (1.5–5.0) $\times 10^{-2}$ e.v./molecule.

B. Side Effects from the Reaction of Nitric Oxide with Non-radical Species.—To test for effects of nitric oxide on reactions that do not involve free radicals (condition 1), we carried out comparable experiments with other radical scavengers. We measured $G(H_2)$ in methane radiolysis with added nitric oxide, ethylene or propylene. The results are summarized in Table I.

TABLE I

THE EFFECTS OF DIFFERENT SCAVENGERS ON $G(H_2)$ IN METHANE RADIOLYSIS

Scavengers[a]			
None	Nitric oxide	Ethylene	Propylene
5.7 ± 0.6	2.8 ± 0.2[b]	2.9 ± 0.1[b]	2.8 ± 0.2[b]

[a] At a concentration of 10 mole %. [b] $G(H_2)$-values are based on the energy absorbed by methane alone. See text also.

To estimate $G(H_2)$ in the methane–olefin systems, hydrogen from the radiolysis of olefin alone was estimated under the assumption that the presence of methane did not change $G(H_2)$ in olefin radiolysis. This portion was subtracted from the total hydrogen yield. Because of the large deviation in the $G(H_2)$ value in the absence of scavengers, the estimated contribution of radical reactions to its formation ranges from 41 to 59%; however, in the presence of scavengers, the reproducibilities are reasonable, and we can conclude that the three different scavengers gave the same yield of hydrogen. A possible explanation will now be considered.

Important reactions[6] for the formation of molecular hydrogen in methane radiolysis are

$$CH_3^+ + CH_4 \longrightarrow C_2H_5^+ + H_2 \qquad (1)$$

$$CH_4^+ + CH_4 \longrightarrow CH_5^+ + CH_3 \qquad (2)$$

$$CH_5^+ + e^- \longrightarrow CH_4 + H_2 \qquad (3)$$

One of the ways in which nitric oxide could interfere with these ionic reactions is by electron capture

$$NO + NO + e^- \longrightarrow NO^- + NO \qquad (4)[12]$$

The NO^- ion thus formed then could react with the ionic species involved in reactions 1, 2 and 3. In the cases of ethylene and propylene, electron capture is not a possibility. Accordingly, the fact that the same yields of hydrogen were obtained in the presence of nitric oxide, ethylene and propylene indicates either that reaction 4 cannot compete with reaction 3 or that reaction 4 does not ultimately affect the yield of molecular hydrogen. One of these possibilities is needed to explain the results reported in the next section. In either case, however, the possibility of electron capture does not introduce any ambiguity in interpreting the results of experiments in which nitric oxide was used to measure molecular and radical yields.

(12) N. E. Bradburg, *J. Chem. Phys.*, **2**, 827 (1934).

Another way in which nitric oxide could interfere with non-radical processes would be by reacting with positive ions, for example, charge transfer

$$M^+ + NO \longrightarrow M + NO^+ \qquad (5)$$

For such possibilities, however, one would have to explain not only the fact that the same yield of hydrogen is observed in the presence of nitric oxide, ethylene and propylene, but also the experimental observations.

(a) An isotopic method using D_2 and a scavenger method using propylene gave the same molecular yield of hydrogen in the argon sensitized radiolysis of methane.[6]

(b) The molecular yields of methane in the radiolysis of ethane estimated from the results of experiments with $C_2H_6 + C_2D_6$ systems[4] agree well with nitric oxide inhibition data.[1] The proposed reaction is[4]

$$C_2H_3^+ + C_2H_6 \longrightarrow C_3H_5^+ + CH_4 \qquad (6)$$

(c) The energy yields of some products in which it is likely that ionic reactions make significant contributions are not affected by nitric oxide.[13]

If it were assumed that reactions like (5) compete with reactions 1, 2, 3 and 6, a considerable collection of coincidences would have to be invoked to provide explanations for the various cited experimental observations. It is more reasonable to conclude that nitric oxide has a negligible effect on these ion–molecule reactions.

Unfortunately, we cannot use the same method to check whether nitric oxide changed the hydrocarbon yields from non-radical processes, because ethylene and propylene are inefficient scavengers for thermalized hydrocarbon radicals.

C. Nitric Oxide-Independent $G(A)$ Values.—When nitric oxide reduces a $G(A)$-value, additional experimental evidence (such as that described in the previous section) is required to form a definite conclusion as to what kinds of reactions have been affected. If nitric oxide has no effect, however, we may conclude at once that the particular reactions involved in the formation of A are non-radical. Examples are summarized here.

The $G(H_2)$ in propylene and cyclopropane radiolysis was not affected by nitric oxide (Fig. 3). Nitric oxide also had no measurable effect on $G(CH_2{=}CH_2)$ ($\simeq$0.8) in propylene radiolysis and $G(H_2)$ in ethylene radiolysis.[14] It can be concluded that thermalized radical contributions to the formation of these products are nearly zero. Supporting evidence is found in work with the $C_2H_4 + C_2D_4$ system showing that the formation of hydrogen in the radiolysis of ethylene does not involve radical reactions.[15]

D. Formation of Unsaturated Hydrocarbons in the Presence of Nitric Oxide.—Previously[1] we reported that nitric oxide decreases $G(A)$ for saturated products but increases the values for unsaturated products in the radiolysis of hydrocarbons. A probable explanation is that the removal of unsaturated products by radical attack

(13) See Section (C) of this paper.

(14) K. Yang and P. J. Manno, THIS JOURNAL, **63**, 752 (1959).

(15) M. C. Sauer, Jr., and L. M. Dorfman, paper presented at the ACS Meeting at Cleveland, Ohio, 1960.

is inhibited by nitric oxide. Clear experimental evidence supporting this view was found.

Figure 4 shows the rate of formation of ethylene in the γ-radiolysis of cyclopropane. Without nitric oxide, $[CH_2{=}CH_2]$ seems to reach a steady-state value; but when nitric oxide is present, $[CH_2{=}CH_2]$ increases linearly with increasing energy absorption.[16] In the presence of nitric oxide $G(CH_2{=}CH_2)$ is 3.8.

Figure 5 shows the rate of formation of ethane in the nitric oxide-free radiolysis of cyclopropane. It suggests that ethane is a secondary product derived from the radiolysis product, presumably ethylene. With added nitric oxide, $G(C_2H_6) \simeq 0$.

Probable reactions yielding ethylene are

$$(CH_2)_3 \text{---}\sim\!\!\rightarrow (CH_2)_3^+ \qquad (7)$$

$$(CH_2)_3^+ + (CH_2)_3 \longrightarrow (CH_2)_3{}^+H + C_3H_5 \qquad (8)[17]$$

$$(CH_2)_3H^+ \longrightarrow CH_3^+ + CH_2{=}CH_2 \qquad (9)[18]$$

In connection with reaction 8, it is noteworthy that the most abundant ion in cyclopropane mass spectra is the parent ion.[19] In the absence of nitric oxide, ethylene formed in reaction 9 would be removed by radical reactions.

Conclusion

It has been shown that nitric oxide, at concentrations high enough (10 mole %) to suppress reactions involving thermalized free radicals in the radiolysis of various hydrocarbons, does not significantly affect the product yields of many non-radical processes; thus the presence of nitric oxide does not change the yields of hydrogen or ethylene in the radiolysis of propylene. It does not change the yields of hydrogen in the radiolysis of ethylene or cyclopropane, and its effect on the yield of hydrogen in methane radiolysis can be ascribed entirely to suppression of the reactions of thermalized free radicals. In fact in all of the gas phase hydrocarbon radiolysis systems investigated so far where a reasonable test has been possible, no evidence has appeared to indicate that nitric oxide changed the molecular yields of various products.

Acknowledgments.—Mr. J. D. Reedy helped with the experiments. Dr. F. H. Dickey of Continental Oil Company and Dr. M. C. Sauer, Jr., of the Argonne National Laboratory offered valuable suggestions for the preparation of the manuscript.

(16) Similar results were obtained in the cyclopropane–tritium reaction: P. L. Gant and K. Yang, *J. Chem. Phys.*, **32**, 1757 (1960).

(17) The general occurrence of ion–molecule reactions of the hydride-ion transfer type has been reported by F. H. Field and F. W. Lampe, *J. Am. Chem. Soc.*, **80**, 5587 (1958).

(18) P. N. Rylander and S. Meyerson, *ibid.*, **78**, 5799 (1956).

(19) "Catalog of Mass Spectral Data," A.P.I. Project 44, Carnegie Institute of Technology, Pittsburgh, Series No. 115.

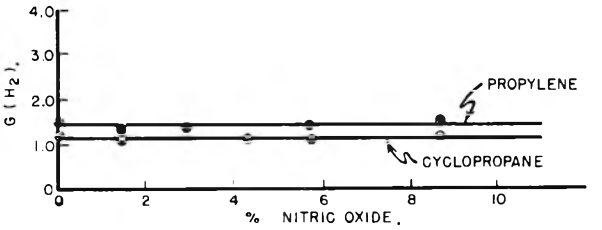

Fig. 3.—Formation of hydrogen in the radiolysis of C_3-hydrocarbons as a function of nitric oxide concentration.

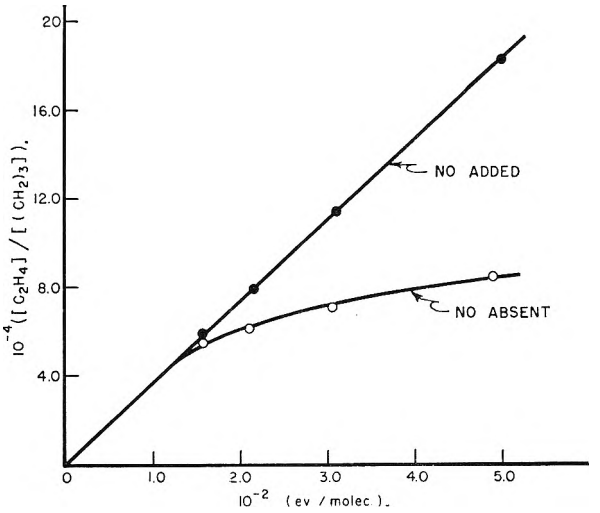

Fig. 4.—Formation of ethylene in cyclopropane radiolysis in the presence and absence of nitric oxide (10 mole %).

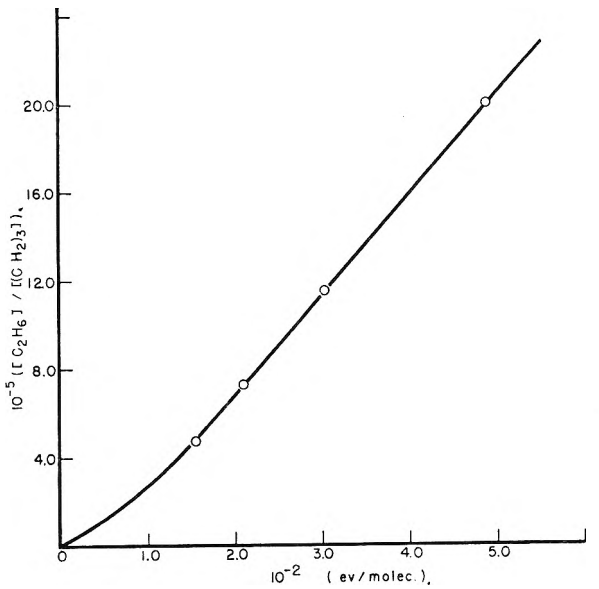

Fig. 5.—Formation of ethane in the scavenger-free radiolysis of cyclopropane: with added nitric oxide, $G(C_2H_6) = 0$.

DIFFUSION CONTROLLED GROWTH OF A MOVING SPHERE. THE KINETICS OF CRYSTAL GROWTH IN POTASSIUM PERCHLORATE PRECIPITATION

BY ARNE E. NIELSEN

Universitetets fysisk-kemiske institut, Copenhagen, Denmark

Received April 22, 1960

The crystals of potassium perchlorate precipitating from aqueous solution were found to grow with a higher velocity than calculated for pure diffusional rate control. This effect is explained by the convection around the falling crystals, which keeps the concentration near the crystals higher than diffusion alone.

Experimental

The supersaturated aqueous solution was prepared by mixing 50 ml. of 0.5 *M* KCl and 50 ml. of 0.5 *M* $NaClO_4$. The mixture was stirred continuously during the experiment. The electric conductance was followed by means of a Philips Recording Conductance Bridge. The readings were converted into the degree of advancement $\alpha = (c_0 - c)/(c_0 - s)$ (where c = concentration of dissolved $KClO_4$, $c_0 = c$ at $t = 0$, s = solubility of $KClO_4$) by means of the results from measurements on solutions having the compositions corresponding to different known values of α. The particle size at the end of the experiment was determined by sedimentation in a mixture of glycerol and water, saturated with $KClO_4$. The weight of the sediment was recorded and, from the relation between weight and time, the weight distribution curve was obtained by differentiation according to Odén.[1] In the following the weight average radius of the crystals (assumed spherical) is used. Since the distribution is rather sharp, the different kinds of average differ only by a few per cent.

The crystals have a rather compact shape so that it will not lead to great errors to treat them as spheres in the calculations of the present work.

Results

In Fig. 1 is shown the degree of advancement α as function of time t. In a previous work[2] it was shown that, in case of pure diffusional rate control the relation between α and t is given by

$$t = K_D I_D$$

where

$$K_D = a_1^2/3vD(c_0 - s)$$

$$I_D = \int_0^\alpha \alpha^{-1/3}(1 - \alpha)^{-1}\mathrm{d}\alpha$$

a_1 = radius at $\alpha = 1$; v = molar volume of precipitate, D = diffusion coefficient, c_0 = initial concentration and s = solubility. I_D is a function of α which has been tabulated.[2] We insert $a_1 = 4.64 \times 10^{-3}$ cm. as found from the sedimentation analysis, $v = 55.0$ cm.^{3}/mole, $c_0 = 2.5 \times 10^{-4}$ mole/cm.^{3}, $s = 1.58 \times 10^{-4}$ mole/cm.^{3}, determined from the final value of the conductivity in the kinetic experiment and $D = 1.61 \times 10^{-5}$ cm.^{2}/sec. (From ionic equivalent conductivities we find $D = 1.88 \times 10^{-5}$ cm.^{2}/sec.; this is corrected to ionic strength 0.5 by means of the factor $1 - 0.5864\sqrt{I}/(1 + \sqrt{I})^2 = 0.858$). This gives $K_D = 88$ sec., and the corresponding curve, $t = 88 I_D(\alpha)$, is shown on Fig. 1.

Discussion

It is clear from this that the crystals have grown faster than possible if the solute can reach the surface of the growing crystals only by diffusion—no matter what is the type of reaction in the surface transferring it from the dissolved to the crystalline state. The only possible explanation is that convection is also contributing to the transport from the bulk of the solution to the crystal.

Mathematical.—The expression quoted for K_D was derived[2] using an approximation, since the concentration gradient at the surface was calculated from the stationary solution of Fick's second law. But when the particles grow it must be a little larger. In order to be sure whether this gives any appreciable contribution to the increased growth rate observed we shall first consider the case of purely diffusional growth. Later on we shall treat the combined diffusion-convection-control of the rate of particle growth.

1. Purely Diffusional Growth of a Sphere.—The diffusion process follows Fick's second law and since the case is spherically symmetric this law can be written, assuming D independent of c

$$\frac{\partial c}{\partial t} = D\left[\frac{\partial^2 c}{\partial r^2} + \frac{2}{r}\frac{\partial c}{\partial r}\right]$$

where c = concentration and r = radius vector. With a = radius of the particle and s = solubility the boundary conditions are

$$c(r,0) = c_\infty;\ c(a,t) = s;\ c(\infty,t) = c_\infty$$

If a and c_∞ are constant the solution is easily obtained by standard methods (*e.g.*, through the Laplace transformation)

$$c = s + (c_\infty - s)\left[1 - \frac{a}{r}\left(1 - \operatorname{erf}\frac{r - a}{\sqrt{2Dt}}\right)\right]$$

where

$$\operatorname{erf} x \equiv \frac{2}{\sqrt{\pi}}\int_0^x \exp(-\xi^2)\mathrm{d}\xi$$

There is a non-trivial stationary solution (this is not true for the analogous one- or two-dimensional cases) obtained for $t \to \infty$

$$c = s + (c_\infty - s)(1 - a/r)$$

The rate of growth must satisfy

$$\mathrm{d}a/\mathrm{d}t = vD(\mathrm{d}c/\mathrm{d}r)_{r=a}$$

and if the stationary value of $\mathrm{d}c/\mathrm{d}r$ is used, we get

$$\mathrm{d}a/\mathrm{d}t = vD(c_\infty - s)/a$$

$$\therefore a = \sqrt{2vD(c_\infty - s)t}$$

This is valid at low concentration only. At high concentration the growth may be so fast that the stationary concentration field cannot be established with sufficient accuracy. We shall therefore derive the exact solution to Fick's second law for a growing sphere.

(1) S. Odén, *Kolloid-Z.*, **18**, 33 (1916).

(2) A. E. Nielsen, *Acta Chem. Scand.*, **13**, 784, 1680 (1959).

The radius a is initially zero. Since no geometric parameter is fixed in advance, the function $c(r, t_I)$ at any time t_I is derived from $c(r,t_{II})$ valid at any other time simply by multiplying all the radii by a common factor. This means that if

$$c(r_1,t_I) = c(r_2,t_{II})$$

and

$$c(r_3,t_I) = c(r_4,t_{II})$$

then

$$\frac{r_1}{r_2} = \frac{r_3}{r_4} = \frac{a_I}{a_{II}}$$

Therefore $c = c(z)$; $z = a/r$; $a = a(t)$.

Inserting this in Fick's second law we get

$$\frac{dc}{dz}\frac{da}{dt} = \frac{Da^2}{r^3}\frac{d^2c}{dz^2}$$

or

$$\frac{a}{D}\frac{da}{dt} = z^3\frac{d^2c/dz^2}{dc/dz}$$

Since

$$\frac{da}{dt} = vD\left(\frac{\partial c}{\partial r}\right)_{r=a} = -\frac{vD}{a}\left(\frac{dc}{dz}\right)_{z=1}$$

we have

$$\frac{a}{D}\frac{da}{dt} = -v\left(\frac{dc}{dz}\right)_{z=1} = K, \text{ a constant} > 0$$

and

$$z^3\frac{d^2c/dz^2}{dc/dz} = K$$

The general solution of this differential equation is

$$c = K_1\left[z\exp\left(-\frac{K}{2z^2}\right) + \sqrt{\frac{K\pi}{2}}\operatorname{erf}\left(\frac{1}{z}\sqrt{\frac{K}{2}}\right)\right] + K_2$$

The arbitrary constants K_1 and K_2 are eliminated by means of the two boundary conditions for $z = 1$

$$c = s, \; dc/dz = -K/v$$

which gives

$$c = s + \frac{K}{v}\left[1 - \frac{a}{r}\exp\left(\frac{K}{2}\left(1 - \frac{r^2}{a^2}\right)\right) - \sqrt{\frac{K\pi}{2}}\left[\operatorname{erf}\left(\frac{r}{a}\sqrt{\frac{K}{2}}\right) - \operatorname{erf}\sqrt{\frac{K}{2}}\right]\exp\left(\frac{K}{2}\right)\right]$$

From the third boundary condition

$$c = c_\infty \text{ for } r = \infty$$

follows

$$v(c_\infty - s) = K\left[1 - \sqrt{\frac{K\pi}{2}}\left(1 - \operatorname{erf}\sqrt{\frac{K}{2}}\right)\exp\left(\frac{K}{2}\right)\right]$$

In the limit $K \to 0$ we find

$$\frac{v(c_\infty - s)}{K} \longrightarrow 1$$

which reproduces the formula

$$a = \sqrt{2Dv(c_\infty - s)t}$$

found by means of the stationary solution to Fick's second law. If we write the exact solution

$$a = \sqrt{2Dv(c_\infty - s)t/q}$$

defining the quantity q by this equation, we may determine the relation between q and $v(c_\infty - s)$ by means of the equations

$$q = 1 - \sqrt{\frac{K\pi}{2}}\left(1 - \operatorname{erf}\sqrt{\frac{K}{2}}\right)\exp\left(\frac{K}{2}\right)$$

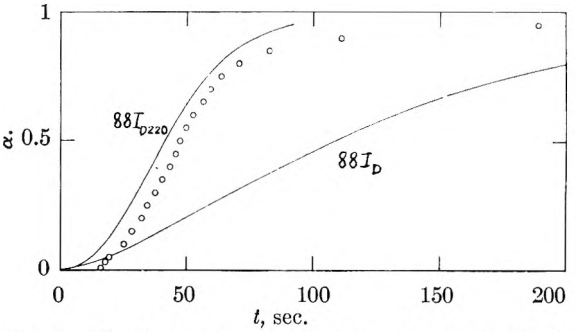

Fig. 1.—The degree of reaction as function of time during the precipitation of potassium perchlorate from supersaturated aqueous solution. "$88I_D$," theoretical curve, assuming that only diffusion is controlling the rate of growth; "$88I_{D220}$," theoretical curve, assuming that both diffusion and convection are controlling the rate of growth; circles, experimental points. The coefficients in the theoretical curves were calculated from the particle size, measured independently.

$$Kq = v(c_\infty - s)$$

Table I gives numerical examples of this relationship.

TABLE I

$v(c_\infty - s)$	q	$v(c_\infty - s)$	q
0.00001	0.996	0.05	0.730
.00002	.994	.1	.626
.00005	.991	.2	.485
.0001	.987	.3	.382
.0002	.982	.4	.300
.0005	.972	.5	.232
.001	.960	.6	.172
.002	.944	.7	.120
.005	.912	.8	.073
.01	.877	.9	.034
.02	.827	1.0	.000

We see that the approximation made when using the stationary concentration gradient is good when $v(c_\infty - s)$ is small. This entity is the ratio between the supersaturation $c_\infty - s$ and the concentration of the matter in the precipitated state, $1/v$. It is also the volume of precipitate originating from a unit volume of the solution. When $v(c_\infty - s) = 1$ the transition from the dissolved to the precipitated state does not require any transport through space, and (neglecting latent heat of phase change, etc.) may proceed infinitely fast.

In the experiments reported above $v = 55.0$ ml./mole, $c_0 = 2.5 \times 10^{-4}$ and $s = 1.6 \times 10^{-4}$ mole/ml., so that in the beginning of the experiment $v(c_\infty - s) = 0.005$, $q = 0.904$. The spheres will thus reach a certain size in 90.4% of the time they would require if the concentration field were of the "stationary" type. Since it will complicate later calculations to take into account the change of q with concentration we shall in the following always assume $q = 1$. The error will not invalidate the conclusions concerning the cause of the great velocity of growth of the particles.

2. **Convection.**—According to Stokes[3] the velocity field in the space around a sphere of radius a falling through the liquid with the velocity U satisfies

(3) G. G. Stokes, *Trans. Cambridge Phil. Soc.*, **9**, 8 (1850), reprinted in "Mathematical and Physical Papers," by G. G. Stokes, Vol. 3, 1, Cambridge Univ. Press, 1901, see pp. 55 ff.

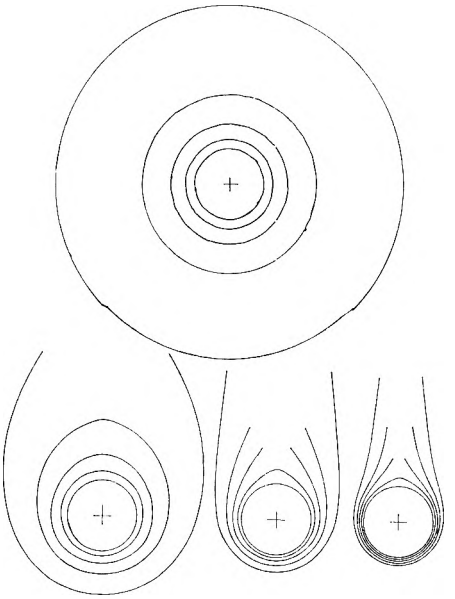

Fig. 2.—Sections of surfaces of equal concentration (z = 0, 0.2, 0.4, 0.6 and 0.8) at different velocities (A = 0, 1, 10 and 100) around a sphere growing with a rate controlled by diffusion and convection whilst falling through the liquid.

$$u_r = U\cos\theta\left[1 - \frac{3}{2}\frac{a}{r} + \frac{1}{2}\left(\frac{a}{r}\right)^3\right]$$

$$u_\theta = -U\sin\theta\left[1 - \frac{3}{4}\frac{a}{r} - \frac{1}{4}\left(\frac{a}{r}\right)^3\right]$$

$$u_\varphi = 0$$

where u_r, u_θ and u_φ are the components in the coordinate directions of the velocity relative to the sphere, r being radius vector (from the center of the sphere), θ the colatitude and φ the longitude; $\theta = 0$ when r points vertically upwards.

These equations describe the velocity fields for Reynold's numbers

$$R \equiv 2aUd/\eta$$

up to about 8. For < 8.15 eddies do not occur.[4] For $R \ll 1$ the force on the sphere caused by the motion through the liquid is given by Stokes' law

$$\text{force} = 6\pi\eta aU$$

When this force equals the pull exerted by gravity

$$6\pi\eta aU = \frac{4}{3}\pi a^3(d - d_0)g$$

the sphere falls with constant velocity, and we derive

$$R = 4a^3gd_0(d - d_0)/9\eta^2$$

In our experiment with $KClO_4$ we had $a_1 = 4.6 \times 10^{-3}$ cm., $d_0 = 1.02$, $d = 2.52$, $\eta = 0.009$, $g = 981$

$$R = 0.81$$

The error introduced by the application of Stokes' law at such large values of R is commented on below.

The vector with the components u_r, u_θ and u_φ (= 0) given above is the flow of liquid volume per unit of area and time. Multiplying it by the concentration we get the flow of matter caused by the convection. Since the flow of matter arising from diffusion is $-D$ grad c we have the total flow of matter

$$\vec{J} = -D\,\text{grad}\,c + c\vec{u}$$

The rate of change of the concentration is given by

$$dc/dt = -\text{div}\,\vec{J} = \text{div}[D\,\text{grad}\,c - c\vec{u}]$$

Neglecting the compressibility and the partial volume of the solute we may use

$$\text{div}\,\vec{u} = 0$$

With a constant D we therefore derive

$$dc/dt = D\,\text{div grad}\,c - \vec{u}\,\text{grad}\,c$$

Introducing the Stokes velocity field we finally get

$$\frac{\partial c}{dt} = D\left[\frac{\partial^2 c}{\partial r^2} + \frac{1}{r^2}\frac{\partial^2 c}{\partial\theta^2}\right] + \left[\frac{2D}{r} + U\left(1 - \frac{3}{2}\frac{a}{r} + \frac{1}{2}\left(\frac{a}{r}\right)^3\right)\cos\theta\right]\frac{\partial c}{\partial r} + \left[\frac{D}{r^2}\cot\theta - \frac{U}{r}\left(1 - \frac{3}{4}\frac{a}{r} - \frac{1}{4}\left(\frac{a}{r}\right)^3\right)\sin\theta\right]\frac{\partial c}{\partial\theta}$$

$c = c(r, \theta, t)$; $c(r, \theta, 0) = c_\infty$; $c(a, \theta, t) = s$; $c(\infty, \theta, t) = c_\infty$. Since we need only the stationary solution we let the left-hand side be zero. Introduction of the dimensionless constant

$$A \equiv aU/D$$

the dimensionless variables

$$\rho = \ln(r/a),\ \zeta = (c - s)/c_\infty$$

and the two functions of ρ

$$\Psi_1 = e^\rho - \frac{3}{2} + \frac{1}{2}e^{-2\rho}$$

$$\Psi_2 = e^\rho - \frac{3}{4} - \frac{1}{4}e^{-2\rho}$$

transforms the equation into

$$\frac{\partial^2\zeta}{\partial\rho^2} + \frac{\partial^2\zeta}{\partial\theta^2} + (1 + A\Psi_1\cos\theta)\frac{\partial\zeta}{\partial\theta} + (\cot\theta - A\Psi_2\sin\theta)\frac{\partial\zeta}{\partial\theta} = 0$$

where $\zeta = \zeta(\rho, \theta)$; $0 \le \rho \le \infty$; $0 \le \theta \le \pi$; $\zeta(0, \theta) = 0$; $\zeta(\infty, \theta) = 1$. A is closely related to Reynolds number

$$A = R\eta/2Dd_0$$

For $KClO_4$ in water at 25°

$$A \cong 270R$$

If the approximations made are regarded good for $R < ca.$ 1 we may as well use the formulae for $A <$ $ca.$ 300.

The equation was solved numerically by relaxation, and some of the results are shown in Fig. 2.

In the case of pure diffusion the total rate of increase of volume is

$$dV/dt = 4\pi a^2 Dv(dc/dr)_{r=a} = 4\pi aDv(c_\infty - s)$$

When also convection is influencing the concentration we write

$$dV/dt = 4\pi aDv(c_\infty - s)F$$

F can be found by integrating the normal component of the flux over a sphere concentric with the growing particle.

$$dV/dt = v\int_S (c\vec{u} - D\,\text{grad}\,c)dS = -v\int_S (cu_i - D\partial c/\partial r)dS$$

$$= -v\int_S (c_\infty U\cos\theta\,\Psi_1\,a/r - D(a/r^2)\partial c/\partial(a/r))dS$$

(4) H. Nisi and A. W. Porter, *Phil. Mag.*, [6] **46**, 754 (1923).

$$F = -\frac{r}{2a}\left[A\Psi_1\int_0^\pi \cos\theta\sin\theta\,d\theta + \int_0^\pi \sin\theta(\partial\xi/\partial\rho)d\theta\right]$$

By calculating F for different values of r a control is obtained of the consistency of the solution. This was tried in several cases and the agreement found to be better than 2%.

The results of these calculations are given in Table II together with $(1 + A)^{0.285}$. This expression was found empirically to agree within the accuracy with F-values found by solving the differential equation and is convenient for interpolation.

TABLE II

A	F	$(1 + A)^{0.285}$
0	1.00	1.00
1	1.21	1.22
3	1.47	1.48
10	2.02	1.98
30	2.62	2.66
100	3.72	3.73

Frisch[5] treated a similar problem "The steady-state diffusion into a streaming sphere at low Reynolds number." But he assumes that $c(r, 0) = c(r, \pi)$. The reason for this is not clear and turns the problem into another one than ours. In order to compare the results we may insert $\lambda R >> 1$ in Frisch's formula (14b), which gives, with our symbols

$$F = 1 + \frac{731}{1152}\left(1 + \frac{5\sqrt{2}}{8}\right)A^2 + \ldots \cong 1 + 1.195A^2 + \ldots$$

whereas the result of the present work can be written

$$F = (1 + A)^{0.285} \cong 1 + 0.285A - 0.1019A^2 + - \ldots$$

These two expressions do not agree, not even approximately.

Chronomals.—We are now able to find how the degree of advancement must change with time when both diffusion and convection carry matter to the growing particles during precipitation. As the particles grow, a and therefore A change. Now a^3 is proportional to α, and so we can write

$$A = R\eta/2Dd_0 = 2a^3g\Delta d/9D\eta = \alpha C$$

where

$$C = 2a_1^3g\Delta d/9D\eta$$

a_1 = radius of the particles when $\alpha = 1$

In the following we shall no longer consider the local variations of c in the solution and will therefore drop the subscript ∞ on c.

The growth follows

$$dV/dt = 4\pi aDv(c - s)F$$

$$d\alpha/dt = -(c_0 - s)^{-1}dc/dt = N(c_0 - s)^{-1}v^{-1}dV/dt$$

$$= N4\pi a_1D\alpha^{1/3}(1 - \alpha)F(\alpha)$$

$$\therefore t = K_D I_{DC}$$

where

$$K_D = 1/4\pi a_1ND$$

$$I_{DC} = \int_0^\alpha \frac{d\alpha}{\alpha^{1/3}(1 - \alpha)F(\alpha)}$$

N = number of particles per unit of volume

Since $(c_0 - s)v = N(4/3)\pi a_1^3$ we may also write

$$K_D = a_1^2/3(c_0 - s)Dv$$

Using $F = (1+A)^{0.285}$, $A = \alpha C$ it is possible to calculate I_{DC} as a function of α by numerical integration for any fixed value of C. The results of such calculations are given in Table III.

TABLE III

α	I_D	I_{D1}	I_{D2}	I_{D10}	I_{D30}	I_{D100}	I_{D300}
0.003	0.03	0.03	0.03	0.03	0.03	0.03	0.03
.01	.07	.07	.07	.07	.07	.06	.06
.03	.15	.15	.15	.14	.13	.12	.10
.05	.21	.21	.20	.20	.18	.16	.13
.10	.34	.33	.33	.31	.28	.23	.18
.15	.45	.44	.43	.40	.35	.28	.22
.20	.56	.55	.53	.48	.41	.33	.26
.25	.67	.65	.62	.56	.47	.37	.29
.30	.77	.75	.71	.63	.53	.41	.32
.35	.88	.85	.80	.70	.58	.45	.35
.40	.99	.95	.88	.77	.64	.49	.38
.45	1.11	1.05	.97	.84	.69	.53	.41
.50	1.23	1.16	1.06	0.91	.74	.57	.44
.55	1.36	1.27	1.17	0.99	.80	.61	.47
.60	1.50	1.40	1.28	1.08	.87	.66	.50
.65	1.66	1.54	1.40	1.17	.94	.71	.54
.70	1.83	1.69	1.52	1.26	1.01	.76	.57
.75	2.04	1.86	1.67	1.37	1.09	.82	.62
.80	2.28	2.07	1.84	1.50	1.19	.88	.66
.85	2.59	2.33	2.05	1.67	1.31	.96	.72
.90	3.01	2.68	2.35	1.88	1.46	1.09	.81
.95	3.72	3.27	2.83	2.24	1.72	1.28	.95

In using Stokes' law an error is introduced since this law is only valid in the limit $R \ll 1$. At $R = 1$ the error in calculating the force from Stokes' law is about 10%.[6] Since the force is almost proportional to R, and A as well, and since $F = (1 + A)^{0.285}$ we find the error on F to be about 3% at $R = 1$. Since the relative error is proportional to R, which during the experiment rises almost proportionally with α until $R = 0.8$ we see that the error introduced with Stokes' law is about 1%, which is negligible.

In the reported experiment on $KClO_4$ we find from the value of a_1, determined by sedimentation analysis, $C = 220$, $K_D = 88$ sec. The corresponding curve $t = K_D I_{DC}(\alpha)$ is shown on Fig. 1. We see that the experimental and the calculated curves have the same shape, but the experimental curve seems to "start" about 7 seconds later. This may be caused by ineffectiveness of the mixing process, or by an induction period in which the crystals are nucleated, or if a mechanism different from diffusion is rate determining. As soon as the crystals have reached a certain very small size they grow according to the theory developed in the present paper.

For $\alpha > 0.80$ the crystals grow more slowly than predicted by the theory. This effect has not been investigated further for $KClO_4$, but a possible explanation is that at these low concentrations the rate is also influenced by the surface reaction transforming the dissolved matter into the crystalline state, as was found with $BaSO_4$.[2]

(5) H. L. Frisch, *J. Chem. Phys.*, **22**, 123 (1954).

(6) See for instance: L. Schiller, *Handbuch der Experimentalphysik* **4.2**, 337 (1932).

THE CONFIGURATION OF THE TETRACHLOROCUPRATE(II) ION

BY B. MOROSIN AND E. C. LINGAFELTER

The Chemistry Department, University of Washington, Seattle, Wash.

Received April 28, 1960

Further refinement of the crystal structure of Cs_2CuCl_4 and a partial analysis of the crystal structure of $[N(CH_3)_4]_2CuCl_4$ have been carried out. The bond angles in the distorted tetrahedral configuration of $CuCl_4^{--}$ are 124.9, 123.3, 102.5 and 102.9°, all ±0.7°.

In 1952, Helmholz and Kruh[1] reported the crystal structure of Cs_2CuCl_4. They found the structure to contain discrete $CuCl_4^{--}$ ions with a configuration intermediate between tetrahedral and planar, the Cl–Cu–Cl bond angles being 104 and 120°. Although it is evident that the reported structure is essentially correct, their reported value of

$$R = \frac{\Sigma\|F_0| - |F_c\|}{\Sigma|F_0|} = 0.19$$

prompted us to carry the refinement further and also to investigate the structure of $[N(CH_3)_4]_2CuCl_4$.[2] The similarity between the axial ratio of Cs_2CuCl_4, $a:b:c = 1.2691:1:1.6137$ and of $[N(CH_3)_4]_2CuCl_4$, $a:b:c = 1.3416:1:1.6766$ suggest that their structures are quite similar.

Experimental

Crystals of both compounds were obtained by evaporation of aqueous solutions containing the stoichiometric proportions of $CuCl_2$ and CsCl or $N(CH_3)_4Cl$. The yellow-orange needles of Cs_2CuCl_4 were similar to those of Helmholz and Kruh[1] while the yellow-orange crystals of $[N(CH_3)_4]_2CuCl_4$ were short rod-like prisms bounded by [011] and terminated by [100].

Precession and Weissenberg photographs taken with Cu radiation ($\lambda = 1.5418$ Å.) of the Cs_2CuCl_4 crystals led to the cell dimensions $a_0 = 9.719$, $b_0 = 7.658$, $c_0 = 12.358$ Å., all ± 0.01 Å., in agreement with Helmholz and Kruh.[1]

Systematic absences of $(0kl)$ for $k + l$ odd and of $(hk0)$ for h odd indicate the space group to be Pnma or $Pn2_1a$.

Similar photographs of the $[N(CH_3)_4]_2CuCl_4$ crystals led to the cell dimensions $a_0 = 36.381$, $b_0 = 9.039$, $c_0 = 15.155$ Å. (all ± 0.01 Å.). However, all but a relatively small number of rather weak reflections could be indexed with $a_0 = 12.127$ Å. Therefore, these weak reflections were ignored in the present treatment and the cell was considered to have $a_0 = 12.127$ Å. These cell dimensions are in satisfactory agreement with those reported by Mellor.[2] Systematic absence of $(0kl)$ for $k + l$ odd and of $(hk0)$ for h odd indicate the space group to be Pnma or $Pn2_1a$.

Integrated photographic intensity data were collected for $(h0l)$ of Cs_2CuCl_4 with MoKα radiation on a Nonius Integrating Weissenberg camera, for $(hk0)$ of $[N(CH_3)_4]_2CuCl_4$ with CuKα radiation on the same camera, and for $(h0l)$ of $[N(CH_3)_4]_2CuCl_4$ with MoKα radiation on an integrating precession camera.[3] In all cases multiple films and a series of exposure times were used. Camera integration was in one direction only and each spot was scanned in the other direction with a Moll type densitometer feeding into a Leeds and Northrup amplifier and recorder having a logarithmic slide wire. The area under the tracing of each spot was measured with a planimeter and these areas were taken as the relative intensities. Lorentz and polarization factors were applied, but no corrections were made for absorption. All calculations were made with an IBM 650 computer. In the calculation of structure factors, Thomas and Umeda[4] scattering factors were used for Cs, Cu and Cl, and McWeeny scattering factors[5] for the other atoms.

Refinement of Cs_2CuCl_4.—Refinement of the projection of Cs_2CuCl_4 on [010] was carried out by difference syntheses to a value of $R = \Sigma \| F_0 | - | F_c \| / \Sigma | F_0 | = 0.10$,[6] using individual atom isotropic temperature factors. The final atomic positions and temperature factors are given in Table I, and bond lengths and angles in Table II. The standard deviation of the Cu–Cl lengths is 0.02 Å. and of the Cl–Cu–Cl angles is 0.7°, calculated by the method of Cruickshank.[7] Thus the changes in bond lengths from those of Helmholz and Kruh are not significant and the changes in bond angles, while significant, are small.

TABLE I

POSITION AND TEMPERATURE PARAMETERS FOR Cs_2CuCl_4

Atom	x/a	y/b[a]	z/c	B
Cs_1	0.1317	0.25	0.1018	3.3
Cs_2	−.0065	.75	.3263	3.1
Cu	.2320	.25	.4178	2.7
Cl_1	.3340	.25	.5745	3.3
Cl_2	.0030	.25	.3935	4.3
Cl_3	.2940	0	.3500	4.3

[a] From ref. 1.

TABLE II

BOND LENGTHS AND ANGLES IN $CuCl_4^{--}$

	In Cs_2CuCl_4	In $[N(CH_3)_4]_2CuCl_4$ From [010]	In $[N(CH_3)_4]_2CuCl_4$ From [001]
$Cu–Cl_1$	2.18 Å.	2.22 Å.	2.28 Å.
$Cu–Cl_2$	2.25	2.20	2.24
$Cu–Cl_3$	2.18	2.23	2.23
$Cl_1–Cu–Cl_2$	124.9°	129.8°	131.5°
$Cl_1–Cu–Cl_3$	102.5	99.6	99.4
$Cl_2–Cu–Cl_3$	102.9	102.2	101.5
$Cl_3–Cu–Cl_3'$	123.3	127.1	127.4

Approximate Structure of $[N(CH_3)_4]_2CuCl_4$.—Neglecting the faint reflections which indicate the tripling of the a axis, the several Weissenberg and precession photographs taken of $[N(CH_3)_4]_2CuCl_4$ are quite similar to those of $[N(CH_3)_4]_2ZnCl_4$,[8] indicating that their structures are similar. Since the $(h0l)$ net shows no indication of the 36 Å. a_0, the effective unit cell in the projection on [010] has $a_0 = 12.127$ Å. Initial atomic positions were obtained from a Patterson projection $P(x,z)$. Refinement of these positions by Fourier and difference syntheses was carried out to a final value of $R = 0.12$, using individual atom isotropic temperature factors, and assuming the space group to be Pnam.

(1) L. Helmholz and R. F. Kruh, *J. Am. Chem. Soc.*, **74**, 1176 (1952).

(2) D. P. Mellor, *Z. Krist.*, **A101**, 160 (1939).

(3) J. M. Stewart and E. C. Lingafelter, *Rev. Sci. Instr.*, **31**, 399 (1960).

(4) L. H. Thomas and K. Umeda, *J. Chem. Phys.*, **26**, 293 (1957).

(5) R. McWeeny, *Acta Cryst.*, **4**, 513 (1951).

(6) Tables of observed and calculated structure factors for both compounds may be obtained from E. C. Lingafelter.

(7) D. W. J. Cruickshank, *Acta Cryst.*, **2**, 65 (1949).

(8) B. Morosin and E. C. Lingafelter, *ibid.*, **12**, 611 (1959).

Refinement of the projection on [001] is expected to be less satisfactory, since the ($hk0$) zone shows the faint reflections corresponding to the 36 Å. a_0. Neglect of these faint reflections can therefore be expected to lead to only approximate coördinates. Fixing the x coördinates at the values calculated from the projection on [010], it was found possible to refine the projection on [001] only to $R = 0.25$. Allowing both x and y coördinates to vary, it was found possible to refine the projection on [001] to $R = 0.18$, with final x coördinates differing somewhat from those obtained from the projection on [010]. The final coördinates are given in Table III. The differences in x coördinates between the two projections range from 0 to 0.085 Å., with a mean value of 0.023 Å., for the heavy atoms, Cu and Cl, and from 0 to 0.45 Å., with a mean value of 0.15 Å., for the light atoms. It therefore seems apparent that the differences between the three sub-cells are primarily in the y-coördinates of the N and C atoms. Since our main interest in $[N(CH_3)_4]_2CuCl_4$ is in the configuration of the $CuCl_4^{--}$, no further attempts have been made to refine the projection on [001] using the faint reflections.

Using y-coördinates from the projection on [001], z coördinates from the projection on [010], and the two sets of x coördinates, two sets of bond distances and angles in $CuCl_4^{--}$ have been calculated and are given in Table II, along with the values from the Cs_2CuCl_4. Because of the uncertainty in the coordinates, no significance should be attached to the differences between the values from the two compounds, but it is apparent that the $CuCl_4^{--}$ is distorted from tetrahedral toward square configuration as described by Helmholz and Kruh.[1]

This intermediate configuration for 4-coördinate Cu(II) has now been found in three cases: the present $CuCl_4^{--}$; the $CuBr_4^{--}$ in Cs_2CuBr_4[9] with

(9) B. Morosin and E. C. Lingafelter, *Acta cryst.*, **13**, 807 (1960).

TABLE III

POSITIONAL AND TEMPERATURE PARAMETERS FOR $[N(CH_3)_4]_2CuCl_4$

	hol (R = 0.119)			$hk0$ (R = 0.181)		
	x/a	z/c	B	x/a	y/b	B
Cu	0.2281	0.4028	3.3	0.2281	0.250	5.9
Cl_1	.0495	.3700	6.5	.0450	.250	6.1
Cl_2	.3100	.5320	6.5	.3170	.250	8.5
Cl_3	.2750	.5490	9.9	.2740	.029	6.5
N_1	.1280	.0970	6.0	.1280	.250	8.0
N_2	.5050	.8330	6.0	.5280	.250	8.0
C_1	.2590	.1130	8.0	.2220	.250	8.0
C_2	.1270	−.0010	8.0	.1270	.250	8.0
C_3	.0770	.1320	9.0	.0600	.121	7.0
C_4	.4210	.7580	7.5	.4210	.250	8.0
C_5	.4500	.9150	7.5	.4500	.250	8.0
C_6	.5710	.8280	9.0	.5920	.121	7.0

angles of 128 and 101°; and in $CuCr_2O_4$,[10] in which the copper ion is surrounded by a set of oxygen ions with O–Cu–O angles of 122 and 103°. The configuration has been quantitatively accounted for on the basis of ligand field theory for $CuCl_4^{--}$ by Felsenfeld.[11]

Some comment should be made with regard to the values obtained for the atomic temperature factors in $[N(CH_3)_4]_2CuCl_4$. The large value for Cu for the $hk0$ zone is due to omission of the dispersion correction as discussed by Stewart, Breazeale and Lingafelter.[12] The large values for Cl may arise from either actual large thermal motion or a small randomness of position associated with the tripling of the small cell.

This work was supported in part by the Office of Ordnance Research (U. S. Army) under Contract No. DA-04-200-ORD-668 and in part by the U. S. Public Health Service under Grant A-2241.

(10) E. Prince, *ibid.*, **10**, 544 (1957).

(11) G. Felsenfeld, *Proc. Roy. Soc.* (*London*), **A236**, 506 (1956).

(12) J. M. Stewart, J. D. Breazeale and E. C. Lingafelter, *Acta Cryst.* (in press).

ON THE VARIATION OF THE SEDIMENTATION RATE OF SPHERICAL PARTICLES WITH CONCENTRATION

BY A. G. OGSTON

Department of Physical Biochemistry, John Curtin School of Medical Research, Australian National University, Canberra A.C.T.

Received May 5, 1960

The results of Cheng and Schachman[1] on dynamic properties of suspensions of uniform polystyrene latex particles are used to test the theory for the concentration dependence of sedimentation rate, based by Fessler and Ogston[2] and Ogston[3] on the treatment of Sullivan and Hertel[4] of the flow of fluid through a porous plug.

Fessler and Ogston[2] and Ogston[3] showed that, with certain assumptions, Sullivan and Hertel's[4] treatment of the flow of fluid through a porous plug can be applied to the sedimentation of solute particles at finite concentration through a fluid medium. Ogston[3] showed that the particle characteristics obtained by this treatment for a variety of types of solute particles were in reasonable agreement with what were believed to be the weights, shapes and hydrodynamic volumes of these particles. However, it has not so far been possible to apply this treatment to any material whose particle characteristics are certainly and accurately known from independent evidence.

The measurements of Cheng and Schachman[1] on a suspension of polystyrene latex particles make such a test possible. These particles are known by

(1) P. T. Cheng and H. K. Schachman, *J. Polymer Sci.*, **16**, 19 (1955).

(2) J. H. Fessler and A. G. Ogston, *Trans. Faraday Soc.*, **47**, 667 (1951).

(3) A. G. Ogston, *ibid.*, **49**, 1481 (1953).

(4) R. R. Sullivan and K. L. Hertel, *Adv. Colloid Sci.*, **1**, 37 (1942).

electron microscopy to be spherical and closely homogeneous, and their radius has been accurately measured. Cheng and Schachman[1] showed that the equation of Einstein for the intrinsic viscosity of a suspension of spheres is obeyed strictly, taking the hydrodynamic volume as equal to the geometric volume of these particles; that is, solvation is negligible. They showed also that the sedimentation coefficient at zero concentration is very close to the value expected for spheres of that size and density; and, finally, that the variation of sedimentation coefficient over the volume fraction (ϕ) range 0–7.5 $\times$ 10^{-2} is expressed by

$$\frac{1}{s} = \frac{1}{s_0}(1 + 4.06\phi + 15.9\phi^2) \qquad (1)$$

where s, s_0 are the sedimentation coefficients at volume fraction ϕ and zero volume fraction of solute.

Theory.—In the expressions given by Fessler and Ogston[2] and by Ogston[3] there is an error in the conversion of the sedimentation rate relative to solvent (which is the quantity given directly by their treatment) to that relative to the cell (which is that directly observed); the former quantity was divided instead of multiplied by the volume fraction of solvent. Equation 9 of Ogston[3] (omitting the factor "ϕ," *q.v.*) should therefore read

$$\frac{1}{s} = \eta S^2 \frac{k}{\zeta} \times \frac{100}{C(1 - \bar{v}\rho)} \times \frac{(CV'/100)^2}{(1 - CV'/100)^4} + \frac{1}{s_0} \qquad (2)$$

where s, s_0 are sedimentation coefficients at concentration C g./100 ml. and zero; S is the surface area/unit hydrodynamic volume and V' is the hydrodynamic volume/g. of solute particles; k and ζ are constants; $\bar{v}$ is the partial specific volume of solute and ρ is the density of solvent and η its viscosity. For comparison with equation 1 it is convenient to convert equation 2 into the same terms. In this case ϕ' ($=CV'/100$), the hydrodynamic volume fraction of solute, is equal to ϕ, since $V' = \bar{v}$, and $1/\bar{v} = \rho_P$ the density of the solute particles; accordingly

$$\frac{1}{s} = \frac{1}{s_0}\left\{1 + s_0\eta S^2 \frac{k}{\zeta} \times \frac{1}{\rho_p - \rho} \times \frac{\phi}{(1 - \phi)^4}\right\} \qquad (3a)$$

Expanding this to the second power of ϕ

$$\frac{1}{s} = \frac{1}{s_0}\left\{1 + s_0\eta S^2 \frac{k}{\zeta} \times \frac{1}{\rho_p - \rho}(\phi + 4\phi^2)\right\} \qquad (3b)$$

TABLE I

VALUES FOR THE AXIAL RATIO J, THE HYDRODYNAMIC SPECIFIC VOLUME V' AND THE MOLECULAR WEIGHT M OF PARTICLES OF POLYSTYRENE CALCULATED BY THE METHOD OF OGSTON[3]

	Value known *a priori*	Value estimated with k = 1.8
10^{-6} M	5.87	5.55
J	1	4
V'	0.95	0.54

Discussion

The forms of equations 1 and 3b are the same and the experimental ratio of the coefficients of ϕ^2 and of ϕ is 3.92 in good agreement with the theoretical value of 4. If the theory is correct there should be complete correspondence between these equations, but comparison is made difficult by uncertainty about the proper values of ζ and k; ζ is probably close to 2/3, but the value of k is rather uncertain. Ogston[3] chose k = 1.8 in preference to the value of 3 used by Fessler and Ogston, on the grounds that this gave better agreement with what were believed to be the molecular characteristics of a number of different types of macromolecular materials.

However, for none of these materials were the molecular characteristics known with certainty. Use of k = 1.8 gives the values for polystyrene latex particles shown in Table I. These are calculated from the data of Cheng and Schachman by the method of Ogston[3] using s_0 = 2410 $\times$ 10^{-13}; η = 0.86 $\times$ 10^{-2}; $[\eta]$ = 0.025; S for spheres = $3/r$ and r, the particle radius = 1300 Å.; ρ_p = 1.052 and ρ = 0.997; $d(1/s)/d\phi$ = 4.06 $\times$ 10^{13}/2410 (from equation 1). Evidently the axial ratio is overestimated and the hydrodynamic specific volume is underestimated. Alternatively, the data may be used to show that k = 1.35 gives agreement with the known dimensions of the polystyrene latex particles, and this value may be used to calculate the molecular characteristics of the substances discussed by Ogston.[3] The results are given in Table II, compared with those obtained with k = 1.8. While the lower value of k gives perhaps more reasonable values for the globular proteins, the axial ratios of the chain polymeric substances are as much less than 1 (the expected value) as they are greater than 1 with k = 1.8.

The present comparison therefore gives only

TABLE II

PARTICLE DIMENSIONS CALCULATED BY THE METHOD OF OGSTON[3]

	k = 1.8			k = 1.35		
	M	J	V'	M	J	V'
Ovalbumin	4.9×10^4	2.5	1.35	4.9×10^4	1/8	0.64
Serum albumin	6.4×10^4	5.2	0.69	6.7×10^4	3.2	1.1
Carboxyhemoglobin	6.2×10^4	5.6	0.61	6.4×10^4	3.7	0.91
Southern bean mosaic virus	6.9×10^6	7.8	0.67	7.5×10^6	3.9	0.96
Myosin	7.1×10^5	16	8.4	7.4×10^5	12	12
Tobacco mosaic virus	4.0×10^7	7.8	2.9	4.2×10^7	5.6	4.2
Polysarcosine viii-75	1.9×10^4	3.2	7.5	2.0×10^4	1/5	6.1
Polyisobutylene F5	1.6×10^6	3.4	120	1.7×10^6	1/3.9	123
F4	7.9×10^5	3.2	74	8.2×10^5	1/5.1	59
LA2	2.2×10^5	3.5	27	2.3×10^5	1/2.5	35
LC2	1.2×10^5	3.1	19	1.2×10^5	1/5.4	15
LD3	4.0×10^4	3.9	7.4	4.2×10^4	1/2.4	11

general support to the treatment and estimates k only for the case of spherical particles. It may be that different values of k are appropriate to different types of particle.

THE DECOMPOSITION OF SOLID H_4N_2 INDUCED BY CHARGED PARTICLE BOMBARDMENT

BY HAROLD A. PAPAZIAN

Convair Scientific Research Laboratory, San Diego, California

Received May 4, 1960

The decomposition of solid hydrazine induced by ion and electron bombardment has been studied. The decomposition was found to proceed through several steps. The stepwise evolution of N_2, H_2 and NH_3 during warmup of the bombarded solid was measured. The absorption spectrum of the bombarded solid showed the absence of NH_2. The results indicate the formation of nitrogen compounds such as triazene which are stabilized at low temperatures and which decompose during warmup of the solid.

Introduction

In a recent study[1] of the photolysis of HN_3 we presented evidence for the existence of the inorganic nitrogen chain compounds. The photolysis of solid HN_3 was shown to proceed through the formation and subsequent decomposition of triazene, tetrazene and perhaps even longer chained compounds. In an attempt to find evidence for these compounds in another system we have studied the decomposition of solid H_4N_2 induced by electron and ion bombardment.

The decomposition of the irradiated solid H_4N_2 was found to be exceedingly complicated, proceeding through several steps. Although it is not possible to state with certainty, the evidence does indicate the existence of the compounds found in HN_3 and also other kinds of nitrogen compounds which are stabilized at low temperatures.

Experimental

Two methods of purifying solid hydrazine were used. Anhydrous hydrazine (95+%) was vacuum distilled from KOH, onto a cold finger containing liquid N_2. The solid was then allowed to warm up by removing the liquid N_2. During this warmup, lower boiling impurities were pumped away. When the white deposit started to disappear from the preparation cold finger, liquid N_2 was reintroduced; a fraction of the remaining H_4N_2 was then sublimed over to the reaction cold finger. The second method of purification was the generation of H_4N_2 from hydrazine bisulfate. There was no difference in the results. The hydrazine was deposited as a transparent glass on the reaction cold finger by careful sublimation of the hydrazine from the preparation cold finger. Approximately 2 mg. of hydrazine was deposited on 2 cm.^{2} of surface yielding solid films on the order of 10^{-2} mm. thickness.

After the deposition on the reaction cold finger, and with the apparatus under continuous pumping, the solid was subjected to ion and electron bombardment by discharging a laboratory Tesla coil against the outer wall of the cold finger for various lengths of time. It has been shown[2] that this procedure subjects the solid to bombardment with 20 Kev. electrons and ions of undetermined energy. After the bombardment the liquid N_2 was removed from the cold finger, allowing the solid to warm up. During this warmup simultaneous mass spectrometer and temperature measurements were made. The temperature was measured by a thermocouple soldered on to the glass cold finger at the deposition surface with a spot of glass-to-metal "Cerroseal-35" solder. A CEC model 620 mass spectrometer was used to analyze the gases evolved from the solid during the warmup.

By adjusting the pumping speed of the system the pressure pulses that occurred during warmup could be discriminated into definite peaks. The pumping speed was controlled by means of a capillary placed between the reaction cold finger and the stopcock leading to the vacuum pump. The inlet to the mass spectrometer was placed between the capillary and the reaction cold finger.

A universal model Perkin-Elmer 112U spectrophotometer was used to study the spectrum of the solid between 3300 and 6300 Å. The sample was deposited on a specially constructed cold finger which consisted of a small flat plate whose edges were in contact with a surrounding volume of liquid N_2; the nitrogen was thus excluded from the light path. After deposition of the hydrazine the absorption was measured. The sample then was bombarded and the difference in absorption caused by the bombardment was measured.

Results

The final products found after warmup of the bombarded solid hydrazine were H_2, N_2 and NH_3. Figures 1, 2 and 3 show the stepwise evolution of these gases during the warmup of the solid, for three different bombardment times.

In these figures the ordinates are proportional to the quantity of gas evolved. Some comparison can be made between the N_2 and H_2 since these are pumped out of the system at roughly the same rate but no comparison can be made with NH_3 since it was found to be pumped much more slowly. In Fig. 1 we also show the temperature *vs.* time warmup curve of the cold finger during the course of gas evolution. A warmup blank also was run with unbombarded hydrazine on the cold finger. The two curves were experimentally identical. It is apparent that the pressure pulses are not rate changes from sudden temperature rises of the cold finger, but that the gas evolution pulses result from stepwise reactions beginning at different temperatures.

Figure 1 shows the evolution of H_2 during warmup from a solid which was bombarded for two seconds. Considerable structure is quite evident. We did not investigate N_2 nor NH_3 evolution for two second bombardment times.

Figure 2 shows the evolution of H_2, N_2 and NH_3, each from separate samples. Different samples had to be used because the mass spectrometer could analyze continuously only one gas at a time. This, however, was no problem because of the excellent reproducibility in the gas evolution from the solid. It should be noted that even though the bombarding

(1) H. A. Papazian, *J. Chem. Phys.*, **32**, 456 (1960).

(2) H. A. Papazian, *ibid*, **29**, 448 (1958).

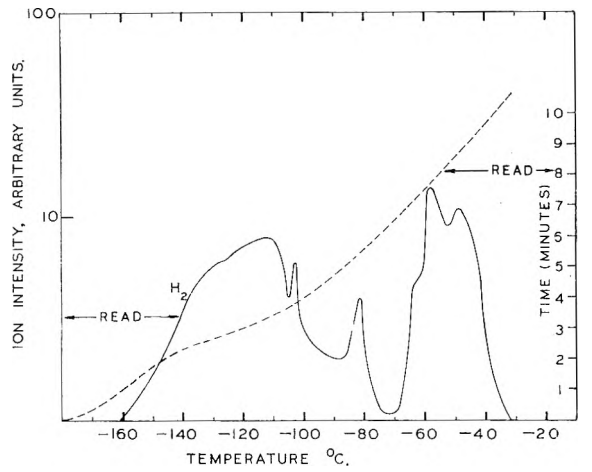

Fig. 1.—Solid line, H_2 evolution from solid H_4N_2 which was bombarded for 2 seconds; broken line, time *vs.* temperature warmup of cold finger.

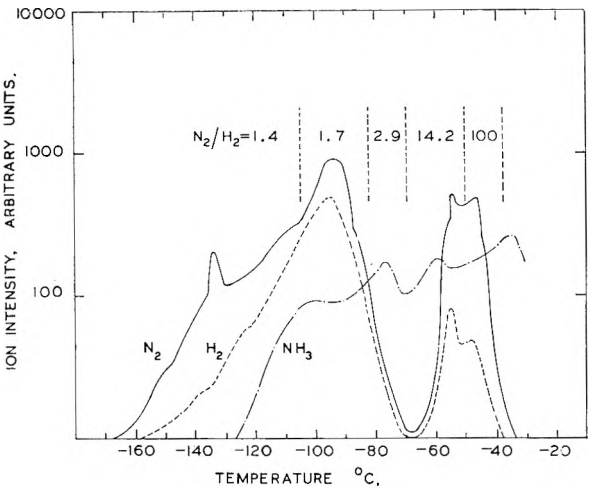

Fig. 2.—Gas evolution from solid H_4N_2 which was bombarded for 10 seconds.

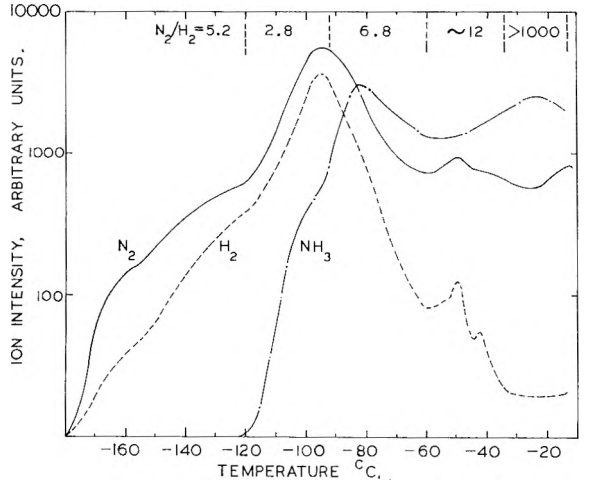

Fig. 3.—Gas evolution from solid H_4N_2 which was bombarded for 30 seconds.

time was increased only 5 times, *i.e.*, to 10 seconds, the H_2 evolution increases by a factor of 100. The structure of the H_2 evolution between -60 and $-40°$ is still clearly present. However, at the lower temperature, *i.e.*, below $-70°$ a new strong evolution appears at $-95°$, and the reaction at $-80°$ has disappeared.

The N_2 evolution appears to be more complex than the H_2. In the region between -60 and $-40°$ there are four pulses of N_2 compared to only two for H_2. Between -170 and $-70°$ the N_2 is again more complex. It should be noted that the NH_3 peaks do not appear at the same temperatures as the N_2 and H_2 peaks.

Figure 3 shows the evolution of H_2, N_2 and NH_3, each from separate samples. Each sample was bombarded for a total of 30 seconds in three 10-second bursts with 10-second intervals between bursts. Here we find that for a threefold increase in bombarding time we get an increase in gas evolution by a factor of about eight.

It was observed that NH_3 would not sublime off of our cold finger below $-120°$ so that it cannot be known with certainty whether or not NH_3 is formed in the reactions occurring below this temperature. Hydrazine began subliming above $-20°$.

In order to gain some insight into the stepwise reactions, a different kind of experiment was carried out. The reactions occurring during warmup were stopped by reintroducing liquid N_2 into the reaction cold finger. If the reaction was stopped at the end of any step, then the next step would not appear until the cold finger was warmed to the temperature of that subsequent step. At the top of Fig. 2 and 3 are given the N_2/H_2 ratios formed over the indicated temperature ranges. These ratios were obtained by allowing a reaction step to proceed, introducing liquid N_2 into the cold finger when the slope of the gas evolution curve indicated the end of the reaction, and then measuring the relative concentrations of H_2 and N_2. With our experimental technique we could not determine the NH_3/N_2 ratios; the NH_3 condensed when liquid N_2 was introduced to stop the reaction. From the N_2/H_2 ratios it is obvious that the chemistry in the different regions studied varies considerably. These ratios cannot be used for the stoichiometry (nor can they be compared closely to the gas evolution traces from the mass spectrometer) because the apparatus is continually pumping up to the time of addition of liquid N_2 and closing of stopcock.

The over-all N_2/H_2 and NH_3/N_2 ratios were determined by bombarding the solid, closing the stopcock to the pump and letting the solid warm up completely. For the 30-second bombardment a series of five experiments were done; the N_2/H_2 ratio varied from 1.7 to 2.3 with an average of 2.0, and the NH_3/N_2 ratio varied from 2.9 to 3.6 with an average of 3.3. Two experiments were done at 10-second bombardment times; the N_2/H_2 ratios were 2.7 and 3.0 with an average of 2.9 and the NH_3/N_2 ratios were 4.2 and 4.4 with an average of 4.3. For the 10-second experiments we measured the total conversion and found approximately 23 and 22% decomposition of hydrazine. We did not measure the total decomposition for the 30-second bombardment but would expect it to be even larger.

We also studied the absorption spectrum of a bombarded sample of solid H_4N_2. The solid line in Fig. 4 shows the difference in absorption between

a bombarded and an unbombarded sample. The spectrum labeled "slight warmup" was obtained by removing liquid N_2 from the absorption cell until gas evolution just began, then quickly stopping reaction by reintroducing liquid N_2 into the cell. The temperature to which the solid was warmed was not measured but from the gas evolution studies we estimate it to be about $-155°$.

At no time did the bombarded solid become permanently colored, even for the longest bombarding times. It did appear to turn slightly blue for an instant but this color could not be stabilized. In an attempt to stabilize the color the solid was bombarded using liquid He as the coolant but no color could be seen. This complete absence of color may have been the inhibition of a reaction by the low temperature.

Discussion

The simultaneous evolution of several substances indicates the complexity in the decomposition process. The N_2/H_2 ratios obtained over the various regions show clearly that different reactions occur during the warmup of the solid. That some chain mechanism is involved is indicated by the comparison of bombarding times with the amount of gas evolved.

One speculation which may not be out of order concerns the region in Fig. 3 where the $N_2/H_2 > 1000$, with NH_3 also being evolved. This may be the decomposition of triazene, $H_2—N—N=N—H \rightarrow NH_3 + N_2$. In Fig. 4 we find an absorption band at 3600 Å. which in ref. 1 we assigned to triazene. In the earlier paper we suggested that the reaction of triazene with HN_3 takes place at $-90°$. It may be that in the absence of a suitable reactant triazene is stable to the higher temperature.

Foner and Hudson[3] trapped the products of hydrazine from an electrodeless discharge. From their cold trap they found the evolution of small quantities of compounds with masses 45 and 60 which they attributed to triazene and tetrazene, respectively. Our inability to find these compounds in the mass spectrometer probably results from their complete decomposition either on the glass walls or in the gas phase. The long distance through glass tubing, at room temperature, that they would have had to travel in our apparatus makes this conclusion reasonable.

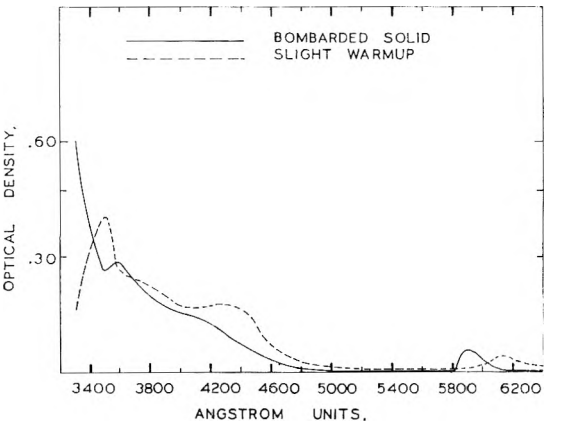

Fig. 4.—Absorption spectrum of a bombarded sample of H_4N_2 before and after some reaction.

NH_2 was not stabilized under the conditions of this study. Robinson and McCarty[4] have studied the absorption spectrum of NH_2 radicals trapped at low temperatures. Among others, they find two strong absorptions at 5150 and 5684 Å. Figure 4 shows that no NH_2 was stabilized before or after some reaction.

Rice has tabulated[5] the reaction temperatures of free radicals stabilized in solids at low temperatures which he has studied in the laboratory and lists these between -125 and $-195°$. Atomic species have only been stabilized at liquid He temperatures.[6] Thus, although it may not be ruled out with certainty, it is unlikely that any of the reactions occurring above $-120°$ are reactions of stabilized free radicals. We must, therefore, assume that the reactions occurring at the higher temperatures are reactions of product molecules with the H_4N_2 matrix and/or the decomposition of these product molecules.

Acknowledgment.—The author wishes to thank Mr. John Pearl for his help in carrying out these experiments.

(3) S. N. Foner and R. L. Hudson, *J. Chem. Phys.*, **29**, 442 (1958).

(4) G. W. Robinson and M. McCarty, *ibid.*, **30**, 999 (1959).

(5) F. O. Rice, *ibid.*, **24**, 1259 (1956).

(6) H. P. Broida and J. R. Pellam, *Phys. Rev.*, **95**, 845 (1954).

HETEROPOLY COMPOUNDS. VI.[1] FURTHER STUDIES ON BASICITIES OF SOME HETEROPOLY ACIDS[2]

BY J. R. KELLER,[3] E. MATIJEVIĆ AND M. KERKER

Clarkson College of Technology, Potsdam, N. Y.

Received May 2, 1960

Using a spectrophotometric technique described previously[4] and the indicators, brom cresol green, methyl red and brom cresol purple, respectively, the basicities of these several heteropoly acids were determined in highly diluted aqueous solutions: 6-molybdochromic(III), 12-tungstosilicic, 9-tungstophosphoric, 12-tungstophosphoric and 12-molybdoceric(IV) acids. The basicities are in agreement with these several formulations of these acids: $H_3CrMo_6O_{21}$, $H_4SiW_{12}O_{40}$, $H_6P_2W_{18}O_{62}$, $H_7PW_{12}O_{42}$ and $H_8CeMo_{12}O_{42}$. The latter two acids become fully ionized only at very low concentrations (6 and 4×10^{-6} *M*, respectively). It was also shown that the 12-tungstophosphate ion absorbs differently from the undissociated acid in the ultraviolet, so that it actually behaves as an acid–base indicator.

Introduction

In an earlier paper[4] we have presented data on the basicities of several heteropoly acids using a spectrophotometric method based on the ionization of methyl orange under the influence of added acids. The concentration range for which the acids may be investigated depends on the *pK* of the indicator employed. Using methyl orange we could establish that the 6-molybdocobaltic(III) and 6-molybdochromic(III) acids are tribasic, that 12-tungstosilicic acid is tetrabasic and that 9-tungstophosphoric acid is hexabasic. However, the 12-molybdoceric(IV) and 12-tungstophosphoric acids showed a steady increase in basicity (number of hydrogen ions in solution per mole of acid) with dilution, indicating that these acids were not fully ionized in the concentration range studied ($\sim 1 \times 10^{-3}$ to 2×10^{-5} *M*). According to the accepted molecular formula, 12-molybdoceric(IV) acid, $H_8CeMo_{12}O_{42}$, should be octabasic. The problem of the basicity of the 12-tungstophosphoric acid has been discussed in previous papers[4,5] where we have shown that in solution the tribasic formulation must be abandoned and a higher basic formulation such as heptabasic acid, $H_7PW_{12}O_{42}$, must be utilized. Since X-ray analysis has indicated the $PW_{12}O_{40}^{-3}$ ion in the crystal, we assume that $H_7PW_{12}O_{42}$ and the ionic species obtained by its dissociation are formed in solution by hydrolysis of the tribasic species. The question then arises as to whether additional waters may be added giving anions containing 43 oxygens, etc., in which case the experimentally observed basicity might be expected to increase beyond 7 upon continued dilution. The same argument could be applied to the 12-molybdoceric-(IV) acid.

In order to work at lower concentrations, indicators having a *pK* higher than that of methyl orange had to be used. Accordingly, we have determined the basicities in the lower concentration range of the 12-molybdoceric(IV) and 12-tungstophosphoric acids using brom cresol green, methyl red and brom cresol purple as indicators. We have also determined the basicity of 9-tungstophosphoric acid, 12-tungstosilicic acid and 6-molybdochromic acid with these indicators in order to test the stability of their ions to hydrolysis of the type discussed and also to provide a check on technique.

In addition, we have found that the optical density of 12-tungstophosphoric acid solutions is strongly *p*H dependent in the near ultraviolet. Thus, this acid behaves as an acid-base indicator. The *p*H dependence of the 12-tungstophosphoric acid is also important from the analytical point of view, since spectrophotometric measurements are often utilized for determining the concentration of heteropoly compounds. These data may be misinterpreted in the case of the 12-tungstophosphoric acid if the *p*H factor is not taken into account.

Experimental

1. Materials.—12-Tungstophosphoric acid, 9-tungstophosphoric acid, 12-tungstosilicic acid, 12-molybdoceric(IV) acid and 6-molybdochromic(III) acid were prepared and purified as described earlier.[4-6] Solutions were prepared by direct weighing and dissolution in doubly distilled water.

2. Basicity Measurements.—Basicity determinations were made utilizing, in principle, the same method as described in detail in our previous paper.[4] Essentially, it is based on measuring the optical density of an indicator in the presence of various concentrations of the heteropoly acid. If the concentrations of the heteropoly acid are chosen to give a *p*H within the critical range for a specific indicator, the optical density varies in a very sensitive way with the hydrogen ion activity. In our previous work we have used methyl orange for which we obtained a calibration curve over a convenient range of HCl for the dependence of the indicator ratio, *R*, upon $[H^+]$, where $R = [A^-]/[HA]$, $[A^-]$ and [HA] being the equilibrium concentrations of the basic and the acid forms of the indicator. *R* can be calculated from optical densities if the optical density of the acid and the basic forms of the indicator are known.[4,7] In addition we have explored the effect of the ionic strength upon the indicator equilibrium and found that below $\mu = 0.001$ *M* the presence of neutral elcctrolytes does not affect the equilibrium. Utilizing these data we were able to determine basicities of heteropoly acids by comparing *R* for a given concentration of a heteropoly acid with the calibration curve.

In the present work, we were interested primarily in obtaining the basicities at very low concentrations of heteropoly acids, hence experiments with brom cresol green (*p*H interval 3.8–5.4), methyl red (4.4–6.2), and brom cresol purple (5.2–6.8) were performed. In the concentration range of heteropoly acids used in these experiments (3×10^{-5} to 1×10^{-6} *M*), the ionic strength effect is negligible. We have also compared the effects of various inorganic electro-

(1) K. F. Schulz, E. Matijević and M. Kerker, *J. Chem. Eng. Data*, in press.

(2) Supported by the U. S. Atomic Energy Commission Contract No. AT(30-1)-1801.

(3) Participant in the N.S.F. Summer Research Project, 1959.

(4) E. Matijević and M. Kerker, *J. Am. Chem. Soc.*, **81**, 5560 (1959).

(5) E. Matijević and M. Kerker, THIS JOURNAL, **62**, 1271 (1958).

(6) E. Matijević and M. Kerker, *J. Am. Chem. Soc.*, **81**, 1307 (1959).

(7) I. M. Klotz, Thesis, The University of Chicago, 1940; see also R. A. Robinson and R. H. Stokes, "Electrolyte Solutions," Butterworth Sci. Publ., London, 1955.

lytes and salts of heteropoly acids upon the absorption of methyl orange. Below $\mu \sim 0.002$ they all behaved identically, indicating that there was no specific interaction between the indicator and the heteropoly anion in the working range. Since the results obtained with indicators used in this paper overlap nicely with those found with methyl orange no specific interaction with the former was assumed.

However, a number of experimental difficulties had to be overcome in order to eliminate the influence of CO_2 on the ionization of the indicator. We modified the experimental procedure because the reproducibility of the results obtained using a calibration curve was quite poor at the lowest concentrations. In the experiments reported here, we always compared the optical density of a solution containing a certain amount of a heteropoly acid and a constant amount of the indicator with that of a number of solutions containing exactly the same amount of indicator but varying amounts of HCl. The concentrations of HCl were chosen so that the solutions had optical densities very close to that of the heteropoly acid solution. When the optical density of solutions containing the heteropoly acid and HCl were exactly the same, the basicity of the heteropoly acid was obtained by direct comparison of molarities of both solutions. When the optical density was slightly different the basicity was calculated from the corresponding R values.

Optical density measurements were determined using the Beckman Model DU spectrophotometer which was equipped with a thermostat jacket in the cell compartment through which was circulated water from a 25° constant temperature bath. Calibrated 1 cm. Corex cells were used in all experiments. The working wave lengths for the different indicators were: brom cresol green 450 and 620 mμ, methyl red 520 mμ, and brom cresol purple 430 and 590 mμ. These wave lengths gave the largest differences in optical absorption between the acid and the basic forms of the indicator. All solutions in one experiment were prepared using the same batch of distilled water. Before taking readings, dry helium or nitrogen was bubbled through solutions for 10 minutes. This bubbling time was found sufficient to eliminate the effects of dissolved CO_2 and to obtain reproducible readings of optical densities. Each measurement was repeated several times using at least two different cells and only results with good internal agreement were used. When two wave lengths were utilized the same procedure was repeated with each.

All solutions were prepared by successive dilution of conconcentrated stock solution using the water from the same batch.

The concentration of all indicators was the same (1.875×10^{-5} M) and kept constant throughout the experiments. The concentration was chosen to give optimal optical density readings. The effect of the ionization of indicator is compensated in the technique employed, since both the heteropoly acid and hydrochloric acid solutions contained the same amount of indicator at very nearly equal activities of hydrogen ions.

All pH measurements have been done using glass electrodes and Model G Beckman pH meter.

Results and Discussion

1. Basicity.—In Fig. 1, the basicities of 6-molybdochromic(III) acid, 12-tungstosilicic acid, 9-tungstophosphoric acid, 12-tungstophosphoric acid and 12-molybdoceric acid are plotted against the molar concentration of the heteropoly acid. These data represent a combination of our earlier results[4] obtained using methyl orange at concentrations of heteropoly acids higher than 2×10^{-5} M and the new data using brom cresol green, methyl red and brom cresol purple for acids in concentration range: 3×10^{-5} to 1×10^{-6} M. The 6-molybdochromic acid, 12-tungstosilicic acid and 9-tungstophosphoric acid maintained the same basicities of 3, 4 and 6, respectively, at the lower concentrations indicating that all three acids were fully ionized in the higher concentration range and that no decomposition or hydrolysis takes place upon dilution.

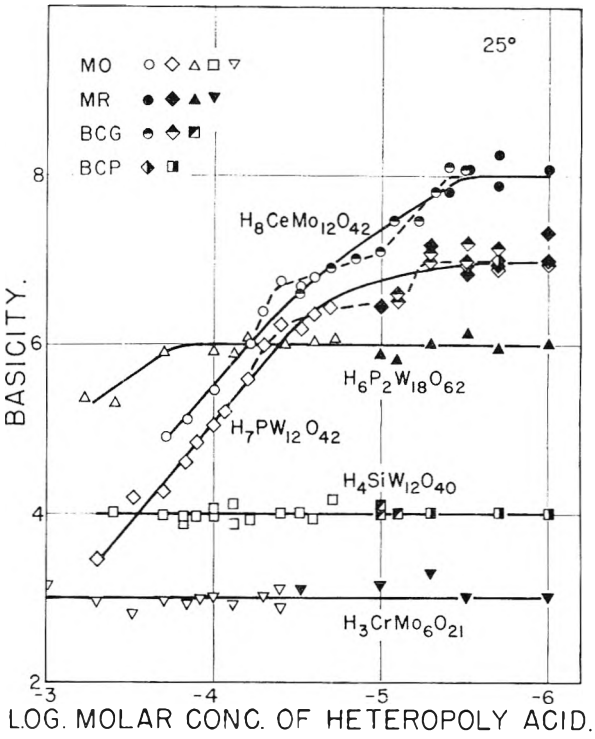

Fig. 1.—Basicities of 6-molybdochromic(III) acid, 12-tungstosilicic acid, 9-tungstophosphoric acid, 12-tungstophosphoric acid and 12-molybdoceric(IV) acid plotted against concentration of investigated solution. Indicators employed: methyl orange (MO), methyl red (MR), brom cresol green (BCG) and brom cresol purple (BCP).

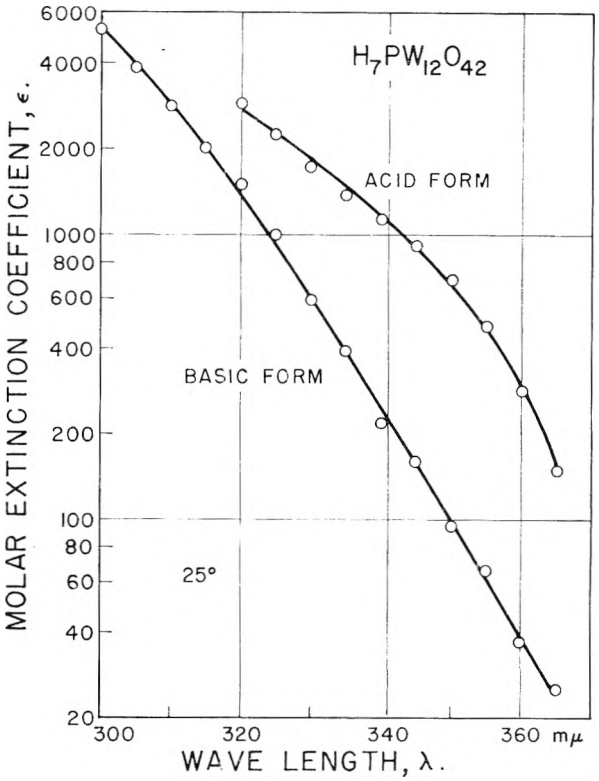

Fig. 2.—Molar extinction coefficients of 12-tungstophosphoric acid in its acid and basic form for the wave length range from 300 to 365 mμ.

In the higher concentration range previously investigated with methyl orange, the 12-tungstophosphoric acid and the 12-molybdoceric acid showed a definite trend toward increasing basicity with dilution. However, the basicities corresponding to structural formulas $H_7PW_{12}O_{42}$ and $H_8CeMo_{12}O_{42}$ were not reached. By extending the measurements to lower concentrations of these acids with the aid of the indicators of higher pK, the basicity values now show further increase until they eventually level off at 7 for the 12-tungstophosphoric acid and 8 for the molybdoceric(IV) acid. Thus, it appears that both of these acids can be obtained fully ionized as free hepta- and octavalent heteropoly ions in these very dilute solutions. In addition, these results further confirm the above formulations for these acids in aqueous solution. The data for 12-tungstophosphoric and 12-molybdoceric(IV) acids at the lowest concentrations suggest that the last stage of the ionization occurs stepwise. In Fig. 1, we have delineated this by the dashed line, the full line being drawn smoothly through all the data.

2. 12-Tungstophosphoric Acid as an Acid–Base Indicator.—In the preparation of the sodium salt of 12-tungstophosphoric acid by ion exchange, we found that although the pH increase upon passage through the column was comparable to that obtained for the 9-tungstophosphoric and 12-tungstosilicic acids, the optical density in the ultraviolet of the steady-state effluent was only a small fraction of that of the free acid. Similar effects were obtained when we attempted to prepare the ammonium and silver salts of the free acid by the same method. However, we found that if dilute nitric acid was added so that the pH of the free 12-tungstophosphoric acid was restored, the optical density returned to a value nearly equal to that for the free acid. This indicates that the ionized form of the acid absorbs differently from the unionized form so that 12-tungstophosphoric acid behaves as an acid-base indicator in the ultraviolet.

We obtained the molar extinction coefficient of the *acid form* of the 12-tungstophosphoric acid from the limit of the optical density of the acid in the presence of increasing concentration of nitric acid. The limiting value was determined from a plot of optical density against the reciprocal of the nitric acid concentration, the optical density of the nitric acid itself being taken into consideration at the highest concentrations. The results are given in Fig. 2.

At very high dilutions, solutions of the sodium salt followed Beer's law, indicating that the anion was completely dissociated so that in this case the optical density was used directly to obtain the absorption index of the *basic form* of the indicator. These results are also given in Fig. 2.

If 12-tungstophosphoric acid were monobasic, the optical density could now be used to calculate the degree of ionization. However, since 12-tungstophosphoric acid is polybasic this problem is complicated by the existence of the various intermediate species between the fully associated and fully ionized acid.

THE ACTION OF OXYGEN ON IRRADIATED POLYVINYL CHLORIDE

BY BILLY R. LOY

Physical Research Laboratory, The Dow Chemical Company, Midland, Michigan

Received May 14, 1960

The formation and decay of the peroxy radical produced in irradiated poly-(vinyl chloride) is studied by electron spin resonance (e.s.r.) spectroscopy over a temperature range from −78 to +45°. The two reactions are studied independently making use of the difference in reaction rates. The exponential formation reaction is thought to be diffusion controlled. The apparent first-order decay reaction is interpreted as an autoöxidation process which gives mobility to the unpaired electron.

Introduction

The effect of air on irradiated poly-(vinyl chloride) has been noted by other workers. Miller[1] has shown by electron spin resonance (e.s.r.) measurements that there is a much more rapid loss of radicals in irradiated PVC that has been exposed to air than similarly treated samples *in vacuo*. Chapiro[2] and Miller[1] both report a lack of coloration of the material when it is exposed to air, presumably through the formation of a peroxy radical.

The e.s.r. spectrum of the peroxy radical is particularly well-suited for study (by e.s.r.). Abraham and Whiffen[3] studied the formation and decay of peroxy radicals in polyethylene and polychlorotrifluoroethylene. They suggest that decay occurs *via* reversible and irreversible processes.

As a result of studying the formation and decay over a temperature range from −78 to +45°, this article proposes that the peroxy radical sites effectively acquire motion through an autoöxidation reaction. In this work, the samples were irradiated with γ-rays at liquid nitrogen temperature. The action of oxygen on the irradiated samples was observed, *in situ*, by e.s.r.

Experimental

Material.—The polyvinyl chloride (PVC) used in these experiments was manufactured by The Dow Chemical Company and is designated PVC-111-4, Lot 11727, Blend 2. The average particle size is about 140 μ, but the surface area as determined by the BET method is 1.24 m.²/g. Therefore, the particles must be regarded as extremely porous. No plasticizers, inhibitors or other additives were used in the manufacture of this material.

(1) A. A. Miller, THIS JOURNAL, **63**, 1755 (1959).

(2) A. Chapiro, *J. chim. phys.*, **53**, 895 (1956).

(3) R. J. Abraham and D. H. Whiffen, *Trans. Faraday Soc.*, **54**, 1298 (1958).

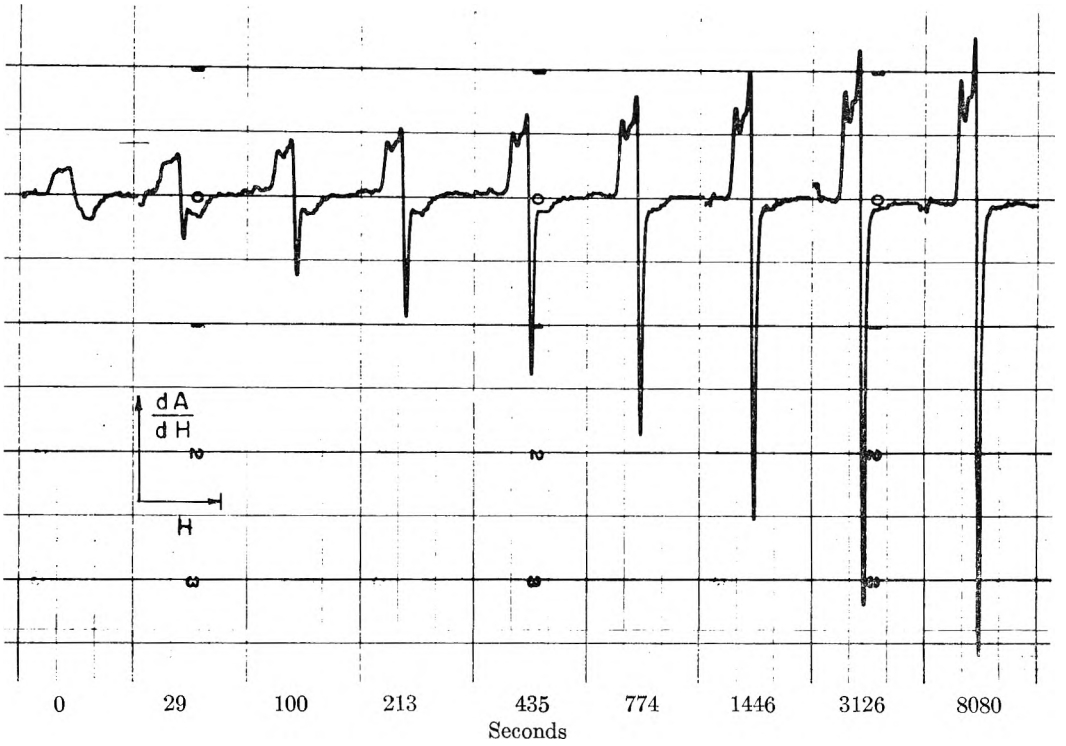

Fig. 1.—Repeated displays showing the conversion of the alkyl radical to the peroxy form at −78° in air. Spectra taken at 0, 29, 100, 213, 435, 774, 1446, 3126 and 8080 seconds, respectively.

QYNV-3317, a product of Bakelite Division, Union Carbide Chemical Company, was used in one experiment to determine the relationship of particle size to reaction rate. The surface area of this material is 6.13 m.²/g. It is reported to be in the form of hard spheres with an average diameter of 0.2145 μ.

Resonance Detection Equipment.—The e.s.r. spectrometer employed was of the conventional 3 cm. type using a reflection type cavity in a slowly varying magnetic field, modulated at a frequency of 700 c.p.s. The spectrum is presented in the form of the first derivative of the absorption signal.

The low temperature cavity consists of two rectangular tanks, made of five mil brass shim stock, which encompass portions of brass wave guide on both sides of the reflection type cavity. A fifty watt Chromalox heater is secured in one end of a piece of copper tubing long enough to keep the heater out of the field. The other end is flattened out and fastened between the two wave guide flanges. Depending upon the temperature range desired, one or both tanks are filled with refrigerant, and varying amounts of heat may be supplied to the system by means of a Variac which supplies power to the heater.

Procedure Irradiation of Samples.—Prior to irradiation, the samples were placed in 6 mm. o.d. Pyrex tubes, flushed three times with nitrogen and evacuated to 10^{-3} mm. While immersed in liquid nitrogen the samples were irradiated with cobalt-60 at a dose rate of 0.425 Mrad. per hour to a total dose of 8.0 Mrad. After irradiation, the end of the tube containing the sample was immersed in liquid nitrogen and the other end was heated nearly to the annealing temperature to eliminate the paramagnetic centers in the glass. After cooling the entire tube to −195°, the sample was transferred to the clear end. The samples were stored in liquid nitrogen for 1–10 days until e.s.r. measurements were made.

The spectra were obtained by transferring the prepared samples from liquid nitrogen to the cavity which was maintained at desired temperatures. After the sample had reached thermal equilibrium,[4] it was opened to air and a series of spectra were recorded. The e.s.r. spectrum of the peroxy radical is typified as an asymmetrical line with the greatest slope on the high field side of the spectrum.

Results and Interpretation

The Formation of the Peroxy Radical.—Figure 1 shows a series of spectra taken after exposure to air at −78°. The small disappearing shoulder on the high field (right hand) side of the spectra is due to the alkyl radical. The peroxy signal reached a maximum amplitude, which was relatively stable, after about 6000 seconds of air exposure.

The peak-to-peak amplitude of the peroxy spectrum may be considered as proportional to the peroxy radical concentration if minor dipolar broadening effects are ignored and a correction is made for the contribution of the alkyl spectrum. The relative concentration of the alkyl radical (R·) reacting with oxygen is considered equal to the final or maximum amplitude of the peroxy spectrum ($RO_2 \cdot)_\infty$ minus the amplitude $(RO_2 \cdot)t$ at any time, t.

$$(R \cdot = RO_2 \cdot_\infty - RO_2 \cdot_t)$$

When plotted against time, the relative alkyl radical concentration seems to fit a logarithmic plot best; although, there is an initial deviation from a linear relationship. Figure 2 shows this relationship for various temperatures from 0 to −78°. Investigating the effect of particle size, the rate of disappearance of the alkyl radical at −78° from irradiated QYNV-3317 is shown by the dashed line in Fig. 2. The ratio of surface areas (about 4.9) is close to the ratio of the rate slopes (4.4).

Peroxy Radical Decay.—As the temperature is

(4) B. R. Loy, unpublished work. When samples are similarly treated *in vacuo*, it has been noted that the alkyl radical decays by at least two different modes. The rate of the first decay was nearly equal to the rate of attaining thermal equilibrium. The slower rate, apparently associated with color formation and dependent upon temperature, has a half-life of several hundred hours at room temperature. After thermal equilibrium has been reached, the fast reaction is complete and the slow reaction is negligible over the period of time required for the formation of the peroxy radical.

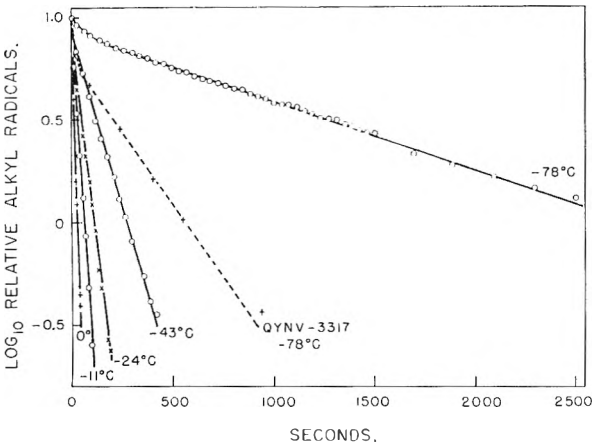

Fig. 2.—Exponential decay of alkyl radical at various temperatures. Dashed curve represents QYNV-3317; all others are PVC-111-4.

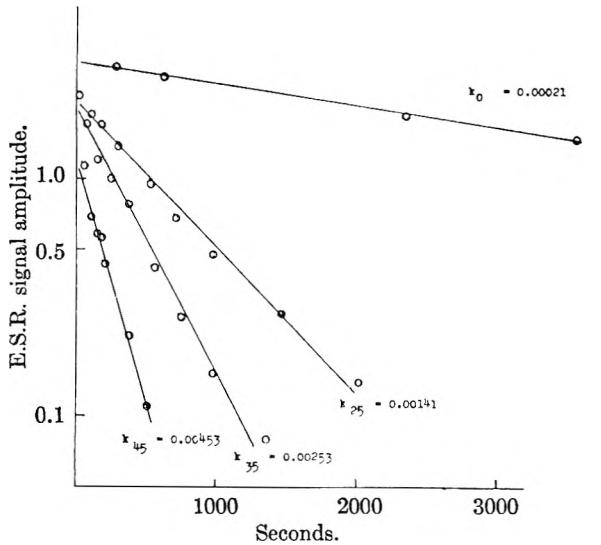

Fig. 3.—Exponential decay of peroxy radical at various temperatures. k's are apparent rate constants and subscripts refer to temperature (°C.).

increased the formation of the peroxy radical becomes so fast that it is not easily measured by e.s.r. techniques. A series of spectra at 25° showed, by disappearance of the alkyl shoulder, that the formation of the peroxy radical was virtually complete when the first spectrum was recorded after 24 seconds of air exposure. Subsequent spectra, taken over a 45-minute period, showed the continuing decrease of the peroxy radical spectrum with no observable change in line shape. The logarithm of the signal amplitude was found to vary linearly with time, indicating the exponential decay of the peroxy radical. Figure 3 shows these plots at different temperatures. An Arrhenius plot of the apparent rate constants yields an activation energy of 12 kcal./mole.

Investigating the behavior of the peroxy radical *in vacuo*, a sample was treated as above except that it was evacuated after 210 seconds of air exposure. After evacuation, a series of spectra, taken over a 45 minute period, showed the reverse of the reaction noted in Fig. 1. The peroxy spectrum decreased exponentially with time with the accompanying increase of the alkyl shoulder until the radical was virtually all in the alkyl form.

Discussion

It was hoped that the data in Fig. 2 would indicate whether the reaction was diffusion controlled or pseudo first order. The exponential decay would fit either case. The initial deviation from linear behavior may possibly represent some open penetration by O_2 before a diffusion barrier is reached. An Arrhenius plot of the slopes of the curves in Fig. 2 indicates an activation energy of 6 kcal./mole. This seems too high for a reaction between an alkyl radical and oxygen but is not unreasonable for diffusion activation energy. The fact that the increase in rate of disappearance of alkyl radical (Fig. 2) is proportional to the increase in surface area indicates, to a first approximation, that the observed reaction rate is diffusion controlled.

The formation of the peroxy radical at room temperature is too fast to be followed by e.s.r. techniques but by extrapolation of the lower temperature data, the half-life of the alkyl radical at room temperature is about 4 seconds. This great difference between the rates of formation and decay make it possible to study one reaction independently of the other, and to relate these observations to proposed mechanisms for the decay of alkyl radicals through peroxy formation.

Abraham and Whiffen[3] describe the decay of the peroxy radical as the result of a reversible

$$R\cdot + O_2 \longrightarrow RO_2\cdot \quad (1)$$
$$RO_2\cdot \longrightarrow R\cdot + O_2 \quad (2)$$

and irreversible process

$$RO_2\cdot + R' \longrightarrow ROOR' \quad (3)$$

or

$$R\cdot + R'\cdot \longrightarrow RR' \quad (4)$$

Step 3 could possibly account for the initial deviation in Fig. 2 but this could play only a minor role, since virtually all of the radicals are in the peroxy form during the major part of the decay period. In keeping with this scheme, R = R′ and step 2 would represent the rate controlling first-order decay observed in Fig. 3b. If the activation energy of step 1 is assumed to be zero, the bond dissociation energy, D(R-O_2). will be equal to the activation energy of step 2. The observed activation energy of 12 kcal. probably is too low for the dissociation energy of this bond.

It might be further argued that if ($RO_2\cdot$ + R·) or (R· + R′·) are spatially in a position to react, the combination of two peroxy radicals should be more favorable in view of the observed relative rates of (1) and (2) and the added length of the (–O–O·) group.

In their studies of the effect of various gases on irradiated PVC, Kuri, *et al.*,[5] have proposed the mechanism

$$r\cdot + O_2 \longrightarrow rO_2\cdot \quad (1)$$
$$rO_2\cdot + O_2 \longrightarrow r{=}O \quad (2)$$

It is not clear what the other reaction products of (2) should be but the method of pairing the un-

(5) Z. Kuri H. Ueda and S. Shida, *J. Chem. Phys.*, **32**, 371 (1960).

paired spin is not apparent. If they were small radicals, such as OH·, this scheme would give the required mobility to the unpaired electron. These more reactive mobile radicals would not be present in sufficient quantity for e.s.r. detection. However, the fact that $RO_2\cdot$ decays both in air and *in vacuo* indicates that the rate-controlling step does not require O_2.

Dr. W. G. Lloyd has suggested[6] that the rate-controlling step might be a pseudo first-order reaction between the peroxy radical and the substrate to form a hydroperoxide plus an alkyl radical. The steps in the decay of the alkyl radical through peroxy formation would be

$$R\cdot + O_2 \longrightarrow RO_2\cdot \text{ (fast)} \quad (1)$$

$$RO_2\cdot + R'H \xrightarrow{k} ROOH + R'\cdot \quad (2)$$

$$R'\cdot + O_2 \longrightarrow R'O_2\cdot \text{ (fast)} \quad (3)$$

$$2R'\cdot \longrightarrow \text{non-radical products (fast)} \quad (4)$$

Analogous reactions,[7] in which R = R′ = H, indicate that the hydrogen abstraction reaction is energetically more favorable than the decomposition of the peroxy radical.

This mechanism would picture the peroxy site moving through the polymer by means of step 2 leaving a trail of hydroperoxide groups until such radicals came close enough to react. The experimental data are consistent with the proposed mechanism: (1) peroxy radical formation (steps 1 and 3) is shown to be fast relative to its decay; (2) the peroxy radical reverts to an alkyl radical in the absence of air; (3) the observed activation energy is within the range of values reported for hydrogen abstraction mechanisms.[8] It is also in harmony with the observations of Lawton, *et al.*,[9] who, in their studies of the reaction of irradiated polyethylene radicals with oxygen, found that the ratio of the total amount of oxygen reacted to polymer radicals was five to one. In an irradiated polymer, most of the radical sites are expected to exist as near neighbors rather than as randomly distributed sites.[10,11] Therefore the hydroperoxide radical ratio is not expected to be very large. The autoöxidation chain length for butadiene rubber, for instance, is reported to be 8–10, while under similar conditions the chain length for tetralin (liquid) is about 400.[12] If the radicals are more randomly distributed as might be expected in the case of an irradiated liquid, a larger ratio is expected.

If the proposed mechanism is correct, it can be shown that the total peroxy as observed by e.s.r. is

$$RO_2\cdot = RO_2\cdot\, e^{-kt} \sum_{n=0}^{n} \frac{(kt)^n}{n!}$$

where $(n + 1)$ is the number of times steps 2 and 3 occur before step 4 terminates the autoöxidative chain. $RO_2\cdot$ represents all of the peroxy radicals except the one represented in step 4 and k is the pseudo first-order rate constant of step 2.

If termination is restricted to isolated near-neighbor radicals, the average n will be constant over the reaction period. Since the distances between near neighbors is expected to be small, n will also be small so that a n approaches zero the reaction appears first order in peroxy radical. A comparison of the rates of peroxy radical decay in air and *in vacuo* indicates an average chain length of 1.5 per radical although simultaneous gas and free radical measurements made in this Laboratory indicate three molecules of oxygen are consumed per peroxy radical.

Conclusion

It is concluded that the rate of formation is diffusion controlled. When the particle size is sufficiently small, the rate of formation of peroxy radical is much faster than its decay. The experimental results are consistent with an autoöxidative scheme in which the decay rate-controlling step is the abstraction of hydrogen from the polymer substrate to leave an alkyl radical. This mobility allows the previously immobilized near-neighbor radical sites to pair off unpaired electrons.

Acknowledgments.—The author wishes to express his appreciation for the aid of Dr. Clifford Thompson, whose interest and advice helped to initiate and continue this work, and also to thank Dr. J. P. Heeschen and Dr. W. G. Lloyd for helpful advice and criticism.

(6) W. G. Lloyd, private communication.

(7) From P. Gray, *Trans. Faraday Soc.*, **55**, 408 (1959)

	Enthalpy increase kcal./mole.
$HO_2\cdot \rightarrow H\cdot + O_2$	47.2 ± 4
$HO_2\cdot + H_2 \rightarrow H_2O_2 + H\cdot$	14.7 ± 4

The abstraction reaction in this case is energetically more favorable by 32.5 kcal./mole.

(8) E. W. R. Steacie, "Atomic and Free Radical Reaction," Reinhold Publ. Corp., New York, N. Y.

(9) E. J. Lawton, R. S. Powell and J. S. Balwit, *J. Polymer Sci.*, **32**, 285 (1958)

(10) A. A. Miller, E. J. Lawton and J. S. Balwit, *ibid.*, **14**, 503 (1954).

(11) B. R. Loy, *ibid.*, **44**, 341 (1960).

(12) L. G. Angert and A. S. Kuzminskii, *ibid.*, **32**, 1 (1958).

THE EFFECT OF PRETREATMENT ON THE ADSORPTION AND DESORPTION OF WATER VAPOR BY LITHIUM AND CALCIUM KAOLINITE[1]

BY J. J. JURINAK

Department of Soils and Plant Nutrition, University of California, Davis, California

Received May 16, 1960

The adsorption and desorption of water vapor by lithium and calcium kaolinite degassed at 33, 70, 100 and 205° was studied. Li-kaolinite degassed at 33 and 70° resulted in the reversible adsorption–desorption of water vapor. Hysteresis became prevalent at the higher degassing temperatures. Reversible dehydroxylation was considered initiated at 205°. Ca-kaolinite adsorbed more water and hysteresis was noted at all pretreatment levels. Factors considered important in the variability of water adsorption by Li- and Ca-kaolinite, in the degassing temperature range studied, are ionic hydration, particle coalescence and surface dehydroxylation.

Introduction

Previous studies have indicated that, following the dehydration of a lithium-saturated kaolinite, the adsorbed lithium ions have no apparent effect on subsequent water adsorption.[2] This property has been attributed to the small ionic size of lithium which permits the unhydrated ion to fit into the surface structure thus becoming sterically hindered from interaction with water vapor. Recent investigations,[3,4] however, have indicated that this view may be oversimplified. Despite the uncertain relation of the lithium ion with kaolinite the attraction of this system as a reference for adsorption studies increases the need for data concerning the availability and stability of Li-kaolinite with regard to the water molecule, particularly in the monolayer region. This paper presents the results of the effect of degassing temperature on the adsorption and desorption of water vapor by lithium kaolinite as compared with a similarly treated calcium kaolinite.

Experimental Methods

The kaolinite was from Dry Branch, Georgia, and was donated by the Georgia Kaolinite Company. X-Ray diffraction analysis showed no visible montmorillonitic contamination which would indicate a minimum purity of about 95%. The exchange capacity was determined as 1.5 meq./100 g. with regard to the lithium as well as the sodium ion which further suggested a minimal, if any, contamination by montmorillonite. The surface area was determined by *n*-butane adsorption at 0.0° and was calculated as 15.0 m.²/g. The kaolinite was saturated with lithium by washing with normal lithium chloride at *p*H 6.8 until the leachate contained only lithium ions and then washed free of chlorides with 95% ethyl alcohol. A similar method was used for calcium kaolinite, except the *p*H of the normal calcium chloride was 6.1. The clay was air-dried, crushed, and the 0.5–1.0 mm. aggregate fraction retained. This material represented the initial state of clay samples used in this study.

The adsorption apparatus has been described previously[5] except that the volume ratio of the manometer to the capillary arm of the Pearson gauge has been modified to give a pressure magnification of better than 50 times. The low pressure equilibrium readings were obtained by the previously described compression method,[6] whereby, after equilibrium is reached between the sample and vapor, the stopcock to the adsorption chamber is closed and the equilibrium vapor is compressed by filling the gas buret with mercury. The resultant pressure is read and the initial equilibrium pressure is calculated, using the ideal gas law. The compression coupled with the Pearson gauge yielded a magnification factor of better than 2000 to the equilibrium pressure with little uncertainty. Pressure as low as $7.6 \times 10^{-4} \pm 3.8 \times 10^{-4}$ mm. could be read. Approximately 2–3 grams of clay were placed in the removable adsorption chamber and the isotherms were determined volumetrically. An agreement of 2–4% was obtained when calculations were checked gravimetrically by periodic weighing of the adsorption chamber plus sample.

The degassing temperatures used in this study were 33, 70, 100 and 205 ± 2° and were maintained by use of a portable furnace. The weight loss associated with each degassing treatment was determined by removing the adsorption chamber from the system and weighing. Duplicate samples were reproducible within ± 0.3 mg. Both the water and *n*-butane in this study were degassed thoroughly by repeated freezing and thawing under vacuum. Adsorption and desorption were carried out at 29.45 ± 0.05°.

Results

Figures 1 and 2 (curve A) show the adsorption and desorption of water vapor by Li-kaolinite degassed for 48 hours at 10^{-6} mm. pressure at the designated temperatures. Pretreatment at 33 and 70° resulted in identical adsorption–desorption isotherms with no hysteresis noted at either pretreatment level. As the degassing temperature was raised to 100°, the adsorption of water decreased and hysteresis became prevalent. Increasing the temperature to 205° not only increased the adsorption of water over the 100° treatment but also changed the nature of the hysteresis curve. The data shown at each temperature are a composite of two or more independently run samples indicating the reproducibility of the system. Figure 3 shows the adsorption of water vapor by Ca-kaolinite which had been degassed in a manner similar to Li-kaolinite. Samples degassed at all four temperatures produced hysteresis upon desorption. The data are not shown. At all pretreatment levels the adsorption of water by Ca-kaolinite was greater than Li-kaolinite. The effect of degassing temperature on *n*-butane adsorption is shown in Fig. 4. The data are a composite of 4 adsorption–desorption cycles by Li-kaolinite which has been degassed at 33, 70, 100 and 205°. No indication of pretreatment effect was noted. A summary comparing the pretreatment effect on the adsorption of water by Li- and Ca-kaolinite is shown in Fig. 5. The primary mechanism considered responsible for the adsorption variability is designated in its appropriate temperature range. Table I gives the total volatile weight loss recorded

(1) Support of this work by a grant (NSF-G10228) from the National Science Foundation is gratefully acknowledged.

(2) (a) A. G. Keenan, R. W. Mooney and L. A. Wood, THIS JOURNAL, **55**, 1462 (1951); (b) R. T. Martin, "Clays and Clay Minerals," monograph #2, Pergamon Press, New York, N. Y., 1959, p. 259.

(3) G. H. Cashen, *Faraday Soc. Trans.*, **55**, 477 (1959).

(4) R. Greene-Kelley, THIS JOURNAL, **59**, 1151 (1955).

(5) F. A. Bettleheim, C. Sterling and D. H. Volman, *J. Polymer Sci.*, **22**, 303 (1956).

(6) J. J. Jurinak and D. H. Volman, *Soil Sci.*, **88**, 6 (1957).

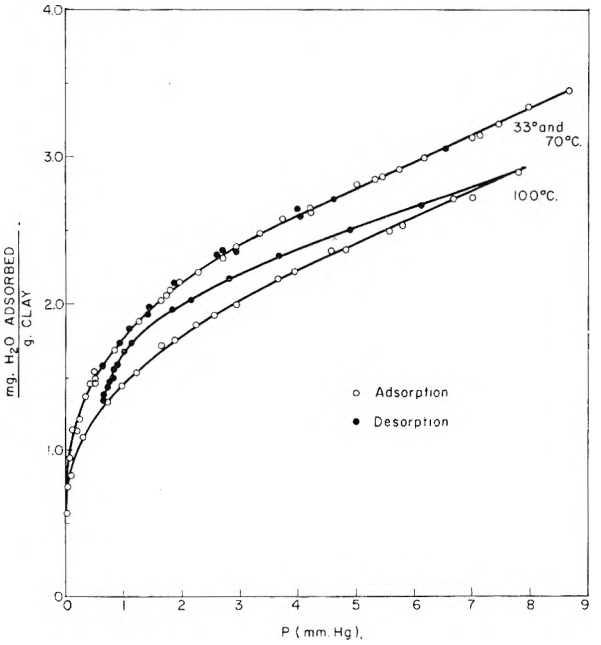

Fig. 1.—Adsorption–desorption isotherms of water vapor at 29.45° by lithium kaolinite degassed at various temperatures.

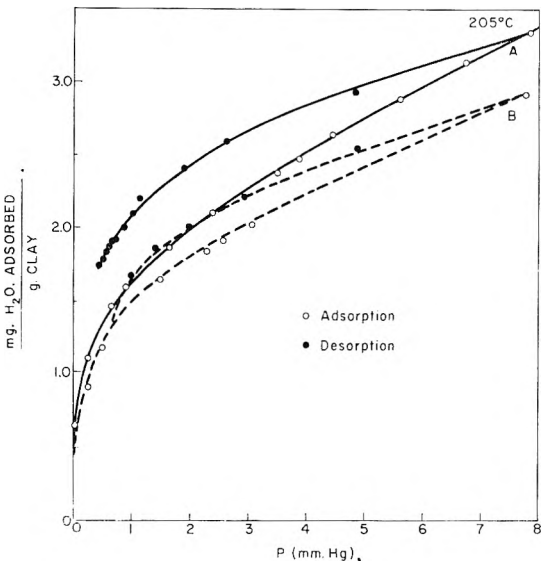

Fig. 2.—Adsorption–desorption isotherm of water vapor at 29.45° by lithium kaolinite degassed at 205° (curve A). Curve B is the adsorption–desorption data of hydroxylated lithium kaolinite degassed at 100° as compared with the corresponding system in Fig. 1 (dash line).

at each degassing temperature and the *p*H of a 1 to 5 clay–water suspension after 24 hours of equilibration.

TABLE I

PRETREATMENT EFFECT ON SAMPLE WEIGHT LOSS AND *p*H

Degassing temp., °C.	Lithium kaolinite Total wt. loss,[a] mg.	*p*H	Calcium kaolinite Total wt. loss,[a] mg.	*p*H
33	16.2	6.80	16.8	6.13
70	17.2	6.80	18.9	6.12
100	17.2	6.45	19.9	6.37
205	20.3	5.35	22.8	6.63

[a] Based on 2-g. sample.

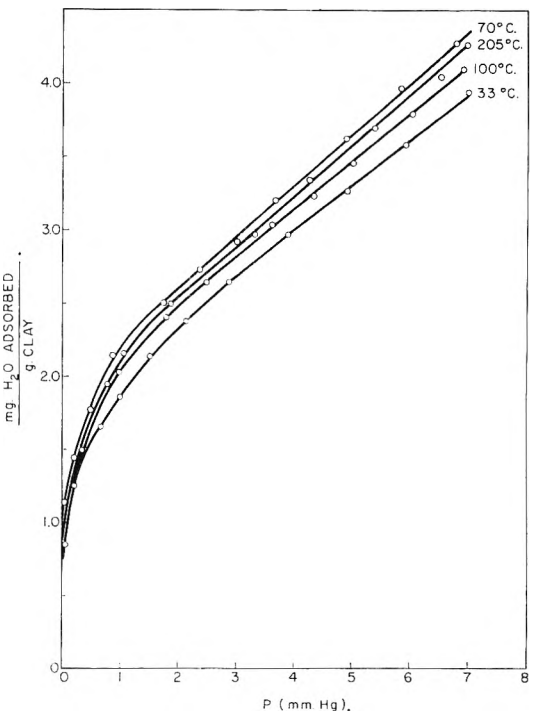

Fig. 3.—Adsorption of water vapor at 29.45° by calcium kaolinite degassed at various temperatures.

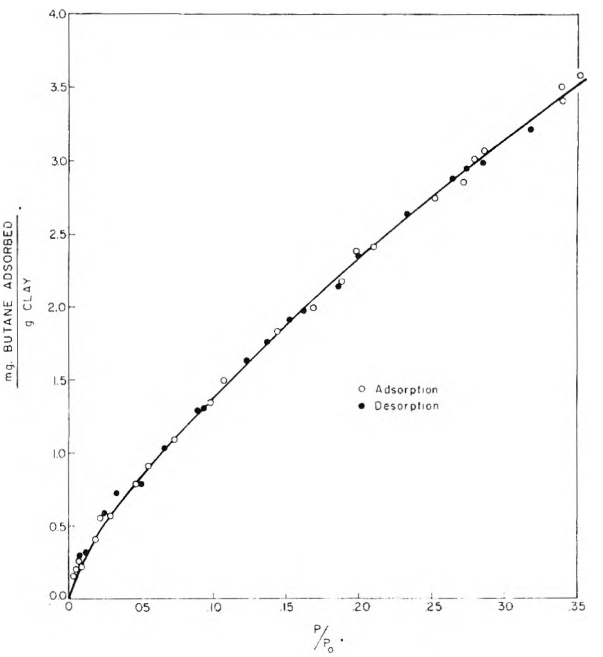

Fig. 4.—Composite adsorption–desorption isotherm of *n*-butane at 0.0° by lithium kaolinite degassed at 33, 70, 100 and 205°.

Discussion

The data in this study are explained on the basis of the difference in the relation of the adsorbed cation with the surface, which in turn depends largely on the relative ionic radii of the cation, *i.e.*, 0.60 and 0.99 Å. for lithium and calcium, respectively.[7]

(7) L. Pauling, "The Nature of the Chemical Bond," Cornell Univ. Press, Ithaca, N. Y., 1948, p. 346.

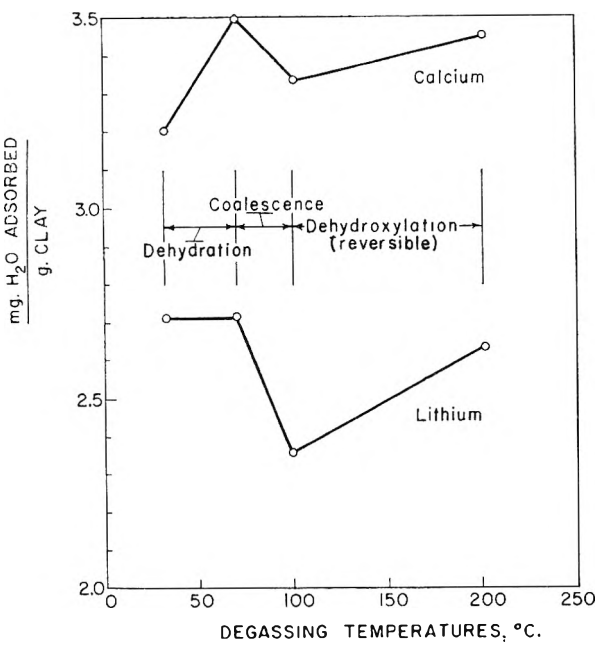

Fig. 5.—Summary diagram comparing the effect of de gassing temperature on the adsorption of water vapor by lithium and calcium kaolinite at P = 4.60 mm. The factors considered important in the variability of water adsorption with degassing temperature are designated in their appropriate temperature range.

The adsorption data for Li-kaolinite shown in Fig. 1 indicate that even degassing at 33° has dehydrated the lithium ion and allowed it to react with the kaolinite in a manner which has no effect on water adsorption. Subsequent degassing at 70°, although some weight loss occurred, did not alter the adsorption of water. This constant adsorption capacity coupled with the complete lack of hysteresis at both degassing temperatures strongly suggest the absence of ionic hydration in water adsorption in the pretreatment range of 33–70°. A contrast to these data was found in the Ca-kaolinite system (Fig. 3) where semi-hydrated calcium ion is considered to be adsorbed on the surface and available to react with water vapor. Although considerable water is removed during degassing at 33° (Table I), sufficient moisture is still associated with the calcium ion to reduce its adsorption capacity. The removal of additional water, by degassing at 70°, induces increased adsorption which is as expected if ion hydration exists. The presence of hysteresis at both lower degassing levels in the calcium system also supports the view of ion hydration. The decrease in water adsorption as shown by both lithium and calcium systems when degassing occurs at 100° is ascribed to particle coalescence. The appearance of hysteresis in the lithium system and the lack of sample weight loss when the degassing temperature was raised from 70 to 100° support this contention. The smaller coalescence effect in the calcium system is explained either by competitive hydration of the calcium ion as additional water is removed or to the protrusion of the calcium ion on the surface which hinders the union of individual clay platelets. These results are in line with the data presented by Martin[8] which showed that prolonged aging of Li-kaolinite, under vacuum, resulted in particle coalescence and reduced water adsorption. The substitution of Cs for Li as the exchangeable ion produced only a slight coalescence.

A degassing temperature of 205° resulted in greater water adsorption in both systems. The increase in adsorption by Li-kaolinite coupled with the hysteresis curve change (Fig. 2, curve A) and weight loss of the sample suggested that the 205° pretreatment initiated surface dehydroxylation and the addition of water resulted in hydroxylation of the surface. Evidence of this reaction and its reversibility was obtained by taking the hydroxylated sample of curve A, degassing it for 48 hours at 100° then measuring an adsorption–desorption cycle of water. The data are shown in Fig. 2, curve B, and indicate the reversible nature of the proposed reaction. The dash line is the adsorption–desorption curve taken from Fig. 1.

The question arose whether the surface variability as shown by water adsorption is reflected by the adsorption of *n*-butane. Figure 4 shows the inertness of *n*-butane adsorption to pretreatment and indicates that the surface of Li-kaolinite available to the *n*-butane molecule (44 Å.^{2}) is unchanged in the temperature range studied. The data of Gregg and Stephens,[9] using oxygen as the adsorbate, showed a decrease in the surface area of kaolinite when the outgassing temperature was varied from 50 to 100°. The area remained constant until the outgassing temperature reached 200° or greater, then a continual downward trend in area was noted. Nitrogen adsorption showed a more general continual decrease in the low outgassing temperature range. These data along with the results of this study suggest that the postulated coalescence of kaolinite manifests itself in the alteration of the microstructure of the system and hence is sensitive to the adsorbate's dimensions.

Figure 5 summarizes the adsorption variability of Li- and Ca-kaolinite as well as the mechanisms involved as a function of degassing temperature. The over-all greater water adsorption by Ca-kaolinite is ascribed to ion hydration, since at least in the dehydrated state the surface area of kaolinite is independent of exchangeable cation.[1] A further indication of the difference in which lithium and calcium ion react with kaolinite is shown by the suspension *p*H given in Table I. Although this *p*H variation has been previously noted,[3] the definite cause remains to be studied.

(8) R. T. Martin, "Clays and Clay Minerals," Nat. Acad. Sci. Nat. Res. Council Pub. 566, p. 23, 1958.

(9) S. J. Gregg and M. J. Stephens, *J. Chem. Soc.*, 3951 (1953).

THERMAL EXPANSION OF ROCK SALT[1]

BY THOR RUBIN, H. L. JOHNSTON AND HOWARD W. ALTMAN

Cryogenic Laboratory of the Chemistry Department, The Ohio State University, Columbus 10, Ohio

Received June 3, 1960

Interferometric determinations of the expansion coefficient of synthetic rock salt were made from 20 to 300°K. Similar measurements for natural rock salt were made from 90 to 300°K. Derivatives for the expansion coefficient were calculated at a variety of temperatures. Grüneisen coefficients were computed as a function of temperatures using measured compressibilities and both measured heat capacities and those computed from Kellerman's frequency spectrum. A correlation of these Grüneisen coefficients with those expected from a nearest neighbor cubic closest packed structure and for a sodium chloride type lattice has been made.

Introduction

The apparatus and experimental technique for determination of expansion coefficients of synthetic rock salt were the same as those described for copper.[2]

The natural rock salt data were determined by a relative method using natural quartz, as a fiduciary material. Here a count of linear interference lines passing a fiduciary mark were measured over a temperature interval. Linear interpolation of the apparent position of interference line at the final temperature, and at the initial temperature was made wherever the total number of fringes passing a fiducial point was not integral.

The synthetic rock salt was obtained from the Harshaw Chemical Company. Natural rock salt was obtained from Cincinnati Chemical Company. No chemical analyses were made. The samples of each material were cut into pillars adjusted to the same length by careful filing. These sets of pillars served as separators between the interference plates. At the completion of the measurements, the samples contained a few cracks which were not present at their preparation.

Results

The data for natural rock salt are shown in Table I. For calculation of the absolute values of the expansion coefficients, coefficients for quartz, determined by Buffington and Latimer,[3] were used. Alpha is the expansion coefficient determined graphically, T_{avg} is the mean absolute temperature and ΔT is the temperature interval of the measurement. These measurements were based on the temperatures read from a standardized thermocouple.

The absolute values for the expansion coefficients of synthetic rock salt are given in Table II. In this table r_1^2, r_2^2 are the squares of the apparent fringe diameter at temperature equilibrium, measured with a filar micrometer eyepiece. The optical constant is a measure of the change of the square of the fringe diameter by an increase of one fringe order, actual values of this quantity are shown in the table, column 5. Smoothed values of this quantity, marked O', are shown in column 4, F is the number of fringes passing a fiduciary mark during the temperature change ΔT, α is the coefficient of expansion, the last column gives the temperature derivative of α. l_0 is the length of the sample at 25°. T°K. average is the mean of the initial and final temperature of a determination.

TABLE I

NATURAL ROCK SALT

l_0 = 1.113 cm., l_0 quartz = 1.099 cm.

$\Delta l \times 10^4$	ΔT	$\frac{1}{l_0}\frac{dl}{dT} \times 10^5$	Quartz corr.	T avg., °K.	First divided dift. $\alpha \times 10^5$
2.417	10.99	2.1987	0.330	92.30	2.245
2.186	9.10	2.3970	.344	102.36	2.462
2.401	9.34	2.5703	.378	111.59	2.649
2.296	8.89	2.5827	.377	111.35	2.659
3.973	14.36	2.7663	.414	122.88	2.857
4.435	15.03	2.9510	.456	137.86	3.061
4.522	14.66	3.0854	.495	152.42	3.217
4.499	14.59	3.0830	.496	152.69	3.215
4.595	14.46	3.1784	.531	167.21	3.333
5.160	15.91	3.2429	.567	182.40	3.423
7.021	21.74	3.2299	.577	178.15	3.402
7.280	21.72	3.3519	.608	199.95	3.558
7.358	21.64	3.4001	.650	218.38	3.639
7.120	20.60	3.4553	.699	239.51	3.732
6.939	19.79	3.5067	.747	259.71	3.822
7.280	20.10	....	.794	279.65	3.968

Measurements marked # in Table II were made by using a standard thermocouple alone. The rest of the results were obtained by using the standard thermocouple in conjunction with a precise resistance thermometer. The resistance thermometer–temperature data were smoothed and tabulated at equal temperature intervals above 30°K. These data then were used to calculate the temperature intervals, ΔT. The thermocouple was calibrated in terms of the Ohio State University Cryogenic Laboratory temperature scale.[4] The runs marked 93 to 104 inclusive and 107 to 118 inclusive were obtained in such a manner that the temperature–length point of one run formed the beginning length point of the next one. The remainder of the data were separate points.

Since the interpolation of the fringe number requires values of the parameter O be known, smoothed values, O', were computed first in order that the effects of random errors be minimized. This was done in the following way: O is inversely proportional to the product of the length of the sample and the refractive index of the helium in the cell. The index of refraction is that for a pressure of 1.3 cm. of helium at room temperature. Since

(1) This work was supported in part by the Air Material Command, Wright Field. Presented in part at the Colorimetric Conference, Chicago, Sept. 1959.

(2) T. Rubin, H. W. Altman and H. L. Johnston, *J. Am. Chem. Soc.*, **76**, 52 (1954).

(3) R. M. Buffington and W. Latimer, *J. Am. Chem. Soc.*, **48**, 2305 (1926).

(4) T. Rubin, H. L. Johnston and H. Altman, *ibid.*, **73**, 3401 (1951).

TABLE II

SYNTHETIC ROCK SALT, l_0 = 0.5570 cm.

Run	ΔT	T, avg., °K.	O' Smoothed	O	τ_1^2	τ_2^2	F	$\alpha \times 10^5$	$\frac{\partial \alpha}{\partial T} \times 10^8$
93	13.215	84.342	28.3	28.1	24.651	37.515	5.4563	2.184	20.6
94	13.720	97.81	28.3	27.8	37.515	48.651	6.3935	2.455	21.1
95	14.414	111.88	28.25	28.1	48.651	33.062	7.4482	2.735	16.5
96	14.530	126.35	28.20	28.7	33.062	35.880	8.0999	2.949	13.4
98	16.212	141.72	28.20	28.3	35.880	25.150	9.6195	3.137	11.8
99	20.248	159.97	28.10	28.2	25.150	44.689	12.6953	3.315	7.3
100	20.082	180.12	28.10	27.7	44.689	47.886	13.1138	3.455	5.3
101	25.183	202.80	28.10	27.4	47.886	50.268	17.0848	3.588	6.2
102	29.746	230.21	28.0	27.6	50.268	49.491	20.9723	3.728	4.4
103	29.746	259.95	27.9	27.9	49.491	37.210	21.5598	3.838	0.7
104	29.841	289.73	27.9	27.9	37.210	48.650	22.4100	3.970	5.7
106	10.48	95.57	...	..	.....	.....	4.7757	2.411	..
107	10.354	26.473‡		28.0	23.620	32.547	3.3154	0.156	20.9
108	9.512	36.41	28.30	28.2	32.547	25.908	0.7654	0.422	29.1
109	7.396	44.86	28.30	28.2	25.908	26.419	1.0181	0.728	43.5
110	8.364	52.74	28.30	28.5	26.419	45.495	1.6741	1.089	42.2
111	8.421	61.13	28.30	28.7	45.495	23.619	2.2270	1.398	36.0
112	8.440	69.56	28.30	28.3	23.619	44.422	2.7351	1.715	36.3
113	7.167	77.37	28.30	28.0	44.422	34.222	2.6396	1.949	24.9
114	12.271	74.83	28.30	28.3	19.448	29.921	4.3714	1.886	..
115	11.685	86.80	28.30	28.0	29.921	27.510	4.9139	2.226	..
49	8.48	19.84‡		28.4	6.864	9.120	0.0794	0.048	..
50	6.92	27.49‡		28.5	5.808	12.350	0.2295	0.176	..
43	9.69	29.05‡		27.6	11.760	22.180	0.3767	0.201	..
51	6.44	34.71‡		28.4	12.350	27.820	0.5447	0.375	..

the cell volume contains most of the gas, the refractive index is thus independent of temperatures and is almost equal to 1.0000. This is because the amount of helium is so small that the refractive index is essentially equal to the value for a vacuum. Thus the optic constant varies with the inverse of the sample length. Values of O were picked at values of the reciprocal of the sample length corresponding to each mean temperature. These are the O' values shown in the table.

Since most of these data may be regarded as continuous sets of length (on an arbitrary scale)–temperature measurements at unequal temperature intervals—first and second temperature derivatives of length were computed from them by the method of divided differences.[5,6] These derivatives were computed at the mean temperature of each interval. Division of the derivatives by l_0 yields the values of α and $\partial\alpha/\partial\tau$ previously mentioned. For α, calculations of divided differences to the fourth order were used. Calculation of $\partial\alpha/\partial\tau$ required divided differences up to the sixth order. Sodium D radiation was used for all the interference measurements.

Errors.—The absolute temperatures are accurate to about 0.03°K. Temperature intervals measured by the thermocouple alone are precise to about 0.02°. Those intervals measured in terms of the resistance thermometer are precise to a few thousandths of a degree.

For the synthetic rock salt, the error in a length measurement is 0.007 fringe order which is the error in values of F.

(5) F. A. Willers, "Practical Analysis," translated by R. T. Beyer, Dover Publications, Inc., 1947, p. 77.

(6) J. B. Scarbrough, "Numerical Mathematical Analyses," Johns Hopkins Press, Baltimore, Md., 1930, p. 115.

Buffington and Latimer[3] have determined the expansion coefficient of natural rock salt from about 120 to 300°K. The data reported here for natural rock salt agree with theirs within 0.3%. The results from this research are always smaller in magnitude. The expansion coefficients for natural rock salt determined in this work are consistently about 0.6% lower above 120°K. than the values of synthetic rock salt. Below 120°K. the values for natural rock salt are progressively lower, becoming about 4% at 90°K. relative to the values for synthetic rock salt.

1. Theory of Grüneisen's Relation and Comparison with Experiment.—The approximate proportionality between thermal expansion and heat capacity at constant volume (Grüneisen's relation) is justified by others[7] on the basis of a simple model which is described below. It is assumed that the partition function for a solid may be obtained with sufficient accuracy on the basis of a model in which (i) the lattice vibrations are harmonic, and (ii) the vibration frequency depends on the volume. Then the derivative of the Helmholtz free energy with respect to temperature gives a formula for the heat capacity at constant volume

$$C_v = \sum_i B_i \qquad (1)$$

while the second derivative with respect to temperature and volumes gives the ratio of the thermal expansion coefficient (α) to the compressibility (β)

$$\frac{\alpha}{\beta} = \frac{R}{V} \sum_i \gamma_i B_i \qquad (2)$$

In these formulas, $B_i = (h\gamma_i/kT)^2/\sinh^2(h\ \gamma_i/2kT)$, $\gamma_i = -\partial \ln \nu_i/\partial \ln V$, V_i is the frequency of the

(7) D. Bilz and H. Pullan, *Physica*, **21**, 285 (1955).

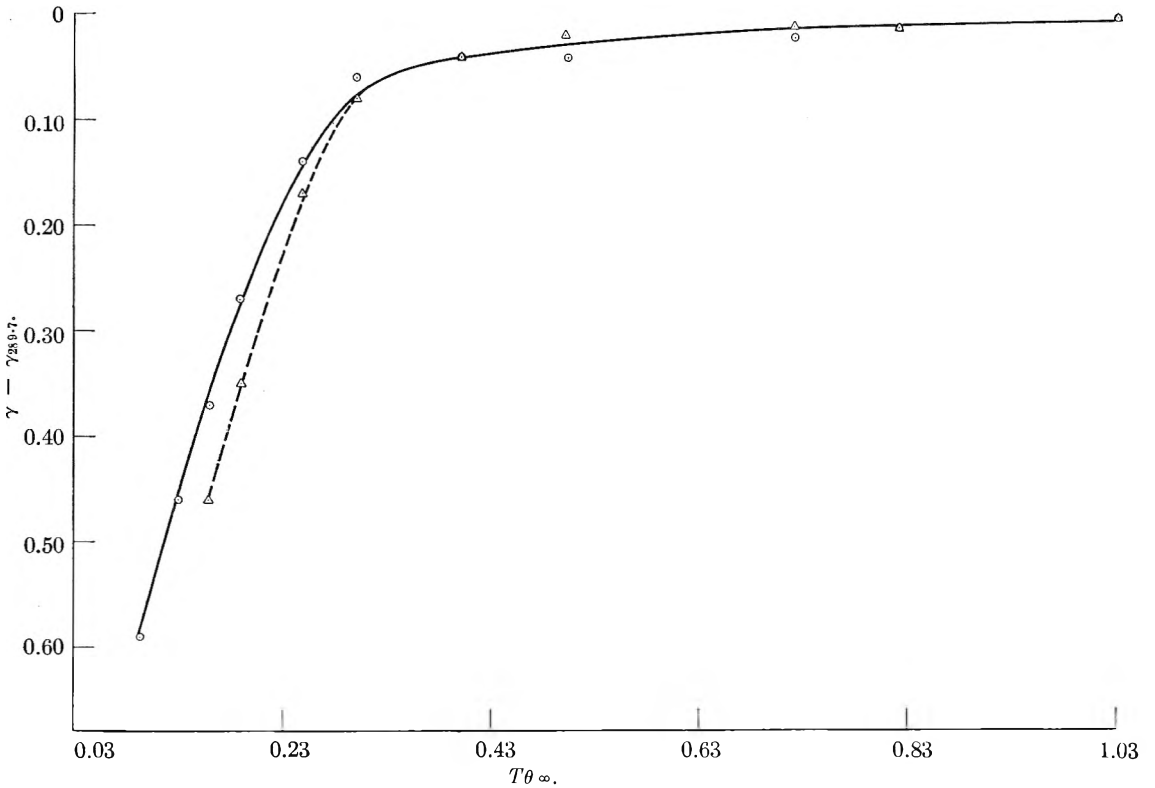

Fig. 1.—Variation of the Grüneisen parameter with temperature.

ith normal mode of vibration, R is the gas constant, V is the molar volume and the other symbols have their usual meanings.

If we define a quantity γ by the equation

$$\gamma = \frac{\sum_i \gamma_i B_i}{\sum_i B_i}$$

then from (1) and (2) it follows that

$$\frac{\alpha}{\beta} = \frac{R\gamma}{V} \sum_i B_i = Kc_v \qquad (3)$$

and $K = R\gamma/V$.

If K were constant, this equation would be the Grüneisen relation. It has been found experimentally that K is very nearly constant at room temperature and higher[8] but decreases at low temperatures.[2] A theory of the variation of γ with temperature has been developed by Barron[9] and it is of interest to compare this theory with experiment. For this purpose it is necessary first to calculate γ from the experimental data.

The results of this work together with the heat capacity results of Clausius, Goldman and Perlick[10] and the compressibilities of Rose,[11] Durand[12] and Galt[13] is sufficient for this computation over the temperature range from 20 to 300°K. The results of this calculation above 40°K. are shown in Fig. 1 as the solid line with circled points. They are expressed as the difference $\gamma - \gamma_{289.7}$. The temperature parameter, T/θ, includes a value of $\theta = 280$°K.[10] The value of R is taken as 82.054 cc. atm./mole, the density of rock salt is the room temperature value of 2.165 g./cc.

For comparison, heat capacities were calculated by graphical integration using Kellerman's frequency distribution and using Einstein functions.[14] The difference γ-$\gamma_{289.7}$ obtained from these also are shown in Fig. 1. (Dotted line with crossed points.) Most of the scatter results from uncertainties in the compressibilities.

The function γ has been expressed as a power series in T^{-1} by Barron[9,15] on the basis of two approximate models. In the first model, the frequency distribution is assumed given with sufficient accuracy by considering only the interaction between nearest neighbors in a cubic crystal whose atoms are all of equal mass. In the second model, an interionic potential for NaCl, consisting of a coulomb term and an inverse 8th power repulsion was assumed but the positive and negative ions were taken to have equal masses. For the first (nearest neighbor) model Barron found expression (4) for $\gamma - \gamma_\infty$, where γ_∞ is the high temperature limit.

$$\gamma - \gamma_\infty = -0.177\sigma^{+2} + 0.035\sigma^{+4} - 0.027\sigma^{-6} + 0.013\sigma^{+8} \qquad (4)$$

where $\sigma = h\nu_{max}/2\pi kT$ where ν_{max} is the maximum lattice vibration frequency. This constitutes the first four terms of an infinite series which converges for $\sigma < 1$ and may converge for larger values of σ.

(8) E. Grüneisen, "Handbuch der Physik," Vol. 101, Springer, Berlin, 1920.

(9) T. H. K. Barron, *Phil. Mag.*, [7] **46**, 720 (1955).

(10) K. Clausius, J. Goldman and A. Perlick, *Z. Naturforschung*, **4a**, 424 (1949).

(11) F. C. Rose, *Phys. Rev.*, **49**, 50 (1935).

(12) M. A. Durand, *ibid.*, **50**, 449 (1936).

(13) J. K. Galt, *Phys. Rev.*, **73**, 1460 (1948).

(14) "Contributions to the Thermodynamic Functions by a Planck–Einstein Oscillator in One Degree of Freedom," H. L. Johnston, L. Savedoff and Jack Beltzer.

(15) T. H. K. Barron, *Ann. Physik*, **1**, 77 (1957).

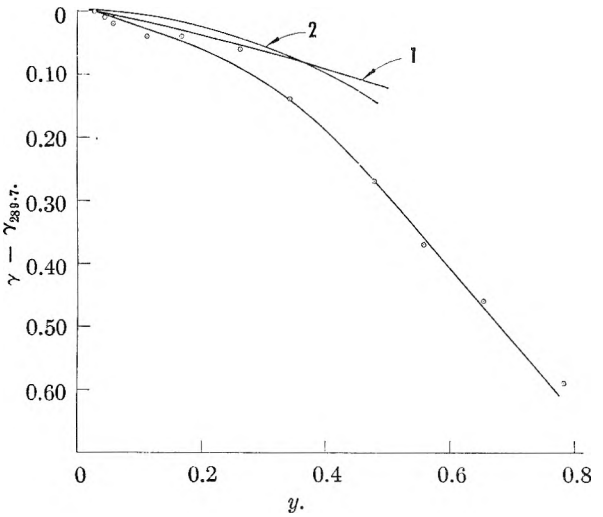

Fig. 2.—Comparison of theoretical and experimental Grüneisen parameters: 1, nearest neighbor model; 2, sodium chloride model.

It has been pointed out recently by Marruddin, Weiss and Sack[16] that the expansion of C_V in a similar series which converges for large values of σ can be made by an application of Euler's transformation.[17] In view of this result, Euler's transformation has been applied to the series of equation 4 giving the series

$$\gamma - \gamma_\infty = -y(0.177 + 0.107y + 0.069y^2 + 0.045y^3) \quad (5)$$

where $y = \sigma^2/(1 + \sigma^2)$. This new variable is a convenient one. It is employed in the subsequent discussion of the data.

(16) A. A. Marruddin, G. H. Weiss and R. Sade, Bull. Am. Phys. Soc. in Detroit, 1960.

(17) Bromwich, "Theory of Infinite Series," The Macmillan Co., New York, N. Y., 1947, pp. 62, 2nd ed.

The second model used by Barron also leads to a series expansion similar to (5) but contains fewer terms since fewer moments were evaluated. This series is

$$\gamma - \gamma_\infty = -0.62y^2 \quad (6)$$

There is a notable difference (6) and (8) in that the term linear in y is missing from equation 6. This arises because two of the moment coefficients, $\gamma(2)$, γ_∞[15] were taken by Barron to be equal and this makes the term in y vanish. y is computed from σ by means of the relation given below.[17]

A comparison between (5) and (6) with the[17] experimental data, is shown in Fig. 2 (curves 1 and 2, respectively). The variation in $\gamma - \gamma_\infty$ predicted by either model is smaller than that observed experimentally. However, the maximum values of $\gamma - \gamma_\infty$ for the nearest neighbor model has been greatly exceeded by the experimental values. This discrepancy cannot be remedied by considering the effects of more neighbors or by adjusting the values of the parameters[15] within reasonable limits.

The NaCl type model seems to be the more promising one since the curvature of the theoretical curve qualitatively appears to be about correct.

It would seem worthwhile to compute some of the higher moments for the NaCl structure so that a more reliable value of the high temperature limit, γ_∞, could be estimated as well as furnishing more terms for the series.[7,13,19,20]

It is a pleasure to acknowledge the help and encouragement offered by E. N. Lassettre of this department.

(18) G. Liebfried and W. Brendig, *Z. Physik*, **134**, 451 (1953).

(19) E. W. Kellerman, *Phil. Trans.*, **A238**, 613 (1940).

(20) E. W. Kellerman, *Proc. Roy. Soc. (London)*, **178A**, 17 (1941).

HIGH TEMPERATURE ADSORPTION STUDIES ON 13X MOLECULAR SIEVE AND OTHER POROUS SOLIDS BY PULSE FLOW TECHNIQUES[1]

By P. E. Eberly, Jr.

Esso Research Laboratories, Esso Standard, Division of Humble Oil & Refining Co., Baton Rouge, Louisiana

Received June 9, 1960

The adsorptive properties of solids at high temperatures are conveniently studied by allowing a pulse of adsorbate to be transported through a packed column of adsorbent by an inert carrier gas stream. The concentration of adsorbate in the effluent stream is continuously measured by a sensitive thermal conductivity cell. Modifications of such a technique permit the detection of an adsorption process and enable one to determine its degree of reversibility. In addition, heats of adsorption can be determined by measuring the pulse retention times at a series of temperatures. This flow method is particularly useful for studying adsorption at high temperature conditions where static methods cannot be used because of the long contact times involved which lead to decomposition of the adsorbates. In this manner, it has been found that materials such as 13X molecular sieve, silica gel, platinum on alumina and alumina itself adsorb significant quantities of benzene at temperatures as high as 427°. The adsorption capacity of 13X molecular sieve (0.632 mmole/g. at 91 mm.) at these conditions is markedly greater than those of the other adsorbents. With the exception of platinum on alumina, the adsorption is readily reversible and the heats of adsorption are typical of those ordinarily associated with a physical adsorption process. The heats of adsorption of benzene on 13X molecular sieve, silica gel and η-alumina were determined to be 15.5, 9.8 and 6.8 kcal./mole, respectively, in the range of 260–454°.

I. Introduction

In the petroleum and allied industries, many chemical reactions and separation processes involving hydrocarbons frequently are conducted in the presence of solid materials at elevated temperatures. Adsorption measurements under such conditions become of interest in elucidating the kinetics and mechanism of the reaction. Also, they are important in determining the various processes which must be taken into account in describing the mass

(1) Presented at the Southwest ACS Regional Meeting, Capitol House, Baton Rouge, Louisiana, December 3, 4 and 5, 1959.

transfer kinetics in gas–solid systems such as fixed-bed or fluidized-solids processes.

Up to the present time, however, very little information has been published on high temperature adsorption of hydrocarbons. Most of the previous experiments were conducted in static systems which limited the study to those lower temperature regions where decomposition did not occur. Hara and Ikebe,[2] however, were successful in studying the adsorption of propane on a silica–alumina catalyst up to 400°. In a series of papers, Emmett and his co-workers[3-5] reported additional studies on the adsorption of hydrocarbons on the silica–alumina catalyst. To minimize decomposition in their high temperature work, they used a flow system in which the hydrocarbon vapor was transported through a packed column of catalyst. After a steady-state had been reached, they disconnected the column and measured its weight from which they were able to calculate the amount adsorbed.

The present report describes a gas–solid chromatographic technique for studying high temperature adsorption. In such a flow system, the contact time of the hydrocarbon vapor with the solid surface can be made quite short, thereby minimizing or even eliminating decomposition reactions. Using a pulse injection technique, an adsorption process can be detected easily. Also, data on the heat of adsorption as well as the adsorption equilibrium constant can be obtained readily. Results are presented on the study of benzene adsorption on 13X molecular sieve, silica gel, alumina and platinum on alumina reforming catalyst in the temperature range of 260–454°.

II. Experimental

Apparatus.—The apparatus used for the pulse injection experiments was similar in basic design to that of a conventional gas chromatograph. Helium, the carrier gas, was allowed to flow in series through a 6-port Perkin–Elmer injection valve, the packed column, and a Perkin–Elmer thermal conductivity cell. The helium flow was accurately measured by observing the movement of a soap film through a graduated buret. The packed columns were constructed of standard 1/4" aluminum tubing (i.d. = 0.18 in.). The adsorbents were pelletized and ground to a 250 to 300 μ particle size to avoid excessive pressure drops. The packed columns were held at the desired temperature by means of a fluidized sand-bath, which was similar to that described by Adams, Gernand and Kimberlin[6] and consisted of a bed of finely divided SiO_2–Al_2O_3 catalyst (40 to 150 μ) fluidized by a stream of hot air. The bath was heated electrically and controlled to a temperature variation of no more than ±2° at the 427° level. The conductivity cell was obtained from the Perkin–Elmer Corporation and had a fast time constant of 0.5 second. It was housed in an oil-bath at an arbitrarily selected temperature of 55 ± 0.05°. A Minneapolis–Honeywell recorder having a pen speed of one second for full-scale deflection was connected to the output of the conductivity cell by a conventional bridge circuit.

Pulses, having a strictly reproducible volume, were injected into the helium stream by means of the 6-port, Perkin–Elmer injection valve. This valve is the type used in their Model 154-C vapor fractometer. The pulse volume was approximately 0.5 cc. In our experiments, the injected pulses consisted of a mixture of about 8 mole % of the hydrocarbon in a non-adsorbable gas such as argon or helium.

Detection of Irreversible Adsorption.—The pulse technique can be used to detect the occurrence of irreversible adsorption provided the process occurs at such a rate that a measurable number of molecules are adsorbed within the contact time allotted. For these experiments, a pulse consisting of a mixture of helium and the hydrocarbon is injected into the helium stream. Thus, the conductivity cell will respond only to the presence of the hydrocarbon. The area of the effluent pulse is directly proportional to the amount of hydrocarbon issuing from the column. If the pulse area obtained when flowing through the packed bed is less than that with a completely empty column, irreversible adsorption has occurred. With our particular system, the disappearance of 0.001 mmole of adsorbate from the helium stream could be detected easily. Using 20 g. of solid, this allowed the measurement of 0.00005 mmole of irreversible adsorption per gram of solid. Those adsorptions, however, which occur at a slow rate would have been beyond the limits of detection of our apparatus. The residence time in a 25 cc. packed bed was estimated to be on the order of 10 seconds at a flow rate of 50 cc./min.

In this report, the only system that exhibited any irreversible adsorption was that of benzene on platinum–alumina reforming catalyst. For the purposes of this investigation, the amount of irreversible adsorption was arbitrarily defined as the material which could not be eluted from the column within an hour's time using a flow rate of 50 cc./min.

Detection of Reversible Adsorption.—A slightly different technique is used to detect a reversible adsorption process. In this case, a pulse consisting of a mixture of argon and the hydrocarbon is injected into the helium stream. The conductivity cell will now respond to either argon (a non-adsorbable gas) or the hydrocarbon. If only one effluent pulse is recorded, it is evident that most of the hydrocarbon molecules traveled through the column at the same rate as argon and, hence, no adsorption occurred. If, on the other hand, the hydrocarbon molecules are retarded in their passage by adsorption on the surface, two peaks will result the first being that of argon and the second that of the hydrocarbon. In this manner, reversible adsorption can be observed for systems exhibiting only a very small adsorption capacity.

It has been found[7,3] that the movement of the maximum of a pulse through a packed column obeys the relation

$$\frac{L}{t_m U_e} = \frac{1}{\beta'} \qquad (1)$$

where

L = length of packed column in cm.
t_m = retention time of pulse maximum in seconds
U_e = superficial linear gas velocity in cm./sec., *i.e.*, velocity that would result if column were completely empty
β' = adsorption equilibrium constant
$= \dfrac{\text{no. of molecules ads./cm.}^3\text{ of column}}{\text{no. of molecules in gas/cm.}^3\text{ of gas}}$ at equilibrium

Equation 1 is important because it relates the chromatographic data to the adsorption equilibrium constant β'. This constant is directly proportional to the slope of the adsorption isotherm and is a true constant only for those systems having linear adsorption isotherms. In the case of Langmuir isotherms, it progressively decreases in value up to a monolayer surface coverage. Since the partial pressures normally involved in gas–solid chromatography are quite small, the value of β' as calculated from equation 1 should be expected to correspond to the limiting slope of the isotherm in the low pressure region. Eberly and Spencer[8] have shown that this is essentially the case.

As previously reported,[9,10] the constant β' can be treated

(2) N. Hara and M. Ikebe, *J. Chem. Soc. Japan, Ind. Chem. Sect.*, **56**, 120 (1953).

(3) R. C. Zabor and P. H. Emmett, *J. Am. Chem. Soc.*, **73**, 5639 (1951).

(4) D. S. MacIver, P. H. Emmett and H. S. Frank, THIS JOURNAL, **62**, 935 (1958).

(5) D. S. MacIver, R. C. Zabor and P. H. Emmett, *ibid.*, **63**, 484 (1959).

(6) C. E. Adams, M. O. Gernand and C. N. Kimberlin, Jr., *Ind. Eng. Chem.*, **46**, 2458 (1954).

(7) A. J. P. Martin and R. L. M. Synge, *Biochem. J.* (*London*), **35**, 1358 (1941).

(8) P. E. Eberly, Jr., and E. H. Spencer, in process of publication.

(9) A. J. M. Keulemans, "Gas Chromatography," Reinhold Publ. Corp., New York, N. Y., 1957.

(10) S. A. Greene and H. Pust, THIS JOURNAL, **62**, 55 (1958).

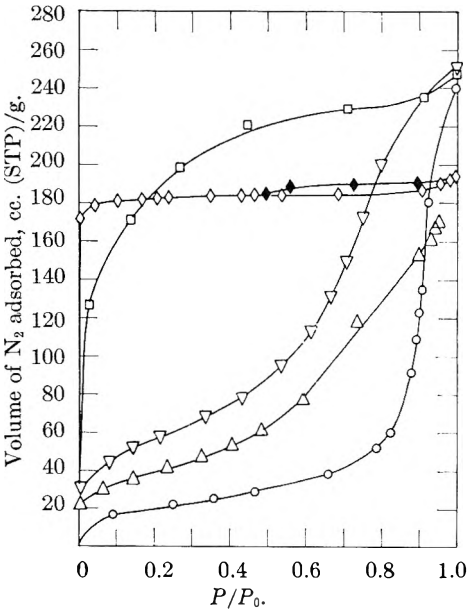

Fig. 1.—Nitrogen adsorption isotherms at −195.8°. The symbols have the following significance: ◇, 13X molecular sieve; □, silica gel; ▽, alumina; ○, alumina calcined at 980°F. for 16 hours; and △, 0.6% Pt on alumina. The dark, solid symbols represent desorption points.

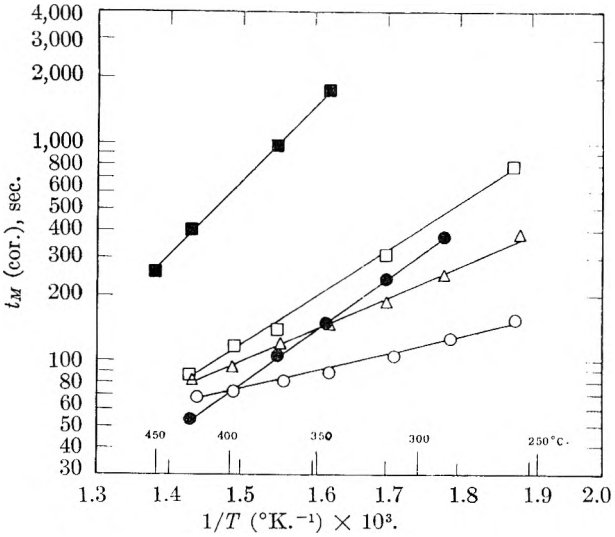

Fig. 2.—Pulse flow retention times as a function of temperature. All experiments were made with helium as the carrier gas flowing at a rate of 50 cc. (STP)/min. The adsorbents having a particle size of 250–300 μ were packed into 0.18 in. i.d. tubing. The symbols have the following significance: ■, benzene on 8.7 cm. long column of 13X; ●, *n*-hexane on 8.7 cm. long column of 13X; □, benzene on 122 cm. long column of silica gel; ○, benzene on 152 cm. long column of the calcined alumina; △, benzene on 152 cm. long column of η-alumina.

as a thermodynamic equilibrium constant and by making the appropriate substitution, equation (2) can be obtained.

$$\log t_M(\text{cor.}) = C - \frac{\Delta H}{2.303R}\frac{1}{T} \qquad (2)$$

where t_M(cor.) represents the observed retention time corrected to 25° and atmospheric pressure in the manner described by Green and Pust.[10] The constant C is a function of the entropy of adsorption, the dimensions of the column and the carrier gas flow rate. If these factors are kept constant, then a plot of the logarithm of the corrected retention time against the reciprocal of the absolute temperature $1/T$ should yield a straight line the slope of which is proportional to the heat of adsorption.

This method is of great value because it represents about the only way in which heats of adsorption can be conveniently measured at high temperatures. The heats of adsorption obtained in this manner are believed to be average values over the range of partial pressures involved. Since the partial pressures of hydrocarbon in the present work were on the order of 1 mm. or less, the heats of adsorption should correspond to those at very low surface coverage. Green and Pust,[10] working at lower temperatures, found good agreement between the heats of adsorption evaluated in this way and those obtained calorimetrically and isosterically.

Materials.—The silica gel and 0.6% Pt on alumina catalyst were obtained from the Davison Chemical Co. The alumina was supplied by the National Aluminate Corporation and consisted essentially of the η-crystalline phase. A portion of this alumina was calcined at 980° for a period of 16 hours. X-Ray diffraction patterns indicated that the calcined alumina contained approximately 20% of the α-Al_2O_3 crystalline phase. The 13X molecular sieve was obtained from Linde Air Products Co. in powder form. The solids existing in powder form were first pelleted and then ground to obtain material in the 250–300 μ particle size range.

Nitrogen adsorption isotherms for these materials at −195.8° are shown in Fig. 1. Pore volumes were determined by measuring the amount of nitrogen adsorbed at saturation pressure. These are listed in Table I together with the calculated B.E.T. surface areas.

The benzene used in this investigation was the reagent grade available from J. T. Baker Chemical Co. The *n*-hexane was the research grade hydrocarbon supplied by Phillips Petroleum Company. Both of these were used without any further purification.

The gases were commercially available. The purities of the helium and argon were 99.99 and 99.995%, respectively. These gases were used as such and no attempt was made for further purification.

III. Results

Table II lists the data obtained with the five different columns of adsorbent. In each case, helium gas was flushed through the column for a period of 16 hours at 427° before the experimental measurements were taken. The amount of material adsorbed at the indicated partial pressures was determined by a continuous flow method reported previously.[11] No decomposition was observed in

TABLE I

ADSORBENT PROPERTIES

Adsorbent	B.E.T. area, $m.^2/g.$	Pore volume, cc./g.
13X molecular sieve[a]	760	0.32
Silica gel	649	.38
Alumina	192	.39
Calcined alumina[b]	69	.37
0.6% Pt on alumina	139	.42

[a] Data were calculated from the isotherm by use of the B.E.T. equation for narrow capillaries (S. Brunauer, P. H. Emmett and E. Teller, *J. Am. Chem. Soc.*, 60, 309 (1938)). [b] Heated to 980° for 16 hours.

any of these runs. This was indicated by a lack of irregularity in the shape of the effluent peak. Also, in the independent measurements in which a continuous flow of hydrocarbon was passed through the column, no decomposition products were observed in a sample of the effluent vapor collected in a liquid nitrogen trap.

With all the solids except the 0.6% Pt on alumina, two distinct and separate peaks were observed. The first corresponded to that of the unadsorbed argon and the second to that of the hydrocarbon. The time difference between the two peaks is listed

(11) P. E. Eberly, Jr., and C. N. Kimberlin, Jr., *Trans. Faraday Soc.*

TABLE II

CHROMATOGRAPHIC DATA WITH VARIOUS ADSORBENT COLUMNS AT 427°[a]

Adsorbent[b]	Column length,[c] cm.	Adsorbate	Difference in retention time of argon and hydrocarbon peak, t_m in sec.	Amount adsorbed, mmoles/g.[d]
13X molecular sieve	8.7	Benzene	186	0.632 at 91 mm.
13X molecular sieve	8.7	*n*-Hexane	25	.....
Silica gel	122.0	Benzene	39	0.053 at 62 mm.
Alumina	152.0	Benzene	29.4	.....
Calcined alumina[e]	152.0	Benzene	17	0.007 at 62 mm.
0.6% Pt on alumina	152.0	Benzene	No hydrocarbon peak obsd.	Rev. 0.042 Irr. 0.02 at 92 mm.

[a] The carrier gas was helium flowing at a rate of 50 cc. (STP)/min. [b] The particle size of the adsorbent was between 250 to 300 μ. [c] Columns were constructed of aluminum tubing having an i.d. = 0.18 in. [d] The amount adsorbed was determined from independent experiments using continuous flow methods as described by Eberly and Kimberlin.[11] [e] Heated to 980° for 16 hours.

in the fourth column. The hydrocarbon retention clearly illustrates the existence of a reversible type of adsorption at this comparatively high temperature. The 13X molecular sieve exhibits an extraordinarily large adsorptive capacity. A 186 second time difference was observed with a column only 8.7 cm. in length. With both silica gel and the aluminas, much longer columns had to be constructed in order to get a detectable time difference between the argon and hydrocarbon pulses. The effect of calcination on the alumina is illustrated by its extremely short retention time and its low capacity for benzene.

The platinum–alumina reforming catalyst was the only material that showed a highly irreversible adsorption of benzene. In fact, no effluent pulse was detected even up to one hour's time with a helium flow rate of 50 cc. (STP)/min. Since the amount of this irreversible adsorption was too large to measure conveniently by the pulse flow technique, independent experiments were made using the continuous flow method reported previously.[11] With a stream containing 91 mm. partial pressure of benzene, the total amount of material adsorbed was found to be 0.062 mmole/g. Approximately two-thirds of this amount was adsorbed reversibly and was eluted easily from the column. The remaining 0.02 mmole/g. was held very tightly to the catalyst surface and represented the extent of irreversible adsorption. This accounts for the absence of an effluent peak in the pulse experiments.

When the temperature of the columns was reduced to successively lower values, it was observed that the retention times of the hydrocarbon pulse increased progressively whereas those of the argon pulse remained essentially constant. The retention times corrected in the previously described manner were found to obey the predicted relationship and increased logarithmically with the reciprocal of the absolute temperature. The data are shown in Fig. 2 and the calculated heats of adsorption are given in Table III.

The calculated heats are representative of those normally associated with a physical adsorption process. Benzene on silica gel gave a value of 9.8 kcal./mole which compares favorably with the 8.5–12.0 kcal. measured previously at much lower temperatures. The η-alumina gave a value which was about 3 kcal./mole lower than that obtained with silica gel. It is also of interest to note the decrease in energy of the alumina surface produced by the calcination process.

TABLE III

HEATS OF ADSORPTION DETERMINED FROM PULSE RETENTION TIMES

Adsorbent	Adsorbate	ΔH of adsorption, kcal./mole: This work	Other work
Silica gel	Benzene	9.8	8.5–12[b]
Alumina	Benzene	6.8	.....
Calcined alumina[a]	Benzene	3.4	.....
13X molecular sieve	Benzene	15.5	16.8[c]
13X molecular sieve	*n*-Hexane	10.8	.....

[a] Calcined at 980° for 16 hours. [b] A. A. Isirikyan and A. V. Kiselev, *Proc. Akad. Sci. U.S.S.R., Sect. Phys. Chem.*, 115, 473 (1957). [c] R. M. Berger, F. W. Bultitude and J. W. Sutherland, *Trans. Faraday Soc.*, 53, 1111 (1957).

The highest value of the heat of adsorption of benzene was obtained with the 13X molecular sieve. This is in good agreement with the 16.8 kcal./mole obtained by Barrer and his co-workers. For comparative purposes, the heat of adsorption of *n*-hexane also was determined and found to be about 5 kcal./mole less than that for benzene.

Due to the occurrence of irreversible adsorption, no attempt was made to conduct similar experiments on the platinum–alumina reforming catalyst.

IV. Discussion

The techniques described in this paper are particularly valuable for the detection of adsorption processes at high temperatures. The low contact times afforded by the flow method permit the study of adsorption without the complicating effects of decomposition frequently encountered in static systems. The method, however, can only detect those processes which occur at a sufficiently rapid rate so that a measurable number of molecules are adsorbed within the allotted contact time. The dependence of the pulse retention time upon temperature permits the evaluation of the heat of adsorption. This quantity would be extremely difficult to measure at these conditions by calorimetric or isosteric methods. The information available from the pulse flow experiment complements that from the previously reported continuous flow method so that a rather complete picture of high temperature adsorption can be obtained.

The existence of a reversible adsorption of this order of magnitude at high temperatures has not been greatly appreciated by previous investigators

in the field. This is due probably to the lack of adequate experimental facilities for measuring adsorption under these conditions. The heats of adsorption determined in the present report are similar to those normally associated with a physical adsorption process. It then becomes interesting to observe that this adsorption occurs at temperatures well in excess of the critical temperatures of benzene and *n*-hexane which are 288.5 and 234.8°, respectively. Similar phenomena, however, have been reported with other systems although not to the degree illustrated in the present paper. For instance, Morris and Maass[12] and Edwards and Maass[13] found that propylene and dimethyl ether are appreciably adsorbed on alumina at temperatures 10 to 15° in excess of the critical temperature. In fact, even multimolecular adsorption was observed.

The unusual nature of the 13X molecular sieve is illustrated by the fact that this solid adsorbs roughly six times the amount of benzene than does the more conventional adsorbent, silica gel. It also exhibited the highest heat of adsorption. Similar effects were recognized previously in moderate temperature regions, and it is interesting to observe their existence even at high temperatures. The platinum–alumina catalyst was the only material examined which exhibited an irreversible adsorption of benzene. This effect must be closely associated with its catalytic properties.

(12) H. E. Morris and O. Maass, *Can. J. Res.*, **9**, 240 (1933).
(13) J. Edwards and O. Maass, *ibid.*, **13B**, 133 (1935).

In a companion report,[11] reversible adsorption of hydrocarbons has been shown to occur on a silica–alumina cracking catalyst and molybdena–alumina reforming catalyst at temperatures as high as 427°. This type of adsorption undoubtedly plays a very important part in mass transfer kinetics of fluidized-solids reactors such as those used in catalytic cracking of petroleum fractions. In order to determine the rate constants of adsorption, Eberly and Spencer[8] solved the mathematics of the pulse process. From an analysis of the shape of the effluent pulse, the magnitude of these rate constants can be determined.

Solid adsorbents should also be useful for analytical purposes. Recently, much work has been reported on the use of gas–liquid partition chromatography for the analysis of high boiling mixtures. The main difficulty encountered in operating columns at high temperature has been either the gradual volatilization and/or decomposition of the substrates. It appears that this difficulty could be overcome by the use of solid adsorbents as packing. These are very stable and probably could be used for indefinite periods of time. Previously, the main objection to the use of solids has been that they give in general asymmetric peaks. The peaks that we have observed are not sufficiently severely asymmetric to exclude solid adsorbents as suitable column packing. Perhaps, more attention should be given to the use of gas–solid chromatography, particularly for the high temperature analyses.

DOUBLE RESONANCE STUDY OF PYRROLE AND OF THE PYRROLE–PYRIDINE INTERACTION

BY JAMES A. HAPPE[1]

Chemistry Division, Research Department, U. S. Naval Ordnance Test Station, China Lake, California

Received June 9, 1960

The self-association of pyrrole has been studied by nuclear magnetic resonance using the double resonance method to overcome interference from the nitrogen quadrupole. The association between pyridine and pyrrole has been studied by the same technique. The pyrrole–pyrrole interaction appears to be of the "π-donor" type while pyrrole and pyridine exhibit an "n-donor" interaction. For the dimerization of pyrrole the equilibrium constant K was 4.3, while for the pyrrole–pyridine association reaction measurements of K at four temperatures gave $\Delta H^0 = -4.3$ kcal./mole and $\Delta S^0 = -8.0$ cal./mole. Chemical shifts were obtained for the associated protons in both hydrogen bonded complexes.

Introduction

Intermolecular association in pyrrole has been demonstrated by the infrared studies of Fuson, *et al.*,[2] who pointed out the presence of an "associated band" at 2.92 μ. An estimate of the over-all extent of the association also was reported as a function of pyrrole concentration in CCl_4. Calorimetric studies by Vinogradov and Linnell[3] supported the self-association of pyrrole. In neither case was the nature of the association clear, however, nor could the results be interpreted in terms of a simple monomer–dimer equilibrium. The latter authors included a quantitative study of the association reaction between pyridine and pyrrole. Some uncertainty existed, however, regarding the compatibility of their calorimetric and infrared results.

Nuclear magnetic resonance studies on the association of pyrrole with various donor solvents have been reported previously.[4,5] These reports gave the effect of association on the chemical shift for pyrrole α and β-ring protons. Also the n.m.r. signals for these protons were reported to separate by about 0.2 p.p.m. on dilution with an inert solvent. The NH proton resonance signal is broadened beyond detection by quadrupole interaction with the nitrogen nucleus.

In view of the above it seemed desirable to carry

(1) Chemistry Division, Lawrence Radiation Laboratory, University of California, Livermore, California.
(2) (a) N. Fuson and M. L. Josien, *J. Chem. Phys.*, **20**, 1043 (1952); (b) N. Fuson, M. L. Josien, R. L. Powell and E. Utterback, *ibid.*, **20**, 145 (1952).
(3) S. N. Vinogradov and R. H. Linnell, *ibid.*, **23**, 93 (1955).
(4) L. W. Reeves, *Can. J. Chem.*, **35**, 1351 (1957); M. Freymann and R. Freymann, *Compt. rend.*, **248**, 677 (1959).
(5) T. Schaefer and W. G. Schneider, *J. Chem. Phys.*, **32**, 1224 (1960).

out a direct investigation of the hydrogen bonding in pyrrole using the double resonance technique to eliminate interference from the nitrogen quadrupole moment.[6] It also appeared that this technique might be well suited for application to the pyrrole–pyridine reaction.

For the pyrrole–pyrrole interaction an equilibrium constant for the dimerization reaction has been obtained. An attempt also has been made to deduce something of the structure of the pyrrole dimer from the magnitude of the association shifts for both NH and α-CH ring protons.

The equilibrium constant for the pyrrole–pyridine association reaction has been measured as a function of temperature. From the results the thermodynamic functions for the reaction have been obtained.

Experimental

Double resonance experiments were carried out with a Varian Associates V-4320 n.m.r. spin decoupler which enabled simultaneous saturation of nitrogen nuclei by irradiation at 2.9 mc. and observation of the proton resonance at 40 mc. The high resolution n.m.r. spectrometer and associated equipment have been described elsewhere.[7] Samples were contained in 5-mm. n.m.r. tubes and rotated. Temperature was controlled to $\pm$ 0.5° by means of a Varian Associates V-4340 Variable temperature n.m.r. probe accessory. The n.m.r. spectra were recorded on a Sanborn −151 recorder and were calibrated by the side-band technique. The chemical shift was taken to be the average of a number of individidual determinations. The α and β protons of pyrrole appear in the spectrum as separate quartets while the NH proton of pyrrole is a 5-fold multiplet in the absence of quadrupole effects. Chemical shifts were measured to the center of the multiplets relative to the cyclohexane solvent and are expressed in terms of the quantity δ defined as $\delta = (H - H_{ref})/H_{ref} \times 10^6$. The accuracy of the measurements was $\pm$0.005 except for the most dilute solutions of pyrrole in cyclohexane.

Twenty-milliliter samples of pyrrole in cyclohexane were prepared in a dry box under an atmosphere of dry nitrogen. One-half milliliter aliquots then were added to n.m.r. tubes and the tubes covered with rubber policemen. Sample tubes were removed from the dry box, the liquid frozen and the tubes sealed off without exposure to air. Cyclohexane solutions containing pyridine and pyrrole were prepared in a similar manner by adding the approximate quantity of pyridine to a 20-ml. aliquot of a stock solution of pyrrole in cyclohexane. The composition of all solutions was determined by weight.

Pyrrole was dried over potassium hydroxide and purified by fractional distillation. Pyridine also was dried and fractionated. Cyclohexane was distilled from P_2O_5 under reduced pressure.

Results and Discussion

Pyrrole–Cyclohexane System.—Proton exchange in cyclohexane solutions of pyrrole is sufficiently slow to allow the resolution of fine structure in the resonance absorption for the NH proton. The splitting of this peak results from spin–spin coupling to the α and β-ring protons. The chemical shift for the multiplet is concentration-dependent reflecting the associated nature of pyrrole. The chemical shift for the α-CH protons of pyrrole moves significantly to lower fields on dilution while the n.m.r. peak for protons in the β-position shifts only slightly relative to the cyclohexane solvent over the major portion of the concentration range. These results are given in Table I together with the extrapolated shifts at infinite dilution.

On dilution with cyclohexane δ for the NH protons is shifted in the direction of *lower* magnetic fields. While this behavior is not expected for the breakup of N-H . . . N bonding it is quite consistent with a decrease in so-called "π interactions" between the N–H proton of a pyrrole molecule and the π-electron ring system of a second molecule.[8] For such an interaction an NH proton located above the mobile π-electrons of a conjugated system experiences a secondary magnetic field opposed to the applied field. Resonance, therefore, occurs at higher applied fields than for an unassociated NH proton. A similar effect, though considerably reduced in magnitude, is expected for the α-CH protons as observed. From a consideration of the bond distances involved it appears, however, that protons in the β-position of a dimeric complex are far enough removed from the donor pyrrole ring to make the corresponding anisotropic effects small.

In view of the anisotropy of the pyrrole molecule there may be some question as to the use of the cyclohexane signal as an internal reference. Although the chemical shift for this signal may be concentration-dependent in such systems, the δ's for other sample signals are expected to exhibit approximately the same concentration shifts in the absence of specific intermolecular interactions.[9] This appears to be confirmed by the minor concentration dependence of the β-CH proton shift. Thus the observed shift in δ_{NH} and $\delta_{\alpha\text{-CH}}$ with concentration are assumed to reflect only the direct effects of intermolecular association, particularly in the low concentration region of interest here.

The Association Constant.—Huggins, Pimentel and Shoolery[10] have described a method for relating the equilibrium constant K for a dimerization reaction to the limiting slope of a plot of resonance shift δ *versus* mole fraction of the associated component. In this method a chemical shift is estimated for the dimeric species. In the present study it was felt that this unknown might also be determined analytically from the general expression for dilute solutions relating observed shift and concentration. The assumption is made that two proton environments exist with chemical shifts δ_1 and δ_2 characterizing, respectively, the unassociated and associated NH protons. The dimer is taken to be open, containing one free and one associated NH proton. Then, for solutions sufficiently dilute to exclude significant concentrations of trimers and higher polymers, the observed shift is given by

$$\delta = \frac{(a - x)}{a}\delta_1 + \frac{x}{a}\delta_2 \qquad (1)$$

or

$$x = a\frac{\Delta}{\Delta_u}$$

$$\Delta = \delta - \delta_1 \quad \Delta_u = \delta_2 - \delta_1$$

(6) For a discussion of the double resonance method see J. D. Roberts, "Nuclear Magnetic Resonance," McGraw-Hill Book Co., Inc., New York, N. Y., 1959, Chapter 5.

(7) J. A. Happe and A. G. Whittaker, *J. Chem. Phys.*, **30**, 417 (1959).

(8) L. W. Reeves and W. G. Schneider, *Can. J. Chem.*, **35**, 251 (1957).

(9) J. R. Zimmerman and M. R Foster, THIS JOURNAL, **61**, 282 (1957).

(10) C. M. Huggins, G. C. Pimentel and J. N. Shoolery, *ibid.*, **60**, 1311 (1956).

TABLE I

CHEMICAL SHIFTS RELATIVE TO CYCLOHEXANE FOR THE PROTONS OF PYRROLE IN CYCLOHEXANE SOLUTION AT 33°

Mole fraction pyrrole	β-CH	α-CH	NH	Mole fraction pyrrole	β-CH	α-CH	NH
0.9675	−4.743	−4.935	−5.863	0.1059	−4.673	−5.018	−5.965
.7102	−4.698	−4.920	−5.825	.0959	−4.673	−5.025	−5.990
.7049	.....	−4.923	.....	.0746	−4.670	−5.035	−6.015
.5642	−4.688	−4.925	−5.825	.0722	.....	−5.040	.....
.5091	−4.678	.....	.....	.0425	−4.670	−5.070	−6.100
.4150	−4.675	−4.935	−5.850	.0422	−4.670	.....	−6.108
.3584	−4.673	−4.945	−5.863	.0335	−4.668	.....	−6.140
.2974	−4.673	−4.950	−5.863	.0212	−4.663	−5.108	−6.198
.2930	−4.665	−4.948	.....	.0106	−4.660	−5.133	−6.238
.2186	−4.663	.....	.....	.0102	−4.660	−5.123	−6.250
.2025	−4.673	−4.965	−5.883	.0080	−4.653	−5.125	−6.263
.1830	−4.670	−4.975	−5.890	.0053	−4.660	−5.139	−6.275
.1569	−4.673	−4.985	−5.910	.0000	(−4.655)	(−5.150)	(−6.318)
.1422	−4.668	−4.993	.....				

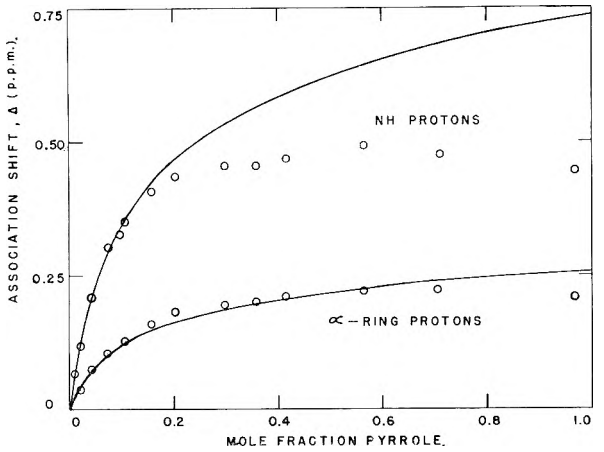

Fig. 1.—Resonance shifts for the α-CH and NH protons of pyrrole in cyclohexane relative to the ∞ dilution shifts. Solid curves are calculated for a monomer–dimer equilibrium.

where moles of dimer are represented by x and stoichiometric moles of pyrrole by a. The coefficients of δ_1 and δ_2 in equation 1 give the fractions of protons in the respective states. The equilibrium constant in mole fraction units is

$$K = x\frac{(a - x + s)}{(a - 2x)^2} \qquad (2)$$

where s is the moles of cyclohexane solvent. Letting X be the stoichiometric mole fraction of pyrrole, equations 1 and 2 may be combined to give

$$\Delta^2\frac{(4K + 1)}{\Delta_u} - \left(4K + \frac{1}{X}\right)\Delta + K\Delta_u = 0 \qquad (3)$$

The solution of equation 3 may be expressed as a converging series

$$\frac{\Delta}{X} = -4K\Delta + K\Delta_u[1 + A + 2A^2 + 5A^3 + \ldots +] \qquad (4)$$

$$A = \frac{K(4K + 1)}{(4K + 1/X)^2}$$

Approximate values of K and Δ_u were obtained from the intercept and initial slope of a plot of Δ/X *versus* Δ neglecting correction terms involving A. The chemical shift for unassociated NH protons was −6.318. Refined values of K and Δ_u were then obtained from similar plots by successive approximations including the correction terms in A. This procedure gave a K of 4.3 and a Δ_u of +1.93.

The concentration dependence of δ for the α-CH protons is also assumed to reflect a rapid exchange between magnetically non-equivalent environments. Here δ_1^1 represents the chemical shift for α-CH protons in an unassociated pyrrole molecule and δ_2^1 characterizes the two α-CH protons above the plane of a donor pyrrole ring. Equation 4 again is appropriate and a Δ_u' may be calculated from the previously determined K and the observed shift for the α-CH protons at a given concentration. The value of δ_1^1 was −5.150 and an average value of $\Delta_u' = 0.66$ was obtained using data up to a mole fraction of 0.1.

The concentration dependence of Δ for both α-CH and NH protons calculated from equation 3 using $K = 4.3$ and the appropriate Δ_u is shown by the solid curves of Fig. 1. The experimental data are included. Deviations from the calculated curves occur above a mole fraction of 0.08 and probably result from significant concentrations of trimers, etc. The direction of the deviation for the NH proton shift indicates that the δ for associated NH protons in higher polymers is considerably more negative than δ_2 for the dimer.

The treatment for a closed dimeric model is very similar to that given above except that the substitution $x = a\Delta/2\Delta_u$ is made in equation 2. The equilibrium constant obtained from this model is again 4.3. The Δ_u's, however, are only half as large, being +0.96 and +0.33, respectively, for the associated NH protons and the α-CH protons of the dimer.

The Pyrrole Dimer.—Waugh and Fessenden[11] have discussed the calculation of chemical shifts arising from the anisotropy of a benzene ring. An expression in terms of elliptic integrals was used for the induced magnetic field of a circular ring around which a current is flowing. If the benzene ring is replaced by a pyrrole ring of radius 1.15 Å. their treatment may be extended to relate the Δ_u for a π-bonded NH proton to its distance above the donor pyrrole ring. For an open dimer in which the associated NH proton is assumed to be directly

(11) J. S. Waugh and R. W. Fessenden, *J. Chem. Phys.*, **24**, 1111 (1956).

above the center of the donor ring, a chemical shift of +1.93 as found here corresponds to a separation of 2.3 Å. between NH proton and donor pyrrole ring. From the bond distances and angles given by Bak, *et al.*,[12] for pyrrole, the α-CH protons of the acceptor pyrrole molecule may then be located about 3.7 Å. above the donor ring and at a displacement of approximately 2.1 Å. from its center. A secondary chemical shift of +0.24 is calculated for protons in this position—lower by about a factor of three than that derived for Δ_u' on the basis of an open dimer.

For the cyclic model of a pyrrole dimer in which both pyrrole rings act as π-donors a separation of 3.0 Å. is calculated between NH proton and donor pyrrole ring by using the derived Δ_u of +0.96. The α-CH protons then may be taken to occupy a position 3.0 Å. above a donor ring at a displacement of 2.5 Å. from its center. For protons in this position a Δ_u' of +0.22 is calculated as compared to the Δ_u' of +0.33 derived experimentally for this model. Thus although the calculations must certainly be considered rough it would appear that a cyclic model for the dimer of pyrrole is most consistent with the n.m.r. results. A summary of the calculations is given in Table II.

TABLE II

COMPARISON OF THE ASSOCIATION SHIFT, Δ_u', DERIVED EXPERIMENTALLY FOR α-RING PROTONS OF PYRROLE WITH THAT CALCULATED ON THE BASIS OF A π-BONDED MODEL OF THE DIMER

Model of dimer	Δ_u NH protons	Δ_u' α-CH protons	NH...Ring separation, Å.	Δ_u' α-CH protons
Open	1.93	0.66	2.3	0.24
Cyclic	0.96	0.33	3.0	0.22

Pyrrole–Pyridine System.—In cyclohexane solutions of pyrrole containing pyridine the NH proton resonance absorption again appeared as a 5-fold multiplet when the sample was subjected to a strong 2.9 mc. R-F signal. The δ for the multiplet was strongly concentration-dependent and shifted to *lower* fields with added pyridine. Large shifts in this direction may be attributed to "n-donor" association here undoubtedly involving the lone pair nitrogen electrons of the pyridine molecule.

The data of Table III give the concentration-dependence for the pyrrole NH chemical shift at four temperatures. The treatment of the data was quite analogous to that given for cyclohexane solutions of pyrrole.[13] Concentration-independent chemical shifts, δ_1 and δ_3, were assumed for the unassociated pyrrole NH proton and the hydrogen bonded proton of the pyrrole–pyridine complex, respectively. For a reaction

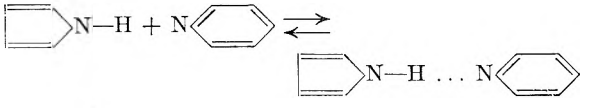

$$K = \frac{x(a - x + s)}{(a - x)(b - x)} \quad \text{and} \quad x = a\frac{\Delta}{\Delta_u}$$

(12) B. Bak, D. Christensen, L. Hansen and J. Rastrup-Andersen, *ibid.*, **24**, 8720 (1956).

(13) See also C. M. Huggins, G. C. Pimentel and J. N. Shoolery, *ibid.*, **23**, 1244 (1955).

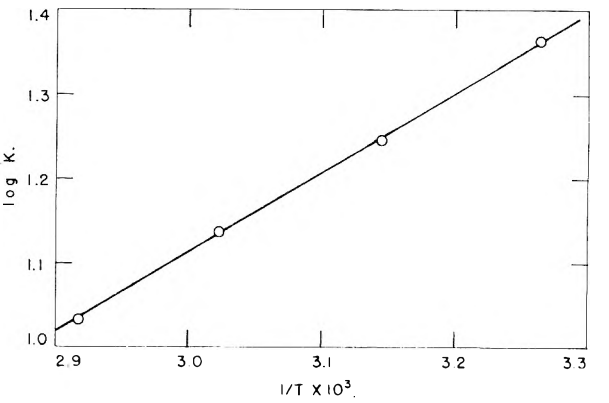

Fig. 2.—Variation of log K with reciprocal temperature for the pyrrole–pyridine reaction.

where the terms have the same meaning as previously defined and b is the number of moles of pyridine added. As before substitution of x into the expression for K gives a quadratic equation in Δ.

TABLE III

EFFECT OF PYRIDINE ON THE CHEMICAL SHIFT FOR THE NH PROTONS OF PYRROLE IN CYCLOHEXANE

Moles pyrrole = 6.0 × 10^{-3}, moles cyclohexane = 0.1778

Moles pyridine × 10^{-3}	Chemical shift (p.p.m.) 33.0°	44.6°	57.6°	69.6°
0.12	−6.185	−6.213	−6.225	−6.233
0.50	−6.293	−6.303	−6.303	−6.303
1.00	−6.448	−6.425	−6.410	−6.383
2.02	−6.718	−6.655	−6.593	−6.533
4.14	.....	.....	−6.910	−6.818
7.83	−7.698	−7.518	−7.343	.....
10.23	−7.985	−7.775	−7.573	−7.393
20.29	−8.593	−8.373	−8.153	−8.935
37.19	−9.028	−8.845	−8.635	−8.413
60.78	−9.290	−9.130	−8.928	−8.728

$$\Delta^2 - \left[\frac{1}{X} + \frac{s}{a(K+1)}\right]\Delta_u\Delta + \frac{K(1-X)}{(K+1)X}\Delta_u^2 = 0 \quad (5)$$

Solution of (5) gives

$$\frac{\Delta}{b} = \frac{(K+1)\Delta}{s(1-X)} + \frac{K\Delta_u}{s}[1 + B + 2B^2 + 5B^3 + \ldots] \quad (6)$$

$$B = \frac{K(K+1)\left(\frac{b}{a}\right)}{\left[(K+1)\left(1+\frac{b}{a}\right) + \frac{s}{a}\right]^2}$$

An estimate of K and Δ_u was obtained from the slope and intercept of a plot of Δ/b *versus* $\Delta/(1-X)$. Improved values of K and Δ_u then were obtained from similar plots by successive approximations including the correction terms in B. The chemical shift for unassociated pyrrole was taken to be −6.318 and thus the observed δ for the lower pyridine concentrations includes a contribution from the still significant pyrrole–pyrrole association. At the higher pyridine concentrations this effect is negligible. The values of K and Δ_u obtained in this manner are included in Table IV. From the plot of log K *versus* $1/T$ shown in Fig. 2, a ΔH^0 of −4.3 kcal./mole is obtained for the pyrrole–pyri-

dine reaction and a standard entropy change of $\Delta S^0 = -8.0$ cal./mole. Thus the present results by the n.m.r. method are quite consistent with the earlier work of Vinogradov and Linnell[3] who obtained for this reaction a ΔH of -3.8 ± 0.2 kcal. from calorimetric measurements and an equilibrium constant of 22 ± 3 at 30° from infrared measurements in CCl_4 solutions.

The significance of the variation of calculated Δ_u with temperature is uncertain. Temperature dependent n.m.r. effects, however, frequently indicate association processes. It may be that the present results arise from a second dimerization reaction between pyrrole and pyridine. Although the most significant interaction is obviously of the n-donor type, association *via* the aromatic pyridine ring is also possible. The variation in Δ_u would then reflect a temperature dependent ratio of π-bonded to n-bonded complexes.

TABLE IV

EQUILIBRIUM CONSTANT AND ASSOCIATION SHIFT FOR THE PYRROLE–PYRIDINE REACTION

Temp., °C.	K (mole fraction)$^{-1}$	Δ_u
33.0	23.1	−3.505
44.6	17.6	−3.483
57.6	13.7	−3.413
69.6	10.8	−3.355

Acknowledgment.—The author wishes to thank Dr. H. F. Cordes for his continued interest in the study and his many helpful suggestions.

THE FREE ENERGY, ENTROPY AND ENTHALPY OF TRANSFER OF SODIUM AND POTASSIUM CHLORIDE FROM METHANOL TO WATER AND FROM ETHYLENE GLYCOL TO WATER[1,2]

BY JAMES K. GLADDEN AND JAMES C. FANNING[3]

School of Chemistry, Georgia Institute of Technology, Atlanta, Georgia

Received June 10, 1960

The major feature of this research is to study the transfer of NaCl and KCl from ethylene glycol and from methanol to water. The thermodynamic quantities of the transfer were measured at three different temperatures, by using the cell: Ag,AgCl|MCl (non-aqueous solvent)‖M(Hg)$_x$‖MCl(water)|AgCl, Ag. The "limiting law" for the transfer process was expressed as a function of $N^{1/2}$. The Born theory was found not to describe completely the transfer process. The deviations between the experimental values of the free energy of transfer and those calculated by use of the Born theory are best explained by considering the order–disorder producing nature of the solute's ions on the solvent. The order–disorder nature of ions can be described by use of the entropy of transfer.

Introduction

By making measurements of the e.m.f. of the cell

$$\text{Ag,AgCl}\,|\text{MCl}\,\left(\begin{matrix}\text{non-aqueous}\\ \text{solvent}\end{matrix}\right)\|\text{M(Hg)}_x\|\,\text{MCl(water)}\|\text{AgCl,Ag} \quad (1)$$

at various temperatures, the thermodynamic properties of the transfer

$$\text{MCl}\left(\begin{matrix}\text{non-aqueous}\\ \text{solvent}\end{matrix}\right) \longrightarrow \text{MCl(water)} \quad (2)$$

can be determined. The free energy of transfer ΔF_t would be the sum of the free energy lost by the water and the free energy gained by the non-aqueous solvent when the ion pair has been removed from it. The entropy of transfer ΔS_t should give some idea as to the ability of the ions to break down or build up the structure of the non-aqueous solvent as compared with this same ability in water.

The measurements will have to be made at certain concentrations of MCl in both the water and the non-aqueous solvent. In order to be free of any potential arising due to cratic effects, both solutions for a single measurement should have the same mole fraction of MCl. This enables an ion pair, undergoing a transfer, to be exposed to an equal number of solvent molecules in both solutions.

Gurney[4] refers to this method as connecting cells "back-to-back." He used this type of cell in order to study the free energy of transfer of several 1–1 chlorides from water to various mixtures of MeOH and water. Others[5] also have investigated the free energy of transfer.

Experimental

Equipment.—The actual apparatus used for making these measurements on cell (1) is similar to that described by MacInnes and Parker[6] and Harned.[7] The silver–silver chloride electrodes used were of the type described by MacInnes and Beattie.[8] The amalgam electrodes were formed by flowing the alkali metal amalgam from capillary tubes into the solution chamber. For the preparation of the alkali metal amalgam triply distilled mercury was used, and the amalgam preparation followed the procedure given by Harned.[7] A K-2 type Leeds and Northrup potentiometer was used for the measurement of the potential.

Chemicals.—Distilled water was redistilled from an alkaline $KMnO_4$ solution with oxygen-free nitrogen bubbling through the solution. Technical grade glycol

(1) Presented in part at the Southeastern Regional Am. Chem. Soc. meeting in Richmond, Virginia, November 5, 1959.

(2) Abstracted in part from the Ph.D. Dissertation submitted by J. C. Fanning to the Georgia Institute of Technology, 1960.

(3) Correspondence concerning this paper should be sent to this author at Department of Chemistry, Tulane University, New Orleans, Louisiana.

(4) R. W. Gurney, "Ionic Processes in Solution," McGraw-Hill Book Co., Inc., New York, N. Y., 1953, Chap. 13.

(5) G. R. Haugen and H. L. Friedman, *J. Am. Chem. Soc.*, **76**, 2060 (1954); THIS JOURNAL, **60**, 1363 (1956); K. Schug, Abstracts of Papers, Division of Physical and Inorganic Chemistry, Am. Chem. Soc., April 13–18, 1958; L. M. Mukherjee, THIS JOURNAL, **60**, 974 (1956).

(6) D. A. MacInnes and K. Parker, *J. Am. Chem. Soc.*, **37**, 1445 (1915).

(7) H. S. Harned, *ibid.*, **51**, 416 (1929).

(8) D. A. MacInnes and J. A. Beattie, *ibid.*, **42**, 1117 (1920).

was purified according to the method given by Smyth and Walls.[9] The methanol was purified by the method of Vogel.[10] NaCl and KCl were purified by the recrystallization of J. P. Baker "Analytical Grade" reagents.

Solutions: The Non-aqueous Solutions.—In every case the solvent was finally distilled into tared 250-ml. erlenmeyer flasks which were sealed with glass stoppers after the proper volume of solvent was distilled into them. The exact weight of solvent in each flask was determined. Since the weight of the solvent was known, the correct amount of salt which would give the desired concentration could be weighed into the flask.

The Aqueous Solutions.—Knowing the exact concentration of a given non-aqueous solution and the weight of the water in the flask, the weight of salt necessary to add to the water was calculated in order to obtain two solutions of equal mole fraction.

Measurements.—Oxygen-free nitrogen was used to force the solutions into their proper cell units. After the cells had remained in the constant temperature bath for about one hour the capillary tubes which formed the amalgam electrode were inserted. After adjusting the potentiometer circuit, the amalgam was passed through the solution and measurements were made quickly. At least three measurements were made on each pair of solutions, and only a small amount of variation was noticed unless the amalgam in the container had a large amount of oxide film on its surface. When this occurred, the last measurement was likely to be somewhat lower than the first and second readings. The temperature was controlled to ±0.05°.

Data.—The potentials of the two cells which were connected back-to-back were measured at three different temperatures and at definite concentrations. The mole fraction of the solute was always the same in the two cells. Table I contains the tabulated results obtained from the experimental measurements.

The concentration range covered by the measurements for the alkali metal chlorides extended from 0.0005 mole fraction unit to a mole fraction which was very close to that of the saturated non-aqueous solution. The minimum value of the concentration range was chosen since it corresponded to a molality of about 0.05. As Robinson and Stokes[11] pointed out, this is about the lowest concentration at which one can obtain reliable results with an alkali metal amalgam electrode.

The results obtained were for NaCl being transferred from glycol to water, NaCl being transferred from MeOH to water, KCl being transferred from glycol to water, and KCl being transferred from MeOH to water. There were only a very few values for KCl transfer from MeOH, because KCl is only very slightly soluble in MeOH.

ΔF_t, ΔS_t and ΔH_t were calculated from the measured potentials and their temperature differentials. The values in each case were for the transfer of one gram formula weight of solute from the non-aqueous solvent to a water solution at the same mole fraction of solute.

The e.m.f. data had an error of about ±0.3 mv. which produced an error in ΔF_t of about one per cent. The estimated error in ΔS_t is ±5 entropy units, and in ΔH_t, about 20% for the transfer of NaCl from glycol to water. The error in ΔS_t and ΔH_t for the other sets of solutes and solvents is much larger, and ΔS_t and ΔH_t values obtained presented only an idea as to the order of magnitude. The reason for this inexactness in these cases is probably the small number of experimental measurements made on these systems.

Initial observation of the data for the transfer of NaCl and KCl from MeOH to water shows that ΔF_t of both is negative. It is found that the values of KCl have larger negative values than those for NaCl. The entropy data for NaCl are found to be positive and of the order of 20 to 30 entropy units. The entropy data for KCl are too inexact to make any definite statement about them, other than that the entropy probably is positive. For NaCl, ΔH_t is opposite in sign to ΔF_t.

The data for the transfer of KCl and NaCl from glycol to water cover a wider concentration range than do the data for the transfer of alkali metal chlorides from MeOH to water. The negative free energy of transfer for KCl is slightly less than that given for NaCl. ΔS_t for the NaCl is positive and of the order of 10 entropy units. Similar data for KCl are also positive, and the magnitude is about the same as for NaCl. ΔH_t for both solutes is opposite in sign to ΔF_t and larger in absolute value. ΔF_t values increase with temperature.

Use of the same solute, except for the transfer from different non-aqueous solvents to water, shows that ΔF_t for MeOH is 3 to 4 times larger than the same quantity for the glycol transfer. The glycol transfer also gives a much smaller change in entropy. The enthalpy change for the glycol transfer is possibly smaller than for the MeOH transfer; however, the data are not accurate enough to make any definite comparison between the two transfers.

If ΔF_t is plotted as a function of the square root of the mole fraction, the resulting curve in each case is a straight line. This holds in the concentration region 0.0005 to about 0.008 mole fraction unit. The slopes of these curves appeared to be independent of temperature over the narrow temperature range studied. The slopes are given in Table II.

TABLE I

ELECTROMOTIVE FORCE DATA. TRANSFER OF SODIUM CHLORIDE FROM METHANOL TO WATER

T = 25°		T = 30°		T = 35°	
$N_2 \times 10^3$	E_t, v.	$N_2 \times 10^3$	E_t, v.	$N_2 \times 10^3$	E_t, v.
0.5011	0.1941	0.5033	0.1965	0.5027	0.2036
.9984	.1876	1.007	.1895	1.004	.1936
1.003	.1861	2.997	.1789	2.989	.1838
2.494	.1749	3.006	.1797	4.799	.1779
3.015	.1733	5.020	.1742	5.938	.1764
5.005	.1691	6.023	.1721		
5.991	.1667				

TRANSFER OF POTASSIUM CHLORIDE FROM METHANOL TO WATER

0.4958	0.2411	0.5044	0.2429	0.5024	0.2424
.9922	.2175	1.004	.2197	1.006	.2321

TRANSFER OF SODIUM CHLORIDE FROM ETHYLENE GLYCOL TO WATER

T = 25°		T = 30°		T = 35°	
$N_2 \times 10^2$	E_t, mv.	$N_2 \times 10^2$	E_t, mv.	$N_2 \times 10^2$	E_t, mv.
0.05060	56.92	0.05012	59.31	0.05008	61.87
.1028	50.80	.05018	58.16	.05022	60.41
.2550	46.78	.09972	54.63	.1001	55.10
.3037	46.52	.1009	52.57	.1011	56.28
.5019	43.44	.3000	48.32	.3001	50.46
.7543	41.55	.5002	45.19	.5020	48.27
1.001	40.53	.5043	45.90	.5083	48.38
1.018	41.11	.7537	44.00	.7532	45.88
1.303	40.00	1.025	42.69	1.003	44.37
1.501	39.27	1.309	41.32	1.307	43.34
1.880	37.50	1.503	40.03	1.509	42.49
2.504	36.53	1.879	38.94	1.870	40.16
4.005	34.53	2.523	37.10	2.506	38.96
		4.045	35.90	2.518	39.77
				4.001	37.70

TRANSFER OF POTASSIUM CHLORIDE FROM ETHYLENE GLYCOL TO WATER

T = 20°		T = 25°		T = 30°	
$N_2 \times 10^2$	E_t, mv.	$N_2 \times 10^2$	E_t, mv.	$N_2 \times 10^2$	E_t, vm.
0.05041	50.17	0.05150	53.45	0.05106	54.55
.1017	46.76	.09991	48.20	.09989	50.43
.2995	42.49	.3001	43.89	.3010	46.65
.7013	38.54	.6951	41.16	.6951	43.40
1.089	37.76	.7058	41.40	1.089	41.17
1.090	37.88	1.087	38.52	1.977	38.60
2.018	35.00	1.969	37.72		

(9) C. P. Smyth and W. S. Walls, *J. Am. Chem. Soc.*, **53**, 527, 2115 (1931).

(10) J. Vogel, "Textbook of Practical Organic Chemistry," Longmans, Green and Co., London, 1951, p. 168.

(11) R. A. Robinson and R. H. Stokes, "Electrolyte Solutions," Academic Press, New York, N. Y., 1955, p. 191.

Discussion

The process shown in equation 1 might be treated by three approaches: (1) the ideal solution approach, (2) the solubility approach, (3) the solvation approach.

Ideal Solution Approach.—The steps in this approach might be illustrated in the manner

$$\mathrm{MCl}\begin{pmatrix}\text{non-aqueous}\\ \text{soln.}\end{pmatrix} \longrightarrow \mathrm{MCl}\begin{pmatrix}\text{Ideal}\\ \text{non-aqueous}\\ \text{soln.}\end{pmatrix} \longrightarrow \mathrm{MCl}\begin{pmatrix}\text{ideal}\\ \text{water}\\ \text{soln.}\end{pmatrix} \longrightarrow \mathrm{MCl}\begin{pmatrix}\text{water}\\ \text{soln.}\end{pmatrix}$$

The free energy change for each step can be found and, in adding these, there would result

$$\Delta F_t = \Delta F_t^0 + 2RT \ln \frac{f_2}{f_2'} \qquad (3)$$

where ΔF_t^0 is the free energy of transfer of the salt from the ideal non-aqueous solution, where the activity coefficient is equal to one, to the ideal water solution, where the activity coefficient is also equal to one. f_2 and f_2' are the activity coefficients of the salt in the real water and non-aqueous solutions, respectively. The free energy at extreme dilution is equal to ΔF_t^0. This value is free of any influence of interionic effects, and it gives a measure of the interaction between the ions and the solvents.

In order to obtain a simple expression for ΔF_t in terms of the mole fraction of the two solutions, the Debye–Hückel[12] limiting expression for the activity coefficient was used along with (3). This produced an equation

$$\Delta F_t = \Delta F_t^0 + kN^{1/2} \qquad (4)$$

which is the "limiting law" for the transfer process. In equation 4

$$k = \frac{5.280 \times 10^8}{T^{1/2}} \left[\left(\frac{d'/D'^3}{M_1'N_1 + M_2N_2}\right)^{1/2} - \left(\frac{d/D^3}{M_1N_1 + M_2N_2}\right)^{1/2}\right]$$

where d, D and M are the density, dielectric constant and molecular weight, respectively. The symbol $'$ represents the values for the non-aqueous case. 1 and 2 are used to designate values for the solvent and solute, respectively. Equation 4 shows that ΔF_t as a function of $N_2^{1/2}$ should be a straight line over the concentration region where the Debye–Hückel theory holds. This would not be expected to cover a very large concentration region. However, it was found that straight lines do represent the data adequately up to $N_2 \sim 0.008$ in glycol and up to $N_2 \sim 0.007$ in MeOH. From Table II the calculated k is found to be of the same order of magnitude as the experimental value of k. k_{calcd} is greater than k_{expt} in each case.

TABLE II

VALUES OF THE SLOPE OF THE EQUATION $\Delta F_t = \Delta F_t^0 + kN_2^{1/2}$

	$k_{\text{calcd.}}$	$k_{\text{expt.}}$
Methanol–water	15.32×10^3	NaCl 8.7×10^3
Ethylene glycol–water	7.30×10^3	NaCl 5.1×10^3
		KCl 5.3×10^3

An empirical value of ΔF_t^0 is found to be needed in order to aid in the explanation of the phenomena. This quantity might be obtained in three ways: (1) by an extrapolation of the data to $N_2 = 0$; (2) by using the extended form of the Debye–Hückel theory and the data for the lowest concentration; and (3) by using the limiting form of the theory and the same piece of data. The three values of ΔF_t^0 found for each set of data agree within 3 to 4%. An average value of ΔF_t^0 was obtained (see Table III).

The best way to obtain a better value of ΔF_t^0 is to make very accurate measurements in very dilute solution. With present experimental methods, this cannot be done.

A relation can be obtained between E_t^0, the standard electrode potential of transfer, and E^0 and $E^{0\prime}$, the standard electrode potentials in both the aqueous and non-aqueous solutions, respectively. This relation is

$$E_t^0 = E^0 - E^{0\prime} - \frac{2RT}{Q} \ln \frac{M_1'}{M_1}$$

Q is Faraday's constant. Thus, if the standard electrode potentials are known for a reaction both in water and in the non-aqueous solvent, E_t^0, ΔF_t^0 can be determined. This method has been used previously to calculate ΔF_t^0 [4,5]

Solubility Approach.—In this treatment the process can be carried out by

$$\mathrm{MCl}\begin{pmatrix}\text{non-aqueous}\\ \text{soln.}\end{pmatrix} \longrightarrow \mathrm{MCl(solid)} \longrightarrow \mathrm{MCl}\begin{pmatrix}\text{water}\\ \text{soln.}\end{pmatrix}$$

The thermodynamic quantities of transfer should be equal to the difference between the thermodynamic properties of solution for MCl in water and those in the non-aqueous solvent. Using the data of Slansky[13] for the heat of solution of NaCl in in water and MeOH, ΔH_t should be equal to +2365 cal./mole. The observed value was approximately +2100 cal./mole.

If the values of the experimental ΔH_t were of sufficient accuracy, then the heats of solution could be calculated for the salts in the non-aqueous solvents.

Solvation Approach.—The third approach involves the process

$$\mathrm{MCl}\begin{pmatrix}\text{non-aqueous}\\ \text{soln.}\end{pmatrix} \longrightarrow \mathrm{MCl(vacuum)} \longrightarrow \mathrm{MCl}\begin{pmatrix}\text{water}\\ \text{soln.}\end{pmatrix}$$

This process requires two solvation phases with different energy requirements. The ions require energy when being removed from a solvent and liberate energy when being placed in a solvent because of their interactions with the solvent molecules.

Since in this section only the interaction of the ions with the solvent molecules is being considered, the free energy, entropy and enthalpy of transfer are the quantities found at extreme dilution.

The free energy change produced can be studied by the application of Born's theory.[14] Born's theory gives a mathematical expression with several limitations for the free energy change for the transfer of an ion from a vacuum to a solvent with a

(12) H. S. Harned and B. B. Owen, "The Physical Chemistry of Electrolytic Solutions," 2nd Edition, Reinhold Publ. Corp., New York, N. Y., 1950, pp. 189 ff.

(13) C. M. Slansky, *J. Am. Chem. Soc.*, **62**, 2430 (1940).

(14) G. Kortum and J. O'M. Bockris, "Textbook of Electrochemistry," Vol. I, Elsevier Publishing, Co., New York, N. Y., 1951, p. 56.

dielectric constant D. The expression for this change is

$$\Delta F_B = -\frac{Nz^2e^2}{2r}\left(1 - \frac{1}{D}\right)$$

where r is the radius of the ion, ze is the charge on the ion, and N is Avogadro's number. The total free energy change for the 1:1 solute transfer would be

$$\Delta F_B = \frac{Ne^2}{2r_M r_{Cl}}(r_M + r_{Cl})\left(\frac{1}{D} - \frac{1}{D'}\right) \qquad (5)$$

According to equation 5 the free energy of transfer, exclusive of any interionic effects, should be equal to the quantity on the right-hand side of the equation. If D is greater than D', which is normally the case, then the total free energy change represented by equation 5 is a negative quantity. Born's equation also implies that as the radius of the ion is increased the negative free energy of transfer of the ion should decrease.

The values of ΔF_t^0 for the transfer of NaCl from MeOH to water are found to be less negative than the value for KCl. This is in accord with the results which Gurney[15] gave. However, this is not what Born's theory might predict. The values of ΔF_t^0 for the transfer of NaCl from glycol to water are found to be more negative than the values for KCl. It then appears that Born's theory is followed for the glycol to water transfer.

What is producing this apparent contradiction between experiment and theory in one case and not in the other? Before this question can be answered, a few brief statements should be made concerning the structure of water and the entropy of solvation.

Several recent authors[16] have used what might be classified as a refined tetrahedral model for the structure of water. Because of its polar nature the water molecule is considered to be a quadrupole with its four charges residing at the corners of an approximate tetrahedron. This tetrahedral charge arrangement of a central water molecule controls the positions of the four neighboring water molecules. By such arrangements being set up throughout liquid water, a liquid structure of some order is produced.

When an ion is placed into solution three possible situations concerning the structure of the water can arise: first, the structure can be broken down; second, the structure can be built up or strengthened; and third, the structure can undergo no change. In water at room temperature there are ions which can perform the first two possibilities, *i.e.*, cause the structure of water to be built up or broken down.

Gurney[17] has given a summary of the experimental evidence for the order-producing and order-destroying nature of ions in water. Gurney[18] also presents a model in order to explain this phenomenon, in brief: An uncharged particle is placed in the water; this particle is able to have a small charge placed on it and then have this charge increased. While the charge is very small, the field which it produces will have only a slight effect on the water molecules; *i.e.*, no breaking or bending of solvent bonds takes place. The charge on the particle is increased slowly, and at a certain value the solvent molecules which are near the particle find their solvent bonds broken. At this stage the molecules are easily disturbed by thermal motions since neither the ion nor neighboring water molecules have enough control to hold them in place. As the charge is increased further, the solvent molecules orient themselves properly around the charge particle and produce order. The first stage, where the charge is so small that it has only a slight influence on the solvent molecules, has not yet been found to occur with ordinary ions. The second situation, where neither the ion nor the neighboring solvent molecules have the dominant influence on a particular solvent molecule, is considered to be the order-destroying ion. In water, large ions, such as Cs^+ and Br^-, are found to be of the order-destroying type; and small ions, such as Li^+ and Na^+, are of the order-producing type.

The order-producing, order-destroying nature of ions in non-aqueous solvents is not too well-known. An indication of this nature can be obtained from the change in the viscosity of the solvent after dissolving the solute in the solvent. If the viscosity is increased, the solute particles have an over-all order-producing effect; if the viscosity is decreased, the solute particles are considered to have an over-all order-destroying effect.

In the derivation of Born's equation no consideration was given to the order-producing, order-destroying nature of ions on the solvent. As Gurney points out in his discussion of the transfer of the alkali chlorides from MeOH–water mixtures to water[15] this effect can account for the inconsistency between the experimental values of the free energy of transfer and the values obtained from the Born theory. If the ions in the non-aqueous solution are order-destroying, then an increase in entropy will take place during the transfer of ions from the non-aqueous solution to the aqueous solution. Previously it was shown that such a process occurred with a negative free energy change; thus by

$$\Delta F_t^0 = \Delta H_t^0 - T\Delta S_t^0 \qquad (6)$$

an increase in entropy means a corresponding increase in the negative free energy. Therefore, in order to understand fully the transfer process, some knowledge of both the entropy and the free energy of transfer is needed.

Since this research deals with a process that occurs in liquids, there is only a slight change in the volume of the system. This situation makes the total energy release or absorption approximately equal to the enthalpy of transfer. By equation 6 it is seen that ΔH_t^0 is a function of ΔF_t^0 and ΔS_t^0 or it is a function of the potential energy of the system and the order-producing, order-destroying nature of the system. If the ΔS_t^0 is a large positive quantity, then ΔH_t^0 can have a sign opposite to that of ΔF_t^0.

In order to apply the above ideas to the experimental values of ΔF_t^0, the free energy might be

(15) R. W. Gurney, ref. 4, p. 225.

(16) R. S. Robinson and R. H. Stokes, ref. 11, pp. 2 ff.; G. Kortum and J. O'M. Bockris, ref. 14, pp. 125 ff.; R. W. Gurney, ref. 4, p. 46 ff.

(17) R. W. Gurney, ref. 4, p. 68 ff.

(18) R. W. Gurney, ref. 4, p. 248 ff.

divided into two parts: (1) the Born free energy of transfer, ΔF_B and (2) the configurational free energy of transfer, ΔF_c. In other words

$$\Delta F_t^0 = \Delta F_B + \Delta F_c$$

ΔF_B is calculated by using equation 5. ΔF_c is obtained by subtracting ΔF_B from the empirical value of ΔF_t^0. These results are shown in Table III.

TABLE III

THERMODYNAMIC DATA

	Free energy, cal./mole					
	Methanol–water			Ethylene glycol–water		
	ΔF_b	ΔF_t^0	ΔF_c	ΔF_b	ΔF_t^0	ΔF_c
NaCl	−3220	−4700	−1500	−2470	−1380	+1090
KCl	−2930	−5600	−2700	−2250	−1300	+ 950

	Entropy, e.u./mole					
	Methanol–water			Ethylene glycol–water		
	ΔS_b	ΔS_t	ΔS_c	ΔS_b	ΔS_t	ΔS_c
NaCl	+20.2	+30	+10	+14.8	+10	−5
KCl	+18.3	?	?	+13.4	+10	−3

It should be noted that for these calculations the values of ionic radii given by Latimer[19] were used. The errors involved in using these values are realized, but in this treatment only an approximation need be used.

It is seen that the ΔF_c for the MeOH case is negative and for the glycol positive. This indicates that if all the solvents had the same dielectric constant, a transfer would occur in the first case, but not in the other. The structure effects in glycol are not favorable for a transfer of ions to water. This is not the case, however, for MeOH. By viscosity studies, certain ions which are order-destroying in water are found to be order-producing in MeOH. This indicates that MeOH is a less ordered solvent than water. Ions appear to favor going from a situation where they are producing order to one where they are order-destroying. It would then appear that glycol is a more ordered solvent than is water because, based on ΔF_c alone, no transfer would occur.

This argument might be extended to ΔS_t^0 where this thermodynamic quantity may also be divided into two parts, ΔS_B and ΔS_c. The Born entropy of transfer can be obtained by using the empirical equation[20]

$$D = D_0 \exp(-(T/\nu)) \qquad (7)$$

which relates the dielectric constant of a solvent to temperature. Equation 7 uses two constants D_0 and ν which are dependent on the nature of the solvent only. ΔS_B is finally calculated by using the equation

$$\Delta S_B = -\frac{\partial \Delta F_B}{\partial T} = \frac{Ne^2}{2}\left(\frac{2}{\nu D} - \frac{1}{\nu' D'}\right)\left(\frac{r_M + r_{Cl}}{r_M r_{Cl}}\right)$$

Table III gives ΔS_B, ΔS_t^0 and ΔS_c. The values for ΔS_c in the MeOH transfer are positive as would be expected. The values for the glycol case are negative even though the over-all value, ΔS_t^0, is positive.

From these considerations a relative order as to the structure of the solvents might be assigned

methanol < water < ethylene glycol

This order lies in the same direction as might be expected by considering Trouton's constant (Table IV).

TABLE IV

DATA FOR THE SOLVENTS USED

	F.p., °C. Experimental	B.p., °C.	D at 25°	ν	Trouton's constant
Methanol	−97.8	64.65	32.6	185	24.95
Water	0	100	78.54	219	26.04
Ethylene glycol	−12	197.2	37.7	194	28.96

Comparing the solutes, the NaCl in both transfers has a more positive ΔF_c than does KCl. This might be expected since the Na ion is an order-producing ion in water but the K ion is an order-destroying ion in water. The Na ion in going from the non-aqueous solvent to the aqueous solution will be entering a solution in which it is producing order. This fact will cause ΔS_t^0 to be more negative than that for the KCl transfer, thus also producing a more positive ΔF_t^0.

The TlCl transfer from glycol to water, in preliminary studies, was found to give a positive value for ΔF_t in the concentration region of 1×10^{-5} mole fraction units. Only a few values were obtained for TlCl and these with rather poor precision. However, a positive value for ΔF_t was observed, and this value is in direct disagreement with Born's theory. When an ion, such as Tl(I) ion, is investigated, quantum-mechanical forces must be considered since Tl(I) is an ion with a non-inert gas type structure. The existence of these forces may lead to some rather unexpected values of ΔF_t. For, not only must ΔF_B and ΔF_c be considered as accounting for the value of ΔF_t; but also, a free energy term must be included which accounts for quantum mechanical forces.

Acknowledgment.—Partial financial support by the Graduate Division of the Georgia Institute of Technology is gratefully acknowledged. Appreciation is extended to Dr. Henry M. Neumann for his very helpful advice. We also acknowledge the aid of Mrs. Sybil S. Fanning in making many of the measurements.

(19) W. M. Latimer, *Chem. Revs.*, **18**, 350 (1936).
(20) R. W. Gurney, ref. 4, p. 16.

SOME THERMODYNAMIC PROPERTIES OF THE SYSTEM $PuCl_3$–KCl FROM ELECTROMOTIVE FORCE DATA[1]

BY R. BENZ

Los Alamos Scientific Laboratory, University of California, Los Alamos, New Mexico

Received June 16, 1960

The molar free energy of formation of plutonium(III) chloride as a function of temperature (650 to 800°) and of composition in liquid $PuCl_3$–KCl solutions was determined from e.m.f. measurements made on reversible galvanic cells of the type Pu(liq)|$PuCl_3$–KCl(liq)|Cl_2(g). The free energy of formation of pure supercooled liquid plutonium(III) chloride at one atmosphere can be represented $\Delta F_1^0 = -206 + 0.03858T$(kcal./mole)(958 to 1014°K.). The standard free energy of formation of solid plutonium(III) chloride can be represented $\Delta F_1^0 = -221 + 0.05328T$(kcal./mole)(958 to 1014°K.).

Introduction

In the development of plutonium power reactors, reprocessing of spent fuels is a vital problem. For economic reasons, reprocessing systems containing liquid alloys or liquid salt solutions at elevated temperatures, is of special interest. Free energies of formation of plutonium compounds and their activities in the solutions involved are indispensable aids in the prediction and the development of possible feasible processes.

From a determination of the heat of solution of plutonium metal in aqueous hydrochloric acid and the heat capacities estimated from similar substances, Brewer, Bromley, Gilles and Lofgren[2] have calculated the free energy of formation of plutonium(III) chloride. A determination of the free energy of formation using an independent method such as that of e.m.f. measurements seems desirable.

Some of the major experimental difficulties encountered in obtaining e.m.f. measurements suitable for reliable determination of the thermodynamic quantities of formation of the general compound MX_m from galvanic cells of the type

$$M(liq)\,|MX_m\text{–}NX_n(liq)|\,X_2(g)$$

are (1) electronic conductivity of the electrolyte, (2) non-unique oxidation state of the ions and (3) mutual dissolution of the metal and electrolyte. It is supposed that the liquid metal and electrolyte are non-volatile and that the compound NX_n, if present, is appreciably more stable than MX_m.

This paper presents the results of a study on the galvanic cells represented by

$$Pu(liq)\,|PuCl_3\text{–}KCl(liq)|\,Cl_2(g) \qquad (1)$$

for which the cell reaction is the formation of plutonium(III) chloride in liquid $PuCl_3$–KCl solutions, *i.e.*, the reaction

$$Pu(liq) + \frac{3}{2}\,Cl_2(g) = PuCl_3(liq, X_1) \qquad (2)$$

Plutonium(III) chloride is ionic and the first effect listed above is negligible. In the region of low concentrations and in the presence of chlorine gas, an appreciable proportion of the plutonium(III) chloride is converted to a second oxidation state. Only data for the solutions in which the concentration of the second oxidation state is negligible—the region of high plutonium(III) chloride concentrations—can be interpreted quantitatively. Although the third effect, the mutual solubility of plutonium metal and $PuCl_3$–KCl solutions, is appreciable, it was found to be possible to make the rate of dissolution negligible with the use of an inert porous partition to separate the electrode and electrolyte. Indeed, for the cell (1), an electrode design incorporating a thoria partition with carefully controlled porosity was found to satisfy for periods as long as 13 hours, conditions (see Procedure) necessary for a reversible cell.

Experimental

Materials.—The plutonium(III) chloride, potassium chloride, hydrogen chloride and argon have been described previously.[3] Chlorine gas (Matheson Co., 99.3% pure) was given no treatment. The pressure of the chlorine gas, which was measured with an accuracy of ±1 mm. in the range 588 to 598 mm., was corrected to one atmosphere by assuming the gas to be ideal and adding $(-RT \ln p)/2$ to the observed e.m.f. values.

The chemical composition of each solution (*ca.* 60 g. total weight) was based upon the composition by weight of the component salts.

Apparatus.—The electrolyte of the galvanic cell proper was contained in the elbow of a 30-cm. long 1.4-cm. bore J-shaped quartz tube. During a run, the elbow of the J-shaped tube was immersed in a liquid metal bath, within a wire wound furnace to ensure uniform temperatures. In order to protect the cell from stray currents, the liquid metal bath in a quartz container was shielded from the furnace by a grounded stainless steel tube. The longer arm of the J-shaped tube was mounted in a Teflon stopper so as to center the cell with the electrolyte about 13 cm. below the surface of the liquid metal bath.

The chlorine electrode was constructed of a 30-cm. long, 6.0 mm. diameter spectroscopic graphite (National Carbon) rod. During an experiment, the electrode was centered in the long arm of the J-shaped cell by means of a tapered joint at the top such that chlorine gas flowing through a 1.5-mm. hole drilled along the axis of the graphite rod continually bubbled over the end of the graphite rod submerged in the electrolyte. Prior to an experiment, the graphite electrode was treated with chlorine gas at a pressure of one atmosphere for a period of 2 to 8 hours at 1000°.

The plutonium electrode located in the second arm of the cell consisted of approximately 3 g. of liquid plutonium metal contained in a 0.43-cm. inside diameter, 0.75-cm. outside diameter and 2.6-cm. long porous thoria crucible centered in the bottom of a 0.8-cm. bore quartz tube which was supported from above. The quartz tube was constricted at the bottom so as to support and contain the thoria crucible.

The thoria crucibles were fabricated from Norton 200F thoria powder (Norton Co.). They were dry pressed and fired for 13 hours at 1750° in a hydrogen atmosphere. The porosity of the thoria crucibles was gauged by the weight per cent. of water absorbable by the crucibles. Values ranged from 4 to 6%. When crucibles with lower values of absorption were used, the cell exhibited a much higher electrical resistance and e.m.f. values usually were

(1) Taken from a dissertation submitted in partial fulfillment of the requirements for the Degree of Doctor of Philosophy in Chemistry at the University of New Mexico.

(2) L. Brewer, L. Bromley, P. W. Gilles and N. L. Lofgren, "The Transuranic Elements," National Nuclear Energy Series, Div. IV, Vol. 14B, McGraw-Hill Book Co., New York, N. Y., 1949, p. 873.

(3) R. Benz, M. Kahn and J. A. Leary, THIS JOURNAL, **63**, 1983 (1959).

erratic. When crucibles with higher values of absorption were used, the e.m.f. values were time dependent.

In its normal position, the bottom of the thoria crucible was located 1 to 3 mm. below the surface of the electrolyte such that electrical contact between the plutonium metal and the electrolyte was made after the electrolyte had passed through the constriction in the end of the quartz tube and the pores of the thoria crucible.

The furnace assembly described above was located in a standard type stainless steel drybox for the protection of personnel against hazards of radioactivity (α-decay of plutonium). The external circuit to the galvanic cell and the thermocouple leads which passed through the wall of the drybox were constructed, respectively, of copper and platinum–rhodium extension lead wire. The external circuit was calibrated for thermoelectric e.m.f.'s which were plotted as a function of temperature to give a small linear correction to the observed e.m.f. values for the cells.

A standard external potentiometric circuit was used to balance the e.m.f. of the galvanic cell. It included an arrangement for electrodeposition and electrodissolution (*i.e.*, electrolytic deposition on and dissolution of the electrodes) within the galvanic cell using a double throw switch for reversing the current from a storage cell.

The temperature measurements were made using two Pt–10% Rh thermocouples located in the bottom of a quartz well, submerged 13 cm. in the liquid-metal bath so as to be adjacent to the galvanic cell. One thermocouple was connected to a Honeywell recorder and served to indicate approximate temperatures. The second thermocouple used for the precise temperature measurements and checked (±0.4°) against the melting point of aluminum (certified by the National Bureau of Standards) before and after the potentiometric measurements, was connected to another thermocouple at 0° and a K-2 potentiometer (Leeds and Northrup Co.) standardized against a calibrated Weston Cell.

Procedure.—To begin an experiment the desired quantities of salts were well mixed by bubbling hydrogen chloride gas through the melt contained in the assembled cell. The graphite electrode with a chlorine-gas flow rate of approximately 5 cc./min. then was introduced and centered so that the tip of the electrode was located at a depth of 2 to 6 cm. below the surface of the electrolyte. The metal electrode finally was introduced and adjusted carefully to the desired depth and the potentiometric measurements were begun. An inert atmosphere in the region above the liquid metal bath was provided by a continuous flow of argon gas. Measurements were repeated every 15 minutes until a steady voltage was obtained. In the temperature region 700 to 800° one to two hours were required for the voltage to reach steady and reproducible values.

A single measurement usually extended over a period of ten minutes. During this period the e.m.f. reading was verified to be reproducible after applying for two seconds an electrodepositing current of 15 ma. at 2.5 v. and, again, after applying for two seconds an electrodissolving current. After a measurement was completed, the furnace temperature was shifted 10 to 30° increasing and decreasing at alternate measurements such that alternate equilibrium temperatures would be approached from above and below. Such a series of potentiometric measurements was carried out on each of the liquid solutions within the temperature region 646 to 741° for the plutonium(III) chloride mole fractions of 0.800 and 0.600. The cells remained reversible over a period from 6 to 13 hours. Galvanic cells containing pure plutonium(III) chloride did not behave reversibly.

Results

Calculations.—The notation employed by Wagner[4] for the thermodynamic mixing properties is followed. Subscript 1 denotes liquid plutonium(III) chloride. X_1 denotes the mole fraction of plutonium(III) chloride. The reference state is that of supercooled liquid plutonium(III) chloride at 973°K. and one atmosphere.

The e.m.f., denoted ϵ, was determined as a function of temperature in the region 646 to 741° for electrolytic solutions at the mole fractions X_1 = 0.600 and 0.800. After having been corrected to that of one atmosphere of chlorine gas (corrections ranged from 0.010 to 0.011 v.) and for thermoelectric effects in the external circuit (corrections ranged from 0.005 to 0.007 v.), these data were represented (least squares fit) by linear equations of the form

$$\epsilon_{X_1} = a_{X_1} + b_{X_1}T \qquad (3)$$

where a_{X_1} and b_{X_1} are constants for the solution of plutonium(III) chloride mole fraction X_1 and T denotes the absolute temperature. The results are given analytically in Table I. Included in Table I are the data for pure plutonium(III) chloride in the supercooled liquid state. These data were obtained by means of an extrapolation described below.

TABLE I

E.M.F. DATA AS A FUNCTION OF TEMPERATURE FOR THE FORMATION OF $PuCl_3$ IN THE LIQUID BINARY SYSTEM $PuCl_3$–KCl

X_1	E.m.f., v.	Max. dev., v.	Temp. range, °K.	No. e.m.f. detns.
1.000	$2.980 - 0.5576\ 10^{-3}T$			
0.800	$2.990 - 0.553\ 10^{-3}T$	±0.004	958 to 1014	12
0.600	$3.056 - 0.5439\ 10^{-3}T$	±0.004	919 to 1010	10

The calculation of the thermodynamic quantities involves, first, extrapolation of the e.m.f. data to the state of pure plutonium(III) chloride at 973°K. in order to obtain the thermodynamic quantities of formation of the supercooled liquid salt. From these results, the partial molar mixing quantities for liquid plutonium(III) chloride are computed. Finally, using these and other data taken from the literature, the standard formation quantities of solid plutonium(III) chloride are calculated. Further details of the calculations are given below.

The free energy (ΔF_1), entropy (ΔS_1) and enthalpy (ΔH_1) of formation of plutonium(III) chloride in the liquid $PuCl_3$–KCl solutions at 973°K. and one atmosphere for X_1 = 0.600 and 0.800 were computed using the formulas

$$\Delta F_1 = -3F\epsilon_{X_1} \qquad (4)$$

$$\Delta S_1 = -\left(\frac{\partial}{\partial T}\Delta F_1\right)_p \qquad (5)$$

$$\Delta H_1 = \Delta F_1 + 973\Delta S_1 \qquad (6)$$

The results are listed in Table II. The data at the mole fraction X_1 = 1.000 represent that for the formation of pure supercooled liquid plutonium(III) chloride. These data were obtained from that for the solutions of plutonium(III) chloride mole fractions X_1 = 0.800 and 0.600 by means of an extrapolation as a function of composition. For the purpose of extrapolation, it was assumed that the functions $F_1''^{E}/X_2''^{2}$ and $S_1''^{E}$ are constants for the binary system $PuCl_3$–K_2PuCl_5 over the region of

TABLE II

MOLAR THERMODYNAMIC QUANTITIES OF FORMATION OF LIQUID $PuCl_3$ AT 973°K.

X_1	ΔF_1, kcal.	ΔS_1, e.u.	ΔH_1, kcal.
1.000	−169	−38.6	−206
0.800	−170	−38.3	−207
0.600	−175	−37.6	−212

(4) C. Wagner, "Thermodynamics of Alloys," Addison-Wesley Press, Inc., 1952, Chap. 1.

K_2PuCl_5 mole fraction $X_2'' = 0$ to 0.333. $F_1''^E$ and $S_1''^E$ denote the excess relative partial molar free energy and entropy, respectively, of mixing supercooled liquid plutonium(III) chloride for this system. Thus, the entropy of formation of supercooled liquid plutonium(III) chloride was taken to be the arithmetic average of the excess entropy of formation of plutonium(III) chloride, *i.e.*, $\Delta S_1'' + R \ln X_1''$, at the K_2PuCl_5 mole fractions 0.125 and 0.333. $\Delta S_1''$ denotes the molar entropy of formation of plutonium(III) chloride for this system. In solutions containing high concentrations of plutonium(III) chloride, it is expected that the mixing quantities for the system K_2PuCl_5–$PuCl_3$ may approximately conform with that of regular solutions (hence, constant $F_1''^E/X_2''^2$ and $S_1''^E$) because there are no intermediate compounds. The enthalpy of formation of pure supercooled liquid plutonium(III) chloride was obtained using the relation

$$\Delta H_1 = \Delta F_1 + 973\Delta S_1$$

The relative partial molar free energy (F_1^M), entropy (S_1^M) and enthalpy (H_1^M) of mixing plutonium(III) chloride at 973°K are listed in Table III. The corresponding activities are given in column 5.

TABLE III

PARTIAL MOLAR THERMODYNAMIC QUANTITIES OF MIXING LIQUID $PuCl_3$ FOR THE SYSTEM $PuCl_3$–KCl AT 973°K

X_1	F_1^M, kcal.	S_1^M, e.u.	H_1^M kcal.	a_1
1.000	0.0	0.0	0.0	1.00
0.800	−1	+0.3	−1	0.59
0.600	−6	+0.9	−5	0.040

The standard molar free energy, entropy and enthalpy of formation of solid plutonium(III) chloride at 973°K. and one atmosphere are given in row (c) of Table IV. These quantities were ob-

TABLE IV

THE CALCULATION OF THE STANDARD MOLAR THERMODYNAMIC QUANTITIES OF FORMATION OF SOLID $PuCl_3$ AT 973°K. AND ONE ATMOSPHERE

	Reaction at 973°K.	ΔF, kcal.	ΔS, e.u.	ΔH, kcal.
a.	$Pu(liq) + \frac{3}{2}Cl_2(g) = PuCl_3(liq)$	−169	−38.6	−206
b.	$PuCl_3(s) = PuCl_3(liq)$	+ 1	+14.7	+ 15
c.	$Pu(liq) + \frac{3}{2}Cl_2(g) = PuCl_3(s)$	−170	−53.3	−221

tained by subtracting the chemical equations (a) and (b). The data for reaction (b), the melting of solid plutonium(III) chloride at 973°K., were computed with the aid of the approximations

$$\Delta S = -\int_{973}^{T_m} \frac{\Delta C_P}{T'}\,dT' + \Delta S_m \approx \Delta S_m,\ \Delta C_p \equiv C_{p(l)} - C_{p(s)} \quad (7)$$

$$\Delta F = \int_{973}^{T_m} \Delta S\,dT' \approx \Delta S_m(T_m - 973) \quad (8)$$

$$\Delta H = \Delta F + 973\Delta S \approx T_m\,\Delta S_m \quad (9)$$

where ΔS_m is the entropy of melting plutonium(III) chloride at the melting point, $T_m = 1042$°K.

Reliability and Discussion of the Data.—An important feature in the design of the galvanic cell is the incorporation of an inert-porous-thoria partition for the purpose of reducing the rate of mutual dissolution of the plutonium electrode and the electrolyte. Experimentally, when a liquid plutonium electrode was exposed directly to liquid $PuCl_3$–KCl solutions in the cell, the e.m.f. value dropped rapidly and continuously from that of a reversible cell. This behavior was interpreted to result from the interdiffusion of the metal and salts during the dissolution of the plutonium(III) chloride in the metal and *vice versa*. Assuming this to be the major irreversible process, the galvanic cell was designed with the aim of reducing the rate of mutual dissolution—in principle, the objective is to extend the period of time during which the virtual half-cell reaction at the metal electrode is essentially Pu (pure liquid) = Pu^{+3} (liq. X_1) + 3e. To this end a thoria wall in the form of a crucible containing the liquid plutonium electrode was used, the function of which was to set up a steady transition interface between the metal and salt phase such that the net virtual cell reaction would be essentially that indicated in equation 2. The fact that the cross section of the used thoria crucibles always had a uniform green color approximately the same shade as the electrolyte—in contradistinction to the black solutions of plutonium dissolved in the electrolyte—indicates that the transitional interface probably was retained near the inner surface of the crucibles. The necessary conditions for reversibility, *viz.*, that the e.m.f. be independent of time and independent of the direction of approach to equilibrium with respect to temperature and chemical reaction (*i.e.*, reproducible after passing a small electrodissolving and electrodepositing current through the cell), were satisfied by all the galvanic cells. This is evidence that the thoria crucibles did function in the manner described above, as well as that the cells were reversible.

Chemical analyses of the electrolytic solutions taken from the galvanic cells at the conclusion of each experiment yielded a chloride to plutonium ratio of 3.0 ± 0.1. This shows that the possible concentration of a second oxidation state of plutonium was not greater than 10% and it is concluded that effects of multiple oxidation states on the derived formation quantities of plutonium(III) chloride is negligible. The effects on the mixing quantities which represent small differences of large quantities may be more pronounced.

The potentiometric measurements for each of the electrolytic solutions were made with a precision of within ± 4 mv. These data were reproducible over a period of several hours during which the temperature of the galvanic cells was varied approximately 75°.

The e.m.f. readings were made with an accuracy within ± 0.1 mv. Contributions to error in the e.m.f. measurements from errors in the temperature measurements were within ± 1 mv. Corrections for thermoelectric effect in the external circuit were made by means of a calibration. The chlorine gas was corrected to its standard state of unit fugacity assuming the ideal gas law. The contributions to the total error in the e.m.f. measurements from these sources are less than the precision within which the measurements were made.

The entropies of formation of liquid plutonium (III) chloride in the various solutions are estimated to be reproducible within 8%. A source of uncertainty in the calculation of the free energy of formation of pure plutonium(III) chloride stems from the extrapolation of the data for the solutions at 700° to the state of pure supercooled liquid plutonium(III) chloride. The extrapolation involves a relatively small correction, *viz.*, 0.5%.

Discussion.—The relative partial molar free energy of mixing the plutonium(III) chloride has large negative values which is consistent with the compound formation observed in the study of phase equilibria.[3] The value of the standard molar free energy of formation of pure plutonium(III) chloride at 700° was determined to be −170 kcal. which is 4% more positive than that estimated by L. Brewer, L. Bromley, P. W. Gilles and N. L. Lofgren.[2]

Acknowledgments.—I wish to thank J. A. Leary and R. D. Baker of the Los Alamos Scientific Laboratory and Milton Kahn of the University of New Mexico for discussions and encouraging interests. I am indebted to A. N. Morgan for the plutonium, J. W. Anderson for the machined plutonium electrodes, C. F. Metz, G. R. Waterbury, C. T. Apel and A. Pullium for chemical analyses, and S. D. Stoddard for the thoria crucibles. This work was done under the auspices of the U. S. Atomic Energy Commission.

STANDARD PARTIAL MOLAL COMPRESSIBILITIES BY ULTRASONICS. II. SODIUM AND POTASSIUM CHLORIDES AND BROMIDES FROM 0 TO 30°[1]

BY BENTON B. OWEN AND PAUL L. KRONICK[2]

Contribution No. 1614 from the Sterling Chemistry Laboratory, Yale University, New Haven, Conn.

Received June 23, 1960

The velocity of sound in pure water and in dilute aqueous solutions of sodium and potassium chlorides and bromides is reported at 5° intervals from 0 to 30°, and at a frequency of 5 megcy./sec. The *isothermal* partial molal compressibilities of the salts at infinite dilution, $\bar{K}_2^0$, are calculated, and found to increase (become more positive) with increasing temperature.

Introduction

The first paper of this series[3] contained a description of the movable-reflector acoustic interferometer and the experimental technique by which sound velocities were measured, and the results of these measurements on solutions of sodium and potassium chlorides were used to illustrate the evaluation of $\bar{K}_2^0$ for these salts at 25°. The present paper reports the results of more extensive measurements on solutions of these salts, as well as sodium and potassium bromides, at 5° intervals from 0 to 30°.

Experimental

In the preparation of the sodium and potassium chlorides, Analyzed C.P. grade salts were used without further purification, but the bromides were recrystallized once from distilled water. The concentration of each solution used in a velocity measurement was determined by withdrawing a portion from the interferometer and performing a differential potentiometric titration[4] against a 0.07 *N* solution of silver nitrate. This silver nitrate solution was standardized periodically against a thoroughly dried sample of sodium chloride purified by the method of Meites.[5]

The operation of the interferometer and associated electronic equipment followed closely the procedure previously outlined,[3] and need not be described again. All velocity measurements were made at 5 megacycles (±5 cycles) per second. Temperature was controlled to ±0.002° during the course of the measurements, so that the variation of the velocity of sound with concentration was obtained "isothermally." The absolute value of the temperature was, however, not known to much better than 0.01° because a discordance of 0.004° developed between the calibrations of two of our three platinum resistance thermometers while the measurements were in progress.

Since our apparatus was designed for precise measurement of changes in velocity rather than absolute magnitudes, the instrumental constant (a function of the angles formed by the screw and the guide rods) was evaluated from the known velocity of sound in pure water at 30°. For this standard of reference, $u_0(30°)$, we used 1509.55 m./sec., the mean of 1509.44 reported by Greenspan and Tschiegg[6a] from the National Bureau of Standards, and 1509.66 reported by Wilson[6b] from the United States Naval Ordnance Laboratory. The instrumental constant at lower temperatures was calculated from the value at 30° and the coefficient of linear expansion of stainless steel (10^{-5} deg.$^{-1}$).

Results of the Velocity Measurements

For each salt at a given temperature, the velocity of sound was determined in from seven to fourteen solutions whose composition ranged from 0 to 0.07 normal. The results of these measurements could be represented within the limits of their reproducibility (±0.02 m./sec.) by the equation

$$u = u_0 + A_u c + B_u c^{3/2} \qquad (1)$$

The coefficient A_u is the quantity which contributes directly to the desired value of $\bar{K}_2^0$, or ϕ_K^0, through the equation

$$\phi_K^0 = 1000A_\delta + \delta_0\phi_V^0 + (2\phi_V^0 - M_2/d_0 - 2000\,A_u/u_0)\beta_{os} \qquad (2)$$

in which β_{os} is the adiabatic compressibility of

(1) This communication contains material from a thesis presented by Paul L. Kronick to the Graduate School of Yale University in partial fulfillment of the requirements for the degree of Doctor of Philosophy, June, 1957.

(2) The Franklin Institute, Philadelphia 3, Pa.

(3) B. B. Owen and H. L. Simons, THIS JOURNAL, **61**, 479 (1957).

(4) N. F. Hall, M. A. Jensen and S. A. Baeckstrom, *J. Am. Chem. Soc.*, **50**, 2217 (1928).

(5) L. Meites, *J. Chem. Ed.*, **29**, 74 (1952).

(6) (a) M. Greenspan and C. E. Tschiegg, *J. Research Natl. Bur. Standards*, **59**, 249 (1957); (b) W. D. Wilson, *J. Acoust. Soc. Am.*, **31**, 1067 (1959).

pure water, and the quantities A_δ and δ_0 are correction terms[3] which convert to isothermal compressibilities. M_2 is the molecular weight of the salt, and d_0 is the density of pure water.

Under the conditions of our measurements the last term in equation 1 contributes so little to u that the value of B_u cannot be determined precisely. Improvement in the evaluation of B_u by using a greater number of solutions and higher concentrations was not attempted because equation 1 is theoretically justified only at extreme dilution, and a statistically significant increase in the number of measurements per run could only be attained by seriously limiting the temperature range, or the number of salts investigated.

TABLE I

PARAMETERS OF EQUATION (1)

t, °C.	u_0[a]	A_u[b]	A_u[c]
	Sodium chloride ($B_u = -3.1$)		
0	1402.99	80.20	80.1
5	1426.73	76.09	76.6
10	1447.79	72.73	73.3
15	1466.40	70.17	70.2
20	1482.75	67.67	67.3
25	1496.70[d]	64.53[d]	64.6
30	1509.64	61.47	62.1
	Potassium chloride ($B_u = -7.2$)		
0	1402.98	73.58	73.1
5	1426.70	69.28	69.2
10	1447.81	65.28	65.6
15	1462.40	62.31	62.3
20	1482.73	60.10	59.3
25	1496.76[d]	57.20[d]	56.6
30	1509.56	53.79	54.2
	Sodium bromide ($B_u = -3.2$)		
0	1402.97	45.88	45.3
5	1426.70	41.69	41.4
10	1447.78	37.83	37.8
15	1466.40	34.41	34.5
20	1482.75	32.49	31.5
25	1497.07	28.54	28.8
30	1509.49	26.18	26.4
	Potassium bromide ($B_u = -5.2$)		
0	1402.99	38.37	38.3
5	1426.70	33.55	34.0
10	1447.79	29.74	30.1
15	1466.40	26.09	26.6
20	1482.73	23.53	23.5
25	1497.05	20.80	20.8
30	1509.51	18.06	18.5

[a] These values differ from those recorded in Table VI of ref. 1 by the factor 0.999874, introduced to change the average value at 30° from 1509.74 to 1509.55 m./sec. [b] From equation 1 and the average values of B_u indicated. [c] Smoothed values obtained graphically from the plot illustrated in Fig. 1. [d] Taken from ref. 3 without change: NaCl ($B_u = -3.0$) and KCl ($B_u = -6.0$).

A preliminary least-square representation of the data by equation 1 showed that there was no consistent trend in B_u with temperature. Accordingly, average values of B_u, independent of temperature, were calculated for each salt and then used to redetermine u_0 and A_u. The values of u_0 were practically unaffected by this second curve-fitting,

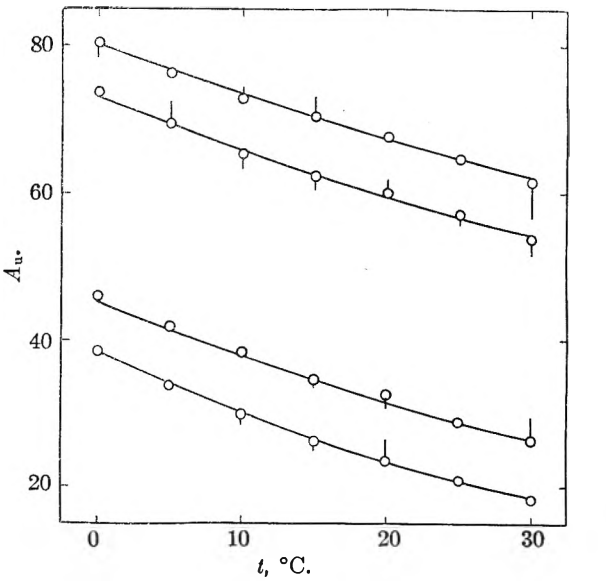

Fig. 1.—Variation of A_u with temperature. Reading from top to bottom, the salts are: NaCl, KCl, NaBr and KBr.

varying less than the difference between values derived from the data on different salt solutions. Unfortunately, A_u is sensitive to a change in B_u, varying as much as 10% in one extreme case. The results of this second curve-fitting are collected in Table I, which also includes smoothed values of A_u read from the plots of A_u against temperature which are illustrated in Fig. 1. The variation in A_u produced by changing B_u from the individual preliminary values to the average values recorded in Table I is indicated by the lengths of the vertical tails on the data points, except for the results at 25° for sodium and potassium chlorides. For these two salts the data at 25° represent results obtained at several frequencies,[3] and the lengths of the tails are equal to the greatest variation in A_u produced by changing from the individual values of B_u, for any one of four series of measurements, to the composite value designated as "com" in Table I of the previous paper.[3]

The variations in A_u may be summarized as follows: 1 unit, or less, for 50% of the points, 2 units for 25%, and about 3 units for the remaining 25% with an outstanding single variation of 5.4 units for sodium chloride at 30°. The larger variations emphasize the extreme difficulty of determining A_u, the individual limiting change in sound velocity with concentration, from the nonlinear equation 1. On the other hand, these extreme variations are much too large to be considered a measure of the uncertainties in the smoothed values of A_u (Table I) which were derived from a whole family of curves, obtained by combining eight from the previous paper[3] with the twenty-eight reported here.

At each temperature we have averaged the four values of u_0 to be found in Table I, and recorded them as u_0(exp.) in the second column of Table II. Values of u_0 calculated from the empirical equation

$$u_0 = 1403.00 + 5.0206t - 0.05700t^2 + 0.0002678t^3 \quad (3)$$

are recorded in the third column, and represent

TABLE II

PROPERTIES OF PURE WATER

t, °C.	u_0 (exp.)	u_0	$10^{6}\beta_{0s}$	$10^{6}\delta_0$	$10^{5}\beta_0$
0	1402.98	1403.00	50.811	0.0300	50.841
5	1426.71	1426.71	49.130	.0017	49.132
10	1447.79	1447.77	47.723	.0522	47.775
15	1466.40	1466.39	46.547	.1567	46.704
20	1482.74	1482.75	45.566	.2998	45.866
25	1497.06	1497.07[a]	44.751	.4726	45.224
30	1509.55	1509.55	44.076	.6695	44.746

[a] The two values at 25° marked with *d* in Table I were excluded from the average because of a change in the instrumental constant.

the experimental values satisfactorily. Because of the temperature smoothing, u_0 calculated from equation 3 will be used in subsequent calculations. The adiabatic compressibility of pure water (expressed as bars^{-1}) was calculated by the equation

$$\beta_{0s} = 100/u_0^2 d_0 \qquad (4)$$

and recorded in the fourth column of Table II. The quantity δ_0, which appears in the fifth column, was calculated from the equation

$$\delta_0 = \beta_0 - \beta_{0s} = T\alpha_0^2/10c_p d_0 \qquad (5)$$

using values for the coefficient of thermal expansion[7], specific heat[8] and density[9] of pure water to be found in the literature.

The isothermal compressibility, β_0, of pure water, calculated from equations 4 and 5, is given in the last column of Table II. We consider these values somewhat more reliable than those calculated from direct measurements of compressions resulting from large pressure increments.[7]

Calculation of ϕ_K^0 ($= \bar{K}_2^0$).—The calculation of ϕ_K^0, and hence $\bar{K}_2^0$, by equation 2 requires knowledge of the two quantities ϕ_V^0 and A_δ at all of the temperatures with which we are concerned. At 25° several sources of data[7] are available for evaluating ϕ_V^0 for the four salts under study, but in order to obtain ϕ_V^0 at 5° intervals from 0 to 30° a very uncertain interpolation must be made between the values available at 0, 25, 35, 45 and 50°. Geffcken[10] extrapolated the data at these temperatures in 1931. Although additional data are now available at 25°, and better extrapolations have been performed at this temperature, it was decided in the interests of smooth and consistent interpolation to use only Geffcken's reported values of ϕ_V^0, and to treat his results for the four salts as a family of very similar curves. This led to the smooth values of ϕ_V^0 recorded in Table III. The uncertainty in these values is high, and probably exceeds that of the smooth values of A_u given in Table I. Fortunately, ϕ_K^0 is very simply corrected by equation 2 for future improvement in the values of ϕ_V^0 at any particular temperature.

The data from which to calculate[7] A_δ, the rate of change of δ with concentration at infinite dilution, are available only at 25°, and at the temperature of maximum density, where A_δ is zero. Since the term $1000A_\delta$ contributes only about 7.5% to ϕ_K^0 at 25°, we have assumed a convenient linear temperature dependence in order to estimate A_δ

$$A_\delta = (t - 3.986)A_\delta(25°)/21.014 \qquad (6)$$

at temperatures other than 25 and 3.986°. Values of $1000A_\delta$ are recorded in Table III, which completes the tabulation of all of the quantities which

TABLE III

STANDARD PARTIAL MOLAL COMPRESSIBILITIES, $\bar{K}_2^0 (= \phi_K^0)$, AND ASSOCIATED QUANTITIES

t, °C.	ϕ_V^0	$10^7 A_\delta$	$10^4 \bar{K}_2^0$
	Sodium chloride		
0	12.4	−0.73	−75.85
5	13.4	.19	−68.12
10	14.3	1.11	−61.47
15	15.1	2.02	−55.69
20	15.8	2.94	−50.65
25	16.35	3.86	−46.28
30	16.8	4.78	−42.44
	Potassium chloride		
0	23.0	−0.58	−68.04
5	23.9	.15	−60.66
10	24.7	.88	−54.38
15	25.4	1.61	−49.00
20	26.0	2.33	−44.38
25	26.45	3.06	−40.44
30	26.8	3.79	−37.06
	Sodium bromide		
0	19.0	−0.87	−66.67
5	20.1	.22	−59.10
10	21.1	1.32	−52.58
15	22.0	2.41	−46.92
20	22.8	3.51	−41.98
25	23.45	4.60	−37.70
30	24.0	5.70	−33.96
	Potassium bromide		
0	29.6	−0.72	−58.86
5	30.6	.18	−51.64
10	31.5	1.09	−45.49
15	32.3	1.99	−40.22
20	33.0	2.90	−35.70
25	33.55	3.81	−31.86
30	34.0	4.71	−28.58

appear in equation 2 except the molecular weights, M_2, and the density of pure water, d_0. Our values of ϕ_K^0 calculated by this equation are given in the last column of Table III. Although the accuracy with which these quantities are presently known might not justify retention of the last two decimal places, we have recorded ϕ_K^0 to four figures so that future improvements in any of the critical quantities A_u, ϕ_V^0 and A_δ may be used very simply to yield more precise values of ϕ_K^0.

These results show that $\bar{K}_2^0$ is negative, and increases rapidly (becomes more positive) with increasing temperature. The rate of increase decreases with rise in temperature, suggesting that $\bar{K}_2^0$ may pass through a maximum above 50°. $\bar{K}_2^0$ is, of course an additive property of the ions. The high degree of additivity observed in the

(7) H. S. Harned and B. B. Owen, "The Physical Chemistry of Electrolytic Solutions," Third Edition, Reinhold Publ. Corp., New York, N. Y., 1958.

(8) N. S. Osborne, H. F. Stimson and D. C. Ginnings, *J. Research Natl. Bur. Standards*, **23**, 197 (1939). Equation 5 requires that c_p be expressed in joules/g. deg. C.

(9) Densities in ref. 7 are g./ml. Equations 4 and 5 require that d_0 be expressed as g./cc.

(10) W. Geffcken, *Z. physik. Chem.*, **155A**, 1 (1931).

values recorded in Table III should be regarded as a necessary condition, but not as a proof of accuracy, for the curves from which ϕ_V^0, A_δ and A_u were read had been carefully constructed to ensure additivity of these quantities, as well as temperature smoothing. The definition[11] and calculation of A_δ make this an additive quantity, and it follows from equation 2 that A_u must also be an additive property of the ions. The application of this principle was very helpful in limiting the positions of the curves in Fig. 1, because it had the effect of increasing the number of data points which had to be considered simultaneously.

(11) Ref. 7, p. 387.

THE SEPARATION OF HYDROGEN, DEUTERIUM AND HYDROGEN DEUTERIDE MIXTURES BY GAS CHROMATOGRAPHY

BY PAUL P. HUNT AND HILTON A. SMITH

Department of Chemistry, University of Tennessee, Knoxville, Tennessee

Received June 20, 1960

The resolution and analysis of the components of hydrogen–deuterium mixtures have been accomplished by gas chromatography at 77°K. Neon was employed as the carrier gas, and the column was chromia deposited on alumina. Orthohydrogen and parahydrogen did not separate on the chromia–alumina column. The separation factor for hydrogen deuteride and deuterium was much greater than that for hydrogen and hydrogen deuteride. The complete separation of deuterium and hydrogen deuteride was also obtained on a silica gel column with hydrogen as the carrier gas, whereas a charcoal column produced very little separation.

Gas chromatography affords a simple method for the analysis of the hydrogen isotopes. Various degrees of separation have been reported by several investigators.[1-5] A recent preliminary communication[6] describes the first complete separation of hydrogen, hydrogen deuteride and deuterium by this method. The resolution was accomplished by means of a chromia–alumina column operated at 77°K. with neon as the carrier gas. Details of this separation as well as experiments with other columns are given in the present contribution.

Experimental

Apparatus.—The chromia–alumina column consisted of a single piece of copper tubing 12 ft. in length and with an outside diameter of $^5/_{16}$ in. Grade F-1, 8–14 mesh, activated alumina, obtained from the Aluminum Company of America, was crushed and screened through a series of standard screens. The column packing was prepared from 225 g. of 20–40 mesh alumina to which 6.7% by weight chromium trioxide was added in 350 ml. of water. The mixture was agitated for three hours and the excess liquid was removed by filtration. The residue was dried and the chromic acid reduced in a stream of hydrogen at 360°. The yellow material turned green upon reduction. Small dust particles were removed by screening following the reduction process. After the column was packed and coiled in a spiral 4 in. in diameter, water was added to the column in order to obtain partial deactivation. Considerable evolution of heat was noted as the water was added. The column was reactivated when desired by passing a stream of nitrogen through the column for three hours at 140–150°.

A circulatory gas flow system with neon as the carrier gas was employed with the chromia–alumina column. A double-acting, piston-type pump furnished sufficient pressure differential for gas flow. The construction of the gas pump was similar to those previously described,[7,8] with the following modifications.

The piston barrel, approximately 5 in. long, was constructed from 12-mm. Pyrex glass tubing. A Teflon-covered magnetic plunger, 1.5 in. in length, was fitted inside the chamber. The outlet and inlet connections to the piston barrel were made of Pyrex tubing with an outside diameter of 6 mm. Valves were constructed from sections of 9-mm. glass tubing approximately $^1/_2$ in. in length, fitted over $^1/_2$-in. sections of 6-mm. capillary tubing. The capillary tubing was ground on the end, and a section of a microscope cover glass was seated in the narrow space between the capillary end and the connection between the 6- and 9-mm. tubing. Indentations were made at the taper seal between the 9- and 6-mm. tubing just above the cover glass to prevent the cover glass from turning edgewise and sticking during the pumping process. The inlet leads from each end of the pump were connected together with glass tubing, as were also the outlet leads.

The plunger was moved by two doughnut-shaped Indox magnets obtained from the Indiana Steel Products Company of Valparaiso, Indiana. The magnets were clamped in a brass carrier. The magnet carrier was connected by means of a string across a pulley to a disc attached to a motor to furnish reciprocal movement of the plunger. A slot cut in a disc allowed the stroke length to be properly adjusted. The motor speed was 45 r.p.m.

The system was prepared for operation by evacuation and flushing with hydrogen and neon. The entire apparatus was then filled with neon to a pressure slightly greater than that of the atmosphere. When the column was immersed in liquid nitrogen, it was necessary to add more neon to maintain this pressure.

The hydrogen and deuterium samples were oxidized in a hot copper tube after the samples had passed through the katharometer. The resulting water was adsorbed in silica gel and charcoal traps. The flow rate was measured by a soap-film meter[9] placed in the circulatory system. Neon was conserved between a series of runs by absorbing the excess from the column in the charcoal trap immersed in liquid nitrogen.

Silica gel columns, 6 and 10 ft. in length, were prepared from 40–60 and 60–80 mesh material obtained from the Davison Chemical Company. The packing was activated at 140–150° before being placed in the column. Hydrogen,

(1) E. Glueckauf and G. P. Kitt, in D. H. Desty, "Vapor Phase Chromatography," Butterworths Scientific Publications, London, 1957, pp. 422–427; E. Glueckauf and G. P. Kitt, in the "Proceedings of the International Symposium on Isotope Separation," Interscience Publishers, Inc., New York, N. Y., 1958, pp. 210–226.

(2) C. O. Thomas and H. A. Smith, *J. Phys. Chem.*, **63**, 427 (1959).

(3) W. R. Moore and H. R. Ward, *J. Am. Chem. Soc.*, **80**, 2909 (1958).

(4) W. A. Van Hook and P. H. Emmett, *J. Phys. Chem.*, **64**, 673 (1960).

(5) S. Ohkoshi, Y. Fujita and T. Kwan, *Bull. Chem. Soc. Japan*, **31**, 770 (1958); S. Ohkoshi, S. Tenma, Y. Fujita and T. Kwan, *ibid.*, **31**, 772 (1958); S. Ohkoshi, S. Tenma, Y. Fujita and T. Kwan, *ibid.*, **31**, 773 (1958).

(6) H. A. Smith and P. P. Hunt, *J. Phys. Chem.*, **64**, 383 (1960).

(7) J. C. Balsbaugh, R. G. Larsen and D. A. Lyon, *Ind. Eng. Chem.*, **28**, 682 (1936).

(8) F. D. Rosen, *Rev. Sci. Instr.*, **24**, 1061 (1953).

(9) C. O. Thomas and H. A. Smith, *J. Chem. Educ.* **36**, 527 (1959).

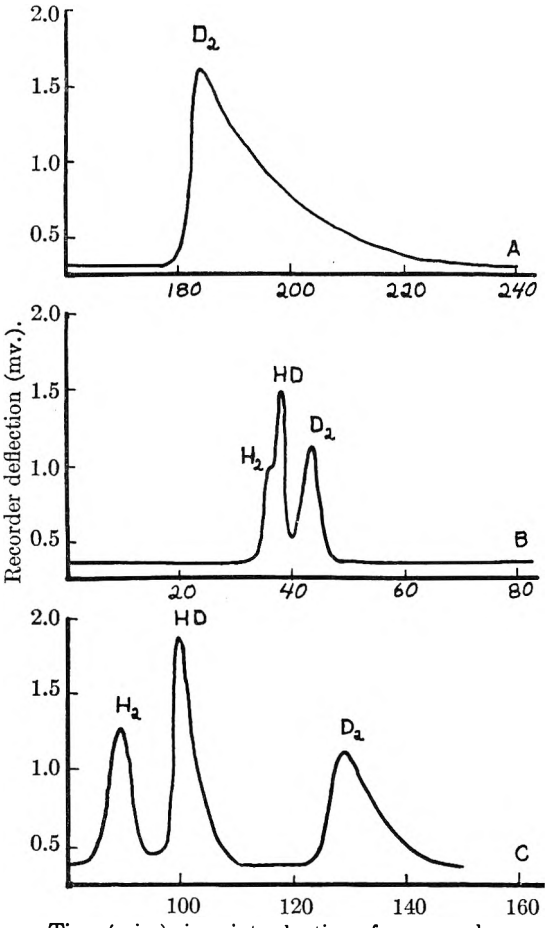

Fig. 1.—Elution curves for hydrogen isotopes on chromia–alumina column with neon carrier at 77°K. and 35 cc. per min. flow rate. (A) Deuterium peak with an activated column after introduction of a mixture of H_2, HD and D_2. The H_2 and HD peaks appeared after 114 and 133 minutes, respectively. (B) H_2, HD and D_2 overlapping peaks when the column is deactivated. (C) H_2, HD and D_2 peaks from mixture introduced into partially deactivated column.

neon and helium were employed as the carrier gases at 77°K. The hydrogen and helium carriers were vented directly to the atmosphere. Silica gel columns were also employed at −161°. This temperature was obtained with boiling methane.

The chamber for the preparation of the mixtures of hydrogen deuterium and hydrogen deuteride consisted of a 100-ml. glass bulb carrying two tungsten leads, which were brazed to a coiled nichrome wire. The flask was connected to a capillary manometer through a three-way stopcock. The samples of hydrogen, deuterium and hydrogen deuteride were prepared by equilibrating mixtures of hydrogen and deuterium over the heated nichrome wire. Samples were injected into the column through a by-pass cell.

The detection and the recording apparatus have been previously described.[2,9]

Gases.—Neon was obtained from the Matheson Company. Ordinary commercial tank hydrogen was purchased from the National Cylinder Gas Company. Deuterium, reported to be 99.5% pure, was obtained from the Stuart Oxygen Company. Commercial nitrogen and argon were used. All gases were employed without further purification.

Results and Discussion

Alumina columns[4] are effective in separating hydrogen and deuterium at 77°K., but orthohydrogen and hydrogen deuteride overlap. A substance which has different adsorption affinities for the isotopes and catalyzes the conversion of ortho- and parahydrogen but does not catalyze the hydrogen–deuterium exchange should make the complete separation of the species possible. Chromia very effectively catalyzes the orthohydrogen-parahydrogen conversion at low temperatures and subsequently no separation of the ortho- and parahydrogen was noted with the chromia–alumina column. The hydrogen peak was effectively sharpened in comparison to the hydrogen deuteride and deuterium peaks. Elution curves for this system with activated and partially deactivated columns are shown in Fig. 1.

The leading parahydrogen is equilibrated with orthohydrogen, and likewise the slower moving orthohydrogen is equilibrated with the parahydrogen at the tail of the peak. For this reason the movement of the peak front should be slowed, while that of the tail should be accelerated.

Pure samples of hydrogen produced only one peak indicating that orthohydrogen and parahydrogen were not separated. Freshly mixed samples of hydrogen and deuterium gave only two peaks, and thus ruled out the possibility of hydrogen–deuterium exchange as the sample passed through the column.

This separation can be very easily adapted to the determination of unknown quantities of the isotopes without either having an equilibrium mixture or a knowledge of the orthohydrogen–parahydrogen ratio. Calibration plots may be obtained for hydrogen, hydrogen deuteride and deuterium from equilibrated mixtures or from samples also subjected to mass spectrographic determination. The percentage composition for unknown mixtures can then be determined from the calibration plots. Neon gives sufficient recorder deflection for small samples and does not require the oxidation of the isotopes before detection.

Samples of pure hydrogen and pure deuterium of constant volume but varying pressures were passed through the columns. When the areas under the peaks shown in the recorder traces (as determined by the product of peak width at half height and peak height) were plotted against the pressure of hydrogen or deuterium, straight lines were obtained for each isotope. When a mixture of hydrogen, deuterium and hydrogen deuteride of the same volume and at a known total pressure were swept through the column, the pressures of hydrogen and deuterium were obtained from the areas under their peaks and the calibration curves. The pressure of hydrogen deuteride was then obtained by subtracting the partial pressures of the hydrogen and deuterium from the total pressure.

A mixture of hydrogen and deuterium of known composition was placed in the equilibration bulb and the nichrome wire heated to approximately 1000°K. The equilibrium constant for the reaction

$$H_2 + D_2 \longrightarrow 2HD$$

is 3.895 at this temperature.[10] An error of 100° in the temperature of the wire makes such a small change in the equilibrium constant that variation in

(10) H. W. Wooley, R. B. Scott and F. G. Brickwedde, *J. Research Natl. Bur. Standards*, **41**, 379 (1948).

the calculated percentages of hydrogen, deuterium and hydrogen deuteride in a mixture are within experimental error. A mixture in which the calculated percentages of hydrogen, deuterium and hydrogen deuteride were 17.7, 34.0 and 48.4 gave experimental values of 18.1, 33.4 and 48.6, with standard deviations of approximately 1%.

The times involved in the analyses could be greatly reduced by increasing the flow rate above the value of 25–35 cc. per minute used in this research. Helium could undoubtedly be used as a carrier gas if the hydrogen were oxidized between the column exit and the katharometer.[3] However, the thermal conductivity of mixtures of hydrogen and helium exhibits a minimum at certain gas concentrations[11] so that direct quantitative analysis without the oxidation process is not feasible.

A column was prepared by depositing chromia on flint quartz and the retention times for hydrogen and deuterium studied under conditions similar to those which resulted in successful isotope separations when chromia–alumina columns were employed. The retention times for pure samples were slightly less than four minutes, and indicated that no separation could be obtained. Thus the chromia alone is not responsible for the separation achieved when the alumina was treated with chromia.

Materials similar to chromia may also be deposited on the alumina for ortho–parahydrogen conversion, and molecules other than water may be employed to deactivate the column. Moore and Ward[12] have now reported separations similar to that reported here with ferric oxide as the coating for the alumina and carbon dioxide as the deactivating agent.

The results obtained with silica gel columns are shown in Fig. 2. The separation of deuterium and hydrogen deuteride at 77°K. with hydrogen as a carrier gas is comparable to that which has been reported when a column containing molecular sieves is employed.[5] Under these conditions, helium and neon failed to elute the isotopes from the silica gel column. The isotopes could be eluted by these carriers at −161° (boiling methane), but the overlapping of peaks prevented quantitative determination of the components of the mixture.

Partial resolution of deuterium and hydrogen deuteride was obtained with hydrogen carrier and a charcoal column at 77°K. This is also shown in Fig. 2.

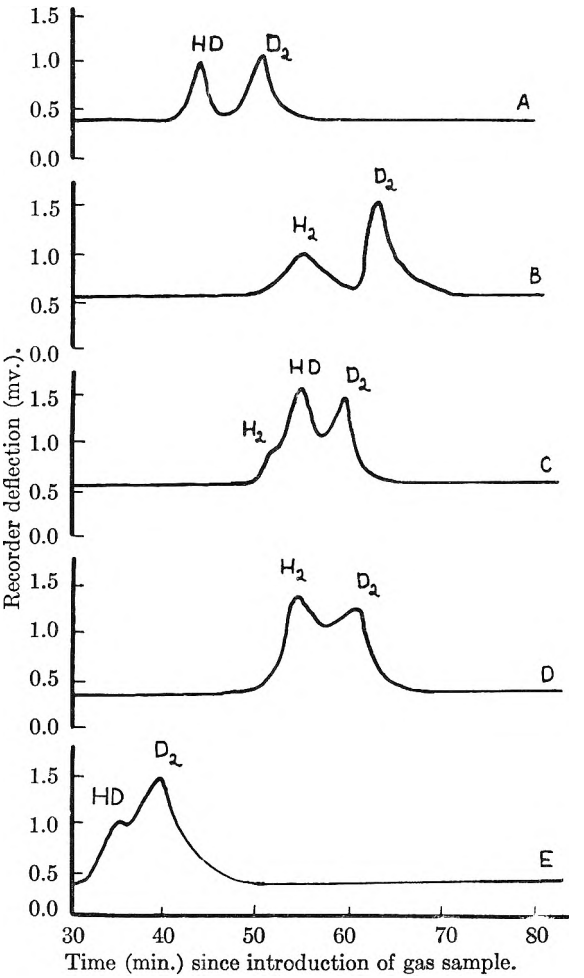

Fig. 2.—Elution curves for hydrogen isotopes on silica gel and charcoal columns. (A) H_2, HD and D_2 on silica gel column at 77°K. Hydrogen carrier at flow rate of 144 ml./min. (B) H_2 and D_2 on silica gel column at 112°K. Helium carrier at flow rate of 58 ml./min. (C) H_2, HD, and D_2 on silica gel column at 112°K. Helium carrier at 60 ml./min. (D) H_2 and D_2 on silica gel column at 112°K. Neon carrier at flow rate of 25 ml./min. (E) H_2, HD and D_2 on charcoal column at 77°K. Hydrogen carrier at flow rate of 75 ml./min.

Acknowledgment.—The authors are grateful to the United States Atomic Energy Commission for support of this research.

(11) J. J. Madison, *Anal. Chem.*, **30**, 1859 (1958).
(12) W. R. Moore and H. R. Ward, *J. Phys. Chem.*, **64**, 832 (1960).

ELECTRICAL CONDUCTIVITY OF SOME ORGANIC SOLUTES IN ANHYDROUS HYDROGEN FLUORIDE[1]

BY LLOYD QUARTERMAN, HERBERT H. HYMAN AND JOSEPH J. KATZ

Argonne National Laboratory, Argonne, Illinois

Received June 24, 1960

Many organic liquids containing oxygen are miscible with anhydrous hydrogen fluoride. Ethanol, acetic acid and diethyl ether are typical proton acceptors and form highly conducting solutions over most of the concentration range. Trifluoroethanol, trifluoroacetic acid and nitrobenzene are much less extensively ionized in this medium. Perfluorobutyl ether is essentially insoluble. The electrical conductivities for these systems are tabulated and compared.

Introduction

We have had an active interest in the behavior of anhydrous hydrogen fluoride as a proton-transfer ionizing solvent. While the properties of solutions in hydrogen fluoride can be studied by optical spectroscopy and allied procedures, measurements of electrical conductivity have an almost unique value in the interpretation of the nature of such solutions. We have therefore carried out an extensive series of electrical conductivity determinations for a number of representative organic solutes.

Most of the literature on the electrical conductivity of hydrogen fluoride solutions is due to Fredenhagen,[2] and has been summarized by Simons.[3] In general, these measurements have been in the concentration range below 1 mole of solute per liter of hydrogen fluoride. For the present research, we have investigated the electrical conductivity for a number of representative solutes over a much larger range of concentration.

Experimental

Materials.—The hydrogen fluoride was purified by a method which has been previously described.[4] After the final distillation, the hydrogen fluoride was not permitted to come into contact with any metal other than platinum, and moisture was rigorously excluded. The electrical conductivity of material so prepared was routinely $<3 \times 10^{-6}$ ohms^{-1} cm.$^{-1}$ at 0°. Acetic acid, reagent grade, was treated with a calculated amount of acetic anhydride to yield essentially anhydrous material. A commercial grade of trifluoroethanol available from Pennsalt Manufacturing Company was purified by a double distillation using a middle cut boiling at 73° at atmospheric pressure. Trifluoroacetic acid was Minnesota Mining & Manufacturing Co. grade distilled at reduced pressure over phosphorus pentoxide. The boiling point observed for this material was 71.2°. A sample of perfluorobutyl ether was kindly provided by Dr. Karl Rapp of the K 25 Division of the Carbide and Carbon Chemicals Company, Oak Ridge, Tennessee, and was used without further purification. It was essentially insoluble in HF and no conductivity data were obtained. All other reagents were commercially available reagent grade chemicals.

Apparatus.—The simple apparatus used for the conductivity measurements has been described previously.[5] Aside from the platinum electrodes the only materials allowed to come in contact with the solutions were polychlorotrifluoroethylene (Kel F) and polytetrafluoroethylene (Teflon).

The Kel-F to Kel-F joints are 45° flares except as noted. Both male and female surfaces are plastic. but the threaded parts are metal (brass or aluminum). Where the male cannot be fabricated in one piece (as in the case of the Kel-F values and tee) a split ring technique is employed. The mixing tube, a machined tube of larger capacity than the molded tubes currently available is sealed with the aid of a Teflon O-ring. A different electrode arrangement was employed for solutions with lower specific conductivities. Two concentric cylinders were used in this case, rather than widely separated plates. The surface area was therefore increased and the distance between the electrodes decreased as compared with the cell shown.

Solution Preparation.—The solute was added to the Kel-F mixing tube and the tube plus valve weighed before and after this addition. The mixing tube was then attached to the vacuum line, the solute frozen with liquid nitrogen, the valve opened, and air removed from the system. The valve was then closed, and the solute alternately warmed to room temperature, refrozen and the system evacuated as often as needed to remove measurable amounts of trapped air. Anhydrous hydrogen fluoride was then distilled into the mixing tube from a weighing tube attached to the vacuum line. The mixture of hydrogen fluoride and the reagent was allowed to warm up slowly while the system was occasionally agitated, and when the mixture reached room temperature, the contents of the cell was thoroughly mixed. The solution was then poured through the flexible Kel-F connecting tubing from the mixing tube into the conductivity cell, filling the conductivity cell up to the middle of the Teflon spacer. Small variations in the filling height produced no effect on the measured conductivity. After the conductivity measurements were completed, the contents of the conductivity cell were poured back into the mixing tube. While the solution in the mixing tube was frozen with liquid nitrogen, the conductivity cell and connecting lines were warmed to return the entire contents to the mixing tube. An additional portion of HF was then distilled into the mixing tube and a solution with a new concentration was then investigated. When no further dilutions could be performed in the mixing tube, the major part of the contents were removed by pouring into a second tube which had replaced the conductivity cell and the series of dilutions continued on the residue. In all cases, the solutions were made up by weight, and aside from the initial introduction of the non-HF component, air was excluded.

The conductivity cell was equipped with a platinum–platinum–10% rhodium thermocouple attached to one of the electrodes and for each solution the conductivity was measured at 0° and at 25 ± 0.2°. The conductivity cell was shaken periodically to assure uniform temperature in the cell during the conductivity measurements.

Conductance measurements were made with an Industrial Instrument RC-16 AC conductivity bridge with an external capacitor in the balancing circuit. Measurements were made at 60 and 1000 cycles to permit corrections for polarization. Such corrections were not usually significant. The precision of the conductivity data is ±1%.

Observations

The data are summarized in Table I. The mole per cent values are calculated directly from the weights of added materials. The cation normalities are calculated at 25° assuming volume additivity in mixing.

It is further assumed that the only ionization process taking place is proton transfer, that the only anion present in the system is the fluoride

(1) Based on work performed under the auspices of the U. S. Atomic Energy Commission.

(2) K. Fredenhagen, G. Cadenbach and W. Klatt, *Z. physik. Chem.*, *A164*, 176 (1933).

(3) J. H. Simons, "Fluorine Chemistry," Vol. 1, Chap. 6, Academic Press, Inc., New York, N. Y., 1950, p. 240.

(4) H. H. Hyman, M. Kilpatrick and J. J. Katz, *J. Am. Chem. Soc.*, **79**, 3668 (1957).

(5) L. A. Quarterman, H. H. Hyman and J. J. Katz, THIS JOURNAL, **61**, 912 (1957).

TABLE I: ELECTRICAL CONDUCTIVITY OF SOLUTIONS OF ORGANIC SOLUTES IN HYDROGEN FLUORIDE

Solute	Concentration		Electrical conductivity		
			Specific conductivity ohm^{-1} cm.$^{-1}$		Equiv. conductance ohm^{-1} cm.^{2}
S	Mole % S	Moles/l.[a] SH$^+$	0°	25°	25°
Ethanol	5.50	2.41	0.250	0.289	120
	6.63	2.84	.269	.308	108.5
	8.43	3.52	.290	.334	94.9
	10.94	4.39	.293	.347	79.0
	17.71	6.44	.275	.325	50.5
	23.71	7.73	.236	.275	35.6
	31.89	9.54	.162	.186	19.5
	39.07	10.98	.0871	.102	9.29
	43.62	11.73	.0470	.0541	4.69
	50.90	12.30	.0259	.0303	2.46
	63.18	8.61	54.0×10^{-4}	66.1×10^{-4}	0.768
	75.05	5.09	8.47	10.7	.210
	85.47	2.75	1.27	1.80	.0655
	92.28	1.38	0.284	0.425	.0308
	97.48	0.44	.0494	.0780	.0178
	100		.0088	.0142	
Trifluoroethanol	5.36	2.27	193×10^{-4}	210×10^{-4}	9.25
	7.01	2.87	214	234	8.15
	9.07	3.56	227	246	6.91
	11.56	4.33	229	249	5.75
	15.56	5.40	213	230	4.26
	29.36	8.18	107	119	1.45
	38.67	9.51	58.4	66.9	0.703
	57.36	8.44	16.2	19.3	.229
	69.11	5.48	5.28	6.13	.112
	77.07	3.67	3.47	3.96	.108
	81.78	2.83	1.80	2.02	.0714
	90.49	1.41	0.626	0.673	.0477
	95.24	0.68	.228	.238	.0351
	100		.007	.012	
Acetic acid	6.61	2.85	0.246	0.263	92.3
	7.99	3.38	.270	.285	84.3
	9.91	4.06	.281	.340	83.7
	14.12	5.44	.259	.276	50.7
	17.5	6.45	.223	.235	36.4
	21.43	7.49	.168	.189	25.2
	27.22	8.87	.113	.130	14.7
	34.47	10.34	.0623	.0701	6.78
	43.19	11.82	.0240	.0267	2.26
	51.46	12.27	65.6×10^{-4}	86.2×10^{-4}	0.703
	65.57	7.70	6.36	9.08	.118
	77.00	4.71		0.896	.019
	89.52	1.96		.0387	.00187
	95.77	0.759		.00532	.00044
	100			.002	
Trifluoroacetic acid	7.01	2.83	88.4×10^{-4}	103×10^{-4}	3.64
	7.85	3.16	61.0	72.4	2.29
	8.18	3.23	59.4	68.8	2.13
	9.80	3.67	57.7	66.4	1.81
	10.67	3.96	44.5	59.6	1.51
	14.39	4.96	47.8	57.1	1.41
	21.09	6.44	27.3	32.2	1.15
	21.87	6.61	24.8	27.9	0.422
	28.81	7.77	12.2	15.0	.193
	30.12	7.98	11.9	13.6	.170
	36.28	8.81	6.69	7.32	.083
	39.24	9.14	5.99	6.96	.076
	44.72	9.73	3.14	3.40	.0349
	56.84	7.91	0.674	0.774	.00979
	73.19	4.33	.111	.146	.00337
	89.59	1.45	.0216	.0304	.00210
	100		.004	.006	

TABLE I (*Continued*)

Solute S	Concentration: Mole % S	Concentration: Moles/l.[a] SH$^+$	Electrical conductivity: Specific conductivity ohm^{-1} cm.$^{-1}$ 0°	Electrical conductivity: Specific conductivity ohm^{-1} cm.$^{-1}$ 25°	Electrical conductivity: Equiv. conductance ohm^{-1} cm.^{2} 25°
Diethyl ether	0.27	0.136	0.0294	0.0364	267.6
	0.54	.266	.0525	.0638	239.8
	1.01	.487	.0768	.0987	202.7
	1.65	.774	.112	.131	169.3
	2.41	1.10	.143	.179	162.7
	3.57	1.56	.179	.213	136.6
	5.20	2.15	.201	.226	105.1
	8.47	3.16	.183	.210	66.5
	10.38	3.67	.159	.179	48.8
	13.02	4.28	.123	.138	32.2
	14.17	4.67	.100	.112	24.0
	18.74	5.36	.0632	.0700	13.1
	22.86	5.97	.0350	.0380	6.37
	31.31	6.95	68.8×10^{-4}	75.2×10^{-4}	1.08
	37.99	7.54	14.5	16.5	0.219
	47.52	8.19	1.56	1.84	.0225
	54.73	6.83	0.349	0.425	.00622
	62.64	5.13	.0963	.116	.00226
	77.24	2.68	.0181	.0185	.00069
	79.75	2.33	.0125	.0112	.00048
	86.76	1.42	.0035	.0030	.00021
	93.48	0.68	.0004	.0004	.00005
Nitrobenzene	6.19	2.39	38.8×10^{-4}	48.9×10^{-4}	2.05
	8.76	3.13	38.8	48.6	1.55
	12.71	4.07	33.1	39.7	0.975
	20.28	5.42	25.9	30.8	.568
	27.74	6.37	19.4	22.3	.350
	34.00	6.99	14.3	16.1	.230
	43.36	7.70	8.21	9.16	.119
	51.60	7.69	4.95	5.50	.0715
	59.22	5.88	2.69	2.95	.0502
	67.14	4.34	1.50	1.65	.0380
	74.83	3.07	0.84	0.914	.0298
	100		0.0024	0.0037	
Acetone	32.74	8.62		76	0.89
	38.01	9.33		46	.50
	46.29	10.26		15.1	.147
	54.35	9.25		5.04	.055
	68.54	5.53		1.04	0.0188
	81.27	2.95		0.318	.0108
	92.90	1.02		.108	.0104
	100			.02	
n-Butyl ether	6.58	2.17	663	915	42.2
	9.26	3.01	487	558	18.5
	11.89	3.12	388	458	14.7
	16.87	3.72	166	180	4.84
	27.10	4.51	76.5	81.4	1.80
	38.85	4.82	2.98	3.59	0.745
	57.19	5.25	0.153	0.202	.0385
	66.28	3.61	.0292	.0348	.00964
	79.25	1.93	.0024	.0025	.00128
	89.14	0.918	.0002	.0002	.00023
	100		.0001		
Tetrohydrofuran	32.67	8.22		67.3×10^{-4}	0.819
	39.00	8.47		15.1	.178
	44.51	9.45		3.07	.0325
	61.71	6.60		0.340	.00515
	73.61	4.04		.134	.00332
	90.12	1.31		.018	.00137
	100			.001	

anion, and that the concentration of cation present is the maximum attainable in the solution. The specific conductivities at 0 and 25° are the measured values. The equivalent conductivities are calculated from the specific conductivity and the maximum equivalent concentration of the cation as given in the Table.

Discussion

Two classes of solutes are readily noted with respect to electrical conductivity. The first group are effective proton acceptors and may be regarded as essentially completely ionized in HF solution. They include most simple oxygen-containing organic molecules whether alcohol, ether or acid. Acetone is in this group. However the protonated acetone is not very stable and in the concentration range where extensive ionization is found, the conductivity changes rapidly with time. When the specific conductivity is plotted as a function of concentration for ethanol, diethyl ether and acetic acid, the specific conductivity rises rapidly as the organic solute is added to the hydrogen fluoride, reaches a maximum in the neighborhood of 90 mole % HF, and then drops to the value of the pure organic compound. With a solvent of a relatively high dielectric constant, such as ethanol (24.2), the maximum is shifted toward a lower hydrogen fluoride concentration. The conductivity falls off more slowly as the organic compound is added than when the organic solute has a low dielectric constant such as in the case of diethyl ether (4.24). Note that acetic acid has a higher conductivity throughout the concentration range than does diethyl ether, so that the contribution of acid strength is clearly not the determining factor in preventing the transfer of a proton to the base.

On the other hand, when the trifluoromethyl group replaces the methyl group in either ethanol or acetic acid, the base strength of the adjacent carbonyl is obviously very much reduced. Neither trifluoroethanol nor trifluoroacetic acid are extensively ionized in anhydrous HF.

Another interesting substance which is not extensively ionized in anhydrous HF is nitrobenzene. This solute has been studied as a Hammett H_0 indicator in fuming sulfuric acid and the pK of the indicator reaction has been given as -11.38.[6] No attempt was made here to observe the conductivity of nitrobenzene at low concentrations comparable to those used in obtaining the spectrophotometric data. At the lowest concentration actually employed, about two moles/l., nitrobenzene appears to be about 2% ionized. Using the equilibrium constant reported by Brand and the H_0 value of anhydrous HF as -10.2,[4] the extent of ionization at infinite dilution might be as much as 6%. The relatively high dielectric constant of nitrobenzene (34.5) leads to a quite significant conductivity in concentration ranges where the much stronger base diethyl ether (dielectric constant 4.24) shows essentially no measurable electrical conductivity.

The proton transfer phenomenon only leads to electrical conductivity if the dielectric constant of the medium is high enough to promote effective charge separation. The electrical conductivity measurements in these HF solutions offer excellent examples of proton transfer with and without ionization.

Hydrogen fluoride is a relatively non-destructive medium. Conductivity measurements such as those reported here offer a simple method of studying the base strength of rather weak bases and therefore the effect of substitution on the base strength of organic molecules. In this respect the conductivity measurements complement spectrophotometric studies.

Hammett pointed out[7] that nitrobenzene is soluble in sulfuric acid under conditions where it is not ionized. Our data suggest that this is true for nitrobenzene in anhydrous HF and for many solute–solvent combinations where the proton transfer reaction takes place only to a slight extent. It may well be true, however, that acid solvents dissolve weak bases without proton transfer only within a limited region of base strength. For still weaker bases, (*e.g.*, perfluorobutyl ether) the solubility drops to very low levels.

Acknowledgments.—The authors are grateful to J. R. Pickhardt for construction of much of the equipment.

(6) J. C. D. Brand, *J. Chem. Soc.*, 997 (1950).

(7) L. P. Hammett, "Physical Organic Chemistry," McGraw-Hill Book Co., New York, N. Y., 1940.

MICROWAVE ABSORPTION AND MOLECULAR STRUCTURE IN LIQUIDS. XXXIV. AN INTERFEROMETRIC METHOD FOR THE MEASUREMENT OF DIELECTRIC CONSTANT AND LOSS AT 4.3 MM. WAVE LENGTH[1,2]

BY W. E. VAUGHAN,[3] K. BERGMANN AND C. P. SMYTH

Frick Chemical Laboratory, Princeton University, Princeton, N. J.

Received June 27, 1960

The theory and apparatus for an interferometric method for the measurement of the dielectric constant and loss of liquids at 4.3 mm. wave length are described. The probable error of the dielectric constant measurements is 1% except for extremely low loss materials, in which case the error increases as the loss decreases. The probable error of the loss measurements is 2%, increasing for both extremely high loss and extremely low loss.

An improved interferometric method has been developed for the measurement of the dielectric constants and losses of liquids at 4.3 mm. wave length using a harmonic from an 8.7 mm. klystron source. The ratio to the incident power of the power reflected at oblique incidence from the air-dielectric interface (of a dielectric backed by a metal sheet) is observed as a function of the dielectric sheet thickness. The dielectric constant and loss may be calculated from the observed curve. Wave guide techniques are used for the production and detection of the microwave power, but the interaction of the plane polarized electromagnetic waves produced with the dielectric sheet occurs in free space.

Apparatus.—A functional diagram of the apparatus is given in Fig. 1. Power for the klystron D (EMI R5146) is supplied by A(FXR Model Z 815 B Universal Klystron Power Supply). The klystron, which generates 8.7 mm. waves, can be tuned both mechanically and electrically. A silicon rectifier B prevents the klystron reflector from becoming positive relative to the cathode. The klystron is air-cooled by a fan C. The output of the klystron is matched to RG-96/U wave guide by two adapting tapers E in series. A harmonic generator F (Microwave Associates MA-435) converts part of the signal to 4.35 mm. wave length and passes the output to RG-99/U wave guide. An E/H tuner G (De Mornay Bonardi DBA-979) is used to match impedances. The frequency is determined using a reaction type frequency meter J (DBA-715-1) with the detector mount modified to accommodate a Sharpless[4] crystal detector M. The detector output is amplified by a standing wave amplifier H(FXR B 810 A). The primary signal is fed into a variable calibrated attenuator K (DBA-430), which regulates the output, isolates generator from load, and permits calibration of the detection system. The wave guide power is converted to a plane wave in free space by a horn L (FXR E 638 A). Power reflected from the cell O is picked up by a similar horn L′, fed to a Sharpless detector M′, amplified and automatically recorded by N (Varian Associates Recorder Model G-10, 0-100 mv., 2″/minute paper speed). The incident and reflected waves form angles of 35° with the normal to the cell. The detector and detector horn were mounted on a movable plate, driven along guide rods against springs by a micrometer drive. The position of the detector assembly relative to the cell could be varied over a range of 2 cm. with a relative accuracy of 0.01 mm.

Figure 2 shows the cell. Two tubes at the bottom of the cell permit water to flow to and from a constant temperature bath. A thermometer indicates the temperature of the water in the cell interior. The cell rests on a tripod with extension legs so that it can be levelled before measurement. A polished silver plate serves as a perfectly reflecting surface beneath the dielectric sheet. The sheet thickness is changed by a micrometer driven plunger, which is forced down into the dielectric reservoir and thus raises the level above the silver disk. The change in dielectric sheet thickness Δd with change in plunger height Δh is given by

$$\Delta d = \Delta h \frac{z_3^2}{z_1^2 + z_2^2 + z_4^2 - z_3^2} \qquad (1)$$

where z_1, z_2, z_3, z_4 are the respective diameters of silver disk, dielectric reservoir, spacer and filling tube. The micrometer is driven by a synchronous motor. Thus distance on the automatic recorder is proportional to dielectric sheet thickness, the constant of proportionality being easily determined with a stopwatch.

Theory

Application of Snell's and Fresnel's equations at the interfaces S, S′ and S″ shown in Fig. 3, for the case in which the incident radiation is normal to the plane of incidence, yields five independent equations in six field intensities ($\vec{E}_0$, $\vec{E}_1$, $\vec{E}_2$, $\vec{E}_3$, $\vec{E}_4$, $\vec{E}_5$). The k_i are the magnitudes of the propagation vectors whose directions are given by the unit vectors $\vec{n}_i$. The θ_i are the angles formed by the propagation vectors and the corresponding normals to the sheet interfaces. L is the thickness of the dielectric layer which is characterized by ϵ_2', ϵ_2'' and d is the thickness of the dielectric layer which is characterized by ϵ_1', ϵ_1''.

Solving for $\vec{E}_{20}/\vec{E}_{00}$, letting

$$\rho e^{i\delta} = \frac{k_0 \cos\theta_0 - k_1 \cos\theta_1}{k_0 \cos\theta_0 + k_1 \cos\theta_1} \qquad (2)$$

and

$$\rho_1 e^{i\delta_1} = \frac{k_1 \cos\theta_1 - k_4 \cos\theta_4}{k_1 \cos\theta_1 + k_4 \cos\theta_4} \qquad (3)$$

we have, on multiplying numerator and denominator by their complex conjugates

$$R = \frac{\begin{array}{c} e^{2\alpha_4 L}[\rho^2 + 2\rho_1\rho e^{-2\alpha d}\cos(2\beta d + \delta - \delta_1) + \rho_1^2 e^{-4\alpha d}] + \\ e^{-2\alpha_4 L}[\rho^2\rho_1^2 + 2\rho_1\rho e^{-2\alpha d}\cos(2\beta d + \delta + \delta_1) + \\ e^{-4\alpha d}] - 2[\rho e^{-2\alpha d}\cos(2\beta d + \delta + 2\beta_4 L) + \\ \rho\rho_1^2 e^{-2\alpha d}\cos(2\beta d + \delta - 2\beta_4 L) + \rho_1 e^{-4\alpha d}\cos(\delta_1 + \\ 2\beta_4 L) + \rho_1\rho^2\cos(\delta_1 - 2\beta_4 L)] \end{array}}{\begin{array}{c} e^{2\alpha_4 L}[1 + 2\rho\rho_1 e^{-2\alpha d}\cos(2\beta d - \delta - \delta_1) + \\ \rho_1^2\rho^2 e^{-4\alpha d}] + e^{-2\alpha_4 L}[\rho_1^2 + 2\rho\rho_1 e^{-2\alpha d}\cos(2\beta d - \\ \delta + \delta_1) + \rho^2 e^{-4\alpha d}] - 2[\rho e^{-2\alpha d}\cos(2\beta d - \delta + \\ 2\beta_4 L) + \rho_1\cos(\delta_1 - 2\beta_4 L) + \rho_1^2\rho e^{-2\alpha d}\cos(2\beta d - \\ \delta - 2\beta_4 L) + \rho^2\rho_1 e^{-4\alpha d}\cos(\delta_1 + 2\beta_4 L)] \end{array}} \qquad (4)$$

(1) This research was supported in part by the Office of Naval Research and in part by the United States Air Force through the Office of Scientific Research of the Air Research and Development Command. Reproduction, translation, publication, use or disposal in whole or in part by or for the United States Government is permitted.

(2) This paper represents a part of the work submitted by W. E. Vaughan to the Graduate School of Princeton University in partial fulfillment of the requirements for the degree of Doctor of Philosophy.

(3) National Science Foundation Fellow, 1957–1960.

(4) The authors wish to thank Dr. William M. Sharpless of the Bell Telephone Laboratories for his assistance in obtaining the crystal detector.

where we have defined R the reflection coefficient as

$$\left|\frac{\vec{E}_{20}}{\vec{E}_{00}}\right|^2 = R \tag{5}$$

ρ^2 is the reflection coefficient for the interface S, while ρ_1^2 is the reflection coefficient for the interface S′. δ and δ_1 give the phase change in the reflected plane waves at the interfaces S and S′ respectively.

Certain special cases are of interest.

If $L = \infty$, $\delta_1 = \pi + \delta$, $\rho_1 = \rho$ we have

$$R = \frac{\rho^2[1 - 2e^{-2\alpha d}\cos 2\beta d + e^{-4\alpha d}]}{1 - 2\rho^2 e^{-2\alpha d}\cos(2\beta d - 2\delta) + \rho^4 e^{-4\alpha d}} \tag{6}$$

a result derived by Rampolla.[5]

If $L = 0$, $\delta_1 = \pi$, $\rho_1 = 1$ we have

$$R = \frac{\rho^2 - 2\rho e^{-2\alpha d}\cos(2\beta d + \delta) + e^{-4\alpha d}}{1 - 2\rho e^{-2\alpha d}\cos(2\beta d - \delta) + \rho^2 e^{-4\alpha d}} \tag{7}$$

This is the configuration used in the present apparatus.

If the radiation in the dielectric sheet has a propagation factor k_1, and is propagated at an angle θ_1 relative to an axis lying in the plane of incidence and perpendicular to the sheet–air interface, one may write the propagation factor along this axis in the sheet as

$$k_1 \cos\theta_1 = \alpha_d + i\beta_d \tag{8}$$

where $\beta_d = 2\pi/\lambda_d$ and λ_d is the "wave length" in the dielectric. Using this definition one can show[6]

$$\epsilon' = \left(\frac{\lambda_0}{\lambda_d}\right)^2\left[1 - \left(\frac{\alpha_d\lambda_d}{2\pi}\right)^2\right] + \sin^2\theta_0 \tag{9}$$

$$\epsilon'' = \left(\frac{\lambda_0}{\lambda_d}\right)^2\frac{\alpha_d\lambda_d}{\pi} \tag{10}$$

where ϵ' = dielectric constant, ϵ'' = dielectric loss, λ_0 = free space wave length of incident radiation, and θ_0 = angle of incidence of the incident radiation to the axis described above. Of the four quantities appearing in equations 9 and 10, θ_0 and λ_0 are functions of the measuring apparatus only and are known in advance. The quantities α_d and λ_d depend on the observed behavior of the reflection coefficient.

Method 1.—From the expression for the reflection coefficient (equation 7) since $\delta \approx \pi$, we may conclude that the reflection coefficient at the maxima touches a maximum envelope given by

$$L = \frac{(\rho + e^{-n\alpha d\lambda d})^2}{(1 + \rho e^{-n\alpha d\lambda d})^2} \tag{11}$$

where n is an integer. The reflection coefficient at the minima touches a minimum envelope given by

$$S = \frac{(\rho - e^{-n\alpha d\lambda d})^2}{(1 - \rho e^{-n\alpha d\lambda d})^2} \tag{12}$$

where n is half-integral. Solving for ρ in these two cases gives

$$\rho = \frac{L^{1/2} - e^{-n\alpha d\lambda d}}{1 - L^{1/2}e^{-n\alpha d\lambda d}} \tag{13}$$

and

$$\rho = \frac{S^{1/2} + e^{-n\alpha d\lambda d}}{1 + S^{1/2}e^{-n\alpha d\lambda d}} \tag{14}$$

(5) R. W. Rampolla, Thesis, Princeton University, 1957.
(6) W. E. Vaughan, Thesis, Princeton University, 1960.

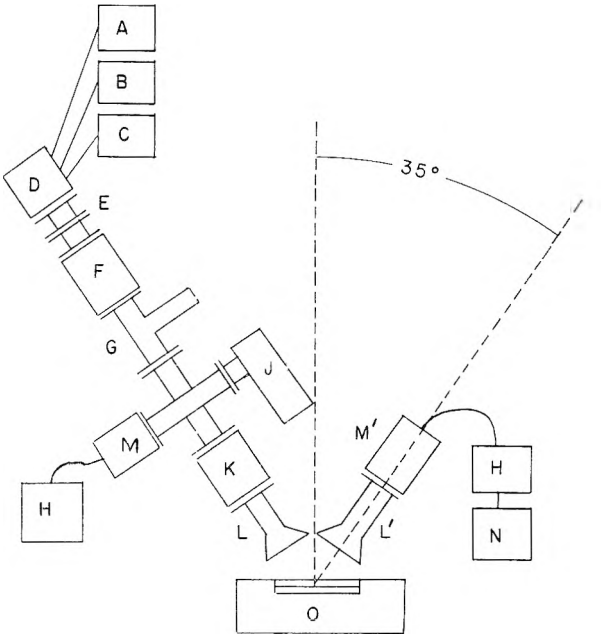

Fig. 1.—Functional diagram of apparatus.

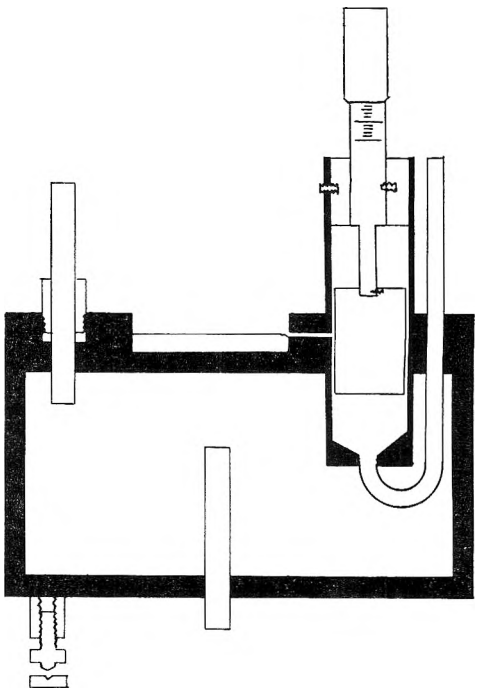

Fig. 2.—Cross section of dielectric cell.

In the latter case it is clear that we must take the positive square root of S when $\rho > e^{-n\alpha d\lambda d}$ (large n), while we take the negative square root of S when $\rho < e^{-n\alpha d\lambda d}$ (small n) since both sides of the equation

$$S^{1/2} = \frac{\rho - e^{-n\alpha d\lambda d}}{1 - \rho e^{-n\alpha d\lambda d}} \tag{15}$$

must have the same sign. Eliminating ρ from equations 13 and 14 and solving for $e^{-n\alpha d\lambda d}$ we have

$$e^{-n\alpha d\lambda d} = \frac{1 - (SL)^{1/2} - [(1 - L)(1 - S)]^{1/2}}{L^{1/2} - S^{1/2}} \tag{16}$$

At the value of n corresponding to $S = 0$, $S^{1/2}$ changes sign. Whether the value of n at a given minimum is larger or smaller than this critical

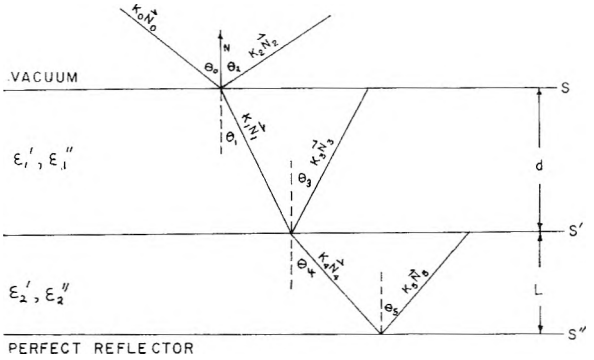

Fig. 3.—Generalized configuration for reflection coefficient measurement.

value of n is in general obvious from the experimental curve. If a question should arise method 2 may be used to get an estimate of ρ. In order to apply equation 16 it is necessary to know the value of the minimum envelope at $n = 1$, $n = 2$. One considers that the minimum envelope as a function of n may be written in the form of a Taylor's series

$$S(n) = S(1.5) + S'(1.5)(n - 1.5) + S''(1.5)\frac{(n - 1.5)^2}{2!} + \ldots \quad (17)$$

Assuming $S''(n)$ equal to a constant, and higher derivatives all zero, we may find $S'(n)$ and $S''(n)$ for $n = 1.5$ from the observed values for the first three minima. From these values one calculates $S(n)$ for $n = 1$ and $n = 2$. Once $S(1)$ and $S(2)$ are known one uses equation 16 to determine $e^{-\alpha_d\lambda_d}$ and $e^{-2\alpha_d\lambda_d}$. The two $\alpha\lambda$ values independently determined are then averaged. ϵ' and ϵ'' may be calculated from $\alpha_d\lambda_d$ and λ_d as previously indicated.

Method 2.—This method was found to be less satisfactory than Method 1 for the determination of ϵ' and ϵ''. From the height of the first maximum

$$L_1 = \frac{(\rho + e^{-\alpha_d\lambda_d})^2}{(1 + \rho e^{-\alpha_d\lambda_d})^2} \quad (18)$$

and the second maximum

$$L_2 = \frac{(\rho + e^{-2\alpha_d\lambda_d})^2}{(1 + \rho e^{-2\alpha_d\lambda_d})^2} \quad (19)$$

we find

$$e^{-\alpha_d\lambda_d} = \frac{L_1^{1/2} - \rho}{1 - \rho L^{1/2}} \quad (20)$$

and

$$e^{-2\alpha_d\lambda_d} = \frac{L_2^{1/2} - \rho}{1 - \rho L_2^{1/2}} \quad (21)$$

whence it follows that

$$\frac{(1 - \rho L_1^{1/2})^2}{(L_1^{1/2} - \rho)^2} = \frac{1 - \rho L_2^{1/2}}{L_2^{1/2} - \rho} \quad (22)$$

or

$$\rho^3 + \rho^2 K + \rho K + 1 = 0 \quad (23)$$

where

$$K = \frac{2L_1^{1/2} - 1 + (L_1L_2)^{1/2}(L_1^{1/2} - 2)}{L_2^{1/2} - L_1^{1/2}} \quad (24)$$

letting

$$\rho = q - K/3 \quad (25)$$

we have

$$q^3 + uq + v = 0 \quad (26)$$

where

$$u = K - K^2/3 \quad (27)$$

and

$$v = {}^2/_{27}\,K^3 - K^2/3 + 1 \quad (28)$$

q is determined by trial and error. The proper value of q (three roots are found) is determined by applying the condition that $L_n > \rho^2 > S_n$ for all n. A glance at the experimental values for the minima sufficed to determine q uniquely in all cases investigated. Once ρ is known $e^{-\alpha_d\lambda_d}$ and $e^{-2\alpha_d\lambda_d}$ may be calculated from equations 20 and 21 and the analysis proceeds as in Method 1.

Correction of Experimental Readings.—In order that the observed reflection coefficient profiles be accurately represented by equation 7 one must compensate experimentally for certain spurious interactions. A serious disturbance is the presence of a horn–horn interaction. Since the VSWR for the horns to air is not unity, power entering the horns is partly reflected, producing a standing wave pattern in the intervening space. If the detector is moved relative to the dielectric sheet a sinusoidal variation of power with detector position of period $\lambda_0/2$ is observed, as expected from theory. Change in the dielectric sheet thickness at fixed detector position also produces an interaction curve superimposed on the reflection coefficient profile. Since the disturbance is approximately sinusoidal the average of two curves with detector positions separated by $\lambda_0/4$ closely approximates the ideal reflection coefficient profile. When four profiles separated by $\lambda_0/4$ are taken, the curves at detector position 0 and $\lambda_0/2$ are internally consistent as are those at $\lambda_0/4$ and $3\lambda_0/4$. The nature of the cell construction causes one face of the dielectric sheet to be exposed to air during a measurement of the reflection coefficient profile. Thus at a fixed micrometer setting one observes a decrease of liquid height with time. In taking the profile, those runs for which the dielectric height is increasing will show increased spacing between the extrema, while, when the liquid height is decreasing, the spacing will be shortened. If evaporation occurs at a constant rate, and if the rate at which the sheet thickness grows is large compared to the rate at which it decreases because of evaporation, the average spacing between extrema over profiles for which the sheet thickness is increasing (spacer driven downward) and decreasing (spacer pulled upward) is that expected in the absence of evaporation. This effect was much reduced by enclosing the cell and the horns in an air-tight plastic bag. For the power incident on the Sharpless detector the response on a log (input) *vs.* log (output) plot is non-linear. In addition the crystal law curve is dependent on the amplifier setting. Thus the amplifier must be set on a fixed scale for any given run, and the detector assembly calibrated as a whole.

Sample Calculation.—The data used to calculate ϵ' and ϵ'' are taken from eight reflection coefficient profiles, pairs from relative detector positions 0, $\lambda_0/4$, $\lambda_0/2$, $3\lambda_0/4$. Each pair is formed from a run with the dielectric sheet thickness increasing and a

run with the sheet thickness decreasing. Automatic recorder deflections for the incident power and the first five extrema are noted. The distance between the first and second maxima is also used.

Measurements on chlorobenzene at 31° will be used as an example.

Av. spacing between 1st and 2nd maxima (dielectric sheet thickness increasing) = 1.459 mm.

Av. spacing between 1st and 2nd maxima (dielectric sheet thickness decreasing) = 1.415 mm.

$\frac{\lambda_d}{2}$ = mean spacing = 1.437 mm.

The recorder deflections for the extrema are converted to actual relative power (in decibels) received by the detector by using the crystal calibration previously mentioned. The input power for reflection coefficient unity is set arbitrarily at 10.00 db. Table I shows the results for the maxima after averaging over pairs has been carried out.

TABLE I

Input power	1st maximum	2nd maximum	Relative detector position
10.00	5.99	2.67	0
10.00	6.71	3.44	$\lambda_0/4$
10.00	5.78	2.62	$\lambda_0/2$
10.00	6.60	3.23	$3\lambda_0/4$

One sees that the data fall into two internally consistent classes, those at relative detector positions 0 and $\lambda_0/2$, and those at positions $\lambda_0/4$ and $3\lambda_0/4$. Averaging over the maxima one calculates the values of the reflection coefficient at the first and second maxima. Assuming the reflection coefficient for the incident power to be unity (perfect reflection from the metal plate alone) we have: $L(0) = 1.0000$, $L(1) = 0.4246$, $L(2) = 0.2000$. The recorder deflections for the minima are treated in a similar manner. We have: $S(0.5) = 0.0679$, $S(1.5) = 0.0000$, $S(2.5) = 0.0649$. Applying equation 17 one finds: $S(1) = 0.0161$, $S(2) = 0.0146$. Now one applies equation 16 at $n = 1$ and $n = 2$. Since the minimum envelope goes to zero at $n \approx 1.5$ we take the negative square root of S at $n = 1$ and the positive square root of S at $n = 2$. We have

$$e^{-\alpha_d\lambda_d} = 0.4242 \text{ (calculation at } n = 1)$$
$$e^{-2\alpha_d\lambda_d} = 0.1799 \text{ (calculation at } n = 2)$$

Squaring $e^{-\alpha_d\lambda_d}$ we find $e^{-2\alpha_d\lambda_d} = 0.1783$, which may be compared with the value 0.1799 determined independently. In general these two calculations of $e^{-2\alpha_d\lambda_d}$ agree within 5%, the agreement becoming worse as the loss decreases. Averaging and solving for $\alpha_d\lambda_d$ we have $\alpha_d\lambda_d = 0.858$. ϵ' and ϵ'' are calculated using equations 9 and 10 from $\alpha_d\lambda_d = 0.858$, $\lambda_d = 2.874$ mm., $\lambda_0 = 4.35$ mm., $\theta_0 = 35°$. One finds $\epsilon' = 2.55$, $\epsilon'' = 0.648$. Two additional runs at 31° gave $\epsilon' = 2.57$, $\epsilon'' = 0.648$; $\epsilon' = 2.58$, $\epsilon'' = 0.641$. Method 2 may also be used to calculate $\alpha_d\lambda_d$. One finds finally: $\epsilon' = 2.60$, $\epsilon'' = 0.49$; $\epsilon' = 2.54$, $\epsilon'' = 0.69$; $\epsilon' = 2.66$, $\epsilon'' = 0.39$. The agreement is much less satisfactory than in the case of Method 1, which has been adopted for use throughout these measurements.

The results of measurements made with this apparatus are discussed elsewhere.[7] Extensive test measurements were made on chlorobenzene, a substance belonging to that class of compounds whose only orientation dispersion is due to over-all molecular rotation. Consequently, it was felt that values of ϵ' and ϵ'' at 4.35 mm. wave length could be predicted successfully from lower frequency data.[8] The observed values at 4.35 mm., $\epsilon' = 2.63$ and $\epsilon'' = 0.739$ are in good agreement with the calculated, $\epsilon' = 2.64$ and $\epsilon'' = 0.726$ at 40°, showing the accuracy of the apparatus and method. The probable error of the dielectric constant measurements is 1% except for extremely low loss materials, in which case the error increases as the loss decreases. The probable error of the loss measurements is 2%, increasing for both extremely high loss and extremely low loss.

(7) W. E. Vaughan and C. P. Smyth, THIS JOURNAL, **65**, 98 (1961).

(8) "Tables of Dielectric Dispersion Data for Pure Liquids and Dilute Solutions," F. Buckley and A. Maryott, NBS Circular 859 (1958).

MICROWAVE ABSORPTION AND MOLECULAR STRUCTURE IN LIQUIDS. XXXV. ABSORPTION BY PURE POLAR LIQUIDS AT 4.3 MM. WAVE LENGTH[1,2]

BY WORTH E. VAUGHAN[3] AND CHARLES P. SMYTH

Frick Chemical Laboratory, Princeton University, Princeton, New Jersey

Received June 27, 1960

The dielectric constants and losses of chlorobenzene, tribromofluoromethane, phenyl ether, benzophenone, anisole, *o*-dimethoxybenzene, *m*-dimethoxybenzene and *p*-dimethoxybenzene have been measured at 4.35 mm. wave length at various temperatures between 20 and 80°. The results are examined in the light of existing lower frequency data. A second dispersion region has been found for benzophenone, which may be explained in terms of an intramolecular mechanism previously suggested to account for the anomalously low relaxation time of phenyl ether. Intramolecular rotation also has been found in the molecules of the four aromatic methoxy compounds.

The study of internal motions in molecules by analysis of their dielectric behavior is facilitated by measurement in the millimeter wave region, where the dielectric loss associated with such motions is a maximum. The apparatus used in the present work[4] permits measurements not previously possible, those on pure polar liquids at temperatures considerably above room temperature. Measurements on chlorobenzene, whose dielectric behavior in the mm. wave region had been previously investigated, were used to test the accuracy of the dielectric constant and loss measurements. Phenyl ether and benzophenone were studied in connection with other work done in this Laboratory.[5] The methoxybenzenes are an example of a system where the contributions of over-all molecular rotation and methoxy group rotation to the dielectric loss overlap in the mm. and cm. wave regions.

Purification of Materials.—The substances investigated were obtained from (A) Matheson, Coleman and Bell, (B) The Eastman Kodak Company, (C) Brothers Chemical Company, (D) Columbia Organic Chemicals Company. The source of each compound, method of purification and boiling or melting point are listed in Table I.

Experimental Results

The dielectric constant and loss of each substance, measured by a method described elsewhere,[4] are listed in Table II.

Discussion of Results

Chlorobenzene.—Three independent measurements of ϵ' and ϵ'' at 31.0° were in agreement to within 1%. Measurements at 40 and 55° were combined with data at 10.0, 3.22 and 1.27 cm.[6] to calculate the optical dielectric constant ϵ_∞, the distribution parameter α, and the critical wave length, λ_m, at which the loss is a maximum. The combined data fit Cole–Cole arcs giving $\epsilon_\infty = 2.42$, $\alpha = 0.02$, $\lambda_m = 1.69 \pm 0.05$ cm. at 40° and $\epsilon_\infty = 2.36$, $\alpha = 0.00$, $\lambda_m = 1.45 \pm 0.10$ at 55°. These values may be compared with the values: $\alpha = 0.03$, $\lambda_m = 1.66$ at 40° and $\alpha = 0.02$, $\lambda_m = 1.37$ at 55°.[6] At 40° using the values of ϵ_∞, α, and λ_m from ref. 6 one calculates $\epsilon' = 2.57$, $\epsilon'' = 0.754$ in good agreement with the observed values at 4.35 mm. of $\epsilon' = 2.63$ and $\epsilon'' = 0.739$. No evidence of a previously reported[7] anomalously high loss in this frequency region was found. The

TABLE I

SOURCES, METHODS OF PURIFICATION, BOILING POINTS AND MELTING POINTS

	Source	B.p., °C. Obsd.	B.p., °C. Lit.
Chlorobenzene[a]	A	132.0	131.7[h]
Anisole[b]	B	154.1	153.8[h]
m-Dimethoxybenzene[c]	C		217[l]
Tribromofluoromethane[d]	D	106	107[i]
		M.p., °C.	
Phenyl ether[e]	A	28	28[m]
Benzophenone[f]	A	48.8	49[k]
p-Dimethoxybenzene[g]	B	56	56[m]
o-Dimethoxybenzene[c]	B	23	22.5[l]

[a] Fractionally distilled and stored over Drierite. [b] Distilled and stored over anhydrous sodium sulfate. [c] Distilled under reduced pressure and stored over anhydrous sodium sulfate. [d] Distilled. [e] Fractionally crystallized at the melting point. [f] Used as received from the manufacturer. [g] Recrystallized from benzene. Purified by E. L. Grubb. [h] A. Weissberger, "Organic Solvents," Interscience Publ. Co., New York, N. Y., 1955. [i] H. Rathsbury, *Chem. Ber.*, 51, 669 (1918). [k] I. Heilbron and H. M. Bunbury, "Dictionary of Organic Compounds," Vol. 1, 1953. [l] *Ibid.*, Vol. 4. [m] *Ibid.*, Vol. 2.

TABLE II

DIELECTRIC CONSTANTS AND LOSSES AT 4.35 MM. WAVE LENGTH

	t, °C.	ϵ'	ϵ''
Chlorobenzene	31.0	2.57	0.639
	40.0	2.63	.739
	55.0	2.55	.723
Tribromofluoromethane	20.0	2.61	.235
Phenyl ether	40.0	2.892	.389
	60.0	2.804	.374
Benzophenone	60.0	3.04	.505
	80.0	2.99	.611
Anisole	20.0	2.452	.389
	40.0	2.530	.465
o-Dimethoxybenzene	25.0	2.82	.463
m-Dimethoxybenzene	60.0	2.64	.494
p-Dimethoxybenzene	60.0	2.82	.737

(1) This research has been supported in part by the Office of Nava Research. Reproduction, translation, publication, use or disposal in whole or in part by or for the United States Government is permitted.

(2) This paper represents a part of the work submitted by Mr. W. E. Vaughan to the Graduate School of Princeton University in partial fulfillment of the requirements for the degree of Doctor of Philosophy.

(3) National Science Foundation Fellow, 1957–1960.

(4) W. E. Vaughan, K. Bergmann and C. P. Smyth, THIS JOURNAL, **65**, 94 (1961).

(5) K. Higasi and C. P. Smyth, *J. Am. Chem. Soc.*, **82**, 4759 (1960).

(6) "Tables of Dielectric Dispersion data for Pure Liquids and Dilute Solutions," NBS Circular 589, 1958.

(7) R. W. Rampolla, R. C. Miller and C. P. Smyth, *J. Chem. Phys.*, **30**, 566 (1958).

values of the distribution coefficient α are so small as to be indistinguishable from zero, which means that the dispersion is Debye-like, and a plot of ϵ' *vs.* ϵ''/λ should be linear.[8] A least squares fit applied to five points gives for the equation of the line for chlorobenzene at 40°

$$\epsilon' - 4.28 = -1.262\,(\epsilon''/\lambda - 0.644) \qquad (1)$$

with a linear regression coefficient of $r = -1.000$. The great usefulness of mm. wave measurements in obtaining ϵ_∞ by extrapolation of the Cole–Cole arc is shown by comparing the values of ϵ' at 40° for 0.435 cm. and 1.27 cm. with ϵ_∞. Here $\epsilon_\infty = 2.42$, $\epsilon'_{0.435} = 2.63$ and $\epsilon'_{1.27} = 3.55$. Thus the length of the extrapolation required is reduced by a factor of five. For most liquids whose only orientation dispersion arises from over-all molecular rotation, ϵ' at 4.35 mm. wave length will be rather close to ϵ_∞, and the extrapolations required from centimeter wave measurements are much reduced.

Tribromofluoromethane.—The data fit a Debye semi-circle with $\epsilon_\infty = 2.47$ and $\lambda_m = 0.94$ cm. The critical wave length calculated from the 4.35 mm. point alone is $\lambda_m = 0.82$ in agreement with the value previously calculated from a 3.1 mm. measurement,[7] but somewhat lower than values from low frequency data.[9] The high frequency intercept ϵ_∞ is consistent with the results of measurements at lower frequencies.

Phenyl Ether.—Although it has been shown that the relaxation of phenyl ether may involve two distinct mechanisms,[5] the data fit a Cole–Cole arc closely at 60°, while the fit is not as satisfactory at 40°. Values for the critical wave length (in cm.) calculated from the 4.35 mm. point and from existing low frequency data[10] are shown in Table III.

TABLE III

CALCULATED CRITICAL WAVE LENGTHS FOR PHENYL ETHER

λ	λ_m 40°	λ_m 60°
10.4	0.923	0.737
3.22	1.021	.733
1.24	0.957	.718
0.435	0.915	.733

At 40° one has $\epsilon_\infty = 2.57$, $\alpha = 0.21$, $\lambda_m = 0.953 \pm 0.06$, and at 60° $\epsilon_\infty = 2.51$, $\alpha = 0.09$, $\lambda_m = 0.729 \pm 0.01$. If one supposes the existence of two relaxation times for phenyl ether, one showing the usual temperature dependence (over-all molecular rotation) and one only slight temperature dependence (internal rotation), then as the temperature increases the two relaxation times should come closer together, and better fit to a Cole–Cole arc would be obtained. Assuming the superposition of two Debye regions the data at 40° are best fitted by $\epsilon_\infty = 2.61$, $C_1 = 0.28$, $\tau_1 = 17.1$ $\mu\mu$ sec., $\tau_2 = 3.4$ where C_1 is the weight factor for the process whose relaxation time is τ_1.[11] Comparison of ϵ' and ϵ'' calculated using these parameters with the experimental values is shown in Table IV.

(8) R. H. Cole, *J. Phys. Chem.*, **23**, 493 (1955).

(9) R. C. Miller and C. P. Smyth, *ibid.*, **24**, 814 (1956).

(10) J. H. Calderwood and C. P. Smyth, *J. Am. Chem. Soc.*, **78**, 1295 (1956).

(11) K. Bergmann, D. M. Roberti and C. P. Smyth, THIS JOURNAL, **64**, 665 (1960).

TABLE IV

CALCULATED AND OBSERVED VALUES OF ϵ' AND ϵ'' FOR PHENYL ETHER AND BENZOPHENONE

	ϵ' obsd.	ϵ' calcd	ϵ'' obsd.	ϵ'' calcd.
Phenyl ether (40°)				
10.4	3.56	3.58	0.123	0.123
3.22	3.43	3.45	.295	.278
1.24	3.17	3.21	.397	.387
0.435	2.89	2.85	.389	.372
Benzophenone (60°)				
10.4	6.21	6.39	3.92	3.73
3.22	3.82	3.80	1.91	1.88
1.24	3.37	3.35	0.95	0.92
0.435	3.04	3.06	0.50	0.49
Benzophenone (80°)				
10.4	7.51	7.54	3.56	3.43
3.22	4.24	4.16	2.33	2.42
1.24	3.38	3.34	1.22	1.17
0.435	2.99	3.01	0.61	0.59

Dividing τ_1 by the macroscopic viscosity η and applying the Powles internal field correction[12] one finds $\tau_1\mu\eta = 6$. The error in this quantity is large as over-all molecular rotation accounts for only 28% of the relaxation for phenyl ether at 40°. Comparing with the corresponding value for benzophenone $\tau_1\mu\eta = 12$ the value for phenyl ether is somewhat lower than expected. The values of τ_2 for benzophenone and phenyl ether are consistent with the internal motion previously proposed.[5] The fraction 0.72 ($= 1 - C_1$) of relaxation attributed to internal rotation requires assignment of a mesomeric moment whose component parallel to the long molecular axis is 0.8 and a net fixed moment of 0.5. These values are close to those previously used.[5]

Benzophenone.—Benzophenone clearly shows two dispersion regions. Previously benzophenone was considered to belong to that class of compounds whose only orientation dispersion was due to over-all molecular rotation. A plot of ϵ' *vs.* ϵ''/λ is non-linear (Fig. 1). Analysis of the data in terms of two relaxation times is shown in Table IV. One has $\epsilon_\infty = 2.88$, $C_1 = 0.94$, $\tau_1 = 67.4$, $\tau_2 = 3.0$ at 60° and $\epsilon_\infty = 2.80$, $C_1 = 0.94$, $\tau_1 = 44.1$, $\tau_2 = 2.7$ at 80°. The percentage relaxation by internal rotation (6%) is the same at 60° and 80° as expected, since the dipole moment components are not significantly temperature dependent. Values of τ_1/η are 16 at 60° and 17 at 80°. This ratio is commonly nearly constant for pure polar liquids when one examines relaxation times corresponding to over-all molecular rotation. τ_2 is not very temperature dependent, decreasing only 14% for a viscosity change from 4.19 to 2.62 cp. If the same mechanism accounts for the high frequency dispersion region in both phenyl ether and benzophenone, then the previous assumption about the slight temperature dependence of τ_2 for phenyl ether seems reasonable. The 94% relaxation corresponding to over-all molecular rotation in benzophenone requires assignment of a net fixed moment of 2.9 and a mesomeric moment whose component

(12) C. P. Smyth, "Dielectric Behavior and Structure," McGraw–Hill Book Co., New York, N. Y., 1955, p. 60.

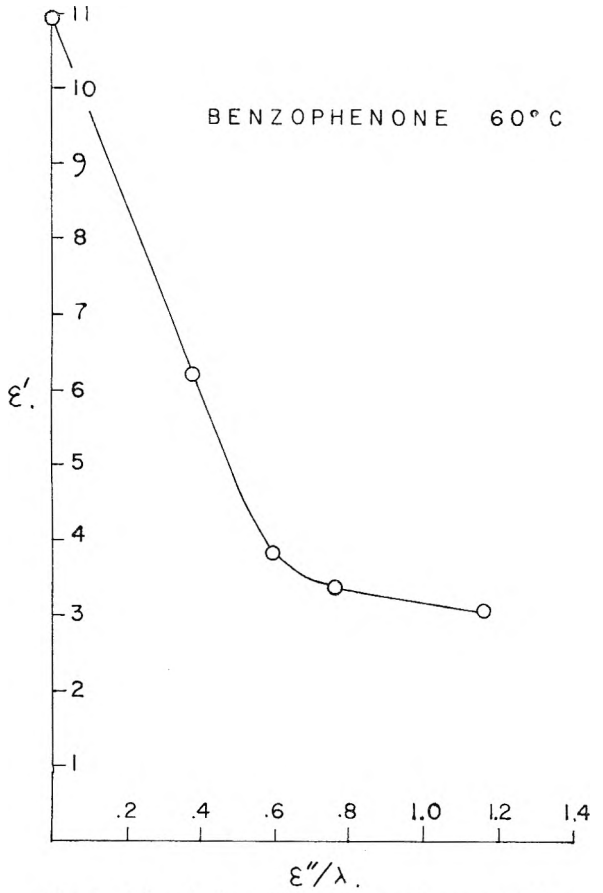

Fig. 1.—Plot of ϵ' *vs.* ϵ''/λ for benzophenone at 60°.

parallel to the long molecular axis is 0.7. Using values of ϵ_∞, α, τ_1 obtained previously[10] one predicts a loss at 4.35 mm. wave length due to over-all molecular rotation alone of $\epsilon'' = 0.289$ at 60° and $\epsilon'' = 0.396$ at 80°. The large differences between these values and the observed losses, $\epsilon'' = 0.505$ and 0.611, respectively, are the contribution of the intramolecular orientation.[5]

Methoxybenzenes.—All these compounds except *p*-dimethoxybenzene gave non-linear plots of ϵ' *vs.* ϵ''/λ and required two relaxation times to explain the data (including points at 10.0, 3.22 and 1.25 cm.).[13] *p*-Dimethoxybenzene fits a Cole–Cole plot with $\epsilon_\infty = 2.65$, $\alpha = 0.05$, $\lambda_m = 1.56 \pm 0.02$ ($\tau = 8.3 \pm 0.1$). Since α is small, a plot of ϵ' *vs.* ϵ''/λ deviates from a straight line by no more than the probable error. A least squares fit to the data gives for the equation of the line

$$\epsilon' - 4.26 = -1.589\,(\epsilon''/\lambda - 0.765) \qquad (2)$$

with a linear regression coefficient of $r = -0.999$. The parameters ϵ_∞, τ_1, τ_2, C_1 required in each case for the other methoxybenzenes are shown in Table V.

ϵ' and ϵ'' could be reproduced within 3% using these values. One may divide the relaxation times for over-all molecular rotation by the macroscopic viscosity to get reduced relaxation times τ_1/η. Anisole has a reduced relaxation time slightly smaller than those of *o*- and *m*-dimethoxybenzene,

(13) D. M. Roberti and C. P. Smyth, *J. Am. Chem. Soc.*, **82**, 2106 (1960).

TABLE V

DISPERSION PARAMETERS FOR THE METHOXYBENZENES

	t°C.	τ_1	τ_2	C_1	τ_1/η	η	ϵ_∞
Anisole	20	13.3	3.7	0.80	12.2	1.091	2.38
	40	9.6	3.2	.80	11.8	0.807	2.39
p-Dimethoxybenzene	60		8.3	.00		2.75	2.65
m-Dimethoxybenzene	60	15.9	2.3	.80	14.0	1.14	2.40
o-Dimethoxybenzene	25	53.1	3.7	.25	16.2	3.281	2.52

as expected from its molar volume. If we apply the Powles internal field correction to these ratios,[12] we may compare them with reduced relaxation times for toluene, *o*-xylene and *m*-xylene. For anisole $\tau_{1\mu}/\eta = 10.3$ while for toluene $\tau_{1\mu}/\eta = 10.6$. These values are about the same, as expected from molar volumes. Similarly for *m*-dimethoxybenzene $\tau_{1\mu}/\eta = 1.16$ and $\tau_{1\mu}/\eta = 1.27$ for *m*-xylene. In the case of *o*-dimethoxybenzene $\tau_{1\mu}/\eta = 1.41$, high compared with $\tau_{1\mu}/\eta = 1.00$ for *o*-xylene. However, in this case only 25% of the relaxation is due to over-all molecular rotation and the error in the calculation of τ_1 is rather large.

One may interpret the short critical wave lengths in terms of methoxy group rotation. The error in determining τ_2 is large for anisole and *m*-dimethoxybenzene where the per cent. relaxation by internal rotation is small. The relaxation times of the methoxy group in *o*-dimethoxybenzene, *m*-dimethoxybenzene and anisole are the same within the large experimental error, while the *p*-dimethoxybenzene seems to have too large a relaxation time to be attributed solely to methoxy group rotation. The slight distribution observed in this case may be due to a small amount of relaxation by over-all molecular rotation in addition to the methoxy group rotation. The relaxation time corresponding to over-all molecular rotation in this compound should be large compared to the other methoxybenzenes if the molecule rotated about its short molecular axes, thus presenting a large effective volume. In addition the macroscopic viscosity is large. Thus a small percentage relaxation by over-all molecular rotation should cause a large shift of the relaxation time, as determined from the Cole–Cole plot, from the value expected for methoxy group rotation alone. On the other hand a shift of the order needed (from 3.7 to 8.3) should cause the distribution parameter to be somewhat larger than that observed. If *p*-dimethoxybenzene has a mesomeric moment μ in the long axis of the molecule when one methoxy group lies in the plane of the ring and the other is perpendicular to it, then the mean square moment along the long axis averaged over all configurations should be approximately $\mu/\sqrt{2}$. If the value of μ is 0.4, 10% of the total relaxation will be due to over-all molecular rotation and the discrepancy between the relaxation time shown by *p*-dimethoxybenzene and that expected for methoxy group rotation may be explained.

The 80% over-all molecular rotation found for anisole and *m*-dimethoxybenzene is consistent with the conventional assignment of bond moments provided the mesomeric moment is small. However the 25% relaxation by over-all molecular rotation in *o*-dimethoxybenzene cannot be explained by the same assignment.

To calculate what per cent. of the relaxation is due to each mechanism one estimates the dipole moment change from the energetically most favorable configuration to the least favorable configuration for each mechanism. Since the intensity of absorption is proportional to this difference squared, the ratio of per cent. of total relaxation for two mechanisms is that of the squares of the dipole moment changes.

Conclusions

Chlorobenzene and tribromofluoromethane show the behavior required by the Debye theory for a single relaxation process corresponding to over-all molecular rotation. Values of ϵ' and ϵ'' at 4.35 mm. wave length may be predicted accurately using the dispersion parameters derived from lower frequency data. The behavior of phenyl ether and benzophenone may be explained by the superposition of two Debye processes, one corresponding to over-all molecular rotation and the other to internal rotation accompanied by a mesomeric shift of charge. The same mechanism appears to be responsible for the short relaxation time in both compounds. The methoxybenzenes also require two relaxation times to explain the data, one due to over-all molecular rotation and the other to methoxy group rotation.

THE REACTIVITY OF HYDROGEN ATOMS IN THE LIQUID PHASE

BY THOMAS J. HARDWICK

Gulf Research & Development Company, Pittsburgh, Pennsylvania

Received June 28, 1960

A method is described in which hydrogen atoms, produced *in situ* by the radiolysis of a saturated hydrocarbon as solvent, are allowed to react competitively with a reactive solute and the solvent. A kinetic expression is derived whereby the relative rate constants for the competing reactions can be calculated from a measurement of the hydrogen gas yield as a function of solute concentration. From previous measurements of the absolute rate constants of H + solute, absolute rate constants for the reaction H + paraffin solvent are obtained. These rate constants show an effect of the molecular structure of the paraffin solvent. Specific values can be assigned to primary, secondary and tertiary groups, from which the absolute rate constant of the reaction of hydrogen atoms with any saturated liquid hydrocarbon may be calculated. If rate constants so measured or calculated are compared with the corresponding published values of H + paraffin in the gas phase, reasonable agreement is found. It is thus concluded that such radical–molecule reactions occur at the same rate in the gas phase as in hydrocarbon solvent.

Introduction

The reactions of hydrogen atoms with the lower hydrocarbons and other simple organic molecules in the gas phase have been studied extensively during the past twenty-five years. Hydrogen atoms have been produced in a variety of ways; *e.g.*, by electric discharge in hydrogen or other suitable gases, by mercury sensitized photolysis, by photolysis of suitable source materials, such as hydrogen sulfide, etc. These techniques, however, are applicable to gas phase reactions only. This restriction has, in turn, limited the reactants which can conveniently be investigated. In addition, many materials cannot be investigated because of interference with the methods of hydrogen atom generation.

The reactions of hydrogen atoms in non-aqueous solutions have received little or no attention. The principal reason appears to be the difficulty of generating hydrogen atoms *in situ*. Most methods applicable in the gas phase cannot, by their nature, be carried out in solution. One of the few feasible methods of hydrogen atom production is the photolysis of formaldehyde, but as this is restricted to temperatures above 100°, the technical problems encountered have limited the value of the method.

Several attempts have been made in which an electric discharge was passed through hydrogen gas just prior to bubbling it through solutions.[1,2] The results are quite scattered, and the method is not considered promising for general application.

(1) F. E. Littman, E. M. Car and A. P. Brady, *Rad. Research*, **7**, 107 (1957).

(2) T. W. Davis, S. Gordon and E. J. Hart, *J. Am. Chem. Soc.*, **80**, 4487 (1958).

The absorption of ionizing radiation in liquid hydrocarbons produces hydrogen atoms. These atoms will react with suitable solutes, and their relative reactivity among various solutes can readily be measured. This paper, the first of a series, outlines the principle and methods of generating hydrogen atoms by ionizing radiation, and develops the kinetics required for a quantitative measurement of reactivity. Data are presented on the rate of reaction of hydrogen atoms with simple alkanes and naphthenes in the liquid phase. By combining these results with absolute measurements in the gas phase, individual rates of reaction have been determined.

Radiolysis of Saturated Hydrocarbons.—The over-all processes which occur on the absorption of ionizing radiation by saturated liquid hydrocarbons are many and varied. However, since the essence of the proposed method involves a measurement of the hydrogen gas produced, all reactions which are unrelated to hydrogen gas formation can be ignored. The method requires the use of a saturated hydrocarbon as a solvent, and, as will be shown later, either alkanes or cycloparaffins may be used. In outlining the method, the term paraffin will be considered to include straight chain and branched chain alkanes and cycloparaffins.

The pertinent characteristics of a liquid paraffin hydrocarbon absorbing ionizing radiation are the following.

(1) Primary products (radicals and some molecules) are formed in proportion to the amount of energy absorbed; *i.e.*, in a zero-order reaction. The amount of chemical change per unit of energy ab-

sorbed, or yield, is expressed in units of molecules per 100 e.v. absorbed, and is designated by the term G.

(2) Hydrogen atoms are produced in the radiolysis of paraffins and disappear by reaction with either solvent or solute. Biradical reactions involving hydrogen atoms appear to be absent.

The experimental method of measuring relative reactivities of hydrogen atoms involves measurements of the radiolytic hydrogen yield (a) from the pure paraffin solvent and (b) from this solvent containing a range of low concentrations of a reactive solute. From the kinetics of the reaction, the relative rate constants for hydrogen atom attack on solvent and solute can be obtained directly from the experimental data.

Kinetics of Hydrogen Gas Formation in Paraffin + Solute Systems.—In the radiolysis of saturated hydrocarbons, hydrogen gas is produced by two general processes. One is influenced by free radical scavengers, the other is not.

The latter process may be represented by the over-all reaction

$$RH \xrightarrow{G_1} H_2 + \text{Products} \qquad (1)$$

In the other process, the first step is hydrogen atom formation

$$RH \xrightarrow{G_2} R + H \qquad (2)$$

When the hydrocarbon contains small amounts of a free radical scavenger S, hydrogen atoms disappear in one of the competitive reactions

$$H + RH \xrightarrow{k_3} H_2 + R \qquad (3)$$

$$H + S \xrightarrow{k_4} HS \qquad (4)$$

where the nature of S is such that hydrogen gas is not produced in reaction 4. In the absence of a scavenger (*i.e.*, pure hydrocarbon) the total amount of hydrogen gas produced, $G_{H_2(O)}$, will be $G_1 + G_2$. With increasing amounts of scavenger present in solution, a decrease in measured hydrogen yield $G_{H_2(S)}$ is observed.

If a steady-state kinetic treatment of the hydrogen atom production is made for the hydrocarbon system with and without scavenger present, the following expression is obtained.

$$\frac{1}{G_{H_2(O)} - G_{H_2(S)}} = \frac{1}{G_2} \times \frac{k_3}{k_4} \frac{[\text{paraffin}]}{[\text{scavenger}]} + \frac{1}{G_2} \qquad (I)$$

Since the rate of product formation is equal to an intensity of radiation term times the yield, the use of yield values in place of rates is permissible and in practice is more convenient.

If the kinetics are correct, a plot of the reciprocal of the difference in the hydrogen gas yield, without and with scavenger, *versus* the ratio of the concentration of paraffin to scavenger, should give a straight line, the slope of which is $1/G_2 \times k_3/k_4$ and the intercept $1/G_2$. From the values so obtained, G_2 and k_3/k_4 may be calculated.

In this kinetic treatment it has been assumed that the reaction of hydrogen atoms with a scavenger does not produce hydrogen gas. This is true for many scavengers, particularly with vinyl monomers.

There are many hydrogen atom scavengers, however, where the hydrogen atom can both add to the molecule and abstract hydrogen atoms. Such behavior is particularly common among olefins. In such cases the reaction

$$H + S \xrightarrow{k_5} M + H_2 \qquad (5)$$

must be considered. Applying this further reaction to the kinetic scheme, equation I becomes

$$\frac{1}{G_{H_2(O)} - G_{H_2(S)}} = \frac{1}{G_2} \times \frac{k_3}{k_4} \frac{[\text{paraffin}]}{[\text{scavenger}]} + \frac{1}{G_2}\left(\frac{k_5}{k_4} + 1\right) \qquad (II)$$

In this case the intercept has a value of $1/G_2(k_5/k_4 + 1)$. With a knowledge of G_2, obtained using other scavengers, k_5/k_4 may be calculated.

Many previous studies have been made on the effect of various solutes on the hydrogen gas yield in paraffin radiolysis.[3] It has not been found possible, however, to use such results for a quantitative estimate of G_1 and G_2, for most data have been presented in graphical form. Tabulated data have not been of sufficient accuracy for a satisfactory determination of G_1 and G_2. However, with the exception of systems containing iodine and hydrogen iodide, the results obtained for scavengers in paraffin solutions give in most cases values which are comparable with those to be reported in this and subsequent papers.

Experimental

Materials.—All hydrocarbons were Phillips Pure Grade. As nearly all contained a degree of unsaturation sufficient to engender erroneous results, removal of these unsaturated materials was necessary. Each hydrocarbon was shaken overnight with 1/10 its volume of concentrated sulfuric acid. The two layers were separated and the organic layer stored over sodium carbonate. In a number of cases the hydrocarbon was further purified by washing, drying and distilling. Experience showed however, that results obtained with and without this last phase of purification were identical. In all cases the unsaturation in the purified material, as measured by bromination, was less than 0.5 mM/l. ($\sim$0.005%).

Rohm and Haas methyl methacrylate monomer was used without further purification. Bromination measurements showed it to be within 1% of the theoretical unsaturation. The stabilizer, 0.006% hydroquinone, was not removed. Hexyl methacrylate, from Rohm and Haas, was used directly. Tetrachloroethylene was supplied by Eastman Organic Chemicals.

Hydrogen Gas Production and Measurement.—The experimental method involved irradiating an evacuated sample of liquid paraffin solution and subsequently measuring the hydrogen gas produced. The technique outlined below is only one of many suitable for this type of experiment.

The techniques used for sample preparation, for irradiation and for hydrogen gas analysis have been described in detail.[4] Briefly, 100 ml. of liquid was placed in an irradiation cell and degassed. Irradiations were made using X-rays from a 3 Mev. Van de Graaff accelerator, with suitable monitoring of the absolute energy absorption. The hydrogen gas produced by the radiolysis was transferred to a gas analysis apparatus, isolated from impurities, and measured quantitatively in a McLeod gauge. The total energy absorbed in each sample was about 0.3 j./g., resulting in the production of 5–15 micromoles of hydrogen gas. The temperature of irradiation was 23 $\pm$ 1°.

At least three determinations of the hydrogen yield were

(3) J. P. Manion and M. Burton, THIS JOURNAL, **56**, 560 (1952); R. H. Schuler, *ibid.*, **61**, 1472 (1957); H. A. Dewhurst, *ibid.*, **62**, 15 (1958); P. J. Dyne and W. M. Jenkinson, *Can. J. Chem.*, **38**, 539 (1960).

(4) T. J. Hardwick, THIS JOURNAL, **64**, 1623 (1960).

TABLE I

COMPARISON OF CALCULATED AND EXPERIMENTAL VALUES OF k_3/k_4[a]

Scavenger, methyl methacrylate; $T = 23°$

Solvent	Molecules/100 e.v. $G_{H_2(O)}$	Molecules/100 e.v. G_2	No. of group types: Primary	Secondary	Tertiary	$k_3/k_4 \times 10^3$: Exptl.	$k_3/k_4 \times 10^3$: Calcd.	% Dev. from calcd. value
n-Pentane	6.35	4.25	2	3		1.83	1.66	+ 9
Cyclopentane	5.78	3.06		5		2.36	2.40	− 1
n-Hexane	5.28	3.16	2	4		1.92	2.14	−10
2-Methylpentane	4.47	2.86	3	2	1	3.67	4.49	−18
3-Methylpentane	4.56	2.90	3	2	1	3.45	4.49	−23
2,2-Dimethylbutane	3.12	1.96	4	1		0.94	0.92	+ 4
2,3-Dimethylbutane	4.02	2.33	4		2	7.50	6.84	+ 9
Methylcyclopentane	4.62	2.63	1	4	1	5.89	5.23	+11
n-Heptane	6.06	3.70	2	5		2.59	2.62	− 1
2,4-Dimethylpentane	4.19	2.60	4	1	2	8.18	7.72	+ 6
Methylcyclohexane	4.76	2.71	1	5	1	5.85	5.91	− 1
n-Octane	6.18	3.33	2	6		3.43	3.10	+10
2,2,4-Trimethylpentane	2.91	1.67	5	1	1	4.33	4.43	− 2
n-Nonane	6.05	3.53	2	7		3.87	3.58	+ 7
							Mean	±10

[a] k_3/k_4 primary $= 0.11 \times 10^{-3}$; secondary $= 0.48 \times 10^{-3}$; tertiary $= 3.20 \times 10^{-3}$.

made for pure paraffins. Agreement was always within ±2%.

In the case of systems containing a scavenger, 100-ml. solutions of appropriate concentration were irradiated. In the usual case, six different concentrations of scavenger ranging between 20 and 80 mmoles/l. were used. Where necessary, minor corrections in the energy absorption were made to allow for the direct absorption of energy by the solute.

Results

Hydrogen Gas Yield from Pure Paraffins.—The radiolytic hydrogen gas yield for a number of pure paraffins is shown in column 1, Table I. In general, the values are somewhat higher than have been reported by others.[5] The possible reasons for this discrepancy are the following.

(1) Presence of unsaturation in the pure liquid. In a previous paper[4] it was shown that 1.8 mM/l. hexene in *n*-hexane would lower the hydrogen yield by 1%. Since preliminary results indicated an effect of similar magnitude in other hydrocarbons, care was taken to reduce the unsaturation below 0.5 mM/l. In previous work purification procedures were given, but the degree of purity achieved was not reported.

(2) Unsaturation is produced as a part of the general radiolytic reactions. At higher doses the measured value of G_{H_2} decreases as a result of the scavenging action of these unsaturates for hydrogen atoms.[4] For instance, with *n*-hexane an energy absorption of 1 Mrad. (10 j./g.) results in a 2% decrease in the measured value of G_{H_2}. Not all previous workers have been cognizant of the magnitude of this decrease in hydrogen yield. It is therefore not advisable to compare the present data with hydrogen yields obtained on irradiation to more than 1 Mrad. energy absorption.

From the results in Table I it is apparent that the radiolytic hydrogen yield from pure paraffins is affected by chemical structure, the more highly branched alkanes having lower hydrogen yields. Such a finding is in qualitative agreement with other work.[5] Detailed comment on this will be reserved for a subsequent paper.

(5) H. A. Dewhurst, *J. Am. Chem. Soc.*, **80**, 5607 (1958).

Kinetic Results—One Paraffin with Several Scavengers.—The addition of a hydrogen atom scavenger decreases the measured hydrogen gas yield (G_{H_2}). A typical curve is shown in Fig. 1, where the hydrogen yield for the system *n*-hexane–methyl methacrylate is shown as a function of scavenger concentration. These same results are shown in a kinetic plot (Fig. 2) where the reciprocal of the difference in hydrogen yield, without and with scavenger, is plotted against the concentration ratio [Hexane]/[Methyl methacrylate]. Similar straight lines were obtained for all systems studied.

From the kinetic scheme, it follows that for a given paraffin solvent, the same value of G_2 should be obtained, regardless of the scavenger used. Confirmation of this is shown in Table II, where for each of three paraffins, the values of G_2 obtained using the various scavengers are in quite good agreement. As a result of this agreement, more confidence can be placed on the kinetics.

Kinetic Results—One Scavenger with Several Paraffins.—Values of G_2 obtained from kinetic plots of the data obtained on the radiolysis of the systems: paraffin plus methyl methacrylate, are shown in Table I. Comment on the individual values of G_2, together with their relation to $G_{H_2(O)}$ will be deferred to a subsequent paper.

The values of the ratio of the rate constants, k_3/k_4, obtained from the product of the slope of the kinetic plot and G_2, are listed in column 6, Table I. The results indicate that methyl methacrylate is 100–1000 times more reactive toward hydrogen atoms than are paraffins. The data also bear out Steacie's statement[6] that the "maximum variation in reactivity at room temperature (of H atoms) for all paraffins other than methane is only a factor of about ten."

Relation of k_3/k_4 to Molecular Structure.—An attempt was made to relate the values of k_3/k_4 to the molecular structure of the solvent. Since the same scavenger (methyl methacrylate) was used through-

(6) E. W. R. Steacie, "Atomic and Free Radical Reactions," Reinhold Publ. Corp., New York, N. Y., 1954, p. 497.

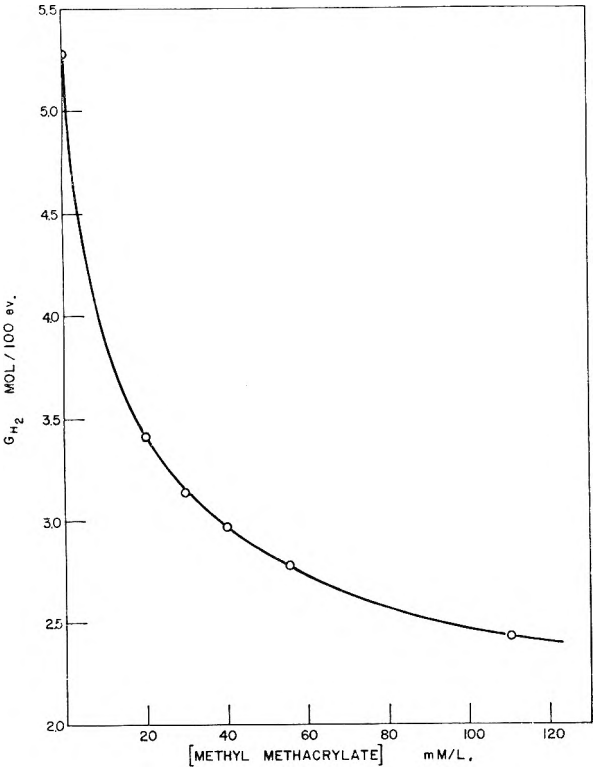

Fig. 1.—Hydrogen yield in *n*-hexane radiolysis as a function of scavenger concentration (methyl methacrylate).

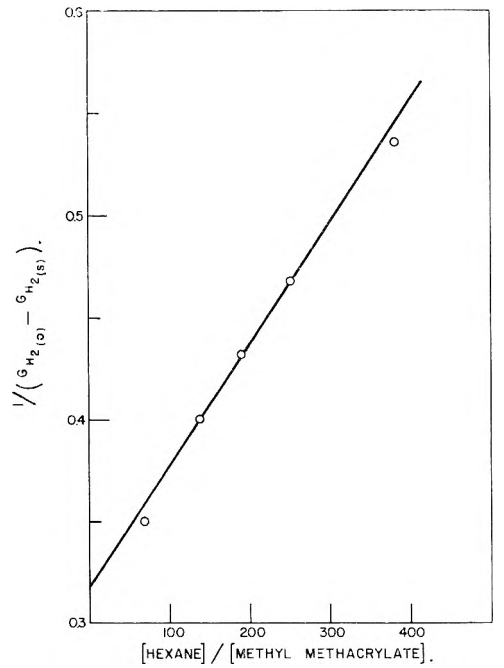

Fig. 2.—Kinetic plot of the data in Fig. 1 to determine hydrogen atom yield (G_2) and the relative reactivity of solvent (*n*-hexane) and solute (methyl methacrylate) toward hydrogen atoms.

out, differences in the values k_3/k_4 reflect differences in the rate constant of reaction 3. The rate constant k_4 is not expected to vary from one paraffin solvent to another, and evidence for this will be presented later in the paper.

Assuming that the reactivity of hydrogen atoms for a particular molecule depends on the total number of primary, secondary and tertiary hydrogen atoms present in the molecule, suitable values of k_3/k_4 were assigned to each of the three structural units, *viz.*, primary 0.11×10^{-3}, secondary 0.48×10^{-3} tertiary 3.40×10^{-3}. These values were so chosen as to give over-all the smallest deviation between calculated and observed data. These values refer to the probability of attack at a given type of carbon atom. The reactivity of an individual primary hydrogen is one-third the primary value; that of an individual secondary hydrogen is one-half the secondary value.

The number of structural groups in each individual molecule is listed in columns 3, 4 and 5, of Table I. In column 7 the values of k_3/k_4, calculated from assigned values, are given. In column 8 the percentage deviation of the experimental from the calculated value is given. The agreement between observed and calculated values is in general quite good, for the mean deviation is only ±10%. It is concluded that using these data for primary, secondary and tertiary groups, the relative reactivity of hydrogen atoms with liquid paraffins may be calculated with reasonable accuracy from a knowledge of the molecular structure.

Absolute Values of the Rate Constants.—It is of course desirable to establish the value of the rate constants on an absolute basis and to determine the effect of temperature on these values. There are several scavengers available for which the rate constants of reaction 4 (and 5 where pertinent), have been measured.

(a) **Methyl Methacrylate.**—Allen, Melville and Robb have measured the rate of the hydrogen atom reaction with a variety of unsaturated compounds in the gas phase at 18°.[7] Among the reactants studied was methyl methacrylate, for which the rate constant for reactivity with hydrogen atoms was determined as 4.4×10^{11} cc. mole^{-1} sec.$^{-1}$. This value, corrected to 23° using an assumed activation energy of 5 kcal., is 5.1×10^{11} cc. mole^{-1} sec.$^{-1}$. Applying this result to the calculated values of k_3/k_4 for paraffins (Table I), individual rate constants for the reaction H + paraffin were found. Values for typical paraffins, *viz.*, cyclopentane and *n*-hexane, are given in Table III.

TABLE II

THERMAL HYDROGEN ATOM YIELDS (G_2) FOR DIFFERENT SCAVENGERS IN PURE ALKANES

Scavenger	G_2, Molecule/100 e.v. *n*-Hexane	*n*-Heptane	Neohexane
Methyl methacrylate	3.18	3.63	1.96
Hexyl methacrylate	3.15	3.75	
Tetrachloroethylene	3.16	3.70	
Carbon tetrachloride	3.13	3.70	1.96

(b) **Cyclohexene, *cis*-Pentene-2 and Benzene.**—In the same paper Allen, *et al.*, investigated the reaction of hydrogen atoms with cyclohexene, *cis*-pentene-2 and benzene, all of which may be conveniently used as scavengers in the present irradiation techniques. To check the data obtained using methyl methacrylate, these materials were used as

(7) P. E. M. Allen, H. W. Melville and J. C. Robb, *Proc. Roy. Soc.* (*London*), **A218**, 311 (1953).

TABLE III

REACTIVITY OF H ATOMS WITH SCAVENGERS IN CYCLOPENTANE AND *n*-HEXANE

$T = 23°$

Scavenger	G_2, atoms/100 e.v.	$\frac{k_3}{k_4} \times 10^3$	$\frac{k_5}{k_4}$	$\frac{k_3}{k_4 + k_5} \times 10^3$	$(k_4 + k_5) \times 10^{-11}$ Cc. mole^{-1} sec.$^{-1}$	$k_3 \times 10^{-9}$ Cc. mole^{-1} sec.$^{-1}$
			Cyclopentane			
Me methacrylate	3.06	2.40	<0.01		5.1	1.2
Benzene		40.7	< .05	40	1.25	5.0
Cyclohexene		7.65	.22	6.3	9.2	5.8
cis-Pentene-2		8.94	.23	7.3	6.7	4.9
					Mean	5.2×10^9
			n-Hexane			
Me methacrylate	3.16	2.14	<0.01		5.1	1.1
Benzene		39.2	< .10	39	1.25	4.9
Cyclohexene		5.75	.25	4.6	9.2	4.2
cis-Pentene-2		9.22	.21	7.6	6.7	5.1
					Mean	4.7×10^9

scavengers in the radiolysis of cyclopentane and *n*-hexane. Data on the hydrogen yield gave straight lines on the kinetic plot.

With cyclohexene and *cis*-pentene-2, and possibly benzene, both addition of hydrogen atoms (reaction 4) and abstraction of hydrogen to form hydrogen gas (reaction 5) may occur. In such a case the kinetic expression II must be used. From the kinetic plot values of k_3/k_4, k_5/k_4, etc., were determined, using values of G_2 obtained previously with scavengers where reaction 5 was absent. The experimental results are shown in the second and third columns in Table III.

Allen, *et al.*,[7] measured the rate of hydrogen atom reaction with the scavengers, regardless of the nature of the products. In comparing the relative rates of reaction of solvent with solute, it is necessary in the case of these solutes to use the sum of the reaction rates 4 and 5 in the denominator. The relative rates, $k_3/(k_4 + k_5)$, were calculated from the experimental data in Table III.

The value of k_3, the rate of the hydrogen atom reaction with this solvent was then calculated. An examination of the data for each solvent (Table III) shows that the values of k_3 obtained for the scavengers benzene, cyclohexene and *cis*-pentene-2 are equal within experimental error, but are higher by a factor of 4 than those obtained from methyl methacrylate.

This difference between the results from methyl methacrylate and the hydrocarbon scavengers may arise from two sources. There may exist an association between methyl methacrylate and the paraffin solvent which in effect produces a scavenger of different reactivity from the pure scavenger. This is considered unlikely, for as has been demonstrated, the values of k_3/k_4 using methyl methacrylate as scavenger are related to the molecular structure of the solvent paraffin.

The second possibility for the discrepancy is an error in the original measurement of the rate of hydrogen atoms with methyl methacrylate. Such a reason would be consistent with the fact that for both *n*-hexane and cyclopentane the value of k_3 using methyl methacrylate is 0.25 of the mean value for the hydrocarbon scavengers. In the determination of the reaction rate in the gas phase it was necessary to know accurately the collision diameter for the reacting molecule. It is perhaps significant that the authors do not consider the geometrical diameter of the molecule to be an entirely satisfactory parameter, but suggest that a sum of reactive groups be used instead. In the case of methyl methacrylate such a discrepancy is expected to be much larger than in the case of simple hydrocarbons. In view of this uncertainty, the mean values of k_3 obtained from the hydrocarbon scavengers are preferred.

Combining the absolute values of k_3 for cyclopentane and *n*-hexane with the relative values of k_3 for primary, secondary and tertiary groups, absolute values for the reactivity of hydrogen atoms with primary, secondary and tertiary groups may be calculated. The results are listed in Table IV. From these data the reactivity of hydrogen atoms with any paraffin may be calculated.

TABLE IV

ABSOLUTE CONSTANTS FOR THE REACTION OF HYDROGEN ATOMS WITH HYDROCARBON STRUCTURAL GROUPS

Reaction of H atoms with		k_3, cc. mole^{-1} sec.$^{-1}$
Primary	CH_3–	0.25×10^9
Secondary group	RCH_2–	1.10×10^9
Tertiary group	R_2CH–	7.75×10^9

Discussion

Effect of Paraffin Solvent on Reaction Rates.—It has been inherently assumed that the rate of reaction 4 is the same throughout all the paraffin solvents studied. This assumption must be true, for if variations occurred from one paraffin solvent to another the results showing the effect of structure on rate of hydrogen abstraction from solvent (reaction 5) would have a marked scatter.

Other hydrogen atom reactions are likewise independent of the solvent. Within experimental error, the value of k_5/k_4 is the same for cyclohexene in both cyclopentane and *n*-hexane. In other experiments the same value of k_5/k_4 was found in the systems *n*-heptane–cyclohexene and neohexane–cyclohexene. In another case, the data in Table III show that the value of k_5/k_4 for *cis*-pentene-2 is the

same in both solvents. Clearly the rate of reaction of hydrogen atoms in solution is unaffected by the paraffin solvent used.

Validity of the Assumption that $k_{(gas)}$ Equals $k_{(solution)}$.—Throughout this discussion it has been assumed that the rate of the hydrogen atom reactions in paraffin solution will be equal to that found in the gas phase. Few reactions have been studied under both conditions. In summarizing the evidence available up to 1950, Laidler[8] concluded that for those reactions occurring in both phases, there is in most cases no difference in the values of the rate of reaction. In many instances cited the values of rates, frequency factors and activation energies were equal. Similar assumptions have been made by other investigators[9] to correlate the results of reactions in the gas phase and in solution. In general, for molecule–molecule, and radical–molecule reactions, quantitative agreement was found for systems of low dielectric constant. Since, of all solvents, paraffins would most likely simulate conditions extant in the gas phase, the assumption of equal rates of hydrogen atom reactions in gas phase and in paraffins seems justified.

Additivity of k_3 Values of Structural Groups.—The calculation of the rate constant of k_3 for paraffins by appropriate summation of individual k_3 values for structural groups is a convenience only, for it reflects the result and not the cause of the difference in rates. Almost certainly the difference in reactivity results from a difference in the bond energies of primary, secondary and tertiary carbon–hydrogen bonds. This difference in turn will be manifested as various values of the activation energy.

If the frequency factors are about the same for the reaction of hydrogen atoms with any carbon–hydrogen bond, and the evidence is that this is so, the postulate the additivity of rate constants is correct. The validity of this reasoning will be checked when experiments on the activation energy for hydrogen atom reactions in solutions have been made.

Activation Energy of the Reaction H + RH → H_2 + R.—There is of course a temptation to combine arbitrary values of the frequency factor with rate constants in order to calculate the activation energy. Rather than indulge in such speculation, we have preferred to await experimental data on this matter which will be forthcoming in a subsequent paper. From the results presented here, however, it can be said that the value of $E_{primary} - E_{secondary} = 1.2$ kcal., while $E_{primary} - E_{tertiary} = 2.7$ kcal. Maximum values of the activation energy (*i.e.*, $P = 1$) are 8.7, 7.5 and 6.0 kcal. for primary, secondary and tertiary bonds, respectively.

Comparison of the Reactivity of Hydrogen Atoms with Paraffins in the Liquid and Gas Phase.—From the arguments that the reactivity of hydrogen atoms is identical in paraffin solution and in the gas phase, it is of interest to compare values of the hydrogen atom reactivity with various paraffin molecules predicted from the present results with those values measured in the gas phase. Such a comparison is made in Table V.

It would of course be desirable to compare directly the rates of reaction in liquid and in gas phase. Unfortunately in reporting results on the gas phase it frequently happens that some of the experimental constants required for an absolute measurement of reaction rates are omitted. As a result data from which absolute rate constants in the gas phase are available are limited.

On the other hand, most results in the gas phase have been found using a Wood's tube in which the collision yield of hydrogen atoms with reactant is measured directly, taking into account molecular diameters, pressure, temperature, etc. For consistency it is therefore more convenient to compare collision yields in the two phases.

In the present case of the liquid phase this collision yield is the probability of reaction on collision between a hydrogen atom and a paraffin solvent molecule. The frequency of collisions of one solute molecule with those of the solvent is calculated from the formula

$$ {}_1Z_S = \frac{3\pi\eta\sigma}{2m_1} \qquad \text{(III)} $$

where

${}_1Z_S$ is the no. of collisions of one solute molecule with solvent molecules in 1 sec.
η is the viscosity of the solvent
σ is the diameter of the solute molecule
m is the mass of one solute molecule

Although this formula was developed for a situation in which the solute molecules were larger than those of the solvent, there does not appear to be any reason why it should not apply in the present case, *i.e.*, large solvent molecule, small solute molecule.

The diameter of a hydrogen atom in solution is not accurately known. The value used in calculations is that used by Allen, Melville and Robb[7] in the gas phase—2.74 Å.

In calculating the collision frequency between hydrogen atoms and ethane, propane and the butanes in the liquid state, it is necessary to know the viscosities of such liquids at room temperature. Under such conditions the viscosities of these liquids change with changing external pressure.[10] As a result it is not clear which value should be considered the true viscosity at room temperature.

There is a more serious problem however. Regardless of the pressure used, the viscosity of ethane, and to a certain extent propane, is considerably lower than that of the solvents used experimentally. In view of this it was not felt advisable to use experimentally measured values of the viscosity. An arbitrary lower limit of $\eta = 2.0 \times 10^{-3}$ g. cm.$^{-1}$ sec.$^{-1}$ was chosen for the theoretical viscosity at room temperature. Such a value is probably quite close to the correct one for the butanes but is much higher than the true values for the other compounds.

For the purposes of comparing results in the liquid and the gas phase, the choice of viscosity values in these cases is not critical.

The collision yield in solution has been obtained from the equation

(8) K. J. Laidler, "Chemical Kinetics," McGraw-Hill Book Co., New York, N. Y., 1950, pp. 112–115.

(9) D. B. Peterson and G. J. Mains, *J. Am. Chem. Soc.*, **80**, 3510 (1959).

(10) A. S. Smith and G. G. Brown, *Ind. Eng. Chem.*, **35**, 705 (1943).

TABLE V

COMPARISON OF THE COLLISION YIELDS FOR THE REACTION H + PARAFFIN IN SOLUTION AND IN THE GAS PHASE

Room temperature

Reaction	Viscosity $\times 10^3$ g. cm.$^{-1}$ sec.$^{-1}$	Molar concn. of solvent, moles/l.	Collision frequency $\times 10^{-9}$, sec.$^{-1}$	k_3, cc. mole^{-1} sec.$^{-1}$	Collision yield: Soln.	Collision yield: Gas phase	Gas phase ref.
H + C_2H_6	2.0	7.3	1.5	5.0×10^7	1.4×10^{-3}	1.8×10^{-8}	11
						3.3×10^{-8}	12
						2.0×10^{-8}	13
						4.6×10^{-8}	14
H + C_3H_8	2.0	11.4	1.5	1.6×10^8	5.4×10^{-3}	5.8×10^{-8}	15
						6.0×10^{-8}	14
						4.5×10^{-8}	16
H + cyclo-C_3H_6	2.0	15.5	1.5	3.3×10^9	2.0×10^{-3}	1.1×10^{-8}	16
						3.4×10^{-8}(D)	16
H + n-C_4H_{10}	2.0	10.0	1.5	2.7×10^9	1.05×10^{-7}	2.4×10^{-7}	17
						0.3×10^{-7}	16
						0.65×10^{-7}(D)	16
H + i-C_4H_{10}	2.0	9.5	1.5	8.5×10^9	3.4×10^{-7}	2×10^{-7}–2×10^{-9}	18
H + cyclo-C_4H_8	3.3	12.5	2.5	4.4×10^9	0.72×10^{-7}	2.5×10^{-7}(D)	16
H + n-C_5H_{12}	2.3	8.6	1.7	3.8×10^9	0.71×10^{-7}	0.59×10^{-7}	16
						0.66×10^{-7}	16
H + neo-C_5H_{12}	2.35	8.1	1.8	1.0×10^9	1.4×10^{-8}	1.9×10^{-8}	13
H + cyclo-C_5H_{10}	4.2	10.6	3.3	5.5×10^9	0.94×10^{-7}	3.0×10^{-7}	16
						5.2×10^{-7}(D)	16
H + n-C_6H_{14}	3.1	7.6	2.4	4.9×10^9	1.56×10^{-7}	0.22×10^{-7}	16
						0.94×10^{-7}(D)	16
H + cyclo-C_6H_{12}	9.3	9.3	7.1	6.6×10^9	0.44×10^{-7}	1.4×10^{-7}	16
						3.3×10^{-7}(D)	16

$$\text{Collision yield} = \frac{k_3 \times [\text{paraffin}]}{\text{collision frequency}}$$

Values of k_3 were obtained by summing the appropriate values for the structural units of the paraffin molecule (Table IV).

The values of the collision yield in the gas phase (Table V), are those appearing in the literature. The numbers are those reported by the authors; no attempt has been made to make corrections for non-uniformity of values such as hydrogen atom and molecular diameters, different formulas used for calculating collision frequency, etc.

Those values of collision yield in the gas phase which are followed by (D) are the collision yields obtained when deuterium atoms are used instead of hydrogen atoms. In general, the collision yields measured with deuterium atoms are larger than those found with hydrogen atoms but Schiff and Steacie[16] indicate that such differences are within experimental error.

Darwent and Roberts[19] studied the reaction of deuterium atoms on alkanes, using photolyzed D_2S as a source of deuterium atoms. It is difficult to compare these results with those in Table V, since activation energies were measured relative to an assumed value $E = 5$ kcal. for the reaction

$$D + H_2 \longrightarrow HD + H \qquad (6)$$

As small changes in activation energy cause large changes in the collision yields calculated therefrom, the values obtained from the results of Darwent and Roberts are not indicative of agreement or lack of it.

Considering the many sources of error in both the liquid and gas phase measurements, there is remarkable agreement between the collision yields obtained in the two phases. The number of gas phase results having values greater than those in liquid are about equal to those with smaller values. As a result, some confidence can be placed on the general use of the data obtained in solution for the prediction of results in the gas phase.

For purposes of comparison, Table VI shows the values of various parameters for reaction in the gas phase and the liquid phase. In the latter case a typical rate of energy input from X-rays is shown, together with a representative power input for fast electrons. The most noticeable difference between the two phases is the average hydrogen atom concentration and the life time of the hydrogen atoms. The fraction of hydrogen atoms recombining in the liquid phase is negligible.

Merits of the General Method

This paper has outlined a new method for measuring the relative reactivity of hydrogen atoms with suitable reactants. Combining this value with the absolute rate constants determined in separate experiments, the reactivity of hydrogen atoms with any organic compound may be measured. Among the advantages of the experimental method are the following.

(11) H. M. Chadwell and T. Tetani, *J. Am. Chem. Soc.*, **55**, 1363 (1933).
(12) E. W. R. Steacie, *J. Am. Chem. Phys.*, **6**, 37 (1938).
(13) W. R. Trost and E. W. R. Steacie, *ibid.*, **16**, 361 (1948).
(14) M. R. Berlie and D. J. Leroy, *Disc. Faraday Soc.*, **14**, 50 (1953).
(15) E. W. R. Steacie and N. M. D. Parlee, *Trans. Faraday Soc.*, **35**, 854 (1939).
(16) H. E. Schiff and E. W. R. Steacie, *Can. J. Chem.*, **29**, 1 (1951).
(17) E. W. R. Steacie and E. W. Brown, *J. Chem. Phys.*, **8**, 734 (1940).
(18) W. H. White, C. A. Winkler and B. J. Kenalty, *Can. J. Research*, **B20**, 255 (1942).
(19) B. de B. Darwent and R. Roberts, *Disc. Faraday Soc.*, **14**, 55 (1953).

TABLE VI

COMPARATIVE DATA FOR LIQUID AND GAS PHASE REACTIONS OF H ATOMS

Reaction H + *n*-hexane; temp. 23°

	Liquid		Gas phase
H atom source	X-rays 3 krad./min.	Electrons 100 watts/cc.	0.05 mm. H 0.002 mm. C_6H_{14}
Rate of H atom formation, moles/cc./sec.	1×10^{-10}	3.3×10^{-5}	
molecules/cc./sec.	6×10^{13}	2.0×10^{19}	
Av. H atom concn., moles/cc.	2.7×10^{-18}	8.9×10^{-13}	2.7×10^{-9}
molecules/cc.	1.6×10^{6}	5.4×10^{11}	1.6×10^{15}
Frequency of collisions between two H atoms, coll./cc./sec.	1.1×10^{4}	1.2×10^{15}	1.1×10^{22}
Frequency of collisions 1 H atom with *n*-hexane, coll./sec.	2.4×10^{14}	2.4×10^{14}	3.1×10^{8}
Frequency of collisions all H atoms with *n*-hexane, coll./cc./sec.	3.9×10^{20}	1.3×10^{26}	5.1×10^{21}
Fraction of H atoms recombining to give H_2	1.8×10^{-10}	6.0×10^{-5}	Large fraction
Lifetime of H atoms, sec.	2.7×10^{-8}	2.7×10^{-8}	Seconds

(1) It is technically simple. The preparation, irradiation and analysis of samples for hydrogen gas involve established techniques in the field of radiation chemistry and microgas analysis.

(2) The over-all error in making measurements of the relative rate constants is sufficiently small that effects of structure can be determined in a precise way.

(3) The number of hydrogen atoms produced can be accurately measured. This in turn leads to information as to their fate on reactions from a mass balance.

(4) It is possible to learn something of the type of reaction which occurs on hydrogen atom attack on the solute. As an example, about 18% of the hydrogen atoms reacting with cyclohexene do so by hydrogen abstraction; the remainder react by addition to the double bond (Table III). In the same manner the relative modes of reactivity may be found on other types of compounds such as alcohols, aldehydes, acids, ketones, etc.

(5) Very small conversions are made. In the average irradiation, to produce 10 micromoles of gas from 100 ml. of liquid, the conversion is 10–20 p.p.m. Little change occurs in the gross properties of the system during such conversions. On the other hand, reactive impurities, if not carefully eliminated, may mask the true effect sought.

(6) Solvents may be selected in order that the precision of the measurements of k_3/k_4 is maximum. For highly reactive solutes, a good choice of solvent is 2,3-dimethylbutane; for solutes reacting less rapidly, neohexane would be a preferred solvent.

(7) The yield of hydrogen atoms from a particular solvent is independent of temperature in the range −25° to +40°.[20] Irradiations at different temperatures will affect the relative values of k_3/k_4. G_2 is unaffected. Since the temperature of a liquid system is easily controlled, a more precise determination of the temperature coefficient for hydrogen atom reactions can be made.

(8) In contrast to most gas phase work, a reactive molecule undergoes only one collision with hydrogen atom. This makes interpretation of the results much more reliable. Hydrogen gas is formed by hydrogen abstraction only and not by hydrogen atom recombination.

(9) As nearly all organic molecules are unreactive towards saturated hydrocarbons, the reactivity of such molecules with hydrogen atoms may be studied. Where the solubility is less than 1%, a suitable ether may be used instead, although this is not to be preferred.

Acknowledgment.—The author wishes to thank the Nuclear Physics Section for the operation of the Van de Graaff accelerator.

(20) T. J. Hardwick, unpublished results.

ADSORPTION OF WATER AND POLAR PARAFFINIC COMPOUNDS ONTO RUTILE[1]

BY C. M. HOLLABAUGH[1] AND J. J. CHESSICK

Surface Chemistry Laboratory, Lehigh University, Bethlehem, Pa.

Received June 30, 1960

The heats of immersion of temperature activated rutile have been measured in water, *n*-propyl alcohol and *n*-butyl chloride as a function of the amount of wetting liquid preadsorbed. Vapor phase adsorption isotherms were Type II for water and *n*-butyl chloride and Type I for *n*-propyl alcohol. Isosteric heats of adsorption were calculated. These data showed the futility in comparing values of the heat of immersion of a clean solid, $h_{I(SL)}$, immersed in several liquids without further data. The assumptions made too often in the past in studies where adsorption and calorimetric data were incomplete that physical adsorption predominates, orientation and monolayer capacities can be estimated, and that $h_{I(SL)}$ near monolayer coverage is equal to h_L, *etc.*, in order to estimate heats of adsorption were shown to be invalid for some and perhaps many other systems reported in the past.

Introduction

Many investigators have reported heats of immersion of several evacuated solids in water and a variety of organic liquids. In most cases, no adsorption data were available to determine the amounts adsorbed. As a consequence, assumptions have been made regarding the monolayer capacity, nature of the energetics of the adsorbed film and orientation, the heat of immersion value of the monolayer covered surface and others. The present investigation was initiated to evaluate the validity of these assumptions by obtaining detailed data and descriptive models for the adsorption of water, *n*-propyl alcohol and *n*-butyl chloride on rutile (TiO_2) activated *in vacuo* at about 500°.

Experimental

Adsorbates.—The adsorbates used in this study were *n*-butyl chloride, *n*-propyl alcohol and water. Water was purified by distillation and had a specific conductance of 2×10^{-6} ohm^{-1} cm.$^{-1}$. The two organic liquids, obtained from Matheson, Coleman and Bell, East Rutherford, New Jersey, were fractionally distilled. Middle fractions of *n*-butyl chloride and *n*-propyl alcohol boiling at 77.4–77.5° and 97.5–97.8°, respectively, were used. The boiling points by Stull[2] are 77.8 and 97.8° for pure *n*-butyl chloride and *n*-propyl alcohol. Trace amounts of water remained in *n*-butyl chloride even after distillation. This water was removed by storing over activated silica in a dry box.

Adsorbent.—The rutile (TiO_2) sample was furnished by the New Jersey Zinc Company, Palmerton, Pennsylvania. This sample was prepared from purified $TiCl_4$ and water. After calcining at 850°, the powder was ball-milled in methanol, dried and remilled in the dry state. The results of chemical analysis showed the following per cent. impurities: Si, 1.0; Ca, 0.01; Al, Sn, Mg, 0.001; B, 0.001; Cu, Fe, Pb, 0.0001. X-Ray analysis showed the sample to be almost entirely in the rutile modification. A surface area of 13.4 m.^{2}/g. was determined from nitrogen adsorption data by the conventional BET method.

Three groups of samples were activated at a number of different conditions by evacuation to a final pressure of 10^{-6} mm. on a high vacuum apparatus. Heats of immersion in water were measured next to determine the effect of varying activation conditions and to define the conditions necessary to yield a reproducible surface.

The first group was activated at 450° without further precautions. All samples in this group turned slightly grey when heated *in vacuo*. Since evidence[3] exists to show that the surface titanium ions are reduced when heated in the presence of organic contaminants, this discoloration probably results from the reduction of the sample by the alcohol adsorbed in the preparation of the rutile or organic contaminants such as stopcock grease.

The second group of samples was activated at 450° on a vacuum apparatus employing a liquid nitrogen trap to condense stopcock grease vapor and facilities for treating the sample with oxygen to remove organic contaminants present on the surface. The oxygen treatment oxidized the organic contaminants and reoxidized the sample to the white form. The following procedure was used. A sample was evacuated for 30 minutes at 450°, then oxygen was admitted to a pressure of 1 atmosphere. After 5 minutes, the sample was evacuated for 2 hours. Oxygen was again added and allowed to remain in contact with the sample for 5 minutes. The sample was re-evacuated for 1.5 hours. Oxygen was added for a third time and allowed to remain in contact with the sample for 10 minutes. Final evacuation was carried out to a pressure of 10^{-6} mm. The temperature of the sample was maintained at 450° throughout this process. These conditions are the standard activation conditions adopted for this investigation. The third group of samples was activated using conditions similar to those for the second group except that the liquid nitrogen trap was not used.

Table I lists heat of immersion values for samples activated under these three conditions. The heat values for Group I samples are manifestations of the reduced-state of the surface. Oxygen treatment at elevated temperatures lowers significantly the heat of immersion in water.

TABLE I

EFFECT OF ACTIVATION CONDITIONS ON THE HEAT OF IMMERSION OF RUTILE IN WATER

Group no.	Activation conditions	$h_{I(SL)}$ (ergs/cm.^{2})
1	No O_2 No trap	-708 ± 19
2	O_2 Trap	-588 ± 9
3	O_2 No trap	-628 ± 16

Group 3 samples were not protected from stopcock grease vapor by a liquid nitrogen trap. Although the samples were not grey after activation, the high heat value of 628 ergs/cm.^{2} clearly indicates the influence of organic vapors in the vacuum system on the final oxidation state of the surface, even though oxygen treatment was used. The results point out the care necessary when temperature activated samples are to be studied by calorimetric or adsorption techniques.

Adsorption Apparatus.—A sensitive Bourdon-type pressure gauge[4] was constructed and incorporated into a volumetric vapor adsorption apparatus specially designed[5] to eliminate dissolution of organic vapors by stopcock grease or manometer oil used with conventional adsorption systems. The simplicity of operation in conjunction with the sensitivity of the pressure gauge makes this apparatus very useful in obtaining adsorption isotherms of organic vapors which

(1) Presented at the A. C. S. Meeting, Colloid Division, Boston, Mass., 1959. This material was used as part of the thesis submitted by C. M. H. in partial fulfillment of the requirements for the degree of Doctor of Philosophy.

(2) D. R. Stull, *Ind. Eng. Chem.*, **39**, 517 (1947).

(3) J. Gebhardt and K. Herrington, THIS JOURNAL, **62**, 120 (1958).

(4) S. Dushman, "Scientific Foundations of Vacuum Technique," John Wiley and Sons, Inc., New York, N. Y., 1949, p. 273.

(5) Yung-Fang Yu, J. J. Chessick and A. C. Zettlemoyer, THIS JOURNAL, **63**, 1626 (1959).

have room temperature vapor pressures from 1 to 10 cm. The dosing and equilibrium pressures could be determined to ±0.003 cm.

Adsorption isotherms for water, *n*-propyl alcohol and *n*-butyl chloride were determined at 26° on the activated sample. Amounts irreversibly adsorbed were determined by evacuating a sample which had previously been exposed to vapor at relative equilibrium pressure greater than 0.5. After evacuating at a selected temperature until a pressure of 10^{-6} mm. was obtained, the amount of vapor readsorbed at 26° was measured as a function of equilibrium pressure. The difference in the volume adsorbed at a relative pressure of 0.2 under these conditions and those used to obtain the original isotherms was calculated. This difference is the volume of vapor retained at the degassing temperature employed.

Evacuation temperatures used for desorption were 26 and 90° for both *n*-propyl alcohol and water, and 26 and 50° for *n*-butyl chloride. The degassing times necessary to obtain a final pressure of 10^{-6} mm. varied with adsorbate and temperature. Table II lists the times used in these experiments to obtain a final pressure of 10^{-6} mm.

TABLE II

EVACUATION TIME USED TO DESORB VAPORS

	Time of evacuation (hr.)		
Adsorbate	26°	50°	90°
n-Butyl chloride	120	24	..
n-Propyl alcohol	20	..	20
Water	96	..	12

Calorimeter.—The thermister calorimeter used to measure the heats of immersion has been described previously.[6] Since any electrical current carried by the liquid in which the thermistor is immersed causes erratic behavior of this element, the thermistor and leads were coated with a thin layer of an epoxy resin (Bakelite Company, Resin BV 1600) and cured for 12 hours at 150° to prevent electrical contact with the liquid. This resin was inert to the liquids used. The entire calorimeter was coated with this resin when *n*-butyl chloride was used as the wetting liquid to reduce the amount of water adsorbed on interior surfaces. It was found that trace amounts of water greatly affected the heat of immersion values obtained with this liquid.

Heats of immersion of rutile into each of the three liquids were measured as a function of the amount of preadsorbed vapor.[6] In order to dry completely both the calorimeter and *n*-butyl chloride, a technique used by Bartell and Suggitt[7] was adopted. This consisted of adding one gram of activated silica by breaking an evacuated glass bulb directly into the calorimeter immediately prior to final assembly. A dry box was used for transferring the liquid and for assembling the calorimeter. The heat of immersion values for rutile in *n*-propyl alcohol were not altered by this drying procedure. Isosteric heats of adsorption were calculated from both the heat of immersion data and the adsorption data measured at 32 and 18°.

Heat of Bulb Breaking.—The heat of breaking of sealed sample bulbs was determined in each liquid. All the bulbs were initially evacuated at 450° for 6 hours. Measurements made with completely evacuated bulbs and with bulbs containing saturated vapor of the liquid.

The results of these measurements are presented in Table III. The values in the second column represent the total heat envolved in breaking a sealed evacuated bulb and include the strain energy for cracking the glass, a $P\Delta V$ work term, and the heat effects due to evaporation and condensation. The latter effects are a consequence of such processes as desorption from the walls of the calorimeter resulting from lowering of the liquid level and resaturation of the vapor which has been diluted by incoming air.

The values in column three result from a combination of the heat evolved with an evacuated bulb and the heat evolved in condensing the saturated vapor contained in the bulb. Differences in the values of columns 2 and 3 represent the heat of condensation of 6 ml. of saturated vapor at 26° which are tabulated in column 4. Theoretical heat of vaporization values calculated for these vapors are shown for comparison in column 5. The significant difference found for *n*-butyl chloride is due to its high vapor pressure (10.5 cm.) at 26°. At this pressure a large *n* number of molecules are present in the vapor phase. Condensation of the small number of vapor molecules of *n*-propyl alcohol and water contained in those bulbs yields insignificant contributions to the correction terms.

TABLE III

HEAT OF BULB BREAKING (CALORIES)

Liquid	Relative pressure $P/P_0 = 0$	$P/P_0 = 1$	Difference	$-\Delta H_v$
n-Butyl chloride	−0.25	−0.57	−0.32	−0.27
n-Propyl alcohol	− .41	− .42	− .01	− .07
Water	− .16	− .16	− .00	− .08

Exptl. values ± 0.07 cal.

Bulb volume 6.0 ± 0.5 ml.

Heat of immersion values were corrected by subtracting the heat of breaking from the total heat evolved in each run. Since the difference in the heat of breaking for the evacuated bulb and the bulb containing saturated vapor of *n*-propyl alcohol and water was within the limits of experimental error, a constant value was used with these adsorbates. The heat of breaking in *n*-butyl chloride varied depending on the vapor pressure in the bulb. It was assumed that the variation in the heat of breaking was a linear function of vapor pressure and the correction applied depended on the equilibrium pressure above the sample.

Results

Adsorption of *n*-Butyl Chloride, *n*-Propyl Alcohol and Water on Rutile (TiO_2).—The adsorption isotherms for *n*-butyl chloride, *n*-propyl alcohol and water determined at 26° are shown plotted in Fig. 1. Curves I represent the amount initially adsorbed as a function of equilibrium relative pressure on the activated and oxygen treated rutile surface. Thereafter, the sample was evacuated at a specified temperature, 50° for *n*-butyl chloride and 90° for both water and *n*-propyl alcohol, to an ultimate vacuum of 10^{-6} mm. to remove as much of the adsorbate as possible. Curves II represent the amount at 26° after evacuation.

The differences in curves I and II of the isotherms of Fig. 1 can be taken measure of the volumes of vapor irreversibly adsorbed at the temperature used for desorption because of the parallelism of the isotherms for a given adsorbate. The calculated V_m values and amounts irreversibly adsorbed are listed in Table IV. Heat data in combination with the values in Table IV will be used to distinguish between the processes of physical and chemisorption.

TABLE IV

VOLUME OF ADSORBED VAPORS ON RUTILE UNDER VARIOUS CONDITIONS ml. (S.T.P.)/g.

Volume	*n*-Butyl chloride	*n*-Propyl alcohol	Water
V_m	1.08	1.80	3.31
Vol. retained at			
26°	0.18	1.42	1.66
90°	..	1.20	1.20
50°	0.18	..	..

The type II isotherms found for the adsorption of *n*-butyl chloride and water on rutile are typical of multimolecular adsorption. The shape of the isotherm for *n*-propyl alcohol is quite unusual for these types of systems. The insignificant increase in the amount adsorbed over a wide range of relative

(6) A. C. Zettlemoyer, G. J. Young, J. J. Chessick and F. H. Healey, *J. Phys. Chem.*, **57**, 649 (1953).

(7) F. E. Bartell and R. M. Suggitt, *ibid.*, **58**, 36 (1954).

pressure is characteristic of monomolecular adsorption. BET plots for *n*-butyl chloride and water were used to estimate the monolayer capacities of these two adsorbates. The V_m value for *n*-propyl alcohol was calculated from the slope of a Langmuir plot of these data.

Heats of Immersional Wetting.—Corrected heat of immersion values obtained for *n*-butyl chloride, *n*-propyl alcohol and water are plotted in Fig. 2 as a function of the amount of vapor preadsorbed on the sample before immersion. These plots show the characteristic large decrease in heat values at small volumes adsorbed. The initial change in the heat of immersion with volume adsorbed is linear for both *n*-propyl alcohol and water up to a coverage of 1.2 ml./g. With *n*-butyl chloride, however, an exponential decrease in the heat values with increasing adsorption is observed.

The heat of immersion of activated samples into freshly distilled *n*-butyl chloride was 621 ± 31 ergs/cm.^{2}. After rigorous drying of the liquid, the heat of immersion decreased to 280 ± 12 ergs/cm.^{2}. The large change in heat values due to small amounts of water made imperative the use of a completely dry system. No changes were found after drying *n*-propyl alcohol in a similar manner, probably because the alcohol shows a larger heat of adsorption than water and is preferentially adsorbed at the very low concentrations of water present as an impurity in the wetting liquid.

Heats of Adsorption.—Differential heats of adsorption were calculated in two different manners. First, the conventional isosteric heat values, q_{st}, were obtained from equilibrium vapor adsorption data at 18 and 32° for θ values near unity. The low equilibrium pressures at 18° precluded the extension of the calculation of these heat values to lower surface coverages. Second, graphical differentiation of the heat of immersion curves yielded differential heat values, q_d, not only near the monolayer but at very low surfaces coverages as well. These results are shown plotted in Fig. 3.

Discussion

Surface of Rutile (TiO_2).—Although the composition and array of constituents in a surface cannot be determined exactly, the spacing of surface ions can be estimated from crystal lattice parameters. The bulk rutile structure consists of units with a titanium ion surrounded by six oxygen ions in the form of an octahedron. Two of the Ti–O bond distances are 2.01 Å. and the other four 1.92 Å.[8] Using an average value of 1.95 Å. a model of the surface was constructed which contained 8.8×10^{19} titanium ions per gram of sample of area 13.4 m.^{2}/g. With the further assumption that an unactivated rutile surface is completely hydroxylated, a model can be presented which explains adequately the experimental adsorption and calorimetric data.

When a sample of rutile is evacuated most physically adsorbed gases are removed near room temperature when an ultimate vacuum of 10^{-6} mm. is achieved. As the temperature is increased, neighboring hydroxyls are assumed to interact to form water vapor and reactive Ti–O–Ti groups. Isolation of some hydroxyls occurs because of the random nature of the interaction of neighboring OH groups. The surface after activation at 450° would then be composed of active Ti–O–Ti linkages and isolated hydroxyl groups if precautions were taken to prevent reduction of Ti^{+4} ions by organic contaminants or if a reduced surface were reoxidized according

(8) W. Hückel, "Structural Chemistry of Inorganic Compounds," Vol. II, Elsevier Publishing Co., New York, N. Y., 1951, p. 683.

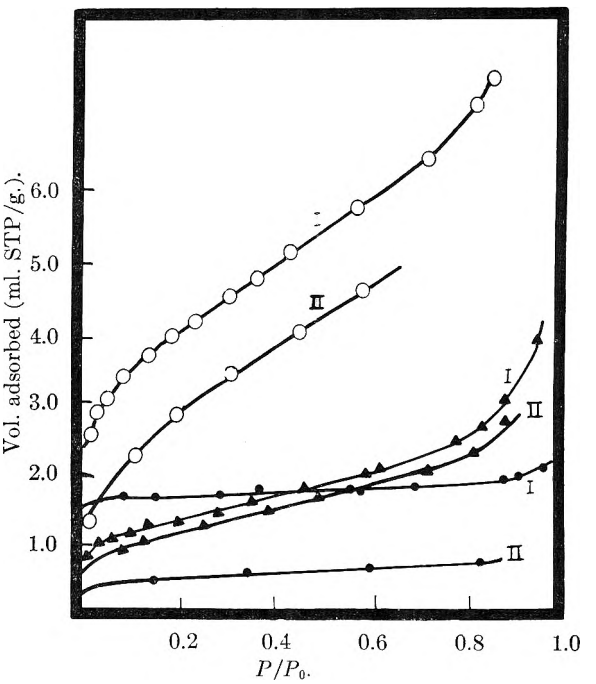

Fig. 1.—Adsorption isotherms for the adsorption of vapors on rutile (TiO_2) at 26°: O, water; △, *n*-butyl chloride; ●, *n*-propyl alcohol. Upper curve of a given set determined after activation at 450°; lower curve obtained with the same sample after evacuation at 90°.

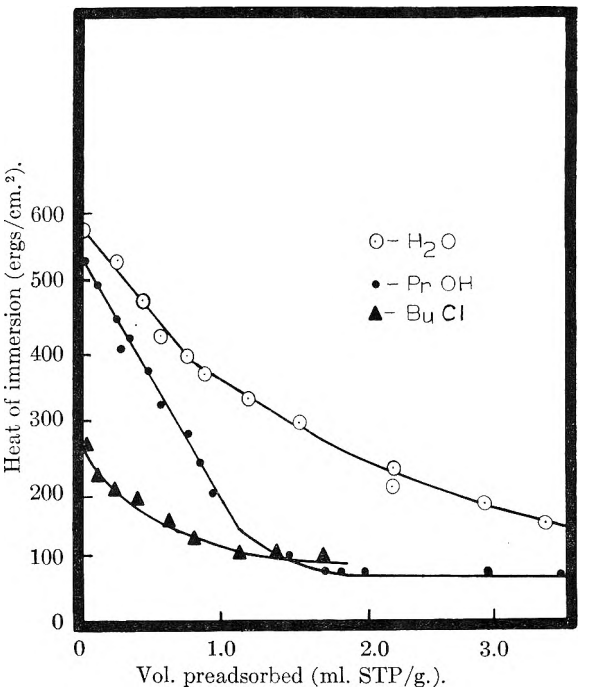

Fig. 2.—Heat of immersion of activated rutile (TiO_2) in several liquids at 26°.

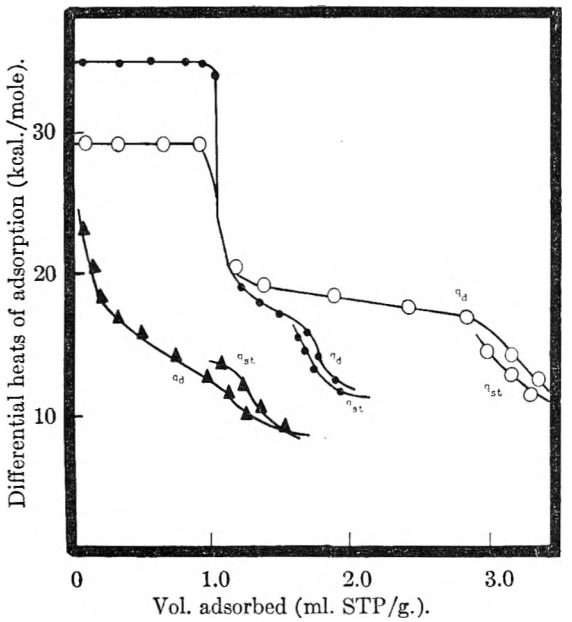

Fig. 3.—Differential heats of adsorption of vapors on activated rutile (TiO_2) at 25°: ●, *n*-propyl alcohol; ▲, *n*-butyl chloride; ○, water.

to the procedure adopted here to yield a reproducible surface.

Adsorption of Water.—The adsorption isotherms for water are Type II showing multilayer adsorption. The calculated area per water molecule on the activated surface is 15.1 Å.² based on a V_m of 3.34 ml. (STP)/g. This value is higher than the 10.8 Å.² usually obtained for physical adsorption of water on polar surfaces. A cross-sectional area of 15.1 Å.² is further surprising when it is considered that the V_m value on which it is based contains water irreversibly adsorbed at 90° and 10^{-6} mm. vacuum.

The adsorption process can be explained conveniently by considering surface dehydroxylation to occur as a result of thermal treatment at 450°. For comparison, Table V lists the number of sites on rutile based on the proposed model and experimental results. After high temperature evacuation the surface consists of active Ti–O–Ti linkages formed by condensation of adjacent hydroxyl groups as well as isolated Ti–OH groups.[9] A water molecule is chemisorbed by reaction with one Ti–O–Ti to form two hydroxyl linkages. The number of such active sites based on the amount of water irreversibly adsorbed at 90° is 3.2×10^{19} per gram of solid.

Physical adsorption over the hydroxylated surface, judged by the large C.S.A. of 23.5 Å.²/water molecule in the monolayer, apparently occurs by localization of a water molecule over two surface hydroxyl groups. Using the BET V_m and subtracting out the initial strong adsorption, a value of 5.7×10^{19} water molecules was calculated as the amount of water adsorbed in this manner. This amount physically adsorbed corresponds to the

(9) No independent data such as infrared or n.m.r. measurements have been obtained which support the view that an unactivated rutile surface is hydroxylated. Nevertheless, the adsorption processes described here for rutile parallel remarkably the results found for silica which is known to contain surface silanol groups.

TABLE V

NUMBER OF ADSORPTION SITES AND MOLECULES ADSORBED PER GRAM OF RUTILE ($\times 10^{-19}$)

Adsorbate	Molecules ads. Chemical	Molecules ads. Physical	Surface sites: Activated Ti–O–Ti	Surface sites: Activated TiOH	Surface sites: After chemisorption Ti–O–Ti	Surface sites: After chemisorption TiOH
Water	3.2	5.7	3.2	4.9	0.0	11.3
n-Propyl alcohol	3.2	1.6	3.2	4.9	0.0	8.1
n-Butyl chloride	0.5	2.4	3.2			

11.4×10^{-19} surface hydroxyl groups and was assumed to be the OH population on a fully hydroxylated surface. From this total population and the amount chemisorbed it was calculated that 4.9×10^{19} OH groups remained on the surface after thermal treatment at 450°. These values for Ti–OH and Ti–O–Ti population based on water data are important since results consistent with these findings should be observed for *n*-propyl alcohol adsorption.

The interatomic spacings used in constructing the model TiO_2 surface gives a total TiOH population of 8.8×10^{19}/gram. The larger amount taken up determined experimentally suggests the values assumed for the interatomic spacings were too large.

The presence of hydroxy groups on rutile appears to be substantiated by treating the solid with dimethyldichlorosilane. A sample was first evacuated at room temperature to remove the physically adsorbed water. After saturating with liquid dimethyldichlorosilane, the sample was heated to 100°. It was washed with alcohol and then with water. Drying at either 26, 100 or 200° left a powder that was hydrophobic. The well known fact that $(CH_3)_2SiCl_2$ reacts readily with OH groups has been utilized by Kiselev[10] and others to methylate the hydroxyl groups on silica.

Adsorption of *n*-Propyl Alcohol.—The Type I isotherm obtained for the adsorption of *n*-propyl alcohol on rutile has *not* been observed previously for systems of this type. The calculated area per molecule in the monolayer of 26.6 Å.² is larger than the value of about 21 Å.² often found for long chain but similar organic molecules physically adsorbed on many substrates. This large C.S.A. is likely caused by localized adsorption over specific sites.

Similarities of adsorption results for water and *n*-propyl alcohol suggests the same type of adsorption mechanism; chemisorption of an alcohol molecule could take place by reaction with Ti–O–Ti group to form Ti–OR and Ti–OH groups. Indeed the same number of water and alcohol molecules (3.23×10^{19}/g.) were chemisorbed on reactive Ti–O–Ti groups.

Physical adsorption of *n*-propyl alcohol occurs by the formation of hydrogen bonds with the surface hydroxyl groups also. Some of these surface hydroxyl groups remain after activation and the remainder (one-half those formed by chemisorption of water) are formed during chemisorption

(10) A. V. Kiselev, "Proceedings of the Tenth Symposium of the Colston Research Society," Butterworths Scientific Pub. London, 1958, p. 195.

of the alcohol. Table V lists the number of molecules adsorbed and the number of sites available. The number of OH groups on the surface after completion of alcohol chemisorption is approximately 8.1×10^{19} per gram. Some of these hydroxyls are not available for bonding with the physically adsorbing alcohol molecules because of steric hindrance of neighboring Ti–OR groups and the necessary presence of some isolated OH groups now. Hence, the number of physically adsorbed molecules is 1.6×10^{19} per gram. Formation of two hydrogen bonds with each of these molecules requires only 3.2×10^{19} of the 8.1×10^{19} surface hydroxyls.

Although the surface presented after completion of the monolayer is not a close packed film, it has properties that are essentially of hydrocarbon character onto which further adsorption does not occur. This type of autophobic surface typified by the type I isotherm for this adsorbate has not been found previously for the adsorption of short chain, polar, paraffinic compounds onto a solid surface. The autophobic surface is a direct consequence of both chemisorption and strong physical adsorption in which the molecules are oriented with the polar and toward the surface. Similar surfaces are found when long chain, polar molecules are adsorbed onto glass and platinum because of the lateral interaction energy.[11] The small increase in volume adsorbed near saturation is probably due to condensation in the capillaries between particles.

Adsorption of *n*-Butyl Chloride.—Adsorption of *n*-butyl chloride onto rutile takes place principally by physical forces. Unlike *n*-propyl alcohol, multilayer adsorption occurs as indicated by the Type II isotherm. The calculated area per molecule is 46.2 A.^{2} at monolayer coverage. Orientation of the molecules must be "flat" on the surface since an area of 20 to 25 Å.^{2} would be expected if vertical orientation occurred. An area of 43.8 Å.^{2} per molecule for flat-wise adsorption is calculated from liquid density by assuming that the molecule is a rigid rod with a cross-sectional area of 20 Å.^{2}. The length of the molecule based on these calculations is 8.7 Å. compared to 8.3 Å. calculated using Pauling's[12] values for bond angles and bond lengths. Area values for similar molecules adsorbed on solid surfaces are in good agreement. For example, areas of 49.3 Å. for 1-pentene adsorbed on anatase[13] and 42 Å. for *n*-butyl alcohol on graphon from aqueous solutions[14] have been reported.

The surface states or rutile after activation consists of 3.2×10^{19} active Ti–O–Ti groups and 4.9×10^{19} OH groups per gram of solid. A small volume of *n*-butyl chloride is chemically adsorbed probably by dissociative reaction with the most active Ti–O–Ti linkages forming Ti–Cl and Ti–OR groups. At the completion of the chemisorption process, there are only 0.5×10^{-9} molecules per gram adsorbed.

Heat Data.—The differential heat data of Fig. 3 for the adsorption of water, alcohol and the chloride may not be quantitative since they were obtained from graphical differentiation of $[h_{I(SL)} - h_{I(SfL)}]$ values in cal./g. *vs.* amount adsorbed in moles/g. Nonetheless, the magnitude of the heat values for the adsorption of water and *n*-propyl alcohol on activated rutile support the desorption data at 90° that chemisorption occurs to a fairly considerable extent for these adsorbates compared to the chloride. The chloride is essentially physically adsorbed. It is interesting to note that isosteric heat values obtained from heat of wetting values and from isotherm data at two temperatures agree well. The utility of heat of immersion technique for obtaining heats of adsorption values becomes obvious when it is pointed out the very limited range of adsorption where pressures were large enough to calculate isosteric heats by conventional means. This limited range is illustrated in Fig. 3 and omits all adsorption except that near monolayer coverage or above for the systems studied here.

Another point of interest is the fact that heat of wetting values shown in Fig. 2 do not necessarily, as often assumed, approach h_L, the heat required to destroy a monomolecular film of wetting liquid near monolayer coverage. The value of h_L for *n*-butyl chloride, for example, is 54 ergs/cm.^{2} at 25° whereas the heat of immersional wetting value near $\theta = 1$ is very nearly double this value.

Comparison of Adsorption and Heat of Wetting Data with Previously Reported Work.—The comprehensives adsorption and heat of immersional wetting results presented here are both necessary and instructive. Too often in the past, workers have drawn, oft-times, profound conclusions concerning wetting and adsorption processes from single heat of wetting values for activated solids in numerous wetting liquids. Prior workers[15] on the basis of heat measurements alone of rutile (TiO_2) activated at 500° immersed in a large number of *n*-butyl compounds of varying functionality calculated interaction energies for the first layer of adsorbate onto the solid surface. Further, these workers broke down these calculated interaction energies into contributions from dipole–dipole interactions, polarization effects and London dispersions force effects. With their limited data it was necessary to assume physical adsorption predominated, all molecules oriented polar group down, the C.S.A.'s in the monolayer of the diverse group of molecules of wetting liquid were the same and that the heat of wetting of the monolayer covered solid was equal to h_L, the enthalpy change on destroying a unit area of wetting liquid.

Their work included studies of the immersion of rutile (TiO_2) in water, alcohol and chloride, the same liquids used in this work. The results presented here indicate extensive chemisorption of water and alcohol, C.S.A.'s representative of localized adsorp-

(11) E. F. Hare and W. A. Zisman, THIS JOURNAL, **59**, 335 (1955).

(12) L. Pauling, "Nature of the Chemical Bond," Cornell University Press, Ithaca, N. Y., 1940, Chap. 3, 5.

(13) W. D. Harkins, "The Physical Chemistry of Surface Films," Reinhold Publ. Corp., New York, N. Y., p. 227.

(14) G. J. Young, J. J. Chessick and F. H. Healey, THIS JOURNAL, **60**, 394 (1956).

(15) F. H. Healey, J. J. Chessick, A. C. Zettlemoyer and G. J. Young, THIS JOURNAL, **58**, 887 (1954); J. J. Chessick, A. C. Zettlemoyer, F. H. Healey and G. J. Young, *Can. J. Chem.*, **33**, 251 (1955).

tion and dependent, in the case of the alcohol, on steric hindrance. While the alcohol oriented polar end down, both in physical and chemical adsorption, the chloride did not. This compound was predominantly physically adsorbed and oriented flat-wise with the very large C.S.A. of 46.2 Å.^{2}. Obviously, the assumptions made by the workers utilizing single heat measurements are unsound.

Many more criticisms could be leveled. Unfortunately, it appears that the practice of drawing conclusions from heat of immersional values of clean samples originated with Harkins and has persisted too long. For example, Harkins[16] concluded that physical adsorption alone occurred on Anatase (TiO_2) activated at 500°. The Russian School headed by Il'in[17] were also guilty of assuming, amongst other things, only physical adsorption, occurred on high temperature activated $BaSO_4$ and proceeded to make extensive calculations of physical interaction energies. Perhaps their assumptions were correct but the work presented here points out the dangers of such assumptions as well as the conclusion that in all likelihood they were incorrect.

Acknowledgment.—The authors greatly appreciate the support provided by the Office of Ordnance Research, U. S. Army.

(16) W. D. Harkins, "The Physical Chemistry of Surface Films," Reinhold Publ. Corp., New York, N. Y., 1952.

(17) B. V. Il'in and V. F. Kiselev, *Doklady Akad. Nauk, S. S. S. R.*, **82**, 85 (1952).

THE STUDY OF THE FRAGMENTATION OF LONG-CHAIN PARAFFINS UNDER ELECTRON BOMBARDMENT USING ISOTOPICALLY LABELLED COMPOUNDS

BY J. H. BEYNON, R. A. SAUNDERS, A. TOPHAM AND A. E. WILLIAMS

I.C.I. Dyestuffs Division, Research Department, Manchester 9, England

Received July 7, 1960

Study of ^{13}C abundance in the various fragments obtained from labelled compounds enables various hypotheses as to the mode of fragmentation to be tested. It is shown that results obtained on samples of *n*-heptadecane-1-^{13}C and *n*-eicosane-4-^{13}C do not support the postulate that abundant peaks are formed by simple carbon–carbon bond rupture. It appears that a multi-stage fragmentation process involving ring formation may be occurring.

Introduction

The factors important in determining the route of fragmentation of an isolated positively-charged ion have been studied by many workers. Attempts to explain the fragmentation pattern of paraffinic ions in terms of the electron densities at the various bonds[1] give results which conflict with experimentally observed intensities especially for C_3 and C_4 ions from long-chain molecules.[2,3]

Attempts have also been made to relate the fragmentation pattern with the bond strength in the parent molecule[4] but here, too, it is not possible to explain the very large peaks occurring at small numbers of carbon atoms.

The quasi-equilibrium theory of mass spectra[5–7] provides the only means of calculating complete mass spectra but has not been employed in this way for molecules larger than C_5 paraffins although it has been used in comparative studies of more complicated molecules.[8–12]

The present work was carried out in order to obtain information concerning the relative importance of different mechanisms in the formation of the various fragments and in particular, to obtain information about the very abundant $C_3H_7^+$ and $C_4H_9^+$ ions in long-chain paraffin spectra. The method employed was to prepare a hydrocarbon isotopically labelled with ^{13}C in a single position and to deduce from the degree of labelling found in various fragments, which processes could have been important in the formation of the fragment. The simplifying assumption had to be made that the probability of fracture of a C–C bond was equal to that of a C–^{13}C bond. (The convention is employed that the symbol C is used to represent the isotope ^{12}C and H to represent the isotope ^1H.) Since the work described here was completed we have learned of some work carried out by Gur'ev, Tikhomirov and Tunitskiĭ[13] using *n*-nonane-5-^{13}C, who have investigated ^{13}C-labelling of C_2, C_3 and C_4 fragments.

Let us consider hypothetical paraffinic compounds, the molecules of which contain only C and H atoms except at one position where the C atom is entirely replaced by ^{13}C. We shall be particularly concerned with the molecules *n*-heptadecane-1-^{13}C and *n*-eico-

(1) J. Lennard-Jones and G. G. Hall, *Trans. Faraday Soc.*, **48**, 581 (1952).

(2) N. D. Coggeshall, *J. Chem. Phys.*, **30**, 595 (1959).

(3) W. M. Fairbairn, *Nature*, **186**, 151 (1960).

(4) G. R. Lester, "Advances in Mass Spectrometry," Pergamon Press, London, 1959, p. 287.

(5) H. M. Rosenstock, M. B. Wallenstein, A. L. Wahrhaftig and H. Eyring, *Proc. Natl. Acad. Sci. U. S.*, **38**, 667 (1952).

(6) H. M. Rosenstock, A. L. Wahrhaftig and H. Eyring, "The Mass Spectra of Large Molecules: Part II, The Application of Absolute Rate Theory," Tech. Rept. No. 2, Institute for the Study of Rate Processes, University of Utah, June 25, 1952.

(7) M. Kraus, A. L. Wahrhaftig and H. Eyring, *Ann. Rev. Nuclear Sci.*, **5**, 241 (1955).

(8) J. Collin, *Bull. Soc. Roy. Sci. Liege*, **25**, 520 (1926).

(9) L. Friedman, F. A. Long and M. Wolfsberg, *J. Chem. Phys.*, **27**, 613 (1957).

(10) L. Friedman, F. A. Long and M. Wolfsberg, *ibid.*, **30**, 1605 (1959).

(11) A. B. King and F. A. Long, *ibid.*, **29**, 374 (1958).

(12) J. H. Beynon, G. R. Lester and A. E. Williams, THIS JOURNAL, **63**, 1861 (1959).

(13) M. V. Gur'ev, M. V. Tikhomirov and N. N. Tunitskiĭ, *Zhur. Fiz. Khim.*, **32**, 2847 (1958).

sane-4-^{13}C. The argument presented below is concerned entirely with the relative numbers of unlabelled and labelled ions in each group of peaks (which ratio is designated R), and not with the absolute abundances of the peaks.

In the following section the percentage labelling for each carbon number corresponding to a variety of hypothetical modes of breakdown of the parent ion have been considered and the results compared with the actual pattern of labelling found in practice. Consider the following specific modes of breakdown.

(1) Simple Cleavage of a Single Carbon–Carbon Bond in the Parent Ion to Give an Ion and a Neutral Fragment.—If we consider an end-labelled paraffin such as n-heptadecane-1-^{13}C, since we are assuming the probability of fragmentation to be the same from both ends of the chain, fragment ions will have a 50% probability of containing the labelled atom, *i.e.*, $R = 1$ for all carbon numbers except C_{17}; for the parent ion $R = 0$. If we consider instead n-eicosane-4-^{13}C, by a similar reasoning the groups C_{17}, C_{18}, C_{19} and C_{20} must always contain the ^{13}C atom so that $R = 0$ for these groups; at all other groups down to C_4 $R = 1$. Below C_4, $R = \infty$.

(2) Rearrangement of the Parent Ion into a Ring Structure Cationated to a Proton.—It is assumed that if this process occurred a fragment ion would be formed by breaking any pair of bonds in this rearranged ion. Then calling R_n the ratio of unlabelled to labelled ions at a carbon number n, we have for any straight chain paraffin containing N carbon atoms that the total number of ways of forming a C_n fragment is N and that of these, $(N - n)$ are unlabelled.

Thus

$$R_n = \frac{(N - n)}{N}$$

The values of R which would be obtained if such a mechanism of fragmentation were dominant are shown graphically in Fig. 1.

(3) Complete Randomization of the Carbon Skeleton before Fragmentaton.—The chance of choosing n carbons under these circumstances all of which are unlabelled is also given by $(N - n)/N$. Thus in an n-carbon fragment the ratio of unlabelled to labelled material is the same as in (2) above, *viz.*, $R_n = (N - n)/N$, so that fragmentation modes (2) and (3) cannot be distinguished by measurements of R when only a single carbon atom is labelled.

(4) The Selection of Any Given Number of Adjacent Carbon Atoms from the (Linear) Parent Ion.—In this fragmentation scheme it is necessary to break two C–C bonds in order to remove a fragment from the inner carbon atoms of the ion and only one for removal of an end. For reasons of simplicity the probabilities of these two processes have been assumed identical.

The number of ways of choosing n atoms from n-eicosane-4-^{13}C in this way is $(21 - n)$. The number of these which are labelled is 1 when $n =$ 1 or 20, 2 when $n = 2$ or 19, 3 when $n = 3$ or 18 and 4 when $4 \leqslant n \leqslant 17$, enabling R to be calculated.

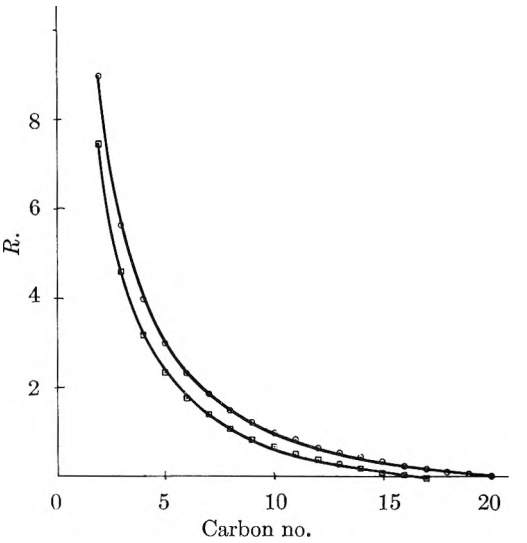

Fig. 1.—Plot of R *versus* carbon number assuming formation of a cyclic form of parent ion or complete randomization before fragmentation: ○, n-eicosane-4-^{13}C; □, n-heptadecane-1-^{13}C.

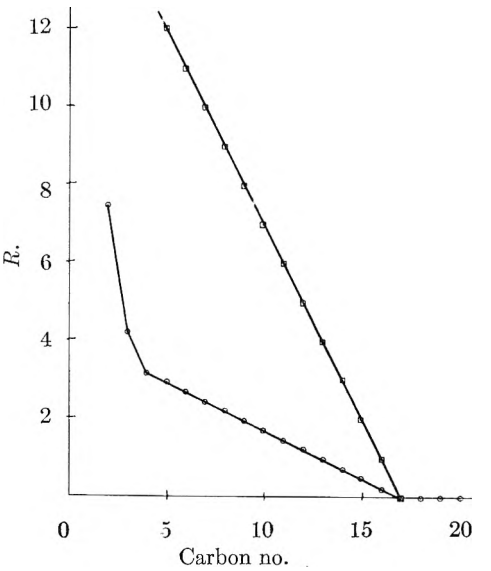

Fig. 2.—Plot of R *versus* carbon number assuming cleavage of a C_n fragment from a linear chain: ○, n-eicosane-4-^{13}C; □, n-heptadecane-1-^{13}C.

From n-heptadecane-1-^{13}C, the total number of ways of choosing n atoms is $(18 - n)$ and for all carbon numbers only one fragment can be labelled so that $R = (18 - n)$.

The values of R for each compound are shown in Fig. 2.

(5) Fragmentation of the Parent Ion by Simple Cleavage of a Carbon–Carbon Bond, as in (1) Above Followed by Rearrangement of the Fragment Ion into a Ring Structure with Further Fragmentation as in (2) Above.—Let us assume that the probability of the initial breaking of the carbon–carbon bond is x and that the probability of losing successive fragments from the rearranged ion is y.

Then for n-heptadecane-1-^{13}C, the total probability of forming fragments (whether labelled or not) is

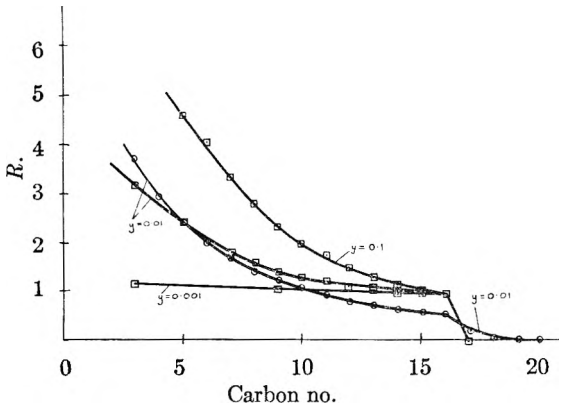

Fig. 3.—Plot of R *versus* carbon number assuming simple cleavage followed by rearrangement of the fragment ion into a cyclic configuration which can fragment further: ○, *n*-eicosane-4-^{13}C; □, *n*-heptadecane-1-^{13}C.

For C_{16}, $2x$
For C_{15}, $2x(1 + 16y) = 2xA_1$
For C_{14}, $2x(A_1 + 15A_1y) = 2xA_2$

For C_n, $2x(A_{15-n} + (n + 1)A_{15-n}y) = 2xA_{16-n}$

The number of these fragments which are labelled with ^{13}C is proportional to

For C_{16}, x
For C_{15}, $x(1 + 15y)$
For C_{14}, $x[1 + 2(14)y + 15(14)y^2]$
For C_{13}, $x[1 + 3(13)y + 15 + 2(14)(13)y^2 + 15(14)(31)y^3]$
For C_n, $x[1 + n(16 - n)y + n[15 + 2(14) + \ldots (n + 1)(15 - n)]y^2 + n\{15(14) + (15 + 2(14)), 13 + \ldots. [15 + 2(14) + \ldots\ldots (n + 2)(14 - n)](n + 1)\}y^3 + \frac{}{} 15(14)(13)(12) \ldots. ny^{16-n}]$

From these values, the ratio of unlabelled to labelled fragments can be calculated at each carbon number for various values of x and y. The results are plotted in Fig. 3 for values of y of 0.001, 0.01 and 0.1. It should be noted that the value of R obtained is independent of x, and in each case, the curve begins at the value $R = 1$ at C_{16}.

This behavior should be contrasted with that which obtains in the case of *n*-eicosane-4-^{13}C. The total number of fragments both labelled and unlabelled is of similar form to that obtaining for the C_{17} hydrocarbon and is

For C_{19}, $2x$
For C_{18}, $2x(1 + 19y) = 2xA_1$
For C_{17}, $2x(A_1 + 18yA_1) = 2xA_2$

For C_n, $2x(A_{18-n} + (n + 1)A_{18-n}y) = 2xA_{19-n}$

In this case, however, the number of labelled fragments is given by

For C_{19}, $2x$
For C_{18}, $2x(1 + 18y) = 2xA$
For C_{17}, $2x[1 + 17y(1 + A)] = 2xB$
For C_{16}, $x + 2x\ 16y\{(1 + A) + 1 + 17y(1 + A)\} = 2x[1/2 + 16y\{(1 + A) + 1 + 17y(1 + A)\}] = 2xC$
For C_{15}, $2x\ [1/2 + 15y(1 + A + B + C)] = 2xD$ and so on

The results are again independent of x. A typical curve, for which $y = 0.01$ is also shown in Fig. 3. In this case, however, R is finite at C_{18} and reaches the value 0.54 at C_{16}. The shape of the curve should be contrasted with the case in which only simple cleavage is permitted. The value of R at C_{16}, C_{17}, C_{18} provides a sensitive measure of whether rearrangement followed by further fragmentation is occurring.

(6) **Simple Cleavage Followed by Successive Loss of C_2H_4 Fragments.**—Another possible form of fragmentation which was examined was that in which cleavage of the carbon chain as in (1) above (with probability x) is followed by successive loss of C_2H_4 fragments from either end of the chain with probability y for each such fragmentation. Such a fragmentation mode is suggested by the large number of metastable transitions involving loss of C_2H_4 which occur in hydrocarbon spectra. Taking various values for x and y, it is found that this stepwise fragmentation leads to steps in the curve of R against carbon number. The values for *n*-eicosane also lie below those for *n*-heptadecane, contrary to what is observed in practice.

Experimental

In order to test the various hypotheses advanced above, samples of *n*-heptadecane-1-^{13}C and of *n*-eicosane-4-^{13}C in which the labelled atom indicated was enriched to almost 50% ^{13}C and also the corresponding unenriched materials were prepared by the following route.

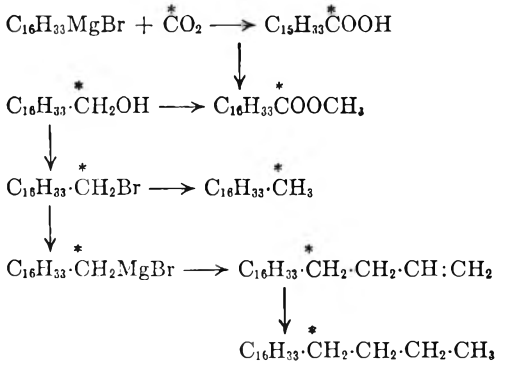

Margaric acid was prepared from cetyl bromide (purified by fractionation using a 14″ column packed with stainless steel gauze rings, collecting at 160–161° (2.4–2.5 mm.)) by reaction of the Grignard reagent with carbon dioxide made from either ordinary barium carbonate or barium carbonate enriched with ^{13}C.[14] The margaric acid was purified by extraction from ether with aqueous triethanolamine using methanol to break the emulsion; yield 83% calcd. on $BaCO_3$; m.p. 57–59.5°. After esterification with methanol and sulfuric acid, reduction with lithium aluminum hydride[15] and recrystallization from acetone, heptadecanol, m.p. 53.5–54°, was obtained in 82% yield. This on heating with hydrobromic acid and sulfuric acid[16] and recrystallization from acetone–methanol gave heptadecyl bromide, m.p. 29–29.5°, in 85% yield. This was reduced with lithium aluminum hydride in tetrahydrofuran[17] to give *n*-heptadecane, m.p. 23°, in 98% yield. Heptadecyl bromide was converted to eicosane by reaction of the Grignard reagent with allyl bromide[18] followed by hydrogenation of the resulting eicosene using palladium charcoal as catalyst. The eicosane was recrystallized from acetone, m.p. 36–36.5°. The over-all yield from heptadecyl bromide was 64%.

The mass spectra of the two labelled compounds were plotted in a double-focussing mass spectrometer using an electron bombarding energy of 50 ev., an accelerating voltage of 4KV and scanning of the magnetic field to produce the spectra. A correction was then applied to the

(14) W. G. Dauben, *J. Am. Chem. Soc.*, **70**, 1376 (1948).
(15) R. F. Nystrom and W. G. Brown, *ibid.*, **69**, 1197 (1949).
(16) O. Kamm and C. S. Marvel, "Organic Syntheses," Coll. Vol. 1, p. 25.
(17) J. E. Johnson, R. H. Blizzard and H. W. Carhart, *J. Am. Chem. Soc.*, **70**, 3664 (1948).
(18) A. P. Kozacik and E. E. Reid, *ibid.*, **60**, 2436 (1938).

spectra for the natural level of ^{13}C and ^{2}H. After subtraction of this correction each spectrum corresponds to that of a mixture, one component being that of the hydrocarbon containing only C and H atoms, (which we shall designate compound X), the other component being a hydrocarbon containing no ^{13}C except at one position in the chain which position consists of ^{13}C (which we shall designate compound Y). From this spectrum was calculated the ratio of unlabelled to labelled ions at each carbon number.

The ratio is calculated in the following way. Let us consider the group of peaks at masses 53, 54, 55, 56, 57, 58 and let us assume that they are all due to ions of the same carbon number (in this case, C_4). Let the abundances of the ions $C_4H_5^+$, $C_4H_6^+$, $C_4H_7^+$, $C_4H_8^+$ and $C_4H_9^+$ be A, B, C, D and E, respectively, and let us assume that the ratio of unlabelled to labelled ions from each ion species is R_1. That is to say, for example, that the mass 54 peak consists of a mixture of ions $^{13}CC_3H_5^+$ and $C_4H_6^+$ and that the height of this peak is given by

$$H_{54} = \left(\frac{A}{R_1} + B\right)$$

Similarly

$$H_{55} = \left(\frac{B}{R_1} + C\right);\quad H_{56} = \left(\frac{C}{R_1} + D\right);$$

$$H_{57} = \left(\frac{D}{R_1} + E\right) \text{ and } H_{58} = \frac{E}{R_1},\ H_{53} = A$$

Solving these equations we obtain: $H_{58}R_1^5 - H_{57}R_1^4 + H_{56}R_1^3 - H_{55}R_1^2 + H_{54}R_1 - H_{53} = 0$ from which R_1 can be calculated. From this ratio R_1, one can calculate the corresponding ratio for compound Y alone as follows:

Suppose that the ratio of unlabelled to labelled ions in any group due to compound Y only is R, and let the ratio of the quantity of X to that of Y in the mixture, the spectrum of which we have obtained, be Q. Then in any group of peaks, $Q/(Q + 1)$ of the ions are due to compound X and $1/(Q + 1)$ to compound Y. Of the ions due to compound Y, $1/(Q + 1) \times R/(R + 1)$ are unlabelled and $1/(Q + 1) \times 1/(R + 1)$ are labelled with ^{13}C.

Thus we have

$$R_1 = \frac{\text{Total unlabelled ions}}{\text{Total labelled ions}}$$

$$= \frac{\left(\frac{Q}{Q+1}\right) + \left(\frac{1}{Q+1}\right)\left(\frac{R}{R+1}\right)}{\left(\frac{1}{Q+1}\right)\left(\frac{1}{R+1}\right)}$$

$$= R(Q + 1) + Q$$

$$\therefore R = \frac{R_1 - Q}{Q + 1}$$

Now at the parent group all those ions due to compound Y are labelled, *i.e.*, $R = 0$ so that $R_1 = Q$ at this group. This enables Q to be estimated; in our case Q was 1.08. Knowing this value the ratios R for compound Y can be found. The values calculated for the hypothetical compounds *n*-heptadecane-1-^{13}C and *n*-eicosane-4-^{13}C monoisotopic except as indicated calculated from the spectra obtained, are shown in Fig. 4. This figure also shows the reproducibility attainable, two of the plots being recorded 3 months apart. This shows that no significant change in R has occurred in the intervening time. The ratio R for the C_4 group of ions in both compounds has also been plotted as a function of the ion-repeller voltage. The results obtained are illustrated in Fig. 5 and show that the measured ratio is not sensitive to the tuning of the mass spectrometer. Varying the ion-repeller voltage from +0.4 to +6.0-volt relative to the walls of the ionization chamber (the range shown) without adjusting any of the other controls was sufficient to change the beam intensity by a factor of 50.

The results show clearly that the smaller ions are not largely formed by simple cleavage of the carbon chain. For example, in the case of *n*-eicosane-4-^{13}C where one would expect 50% of the C_4 ions to be labelled if these ions were formed by breaking a single C–C bond, in fact only about 14% are labelled. At high masses on the other hand, cleavage at a single C–C bond explains the percentage labelling found ($R = 1$). The deviation of R from the value unity is not appreciable until a carbon number of about 10 and

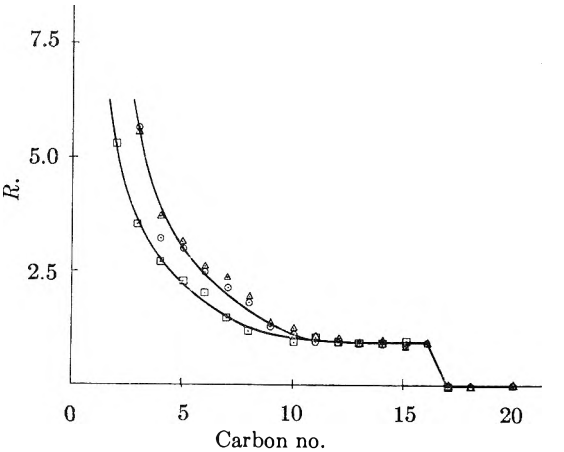

Fig. 4.—Values of R against carbon number calculated from the mass spectra obtained from the synthesized hydrocarbons: ○, *n*-eicosane-4-^{13}C; □, *n*-heptadecane-1-^{13}C (both obsd. in Jan. 12, 1960); △, *n*-eicosane-4-^{13}C (obsd. in April 26, 1960).

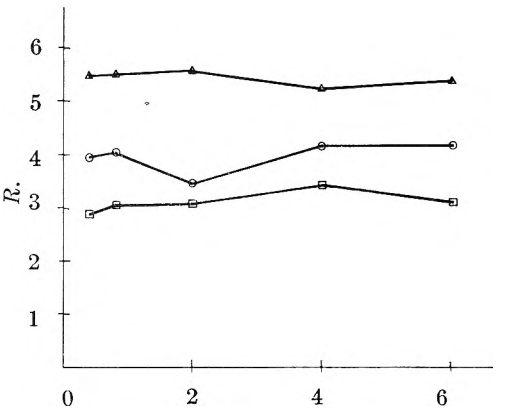

Fig. 5.—Plot of R *versus* ion repeller voltage for various peaks: △, mass 29, *n*-heptadecane-1-^{13}C; ○, mass 57, *n*-eicosane-4-^{13}C; □, mass 57, *n*-heptadecane-1-^{13}C.

increases smoothly for smaller ions. The comparative smoothness of the curve disposes of the argument that further fragmentation occurs mainly by loss of a particular number of carbon atoms, for example, C_2 (see Section 6).

At low masses, the R value found for *n*-eicosane-4-^{13}C is always higher than that for *n*-heptadecane-1-^{13}C. This is contrary to the behavior to be expected if neutral fragments could be removed at random from a linear chain. The only fragmentation modes which can explain this fact are those involving ring formation or complete randomization of the carbon skeleton. Although the latter scheme would seem to be ruled out on energetic considerations alone, it cannot be distinguished in its effect on the ratio of unlabelled to labelled ions at any carbon number except by multiple labelling. Figure 1 which supposes that it is the parent ion which forms a ring structure does not fit the observed ratios at high mass numbers. The computed curve, which comes closest to actuality is that of Fig. 3 but even here (as is shown with particular sensitivity by the 4-^{13}C-labelled hydrocarbon) it would be necessary to assume that the tendency to ring formation was small at high carbon numbers in order to fit the observed curve. It would seem reasonable on steric considerations that rings containing about 5 or 6 carbon atoms would be most likely to form and some such assumption would in fact enable the practical curve to be approached even more closely.

Figure 2 shows the values of R as a function of carbon number assuming that a C_n fragment is formed by cleavage of two carbon–carbon bonds in the chain and rearrangement of a single hydrogen atom. This is the mechanism suggested to be taking place by Gur'ev, *et al.*, from their results on *n*-nonane-5-^{13}C, but it is shown in the present work not

to be the dominant process, the curve for *n*-heptadecane-1-^{13}C providing a particularly sensitive test.

The method of using ^{13}C-labelled paraffins to investigate fragmentation processes is of very wide application and further work using shorter and also branched hydrocarbons is planned.

THE THIRD DISSOCIATION CONSTANT OF ORTHOPHOSPHORIC ACID[1]

BY CECIL E. VANDERZEE AND ARVIN S. QUIST[2]

Avery Laboratory of Chemistry of the University of Nebraska, Lincoln, Nebraska

Received July 7, 1960

Comparison of carbonate–bicarbonate buffers and phosphate–monohydrogen phosphate buffers against an indicator by spectrophotometry leads to $pK_3^0 = 12.375 \pm 0.010$ for HPO_4^{-2}, based upon $pK_2^0 = 10.329$ for HCO_3^{-1}, both values at 25°. The ion-size parameter $a = 4.8$ Å. produced the best representation of the activity coefficients by the Debye–Hückel equation. The indicator 3-carboxy-4-hydroxy-4′-(4-sulfophenylazo)-azobenzene, disodium salt, Schultz number 567, C.I. 274, has the indicator constant $pK^0_{in} = 11.495$ with a Debye–Hückel ion-size parameter $a = 8.0$ Å.

Introduction

Although indicators have been used for many years for estimating the dissociation constants of acids, few attempts have been made to refine these methods to the accuracy obtainable by the electrometric procedures which must ultimately serve as reference standards. When electrometric methods cannot be applied, as with acid–base systems which cause irreversible electrode behavior, indicator methods are especially useful, provided that suitable stable indicators are available.

In the course of some studies on indicators whose color changes occur above *p*H 11, we found the dye 3 - carboxy - 4 - hydroxy - 4′ - (4 - sulfophenylazo)-azobenzene, sodium salt, Schultz number 567, C.I. 274, to possess many of the qualities desirable for accurate spectrophotometric studies of acid–base equilibria in the *p*H range 10 to 13.

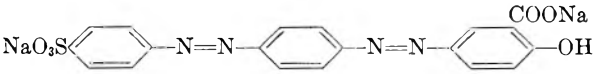

C.I. 274

The substance has a relatively simple structure, and as shown in Fig. 1, an uncomplicated absorption spectrum in the visible ultraviolet range. The response to *p*H changes is very desirable in two broad wave length regions, and the sharp isosbestic point at 428.4 mμ quite clearly indicates only two different absorbing species in this general wave length range. There is little *p*H dependence below wave lengths of 335 mμ. The indicator is completely in its acidic (orange-yellow) form below *p*H 8 and completely in its basic (blue) form above *p*H 13.3. The absorbancy indexes of the acid and base forms were found to be remarkably free from salt effects over ionic strengths up to 1 in NaCl as the inert salt, and between 0.1 and 1.0 NaOH no change in spectrum was observed. The isosbestic point is not disturbed by changes in ionic strength, regardless of *p*H. Aqueous solutions of the indicator were stable over long periods; identical spectral curves were obtained when solutions freshly prepared were compared with solutions two months old. These observations on the properties of the indicator are in accord with those of Konopik and Leberl.[3]

It was our purpose to show that by careful selection of a suitable indicator, together with careful choice of experimental conditions and proper treatment of the experimental data, modern spectrophotometric methods could yield thermodynamic equilibrium constants with accuracy approaching that of modern electromotive force methods, but with one reservation: the values so obtained will ultimately rest upon some reference equilibrium constant determined by electrical measurements, these being the primary means of studying ionic equilibria. We were particularly interested in determining the third dissociation constant of orthophosphoric acid, which as yet has not been determined by modern electrical methods free of liquid junction potentials.

Procedure.—In the experimental approach used in this research, the third dissociation constant of orthophosphoric acid was determined using the second dissociation constant of carbonic acid as a reference standard and the indicator as a means of comparison. The only necessary assumption concerning the indicator is that the activity coefficients of its acidic and basic forms are functions only of the ionic strength and not of the specific ions involved.

For the equilibria concerned we can write the general reaction[4] and the general equilibrium con-

$$OH^- + HB \rightleftharpoons B^- + H_2C \qquad (1)$$

stant expression

$$\frac{K_i^0}{K_w^0} = \frac{C_{B^{-1}}}{C_{HB}C_{OH^-}} \times Y_i \qquad (2)$$

where K_i^0 and K_w^0 are the usual thermodynamic equilibrium constants and Y_i is the appropriate function of the activity coefficients. In terms of the Debye–Hückel equation[5]

(1) In part from the M.S. Thesis of Arvin S. Quist, January, 1957. Presented before the Division of Physical and Inorganic Chemistry, Chicago Meeting of the American Chemical Society, September, 1957.

(2) Minnesota Mining and Manufacturing Fellow, 1956–1957; Du Pont Teaching Fellow, 1957–1958; National Science Foundation Fellow, 1958–1959.

(3) N. Konopik and O. Leberl, *Monatsh. Chem.*, **79**, 586 (1948); **80**, 420, 655, 781 (1949).

(4) For simplicity in notation the actual charges on HB and B are not specified, and because of the restriction to moderately dilute solutions the activity of the water is practically equal to unity. As usual, $-\log K^0 = pK^0$, and the superscript notation K^0 is used for the thermodynamic equilibrium constant. For convenience the molar scale of concentration was used; with water as solvent, the difference between molar and molal scales changes pK_i by about 0.001.

In the *p*H range of these studies, only the final stage of dissociation of H_2CO_3 and H_3PO_4 need be considered.

(5) P. Debye and E. Hückel, *Physik. Z.*, **24**, 185 (1923).

$$\log Y_i = -D_i = \frac{-2nA\sqrt{\mu}}{1 + aB\sqrt{\mu}} \quad (3)$$

where n is the charge on species HB in the general reaction 1, and the constants A and B have the values 0.5092 and 0.3286 $\times 10^{-8}$, respectively, at 25° for the molar concentration scale.[6] Then for the specific equilibria involved in this research, we can write

$$pK_{in}^0 = pK_w^0 - \log \frac{C_{In^-}}{C_{HIn}} + D_{in} + \log C_{OH^-} \quad (4)$$

$$pK_2^0 = pK_w^0 - \log \frac{C_{CO_3^{-2}}}{C_{HCO_3^-}} + D_2 + \log C_{OH^-} \quad (5)$$

$$pK_3^0 = pK_w^0 - \log \frac{C_{PO_4^{-3}}}{C_{HPO_4^{-2}}} + D_3 + \log C_{OH^-} \quad (6)$$

When the indicator and carbonate equilibria are coupled together in carbonate buffer solutions, equations 4 and 5 combine to yield

$$pK_{in}^0 - D_{in} = pK_2^0 + \log \frac{C_{CO_3^{-2}}}{C_{HCO_3^{-1}}} - \log \frac{C_{IN^-}}{C_{HIN}} - D_2 \quad (7)$$

and similarly, when the indicator and phosphate equilibria are coupled together in phosphate buffer solutions, equations 4 and 6 yield

$$pK_3^0 = pK^0_{in} - D_{in} + \log \frac{C_{IN^-}}{C_{HIN}} - \log \frac{C_{PO_4^{-3}}}{C_{HPO_4^{-2}}} + D_3 \quad (8)$$

Two alternative procedures are available for representation of the indicator function, $pK_{in}^0 - D_{in}$, from equation 7 for use in solving equation 8. In the first, the function is represented graphically as a function of ionic strength, and the appropriate values required for equation 8 are read directly from the graph. In the second, the function is represented analytically using an appropriate Debye–Hückel expression for D_{in} which best fits the data, and then the necessary values of the function are computed at the respective ionic strengths associated with equation 8. Both procedures involve the assumption that D_{in} is a function only of the ionic strength.

Although the activity coefficient functions D_i are more accurately representable by the Hückel equation[7] which includes a term linear in the ionic strength, it is not practical to attempt to include the additional terms in equations 4 and 5. The effects of these terms then accumulate in equation 8, so that the standard procedure for evaluating pK_3^0 is to plot the right-hand member of equation 8 against the ionic strength, seeking the values of the ion-size parameter a which gives the best straight line as a criterion of fit, and remembering that increasing a is to a first approximation equivalent to subtracting a linear term as needed for the Hückel equation.

The concentration ratio for the acidic and basic forms of the indicator is taken equal to the ratios of the colored forms as obtained from spectrophotometry, *viz.*

$$\frac{C_{In^-}}{C_{HIn}} = \frac{A_s^a - A_s}{A_s - A_s^b} = R_i \quad (9)$$

where A_s is the observed absorbancy and A_s^a and A_s^b are the absorbancies of the acidic and basic forms at the same wave length, all for the same cell length and concentration of the indicator. The ratio of concentrations, R_i, can be determined with maximum accuracy when its value is 1, but with quite satisfactory accuracy for $0.3 < R_i < 3$. When R_i is less than 0.1 or greater than 10, errors in the measured absorbancies are greatly magnified in R_i. In a similar way the base/acid ratio, C_B-/C_{HB}, should lie near unity for optimum accuracy, but can safely fall between 0.1 and 1.0 since this ratio can usually be determined with somewhat more accuracy than the indicator ratio R_i. In a practical sense, pK_{in}^0 and pK_a^0 should lie within 1.3 units of each other, and preferably within 1 unit, for successful application of this method. With these considerations in mind, combinations of the acid–base and indicator ratios were chosen, based on preliminary measurements, to minimize resultant errors in the derived equilibrium constants. Likewise, the concentration of the indicator itself was chosen to maximize the accuracy with which the absorbancies could be measured.[8,9] (Maximum accuracy would be for $A_s = 0.43$.)

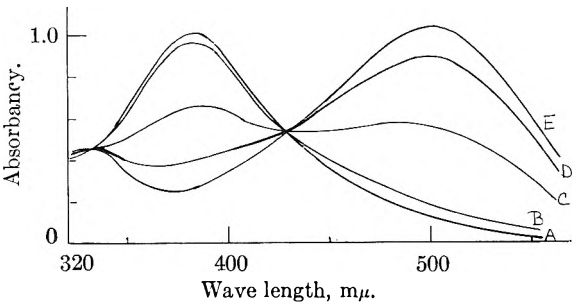

Fig. 1.—Absorption spectra of indicator, C. I. 274. Curves A, B, C, D, E correspond to pH 9.18, 10.02, 11.04, 11.72, 13, respectively. The spectrum for pH 8.04 was little different from A.

The second dissociation constant of carbonic acid was selected as the reference equilibrium constant for a number of reasons. First, it lies sufficiently close to the indicator constant of the chosen indicator to meet the criteria for accuracy just outlined. Second, it is a most convenient system to use in the low alkaline range. Third, the value of the dissociation constant, $K_2^0 = 4.69 \times 10^{-11}$, $pK_2^0 = 10.329$ at 25°, appears to be reliably established by the work of Harned and Scholes[10] and by MacInnes and Belcher.[11] To make the fullest use of the substitutional nature of our procedure, much the same technique was used in preparing solutions, and the same ion-size parameter (a = 4.3 Å.) was used to evaluate D_2, as was used by Harned and Scholes.[10]

Experimental

Properties of the Indicator.—Samples of the dye stuff Schultz number 567, C.I. 274, were obtained from General Dyestuff Company under the trade name "Wool Fast Orange GACF" and from the American Cyanamid Company under the trade name "Calcochrome Orange GR."[12] The

(6) G. G. Manov, R. G. Bates, W. J. Hamer and S. F. Acree, *J. Am. Chem. Soc.*, **65**, 1765 (1943).

(7) E. Hückel, *Physik. Z.*, **26**, 93 (1925).

(8) I. M. Kolthoff and E. B. Sandell, "Textbook of Quantitative Inorganic Analysis," The Macmillan Co., New York, N. Y., 1952, p. 614–631.

(9) C. F. Hiskey, *Anal. Chem.*, **21**, 1440 (1949).

(10) H. S. Harned and S. R. Scholes, Jr., *J. Am. Chem. Soc.*, **63**, 1706 (1941).

(11) D. A. MacInnes and D. Belcher, *ibid.*, **55**, 2630 (1933); **57**, 1683 (1935).

material is sparingly soluble in water and slightly soluble in the common organic solvents. The most effective procedure for purification consisted of washing the material alternately with water and with ethyl alcohol. Most of the impurities were removed after one cycle of washing, and no changes in spectral characteristics were observed after two cycles of washing. After three cycles of washing the material was dried under vacuum at room temperature for several hours. Identical spectra were obtained from different sources of the material after the above washing procedure.

Solutions of the indicator showed no change of spectra upon standing, either in neutral or alkaline buffer solutions, for periods of over two months. Studies of short-term stability over the first hour after preparation showed absolutely no drift in absorbancy at any wave length.

Data showing the response to *p*H changes, shown in Fig. 1, were obtained at 25° with a Beckman Model DU Spectrophotometer, with the indicator concentration 0.02 g./l. in each case. Temperature was held constant within ± 0.01°, using a cell compartment equipped with thermospacers; the cells were allowed 15 minutes to reach thermal equilibrium before readings were taken.

Studies of the salt effects on the indicator showed no displacement of the isobestic point up to ionic strengths of 1 with NaCl as the inert salt. In its acid form at a *p*H 6.8 to 7.0 there was no change in spectrum at any point for ionic strengths up to 0.3, and in its basic form identical spectra were found in solutions 0.1 and 1.0 *M* in NaOH. No evidence of variation of absorbancy indexes with ionic strength could be found for either the acidic or basic form at any wave length within the ranges chosen for measurement; this condition is mandatory if thermodynamic dissociation constants are to be obtained by spectrophotometric methods.

Apparatus.—Exploratory studies and two of the series of carbonate–bicarbonate buffer studies were made using a Beckman Model B spectrophotometer, in which the cells were kept at 25° by means of a stream of air, previously thermostated, flowing through the cell compartment. The remaining studies were done with a Beckman Model DU spectrophotometer equipped with thermospacers, which gave better temperature control (±0.04°). To some extent the use of both instruments was deliberate, to establish that equivalent results could be obtained.

The same two matched Beckman Corex absorption cells (1 cm.) were used with both spectrophotometers throughout the entire series of measurements. One cell was always used to contain the blank and the other was always used to contain the sample, to avoid any possible error due to variation in cell length during a series of observations.

The absorbancies of all solutions were determined at 510, 500, 490, 390, 380 and 370 mμ and at the isobestic point. The first three wave lengths are near the maximum absorbancy of the alkaline form while the last three are near the maximum absorbancy of the acid form of the indicator. Since the absorbancy at the isobestic point should be the same for all solutions, measurements of the absorbancy of each solution at this wave length furnished a convenient check on the indicator concentration and the cleanliness of the absorption cells for the particular solution being measured. From these observations, six values of the indicator ratio R_i could be obtained for each solution.

Solutions.—Conductivity water, collected near its boiling point from a Barnstead still, was used throughout the investigation for all solutions. Usually the water was distilled a short time prior to use; it was protected from carbon dioxide by a soda lime tube. All solutions were prepared and stored in Pyrex flasks.

The stock solution of indicator C.I. 274 contained 0.4000 g. of purified indicator per liter of solution. All solutions used in the equilibrium measurements contained 3.000 ± 0.005 ml. of indicator stock solution (dispensed by means of a 10-ml. microburet) per 100.0 ml. of final buffer solution.

Reference solutions to determine the absorbancies of the indicator in its acidic form were mono- and dihydrogen phosphate buffers[13] having a *p*H of 6.86 and ionic strength 0.1. Reference solutions for the alkaline form were 0.2 molar carbonate-free NaOH solutions.[14]

Stock solutions for the carbonate–bicarbonate buffer studies were prepared by dissolving weighed amounts of reagent grade sodium carbonate in water, then adding aliquots of standard HCl solutions, delivered below the surface of the solution to avoid any loss of carbon dioxide. Four different solutions were prepared, having carbonate/bicarbonate ratio of 1.3, 10, 13 and 6.7. On dilution, these ratios decrease due to hydrolysis. The standard HCl solutions were prepared from constant-boiling hydrochloric acid,[15] using weight burets to prepare 2-liter batches. The concentration was checked against potassium hydrogen phthalate by comparison against carbonate-free NaOH solution. The Na_2CO_3 (Baker Analyzed Reagent) was dried 2 to 4 hours at 120°, and was found to be at least 100.0 ± 0.1% pure in comparison against the standard HCl solution. The solutions were either used immediately after preparation or stored in paraffin-coated bottles.

Solutions used in the phosphate series were prepared in 1 or 2-liter quantities from weighed portions of reagent grade Na_2HPO_4 (dried 4 hours at 110°) and aliquots of standard carbonate-free NaOH. The first series was prepared from Baker Analyzed Reagent Na_2HPO_4, the other three from Fisher Certified A.C.S. Reagent Na_2HPO_4. Ratios of 0.23, 0.27, 0.31 and 0.32 for PO_4^{-3}/HPO_4^{-2} were selected to give indicator ratios near unity.

In the measurements to determine the equilibrium constants, the several stock solutions were appropriately diluted to give a series of solutions with ionic strengths varying from 0.5 down to 0.01. In making the absorbancy measurements on these solutions, and for the determination of the absorbancy of the acidic and alkaline forms, in all cases duplicate solutions were prepared. One contained the indicator; the other contained no indicator and was used as the blank for 100% transmission. All of the solutions were brought to 25 ± 0.1° before being placed in the absorption cells to reduce the time required to reach thermal equilibrium in the cell compartment. In all of these solutions, the indicator concentration was 2.60×10^{-5} moles per liter, with an absorbancy of 0.324 ± 0.001 at the isobestic point, using a cell length of 1.002 cm.

Results and Discussion

The Indicator Constant, K_{in}^0.—In Table I the absorbancies of the acidic and basic forms of the indicator C.I. 274 are recorded for several wave lengths, obtained with a Beckman Model DU spectrophotometer; for this instrument the isosbestic wave length was 428.4 mμ.

TABLE I[a]

SELECTED ABSORBANCIES OF INDICATOR C.I. 274

λ, mμ	A^a, acid form	A_b, basic form
510	0.042	0.618
500	.064	.632
490	.091	.619
430	.315	.332
429	.320	.326
428	.325	.322
390	.606	.175
380	.625	.147
370	.589	.136

[a] Data obtained with Beckman Model DU spectrophotometer.

Table II presents the data obtained with the carbonate–bicarbonate buffer solutions. In the first two columns, *b* and *a* represent the stoichiometric concentrations of CO_3^{-2} and HCO_3^-, respectively. The third column, log R_i, gives the logarithm of the average value of R_i for the six chosen wave lengths. No significant difference could be found between groups of R_i values at different wave lengths. The average deviation in log R_i was found to be 0.008 for series 2, 3 and 4, but was about 0.020

(12) The authors gratefully acknowledge the courtesy of the above companies in making samples of this dyestuff available.

(13) R. G. Bates, *Chem. Revs.*, **42**, 1 (1948).

(14) Ref. 8, p. 526.

(15) C. W. Foulk and M. Hollingsworth, *J. Am. Chem. Soc.*, **45**, 1220 (1923).

TABLE II

EXPERIMENTAL DATA FOR CO_3^{-2}–HCO_3^- BUFFER SOLUTIONS[a]

$b \times 10^3$, moles/l.	$a \times 10^3$, moles/l.	log R_i	μ, true
	Series 1[b]		
42.422	32.352	−0.907	0.1918
28.281	21.568	− .914	.1278
21.211	16.176	− .920	.0958
14.141	10.784	− .924	.0638
11.312	8.627	− .928	.0510
7.070	5.392	− .939	.0318
5.656	4.314	− .963	.0254
2.828	2.157	−1.006	.0126
	Series 2[b]		
54.116	5.392	−0.103	0.1722
40.587	4.044	− .130	.1289
32.469	3.235	− .166	.1029
27.058	2.646	− .180	.0856
21.646	2.157	− .217	.0683
16.235	1.618	− .261	.0511
10.823	1.078	− .335	.0338
4.059	0.4044	− .566	.0124
	Series 3[c]		
106.02	8.124	+0.021	0.3335
70.68	5.416	− .010	.2220
53.01	4.062	− .046	.1662
42.41	3.250	− .065	.1327
35.34	2.708	− .089	.1104
28.272	2.166	− .123	.0882
21.204	1.625	− .182	.0659
17.670	1 354	− .212	.0548
14.136	1.083	− .246	.0437
8.835	0.6770	− .355	.0271
3.534	0.2708	− .564	.0106
	Series 4[c]		
54.566	8.124	−0.244	0.1792
43.650	6.499	− .252	.1432
36.378	5.416	− .268	.1193
29.102	4.333	− .295	.0952
25.464	3.791	− .305	.0832
21.826	3.250	− .322	.0713
18.189	2.708	− .336	.0593
14.551	2.166	− .374	.0473
7.276	1.083	− .482	.0234
3.638	0.5415	− .600	.0115

[a] The last digit in the concentration values is not necessarily significant but is carried to avoid errors due to "rounding off." [b] Obtained with a Beckman Model B spectrophotometer. [c] Obtained with a Beckman Model DU spectrophotometer.

for series 1, in which a less favorable ratio R_i was chosen. The fourth column gives the actual ionic strength, μ, which is given by

$$\mu = 3b + 2a - C_{OH^-} \quad (10)$$

The actual ionic concentrations of CO_3^{-2} and HCO_3^- are obtained from the relations

$$C_{CO_3^{-2}} = b - C_{OH^-} - 2.6 \times 10^{-6} R/(1 + R) \quad (11)$$

and

$$C_{HCO_3^-} = a + C_{OH^-} + 2.6 \times 10^{-6} R/(1 + R) \quad (12)$$

where the last term in the above equations represents the perturbation by the indicator as a disodium salt. In most cases this term was trivial. To obtain the hydroxide ion concentration term in equations 10, 11 and 12, it was necessary to solve equations 5, 10, 11 and 12 for log C_{OH^-} by successive approximations. In these calculations, pK_2^0 and pK_w^0 were taken equal to 10.329 and 13.9965, respectively.[10,16] Two series of computations were made, one using the ion-size parameter a = 4.3 Å. and one using a = 6.0 Å to evaluate the Debye–Hückel term D_2, to yield two slightly different sets of values for C_{OH^-}.

These two sets consequently produced two slightly different sets of values of the indicator function, $pK_{in}^0 - D_{in}$, from equation 7; these different sets arose mainly from the differences in D_2 for the two ion size parameters, and it was significant that the function

$$pK_{in}^0 - D_{in} + D_2 = pK_{in}' = pK_{in}^0 + C\mu \quad (13)$$

was decreased only very little (0.001 to 0.005) in going from 4.3 to 6.0 Å. for a, the least effect being noticed in the first series where the hydrolysis correction was least. Furthermore, plots of pK_{in}' against ionic strength were linear within experimental error (0.008) down to ionic strengths of 0.05. Below that, the points lay slightly above the line by amounts up to 0.060. These deviations could be ascribed to errors in measuring R_i combined with errors due to small amounts of absorbed CO_2 perturbing the system at low concentration and especially at lower buffer capacities. Amounts of CO_2 up to 6×10^{-5} mole per liter would have been required to account for the systematic deviations. The plots of equation 13 suggested strongly that $D_2 = D_{in}$, and that the indicator was in effect going from a singly to doubly charged species in equation 1. This amounts to treating the sulfonic acid end of the molecule, with its charge, as part of the general solvent environment, and considering the activity coefficient factor D_{in} as being determined primarily by the change in the ion atmosphere around the phenolcarboxylate end of the dye molecule, with the reasonable ion-size parameter 4.3 to 6.0 Å. Based on this interpretation, the value 11.375 was obtained for pK_{in}^0 with either choice of ion-size parameter.

The alternative interpretation of the indicator function accepts the indicator as going from doubly to triply charged in equation 1 and then seeks the Debye-Hückel parameters leading to best agreement with the data. Using the relation

$$pK_{in}'' = pK_{in}^0 - D_{in} - \frac{4A\sqrt{\mu}}{1 + aB\sqrt{\mu}} = pK_{in}^0 + C\mu \quad (14)$$

which is equivalent to

$$D_{in} = -\frac{4A\sqrt{\mu}}{1 + aB\sqrt{\mu}} - C\mu \quad (15)$$

an excellent fit could be obtained for all of the data over the entire range of ionic strength by taking a = 8.0 Å. While this at first appeared somewhat large for the ion-size parameter, it is not inconsistent with the total charge being spread over the whole region occupied by the ion, but lacking in symmetry and uniformity of distribution. The use of

(16) H. S. Harned and B. B. Owen, "The Physical Chemistry of Electrolytic Solutions," 3rd Ed., Reinhold Publ. Corp., New York, N. Y., 1958, p. 638.

TABLE III

EXPERIMENTAL DATA FOR PO_4^{-3}–HPO_4^{-2} BUFFER SOLUTIONS[a,b]

$b \times 10^3$, moles/l.	$a \times 10^3$, moles/l.	log R_i	μ, true
	Series 1		
9.145	39.340	0.040	0.1700
7.316	31.472	.023	.1354
6.402	27.530	.010	.1181
5.487	23.600	.000	.1008
4.572	19.670	− .029	.0836
3.658	15.736	− .064	.0664
2.744	11.800	− .128	.0494
1.829	7.867	− .245	.0326
	Series 2		
13.808	52.939	0.090	0.2386
11.045	42.351	.087	.1903
9.204	35.292	.081	.1581
7.364	28.234	.058	.1258
5.891	22.587	.040	.1000
4.602	17.646	− .017	.0778
3.682	14.117	− .060	.0618
2.945	11.294	− .090	.0490
1.841	7.058	− .226	.0302
0.920	3.529	− .476	.0149
	Series 3		
17.470	55.588	0.167	0.2681
11.033	35.108	.157	.1679
9.194	29.257	.144	.1392
7.356	23.406	.118	.1108
5.884	18.724	.087	.0880
4.597	14.628	.052	.0681
3.678	11.703	.001	.0541
1.839	5.851	− .210	.0265
	Series 4		
32.791	104.430	0.146	0.5070
29.339	93.435	.151	.4532
25.888	82.443	.159	.3995
24.162	76.947	.161	.3726
20.710	65.954	.163	.3188
17.258	54.962	.165	.2650
13.807	43.970	.163	.2112
10.355	32.977	.150	.1574
6.903	21.985	.113	.1038

[a] The last digit in the concentration values is not necessarily significant but is carried to avoid errors due to "rounding off." [b] All data were obtained with the Beckman Model DU spectrophotometer.

$a = 4.3$ Å. in the carbonate function D_2 led to the relation

$$pK_{in}'' = 11.495 + 0.015\mu \quad (16)$$

while $a = 6.0$ Å. in computing D_2 gave

$$pK_{in}'' = 11.495 + 0.180\mu \quad (17)$$

Both equations fit the data with an average deviation of 0.008 (the same as that associated with log R_i) but the pattern of deviations for equation 17 suggested slight curvature. Values of 7 and 9 Å. for a in D_{in} gave slightly poorer fit, with curvature and rather large slopes, but led to the same intercept within the limits of the data.

A comparison of the alternative treatments of the indicator function is shown in Fig. 2. The results indicate that the second interpretation is most appropriate, giving $pK_{in}^0 = 11.495$ and $K_{in}^0 = 3.20 \times 10^{-12}$ at 25°. Either interpretation should of course lead to the same value of K_3^0 for H_3PO_4.

The Third Dissociation Constant of Orthophosphoric Acid.—Data from series 1, 2, 3 and 4 for the four phosphate–monohydrogen phosphate buffer solutions are presented in Table III. Again, b and a represent the stoichiometric amounts of PO_4^{-3} and HPO_4^{-2}, respectively, at preparation; log R_i values were obtained in exactly the same manner as in Table II and showed again a mean deviation of 0.008. The actual ionic strength reported in the fourth column was computed from the equation

$$\mu = 3a + 6b - 2C_{OH^-} \quad (18)$$

The hydroxide concentration for these series was obtained from equations 4 and 18 by successive approximations. This procedure requires only a few cycles. The actual concentrations of the phosphate species were computed from

$$C_{PO_4^{-3}} = b - C_{OH^-} - 2.6 \times 10^{-5} R/(1 + R) \quad (19)$$

$$C_{HPO_4^{-2}} = a + C_{OH^-} + 2.6 \times 10^{-5} R/(1 + R) \quad (20)$$

where the last term represents the perturbation due to the indicator (as disodium salt).

Three possible procedures were used in acquiring values of the indicator function, $pK_{in}^0 - D_{in}$, for these computations: method A consisted of selecting appropriate values from a large graph; method B utilized pK_{in}' from equation 13; method C utilized pK_{in}'' from equation 16 or 17. Using a given set of data, the right-hand member of equation 8, designated by pK_3', was computed and plotted against the ionic strength, the intercept being pK_3^0. The results of several such analyses of the data are shown in Fig. 3, where the solid curves are based on $a = 4.3$ A. for D_2 and D_3, and the dotted curves show results for $a = 6.0$ Å. At the lower ionic strengths, errors in log R_i are magnified in their influence on pK_3; thus at $\mu = 0.0265$, an error of 0.008 in log R_i produces an error 0.023 in pK_3'. The presence of as little as 7×10^{-6} mole of CO_2 per liter in the solution would produce the same deviation at this point. Quite obviously the points below $\mu = 0.05$ must be given less weight. It was found that method C gave conclusively the best fit and method B the poorest. The superiority of method C over method A arises mainly from its objectivity and the analytical smoothing of the indicator function. The results strongly support the description of the indicator behavior by equations 14 and 15. All three methods, however, yield the same value, 12.375, for pK_3^0 for both choices of the ion-size parameter. A re-examination of Harned and Scholes[10] data together with our own indicated than an ion-size parameter of 4.8 Å. would be an optimum value for both the carbonate and phosphate systems and lead to practically horizontal plots of all the D_i functions against μ, with maximum internal consistency throughout the calculations.

The final value chosen for the third dissociation constant is taken to be

$$pK_3^0 = 12.375 \pm 0.010$$

$$K_3^0 = 4.22 \times 10^{-13} \text{ at } 25° \quad (21)$$

This value is close to that obtained by Bjerrum and

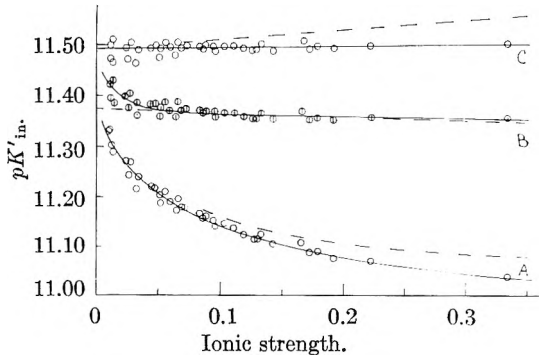

Fig. 2.—Behavior of the indicator function. Curve A, $pK^0_{in} - D_{in}$, eq. 7; curve B, pK'_{in}, eq. 13; curve C, pK'_{in}, eq. 16. Solid curves based on ion size parameter 4.3 Å. for the carbonate system, dashed curves based on 6.0 Å. (See Discussion.) Diameter of circles equals 0.008 in pK_{in}.

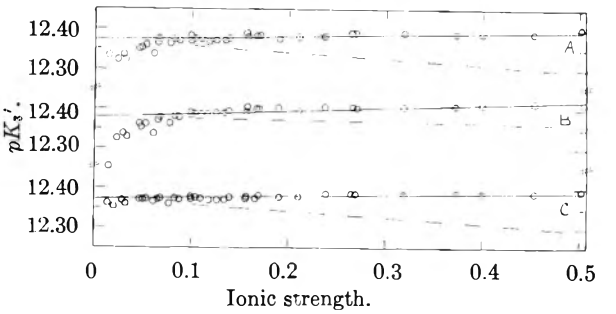

Fig. 3.—Extrapolation of the phosphate function, pK_3'. Curve A, method A; curve B, method B; curve C, method C. (See Discussion.) Solid curves based on ion size parameter 4.3 Å. for carbonate and phosphate systems dashed curves based on 6.0 Å. Diameter of circles equals 0.008 in pK_3'.

Unmack,[17] $pK_3^0 = 12.325$, from cells with liquid junctions. The high quality of their work has been borne out by the close agreement of other constants reported in their paper[17] with values obtained later by improved methods. An examination of their data indicates that it would readily support a value close to ours if points below $\mu = 0.02$ are given appropriately less weight than the rest. The only later attempt at measurement of pK_3^0 is that of Konopik and Leberl,[18] who reported a value between 11.70 and 11.95 from colorimetric data but with very insecure treatment of activity coefficients. Both references[17,18] summarize older data for historical interest.

Acknowledgments.—We wish to express our appreciation to the sources listed in Ref. 2 for fellowships supporting the junior author (A.S.Q.). The senior author (C.E.V.) wishes to thank E. I. du Pont de Nemours and Company for a Grant-in-Aid under which this manuscript was completed.

(17) N. Bjerrum and A. Unmack, *Kgl. Danske Videnskab. Selskab, Math-fys. Medd.*, **9**, 5 (1929).

(18) N. Konopik and O. Leberl, *Monatsh. Chem.*, **80**, 655 (1949).

THE HYDROGEN FLUORIDE–ANTIMONY PENTAFLUORIDE SYSTEM[1,2]

BY HERBERT H. HYMAN,[3] LLOYD A. QUARTERMAN, MARTIN KILPATRICK AND JOSEPH J. KATZ

Argonne National Laboratory, Argonne, Illinois

Received July 15, 1960

Antimony pentafluoride and hydrogen fluoride as liquids are miscible in all proportions. Observations on the reactivity of mixtures have been interpreted in terms of fluoride ion acceptor behavior to form an octahedrally symmetrical SbF_6^-. Nickel and other base metals as well as siliceous materials are attacked rapidly by hydrogen fluoride solutions containing several mole per cent. antimony pentafluoride. Platinum, polychlorotrifluorethylene, sapphire and silver chloride can be used in constructing optical equipment. Suitable cells have been devised and the electrical conductivity, and the infrared and Raman spectra have now been observed throughout the concentration range. Spectral patterns have been identified for pure SbF_5, pure HF, a highly symmetrical species, presumably SbF_6^-, and a more complex species, possibly the ion pair $H_2F^+SbF_6^-$. The observations can be described by a set of equations $2HF + SbF_5 \overset{(1)}{\rightleftharpoons} H_2F^+SbF_6^- \overset{(2)}{\rightleftharpoons} H_2F^+ + SbF_6^-$. At 20 mole % SbF_5, $K_1 \cong 4.4 \times 10^{-4}$ and $K_2 \cong 1.7 \times 10^2$. At lower SbF_5 concentrations the ionic dissociation becomes essentially complete. The electrical conductivity is at a maximum near 10 mole % SbF_5. At higher concentrations the amount of ionization drops off rapidly and the complex becomes the predominant species.

Introduction

We have had an active interest in the behavior of anhydrous hydrogen fluoride as an ionizing solvent. Hydrogen fluoride is a strongly acidic material and as such by far the overwhelming number of solutes behave as proton acceptors. It has long been known however, that certain solutes in hydrogen fluoride such as boron trifluoride and antimony pentafluoride behaved as if they were fluoride ion acceptors, and therefore acids (or co-acids)[4] rather than proton acceptors. Clifford[5] for example has discussed the chemical behavior of a number of possible fluoride ion acceptors and came to the con-

(1) Based on work performed under the auspices of the U. S. Atomic Energy Commission.

(2) Presented before the Inorganic Division Symposium on Aqueous and Non-aqueous Solution at the 136th Meeting of the American Chemical Society, Atlantic City, N. J., Sept. (1959).

(3) From the thesis submitted by Herbert H. Hyman in partial fulfillment of the requirement for the Doctor of Philosophy degree at Illinois Institute of Technology.

(4) The term co-acid was introduced by M. Kilpatrick for compounds which increase the acidity of a protonic solvent, without contributing a proton. In water such familar oxides as CO_2 and SO_3 that add an oxide or hydroxide ion to form the anionic CO_3^- (or HCO_3^-) and SO_4^- (or HSO_4^-) and increase the H_3O^+ concentration, would be classified as co-acids. While it is obvious that the familiar term "Lewis Acid" may be applied to these compounds the terms are used in a slightly different context. The term co-acid is restricted to compounds which increase the acidity of a proton acid, while Lewis Acids may react directly with bases.

(5) A. F. Clifford, H. C. Beachell and W. M. Jack, *J. Inorg. Nucl. Chem.*, **5**, 57 (1957).

clusion that antimony pentafluoride was the most acidic of the substances he investigated although he believed that fluoride ion transfer was very incomplete even for antimony pentafluoride. Clifford's observations were almost entirely qualitative and he ranked acids as to relative strength depending on the ability of HF solutions of the potential co-acid to dissolve cobalt trifluoride and chromium and manganese and magnesium metals. He based his estimate of the absolute strength of antimony pentafluoride as a weak acid on the ease of solvolysis of cobaltic hexafluoro-antimonate.

Kilpatrick and Lewis[6] on the other hand measured the electrical conductivity of dilute solutions of antimony pentafluoride and sodium hexafluoroantimonate in hydrogen fluoride. These investigators found that the molar conductivity of these two materials was essentially identical. They therefore suggested that antimony pentafluoride was a strong acid (or rather co-acid) that is essentially completely converted to an anionic species in HF, that the conductivity of the sodium ion and the H_2F^+ cation were roughly comparable, and that these conductivities are substantially less than the conductivity of fluoride ion in sodium fluoride solutions in HF. Kilpatrick and Lewis investigated only very dilute solutions and their results seemed to disagree with Clifford's conclusion that antimony pentafluoride was a weak acid. Because of this, the possibility that the measured conductivity was that of an SbF_6^- salt due to an impurity could not be dismissed. Water would serve as a cationic impurity. The present investigation was aimed at establishing the nature of the ionic processes taking place in solutions of hydrogen fluoride and antimony pentafluoride in a concentration range where the effect of small quantities of undetected impurities could not affect the data.

In addition to electrical conductivity data, primarily aimed at establishing an ionization process, it was possible to employ both infrared spectroscopy and Raman spectroscopy to obtain some information about the structure of the ionic species present.

Since measurements of the Hammett acidity function for anhydrous hydrogen fluoride and solutions of anhydrous hydrogen fluoride containing proton acceptors had proven useful in describing the properties of these solutions,[7,8] some Hammett acidity measurements were made on solutions containing fluoride ion acceptors.

Experimental

Materials. Hydrogen Fluoride.—The hydrogen fluoride was purified by distillation as has been previously described.[9] Antimony pentafluoride was a commercial grade distilled at reduced pressure through an all-glass system, collecting the middle third in a Kel-F vessel. Solutions of antimony pentafluoride and HF were then made up by pouring the antimony pentafluoride from this vessel through evacuated flexible Kel-F lines. For studies involving pure antimony pentafluoride alone, the material was redistilled through a nickel system in a heated box directly into the cell appropriate to the investigation.

Niobium pentafluoride was prepared from reagent grade niobium pentachloride by reaction with anhydrous hydrogen fluoride and tantalum pentafluoride was prepared similarly from reagent grade tantalum pentachloride. Solutions of these pentafluorides in HF were refluxed vigorously to remove traces of hydrogen chloride. Examination of the near infrared spectrum of resulting solutions in hydrogen fluoride showed no detectable absorption attributable to OH.

The *p*-nitrotoluene used as an indicator was a reagent grade chemical used as received and 2,4,6-trinitroaniline was one of the Aldrich Company Hammett indicators, also used as received.

Equipment.—Pure antimony pentafluoride is not particularly corrosive, attacking neither glass nor the usual metals employed in vacuum line work with fluorine systems. No reaction was observed with nickel, copper, aluminum or monel metal and certainly not with the noble metals. Anhydrous hydrogen fluoride containing antimony pentafluoride is extremely corrosive, reacting vigorously not only with silica containing materials but also nickel and copper and their alloys. As a result all equipment items used in contact with solutions of hydrogen fluoride and antimony pentafluoride were fabricated from platinum and polychlorotrifluoroethylene. Teflon gaskets could be employed and sapphire windows are suitable for optical cells in the visible, ultraviolet and near infrared regions. Silver chloride was employed as a window for transmission of infrared radiation although it is not inert to all mixtures of hydrogen fluoride and antimony pentafluoride. In the concentration region associated with high electrical conductivity, a thin film of white powder appeared on the silver chloride window. This powder did not appreciably affect transmission in the infrared region and appeared to be as transparent as silver chloride itself. This white powder may be $AgSbF_6$.

The conductivity equipment has been described previously.[9] The cells employed for infrared absorption spectroscopy represented the latest in a number of similar designs which have been described earlier. For pure antimony pentafluoride solutions a nickel diaphragm variable spacer cell was employed similar to that described by Adams and Katz.[10] For the more corrosive mixtures of antimony pentafluoride and hydrogen fluoride a smaller cell based on the design described by Quarterman, Hyman and Katz[9] was employed. The outer body of the cell was fabricated from platinum and the inner barrel from polychlorotrifluoroethylene. Both sapphire and silver chloride windows were used in these cells. With silver chloride windows there is no possibility of cracking the windows on bringing them too closely together and path lengths as low as 5–10 μ were used. With the large nickel cell, windows are reasonably parallel down to at least 10 μ and extinction coefficients may be duplicated to within 10%. With the Teflon gasketed smaller cell the faces cannot be maintained sufficiently parallel to permit calibration by counting fringes and estimates of the light path in the 10 μ region may well be in error by 50 or 100%.

The bulk of the spectra discussed were obtained with a Beckman IR 4 using either sodium chloride or cesium bromide optics. In the near infrared region overlapping data were obtained with a Beckman DK recording spectrophotometer using the platinum and polychlorotrifluoroethylene cells. With the sapphire windows, cell path lengths of less than 50 μ cannot be used safely, since the windows will crack on contact. However, light path lengths of about 100 μ could be determined quite accurately and the most accurate extinction coefficients reported below were obtained by a sequence of internal comparisons starting with accurately determined molar absorption coefficients for bands in the near infrared. The same solution could be compared in a cell with sapphire windows and one with silver chloride windows.

A number of Raman cells were devised for this investigation. These were operated with the Hilger photographic Raman spectrograph, using Eastman Kodak 103 a-J plates, a high intensity Applied Research Corporation power supply, and a laboratory fabricated straight tube mercury arc. A nickel cell with a large flat Kel-F window facing the arc and a small sapphire window facing the spectrograph was employed in some parallel studies with hydrogen fluoride solutions. However, when the antimony pentafluoride hydrogen-fluoride solutions were found to attack nickel cells and gold

(6) M. Kilpatrick and T. J. Lewis, *J. Am. Chem. Soc.*, **78**, 5186 (1956).

(7) H. H. Hyman, M. Kilpatrick and J. J. Katz, *ibid.*, **79**, 3668 (1957).

(8) H. H. Hyman and R. A. Garber, *ibid.*, **81**, 1847 (1959).

(9) L. A. Quarterman, H. H. Hyman and J. J. Katz, THIS JOURNAL, **61**, 912 (1957).

(10) R. M. Adams and J. J. Katz, *J. Opt. Soc. Am.*, **46**, 895 (1956).

plating failed to provide adequate protection, a much simpler all Kel-F tube was devised. The background from this cell was somewhat greater than from the earlier metal cells, but the ease with which new cells could be fabricated more than compensated for the slightly lessened convenience in obtaining spectra. All of the spectra employed observed refer to the mercury line at 4358 Å. and no filters were found necessary in view of the simple nature of the spectrum observed in each case.

Observations

Electrical Conductivity.—The electrical conductivity data are given in Table I. Pure antimony pentafluoride is a non-conductor and apparently has a low dielectric constant. The addition of hydrogen fluoride to antimony pentafluoride raises the conductivity, but the maximum specific conductivity is not reached until about 90 mole % hydrogen fluoride is present. At this point, the equivalent conductivity of antimony pentafluoride is somewhat less than 40% of the infinite dilution value in anhydrous hydrogen fluoride as described by Kilpatrick and Lewis.[6] They suggest 275 ohm^{-1} cm.^{2} mole^{-1} as the extrapolated equivalent conductivity at 0°. From this number and their value at 20° the equivalent conductivity at infinite dilution at 25° may be estimated as 375 ohm^{-1} cm.^{2} mole^{-1}.

TABLE I

ELECTRICAL CONDUCTIVITY OF HF–SbF_5 SOLUTIONS

Concn. HF Mole %	Concn. HF Moles/l.	Concn. SbF_5 Mole %	Concn. SbF_5 Moles/l.	Cond. (ohm^{-1} cm.$^{-1}$) 0°	Cond. (ohm^{-1} cm.$^{-1}$) 25°
0	0.0	100	13.7	2.4×10^{-8}	7.4×10^{-8}
9.92	1.44	90.08	13.1	2.1×10^{-6}	6.4×10^{-6}
13.10	1.96	86.90	13.0	2×10^{-6}	6.2×10^{-6}
27.03	4.48	72.97	12.2	0.597×10^{-3}	1.22×10^{-3}
48.20	10.00	51.80	10.8	1.77×10^{-2}	2.98×10^{-2}
76.12	22.62	23.88	7.10	0.146	0.200
79.09	24.71	20.91	6.53	.173	.240
85.01	29.57	14.99	5.21	.264	.322
92.13	36.6	7.87	3.13	.35	.40
100	47.7	0.00	0.0	10^{-6}	10^{-5}

Infrared Absorption.—The infrared absorption spectrum of antimony pentafluoride vapor has been reported by Gaunt, Ainscough and Deane.[11] They also show the spectrum of a rather thick liquid layer which is opaque below 900 cm.$^{-1}$. In this work only the liquid has been studied. However, path lengths as short as 14 μ were used and the spectrum of the liquid was determined in the wave length range 2–25 μ, 5000–400 cm.$^{-1}$. Table II lists the peaks found by Gaunt, *et al.*, and those found in this work for antimony pentafluoride. There are minor discrepancies. The 1140 cm.$^{-1}$ peak reported by them was not found in this work. There are four peaks in the spectrum of both the liquid and vapor between 600 and 800 cm.$^{-1}$ but only 2 peaks coincide within the precision of the spectrophotometer.

In the infrared spectrum of mixtures three separate wavelength ranges of interest can be discussed. In the 3μ region the HF vibrations modified by environment are the most prominent feature. The most prominent feature of the pure hydrogen fluoride spectrum itself is the very intense absorption band near 3450 cm.$^{-1}$ due to the group of polymers that make up liquid hydrogen fluoride. There is also present a small satellite peak at 4100 cm.$^{-1}$ that corresponds to the monomer vibration and a 6900 cm.$^{-1}$ overtone of the principal vibration. As antimony pentafluoride is added to this system, the first change noted seems to be a substantial reduction of the relative height of the 6900 cm.$^{-1}$ peak. The polymer absorption band is broadened and reduced in height and as more antimony pentafluoride is added the wave length of maximum absorption shifts to longer wave lengths. An absorption maximum is found at about 3250 cm.$^{-1}$ for a 20% antimony pentafluoride solution. As the antimony pentafluoride concentration increases the band at this frequency is reduced to a shoulder on a new band with a maximum at 3000 cm.$^{-1}$. The intensity of this 3000 cm.$^{-1}$ band appears to be directly proportional to the intensity of the much more intense 1560 cm.$^{-1}$ band observed in the 800–1800 cm.$^{-1}$ region.

TABLE II

INFRARED ABSORPTION PEAKS FOR SbF_5 (cm.$^{-1}$)

Peaks obsd. by Gaunt, *et al.*[11] Gas	Liquid	This work Liquid
1420	1420	1420
	1140	..
760		
		745
727		
710		710
684		685
		655
517		
491		490
478		
439		
335		
326		
~300		

In the middle of the sodium chloride spectral region, a number of absorption bands are observed. The peak at 1420 cm.$^{-1}$ is attributable to pure antimony pentafluoride. In a solution containing 10 mole % HF it is much weaker than the 1560 cm.$^{-1}$ peak. The latter has a molar absorption coefficient of 350 if the concentration of the absorbing species is taken as equal to the hydrogen fluoride concentration. Absorption in the region 950 to 1150 cm.$^{-1}$, which is probably best interpreted as a triplet with peaks at 980, 1020 and 1090 cm.$^{-1}$, is observed only in antimony pentafluoride-hydrogen fluoride. The absorption in this region seems to parallel in intensity the more strongly absorbing band at 1560 cm.$^{-1}$. The broad and intense absorption in 50 mole % HF at ~ 1400 cm.$^{-1}$ cannot be attributed to the pure SbF_5 band at 1420 cm.$^{-1}$, though the latter may contribute. In the concentration range close to 80 mole % HF, the predominant absorption band is a broad peak, or more likely a doublet, at 1220–1300 cm.$^{-1}$. In the cesium bromide region, four sharp strong peaks attributable to pure antimony pentafluoride are observed. Unfortunately, these peaks are obscured by the intense hydrogen fluoride absorption in this region for solutions in which the antimony pentafluoride content is lower than 70 or 80 mole %. An absorption band at 600 cm.$^{-1}$ is observed in each solution. In 20 mole % antimony pentafluoride solutions this band shows rather

(11) J. Gaunt, J. B. Ainscough and A. M. Deane, A.E.R.E. C/R 2292, May (1957).

prominently and at 80 mole % antimony pentafluoride solutions the 600 cm.$^{-1}$ extinction coefficient is very much less. It appears to be present however even in antimony pentafluoride with no added hydrogen fluoride and there may actually be two different absorption bands close to this same point. The 490 cm.$^{-1}$ peak is perhaps the best one for determining the concentration of un-ionized and uncomplexed antimony pentafluoride present and the equilibrium constants given below depend heavily on the extinction coefficient found for this 490 cm.$^{-1}$ peak. The molar absorption of antimony pentafluoride is 40 at 490 cm.$^{-1}$ in liquid antimony pentafluoride containing no added hydrogen fluoride. Hydrogen fluoride is transparent in this region so that fairly low intensity absorptions may be studied. There appears to be a weak absorption peak at 440 cm.$^{-1}$ in liquid antimony pentafluoride and there may be others at still longer wave lengths, but the silver chloride cells become less transparent as the frequency increases and no reliable data were obtained below 450 cm.$^{-1}$.

Raman Spectrum.—Raman spectra were obtained for each of the solutions prepared and listed in Table I. Table III shows the peaks found for pure antimony pentafluoride. When hydrogen fluoride is added this pattern tends to disappear more rapidly than simple dilution would suggest. In solutions containing more than 20 or 30 mole % hydrogen fluoride none of the lines attributable to antimony pentafluoride were observed in the Raman spectrum. This behavior is not characteristic of hydrogen fluoride when it acts as an inert solvent. Liquid SO_2, for example, has a Raman spectrum which for the pure material is no more readily excited than antimony pentafluoride. However the entire liquid SO_2 Raman spectrum may be observed in a 20 mole % solution in hydrogen fluoride with little difficulty, and the principal line of sulfur dioxide was observed in the same equipment with no change in wave length in a 2 mole % solution.

In a 10–20 mole % antimony pentafluoride solution in hydrogen fluoride the characteristic spectrum is a single rather faint line at about 650 cm.$^{-1}$. While this is close to the most prominent line in the pure antimony pentafluoride spectrum there seems to be no doubt that it is not due to the same species. There is no trace of the 710 cm.$^{-1}$ line which is almost as strong in the pure antimony pentafluoride. Some evidence was found for a second, very faint line in the Raman spectrum at around 550 cm.$^{-1}$ but this point could not be unequivocally established with the cells and apparatus available.

TABLE III

THE RAMAN SPECTRUM OF LIQUID SbF_5 IN CM.$^{-1}$

Reported by Gaunt, *et al.*[11]	This work
716s	712s
667s	668s
264m	265m
228m	228m
ca. 90v.w.	150v.w.

Hammett Acidity Values.—The direct measurement of H_0 values of the HF-SbF_5 system poses serious problems. An indicator less basic than the one employed in anhydrous HF is required.[7] For this purpose, *p*-nitrotoluene ($pK = -10.46$)[12] was employed.[12] Antimony pentafluoride appears to react chemically with this indicator in an irreversible fashion, and direct measurements are thus excluded. With NbF_5 and TaF_5 the situation is more favorable in this respect, since chemical reactions do not appear to occur with the indicator under the experimental conditions employed. However, since questions arise, which at present cannot be answered unequivocally, it is not clear that the use of nitro compounds as indicators permits a smooth extension of the H_0 function.

Using *p*-nitrotoluene as an indicator, and NbF_5 as the co-acid, a concentration of as little as 0.02 M converted the indicator almost completely to the acidic form ($H_0 \sim -12.5$). By making assumptions as to the ionization process and the relationship between H_0 value and the concentration of H_2F^+, it is possible to connect H_0 values and electrical conductivity in HF solutions. On this basis, a saturated NbF_5 solution (0.36 M) would have an H_0 value of -13.5, and an SbF_5 solution at this concentration would have an H_0 value of -14.3. For 3.0 M SbF_5 (near the concentration where the specific conductivity is a maximum) an H_0 value of -15.2 may be calculated on this basis. There appears to be little doubt, therefore, despite indicator problems, that there are co-acids that strongly increase the acidity of HF solutions.

Discussion

Both the spectral data and the conductivity data appear to be consistent with the postulated ionization of antimony pentafluoride in dilute solution in hydrogen fluoride to give a hexafluoroantimonate anion and a protonated hydrogen fluoride cation according to the equation

$$2HF + SbF_5 \rightleftarrows H_2F^+ + SbF_6^-$$

Perhaps the most important single piece of evidence is the complete absence of the well established absorptions due to the HF_2^- anion[13] in solutions with high electrical conductivity. The infrared absorption spectrum and the Raman spectrum of solutions in the region where the hexafluoroantimonate ion is prominent, while not sufficient to define completely the structure of the octahedral ion, seem to be very close to what would be predicted for such an anion.

The infrared spectra of a number of hexafluorides have now been established.[14] All the hexafluorides studied have octahedral symmetry and their infrared spectra can be interpreted on this basis. The hexafluoroantimonate ion should show a similar structure and spectrum. One characteristic absorption band for the hexafluorides is a doublet in the 1200–1500 cm.$^{-1}$ region, which is attributed to the combination bands $\nu_2 + \nu_3$ and $\nu_1 + \nu_3$. For example gaseous tellurium hexafluoride has absorption bands at 1425 and 1450 cm.$^{-1}$, respectively. The fundamental absorption band ν_1 is found only in the Raman spectrum of hexafluorides. For tellurium hexafluoride ν_1 is 701 cm.$^{-1}$, for the hexafluoroantimonate ion ν_1 is

(12) M. A. Paul and F. A. Long, *Chem. Revs.*, **57**, 1 (1957).
(13) R. M. Adams and J. J. Katz, *J. Mol. Spect.*, **1**, 306 (1957).
(14) J. Gaunt, *Trans. Faraday Soc.*, **49**, 1122 (1953).

650 cm.$^{-1}$. The ν_2 and ν_3 bands are infrared active, but in solution in hydrogen fluoride they would be hidden by the hydrogen fluoride absorption. Woodward and Anderson[15] have investigated iso-electronic series in which the central atom changes, for example, PF_6^- (ν_1 = 741 cm.$^{-1}$) and SF_6 (ν_1 = 775 cm.$^{-1}$). If the observed absorption at 1220–1350 cm.$^{-1}$ in the hydrogen fluoride–antimony pentafluoride solutions is attributed to the hexafluoroantimonate ion, the shift to lower frequency from the tellurium hexafluoride absorption is in the right direction and of the right magnitude. This doublet absorption is observed only in electrically conducting solutions containing at least 50 mole % hydrogen fluoride. The relative intensity of these bands per mole of antimony pentafluoride decreases with increasing concentration. It is concluded that the 1200–1300 cm.$^{-1}$ absorption peak is due to the ionic species produced on the addition of antimony pentafluoride to hydrogen fluoride and it is almost certainly due to the hexafluoroantimonate ion. The absorption band in the 1400 cm.$^{-1}$ region in 50 mole % HF probably contains a contribution from the 1560, 1420 and 1350 cm.$^{-1}$ absorption bands attributable to the three species known to be present, but may well include a contribution from an additional species not otherwise observed.

The single Raman line is approximately what one would expect from the observed ν_1 for tellurium hexafluoride and the predictions of Woodward and Anderson as to the effect of a unit nuclear charge difference in iso-electronic species.

It is clear however, that ionization is not an important process below 40 or 50 mole % hydrogen fluoride. However, antimony pentafluoride is not present simply diluted by an inert solvent but rather hydrogen fluoride and antimony pentafluoride combine to form a molecular complex with a distinct absorption spectrum and presumably existence as a discrete molecule. The absorption bands at 3000 and 1560 cm.$^{-1}$, the triplet in the 950 to 1150 cm.$^{-1}$ region and possibly an absorption at 600 cm.$^{-1}$ are all attributable to this molecular complex. It is probably not a species of very high symmetry and sufficient data to work out a detailed structure do not exist. The equilibrium in 70–100 mole % hydrogen fluoride seems to be substantially in favor of ionization. At 20 mole % antimony pentafluoride enough absorption from bands attributable to each of the species in the equilibrium occurs to make possible a rough guess at equilibrium constants. The calculation below is based on the assumption that only a single complex is formed which corresponds to the ion pair.

(15) L. A. Woodward and L. E. Anderson, *J. Inorg. Nucl. Chem.*, **3**, 326 (1956).

The equilibria in the HF–SbF_5 system are assumed to be

$$2HF + SbF_5 \underset{}{\overset{K_1}{\rightleftharpoons}} H_2F^+ SbF_6^- \overset{K_2}{\rightleftharpoons} H_2F^+ + SbF_6^-$$

$$K_1 = \frac{C_{H_2F^+SbF_6^-}}{(C_{HF})^2(C_{SbF_5})}$$

$$K_2 = \frac{(C_{H_2F^+})(C_{SbF_6^-})}{C_{H_2F^+SbF_6^-}}$$

$$K = \frac{(C_{H_2F^+})(C_{SbF_6^-})}{(C_{HF})^2(C_{SbF_5})}$$

The concentration of the species SbF_5 is determined from the infrared absorption at 490 cm.$^{-1}$ (A_m = 40).

The concentration of the species H_2F^+ SbF_6^- is determined from the infrared absorption at 1560 cm.$^{-1}$ (A_m = 350).

The molar absorption for the 490 cm.$^{-1}$ peak is based on the adsorbance of pure antimony pentafluoride. The molar absorbance of the 1560 cm.$^{-1}$ peak is based on the absorbance of a 9.92 mole % hydrogen fluoride solution. The absorbance of 1 cm. of this solution at 1560 cm.$^{-1}$ is 500 and the concentration of addition compound is taken as essentially that of the hydrogen fluoride present (1.4 *M*).

TABLE IV

SPECIES CONCENTRATIONS IN 20 MOLE % SbF_5 IN HF

Species	HF	SbF_5	H_2F^+ SbF_6^-	H_2F^+ SbF_6^-
Stoichiometric concn. *M* (20 mole % SbF_5)	25	3.5		
Absorption band, cm.$^{-1}$		490		1560
Molar absorbance, A_m		40		350
Absorbance of 1 cm. of 20 mole % SbF_5		60		50
Concn., *M*	15[b]	1.5[a]	5[b]	5[b] 0.15[a]

[a] Concentration calculated from absorbance. [b] Concentration calculated from numerical proportions.

The concentration of the species SbF_6^- (and therefore H_2F^+) is the stoichiometric concentration of SbF_5 minus the sum of the concentrations of the species SbF_5 minus the sum of the concentrations of the species SbF_5, and H_2F^+ SbF_6^-. The concentration of the species HF is taken as the stoichiometric hydrogen fluoride concentration less the HF present as H_2F^+ and H_2F^+ SbF_6^-. The concentration data for this solution are summarized in Table IV. $K_1 = 4.4 \times 10^{-4}$, $K_2 = 1.7 \times 10^{-2}$ and $K = K_1K_2 = 7.3 \times 10^{-2}$.

THE EXCHANGE OF DEUTERIUM GAS WITH THE HYDROGEN ASSOCIATED WITH SOLID CATALYSTS. II. KINETICS AND MECHANISM OF THE REACTION WITH HYDROGENATED TANTALUM

BY W. KEITH HALL, W. E. WALLACE AND F. J. CHESELSKE

Contribution from Mellon Institute, Pittsburgh, Penna.

Received July 18, 1960

The rate of the transport of hydrogen from solid tantalum hydride to gas has been found to be proportional to pressure while the solubility of hydrogen in tantalum varies as the square root of pressure. These facts, together with the previously determined activation energy (14.9 ± 0.5 kcal./mole) and the absolute magnitude of the rate can be satisfactorily rationalized if it is assumed that the rate-determining step involves desorption of hydrogen molecules from the surface. When deuterium is present, this corresponds to a Bonhoeffer–Farkas-type mechanism for the exchange reaction. A Rideal-type mechanism, involving an exchange between a molecule and an adsorbed atom, would appear to be ruled out on the grounds that the observed pressure dependence would require that the surface be nearly completely covered with adsorbed hydrogen atoms; evidence has been obtained indicating that this probably is not the case.

Introduction

A study of the kinetics of the exchange reaction between deuterium gas and hydrogen held interstitially in the tantalum lattice was undertaken in order to learn something about the nature of the hydrogen held by solids. The tantalum–hydrogen system was selected for study because it approximates a model amenable to simple mathematical treatment. This treatment was presented in detail in an earlier paper[1] (hereinafter referred to as Part I). In this development, the hydrogenated tantalum was pictured as a box filled with hydrogen atoms surrounded by deuterium gas. Neglecting small differences in reactivity of the isotopes, it was found that if both phases are well stirred, the apparent kinetics may be described by the equation

$$V_g(dx/dt) = R(V_g/V_s + 1)(x_\infty - x) \qquad (1)$$

where V_g and V_s are the number of moles (NTP volumes) of the hydrogen plus the deuterium in the vapor and solid phases, respectively, and x is the atom fraction of hydrogen in the gas phase at any time t; x_∞ is the value of x at equilibrium at the end of the experiment; R is the equilibrium rate at which molecules cross the boundary between the two phases; when both contain only hydrogen, it is the equilibrium rate of sorption and of desorption of this gas.

In Part I, it was shown that the integrated form of (1) was obeyed over a wide temperature range. From the slope of these first-order plots, a parameter k could be determined at constant temperature, where $k = R(V_g + V_s)/V_gV_s$. Further, since V_g and V_s could be evaluated independently, R could be calculated for each experiment. From experiments carried out at different temperatures, two activation energies were evaluated. The first of these, corresponding to the temperature coefficient of k, has a value of 22.3 kcal./mole while the latter, corresponding to the temperature coefficient of R or the true activation energy for the equilibrium rate process, amounted to 14.9 kcal./mole. It was further shown that the difference between these two activation energies was approximately equal to the heat of solution of hydrogen in tantalum.

(1) F. J. Cheselske, W. E. Wallace and W. K. Hall, THIS JOURNAL, **63**, 505 (1959). Most of the pertinent related literature is reviewed here.

In the present study, the pressure dependence of the equilibrium rate, R, and of the solubility of hydrogen in tantalum have been determined. These data, together with those obtained in Part I, are interpreted to show that the rate, R, is limited by a surface process and probably involves a microscopically reversible step in which hydrogen adsorbs with dissociation and desorbs with recombination.

Experimental

The same materials and equipment were used in the present study as in Part I. For sake of brevity, therefore, only a few details essential to the reader's understanding will be repeated here.

Experiments were carried out in an all-glass circulating system,[1] so designed that the atom fraction of H could be followed continuously [*i.e.*, $x = f(t)$] and the data treated as if they had been obtained from a static reactor. The 1.72-g. sample of tantalum was in the form of 15 mil wire having a geometric surface area of 18.7 cm.^{2}.

The thermal conductivity method used could not simultaneously provide invididual analyses for H_2 and HD. The bridge unbalance was found to be an exact linear relation of the % H with the two component H_2, D_2 mixtures. The three component equilibrium mixtures also provided a linear calibration over the range (0 to 30% H) used in the experiments, but with a 10% lower slope. Since the choice of this slope parameter affects only the intercept of the first-order plots whose slopes in turn provide the kinetic data, values of R could be obtained without introducing appreciable error due to the actual distribution of isotopes.

The customary procedure was to pre-equilibrate the tantalum in pure hydrogen gas at the same temperature and pressure at which the exchange experiment was to be carried out. When equilibrium had been obtained, the stopcocks on the sample tube were closed and the sample was quenched to the temperature of liquid nitrogen. At this temperature, the gas phase was removed by evacuation and replaced with pure deuterium gas at the same pressure. After circulation of the latter was commenced, the furnace was quickly replaced around the sample and temperature equilibrium was re-established within a period of about three minutes. Any errors introduced by the short heating period were neglected in the treatment of the data. This procedure served to minimize the transport of gas between the two phases during the course of the experiment.

Results

A series of experiments was carried out to test the validity of the two assumptions made in the derivation of (1) as well as an additional assumption, (c) usually made in the treatment of the data. Specifically, these assumptions were that: (a) small differences in isotopic reactivity may be neglected; *i.e.*, $x_\infty = y_\infty$; (b) a single value of R is adequate to characterize the data; and (c) no net mass transport of gas takes place between the two phases

during an experiment; *i.e.*, δ may be taken as zero in the parametric equations

$$V_g = V^0_{D_2} + \delta \text{ and } V_s = V^0_{H_2} - \delta \qquad (2)$$

If the first assumption is true, when a solid containing hydrogen is exchanged with pure deuterium gas, its residual hydrogen content at equilibrium is given by $V_g x_\infty$. This amount of hydrogen may be experimentally determined, provided δ is known, by exchange with a fresh sample of pure deuterium. Alternatively, given the results of the first step, the results of all such repeat experiments may be calculated provided that (c) is also valid. The data collected in Table I compare the experimentally determined values, V_1, with values calculated in two different ways, V_2 and V_3. V_2 for the ith step is taken as the amount of hydrogen left in the solid at the end of the $(i-1)$th step, while V_3 is the difference between the initial hydrogen content, found in the first step, and the sum of all the hydrogen actually recovered in the gas phase (and discarded) in all previous steps. Also, the observed values of x_∞ are compared with those calculated on the basis of assumption (c), using values of V_2 and the volumes of D_2 measured in each step. In these calculations, the V_2 and x_∞ values were calculated exclusively from the results of the first step and the new volumes of deuterium; for the V_3 values, the experimentally determined x_∞ values were used also. The agreement obtained in all cases shows that errors introduced through these assumptions are negligible and not cumulative. It is also of interest to note (V_3) that 98% of the hydrogen initially held by the solid was recovered in the gas by the end of the experiment. The reproducibility obtainable with this system is indicated by comparing these values with those obtained by repeating the experiment (first two rows of data below the dashed line of Table I).

The pre-equilibrium and quenching procedure used in carrying out the experiments was designed to maintain δ near zero. Since the solubility of deuterium in the tantalum lattice may be appreciably less than the solubility of hydrogen under similar conditions of temperature and pressure, some hydrogen transport across the phase boundary could take place; from the results already reported in Part I, δ might reasonably amount to 10% of $V^0_{H_2}$.

At the end of the first step of the repeat experiment, the sample was quenched to $-195°$ and the gas phase was removed with an automatic Toepler pump and measured. It was found that 3.5 cc. more gas was recovered than the initial amount of the pure deuterium introduced into the system. When this procedure was again repeated, it was observed that 0.2 cc. more gas was recovered than had been introduced at the start. Thus, in agreement with the results of Part I, it was found that the solubility of the mixture of isotopes decreases as the deuterium content increases. This, of course, is as expected from the difference in zero point energies of the gaseous molecules.

In Part I, an exact equation was derived taking into account both the isotope effect and the nonzero value of δ, *viz.*,

$$V^0_{H_2} = \frac{[V^0_{D_2} + \delta(1 - K')]x_\infty}{(1 - K'x_\infty)} \qquad (3)$$

Use was made of this equation and the values of δ and K' (Part I) to establish more accurate values of the hydrogen contents. The results of these calculations are listed in the bottom two rows of Table I. Comparison of these with all the other results (calculated with $\delta = 0$ and $K = 1$) indicates that these simplifying assumptions cause negligible error; all results agree within 3%.

TABLE I

EXHAUSTIVE DEUTERATION OF HYDROGENATED TANTALUM AT 600° AND 100 MM.

Equilibrium gas Compn., x_∞ atom fraction		Hydrogen held by solid,[a,b] cc. (NTP)			δ,[c] cc. (NTP)
Obsd.	Calcd.[d]	V_1	V_2	V_3	
0.287	...	29.4	..	..	..
.085	0.082	8.7	8.4	8.4	..
.042	.044	2.1	2.4	2.2	..
.027	.029	1.3	1.3	1.4	..
...	...	..	0.7	0.8	..
.286	...	29.4	..	..	..
.084	.083	8.5	8.4	8.5	..
.286	...	30.2	..	..	3.5
.084	.083	8.6	8.2	8.3	0.22

[a] Hydrogen and deuterium dissolve in tantalum as atoms. Nevertheless, it is convenient to evaluate the initial hydrogen contents as cc. (NTP) or moles of H_2 gas. [b] V_1 is the value experimentally determined for each step and V_2 and V_3 are corresponding values calculated from the results of the first step by alternative paths. V_2 is the amount of hydrogen left in the solid at equilibrium in the previous step and V_3 is the difference between the amount of hydrogen originally held by the solid and the total amount actually recovered in the gas. Except for the bottom two rows, isotope effects were ignored and δ was taken as zero. [c] Defined by: $V_g = V^0_{D_2} + \delta$ and $V_s = V^0_{H_2} - \delta$. [d] Values of x_∞ were calculated from hydrogen left in solid at the end of previous step and total gas in the system; all values are calculated from results of first step.

The remaining assumption, (b), was tested with the isothermal rate data shown in Fig. 1. In this experiment, the exchange reaction was carried to about half completion before it was stopped by quenching to the temperature of liquid nitrogen. The gas phase was then removed, a new sample of pure deuterium gas introduced and the experiment continued. When these results were compared with those from a similar experiment, it was found that in both instances a rate value of 1.77 cc. per minute was obtained for the first part of the experiment, R_1, and 1.40 and 1.36 cc. per minute for the latter part, R_2. Thus, R_1 was found to be about 20% higher than R_2. It is tempting to suppose that this relatively minor diminution in rate is the result of an isotope effect, *i.e.*, that the process becomes more sluggish as more and more deuterium enters the solid. That this is probably not the case, however, was established by exhaustively deuterating the sample and carrying out the exchange using pure hydrogen gas. The results from this experiment showed that the averaged value of R for the reverse experiment was identical with that obtained in the normal way. Thus, the small decrease is observed, probably because the hydrogen held within the tantalum lattice does not remain

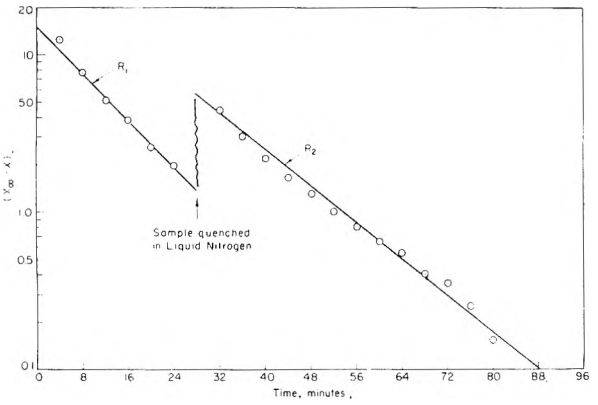

Fig. 1.—Effect of partial deuteration on the exchange kinetics of D_2 with Ta_xH.

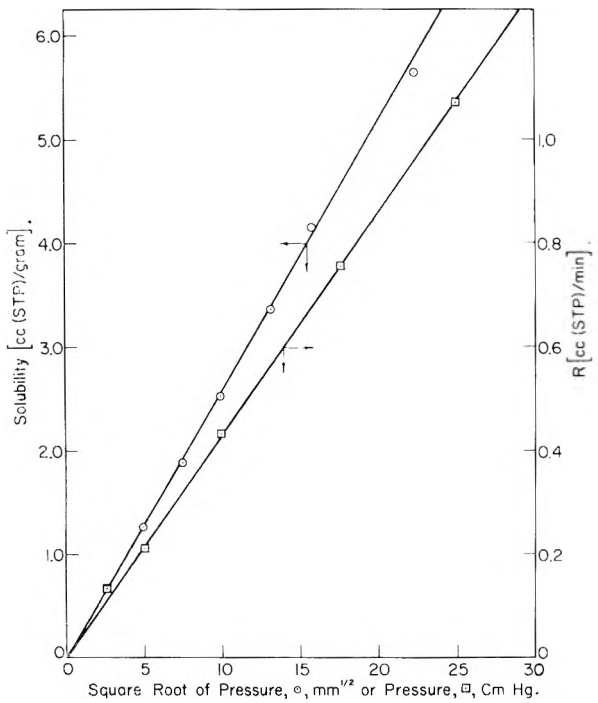

Fig. 2.—Dependence of the reaction rate and the solubility of hydrogen in tantalum on pressure at 610°.

quite uniformly distributed as the reaction proceeds.

The exchange reaction was studied over the pressure range 25–250 mm. The data obtained are plotted in Fig. 2 showing that R is directly proportional to pressure, while the solubility of hydrogen in tantalum varies as $P^{1/2}$, accurately obeying Sievert's law over the pressure range investigated. Due to insufficient accuracy, inconclusive results were obtained from experiments where attempts were made to obtain additional information about the mechanism by examining the initial distribution of isotopes in samples sent to an external mass spectrometer.

Discussion

The data from Part I and the present paper describe the changes in the equilibrium rate process with temperature and with pressure and provide certain auxiliary information. In considering possible interpretations of these data, it should be noted that the rate process characterized by R does not depend upon the presence of an isotope. Rather, the use of deuterium makes possible the evaluation of the magnitude of R.

The criteria which are available to characterize the reaction mechanism are listed as follows: (1) Only a single value of R is necessary to fit the experimental data with sufficient accuracy; thus, plots of $\log (x_\infty - x)$ *vs.* t are linear over the entire range of the independent variable; (2) R varies exponentially with the reciprocal of the absolute temperature; the determined activation energy was 14.9 kcal./mole; (3) R is directly proportional to pressure, *i.e.*, $R = k_f P_{H_2}$; (4) Sievert's law is obeyed, *i.e.*, $S = V^0_{H_2} = K_3 P^{1/2}_{H_2}$; (5) At 610° and 100 mm. pressure, 1.0×10^{16} molecules per second per cm.^{2} cross the boundary (10.9 cm.^{2}/g.) between the two phases. Under the same conditions, there are 1.8×10^{19} collisions per cm.^{2} per second, having an energy greater than the activation energy. Thus, there are about 1800 collisions with energy greater than the activation energy per penetration; (6) Finally, as noted in Part I, the absolute magnitude of R has been found to be somewhat sensitive to the history of the sample.

The over-all process of transport of gaseous hydrogen molecules into the interior of the tantalum lattice as atoms may be described by a series of steps including: adsorption or reaction on the surface, diffusion from the surface into the interior of the lattice, diffusion from the interior to the surface and desorption from the surface. Of these, the process involving the adsorption–desorption equilibrium corresponds to the so-called Bonhoeffer-Farkas mechanism of the hydrogen–deuterium exchange reaction. An alternate possibility, involving reaction of hydrogen molecules with adsorbed atoms (Rideal mechanism[2]), must also be considered.

The first-listed criterion eliminates diffusion through the lattice as a rate-controlling process as it is well known[3] that, in this instance, the distance from equilibrium would be proportional to a sum of a near infinite series of exponential functions of time. The same conclusion could be reached from a simple analysis which shows that the observed pressure dependence of R requires that a hydrogen molecule be involved in the rate-limiting process. If hydrogen gas is dissociatively adsorbed on the surface of the tantalum metal, as must certainly be the case, the fraction of the surface covered by hydrogen atoms, θ, will be a function of $P^{1/2}$. The rate of adsorption of hydrogen molecules will then be a function of $(1 - \theta)^2$ and the rate at which they are desorbed will be a function of θ^2. These relations simply reflect the fact that pairs of adjacent empty or covered sites are required for adsorption and desorption, respectively. If the adsorption–desorption process is followed by diffusion from the surface into the lattice, coupled with diffusion from the interior to the surface, the concentration of hydrogen atoms at the surface, θ, will determine the rate. Thus, were the diffusion process rate-determining, R would vary as P^n where $(0 < n < 1/2)$.

(2) B. M. W. Trapnell, "Catalysis III," Edited by P. H. Emmett, Reinhold Publ. Co., New York, N. Y., 1955, p. 14 *ff.*

(3) J. Crank, "The Mathematics of Diffusion," Clarendon Press, 1956, p. 84 *ff.*

The several possible situations which can lead to the observed pressure dependence are discussed below. Following Trapnell,[4a] we write for the adsorption step

$$R = \sigma Z(1 - \theta)^2 e^{-E_1/RT} \qquad (4)$$

and for the desorption step

$$R = K\theta^2 e^{-E_b/RT} \qquad (5)$$

The adsorption rate involves four factors, *viz.*, the rate at which molecules collide with the surface, Z; the fraction of the surface that is made up of pairs of adjacent vacant sites, $(1 - \theta)^2$; the fraction of the collisions having more than the required activation energy (given by the exponential function); and the condensation coefficient, σ. The last quantity represents the chance that adsorption will occur whenever a gas molecule possessing the necessary activation energy collides with the surface. The collision frequency, Z, is given by

$$Z = \frac{P}{\sqrt{2\pi mkT}} \qquad (6)$$

Equations 4 and 6 show that if θ is very much less than unity, the correct pressure dependence will be obtained; otherwise, a complex order will emerge. When the surface is sparsely populated, *i.e.*, θ is small, θ becomes proportional to $P^{1/2}$, so that, also in this region of coverage, the correct pressure dependence will be obtained for the desorption process, as shown by 5.

Numerically, it is found that the number of collisions having more than the required activation energy is 1.8×10^{19} molecules per cm.^{2} per second at 610° and 100 mm. Thus, for equation 4 to hold, a value of σ of the order of 10^{-3} is required. As shown by Trapnell,[4b] values of this parameter less than unity are usually not obtained unless the adsorbed atoms are immobile. In view of the demonstrated free mobility of the hydrogen atoms within the tantalum lattice, it is highly probable that they move freely over the surface. It seems much more likely that the factor of 10^{-3} corresponds to a steric factor, implying that only collisions with certain active regions of the total surface area should be counted in evaluating the number of molecules crossing the boundary per unit time per unit surface area. If most of the surface of the tantalum wire were covered by a stable oxide coat, reasonable agreement would be obtained.

The parameter K of (5) can be estimated by a number of methods and it is usually found[4b] to have a value $\sim 10^{28}$. As the exponential function of (5) has a value $\sim 10^{-8}$ (see later) a value of $\theta \sim 10^{-2}$ will provide quantitative agreement with the observed rate if the geometric surface is considered. If, on the other hand, the "effective surface" is smaller by a factor of about 10^3, then a value of $\theta \sim 10^{-1}$ would be required. Either result is acceptable within the limits of uncertainty.

In interpretating equations 4 and 5, it was assumed that Langmuir's adsorption isotherm is obeyed in our experiments and, hence, that the heat of adsorption is independent of coverage. The limiting forms of a number of other adsorption isotherms (at small θ) lead to the same conclusions when inserted in (4) and (5). Most of these can be derived from the treatment given in ref. 4; these include mobile layers with lateral interaction (heat of adsorption decreasing with coverage), cases where rates of adsorption and desorption are exponentially dependent on θ, as well as those situations in which the adsorption takes place on a heterogeneous surface and the process is described by a Freundlich isotherm. The equation derived and experimentally shown by Schuit and de Boer[5] to describe the adsorption of H_2 on Ni between −80° and 400° also yields the same result.

The remaining possible rate-determining process differs from the one discussed above, in that it is supposed that a hydrogen molecule reacts with a chemisorbed atom. In this case, it follows that

$$R = \sigma' Z\theta e^{-E/RT} \qquad (7)$$

where σ' now becomes a steric factor. As shown by (6), Z contains pressure as a factor; therefore, the only way in which the observed pressure dependence could be obtained is for θ to be independent of pressure, *i.e.*, for the surface to be extensively covered. Quantitatively, comparison of (7) with (4) shows that the calculated rate is too high, a steric factor of 10^{-3} being required to provide agreement. Here again, only a very small fraction of the total surface area may be available for the chemisorption of hydrogen.

The principal distinguishing feature between these two possible mechanisms is that the one requires that the available surface be sparsely populated while the other requires that it be extensively covered. The evidence concerning which of these two situations is operative will now be examined. The samples of tantalum hydride studied were relatively dilute alloys, running from about 2 to 8 atom % hydrogen. As already indicated, surface coverages corresponding to this concentration level (or lower) will provide satisfactory quantitative agreement with the Bonhoeffer–Farkas-type mechanism. For the Rideal-type mechanism, on the other hand, a substantial enrichment of the surface over the bulk composition would be required to raise θ to near unity. The only way in which a surface enrichment could come about would be if the heat of adsorption of hydrogen (on a surface near unit coverage) were greater than the heat of solution (8.0 kcal./g. atom). Although the initial heats of adsorption on evaporated tantalum films are known to be quite high (~45 kcal./mole of H_2 or 22.5 kcal./g. atom),[4c] it does not seem likely on the relatively dirty surface used in our experiments and at the equilibrium coverages, that the two heats would differ sufficiently to cause much surface enrichment. Support for this contention is found in the work of Kofstad, Wallace and Hyvönen,[6] who have shown that the heat of vaporization of hydrogen from tantalum hydride increases from about 5 to nearly 10 kcal./g. atom of hydrogen as the atomic composition is increased from very low values to the neighborhood of 1 atom %; it then remains fairly constant as the

(4) B. M. W. Trapnell, "Chemisorption," Academic Press, Inc., New York, N. Y., 1955, (a) p. 49 *f.*, (b) p. 86 *ff.*, and (c) p. 149.

(5) G. C. A. Schuit and N. H. de Boer, *Recueil*, **72**, 909 (1953).

(6) P. Kofstad, W. E. Wallace and L. J. Hyvönen, *J. Am. Chem. Soc.*, **81**, 5015 (1959).

hydrogen content of the alloy is increased. Were hydrogen concentrating at the surface, the opposite effect would be expected at high dilution, *i.e.*, that the heat vaporization would fall as the amount of hydrogen in the sample is increased. A similar conclusion can be arrived at from our experimental data in the following way. Figure 2 shows that the total hydrogen being exchanged obeys Sievert's law over the range studied. Sievert's law itself holds for a gas dissolved in a metal under conditions of ideal behavior. If the process of dissolving gaseous hydrogen in the tantalum metal is described by the two steps of adsorption–desorption and surface-bulk equilibrium, it seems only reasonable to expect ideal behavior to be followed in both of these. For the step involving adsorption with dissociation, ideal behavior may be represented by a Langmuir isotherm

$$K_1 = \theta/(1 - \theta)P^{1/2} \qquad (8)$$

The surface–bulk equilibrium may be described by

$$K_2 = S/\theta \qquad (9)$$

and Sievert's law for the over-all process as shown 2 requires that

$$K_3 = S/P^{1/2} \qquad (10)$$

However, $K_1K_2 = K_3$, and inspection shows that the only way that this can come about is if $\theta << 1$, indicating that the surface is sparsely covered. Thus, since all of the available evidence points toward the sparsely covered surface, it is concluded that, in all probability, the rate-determining process involves the microscopically reversible act of adsorption with dissociation and desorption with recombination.

The data of Fig. 2 show that

$$R = k_f P_{H_2} \qquad (11)$$

Since the pressure was held constant as the temperature was varied, it is clear that

$$\frac{E_f}{\Re} = \frac{d(\ln k_f)}{d(1/T)} = \left(\frac{\partial \ln R}{\partial (1/T)}\right)_P \qquad (12)$$

where $\Re$ represents the gas constant. If now, (11) is identified with (4), *i.e.*, if it is taken as the rate of the forward reaction, it can be seen that E_f corresponds to the activation energy for the adsorption process. For desorption, therefore, it would be necessary to write

$$R = k_b\theta^2 = k_b K_1^2 P_{H_2} \qquad (13)$$

corresponding to (5). From (11), (12) and (13) it is at once obvious that

$$E_0 = E_f = (E_b - 2\lambda) = 14.9 \text{ kcal./mole} \qquad (14)$$

where λ is the heat of adsorption and corresponds to the temperature coefficient of K_1. Thus, if the activation energy for adsorption is 14.9 kcal./mole and if it is supposed that the heat of adsorption is of the same order of magnitude as the heat of solution (16 kcal./mole), *i.e.*, that K_2 is not a strong function of temperature, then it follows that the activation energy for the backward step is approximately 31 kcal./mole, providing the estimate used in calculating the theoretical desorption rate.

Acknowledgment.—This work was sponsored by the Gulf Research & Development Company as a part of the research program of the Multiple Fellowship on Petroleum.

HEAT CAPACITY AND THERMODYNAMIC PROPERTIES OF TITANIUM TETRAFLUORIDE FROM 6 TO 304°K.[1]

BY ROBERT D. EULER AND EDGAR F. WESTRUM, JR.

Department of Chemistry, University of Michigan, Ann Arbor, Michigan

Received July 18, 1960

The low temperature heat capacity of titanium tetrafluoride has been determined by adiabatic calorimetry and found to be without thermal anomalies. The thermodynamic properties have been computed by numerical quadrature from these data. The values of the thermodynamic functions at 298.15°K. are: C_p = 27.31 cal./(deg. mole), S^0 = 32.02 cal./(deg. mole), $H^0 - H_0^0$ = 4841 cal./mole, and $(F^0 - H_0^0)/T$ = −15.78 cal./(deg. mole). Comparison of the heat capacity of TiF_4 with other tetrafluorides supports the view that its crystal structure is intermediate between the molecular carbon tetrafluoride type and the coördinative zirconium tetrafluoride type.

Introduction

From the endeavor to improve the resolution of the lattice and magnetic contributions to the heat capacity of UF_4[2,3] interest developed in the heat capacity of the Group IV tetrafluorides. Because TiF_4 is the only member of this family that apparently is not isostructural, it was considered desirable to study its low temperature heat capacity.

(1) Submitted in partial fulfillment of the requirements for the Doctor of Philosophy degree in chemistry at the University of Michigan.

(2) H. R. Lohr, D. W. Osborne and E. F. Westrum, Jr., *J. Am. Chem. Soc.*, **76**, 3837 (1954).

(3) D. W. Osborne, E. F. Westrum, Jr., and H. R. Lohr, *ibid.*, **77**, 2737 (1955); J. H. Burns, D. W. Osborne and E. F. Westrum, Jr., *J. Chem. Phys.*, **28**, 387 (1960).

Experimental

Preparation and Purity of the TiF_4 Sample.—The titanium tetrafluoride sample was obtained from the General Chemical Division of Allied Chemical and Dye Corporation. It was prepared by reaction of elemental fluorine on pure titanium dioxide and purified further by sublimation in nickel reactors. Analysis for fluorine by the method of Saylor and Larkin[4] (utilizing titration of aqueous fluoride ion with $AlCl_3$ solution and Eriochromcyanine R as an internal indicator), together with determination of titanium by dissolution in concentrated sulfuric acid, followed by subsequent precipitation and ignition, indicated that the material assayed approximately 99.9% TiF_4. Because the sample was very hygroscopic and finely divided it was handled and loaded entirely within a nitrogen-filled dry box. The sublimate (52.494 grams (*in vacuo*)) was sealed into the calorimeter. Correc-

(4) J. H. Saylor and M. E. Larkin, *Anal. Chem.*, **20**, 194 (1948).

tions for buoyancy were made on a density of 2.798 for TiF_4.

Calorimetric Technique.—The Mark I liquid helium cryostat and circuits employed in these measurements were quite similar to those described by Westrum, Hatcher and Osborne.[5] Temperatures were measured with a platinum resistance thermometer (laboratory designation A-3) calibrated by the National Bureau of Standards above 10°K., and against a provisional scale at lower temperatures. Accuracy of the adiabatic calorimetric technique was tested with a Calorimetry Conference sample of benzoic acid.[6] The copper calorimeter (laboratory designation W-5) was gold-plated on the exterior surface and had an internal volume of approximately 90 cc. Eight radial vanes of thin copper foil aided rapid achievement of thermal equilibrium. Helium gas (3 cm. pressure) was added to the sample space to facilitate thermal conduction. Lubriseal N stopcock grease was used to establish thermal contact between the calorimeter, thermometer and heater, as well as with the differential thermocouple for adiabatic shield control. The heat capacity of the empty calorimeter assembly with identical amounts of Lubriseal and solder was determined in a separate series of determinations and represented about 20% of the total heat capacity at 10°K., gradually increased, and averaged about 44% above 40°K.

Results

Heat Capacity Data.—Experimental determinations of the heat capacity are presented in chronological order in Table I. The approximate temperature increment of each measurement can usually be inferred from the adjacent mean temperature values. Heat capacities are reported on a basis of a mole weight equal to 123.90 g., the defined thermochemical calorie equal to 4.1840 absolute joules, and an ice point of 273.15°K. Corrections have been applied to the heat capacity values for curvature (*i.e.*, for the finite temperature increments employed in the measurements). While the finely divided sample, essentially a white powder, does not represent the most desirable thermodynamic reference state, the heat capacity data are considered to have a probable error of about 5% at 6°K. decreasing to 1% at 10°K. and decreasing further to 0.1% above 30°K. Thermodynamic functions, S^0 and $H^0 - H_0^0$, were computed by numerical quadrature of the heat capacity *vs.* log T and T, respectively; but all values were obtained from a single large scale plot. These functions, the derived free energy function, and values of the molal heat capacity read from the smooth curve through the experimental points are shown at selected temperatures in Table II. The thermodynamic functions are considered to have a probable error of less than 0.1% at temperatures above 100°K. Extrapolation below 6°K. was done by means of the Debye T^3 law. S_0^0 is assumed to be zero. No contribution from isotope mixing or from nuclear spin has been included in the entropy and free energy functions. Hence, these values are practical entropies suitable for use in chemical calculations. In order to make Table II internally consistent and to permit interpolation, one more digit is given in some of the thermodynamic functions than is justified by the experimental accuracy.

A calculation of the entropy of TiF_4 has been reported[7] on the basis of vapor pressure measurements on TiF_4, an estimated ΔC_p of vaporization, and a calculated entropy of gaseous TiF_4 using an estimated Ti–F distance. The resulting value, 31.3 ± 0.40 e.u., agrees as well as can be expected with the present determination although it is definitely outside the assigned precision indices of both measurements.

TABLE I

HEAT CAPACITY OF TITANIUM TETRAFLUORIDE

[TiF_4, mol. weight = 123.90 g.; in cal./(deg. mole)]

T, °K.	C_p	T, °K.	C_p	T, °K.	C_p
Series I		233.81	24.12	20.52	1.500
59.43	7.364	243.02	24.64	22.80	1.805
64.57	8.157	252.21	25.06	25.01	2.106
70.02	8.951	261.69	25.56	27.60	2.467
76.58	9.905	271.80	26.06	30.53	2.897
84.02	10.97	282.34	26.59	33.59	3.361
91.68	12.02	292.74	27.06	36.93	3.877
99.40	12.95	301.54	27.56	40.63	4.442
107.44	13.91			44.75	5.075
116.12	14.91	Series II		49.43	5.810
125.04	15.90	6.32	0.075	54.70	6.629
133.96	16.80	7.06	.106	60.38	7.505
142.87	17.64	7.68	.120		
151.90	18.43	8.35	.189	Series III	
161.26	19.24	9.26	.266		
170.85	20.01	10.21	.348	246.39	24.75
180.15	20.71	11.35	.461	255.26	25.23
189.34	21.35	12.68	.583	264.83	25.74
198.31	21.97	13.94	.713	274.54	26.14
207.09	22.53	15.28	.866	284.09	26.67
215.89	23.07	16.76	1.037	292.34	27.05
224.78	23.62	18.42	1.239	300.45	27.42

Free Energy of Formation.—Utilizing the enthalpy of formation of TiF_4 reported by Gross, Hayman and Levi[8] of −392.5 ± 0.3 kcal./mole at 298.15°K. and entropies of the elements[9] yield a free energy of formation for TiF_4 of −360.3 kcal./mole at 298.15° K.

Discussion

Since low temperature thermal data are available for three other tetrafluorides of the Group IV elements, it is interesting to compare the heat capacity of TiF_4 with those of ZrF_4,[10] ThF_4[2] and UF_4.[3] The result of this comparison may be seen readily in Fig. 1 which shows the experimental values of the heat capacity of TiF_4 and those of the three other substances. As might be expected, the heat capacities of isostructural ZrF_4, ThF_4 and UF_4 increase with increasing molecular weight. If TiF_4 were to follow this pattern, it should have a heat capacity lower than any of them. Instead, TiF_4 has a higher value than does ZrF_4 over the entire range. Indeed, from 10 to 30°K. TiF_4 has the highest heat capacity of the four.

A comparison of the known physical properties of the various tetrafluorides illustrates the intermediate behavior of TiF_4. Tetrafluorides of lower molecular weight than TiF_4 (such as CF_4 and SiF_4) have a cubic structure, tend to be plastic crystals

(5) E. F. Westrum, Jr., J. B. Hatcher and D. W. Osborne, *J. Chem. Phys.*, **21**, 419 (1953).

(6) G. T. Furukawa, R. E. McCoskey and G. J. King, *J. Research Natl. Bur. Standards*, **47**, 256 (1951).

(7) E. H. Hall, J. M. Blocher, Jr., and I. E. Campbell, *J. Electrochem. Soc.*, **105**, 275 (1958).

(8) P. Gross, C. Haymann and D. L. Levi, Transactions XVIIth International Congress of Pure and Applied Chemistry, Munich, September, 1959, p. 90.

(9) "Selected Values of Chemical Thermodynamic Properties," Circular 500, National Bureau of Standards, Washington, D. C., 1952.

(10) E. F. Westrum, Jr., and D. H. Terwilliger, unpublished data.

TABLE II

THERMODYNAMIC FUNCTIONS OF TITANIUM TETRAFLUORIDE
(TiF_4, mol. weight = 123.90 g.)

T, °K.	C_p, cal./(deg. mole)	S^0, cal./(deg. mole)	$H^0 - H_0^0$, cal./mole	$-(F^0 - H_0^0)/T$, cal./(deg. mole)
10	0.329	0.110	0.82	0.028
15	0.834	.335	3.68	.090
20	1.440	.656	9.33	.189
25	2.104	1.048	18.16	.321
30	2.819	1.494	30.44	.479
35	3.580	1.985	46.43	.658
40	4.345	2.513	66.24	.857
45	5.116	3.069	89.89	1.071
50	5.898	3.649	117.43	1.300
60	7.453	4.862	184.20	1.792
70	8.968	6.126	266.39	2.320
80	10.41	7.418	363.30	2.877
90	11.78	8.725	474.36	3.454
100	13.03	10.031	598.5	4.046
110	14.21	11.328	734.7	4.649
120	15.35	12.614	882.5	5.260
130	16.41	13.885	1041.3	5.875
140	17.37	15.137	1210.3	6.492
150	18.28	16.366	1388.6	7.109
160	19.14	17.574	1575.7	7.726
170	19.95	18.757	1771.1	8.341
180	20.70	19.921	1974.4	8.952
190	21.40	21.058	2184.9	9.558
200	22.08	22.173	2402.3	10.161
210	22.72	23.266	2626.3	10.760
220	23.32	24.337	2856.5	11.353
230	23.90	25.388	3092.7	11.942
240	24.44	26.416	3334.4	12.523
250	24.96	27.424	3581.5	13.098
260	25.47	28.413	3833.6	13.668
270	25.97	29.384	4090.9	14.233
280	26.47	30.337	4353.1	14.790
290	26.94	31.274	4620.1	15.343
300	27.39	32.195	4891.4	15.889
273.15	26.13	29.69	4173.	14.41
298.15	27.31	32.02	4841.	15.78

with low heats of fusion, and tend to melt at very low temperatures, whereas those of higher molecular weight, including the monoclinic group IV tetrafluorides, tend to melt at very high temperatures. With respect to the other titanium tetrahalides, TiF_4 occupies a relatively unique position. The density of the solid TiF_4 and the persistence of the solid state and of the liquid state as well are out of line with the trend for the rest of the series.

Crystal structure determinations[11] show SiF_4, $TiBr_4$ and TiI_4 to be cubic and tetrahedrally symmetrical with molecular type structures. ZrF_4, ThF_4 and UF_4, as well as HfF_4 and CeF_4, are isostructural[12] and have a monoclinic holohedral lattice in which the metal atom has a coördination number of 12. Presumably then, TiF_4 will exhibit some structure intermediate between the molecular type lattice of SiF_4 and the coördinative type characteristic of ZrF_4. Hückel[13] suggests the existence of a chain type structure in which TiF_6 octahedra are joined to each other along an edge, giving the titanium a coördination number of six except at a chain terminus. This value lies between four for Si in SiF_4 and twelve for Zr in the monoclinic structure and would be consistent with the intermediate density value. Four of the six fluorine atoms in each octahedron would be held jointly by two titanium atoms and two by one titanium atom. This would lead to two different TiF crystalline distances and resulting distorted octahedra. This hypothesis would explain the relatively high density and the moderately high boiling point characteristic of TiF_4. The fact that the heat capacity of TiF_4 exhibits a temperature dependence somewhat less than T^3 below 30°K. would also be consistent with the hypothesis of a chain type structure.[14]

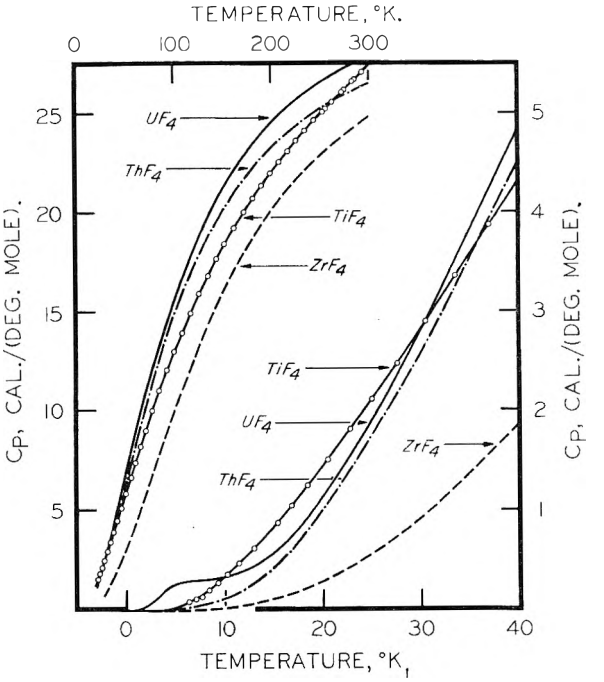

Fig. 1.—Heat capacities of Group IV tetrafluorides.

Acknowledgment.—The authors thank Mrs. Emilia Martin for her assistance with the calculations, and the Division of Research of the United States Atomic Energy Commission for partial financial support.

(11) R. W. G. Wyckoff, "Crystal Structures," Vol. I, Interscience Publishers, Inc., New York, N. Y., 1951.

(12) W. H. Zachariasen, *Acta Cryst.*, **2**, 288 (1949).

(13) W. Hückel, "Structural Chemistry of Inorganic Compounds," Vol. II, Elsevier Publishing Co., Amsterdam, 1951, p. 470.

(14) V. V. Tarassov, *Zhur. Fiz. Khim.*, **24**, 111 (1950).

STUDIES ON THE ELECTROCHEMISTRY OF CARBON AND CHEMICALLY-MODIFIED CARBON SURFACES

BY BILL B. ARNOLD AND GEORGE W. MURPHY

Department of Chemistry, University of Oklahoma, Norman, Oklahoma

Received July 19, 1960

Some factors which influence the behavior of carbon electrodes in contact with aqueous sodium chloride solutions are analyzed. A concentration cell method for identifying finely divided carbon electrodes as cation- and anion-responsive types has been developed. Commercial graphites investigated have been found to be cation-responsive; however, anion-responsive electrodes have been prepared by the adsorption on graphite of certain organic compounds. Possible half-cell reactions are discussed for both electrode types and the electrochemical capacities of some electrodes are reported.

The potentials of carbon electrodes in aqueous solution are determined by the nature of the chemical groups forming the partly-oxidized surface, by impurities, and by electrochemically-active additives. As part of the development of an electrochemical water demineralization process,[1] a systematic study of carbon electrode behavior has been undertaken.

It is convenient to classify electrodes in accordance with their ion responsiveness, that is, their reversibility to one general ion type, cation or anion, whether complete or not. Thus in sodium chloride solution the half cell reaction of a cation-responsive electrode is

$$C + Na^+ + e = C^-Na^+$$

and for an anion responsive electrode

$$A + Cl^- = A^+Cl^- + e^-$$

The solid non-consumable electrode material C can, in the reduced state, form a bond (usually ionic) with the cation. Similarly, the non-consumable anion-responsive electrode A can form a bond with the anion in the oxidized state. It will be noted that reduced C and oxidized A are ion-exchangers; if carbon-based they are also electronic conductors, an interesting and useful combination of properties. Coupling electrodes A and C in a suitable cell leads, with the passage of current at appropriate applied potential, to the removal of salt from solution, a practical application of the classical "cell with transference."

Implementation of the classification scheme calls for a rapid experimental means of electrode characterization. With reversible electrodes of established properties, a concentration cell method has been employed to establish selectivity coefficients (as transference numbers) of ion-permeable membranes. The basic theory of this method was developed by Teorell[2] and Meyer and Sievers[3] and applications have been made by several later workers.[4,5]

In the present work the method has been inverted to establish electrode responsiveness with the aid of membranes having known properties.

The concentration potentials at 25° expected from cells with various perfect cation- and anion-responsive electrode and perfectly-selective cation- and anion-permeable membrane (M) configurations in 1-1 electrolyte solutions of activities a_1 and a_2 are listed in Table I.

TABLE I

Anion-permeable membrane	Concn. potential
$C/a_1/M/a_2/C$	$0.1183 \log (a_1/a_2)$
$A/a_1/M/a_2/A$	0
Cation-permeable membrane	
$A/a_1/M/a_2/A$	$0.1183 \log (a_2/a_1)$
$C/a_1/M/a_2/C$	0

Electrodes with imperfect ion-responsivity would yield intermediate potentials between these extremes. The selectivity of available commercial membranes is almost perfect under experimental conditions to be described.

Great strides have been made in recent years in the interpretation of the chemical, electrochemical and adsorptive properties of carbons in terms of functional groups on the surface.[6-10] Although other groups may be present or even dominant on carbons arising from different sources and prepared in different ways, the quinone–hydroquinone theory of Garten and Weiss[6] is sufficient for our purposes. The cation-responsive character of "as received" graphites described later will be assumed to arise through the half cell reaction

$$\rangle C{=}O + Na^+ + e = \rangle CO^-Na^+$$

where C represents an edge carbon atom in the graphite lattice. The electrode capacity would thus be determined by the numbers of carbonyl and phenolic groups, that is, by the extent of surface oxidation. It has been found that chemical oxidation of graphite does increase its cation capacity.[1]

Anion-responsive electrodes can be prepared by adsorbing on graphite organic molecules which undergo oxidation–reduction reactions with participation of anions. Consider the assumed oxidation–reduction reaction of prototype molecule A

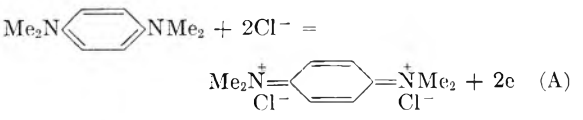

(A)

(1) J. W. Blair and G. W. Murphy, 1960 Symposium on Saline Water Conversion, American Chemical Society Advances in Chemistry Series, in press.

(2) T. Teorell, *Proc. Soc. Exp. Biol. Med.*, **33**, 282 (1935).

(3) K. H. Meyer and J. F. Sievers, *Helv. Chim. Acta*, **19**, 649, 665, 987 (1936).

(4) H. P. Gregor and K. Sollner, THIS JOURNAL, **50**, 53, 88 (1946).

(5) W. Juda, N. W. Rosenberg, J. A. Marinsky and A. A. Kaspar, *J. Am. Chem. Soc.*, **74**, 3736 (1952).

(6) V. A. Garten and D. E. Weiss, *Asutralian J. Chem.*, **8**, 68 (1955).

(7) V. A. Garten and D. E. Weiss, *ibid.*, **10**, 295, 309 (1957).

(8) V. A. Garten and D. E. Weiss, *Revs. Pure and Appl. Chem. (Australia)*, **7**, 70 (1957).

(9) J. V. Hallum and H. V. Drushel, THIS JOURNAL, **26**, 110, 1502 (1958).

(10) M. L. Studebaker, *Rubber Chem. Technol.*, **30**, 1401 (1957).

Upon oxidation the molecule would acquire a double positive charge and take up two anions; however, there is evidence that prototype A molecules may undergo step-wise oxidation involving semiquinone formation.[11] On the other hand, a typical triphenylmethane dye (prototype B) might undergo the reaction

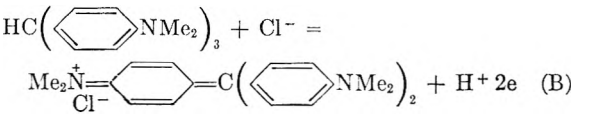

taking up an anion, but giving up a cation in the process. (A partly oxidized semiquinone product molecule should also be considered). Prototype A should yield an electrode responsive to the anion, while B should yield one responsive to both ions. It has been found that two prototype A molecules tetramethylphenylenediamine (TMPD) and tetramethylbenzidine (TMB) are indeed anion-responsive, while the dye neocyanine is responsive to both ions in accordance with prediction for prototype B molecules.

Experimental

Electrodes.—The electrodes were prepared by depositing aqueous dispersions of colloidal graphite on 1/16 inch thick Dacron felt backing material obtained from Troy Blanket Mills, New York, N. Y. The electrode was then dried at 100° for two to four hours to break the dispersion. Aquadag, a predispersed graphite manufactured by Acheson Colloids Corporation, Port Huron, Michigan, was employed as received; the identity of the dispersing agent is not available. The other dispersions were made in the laboratory from Dixon's (Joseph Dixon Crucible Co., Jersey City, N. J.) Air-Spun Graphite Type 200–10, with the aid of Mallinckrodt's analytical reagent tannic acid, Monsanto's Lustrex m-710 polystyrenesulfonic acid (PSA), and Badische Anilin and Soda Fabrik AG (Ludwigshafen, Germany) poly-N-vinylimidazol (PVI) which was quaternized in the laboratory.[1] Details of the preparation of graphite dispersions and of the silver–silver chloride, Aquadag, mixed-acid-treated graphite, oleum-treated graphite, PSA, and PVI electrodes used in the experiments reported below are given elsewhere.[1]

The neocyanine electrode was made by soaking an Aquadag electrode in a saturated solution of neocyanine (Eastman) in water and drying at 100°. The amount of neocyanine adsorbed on the electrode was not determined.

The TMPD electrode was prepared by soaking an electrode made from Dixon's Air Spun Graphite Type 200–10 dispersed with PVI in 20 ml. of a 1.1% aqueous solution of tetramethylphenylenediamine dihydrochloride. The electrode was then dried in the oven for four hours, soaked in a solution of 4 *N* NH_4OH for conversion to the insoluble amine form, dried in the oven again, washed with distilled water and dried again.

Tetramethylbenzidine (Eastman) was adsorbed on another electrode in similar fashion, starting with the dihydrochloride.

Concentration Cell.—Two difficulties were encountered in the early development of the concentration cell method. Some erratic and unpredictable potentials were attributed to the absence of a definite electrode reaction involving the ions in the solution. In many cases preconditioning of electrodes by electrolysis, first in one direction, then the other, stabilized the potentials.

The second difficulty was a slow but steady drift in potential. The two initially identical electrodes take on a bias potential when put in solutions of different concentration, apparently due to a slow oxidation–reduction reaction. This bias is exhibited when solution of the same concentration is directed into both electrode chambers, and can be removed by shorting the electrodes under the latter condition.

The concentration cell reported here is a refined version which enables the experimenter to overcome the aforementioned difficulties with ease. This cell, designated as CC-2, is illustrated in Fig. 1. The cell has four electrode positions, two on each side of the membrane so that electrical preconditioning and concentration potential measurements can be carried out in the same cell. Electrical contact is made by platinum wires in the four long tubes labeled A, A′, B and B′. The wires were sealed into the tubes with Epibond resin No. 122, (Furan Plastics, Inc., Los Angeles, California). The solutions enter the cell through the four tubes labeled C and must pass through the porous electrodes to leave through the two tubes marked D. The position of the membrane is indicated by M.

Membranes used were Nalfilm 1 (cation-permeable) and Nalfilm 2 (anion-permeable), manufactured by National Aluminate Co., Chicago. At the NaCl concentrations employed, manufacturer's specifications indicate minimum permselectivities of 95 and 96% respectively.

In all experiments three small electrodes $1/2'' \times 1/2''$ cut from a larger electrode patch were placed in each of the four positions; the cell was then assembled with the appropriate type of membrane separating the two halves of the cell. The flow of the sodium chloride solutions, the electrolyte used in all experiments, was controlled by a manifold of glass needle valves. During an experiment, steady solution flows were maintained. In all experiments the solutions were 0.01 and 0.1 *N* NaCl.

The electrical conditionings were all carried out with 0.1 *N* NaCl flowing on both sides of the membrane. The conditioning potentials varied between 0.4 and 0.6 volt from experiment to experiment but were held constant for any given experiment. The polarity was reversed every 30 minutes by a time switch. The contacts A and A′ were of one polarity and B and B′ of the opposite. The electrode pair which was negative after the last polarity reversal will be referred to as the reduced electrodes and the pair which was positive as the oxidized electrodes.

After conditioning, one of the electrode pairs (either oxidized or reduced) was shorted together with 0.1 *N* NaCl solution on both sides of the membrane until zero potential was obtained upon opening the circuit. The 0.01 *N* NaCl solution was then introduced on one side of the membrane and the potential which developed was measured on a Sargent recording potentiometer Cat. No. S-72150.

Demineralization Experiments.—The demineralization experiments were carried out in a small Lucite cell (DC-1) which held two parallel electrodes (1.7 by 1.1 inches) with a separation of 1/8 inch. Details of DC-1 and the experimental procedure are given elsewhere.[1] The electrode being tested was placed in DC-1 with a counter electrode of the opposite type of ion responsiveness. A potential of 0.45 volt was applied first in one direction for demineralization and 0.80 volt (reversed polarity) for regeneration. In all experiments 0.03 *N* NaCl solution was pumped through the cell at flow rates which varied between 5 and 7 ml. per hour from cycle to cycle but were held constant for any given cycle. The variation of the effluent solution concentration with time was recorded, and from a plot of concentration *vs.* volume (assuming a constant flow rate) the demineralization capacity (number of equivalents of salt removed by the electrodes) was determined by graphical integration.

Results

The effect of the potential drifts mentioned previously are illustrated in Fig. 2, which is a plot of concentration cell potentials *vs.* time for a typical experiment with two Aquadag (cation responsive) electrodes separated by an anion selective membrane. The cell had been left with 0.01 *N* NaCl solution in one compartment and 0.1 *N* NaCl solution in the other for some time before measurements were begun. Because of the bias potential introduced by the electrodes being in solution of different concentrations, the potential is lower than theoretical in Step 1 and continues to decrease with time. The bias of 39 mv. with opposite polarity is exhibited in Step 2 with 0.1 *N* NaCl solution directed on both sides of the membrane. This bias is approximately equal to the difference between the poten-

(11) L. Michaelis and M. P. Schubert, *Chem. Revs.*, **22**, 437 (1938).

tial obtained in Step 1 and the theoretical value. The bias was removed in Step 3 by shorting the electrodes together as verified by the zero potential found in Step 4 upon opening the circuit. In Step 5 the 0.01 *N* NaCl solution was reintroduced on one side of the membrane; it will be observed that the nearly theoretical potential of 104 mv. is obtained before the bias develops.

The results of a number of concentration cell experiments are shown in Table II. The potentials represent averages between the values obtained for the oxidized and reduced pair, since these values varied by one or two mv. at most. Experiments 1 and 2 were controls to establish the behavior of the concentration cell with electrodes of known ion-responsiveness (anion). The results are in agreement with the theoretical prediction if the differences between activities and concentrations and small membrane imperfections are taken into account.

TABLE II

CONCENTRATION POTENTIALS FOR THE CELL

Experiment no.	Electrode tested	Selectivity of membrane	Potential, mv.
1	Ag–AgCl	Cation	102
2	Ag–AgCl	Anion	Zero
3	Aquadag	Anion	104
4	Mixed-acid-treated	Anion	105
5	Oleum-treated	Anion	108
6	Neocyanine	Cation	50
7	PSA	Anion	96
8	PVI	Cation	88
9	PVI	Anion	10
10	TMPD	Cation	102
11	TMB	Cation	100

Experiments 3, 4 and 5 show that Aquadag, mixed acid-treated, and oleum-treated electrodes yield very close to theoretical potentials for cation responsive electrodes. Experiment 6 indicates that the neocyanine-treated graphite is about equally cation- and anion-responsive, thus confirming Prototype B oxidation–reduction behavior. Experiments 7, 8 and 9 were designed to investigate the effect of dispersants on ion-responsiveness. Evidently PSA-dispersed graphites retain cation-responsiveness, while PVI as a dispersant imparts anion-responsiveness which is not quite complete. Experiment 10 and 11 shows that TMPD and TMB adsorbed on a PVI-dispersed electrodes are for practical purposes anion-responsive.

In Fig. 3 are shown four demineralization and three regeneration cycles for TMPD *vs.* mixed-acid electrodes. It will be noted that the demineralization capacity increases significantly for each of the first three cycles, but did not change for the fourth. The apparently larger capacity observed during regeneration is known to be due to a slow anodic release of hydrogen ions from the mixed-acid-treated electrode. The demineralization experiments clearly confirm the anion-responsive nature of TMPD electrodes.

The demineralization cell capacities of three electrodes are given in Table III. The oleum-treated electrode was tested *vs.* a silver–silver chloride electrode and the TMPD and TMB electrodes

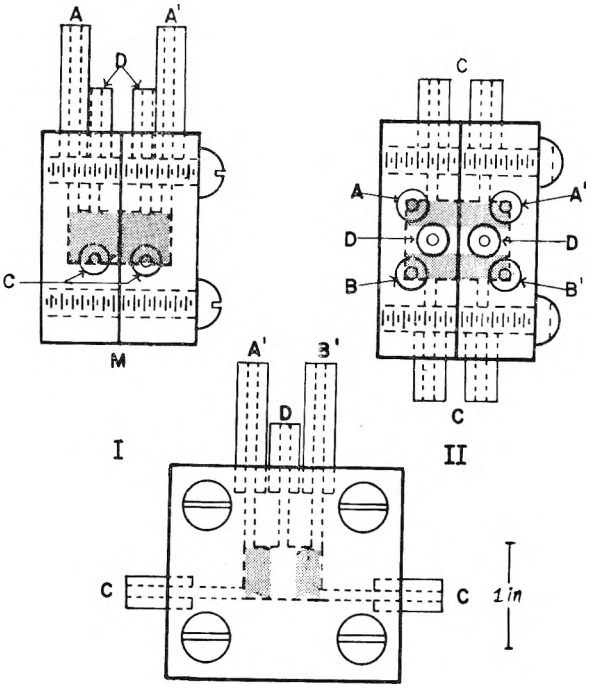

Fig. 1.—Concentration Cell CC-2, I side view, II top view, III front view; (A, B, A′, B′) electrical contact tubes, (C) solution entry tubes, (D) solution exit tubes, (M) membrane; shaded area, electrode positions.

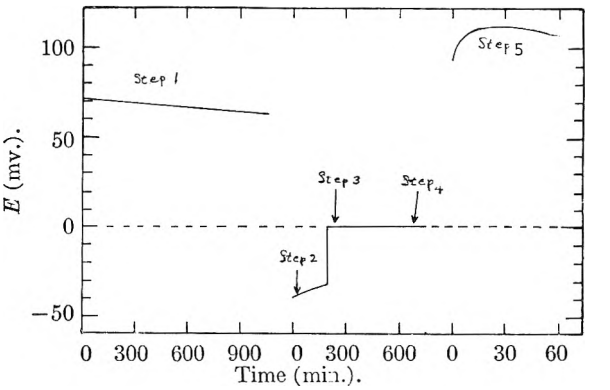

Fig. 2.—Concentration potentials for cell; cation electrode/0.1 *N* NaCl/anion membrane/0.01 *N* NaCl/cation electrode, illustrating potential drifts and biases.

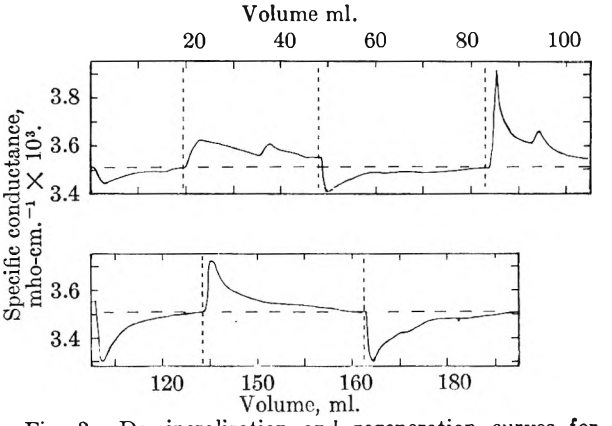

Fig. 3.—Demineralization and regeneration curves for TMPD *vs.* mixed-acid-treated electrodes. Horizontal dashed line represents conductance of feed solution.

TABLE III

DEMINERALIZATION CELL CAPACITIES

Electrode tested	Cap. in equiv. per sq. in. × 10^5
Oleum-treated	1.8
TMPD	0.79
TMB	0.37

were tested *vs.* a mixed-acid-treated electrode. Both of these counter electrodes have capacities which are known[1] to be greater than those reported in the table. The capacity of the oleum-treated electrode has the same order of magnitude as the mixed-acid-treated electrode, while the capacities of the TMPD and TMB electrodes compare with that of Aquadag.

The above experiments establish the concentration cell method as a means of determining the ion-responsiveness of electrodes. It has been found that the ion-responsiveness of graphite electrodes is influenced by chemical treatment of graphite, such as oxidation, by the nature of the dispersing agents used in preparing the electrodes and by the adsorption of electrochemically active molecules.

Acknowledgment.—This research was supported by the United States Department of the Interior, Office of Saline Water, under Contract No. 14-01-001-160 with the University of Oklahoma Research Institute.

THE HEAT CAPACITY OF SOLID IRON(II) CHLORIDE ABOVE ROOM TEMPERATURE

BY FRANKLIN L. OETTING AND N. W. GREGORY

Department of Chemistry at the University of Washington, Seattle, Washington

Received July 19, 1960

The heat capacities of CCP and random-packed forms of $FeCl_2$ between room temperature and 500° have been measured in a constant heating adiabatic calorimeter and found identical (within ±1%). After the random-packed form has been heated to 500° it is found to have changed to the CCP form; no energy effect associated with this transition could be detected. The heat capacities are in good agreement with results reported earlier by Moore.[1]

The heat capacity of solid iron(II) chloride above room temperature has been reported by Moore[1] and by Krestovnikov and Karetnikov.[2] The two sets of data are not in close agreement. Recent heat capacity measurements in our laboratory on the structurally similar compound $FeBr_2$[3] have revealed a transition near 380°. No evidence for a similar transition in $FeCl_2$ is seen in the results of either of the previous studies. However in Moore's work, for example, the "drop" method was used to measure the difference in enthalpy of the sample at a selected temperature (chosen at intervals of from one to two hundred degrees) and 298°K. Since the energy associated with the transition in $FeBr_2$ was very small, of the order of the experimental uncertainty estimated by Moore for the relative enthalpies measured in his study of $FeCl_2$, it seemed possible that a minor transition in $FeCl_2$ might not have been detected. To investigate this question and to provide evidence to aid in resolving the discrepancy between the two sets of data reported,[1,2] we have made a further study which includes a comparison of the heat capacities of $FeCl_2$ in the cubic close-packed form with that of the random-packed form.[4]

Experimental

Anhydrous iron(II) chloride was prepared by vacuum dehydration at 110° of $FeCl_2 \cdot 4H_2O$ (Mallinckrodt Chemical Co., Analytical Reagent), followed by sublimation at 500° in high vacuum. Samples were analyzed by standard methods; the following result is representative: % Fe, 43.84 (44.06); % Cl, 55.70 (55.94); Cl/Fe, 2.001 (theoretical values for $FeCl_2$ in parentheses). X-Ray powder patterns of the sublimed material were typical of the cadmium chloride type structure in which the chlorine atoms are in a cubic close-packed (CCP) array.[4] Crystals in which the halogen layers are packed randomly (RP) may be prepared by allowing oxygen free distilled water to dissolve a sublimed sample and subsequently dehydrating the solution and salt under vacuum. Analysis of the RP material for Fe and Cl gave results similar to those for the original sublimed sample. Powder patterns of the RP phase differ markedly from those of CCP material[4,5] and were used for identification of the nature of the phases prepared (see Fig. 3).

Heat capacities were measured in the vacuum adiabatic constant heating calorimeter described in detail in a recent publication.[6] The sample was sealed in a uranium glass sphere, *ca.* 1 and 3/4 in. o.d., in the center of which was a nichrome heating element also encased in a small uranium glass sphere, which provided a net volume of *ca.* 60 ml. The outer surface of the cell was coated with silver and the cell was suspended by its heater leads inside a series of three cylindrical heated jackets, designed so that the temperature of all surfaces of the innermost jacket exposed to the cell could be controlled automatically to within ±0.1° of the cell surface. Jacket heating elements described earlier were reconstructed so that the elements were insulated with quartz; platinum–platinum-10% rhodium thermocouples were used for measurement of cell temperatures in the present work. The cell was heated continuously; time, current and cell heater voltage were measured carefully to determine energy input. As soon as a nearly constant gradient (about six degrees near room temperature, changing slowly to about three degrees at the highest temperatures) across the sample was established and the jacket temperatures were properly controlled, the energy required to raise the temperature of the cell and its contents through each *ca.* ten degree interval was measured from which mean heat capacities were calculated. The calibration of the empty cell and general performance of the calorimeter were tested with α-aluminum oxide and were checked before and after measurements on $FeCl_2$.[7]

(1) G. E. Moore, *J. Am. Chem. Soc.*, **65**, 1700 (1943).

(2) A. N. Krestovnikov and G. A. Karetnikov, *J. Gen. Chem. U.S.S.R.*, **6**, 955 (1936).

(3) H. E. O'Neal and N. W. Gregory *J. Am. Chem. Soc.*, **81**, 2649 (1959).

(4) R. O. MacLaren and N. W. Gregory, *ibid.*, **76**, 5874 (1954).

(5) G. Hagg and E. Linden, *Arkiv Kemi, Mineral., Geol.*, **B16**, No. 5 1 (1943).

(6) H. E. O'Neal and N. W. Gregory, *Rev. Sci. Instr.*, **30**, 434 (1959).

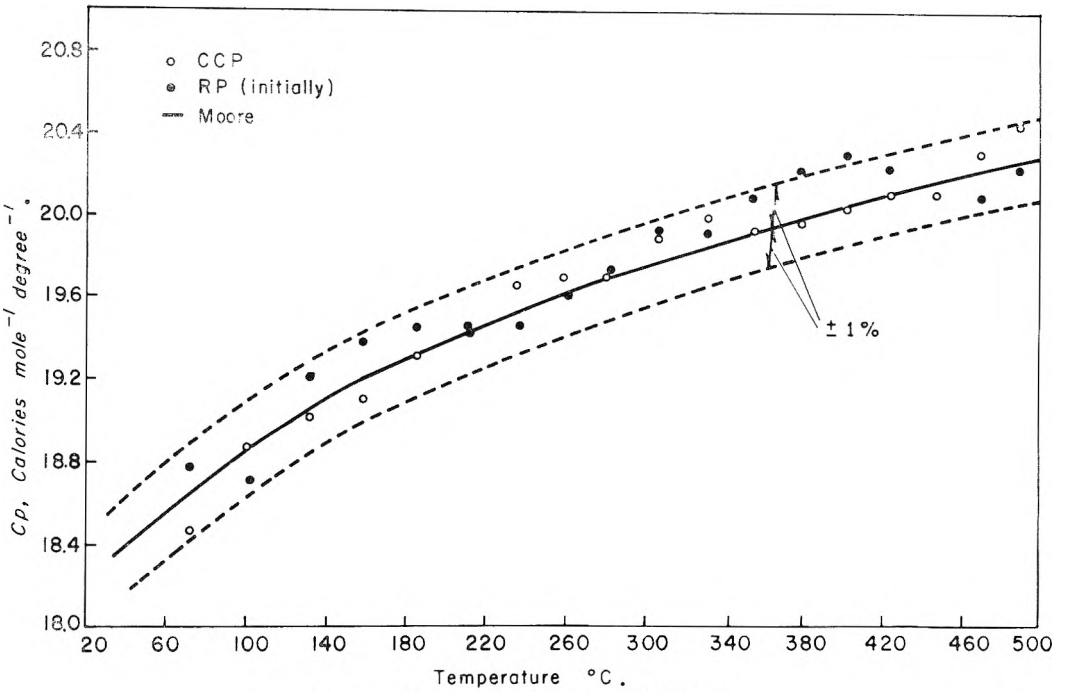

Fig. 1.—Heat capacity of iron(II) chloride.

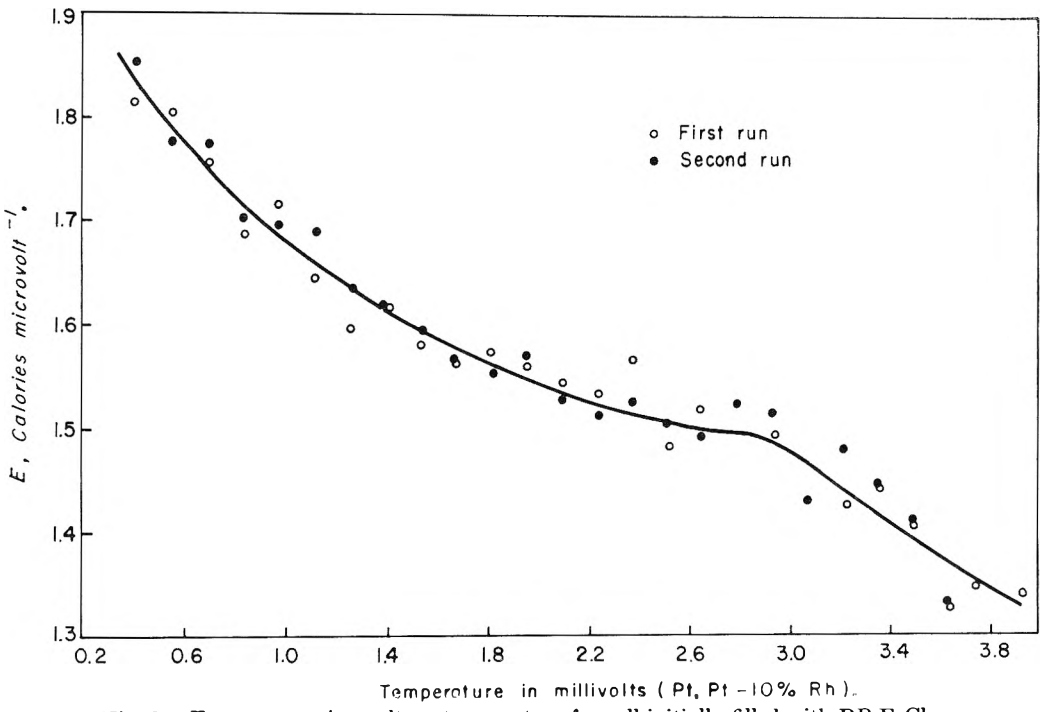

Fig. 2.—Energy per microvolt *vs.* temperature for cell initially filled with RP $FeCl_2$.

Results and Discussion

Results are summarized in Fig. 1. The points labelled CCP were obtained from 67.35 g. of vacuum sublimed material for which X-ray powder patterns indicated the CCP structure. The cell was loaded in a nitrogen filled dry box, evacuated, heated under high vacuum at 450° for six hours, cooled, filled (voids between crystals) with argon at 200 mm. pressure, sealed and placed in position in the calorimeter assembly. Three consecutive runs were made; in each the energy necessary to raise the temperature of the cell and its contents through each *ca.* ten degree interval between 60 and 500° was measured. A smooth curve was drawn through the combined results of the three runs. The maximum deviation of any point from this curve was 2%; the average deviation was 0.9%. Points were taken from this curve at thermocouple temperature intervals of two tenths millivolts and used to calculate the heat capacities shown in Fig. 1. The results are seen to be in good agreement with the data of Moore.[1] The results of Krestovnikov and

(7) For details see the Ph.D. thesis of F. L. Oetting, University of Washington, 1960.

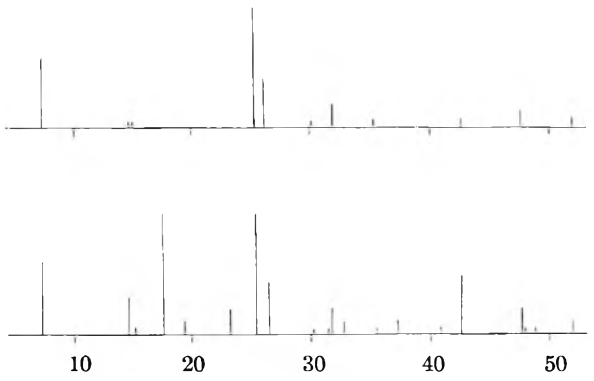

Fig. 3.—Representation of powder patterns for RP (top) and CCP (bottom) forms of $FeCl_2$. Line heights indicate relative intensity. After one run in heat capacity calorimeter, the pattern for the RP sample changed to that characteristic of the CCP material.

Karetnikov[2] cross this line at about 270° but deviate by from 5 to 15% at higher and lower temperatures.

No evidence for a transition of the type found in $FeBr_2$ is seen in the data represented in Fig. 1. Differential cooling experiments, in which the rate of cooling of a sample of $FeCl_2$ was compared with that of NaCl, also failed to show the existence of a transition at higher temperatures (between 660 and 500°).

The points on Fig. 1 labelled RP were obtained from a sample treated in the following manner: 47.07 g. of random-packed $FeCl_2$ was prepared by vacuum dehydration of the commercial hydrate at 110°; pumping was continued for two days until a vacuum of 1×10^{-6} mm. had been attained. The material was transferred to the calorimeter cell and pumping resumed for an additional four hours at 110°, after which argon was added until its pressure in the cell was 200 mm. A sample of the solid taken when the cell was filled gave an X-ray pattern typical of the random-packed structure.

The heat capacity of this material was then measured between 70 and 500° in a continuous run (#1). The sample was then permitted to cool and the heat capacity again measured (#2). These two runs are compared on Fig. 2 and results are seen to be the same within experimental error. Heat capacities calculated from the smoothed curve are compared with those of the sublimed material in Fig. 1. A sample of the RP material taken after the heat capacity measurements gave an X-ray pattern typical of CCP $FeCl_2$, showing that a transition from the RP to CCP form had occurred.

In preliminary experiments it was found that after RP $FeCl_2$ had been heated once to 500° in a regular run in the calorimeter, powder patterns characteristic of the CCP structure were obtained. Hence in the comparison shown in Fig. 2, it is suggested that run #2 is typical of CCP material whereas in run #1 the sample was initially RP but changed to CCP as the temperature increased. Hence we conclude that (a) in this temperature interval the heat capacity of the two forms cannot be distinguished (within our experimental error) and (b) the difference in energy of the two forms is so small that the transition from RP to CCP cannot be detected in our experiments. The total energy input required to raise the temperature of the cell from 70 to 500° for runs #1 and #2 differed by only 0.4% (*ca.* 20 cal.), a difference within our experimental error. If the RP form were to release as much as 20 cal. of energy per mole on changing to the CCP form, it would have been detected even though the transition might be spread out over as much as a fifty degree interval.

It is believed that the major portion of the RP sample changed to the CCP form during the heating period as measurements were made. The RP form is apparently stable for an indefinite period at room temperature. It does not change to the CCP form at an appreciable rate until the temperature reaches the vicinity of 400–500°. At 500° the vapor pressure is still small, *ca.* 2×10^{-2} mm., but sublimation provides mechanism for the transformation. It has been observed that X-ray diffraction lines of the CCP form appear in a pattern of a sample of RP material which was heated rapidly (five minutes) to 480°, held there for 20 minutes, and then cooled rapidly to room temperature. At the heating rate used in heat capacity measurements, *ca.* 1 degree minute^{-1}, the sample was between 400 and 500° for about 100 minutes. Cooling back through this interval required a somewhat shorter time.

The heat capacity of $FeCl_2$(s) between 60 and 500° may be represented by the equation[1]

$$C_p = 18.94 + 2.08 \times 10^{-3}\, T - 1.17 \times 10^{5}\, T^{-2}\ (°K).$$

This work was supported by the Office of Ordnance Research, U. S. Army.

MEASUREMENT OF DONNAN RATIO BY RADIOACTIVE TRACERS AND ITS APPLICATION TO PROTEIN-ION BINDING[1]

BY ABRAHAM SAIFER AND JOSEPH STEIGMAN

Department of Chemistry, Polytechnic Institute of Brooklyn, Brooklyn, N. Y.

Received July 20, 1960

Binding of iodide ion from solutions of sodium or potassium iodide to deionized bovine serum albumin and to bovine serum mercaptalbumin has been studied by equilibrium dialysis using radioactive I^{131} as a tracer. The Donnan effect was evaluated by introducing another radioactive ion, *e.g.*, Na^{24}, into the system which does not bind to these proteins. In acid solutions of BSA unbound hydrogen ions measured by *p*H showed the same distribution across the membrane as did the Na^{24} ions. In addition at *p*H 12, where iodide ion should not bind, the I^{131} ratio across the membrane was equal to the reciprocal of the Na^{24} ratio. Finally at isoionic *p*H the binding constants for iodide ion to BSM determined by this method were shown to be in close agreement with those obtained by other workers by means of e.m.f. measurements.

The different experimental techniques employed in the study of ion binding to proteins have been summarized in a review article by Klotz.[2] Of these, the equilibrium dialysis procedure[3] and those employing e.m.f. measurements with electrodes which measure the activity of the ion under investigation[4,5] have been among the most widely used. The equilibrium dialysis technique is generally performed in strong salt or buffer solutions so as to reduce the Donnan effect to negligible proportions. This experimental approach disregards the effect of the competitive binding to the protein molecule of salt or buffer ions present in high concentration. On this account this method of measuring ion binding has been criticized by Scatchard.[6] In addition Scatchard and Black[7] have shown that a large change occurs in the concentration of bound hydrogen ion in the presence of neutral salts.

E.m.f. measurements of protein systems by means of indicator or ion-exchange electrodes are not subject to this criticism since they can be performed in the absence of buffer and at low salt concentrations. These measurements, which are otherwise quite satisfactory, suffer from a minor drawback, *i.e.*, satisfactory measurements cannot usually be made at ion concentrations less than 10^{-4} *M*. These regions of higher dilution are important in the evaluation of intrinsic binding constants and certain other thermodynamic data,[8] and these must be determined by extrapolation rather than by direct measurement.

This paper describes the binding of iodide ions to bovine serum albumin (BSA) and bovine serum mercaptalbumin (BSM) using trace amounts of Na^{24} of high specific activity as the Donnan ion, *i.e.*, as the unbound ion whose distribution across a semi-permeable membrane yields the Donnan ratio for the solution. Previous investigators, using a variety of techniques including potentiometric measurements, have concluded that sodium ion is not bound to serum albumin.[2,8] In addition, diffusion study has shown that sodium ion at the trace level is not bound to a polyelectrolyte which has a much higher charge density than proteins.[9] It has, therefore, been assumed in this work that Na^{24} is not bound to the serum albumins.

In the study of the binding of an anion A of charge $-n$ to a protein in the presence of an unbound cation M of charge, $+m$ the equations apply

$$A_b = A_t - \frac{A_0 \gamma_0}{r \gamma_i} \qquad (1)$$

where

A_t = total concn. of anion found by analysis inside
A_b = concn. of bound anion
A_0 = total concn. of anion found by analysis outside
γ_0, γ_i = activity coefficients of the ion in the outside and inside soln.

$$r = (A_0\gamma_0/A_i\gamma_i)^{1/n} = (M_i\gamma_i/M_0\gamma_0)^{1/m} \qquad (2)$$

where

A_i, A_0 = total molal concn. of any unbound *n*-valent anion inside and outside the membrane, resp.
M_i, M_0 = total molal concn. of any unbound *m*-valent cation inside and outside the membrane, resp.

It is generally assumed that the activity coefficients of the ions being measured are unaffected by the presence of the protein and that in sufficiently dilute solutions concentrations may be used instead of activities.[10] Appropriate activity coefficient corrections were applied whenever they were found to be necessary.

This equilibrium dialysis-tracer technique was employed to show that in acid solutions of BSA, unbound hydrogen and sodium ions had the same distribution across the membrane, *i.e.*, Na^{24} was not bound. In addition the binding of iodide ions to BSA was investigated over a wide range of *p*H and the iodide binding constants of BSM in the isoionic *p*H region were determined using both Na^{24} and I^{131} as the tracer ions.

(1) From a thesis submitted by Abraham Saifer to the Graduate School of the Polytechnic Institute of Brooklyn in partial fulfillment of the requirements for the degree of Doctor of Philosophy.

(2) I. M. Klotz in H. Neurath and K. Bailey, eds., "The Proteins. Chemistry, Biological Activity, and Methods," Vol. I, Part B, Academic Press, New York, N. Y., 1953, p. 727.

(3) T. R. Hughes and I. M. Klotz in D. Glick, ed., "Methods of Biochemical Analysis," Interscience Publishers, Inc., New York, N. Y., 1956, Vol. 3, p. 265.

(4) (a) C. W. Carr, *Arch. Biochem. Biophys.*, **40**, 286 (1952); (b) **43**, 147 (1953); (c) **46**, 417, 424 (1953); (d) C. W. Carr and L. Topol, THIS JOURNAL, **54**, 176 (1950).

(5) G. Scatchard, I. H. Scheinberg and S. H. Armstrong, Jr., *J. Am. Chem. Soc.*, **72**, 535, 540 (1950).

(6) G. Scatchard, W. L. Hughes, Jr., F. R. N. Gurd and P. E. Wilcox in F. R. N. Gurd, ed., "Chemical Specificity in Biological Interactions," Academic Press, New York, N. Y., 1954, p. 193.

(7) G. Scatchard and E. S. Black, THIS JOURNAL, **53**, 88 (1949).

(8) F. R. N. Gurd and P. E. Wilcox in M. L. Anson, K. Bailey and J. T. Edsall, eds., "Advances in Protein Chemistry," Academic Press, Inc., New York, N. Y., 1956, Vol. 11, p. 311.

(9) J. P. Dux and J. Steigman, THIS JOURNAL, **63**, 269 (1959).

(10) (a) J. H. Northrup and M. Kunitz, *J. Gen. Physiol.*, **7**, 25 (1924–1925); (b) **9**, 351 (1925–1926); (c) **11**, 481 (1927–1928).

Experimental

I. **Deionization of Proteins.**—Two to 10% protein solutions were deionized by passage through the multi-bed ion-exchange resin column proposed by Dintzis.[11] The appearance of the protein solution in the column effluent was determined by means of the color produced with biuret reagent. Deionized, redistilled water was used for the preparation of the protein and salt solutions. Passage through the column of protein solutions containing 10^{-4} *M* (plus tracer) iodide ion added as an impurity showed that a single pass reduced its concentration to less than 10^{-8} *M*. Deionized preparations of BSA and BSM gave isoionic *p*H values of 5.05 and 5.15, respectively, in the absence of salts. The latter value for BSM is identical with that reported by Scatchard, *et al.*,[12] whereas, the isoionic *p*H of the BSA sample (5.05) is somewhat lower than that reported by others[13,14] in the presence of salts.

II. **Equilibrium Dialysis Procedure.**—The technique used for the preparation of the dialysis bags (Visking casing, 20/32 inches) is essentially that described by Hughes and Klotz.[3] Whenever the casings were to be used for binding measurements in the presence of a supporting electrolyte, they were soaked in such solutions for at least 12 hours prior to their use as dialysis membranes.

A 5.00-ml. aliquot of the deionized protein solution was transferred to the dialysis bag which had been sealed off at one end with a double knot. The other end of the bag was twisted so as to leave as little air space as possible and was then also sealed off with a double knot. A length of fiberglass or suture thread was attached to one end of the bag and any excess tubing was cut away. The bag was held suspended by the thread and the outside surface rinsed free of any protein by washing with distilled water and then blotted dry with cotton gauze.

The bags were then lowered into polyethylene tubes (30 × 200 mm.) containing 50.00 ml. of freshly prepared dilute potassium iodide solutions of known concentration and trace amounts of I^{131} (about 50,000 cts./min./ml.) and of Na^{24} (about 100,000 cts./min./ml.). The tubes were tightly stoppered with corks wrapped in Saran Wrap (polyethylene) and the ends of the threads were allowed to pass outside the stoppers to facilitate removal of the bags. Finger cots rinsed in distilled water were worn while manipulating the bags and the radioactive solutions so as to avoid contaminating the samples with sweat.

The tubes were shaken with a wrist-action type of shaker for about 12–15 hours at room temperature (22 ± 3°) in order to establish equilibrium between the internal and external solutions. The bags were then lifted out of tubes by the fiberglass thread, their outside surfaces quickly rinsed with distilled water and the bags dried with a gauze sponge. Each bag was then placed in a clean, dry test-tube and punctured with an applicator stick to transfer its contents to the tube. The *p*H of the internal protein solution was measured with a Beckman Model G *p*H meter using a glass–calomel electrode system. Spectrophotometric measurements of the protein solutions were made with a Beckman D.U. spectrophotometer at 279 mμ after diluting 1.00-ml. aliquots to 50.00 ml. with 0.9% NaCl. The protein concentrations were calculated by means of the relationship, $E^{1\%}_{1\ cm.} = 6.67$.[13]

Sodium-24 of high specific activity was obtained from Brookhaven National Laboratories. Iodide-131 was a carrier-free material from Oak Ridge. One-ml. aliquots of the solutions of these isotopes were counted with a scintillation counter using a well-type sodium iodide crystal. A minimum of 100,000 counts were recorded for each sample run in duplicate. Iodide-ion binding was determined by counting the combined activities of I^{131} and Na^{24} allowing the sodium to decay ($T_{1/2}$ = 14.5 hours) for one week or longer and then counting the iodide activity alone. The iodide decay ($T_{1/2}$ = 8.1 days) was corrected by means of measurement against a reference solution. Frequent background counts were made.

The *p*H of the external solutions was determined by a glass electrode in alkaline *p*H and by either a glass or a quinhydrone electrode in acid *p*H.

Preliminary experiments with BSA solution in the internal phase and iodide solutions plus I^{131} in the external phase showed that equilibrium in dialysis was established at room temperature after four hours of shaking.

In order to obtain results comparable with those of other investigators, a molecular weight of 69,000 was assigned both to BSA (Pentex, 1X recrystallized) and BSM (Pentex, 10X recrystallized).

Results and Discussion

I. Comparison of Sodium Ion and Hydrogen Ion Distribution in Acid BSA Solutions.—Small quantities of Na^{24} (about 100,000 cts./ml./min.) were added to the external solutions whose acidity had been adjusted with standard HCl to *p*H values which ranged from 1.0 to 5.0. The concentration of BSA in the inner solution was maintained at 5%. After the dialysis had reached equilibrium, the *p*H and the radioactivity of each solution were measured. Figure 1 shows the change in the negative logarithm of the Donnan ratio as a function of the *p*H of the inner solution. The ratios at various *p*H's were calculated from the activities of the free H^+ ions as well as from the activities of the sodium ions. Since the radioactivity measurements give relative concentrations, it was assumed that the relative concentrations of the Na^+ ions were the same as their activities at *p*H values greater than 3.4. In all other cases activity coefficients as given by MacInnes[15] were used to calculate the Na^+ ion activities.

From the curve illustrated in Fig. 1 it can be seen that the ratio of Na^+ ion activities inside and outside the membrane are virtually identical with the ratio of their corresponding free hydrogen ion activities. This constitutes additional evidence for the lack of appreciable binding of Na^+ ions to BSA on the acid side of the isoionic point. Similar results were obtained for BSM in the same *p*H range. Accordingly it was concluded that Na^{24} distribution measurements would provide direct and accurate Donnan ratio values and thereby permit quantitative evaluation of the binding of various ions to the serum albumins. The validity of this conclusion for the alkaline side of the isoionic point will be discussed in a later section.

II. Effect of *p*H on Iodide Ion Binding to BSA.—Deionized 5% BSA solutions were subjected to equilibrium dialysis against external solutions which contained 10^{-5} *M* sodium iodide plus I^{131}, a trace of Na^{24} and different concentrations of HCl or NaOH. After equilibration the *p*H of each internal solution was measured and the distribution of the radioactive cations and anions in each phase determined by means of the previously described scintillation counting techniques. Figure 2 shows the variation with *p*H of the negative logarithm of $(Na^{24})_i/(Na^{24})_0$ and $(I^{131})_0/I^{131})_i$ in the *p*H range from 1.5 to 12.0. No attempt was made to maintain constant ionic strength in these experiments.

The differences between the two curves at various *p*H's *i.e.*, between the ratios of sodium ions and those of iodide ions, are related to the extent of iodide ion binding to the protein. The maximum iodide ion binding appears to be at about *p*H 4.5,

(11) H. M. Dintzis, Ph.D., Thesis, Harvard University, 1952.

(12) G. Scatchard, J. S. Coleman and A. L. Shen, *J. Am. Chem. Soc.*, **79**, 12 (1957).

(13) J. F. Foster and M. D. Sterman, *ibid.*, **78**, 3656 (1956).

(14) C. Tanford, S. A. Swanson and W. S. Shore, *ibid.*, **77**, 6414 (1955).

(15) D. A. MacInnes, "The Principles of Electrochemistry," Reinhold Publ. Corp., New York, N. Y., 1939.

which is to be expected because of the increased positive charge on the protein. At *p*H's lower than 4.5 there is a reduction in the binding of iodide ion which is in part due to the competition for the same binding sites of the increasing chloride ion concentration[5] and also results from a decrease in charge due to the expansion of the albumin molecule at acid *p*H.[16,17] The binding of the iodide ion on the alkaline side of the isoionic *p*H of BSA is of greater interest. Firstly, there is the indication of extensive binding of iodide ion in the *p*H range from 7 to 9 although the net charge on the protein is negative. This means that serum albumin can function as a anion transport agent at physiological *p*H. Secondly, at *p*H 12 the ratio of the iodide ions is almost identical with the reciprocal ratio of the sodium ions. In this strongly alkaline solution the binding of iodide ions would be negligible because of the high negative charge on the protein. There are two alternative explanations for the identity of the tracer ion ratios at this *p*H. The first one is that although some Na^+ ions may be bound, the extent of the iodide ion binding is exactly parallel at the same *p*H. The second possibility is that Na^+ ion is not bound at this *p*H and hence neither is iodide. The general chemistry of the system makes this simpler hypothesis the more likely one. While it would appear possible to calculate $\bar{\nu}/\alpha$ as a function of Z_p for nearly zero $\bar{\nu}$ for BSA at *p*H's > 5 from the data given in Fig. 2, the measurements of *p*H and protein concentration were not made with sufficient accuracy to warrant such calculations. In addition the results at acid *p*H would have been more useful if HI had been used instead of HCl. Experimental difficulties in keeping HI free of I_2 for the prolonged time periods necessary to establish equilibrium conditions prevented us from successfully carrying out such experiments.

III. Iodide Ion Binding to BSM at Isoionic *p*H.—Equilibrium dialysis measurements were performed on 5% deionized BSM in the presence of iodide salts whose concentrations ranged from the trace level ($> 10^{-5}$ *M*) to 5×10^{-3} *M*, using Na^{24} as the Donnan ion and I^{131} as the determinant of the iodide ion distribution. The ratio of Na^{24} outside to Na^{24} inside was the same in solutions of 5×10^{-3} *M* NaI and 5×10^{-3} *M* KI containing tracer Na^{24}, pointing to the negligible binding of Na^+ ions to BSM even at the higher Na^+ ion concentrations as was found by Scatchard, *et al.*,[18] for human serum albumin.

From equation 1 the bound iodide ion concentration, $(I)_B$, can be calculated

$$(I)_B = (I)_T - (I)_F \qquad (3)$$

but

$$(I)_F = \frac{(I)_0}{r} = (I)_0 \times \frac{(Na^{24})_0}{(Na^{24})_i} \qquad (4)$$

and hence

$$(I)_B = (I)_T - (I)_0 \times \frac{(Na^{24})_0}{(Na^{24})_i} \qquad (5)$$

(16) J. F. Foster and J. T. Yang, *J. Am. Chem. Soc.*, **76**, 1015 (1954).

(17) C. Tanford, J. Buzzell, D. Rands and S. Swanson, *ibid.*, **77**, 6421 (1955).

(18) G. Scatchard, A. C. Batchelder and A. Brown, *ibid.*, **68**, 2320 (1946).

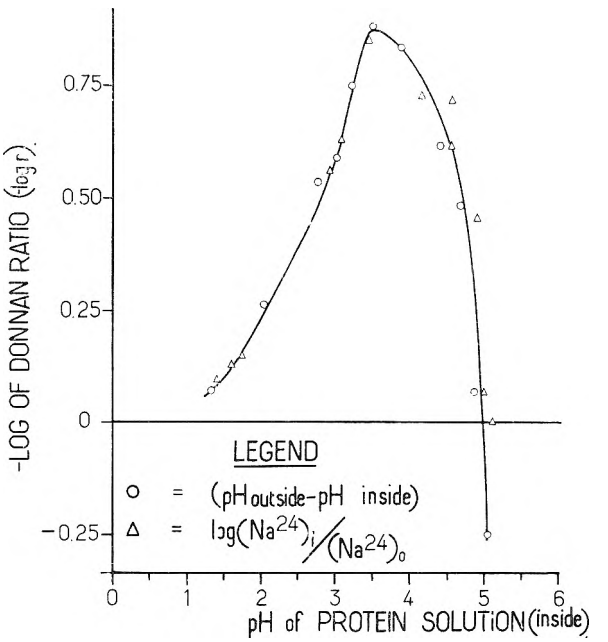

Fig. 1.—Variation of Donnan ratio-(pH outside − pH inside) and − log $(Na^{24})_i/(Na^{24})_0$ with pH of BSA (5%) after attainment of equilibrium by dialysis.

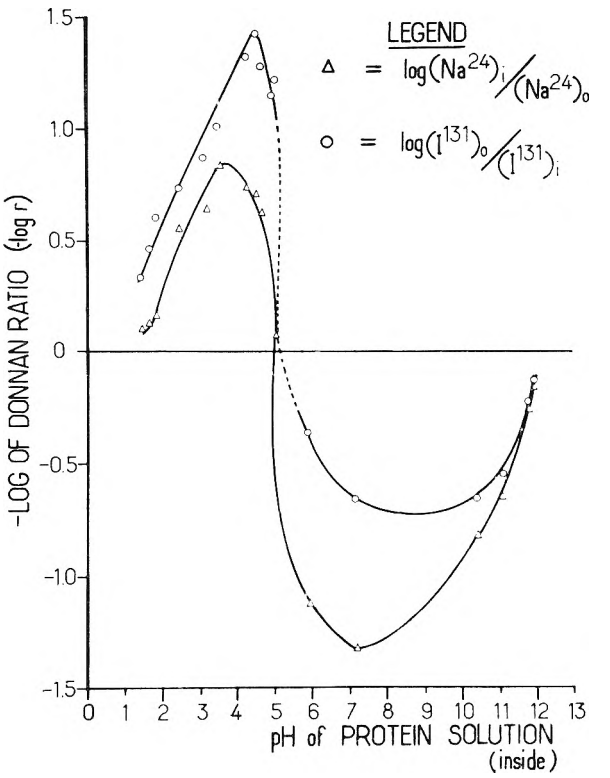

Fig. 2.—Variation of Donnan ratio-log $(Na^{24})_i/(Na^{24})_0$ and $-\log (I^{131})_i/(I^{131})_i$ with pH of BSA (5%) after attainment of equilibrium by dialysis as an index of iodide ion binding.

From these data (Table I) a plot was made of $\bar{\nu} = (I)_B/(P)$ and of $\bar{\nu}/\alpha$ where $\alpha = (I)_F\,(e^{-2.303\,w'Z_pZ_A})$ as is illustrated in Fig. 3. The symbols $\bar{\nu}$ and α correspond to those employed by Scatchard and his co-workers[12] who investigated the same system with ion-exchange electrodes. Z_A is the

TABLE I

IODIDE ION BINDING TO ISOIONIC BOVINE SERUM MERCAPTALBUMIN

$(I^-)_T$, molality	$(I^-)_F$, molality	$(I^-)_B$, molality	$\bar{r}$ (Donnan ratio)	$\bar{\nu} = (I)_B/(P)$	$\bar{\nu}^a/\alpha$	α^a
1.46×10^{-5}	3.64×10^{-6}	1.09×10^{-5}	0.414	4.27×10^{-2}	11,850	3.603×10^{-6}
2.49×10^{-5}	6.51×10^{-6}	1.83×10^{-5}	.290	7.62×10^{-2}	11,758	6.481×10^{-6}
6.79×10^{-5}	1.86×10^{-5}	4.94×10^{-5}	.422	2.09×10^{-1}	11,747	1.779×10^{-5}
3.86×10^{-12}	8.05×10^{-13}	3.05×10^{-12}	.234	9.00×10^{-9}	11,174[b]	8.054×10^{-13}[b]
3.06×10^{-4}	1.02×10^{-4}	2.04×10^{-4}	.463	8.55×10^{-1}	7,948	1.076×10^{-4}
1.59×10^{-3}	4.58×10^{-4}	1.14×10^{-3}	.527	2.09	6,789	3.079×10^{-4}
1.24×10^{-3}	6.39×10^{-4}	5.99×10^{-4}	.727	2.42	6,012	4.025×10^{-4}
1.20×10^{-3}	6.41×10^{-4}	5.59×10^{-4}	.729	2.34	5,529	4.232×10^{-4}
1.05×10^{-3}	6.49×10^{-4}	4.06×10^{-4}	.733	2.30	5,390	4.267×10^{-4}
2.70×10^{-3}	1.81×10^{-3}	8.86×10^{-4}	.798	3.71	3,893	9.529×10^{-4}
5.11×10^{-3}	4.06×10^{-3}	1.06×10^{-3}	.889	4.86	2,593	1.874×10^{-3}

[a] These quantities are defined in the text of the paper. [b] This point was not included in plotting the data shown in Fig. 3 because of the greater possibility of the oxidation of tracer iodide ion in a carrier-free system.

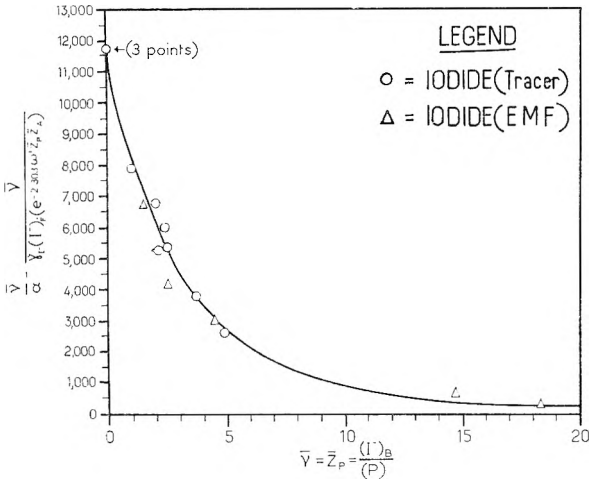

Fig. 3.—Iodide ion binding to isoionic BSM (5%).

charge on the anion and $\bar{Z}_p$ is the average charge on the protein and $w' = 2w/2.303$ where w is a constant calculated from the Debye equation[16] for a spherical protein molecule.

The present data for the BSM–NaI system, obtained with the equilibrium dialysis-tracer technique, are superimposed in Fig. 3 on Scatchard's published data (Table I, last column)[12] for the same system. This figure shows that the results obtained with the two methods are in good agreement. The fact that the shape of the curve is concave upwards shows that the iodide ion is binding to more than one class of sites. At $\bar{\nu}_I = 0$, the intercept is $\bar{\nu}_I/\alpha_I = \Sigma_i n_i K^0_{iI}$ and the asymptotic slope is $-\Sigma_i n_i K^{02}_{iI}/\Sigma_i n_i K^0_{iI}$. At $\bar{\nu}_I/\alpha_I = 0$, the intercept is $\bar{\nu}_I = \Sigma_i n_i$ and the asymptotic slope is $-\Sigma_i n_i/(\Sigma_i n_i/K^0_{iI})$. The limits at $\bar{\nu}_I/\alpha_I = 0$ are usually indeterminate but those at $\bar{\nu}_I \cong 0$ ($< 10^{-5}$ M I^-) are now directly determinable experimentally with the equilibrium dialysis-tracer method.

Scatchard, *et al.*,[12] found that the data for the binding of chloride or iodide ions to BSM in dilute solution could be interpreted as binding to three classes of sites with the number, n_i, of groups in successive classes being $n_1 = 1$, $n_2 = 7 \pm 1$ and $n_3 = 18 \pm 4$. They reported the following values for the various binding constants for iodide ion: $K_1 = 9200 = 24K_2 = 720K_3$. Other anions, like chloride, fluoride and thiocyanate, were bound to these same sites but with different binding constants. The present data best fit the lower limits of the number of binding sites proposed by them, *i.e.*, $n_1 = 1$, $n_2 = 6$ and $n_3 = 14$ and $\Sigma n_i K_i = 11{,}680$ (calculated) compared to 11,788 (experimental).

The present investigation was designed with a view toward an intensive study of a few well-characterized, water soluble proteins, *i.e.*, bovine serum albumin and mercaptalbumin, with a single radioactive ion (I^{131}) in order to firmly establish the validity of this new experimental approach to the quantitative determination of the binding of ions to proteins in buffer-free systems. The principle involved should be applicable to other water or salt-soluble proteins and to many other radioactive ions which are available as relatively carrier-free salts.

Acknowledgments.—We wish to thank Dr. Bruno W. Volk, Director of Laboratories of the Isaac Albert Research Institute, Brooklyn, N. Y., for permitting this work to be done in its laboratories. We also wish to acknowledge the assistance of Mr. Arthur Hyman with some of the measurements.

A SPECTROPHOTOMETRIC STUDY OF THE NIOBIUM SULFOSALICYLATO COMPLEXES[1]

BY ORVAL E. AYERS AND JAMES E. LAND

Contributed from the Ross Chemical Laboratory, Auburn University, Auburn, Alabama

Received July 21, 1960

Niobium pentoxide, dissolved in NaOH solution, was found to react with sulfosalicylic acid in a stepwise fashion to form a water-soluble complex compound, which produced a greenish-yellow solution with maximum absorption at 310 mμ. By using spectrophotometric data, the Nb:(SSal) ratio was postulated to be 1:2 in the predominant species and 1:1 in the minor species present in a solution 10^{-5} to 10^{-3} *M* in sulfosalicylic acid. The stepwise formation constants, k_1 and k_2, and the over-all formation constant, *K*, for the complexes in these solutions at *p*H 2–4 were calculated to be 1.08×10^4, 4.18×10^3 and 4.52×10^7, respectively. A solid compound was isolated from solution but its formula could not be determined.

Introduction

The use of sulfosalicylic acid to form a coördination compound with niobium has been previously reported but mainly in connection with analytical schemes. Schwartz[2] effected the separation of niobium and tantalum with it while Das Gupta and Dhar[3] employed it for estimating microgram quantities of niobium in the presence of moderate excesses of tantalum and titanium. Sudarikov and Busarov[4] reported that solutions of niobium(V) sulfate and niobium(V) chloride became greenish-yellow in color when sulfosalicylic acid was added and from these solutions isolated a compound to which they assigned the formula, $(NbO)_2(SSal)_3 \cdot 4H_2O$.[5]

It was our aim in this study to determine the chemical constitution of the niobium sulfosalicylato complex species in aqueous solution. From absorption measurements in the ultraviolet and by using a modification of the methods developed by Newman and Hume,[6] along with those of Mukherji and Dey,[7] and Brown and Land[8,9] it was possible to postulate that two complex species were present in the concentration range studied and to calculate formation constants for the equilibria involved.

Experimental

Measurements.—The equipment and conditions for obtaining the measurements were the same as previously described,[8] except that for the ultraviolet absorption measurements 2 cm. matched silica cells were used.

Materials.—The sulfosalicylic acid (Merck and Co., Inc., Rahway, N. J.), labeled 99.5–100.3% pure, was used without further purification.

Solutions for ultraviolet absorption studies were prepared as follows: 0.066 g. of Nb_2O_5 (Fairmount Chemical Co., Newark, N. J.) and 1–2 g. of $KHSO_4$ were fused together in a Vycor crucible until a clear melt was obtained. The hot crucible was removed from the heat and rotated in such a manner that the melt solidified on the sides of the crucible. The slightly cooled crucible with its contents was placed in about 200 ml. of hot 2 *N* HCl solution which was maintained just below the boiling point. The precipitated oxide was allowed to digest for about 20 minutes and then filtered on a büchner funnel using No. 50 Whatman filter paper. The freshly precipitated oxide was washed with 200 ml. of hot water and rinsed thoroughly with acetone. The precipitate was then dried by drawing air through it until all the acetone was removed.

The dried Nb_2O_5 was added to 100 ml. of a 0.6% NaOH solution and refluxed for about one hour to effect solution of the oxide. This NaOH–niobate solution was allowed to cool to room temperature, filtered to remove any particles of filter paper or unreacted oxide and the volume made up to 500 ml. with distilled water. An aliquot of this solution was analyzed for Nb.

A 10^{-3} *M* sulfosalicylic acid solution was prepared by dissolving 0.1271 g. of sulfosalicylic acid dihydrate in a small quantity of water and then diluting to 500 ml.

Solutions having a constant Nb concentration and varying sulfosalicylic acid concentrations were prepared for spectrophotometric scan as follows: using a buret, seven constant volume portions of the NaOH–niobate stock solution were measured into 25-ml. volumetric flasks. Varying amounts of standard sulfosalicylic acid solution and approximately 2 *N* $HClO_4$ were then added in order to make, when each solution was diluted with water, final solutions between *p*H 2–4 and the sulfosalicylic acid concentrations of the respective solutions 1.0×10^{-4}, 2.4×10^{-4}, 3.2×10^{-4}, 4.0×10^{-4}, 6.0×10^{-4}, 8.0×10^{-4} and 1.0×10^{-3} *M*. Seven reference solutions were prepared in a similar manner except that they contained no Nb. Perchloric acid was used to make the final solution acidic because the perchlorate ion is known to show little, if any, tendency to form complexes with metal ionic species. The concentration of the Nb in a given series of solutions was between 1×10^{-3} and 2×10^{-6} molar.

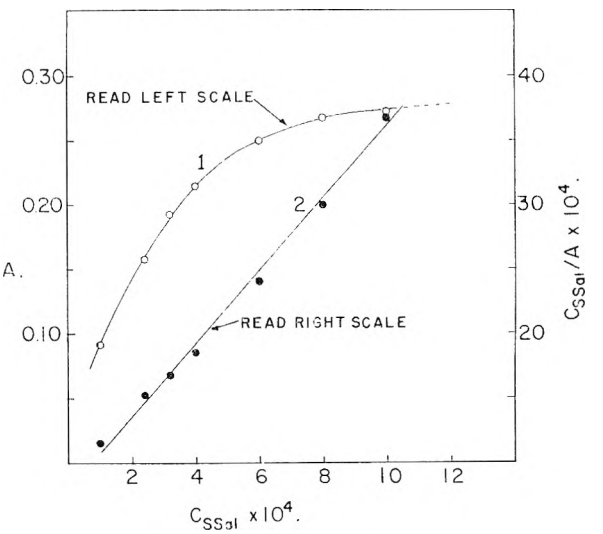

Fig. 1.—Curve 1, absorbance as a function of sulfosalicylato ligand concentration; curve 2, ligand concentration divided by absorbance as a function of ligand concentration.

(1) Based upon Orval E. Ayers' M.S. thesis research. Presented at the Southeastern Regional Meeting of the American Chemical Society, November 5–7, 1959.

(2) V. Schwartz, *Z. angew. chem.*, **47**, 228 (1934).

(3) A. K. Das Gupta and S. K. Dhar, *J. Sci. Ind. Res.*, **12B**, 396 (1953).

(4) B. N. Sudarikov and Yu. P. Busarov, *Neorg. Khim. (U.S.S.R.)*, **2**, 702 (1957).

(5) The symbol (SSal) has been employed throughout this paper for the sulfsalicylato ligand.

(6) L. Newman and D. N. Hume, *J. Am. Chem. Soc.*, **79**, 4571 (1957).

(7) A. K. Mukherji and A. K. Dey, *J. Inorg. Nucl. Chem.*, **6**, 314 (1958).

(8) S. A. Brown and J. E. Land, *J. Am. Chem. Soc.*, **81**, 3185 (1959).

(9) S. A. Brown and J. E. Land, *J. Less-Common Metals*, **1**, 237 (1959).

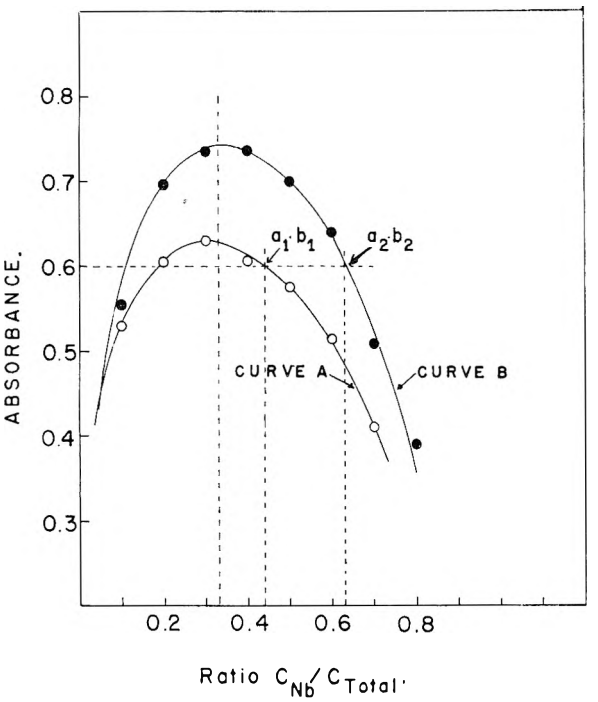

Fig. 2.—Continuous variations plots for niobate sulfosalicylato mixtures.

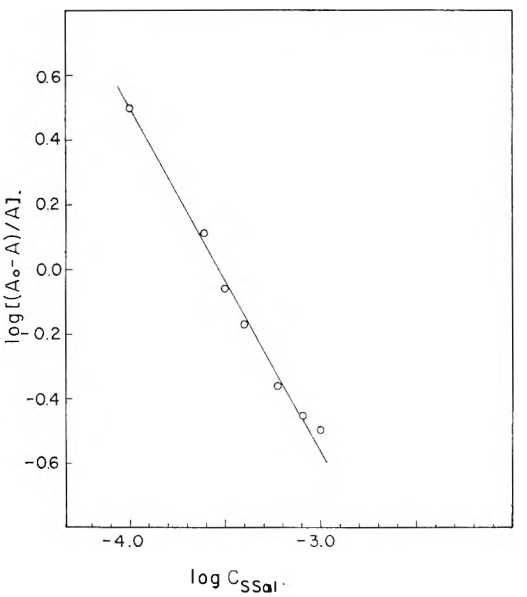

Fig. 3.—Determination of the formation constant k_n with two species present and one absorbing.

The solutions prepared by this procedure were placed in matched 2 cm. silica absorption cells and scanned from 400 to 290 mμ. The resulting curves showed the complex to absorb at 310 mμ and the absorption at this wave length increased as the concentration of the sulfosalicylic acid increased. Data taken from a typical set of curves are plotted in Fig. 1, curve 1.

For the continuous variation studies, solutions of the NaOH–niobate and the sulfosalicylic acid solutions were prepared by dilution so that the molarity of each solution was the same. A series of 7 to 9 solutions for absorption measurements were then prepared by mixing varying amounts of these two solutions so that in each case the combined volume was constant. The *p*H was adjusted to approximately 4 by adding small amounts of $HClO_4$, but the quantity added did not cause any significant volume change in the niobium sulfosalicylic acid solution. Reference solutions in each case were the same in composition and concentration except that the niobium was absent. Data from two typical runs are plotted in Fig. 2.

Analytical.—Analysis of the NaOH–niobate solutions used in forming the niobium sulfosalicylic acid complex was accomplished gravimetrically. An aliquot of the solution to be analyzed was acidified with 2 *N* HCl solution whereupon the Nb_2O_5 precipitated. After a short period of digestion, the precipitate was filtered with suction, using Whatman No. 42 paper, and thoroughly washed with hot water. The filter paper and precipitate were placed in a previously weighed crucible and heated slowly at first, and finally to red heat to drive off all the carbon and volatile matter. The residue was weighed as Nb_2O_5 and then converted to Nb by the gravimetric factor 0.6990.

Results and Discussion

Although it is known that the method of continuous variations possesses certain limitations it was tried for the determination of the maximum number of ligands per metal atom in the complex species. The results presented in Fig. 2 indicate a 1:2 ratio of the niobium to the sulfosalicylato group in the 10^{-3} to 7.5×10^{-4} *M* concentration range.

Only one absorption peak at 310 mμ was noted in the absorbancy measurements made on the solutions used in these continuous variations studies and it was reasoned that it indicated only the concentration of the highest complex species in the over-all equilibrium constant equation

$$K = C_{[NbO(SSal)_2]}/(C_{Nb})(C_{SSal})^2 \qquad (1)$$

For the calculation of this over-all constant K we modified a method previously employed by Mukherji and Dey.[7] For simplicity, let "x" equal the concentration of the complex species and "a" and "b" the initial concentrations of the niobium species and the chelating agent, respectively, in a given solution.

Using two concentrations, a_1, a_2 and b_1, b_2, of the reactants, having the same value of x, *i.e.*, the same absorbancy ($A = 0.6$ in Fig. 2), we have

$$K = x/(a_1 - x)(b_1 - 2x)^2 = x/(a_2 - x)(b_2 - 2x)^2 \qquad (2)$$

or

$$4(a_2 + b_2 - a_1 - b_1)(x)^2 + (4a_1b_1 - 4a_2b_2 + b_1^2 - b_2^2)(x) + (a_2b_2^2 - a_1b_1^2) = 0 \qquad (3)$$

From the graph (Fig. 2) it was determined that $a_1 = 3.3 \times 10^{-4}$, $b_1 = 4.2 \times 10^{-4}$, $a_2 = 6.3 \times 10^{-4}$ and $b_2 = 3.7 \times 10^{-4}$. So equation 3 becomes

$$10^{-3}(x)^2 - 3.385 \times 10^{-7}(x) + 2.803 \times 10^{-11} = 0 \qquad (4)$$

and x was calculated to be 1.94×10^{-4} or 1.444×10^{-4}. Using the latter value for substitution into equation 2, since the other value gives an unreasonable answer, K was computed to be 4.52×10^7.

This over-all formation constant can be considered to represent the product of the two separate formation constants, k_1 and k_2, for the equilibrium involved in the formation of this complex species. For the evaluation of these individual step constants, absorption measurements were made on a series of solutions where the concentration of the niobium was constant and the concentration of the sulfosalicylic acid was progressively increased. Curve No. 1 of Fig. 1 shows the increasing absorbance at 310 mμ with increasing concentration of the ligand. As no other absorption peak than the 310 mμ was noted in these solutions and since the relative concentration of the ligand was so much

greater than that of the niobium, it was considered that the main equilibrium would be the step, NbO $(SSal)_{2-m} + m(SSal) = [NbO(SSal)_2]$, and $k_2 = C_{[NbO(SSal)_2]}/(C_{NbO(SSal)_{2-m}})\ (C_{SSal})^m$.

Using a method previously described[8,9] it was possible to calculate A_0, the limiting absorbance, for this complex species from the straight line plot of A *vs.* C_{SSal}/A. With A_0 known a modification[9] of equation C13 of Newman and Hume,[6] $\log(A_0 - A)/A = -(m)\log C_{SSal} - \log k_n$, could be used under these circumstances to evaluate k_n, and here $n = 2$.

In Fig. 3 a plot of $\log (A_0 - A)/A$ *vs.* $\log C_{SSal}$ is noted to give a straight line with a slope for m of unity (actually 1.025 using the method of least squares), which indicates that one (SSal) group is being added in this equilibrium step. From this plot k_2 was calculated to be 4.18×10^3, then k_1 is given by K/k_2 and equals 1.08×10^4.

When the NaOH–niobate solution was treated with the sulfosalicylic acid solution the greenish-yellow color reported by Sudarikov and Busarov[4] was observed. Treating this resultant solution with an equal volume of acetone caused a finely divided greenish-yellow solid to precipitate. The results of the analysis of this precipitate, however, could not be interpreted to indicate any definite empirical formula.

The infrared spectrum of this solid precipitate, using the KBr wafer technique, showed a small absorption peak at 10.9–11.0 μ which was believed to represent the NbO bond.[8]

THERMODYNAMICS OF THERMOCELLS WITH FUSED OR SOLID ELECTROLYTES

BY KENNETH S. PITZER

Department of Chemistry and Lawrence Radiation Laboratory, University of California, Berkeley 4, California

Received July 21, 1960

The thermodynamic principles related to thermocells are reviewed. The equation for the potential of a cell with a single component electrolyte, such as a fused or solid salt, is similar to that for a cell with aqueous solution electrolyte after the Soret equilibrium has been established. In particular the total "transported entropy" of the ionic species reacting at the electrodes may be obtained without any complication from transference numbers, and values of this quantity are given for several cells. The meaning and measurability of the partial molal entropies of single ions in electrolytes are considered. It is found that the transported entropy of metal ions in fused salts is approximately equal to estimated values of the partial molal entropies of these ions; hence the entropies of transfer are small. In solid electrolytes the entropies of transfer are sometimes large and are discussed in terms of the probable conductance mechanisms.

Through the years several thermocells with fused salt or solid salt electrolytes have been investigated.[1-5] Recent work in other fields gives us now a clearer picture of the conduction mechanism in the solid electrolytes as well as additional data for the liquids. Also some of the previous discussions of these thermocells are confused unnecessarily by apparent uncertainties in transference number. Hence it seems worthwhile to look again at the information on these systems.

Thermodynamic Relationships.—The thermodynamics of a thermocell was derived by Eastman[6] and in greater detail by Wagner.[7] We shall follow the definitions and terminology of Agar and Breck[8] and confine our attention to cells with pure metal electrodes and simple MX_ν electrolytes where X is a halogen or nitrate. The e.m.f. of the cell $\mathcal{E}$ is defined as the electrical potential of a wire attached to the hot electrode less the potential of a similar wire attached to the cold electrode. The electrical work for ν equivalents of electricity is determined by the entropy absorbed from the heat reservoir surrounding the hot electrode when this positive electricity passes through the cell from the cold to the hot electrode. This entropy is equal to the sum of the entropy absorbed in the electrode reaction, in this case $\bar{S}_M - \bar{S}_{M^{+\nu}} - \nu\bar{S}_{e^-(M)}$ and the entropy transported away from the hot electrode region, in this case $-S^*_{M^{+\nu}} - \nu S^*_{e^-(M)}$. Here S_M is the molal entropy of the metal, $\bar{S}_{M^{+\nu}}$ and $S^*_{M^{+\nu}}$ are the partial molal entropy and the entropy of transfer, respectively, of the $M^{+\nu}$ ion, and $\bar{S}_{e^-(M)}$ and $S^*_{e^-(M)}$ are the corresponding properties of the electron in the metal M. These terms may be combined to yield

$$\nu \mathfrak{F} \frac{d\mathcal{E}}{dT} = S_M - \bar{S}_{M^{+\nu}} - \nu\bar{S}_{e^-(M)} \qquad (1)$$

where $\bar{S}_{M^{+\nu}}$, the total "transported entropy" of the ion $M^{+\nu}$, is the sum of the partial molal entropy of the ion and the entropy of transfer. The quantity $\bar{S}_{e^-(M)}$ is, similarly, the "transported entropy" of electrons in the metal M.

It is desirable to note at this point the relationship to aqueous solution thermocells. After the Soret equilibrium is established, equation 1 is applicable to the corresponding aqueous solution cell, but at uniform electrolyte concentration in each half cell the expression contains the additional term $t_- \times (S^*_{M^{+\nu}} + \nu S^*_{X^-})$ where t_- is the transference number of the negative ion. In the aqueous solution the sum of the two ionic entropies of transfer is the

(1) L. Poincaré, *Ann. chim. phys.*, [6] **21**, 289 (1890).

(2) H. Reinhold and A. Blachny, *Z. Elektrochem.*, **39**, 290 (1933); H. Reinhold, *Z. anorg. allgem. Chem.*, **171**, 181 (1928).

(3) H. Holtan, Thesis, Utrecht, 1953; *Tids. Kjemi Bergvesen Met.*, **12**, 5 (1952).

(4) B. R. Sundheim and J. Rosenstreich, THIS JOURNAL, **63**, 419 (1959).

(5) B. F. Markov, *Doklady Akad. Nauk S.S.S.R.*, **108**, 115 (1956).

(6) E. D. Eastman, *J. Am. Chem. Soc.*, **50**, 292 (1928).

(7) C. Wagner, *Ann. Physik*, **3**, 629 (1929); **6**, 370 (1930).

(8) J. N. Agar and W. G. Breck, *Trans. Faraday Soc.*, **53**, 167 (1957).

quantity which governs the Soret equilibrium. However, in a pure salt the transfer of both ions equally in the same direction is just the gross linear movement of the salt which has no net entropy of transfer. Hence the sum $(S^*_{M^{+\nu}} + \nu S^*_{X^-})$ is zero and it is apparent that the transference number drops out of the equation for the pure salt cell. Indeed a tranference number in a single component fused salts can only be defined in an arbitrary manner. While the transference measurements for solid electrolytes by Tubandt[9] yield information of interest for interpretation of the conduction mechanism, there is no need to introduce a transference number in the thermodynamic equation for a pure salt either solid or liquid.

In equation 1 the first quantity on the right is just the molal entropy of the metal which is available from heat capacity data and the third law.[10] Recently Temkin and Khoroshin[11] have given values for $\bar{S}_{e^-}$ in several metals; these values are zero within the uncertainty of presently available thermocell data. Thus equation 1 yields $\bar{S}_{M^{+\nu}}$ from experimental thermocell potentials. Several values obtainable from the literature for fused salts are listed in Table I and similar values for solid electrolytes are given in Table II.

TABLE I

THERMOCELLS WITH FUSED SALT ELECTROLYTES

Electrolyte	Ref.	T, °K	S_M	$-\nu\mathfrak{F}\frac{d\varepsilon}{dT}$	$\bar{S}_{M^{\nu+}}$	$\bar{S}_{M^{\nu+}}$	$S^*_{M^{\nu+}}$
$AgNO_3$	3, 4	500	13.37	7.6	21.0	19	2
AgCl	2, 3, 5	800	16.43	9.3	26	22	4
AgBr	2, 5	750	16.00	11	27	22	5
AgI	2, 5	850	16.84	10	27	24	3
$ZnCl_2$	1	~600	14.41	−6	8	14	−6
$SnCl_2$	1	~600	20.59	+1	22	16	+6

Absolute Ionic Entropies in Fused Salts.—While it is not yet experimentally feasible to measure directly the partial molal entropies of individual ions, a rather convincing theoretical calculation seems possible in favorable cases. Consider first a fused salt wherein the positive and negative ions are identical in every respect except for the sign of the net electrical charge on each. In this case clearly the symmetry of the situation allows one to divide the measured molal entropy equally between the positive and negative ions.

Next let us consider the effects of various differences between the ions. The mass effect on the translational entropy[11a] gives a difference $(3/2)\ R \ln (M_2/M_1)$ between the entropies of species of molecular weights M_2 and M_1. Moderate differences in the short range forces which determine ion size should have no effect since ions of the same sign will seldom contact one another. Consequently the entropy of the metal ion in a simple binary salt is given by the expression

$$\bar{S}_{M^+} = \frac{1}{2}\left(S_{MX} + \frac{3}{2} R \ln \frac{M_M}{M_X}\right) \qquad (2)$$

Wagner[7] estimated the entropy of the ion to be just one-half that of the salt which is our result except for the omission of the mass correction term.

The entropies of free rotation and of vibration of polyatomic ions are readily calculated by standard methods and can be subtracted from the total entropy before apportionment of the translation entropy. In actual cases, however, the rotation will usually be somewhat restricted. If a reasonable estimate can be made of the potential barrier restricting the rotation, then the net internal entropy can also be estimated.

If one type of ion is very much larger than the other, then there will be direct short range repulsive contacts of the large ions. This effect is well known in ionic crystals such as LiI where the anion–anion contacts primarily determine the size of the unit cell. In such cases one expects the freedom of translational motion of the large ions to be less than that of the small ions. It is difficult to calculate the magnitude of this difference but it seems unlikely to exceed a few cal./degree mole except in most extreme cases.

If we apply these methods to $AgNO_3$ at 500°K. and assume a 4.5 cal./deg mole reduction in rotational entropy of NO_3^- from restriction of rotation, the net internal entropy of NO_3^- is 19.7 cal./deg.

TABLE II

THERMOCELLS[2] WITH SOLID SALT ELECTROLYTES

Electrolyte	T, °K	S_M	$-\nu\mathfrak{F}\frac{d\varepsilon}{dT}$	$\bar{S}_{M^{\nu+}}$
AgCl	400	11.98	32	44
	500	13.37	27.6	41.0
	600	14.55	23.1	37.6
	700	15.55	16.2	31.8
AgBr	400	11.98	34	46
	500	13.37	25.8	39.2
	600	14.55	18.2	32.8
AgI (II)	400	11.98	28.6	40.6
AgI (I)	500	13.37	12.9	26.3
	600	14.55	12.9	27.4
CuCl	400	9.70	23	33
	500	11.07	21.5	32.6
	600	12.22	19.8	32.0
CuBr	400	9.70	36	46
	500	11.07	29.5	40.6
	600	12.22	22.8	35.0
CuI (III)	400	9.70	23	33
	500	11.07	21.5	32.6
	600	12.22	19.8	32.0
CuI (I)	750	13.66	8	22
$PbCl_2$	500	18.87	27	46
$PbBr_2$	500	18.87	21	40
PbI_2	550	19.55	−18	2
	650	21.65	− 9.2	12.5

(9) C. Tubandt, *Handbuch Exp.-Physik* **XII**, 1, 394 ff., Leipzig (1932).

(10) D. R. Stull and G. C. Sinke, "Thermodynamic Properties of the Solvents," American Chemical Society, Washington, D. C., 1956.

(11) M. I. Temkin and A. V. Khoroshin, *Zhur. Fiz. Khim.*, **26**, 500 (1952).

(11a) This mass relationship is valid for the solid, liquid or gas state, regardless of restraining forces, provided the particles are heavy enough to eliminate quantum effects at the temperature of interest. The integration of the classical partition function for the kinetic energy yields a factor $m_i^{3n_i/2}$ for n_i particles of mass m_i (see R. H. Fowler and E. A. Guggenheim, "Statistical Thermodynamics," Cambridge University Press, 1939, p. 257) and the usual relationship of partition function to entropy yields the result given.

mole. The heat capacity of silver nitrate has been measured and the data as summarized by Kelley[12] yield the entropy value 54.04 cal./deg. mole at 500°K. With the mass correction of equation 2 one then finds $\bar{S}_{Ag^+} = 19.0$ cal./deg. mole in fused $AgNO_3$ at 500°K.

The calculation of the partial molal entropy of silver ion in the fused halides follows the same principles but is simplified by the absence of internal entropy for the anions. The results, based upon Kelley's tables, are given in Table I. No correction has been made for anion–anion repulsions in these values; such effects would further restrict anion motion and reduce the anion entropy. Consequently, the cation entropies would be increased by this effect which may or may not be significantly large.

Entropies of Transfer in Fused Salts.—The last column in Table I gives the values of the entropy of transfer which follow from the experimental data and our calculation of the absolute ion entropies. In a simple MX salt in the liquid state all of the ions are presumably free to migrate without large activation energy. Nothing in the nature of the fused salt seems to indicate any other source of significant heat of transfer. Consequently, we expect the heat and entropy of transfer to be small for the various silver salts. The values of S^* in Table I are indeed small and may be further reduced by a modest correction to $\bar{S}$ for anion–anion repulsion effects.

Ionic Entropies in Solid Electrolytes.—In accordance with the usual definition the partial molal entropy of an ion in a solid electrolyte is the increase in the total entropy of the solid upon addition of extra ions divided by the molal amount of ions added. Space charge effects will actually limit additions to very small amounts in the case of ions. If the lattice of the solid electrolyte were perfect, this process of addition would be difficult to interpret, but actual crystals at finite temperatures contain significant numbers of defects such as vacancies. The actual addition process is readily interpreted in terms of these defects. For example in the silver halides the defects are predominantly vacancies in the positive ion lattice and interstitial positive ions. Suppose there are N_1 vacancies and correspondingly N_1 interstitials per mole of silver halide. The addition of N_2 excess silver ions, where $N_2 << N_1$, will yield a final state in which there are N_2 more interstitials than vacancies. One can easily show that the equilibrium state after the addition will have approximately $(N_1 + 1/2\ N_2)$ interstitial atoms and $(N_1 - 1/2\ N_2)$ vacancies.

While it is possible to define equilibrium entropies of interstitial ions, vacancies, etc., and to express the partial molal entropy of ions in the solid in these terms, there are no experimental values now available for comparison. However, this discussion indicates the mechanisms by which extra ions may be accommodated in crystals containing defects.

Transported Entropy of Ions in Solids.—We now turn to the discussion of the experimentally measured total transported entropy of the positive ion. The actual conduction mechanism must be considered. Mott and Gurney,[13] Wagner[14] and Hauffe[15] have reviewed work which indicates for the systems of Table II conductance by three types of carriers: (a) interstitial cations, (b) cation vacancies, (c) anion vacancies. In the case of conduction by interstitial cations the transported entropy is just the sum of the partial molal entropy of the interstitial ion and its entropy of transfer. In the other cases the cation produced at the electrode either fills a cation vacancy in case (b) or extends the lattice and creates ν anion vacancies in case (c); also there are the entropies of transfer of the respective vacancies. These results are summarized by the equations

$$\text{(a)}\quad \bar{S}_{M^{+\nu}} = \bar{S}_{M,\bigcirc} + S^*_{M,\bigcirc} \tag{3a}$$

$$\text{(b)}\quad \bar{S}_{M^{+\nu}} = (\bar{S}_M{}^i - S_{M,\square}) - S^*_{M,\square} \tag{3b}$$

$$\text{(c)}\quad \bar{S}_{M^{+\nu}} = (\bar{S}_M{}^i + \nu\bar{S}_{X,\square}) + \nu S^*_{X,\square} \tag{3c}$$

where $M,\bigcirc$ indicates an interstitial cation, M, $\square$ or X, $\square$, cation or anion vacancies, respectively, and $\bar{S}_M{}^i$ is the entropy of a cation in an ideal lattice site.

While it is not feasible to calculate these various entropy quantities accurately, certain properties may be defined which make estimates possible. The partial molal entropies of defects all contain terms for the entropy of distribution over the possible sites which have the form $-R \ln x_i$ where x_i is the ratio of defects to sites. In many cases $x_i \cong 10^{-4}$ which yields an entropy term of $\sim$18 cal./deg. mole which is a positive contribution in cases (a) and (c) but negative in (b). The entropy of thermal vibration of the cation also enters either in $\bar{S}_{M,\bigcirc}$ or $\bar{S}_M{}^i$ (but not for vacancies), and its magnitude may be estimated to be approximately the same as the entropy of the metal S_M. The entropies of transfer may be expected to be positive and of the order of the energy of activation for ion migration divided by the temperature. In the case of AgBr, Teltow[16] gives energies of activation of approximately 2.5 kcal./mole for interstitial cations and 5.5 kcal./mole cation vacancies. Combination of these values for AgBr in the 400–600°K. range yields the estimates for $\bar{S}_{M^{+\nu}}$ of 35 to 45 cal./deg. mole for case (a) and -5 to -15 cal./deg. mole for case (b).

In the best studied case of AgBr, Teltow's results[16] indicate that at 400°K. the conductance is almost entirely by interstitial ions, case (a), and the value of $\bar{S}$ in Table II is reasonable on this basis. At 500 and 600°K., respectively, the vacancy conduction is reported to constitute approximately 10 and 30% of the total, and this shift of part of the current to mechanism (b) is rather more than sufficient to explain the reduction of $\bar{S}$ with increase in temperature. The properties of the other silver and cuprous halides[13,14] are sufficiently similar to AgBr to indicate a parallel explanation, but the available data are much less detailed.

(12) K. K. Kelley, U. S. Bureau of Mines Bulletins 477 and 584, U. S. Government Printing Office, Washington, D. C., 1950 and 1960.

(13) N. F. Mott and R. W. Gurney "Electronic Processes in Ionic Crystals," Oxford University Press, 1948.

(14) C. Wagner, *J. Electrochem. Soc.*, **99**, 346C (1952).

(15) K. Hauffe, "Reaktionen in und an Festen Stoffen," Springer-Verlag, Berlin–Gottingen–Heidelberg, 1955.

(16) J. Teltow, *Ann. Physik*, [6] **5**, 63, 71 (1949); *Z. Physik. Chem.*, **195**, 197, 213 (1950).

Tubandt[9] reports 100% anion transference for $PbCl_2$ and $PbBr_2$ but about 50% for PbI_2 at the temperature of interest. Since vacancy mechanisms are presumably involved, we may assume mechanism (c) for the chloride and bromide and half (b)–half (c) for the iodide. However, Mott and Gurney[13] show that many of the data indicate conductance on the surfaces rather than through the lattice. Hence it seems best to merely note qualitative agreement between the large values of $\bar{S}$ found for $PbCl_2$ and $PbBr_2$ with the expectation for mechanism (c) and the lower value for PbI_2 with the expectation for the mixture of mechanisms (b) and (c).

This research was carried out under the auspices of the U. S. Atomic Energy Commission.

THERMODYNAMICS OF WATER AND *n*-BUTANE ADSORPTION BY Li-KAOLINITE AT LOW COVERAGES[1]

BY J. J. JURINAK AND D. H. VOLMAN

Department of Soils & Plant Nutrition and Department of Chemistry, University of California, Davis, California

Received July 22, 1960

Differential ΔH and ΔS values are calculated for the adsorption of *n*-butane and water by Li-kaolinite. Experimental ΔS values are compared with ideal standard states of localized and mobile adsorption models. Butane adsorption is described as mobile with modification for surface heterogeneity and adsorbate interaction. Water adsorption is not adequately described by either model. Molecular interaction results in adsorbate orientation which is of the same magnitude as found in ice. Adsorbed water prior to interaction is mobile and after interaction develops surface lens.

Introduction

Preliminary investigations[2] concerning the effect of degassing temperature on water adsorption by Li^+ and Ca^{++} kaolinite have indicated that adsorption by Li-kaolinite which has been degassed between 33–70° is reversible. It was concluded that Li-kaolinite represents a first approximation of a clay mineral surface whose attraction for water is independent of ionic hydration effects. This report represents an attempt to characterize by thermodynamics the nature of water adsorbed by Li-kaolinite and to compare the reaction with the adsorption of n-butane on the same surface.

Experimental

The kaolinite used was from Dry Branch, Georgia, and donated by the Georgia Kaolinite Company. The exchange capacity was determined as 1.5 meq./100 g. with regard to the lithium ion. Surface area was determined by *n*-butane adsorption at 0.0° and was calculated as 15.0 $m.^2/g.$ Clay preparation and adsorption apparatus have been previously described.[2,3] Prior to adsorption the samples were degassed at 65–70° for 48 hours at 10^{-6} mm. pressure. Adsorption data for water were obtained at 29.45 ± 0.05°. Data for *n* butane adsorption were obtained at 0.0° and 15.45 ± 0.15°. Data at both temperature for water adsorption were obtained from a composite of 4 independently run samples. Butane adsorption data were obtained from 2 independent samples. Both adsorbates were thoroughly degassed by alternate freezing and thawing under vacuum.

Calculations

The thermodynamic adsorption model of this study has been used by various workers[4-6] who differ mainly in their choice of the standard adsorbed state. The differential molar free energy, enthalpy, and entropy is defined for the isothermal change in the transfer of one mole of adsorbate from its standard 3 dimensional gas state, 760 mm., to a surface in equilibrium with a vapor, which contains adsorbed molecules at a certain surface concentration. The differential (isosteric) heat, ΔH, of adsorption is calculated by the Clausius–Clapeyron equation and the differential entropy, ΔS, is calculated by the relation between the functions.

Interpretation of entropy calculations as developed by DeBoer and Kruyer[5] is based on the comparison of experimental data with two ideal unimolecular models. If ideal localized or site adsorption occurs the entropy decrease is given by

$$-\Delta S_{\mathrm{Loc}} = {}_3S_t + R \ln \frac{\theta}{1-\theta} \qquad (1)$$

where ${}_3S_t$ is the 3 dimensional translation entropy of the gas, θ is the degree of surface coverage and $R \ln [\theta/[1-\theta)]$ is the differential molar entropy of configuration. To allow comparisons, calculations are based on the same standard states, hence ${}_3S^0/_t$ for the gas phase is calculated by the Sackur—Tetrode equation and $\theta = 1/2$ is chosen as the standard surface coverage. Thus equation 1 becomes

$$-\Delta S^0_{\mathrm{Loc}} = {}_3S^0{}_t \qquad (2)$$

If ideal mobile adsorption occurs, the three dimensional translation entropy is replaced by a two dimensional entropy ${}_2S_t$, hence

$$-\Delta S_m = {}_3S_t - {}_2S_t \qquad (3)$$

The ${}_2S^\circ{}_t$ for the standard state is calculated from the equation of Kemball[7]

$${}_2S^0{}_t = R \ln (MTA^0) + 65.80$$

where M is the molecular weight and A^0 is the standard molecular area which is obtained from the 2 dimensional gas law using the standard spreading pressure of 0.338 dyne/cm. Equation 3 becomes

(1) Support of this work by a grant (NSF-G10228) from the National Science Foundation is gratefully acknowledged.

(2) J. J. Jurinak, THIS JOURNAL, **65**, 62 (1961).

(3) F. A. Bettleheim, C. Sterling and D. H. Volman, *J. Polymer Sci.*, **22**, 303 (1956).

(4) C. Kemball and E. K. Rideal, *Proc. Roy. Soc. (London)*, **A187**, 53 (1946).

(5) D. H. Everett, *Trans. Faraday Soc.*, **46**, 942 (1950).

(6) J. H. DeBoer and S. Kruger, *Proc. Kon. Akad. V. Wet*, **B55**, 451 (1952); **B58**, 61 (1955).

(7) C. Kemball, *Proc. Roy. Soc. (London)*, **A187**, 73 (1946).

$$-\Delta S_m^0 = {}_3S^0_t - {}_2S^0_t \quad (4)$$

The experimental data is compared with the two standard models, equations 2 and 4, using the following

$$-\Delta S^0_{Loc} = -\Delta S - R \ln \frac{\theta}{1-\theta} \quad (5)$$

$$-\Delta S^0_m = -\Delta S - R \ln \frac{A^0}{A} \quad (6)$$

Results

Figure 1 and 2 show the adsorption of *n*-butane and water vapor, respectively, by lithium kaolinite at the designated temperatures. Figure 3 shows the experimental ΔH and ΔS of *n*-butane adsorption by Li-kaolinite as a function of coverage. The variability of the functions at low coverages indicate surface heterogeneity. Figure 4 shows the ΔH and ΔS for the adsorption of water on the same surface. The ΔS values shown in Figs. 3 and 4 were used to calculate $\Delta S°$ for the standard states of the two ideal models of adsorption. The results of the comparison between the experimental entropy values and the theoretical figures are shown in Tables I and II.

TABLE I

ENTROPIES OF *n*-BUTANE ADSORPTION BY LI-KAOLINITE AT $T = 288°K.$

Localized: standard state, $w/w_m = 0.5$. Mobile: standard state $A^0 = 1175 \times 10^{-16}$ cm.^{2}.

w/w_m	$-\Delta S^0_{Loc}$, e.u.	${}_3S^0_t$, e.u.	$-\Delta S^0_m$, e.u.	${}_3S^0_t - {}_2S^0_t$, e.u.
0.01	24.1	37.9	15.2	11.9
.02	23.5	37.9	16.3	11.9
.05	14.6	37.9	8.5	11.9
.10	11.4	37.9	5.0	11.9
.20	16.8	37.9	11.7	11.9
.30	18.8	37.9	13.1	11.9
.40	18.6	37.9	13.1	11.9
.50	18.0	37.9	12.9	11.9
.60	17.5	37.9	12.8	11.9
.70	16.6	37.9	12.6	11.9
.80	15.7	37.9	12.3	11.9
.90	14.1	37.9	12.2	11.9
1.0			12.1	11.9

TABLE II

ENTROPIES OF WATER ADSORPTION BY LITHIUM KAOLINITE, $T = 296°K.$

Localized: standard state, $w/w_m = 0.5$. Mobile: standard state, $A^0 = 1208 \times 10^{-16}$ cm.^{2}

w/w_m	$-\Delta S^0_{Loc}$, e.u.	$3S^0_t$, e.u.	$-\Delta S^0_m$, e.u.	$3S^0_t - 2S^0_t$, e.u.
0.15	6.83	34.5	−1.75	10.7
.2	12.8	34.5	4.1	10.7
.3	34.3	34.5	25.8	10.7
.4	37.0	34.5	28.9	10.7
.5	36.5	34.5	28.7	10.7
.6	34.0	34.5	26.5	10.7
.7	26.5	34.5	19.7	10.7
.8	25.3	34.5	19.4	10.7
.9	22.2	34.5	17.5	10.7
1.0			17.4	10.7

Discussion

The data shown in Table I indicate that, over a large range of surface coverage, the adsorption of *n*-butane by Li-kaolinite agrees favorably with

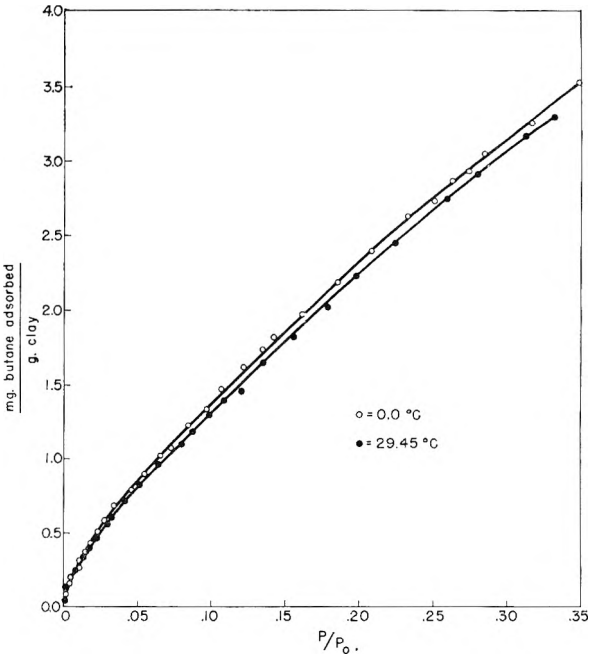

Fig. 1.—Adsorption of *n*-butane by Li-kaolinite at the designated temperatures.

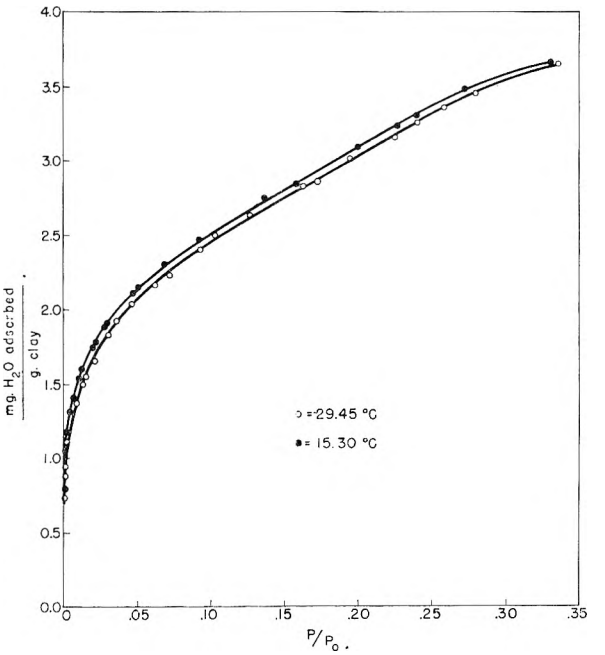

Fig. 2.—Adsorption of water vapor by Li-kaolinite at the designated temperatures.

the mobile adsorption model. The restriction noted in the freedom of the butane molecule at low coverages is ascribed to heterogeneity and is more evident from the data of Fig. 3. At coverages between 0.10 and 0.20, the adsorbate exhibits more freedom than a two dimensional gas, *i.e.*, super mobility, suggesting the presence of a weak vibration perpendicular to the surface replacing the translational entropy loss.[8] The minimum in the ΔH values supports this view. In the coverage range of 0.4 to 0.7, the $-\Delta S^0_m$ values indicate re-

(8) C. Kemball, "Advances in Catalysis," Vol. II, Academic Press Inc., New York, N. Y., 1950, p. 233.

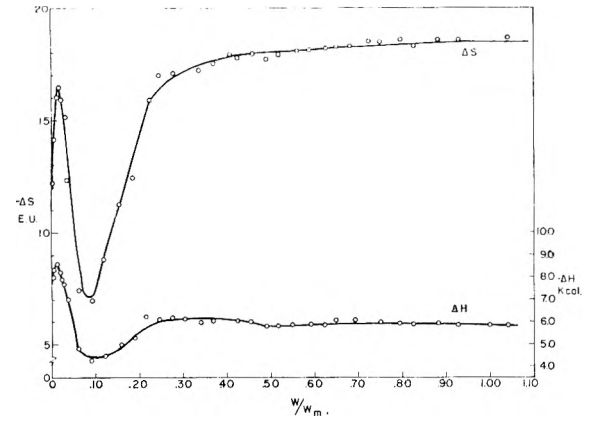

Fig. 3.—Thermodynamics of *n*-butane adsorption by Li-kaolinite at $T = 288°K.$

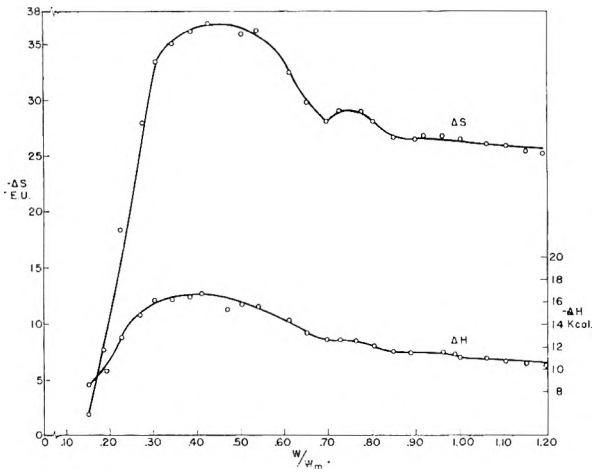

Fig. 4.—Thermodynamics of water vapor adsorption by Li-kaolinite at $T = 296°K.$

stricted freedom suggesting intermolecular attraction which is also reflected by a corresponding increase in the ΔH values. The data further indicate that kaolinite exhibits a surface of considerable homogeneity. Adsorbate interaction during *n*-butane adsorption was also obtained by Ross and Good[9] who used Spheron 6 (2700) carbon black. Adsorption by the carbon black surface produced higher heats of adsorption and greater restriction of butane freedom when compared to the Li-kaolinite surface.

The thermodynamic data of water adsorption by Li-kaolinite as shown by Fig. 3 and Table II is in contrast to corresponding butane adsorption data. Table II shows that between coverages of approximately 0.3 and 0.6 adsorption is described as immobile or localized with an indication that all translation as well as some rotational entropy is lost. However since the loss of translation entropy occurs after an appreciable amount of the surface is covered and is preceded by a region in which water exhibits considerable freedom, the loss of entropy is considered to result from causes other than adsorption site bonding. The characteristic ability of water to associate suggests that as surface coverage increases intermolecular attraction induces mutual orientation of water molecules producing the decrease in entropy noted in Fig 3. The entropy of the adsorbed water in this zone of orientation, calculated by subtracting experimental ΔS values from $S°_{298}$ of the standard gas state, varies from 9.0 to 11 e.u. The entropy of ice[10] at 273°K. is calculated to be 9.9 e.u. From these data it is inferred that the orientation of the water molecules on the surface produces a restriction in freedom of the same magnitude as that experienced in ice. Data indicates a definite structure water layer in the coverage range of 0.3 to 0.6. Whether the structure corresponds to ice, however, remains speculative. Prior to interaction the adsorbed water exhibits a high degree of freedom which occurs at about the same coverage that produces "supermobile" butane adsorption. Adsorbate mobility lends credence to the view that water adsorption by Li-kaolinite can be regarded as physical. However, the recent work of Folman and Yates[11] interjects the possibility that a portion of the variability of the thermodynamic function may be due to solid phase perturbance at low coverages which would be incorporated in the data.

At coverages beyond 0.60, the freedom of the adsorbed water molecule increases to that slightly greater than liquid water. A reasonable explanation is the development of lenses or islands of adsorbate on the surface prior to the development of a true multilayer phase. In the coverage range of lens formation the ΔS value would be expected to be less than 28.4 e.u. which is the S^0_{Vap} at 298°K.[12]

(9) W. Ross and R. J. Good, THIS JOURNAL, **60**, 1167 (1956).

(10) W. F. Giauque and J. W. Stout, *J. Am. Chem. Soc.*, **58**, 1144 (1936).

(11) M. Folman and D. J. C. Yates, *Trans. Faraday Soc.*, **54**, 429 (1958).

(12) D. D. Wagman, J. E. Kilpatrick, W. J. Taylor, K. S. Ditzer and F. D. Rossini, *J. Research Natl. Bur. Standards*, **34**, 143 (1945).

THERMOCHEMISTRY OF THE ACID HYDROLYSIS OF POTASSIUM CYANATE[1,2]

BY CECIL E. VANDERZEE AND RALPH A. MYERS[3]

Avery Laboratory of Chemistry of the University of Nebraska, Lincoln, Nebraska

Received July 21, 1960

The conditions for stoichiometric acid hydrolysis of cyanate, $KNCO + 2H^+ + H_2O \rightarrow K^+ + NH_4^+ + CO_2$, without interference from side reactions, require H^+ concentration above 0.06 *M* to suppress urea formation, and require addition of the acid *to* the cyanate solution; high local concentrations of HNCO lead to cyanuric acid formation. Consistent with these requirements, studies of the acid hydrolysis in a solution calorimeter, together with studies of the heat of solution of KNCO, lead to ΔHf^0 equal to −99.85, −95.01 and −34.97 kcal. mole^{-1} for KNCO(s), KNCO(aq) and NCO^-(aq), respectively, at 25°. The standard deviation of the experimental measurements was ±0.06 kcal. mole^{-1}.

Introduction

In the intervening time since Wöhler's synthesis of urea, the thermodynamic properties of urea and ammonium ion have been reliably established, but those of cyanate ion and cyanic acid retain considerable uncertainty. Considering the borderline position of cyanic acid among the fields of inorganic, organic and biochemistry, with the result that the literature on the compound is widely scattered, and with most of the interest and emphasis focused on its derivatives, it is perhaps not surprising that the thermodynamic properties of the compound itself have not been closely investigated. Examination of the literature reveals much descriptive and qualitative information but little of a quantitative nature.

Lewis[4] took advantage of reversible routes for the formation of cyanic acid and cyanate ion to calculate free energies of formation. The heats of formation reported in Circular 500, National Bureau of Standards,[5] are based on studies of the acid hydrolysis of cyanate ion by Lemoult[6] and some combustion and solution data by Berthelot.[7,8] These early studies were carried out under poorly specified conditions, making correction to present standard conditions difficult if not almost impossible. Recently Lord and Woolf[9] made calorimetric studies on the acid hydrolysis of sodium cyanate. However, due to appreciable dead space in their calorimeter, their final state for the CO_2 formed could not be clearly specified. For reactions in 0.05 to 0.02 *N* HCl they assumed that most of the CO_2 (0.01 *M*) stayed dissolved, while for reaction in 1 *N* H_2SO_4 they assumed practically complete escape of gaseous CO_2 during the run. These contradictory positions for 0.01 *M* CO_2 appear to have been compensated for partly by questionable handling of heats of dilution for H_2SO_4 and partly by differences in stoichiometry, since neither of their conditions for reaction would be free from side reactions, according to the requirements we have found for exact stoichiometry.

The reaction chosen by Lemoult[6] and by Lord and Woolf[9]

$$NCO^-(aq) + 2H^+(aq) + H_2O(l) \longrightarrow NH_4^+(aq) + CO_2(aq) \quad (1)$$

would appear to be most appropriate for determination of $\Delta Hf^0NCO^-(aq)$, since reliable values are known for the heats of formation of the other species. It must first be shown, however, that the conditions for exact stoichiometry have been met, and that these conditions are compatible with accurate calorimetry and accurate corrections to standard states. Examination of recent kinetic studies by Amell,[10] Kemp and Kohnstam[11] and Wyatt and Kornberg[12] suggested that the competing reaction in solution

$$HNCO + NH_3 \longrightarrow CO(NH_2)_2 \quad (2)$$

would be negligible compared to the desired reaction 1, provided that the acidity was kept sufficiently high to supress urea formation. On the other hand, high acidity and high concentration of HNCO lead to polymerization to cyanuric acid

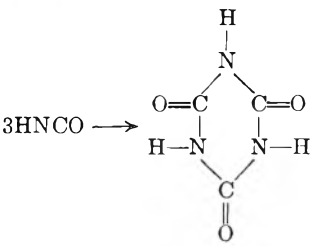

(3)

Both Amell[10] and Lemoult[6] presented analytical evidence that in reaction 1 from 97.5 to 101% of the theoretical amount of acid was used, but neither gave the conditions of reaction, *e.g.*, concentration of acid and of cyanate, or sequence of operations. Lewis and Brighton[13] studied reaction 1 as a possible quantitative procedure for cyanate, but discarded the method when their analyses for acid used and ammonia produced amounted to no more than 92% of the cyanate used, even when the reaction was carried out in sealed tubes at 100° for an hour. They did not report the details of their procedure,

(1) From the Ph.D. Thesis of Ralph A. Myers, October, 1958.

(2) We shall use the common term cyanic acid to denote the acid formed from acidification of the cyanate salts, even though the structure HNCO, isocyanic acid, is more compatible with its reactions, and shall use the expressions KNCO, HNCO and NCO^- in referring to the compounds throughout this paper.

(3) Monsanto Chemical Company Fellow, 1957–1958.

(4) G. N. Lewis and M. Randall, "Thermodynamics and Free Energy of Chemical Substances," McGraw-Hill Book Co., Inc., New York, N. Y., 1923.

(5) "Selected Values of Chemical Thermodynamic Properties," Natl. Bur. Standards, Circular 500, Washington, D. C., 1952.

(6) P. Lemoult, *Ann. chim. et phys.*, [6] **16**, 338 (1899).

(7) M. Berthelot, *ibid.*, [4] **4**, 74 (1873).

(8) M. Berthelot, *ibid.*, [6] **11**, 145 (1897).

(9) G. Lord and A. A. Woolf, *J. Chem. Soc.*, 2546 (1954).

(10) A. R. Amell, *J. Am. Chem. Soc.*, **78**, 6234 (1956).

(11) I. A. Kemp and G. Kohnstam, *J. Chem. Soc.*, 900 (1956).

(12) P. A. H. Wyatt and H. L. Kornberg, *Trans. Faraday Soc.*, **48**, 454 (1952).

(13) G. N. Lewis and T. B. Brighton, *J. Am. Chem. Soc.*, **40**, 482 (1918).

other than the use of "dilute" acid (HCl). We have found that a suitable range of conditions for exact stoichiometry does exist (see Experimental), which requires that the cyanate be first dissolved and then acidified, with the final acidity not less than 0.06 *M* HCl. Apparently lower acidity allows urea formation, reaction 2, while addition of the solid potassium cyanate produces cyanuric acid due to high local concentrations of HNCO.

Two practical considerations limit the amount of cyanate which can be used in a calorimetric run: (a) concentrations greater than 0.03 *M* would produce partial pressures of CO_2 greater than 1 atm. in the final solution, producing problems with its confinement in the calorimeter; (b) concentrations greater than 0.05 *M* would probably yield complicating amounts of cyanuric acid. Accordingly, 0.01 mole of cyanate per liter was judged to be an optimum amount for the calorimetric reaction process.

The need for considerable excess acid in the runs leads to large heat of dilution corrections. Accordingly, these were checked experimentally, as was the heat of "unmixing" the final solution, and the heat of solution of potassium cyanate.

Experimental

All solutions used in this research were prepared from conductivity grade distilled water collected near its boiling point. All analytical apparatus was carefully calibrated, and standard analytical procedures were used throughout. Weighings of large amounts of water or solutions were made on a 5-kg. capacity Sederer–Kohlbusch analytical balance. The primary standard of temperature was a platinum resistance thermometer bearing a NBS certificate with a Leeds and Northrup Type G-1 Mueller Bridge and its manufacturer's certificate of calibration.

Purification of Potassium Cyanate.—Freshly opened bottles of newly purchased potassium cyanate (Baker Analyzed Reagent or Fisher Certified Reagent) all had a distinct odor of ammonia and gave strong tests for carbonate, the result of hydrolysis by traces of water or water vapor either retained during preparation or absorbed during storage.

$$KNCO(s) + 2H_2O \longrightarrow NH_3(g) + KHCO_3(s) \quad (4)$$

The recrystallization procedure outlined in Inorganic Syntheses[14] gave considerable improvement in quality. Briefly this procedure consists of preparation of a saturated aqueous solution of KNCO at 50°, neutralization with acetic acid, filtration, treatment with 5 volumes of alcohol, and then refrigeration for several hours, after which the crystals of KNCO are filtered off, washed with alcohol and stored in a desiccator. No matter how many times the process was repeated, however, it failed to yield a product free of carbonate or ammonia. The procedure was therefore modified, with some sacrifice of yield, by reducing the excess of alcohol from 5 to 1 to about 2 to 1; under these conditions coprecipitation of $KHCO_3$ could be avoided. The solution was cooled in an ice-bath for 3 to 4 hours; the fine crystals were then removed by filtration, washed with alcohol, and dried quickly in a vacuum desiccator.

Material twice recrystallized in this manner gave no test[14] for carbonate or for ammonia. The ammonia test, sensitive to 1 part in 5000, must be carried out with care. It consists of adding a few drops of 0.1 *M* $HgCl_2$ solution to a few ml. of 0.5 *M* cyanate solution and then adding NaOH solution until the solution is alkaline; formation of $Hg(NH_2)Cl$ indicates the presence of NH_3. Since the $HgCl_2$ solution, to prevent its own hydrolysis, must be fairly acidic, an interval of more than 10 seconds between addition of the $HgCl_2$ and the neutralization with NaOH allows production of enough NH_3 from the cyanate to give a distinct positive test; obviously there must be as little delay as possible in the neutralization step, in order to obtain meaningful results.

(14) "Inorganic Syntheses," Vol. II, McGraw-Hill Book Co., Inc., New York, N. Y., 1946, p. 86.

Confirmatory evidence for absence of impurities was obtained from study of the weight loss by samples heated *in vacuo*. Salt recrystallized by the "Inorganic Syntheses" method lost 0.6% at 130° and a total of 1.25% at 250° when heated for 30 minutes at each temperature. Salt purified by the modified procedure lost from 0.04 to 0.18% at 130° but sustained no further loss at 250°. The lower figure was obtained with a sample dried for one week in a vacuum desiccator.

All material used in these studies was purified and stored as indicated. Tests on material two months old showed that no detectible hydrolysis occurred, even though the vacuum desiccator was opened frequently.

Conditions for Proper Stoichiometry.—The procedure adopted for this study consisted of adding an excess of standard HCl to weighed portions of the purified KNCO, allowing 1 to 2 hours for completion of reaction, and titrating the excess acid with standard NaOH using a *p*H meter to determine the equivalence point. Boiling out the CO_2 before back-titration sharpened the equivalence point but did not change its location, so most analyses included prior elimination of the CO_2.

Two series of observations were made. In Series A, the weighed portion of KNCO was first dissolved in water, and the aliquot of standard acid was added to this solution. With 0.03 to 0.045 *M* KNCO initially present and with a final acidity between 0.06 and 0.16 *M* HCl, 100.0 ± 0.25% of the theoretical amount of HCl reacted. The limits of error are imposed by the analytical procedures due to the large excesses of acid present. There seemed to be no point in going to higher acidities. With the final acidities down to 0.014 and 0.0074 *M*, only 99.0 and 98.7%, respectively, of the theoretical amount of acid reacted. Under these conditions it appears that urea formation is not adequately suppressed.

In Series B, the solid KNCO was added directly to the acid solutions. In every case the results were low by 5 to even 20%, the largest errors usually appearing at the lowest acidities, but with no systematic pattern. In these solutions a permanent turbidity was produced, most noticeable with cases showing the largest error. It was immediately suspected, and later established, that the turbidity was due to insoluble cyanuric acid, produced by polymerization of HNCO at the high local concentrations resulting as the solid KNCO dissolved in the acid.

Description of the Calorimeter.—The basic principles of calorimeter design have been thoroughly covered by White,[15] Sturtevant[16] and Rossini,[17] and numerous references to specific designs are given in these sources. Consistent with these principles, the instrument constructed for this work utilized a 1-liter silvered Dewar fitted at the top with a brass flange carrying an O-ring seal against which the lid is clamped. The 1/4-inch thick brass lid was fitted with seven 3-inch-long chimneys, and was permanently mounted with the stirring assembly to movable brackets attached to a large water thermostat. A thin sheet of Lucite was cemented to the bottom of the lid. Somewhat similar arrangements have been used by Southward[18] and by Young and Vogel.[19]

Stirring was accomplished by a centrifugal type impeller driven by a 180-r.p.m. synchronous motor. The impeller was located at the bottom of a concentric glass well which extended almost the depth of the calorimeter vessel. The cross-section area of the well and the annulus were about equal. The arrangement produced forced vertical circulation downward inside the well and upward in the annular space; a cycle was completed in about 4 seconds, and uniform mixing was completed in 3 or 4 cycles with a minimum of turbulence and heat of stirring.

The heater was a loop of 4 mm. glass tubing containing a tightly coiled heating element of No. 30 manganin wire (50 ohms) and filled with silicone oil as a heat transfer medium.

(15) W. P. White, "The Modern Calorimeter," The Chemical Catalog Co., Inc., New York, N. Y., 1928.

(16) J. M. Sturtevant, in "Physical Methods of Organic Chemistry," A. Weissberger, Ed., Vol. I, Part I, Interscience Publishers, Inc., New York, N. Y., 1949, Chapter XIV.

(17) F. D. Rossini, "Experimental Thermochemistry," Interscience Publishers, Inc., New York, N. Y., 1956, Chap. 1, 2, 3, 11, 14.

(18) J. C. Southard, *Ind. Eng. Chem.*, **32**, 442 (1940).

(19) T. F. Young and O. G. Vogel, *J. Am. Chem. Soc.*, **54**, 3030 (1932).

Particular care was taken with placement of the leads and with insulation and shielding.

The electric circuit for determining the energy equivalent was of conventional design,[20] using a 450-ampere hour 32-volt storage battery as the power supply. Two Leeds and Northrup Series 4020 N.B.S. type standard 1-ohm resistors were mounted in parallel for current determination. Both resistors carried manufacturer's certificates; one was new. They were further checked against each other with a G-1 Mueller bridge. Potential measurements were made with a Leeds and Northrup type K-2 potentiometer and a Leeds and Northrup No. 7581 volt box. The volt box ratio was checked by applying a standard potential to the box and comparing input and output voltages with the potentiometer, which itself had been subjected to several checks for internal consistency. The standard cell was an Eppley low-resistance unsaturated type with negligible temperature coefficient at room temperature; it and the K-2 potentiometer as a unit were checked against a standard cell bearing a N.B.S. certificate. The duration of the electrical energy input was measured with a Standard Electric Time Co. Type S-1 electric timer with a direct current clutch synchronized with the heater circuit through a double-pole switch; the timer was driven by the output from an American Time Products, Inc., frequency standard.

For temperature measurements we employed two 2000-ohm thermistors (E. H. Sargent Co.) in opposite arms of a Maier[21] transposed bridge. The other two arms of the bridge were 2000-ohm manganin wire-wound component resistors (Leeds and Northrup Co.) mounted in a long glass well extending into the thermostat. All of the junctions and connections were placed inside this well, and lead wires were paired and shielded. The resistors were chosen so that the temperature corresponding to zero output voltage would lie between 20 and 25°. The input voltage to the bridge was maintained constant and equal to that of a standard cell, and was continuously monitored to within 10 microvolts during temperature measurement. The output from the bridge was measured to 1 microvolt with a Leeds and Northrup type K-3 potentiometer and an unsaturated Eppley standard cell with negligible temperature coefficient. In place of a conventional galvanometer, a Leeds and Northrup 9835-B direct current indicating amplifier was used as the null detector. Once energized, the bridge input circuit was never interrupted, in order to avoid disturbance of the thermistor characteristics, as recommended by Müller and Stolten.[22] The thermistor thermometer was calibrated against a platinum resistance thermometer and a Leeds and Northrup type G-1 Mueller bridge at 20 points between 10 and 35°. The temperatures were representable by the equation (for this particular thermometer)

$$\theta = 21.7375 + 49.18E + 7.40E^2 + 17.88E^3 \quad (5)$$

where θ is the temperature and E the output voltage; the mean deviation of the experimental temperatures from this equation was ±0.0016° over the whole range and ±0.0003° in the range 21 to 28° where several points were taken. In this range, E is small (−0.02 to +0.12 volt) and the function is almost linear. The entire circuit was very stable; most of the "noise" (about 0.5 microvolt) could be traced to the low rate of stirring. Rechecks of the calibration showed no changes beyond the mean deviation over several months.[23]

With this thermometer an operating sensitivity of 5×10^{-5} °C./microvolt was available, corresponding to about 0.06 cal. per microvolt. For very small amounts of energy the temperature rise could be read directly in terms of meter readings on the direct current amplifier to 0.3 microvolts or 1.5×10^{-5} over a range of 0.003°.

The sensing elements of the two thermistors were located diammetrically opposite to each other near the top of the annular region, 1 or 2 cm. below the liquid level and about 1/2 cm. below the top of the stirring well. This location placed them in the steady current of rising liquid in the annular space, yet properly close to the major avenue of heat leakage.[15] The Dewar was filled to within 1.5 cm. of the top, and for the hydrolysis runs a 1 cm. plastic disk was fastened to the underside of the lid to further reduce the dead space above the liquid.

When in use, the calorimeter assembly was submerged in a large well-stirred water-bath controlled at 25° to within 0.003°. Any of the chimneys on the lid which were not in use were sealed, and most of the working surface of the bath was covered to avoid disturbances from air circulation in the laboratory, the temperature of which remained reasonably steady.

For processes of short duration, *e.g.*, mixing, dissolving, or electrical calibration, the corrected temperature rise was obtained by the Dickinson[24] method, using as a "mean time" a time 0.1 minute after opening the sample holder or after the mid-point of the heating period. The 0.1 minute interval was characteristic of the time–temperature response to heat evolution in the calorimeter, being primarily governed by the stirring characteristics. Time–temperature readings for the "after" period were not started until 7 minutes after completion of the process to allow for thermal equilibration of the solid parts of the calorimeter. For these processes, "fore" and "after" periods were normally 15 minutes in length. For those runs which were not rapid or were not characterized by a linear temperature rise, *e.g.*, the hydrolyses of cyanic acid, for which the half-life varied from 0.8 to 1.5 minutes, the corrected temperature rise was obtained by graphical integration of the time–temperature curves according to methods described by Rossini and others.[25] At least 12 half-lives were allowed for the "main" period in these cases; since the reactions were first order they should be 99.98% completed within the main period. For these runs, the "fore" and "after" periods were normally 20 minutes in length. With the total period of observation as long as 60 minutes, the 0.003° control of the water-bath was barely tolerable, according to White.[15]

In determining the energy equivalent by electrical calibration, the duration of the electrical heating period was approximately 120 seconds; the resulting temperature rise was about 0.5°. Energies were computed in terms of the defined calorie. Since the energy equivalent of the system was determined by electrical calibration on the final state of the system for each run, the assigned temperature of the calorimetric process was the initial temperature at the beginning of the reaction period. The initial temperatures were always between 24.95 and 24.97°, and were close to but slightly below the bath temperature. The entire system was allowed to equilibrate for at least 30 minutes before starting observations for the "fore" period; "blank" runs indicated that this was adequate time to bring the sample holders to equilibrium.

Liquid samples were contained in a glass tube about 2 cm. in diameter and about 15 cm. long, giving a volume of about 39 ml. (Fig. 1). The ends were closed with these circular glass plates, all mating surfaces being ground and given a light coating of Vaseline to provide a tight seal. The two plates were joined by links of platinum wire; the sample holder was opened at the desired time by a light steady pull on a nylon filament attached to the upper plate and extending through the capillary bore tubing which served to support the sample holder in one of the chimneys. Experience showed that the sample holder emptied within one stirring cycle. With the plates held in their open position, a continuous flow of liquid circulated through the sample holder for the remainder of the run.

Solid samples were placed in a small hemispherical glass cup which was held up against a plastic "seat" on the lower surface of the lid until it was time to release the sample. The cup was held in place by a spring-loaded "L" shaped glass rod through one of the chimneys and hinged to the underside of the cup (Fig. 1). The hinge and part of the lower surface of the cup were below the liquid level. A light coating of Vaseline provided a liquid- and vapor-tight seal against the seat. When the support rod was momentarily depressed, the cup would tip outward, emptying its contents, and then would hang completely immersed in the liquid.

Periodic checks of the energy equivalent with a standard

(20) Reference 17, page 48.

(21) C. G. Maier, THIS JOURNAL, **34**, 2860 (1930).

(22) R. H. Müller and H. J. Stolten, *Anal. Chem.*, **25**, 1103 (1953).

(23) The thermistor thermometer described in connection with this research stayed within its original calibration limits for 11 months, when one of the thermistors was accidentally broken. A new unit was calibrated in September, 1958, and rechecked several times over a 20-month period, during which it likewise showed similar stability, drifting in that time about 0.002°. It appears that at the low power-levels employed in this application the thermistor thermometer can be quite stable.

(24) H. C. Dickinson *Bull. Natl. Bur. Standards*, **11**, 189 (1914).

(25) Reference 17, pp. 28 ff.

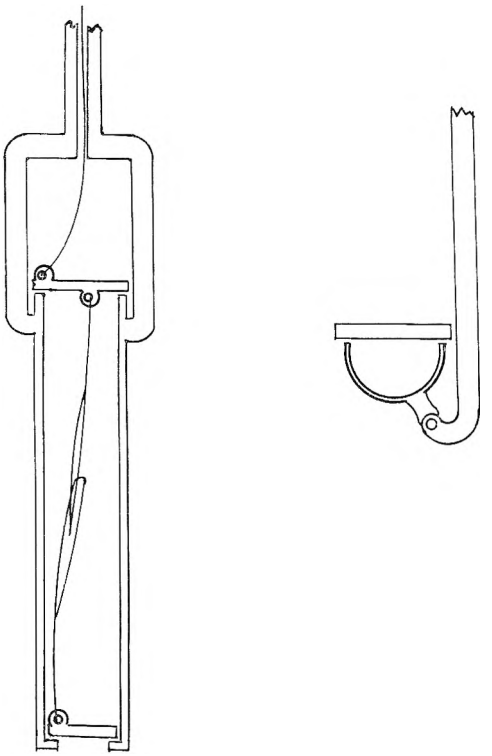

Fig. 1.—Liquid and solid sample holders.

mass of water served to monitor the over-all stability of the apparatus. Initial checks of the equipment included a series of runs on the neutralization of HCl with NaOH(CO_2-free). The mean of the four runs, reduced to the conventional standard state process by heats of dilution taken from the literature,[5] gave for the heat of neutralization $\Delta H^0 = -13{,}397$ cal. mole 1 at 25°, with a mean deviation of ±6 cal. mole^{-1} (±0.2 cal. per 0.02945 mole of material reacting in each run.) In terms of absolute accuracy, the results are limited by the accuracy of the volumetric analysis of the HCl solution (*ca.* 2 parts per 1000).

Dilution and Mixing Studies with Hydrochloric Acid.—These studies were undertaken partly to check the apparatus but mainly to study the heat effects associated with "mixing" or "unmixing" of the final solutions resulting from the acid hydrolyses of potassium cyanate. A 39-ml. liquid sample holder allowed 27-fold dilution of the sample to a final volume of 1065 ml. In the first set of studies the acid was diluted directly into water; in the second set, dilution was made into a 0.02 *m* KCl solution. The results are presented in Tables I and II.

TABLE I

HEATS OF DILUTION OF HCl SOLUTIONS AT 25°

Molal concn. Initial	Final	Moles HCl	Cor. temp. rise, °C.	Energy equiv., cal. deg.$^{-1}$	ΔH_{obs}, cal. mole^{-1}	$\Delta H_{calc.}$, cal. mole^{-1}
2.140	0.0752	0.07994	0.0371	1174.8	−545.2	
2.140	.0749	.07966	.0368	1176.0	−543.3	
				Mean	−544.3	−545.5
3.255	.1120	.1186	.0771	1173.3	−763.0	
3.255	.1109	.1178	.0766	1178.2	−766.0	
				Mean	−764.5	−754.4
4.468	.1504	.1600	.1385	1170.0	−1012.9	
4.468	.1502	.1597	.1382	1171.3	−1013.4	
				Mean	−1013.2	−978.0

In Table I, ΔH_{calc} is derived from data in NBS Circular 500.[5] The discrepancy between our data and the literature values at the two higher concentrations was disturbing, but could not be traced to any experimental source. The combined errors of stoichiometry and temperature measurement should not have exceeded 3 cal. mole^{-1} in these runs.

TABLE II[a,b]

HEATS OF MIXING OF HCl AND KCl SOLUTIONS AT 25°

HCl, molal concn. Initial	Final	Moles HCl	Cor. temp. rise, °C.	Energy equiv., cal. deg.$^{-1}$	ΔH_{obs}, cal. mole^{-1}	ΔH_{calc}, cal. mole^{-1}
2.140	0.0751	0.0796	0.0357	1172.6	−526	−525
3.255	.1117	.1190	.0786	1173.2	−747	−747
4.468	.1497	.1585	.1354	1167.8	−995	−999

[a] The first two dilutions were made with 0.01784 mole of KCl in the calorimeter, the third with 0.01780 mole. In each case, the initial concentration of KCl was 0.0196 molal, the final concentration 0.0189. [b] ΔH_{obs} and ΔH_{calc} are computed in terms of 1 mole of HCl.

In Table II, $\Delta H_{calc.}$ represents the sum of the calculated heats of the processes

$$HCl(m_1) \longrightarrow HCl(m_2,\mu_2) \quad (6)$$

$$a\text{KCl}(0.02m) \longrightarrow a\text{KCl}(m_2,\mu_2) \quad (7)$$

$$HCl(m_2,\mu_2) + a\text{KCl}(m_2,\mu_2) \longrightarrow (HCl + a\text{KCl})(\mu_2) \quad (8)$$

assuming that the heat of mixing at constant ionic strength, process 8, is zero. The heat of process 6 was computed from our dilution data in Table I, while that for process 7 was obtained from NBS Circular 500. It appears that under these conditions the assumption concerning process 8 is not seriously in error. These observations on the HCl–KCl mixing process are consistent with data presented by Young, Wu and Krawetz.[26]

The Carbon Dioxide Correction.—It was vital to establish, through preliminary runs, the length of the reaction period in the cyanate hydrolysis for guidance in making thermal leakage corrections, and to ascertain whether any parasitic processes were present. To this end, the calorimeter was operated as an adiabatic instrument by installing an auxiliary differential thermometer consisting of two thermistors in adjacent arms of a bridge, with one thermistor in the calorimeter and the other in the water-bath. With this arrangement it was possible to regulate manually the power input to the bath with a variable autotransformer and maintain adiabatic conditions within ±0.002° except during the initial minute of reaction. Under these conditions, with no reaction occurring, the rate of temperature rise should be merely that of stirring.

In the first such runs, there was from 80 to 100 ml. of dead space in the calorimeter above the liquid. In these runs it was observed that the apparent heat of stirring was consistently less at the end of the cyanate hydrolysis (12 half-lives) than before the reaction began, as shown by an almost 50% decrease in the rate of temperature rise due to stirring. This difference in rates decreased with time. Two possible kinetic processes were considered: a slow endothermal chemical reaction in the calorimeter, or the slow escape of CO_2 from the solution into the dead space. The second alternative seemed most probable. Accordingly, the dead space was reduced to about 20 ml. by attaching a 1-cm. thick Lucite disk to the underside of the lid, filling most of the dead space, and then bringing the liquid level to within 3 to 5 mm. of this disk. No dead space was available in any of the chimneys. Following this modification, no significant difference could be observed in apparent heats of stirring before and after the reaction. From this we were led to conclude that in the 20 to 30 minutes associated with the main reaction period, the CO_2 distribution had come to equilibrium. It was relatively easy to confirm this by disturbing the equilibrium through removal of some of the saturated air and noting the time of return to equilibrium.

In order to correct the calorimetric data for the distribution of the CO_2, the total volume of the calorimeter was determined, and the dead space volume could then be calculated for each hydrolysis run. The correction for heat absorbed by escape of CO_2 from solution into the dead space was computed by combining Henry's law, the ideal gas law, and the heat of evaporation of CO_2. To a good approximation, since the total amount of solvent was nearly constant (about 1063 g.) and almost a constant fraction (97–98%) of the CO_2 remained dissolved at equilibrium, the correction reduced to the simple form (at 25°)

(26) T. F. Young, Y. C. Wu and A. A. Krawetz, *Disc. Faraday Soc.*, **24**, 37 (1957).

TABLE III

EXPERIMENTAL DATA FOR THE HEAT OF HYDROLYSIS OF POTASSIUM CYANATE IN ACID SOLUTION AT 25°

Run no.[a]	HCl,[b] *m.*	HCl, moles	KNCO, moles	H_2O, g.	$\Delta\theta$ cor., °C.	Energy equiv., cal. deg.$^{-1}$	ΔH_{obs}, cal. mole^{-1}	Q_c, cal. mole^{-1}	ΔH_{10}^0, cal. mole^{-1}	*d*,[c] cal. mole^{-1}
				Series I, starting with solid KNCO						
13	2.140	0.07984	0.009736	1063.2	0.2210	1176.6	−26707	89	−17590	−16
18	2.140	.07982	.009420	1060.3	.2163	1173.1	−26937	105	−17688	+37
3	3.255	.1175	.010205	1059.7	.2709	1172.0	−31112	105	−17647	− 4
5	3.255	.1181	.010319	1064.6	.2726	1178.0	−31120	79	−17684	+33
6	3.255	.1188	.010904	1061.5	.2837	1174.8	−30565	100	−17575	−76
7	4.468	.1598	.008849	1061.1	.3063	1173.5	−40621	100	−17632	−19
8	4.468	.1604	.009202	1061.9	.3143	1173.9	−40094	94	−17740	+89
								Mean	−17651	±46
				Series II, starting with aqueous KNCO						
23	0.07788	0.07964	0.010004	1061.8	0.2320	1174.2	−27230	94	−17647	−19
24	.07760	.07947	.009146	1061.7	.2217	1174.0	−27184	94	−17594	−72
20	.1162	.1187	.009800	1060.4	.2276	1170.7	−27189	105	−17571	−95
21	.1156	.1185	.010143	1063.3	.2357	1179.9	−27325	89	−17695	+29
37	.1157	.1184	.009962	1062.2	.2311	1174.3	−27242	94	−17615	−51
38	.1160	.1188	.009930	1062.3	.2317	1174.8	−27412	94	−17785	+119
39	.1153	.1185	.009984	1065.4	.2314	1179.8	−27344	79	−17700	+34
16	.1557	.1588	.010192	1058.1	.2384	1170.0	−27367	115	−17721	+55
25	.1554	.1589	.009917	1060.5	.2313	1171.7	−27328	100	−17664	− 2
								Mean	−17666	±53

Mean of all runs	−17660 ± 50 cal. mole^{-1}
Mean of 0.075 *m* HCl	−17630 ± 38 cal. mole^{-1}
Mean of 0.11 *m* HCl	−17659 ± 57 cal. mole^{-1}
Mean of 0.15 *m* HCl	−17689 ± 41 cal. mole

[a] Table III contains all of the runs made in the hydrolysis of cyanate, which were interspersed among other studies. [b] Initial concentration, before mixing and reaction. [c] Deviation from mean of Series.

$$Q_c = 5.25V \text{ cal. mole}^{-1} = \Delta H_9 \qquad (9)$$

where V is the dead space volume in ml. and Q_c is given directly in calories per mole of cyanate reacted. In arriving at this correction, the heat of evaporation was taken to be 4640 cal. mole^{-1} for CO_2,[5] and the solubility of CO_2 was taken to be 0.0330 mole of CO_2 per kilogram of water for these solutions.[27,28] Because the dead space volume cannot be defined more closely than 2 ml., the correction cannot be more certain than ±10 cal. mole^{-1}.

The Hydrolyses of Potassium Cyanate.—Consistent with the conditions for proper stoichiometry of reaction 1 as described above, two different patterns of experimental conditions were followed. Series I started with solid KNCO in one sample holder and HCl solution, related to the dilution data in Tables I and II, in the other. After the initial rate period, the solid was dissolved and the temperature monitored for two minutes before opening the acid sample holder. This delay was a precautionary measure to detect any evidence of leakage of the acid sample holder prior to opening it. The hydrolysis reaction was considered complete after 12 half-lives, after which the final rate period was taken and the electrical energy equivalent determined. In this Series, the processes of dissolving and subsequent hydrolysis were included in a single main period; no attempt was made to extract the heat of solution from these data.

In the second pattern of operations, Series II, acid solution was placed directly in the calorimeter at the appropriate concentration, and the liquid sample holder was loaded with a weighed sample of KNCO dissolved in 0.001 *M* NaOH to prevent any hydrolysis of cyanate during the preparations for the run. In these runs, only hydrolysis was involved; to reduce this Series to the standard state process, separate studies of the heat of solution of KNCO(s) were made. The correction for the NaOH neutralized in the process averaged 60 cal. per mole of cyanate used.

Both Series utilized about 0.8 g. (0.01 mole) of KNCO, weighed to the nearest milligram with minimum exposure to air, and reduced to a vacuum weight basis. Hydrolysis began at one of three starting acidities, 0.075, 0.11 and 0.15 *m* HCl. Starting temperatures were between 24.95 and 24.97°. Corrections for thermal leakage varied from −0.0011 to −0.0033°. A summary of the experimental data is presented in Table III, together with the standard state heat of reaction for the process

$$KNCO(s) + 2HCl(aq) + H_2O(l) \longrightarrow KCl(aq) + NH_4Cl(aq) + CO_2(g) \qquad (10)$$

$$\Delta H_{10}^0 = -17{,}660 \pm 60 \text{ cal. mole}^{-1}$$

involving the substances in their conventional standard states. The standard deviation is given as figure of merit.

To facilitate comparison of the two Series, both were reduced to the same standard state process, reaction 10. For this purpose heats of dilution of the dilute HCl solutions (0.05 to 0.16 *m*) were taken from NBS Circular 500[5]; for the concentrated solutions, the heats of dilution were computed from the data in Table I by applying the appropriate corrections to the literature values.[5] Heats of dilution of KCl and NH_4Cl were likewise taken from the literature,[5] and the heat of unmixing the final calorimetric solution at constant ionic strength was taken equal to zero as indicated by the preliminary studies (Table II). Heats of dilution and solution for KNCO were determined experimentally for making appropriate standard state corrections. In the absence of definitive information on the heat of solution of CO_2 in HCl and KCl solutions, the literature[5] value −4640 cal. mole^{-1} was used for all runs in correcting to the gaseous state of CO_2.

Heat of Solution and Dilution of KNCO.—In the heat of solution studies, approximately 0.01 mole of solid KNCO was dissolved in 0.001 *M* NaOH; the use of an alkaline medium was necessary to suppress hydrolysis. Dilutions of the same amount of KNCO from 0.26 to 0.01 molal, using 0.001 *M* NaOH as the solvent and dilution medium, provided data pertinent to Series II of the hydrolyses, and also furnished a characterizing pattern for selecting an appropriate 1–1 salt (CsCl was chosen) as an analog for estimating the heat of dilution from 0.01 molal to infinite dilution

(27) H. S. Harned and R. Davis, Jr., *J. Am. Chem. Soc.*, **65**, 2030 (1943).

(28) A. E. Markham and K. A. Kobe, *ibid.*, **63**, 449, 1165 (1941); *Chem. Revs.*, **28**, 519 (1941).

($\Delta H^0 = -36$ cal. mole^{-1} was taken). Because the concentration of the NaOH did not change in these studies, its effect was simply to contribute to the ionic strength. Data for these studies are given in Tables IV and V; the concentrations m_1 and m_2 refer to the concentration of KNCO. The dilution data in Table V required estimation of the temperature rise in terms of the meter deflection of the DC amplifier, and are probably reliable to ± 2 cal. mole^{-1}.

TABLE IV

HEAT OF SOLUTION OF POTASSIUM CYANATE AT 25° IN 0.001 *M* NaOH

Run no.	KNCO, moles	H_2O, g.	m_2, final	Corr. temp. rise, °C.	Energy equiv., cal. deg.$^{-1}$	ΔH_{obs}, cal. mole^{-1}
17	0.010578	1086.1	0.009740	−0.0429	1198.3	4860
29	.010425	1086.4	.009868	− .0427	1192.5	4885
31	.010193	1085.2	.009393	− .0419	1191.6	4898
32	.009738	1088.8	.008953	− .0396	1195.6	5862
					Mean	4876 ± 15

TABLE V[a]

HEAT OF DILUTION OF POTASSIUM CYANATE AT 25° IN 0.001 *M* NaOH

Run no.	KNCO, moles	m_1, initial	m_2, final	Corr. temp. rise, °C.	ΔH_{obs} cal. mole^{-1}
27	0.01027	0.267	0.00964	−0.00006	7
35	.01010	.263	.00952	− .00005	6
36	.00998	.259	.00941	− .00004	5
				Mean	6

[a] In this series, the calorimeter contained 1060 g. of water; the energy equivalent was not measured but taken as 1175 cal. deg.,$^{-1}$ typical of the type of run.

Discussion

An examination of the heats of hydrolysis gave no evidence of a skewed distribution of errors. Considering the limited amount of cyanate used, we attribute approximately 15 cal. mole^{-1} to instrumental errors, and assign the remaining errors to purity, stoichiometry and correction terms, including about 15 cal. mole^{-1} in the carbon dioxide correction, Q_c, associated with the volume of the dead space. In spite of its large deviation, we have retained run 38; no experimental artifact could be found on which to question its validity. If run 38 were omitted, the two Series would have almost identical average values for ΔH_{19}^0. In any case the concordance between the two Series is gratifying, especially in view of the large dilution corrections in Series I. The slight trend of the data with acidity is probably due to magnification of uncertainties in the heat of dilution data for HCl or a small residual heat of unmixing. The unfavorable ratio of acid to cyanate, required for control of stoichiometry, amplifies greatly the errors in the correction terms associated with the acid.

The data in Tables IV and V, together with the estimate of -36 cal. mole^{-1} for dilution from 0.01 molal to infinite dilution, lead to $\Delta H^0 = 4840 \pm 15$ cal. mole^{-1} for the standard heat of solution at infinite dilution for potassium cyanate. Circular 500[5] gives +5000 cal. mole^{-1}. The heat of dilution data in Table V, though limited, are significant in revealing a slightly endothermal behavior on dilution from 0.26 to 0.01 molal. Examination of the characteristic curves for a number of 1–1 electrolytes[29] suggests that potassium cyanate is quite similar to CsCl in its heat of dilution behavior; its heat of dilution curve should lie between those of KCl and KBr.

TABLE VI

HEATS OF FORMATION OF CYANATE SPECIES AT 25°

Species	ΔHf^0, kcal. mole^{-1} Lord and Woolf[9]	NBS Circ. 500[5]	This work
KNCO(s)		−98.5	−99.85
KNCO(aq)		−93.5	−95.01
NCO^-(aq)	−35.22	−33.5	−34.97

By combining our experimental heats of reaction with supplemental data from NBS Circular 500, we have obtained the heats of formation summarized in Table VI. For comparison we have included the values reported in NBS Circular 500 and also the heat of formation of cyanate ion reported by Lord and Woolf,[9] whose work was discussed in the Introduction.

Acknowledgments.—We wish to express our appreciation to the Monsanto Chemical Company for a Fellowship supporting the junior author (R.A.M.). The senior author (C.E.V.) wishes to thank E. I. du Pont de Nemours and Company for a Grant-in-Aid under which this manuscript was completed.

(29) E. Lange and A. L. Robinson, *Chem. Revs.*, **9**, 105 (1931). Data from reference 5 were also examined.

ION ASSOCIATION. V. DISSOCIATION CONSTANTS FOR COMPLEXES OF CITRATE WITH SODIUM, POTASSIUM, CALCIUM, AND MAGNESIUM IONS[1]

BY MACKENZIE WALSER

The Department of Pharmacology and Experimental Therapeutics, The Johns Hopkins University School of Medicine, Baltimore 5, Maryland

Received July 22, 1960

Titration of citrate in solutions of Me_4NCl, NaCl and KCl, at $\mu = 0.16\ M$, indicates association of Cit^{3-} ions with Na^+ and K^+ ions. Estimated dissociation constants are $K_{NaCit^{2-}} = 0.2\ M$, $K_{KCit^{2-}} = 0.37\ M$. Dissociation constants for the complexes $CaCit^-$ and $MgCit^-$ were measured spectrophotometrically in the presence and absence of sodium ions, allowing for $NaCit^{2-}$ in the latter. Mean values obtained are $K_{CaCit^-} = 0.0007\ M$; $K_{MgCit^-} = 0.00028\ M$, at $\mu = 0.16\ M$ and 25°.

Reported measurements[2-7] of dissociation constants for the complexes $CaCit^-$ and $MgCit^-$ have been made in the presence of sodium ions at concentrations in excess of 0.13 *M*. It has been assumed either explicitly or implicitly that under these conditions sodium ions do not complex a significant fraction of the citrate present. However, evidence obtained by nuclear spin resonance[8] indicates the presence of a complex between Na^+ and Cit^{3-}.

Values for K_{CaCit^-} and K_{MgCit^-} have therefore been obtained in solutions containing less than 0.015 *M* Na^+, using spectrophotometric methods for determining free calcium and magnesium ion concentrations.[9] Estimates of $K_{NaCit^{2-}}$ and $K_{KCit^{2-}}$ are also presented based on titration curves. The new value for K_{MgCit^-} is consistent with earlier values when the latter are corrected for the complex $NaCit^{2-}$. The new value for K_{CaCit^-} indicates somewhat lesser stability of this complex than previously reported.

Experimental

Determination of K_{MgCit^-} and K_{CaCit^-}.—Tetramethylammonium chloride, 0.16 *M*; $MgCl_2$, 0.053 *M*; tris-(hydroxymethyl)-aminomethane ("tris") buffer, *p*H 7.50, 0.16 *M*; and sodium citrate ($Na_3C_6H_5O_7 \cdot 2H_2O$), 0.0267 *M*; freed of heavy metals, were mixed in various proportions in cuvettes, the total volume being 3 ml. The calculated ionic strength of all of these solutions is 0.16 *M*. 0.2 ml. of a freshly prepared solution of Eriochrome Black T, 0.035%, was added to each cuvette with mixing. Absorbancy was determined in a Beckman Model DU spectrophotometer at 530 mμ. *p*H was then determined in selected samples using a Radiometer *pH* meter model 4 equipped with a glass electrode. In order to determine K_{CaCit^-}, solutions of $CaCl_2$, 0.053 *M*, and murexide, 0.03%, were substituted for $MgCl_2$ and Eriochrome, respectively; absorbancy was determined at 475 mμ. In order to measure these constants in the presence of sodium, NaCl, 0.16 *M*, was substituted for tetramethylammonium chloride.

Magnesium or calcium ion concentration, M^{2+}, was calculated from the equation

$$M^{2+} = K_D(A - A_0)/(A_1 - A)$$

where *A* is observed absorbancy; A_0 and A_1 are the absorbancies of solutions containing zero and excess M^{2+}, respectively; K_D is the dissociation constant of the metal–dye complex, derived from standard curves analyzed at the same time. Further details are given elsewhere.[9]

Measurement of Complex Formation between Tris and Citrate.—Fifty-ml. portions of tetramethylammonium chloride, 0.16 *M* and tris, 0.02 *M*, were titrated with either 0.16 *M* HCl or 0.0178 *M* citric acid. The solutions were mixed in a constant temperature bath at 25°. *p*H was determined at intervals with precautions to avoid adding appreciable amounts of saturated KCl to the solutions being titrated.

Determination of $K_{NaCit^{2-}}$ and $K_{KCit^{2-}}$.—Five-ml. portions of sodium citrate, 0.0267 *M*, were mixed with 50-ml. portions of (1) tetramethylammonium chloride, 0.16 *M*, (2) sodium chloride, 0.16 *M* or (3) potassium chloride, 0.16 *M*, and titrated with HCl, 0.1 *N*, at 25°. All solutions were free of CO_2.

Results

K_{MgCit^-} and K_{CaCit^-}.—Derived values for K_{MgCit^-} and K_{CaCit^-} obtained in the virtual absence of sodium are given in Table I. The range of concentrations which can be studied is limited by the fact that errors become magnified when the concentration of the complex approaches the total concentration of either metal ion or of citrate, or when *A* approaches either A_0 or A_1. The assumption of only 1:1 complex formation leads to reasonably consistent values under these conditions. No correction had been applied for the slight change in ionic strength due to complex formation. The dependence of K_D values upon ionic strength is not marked in this region.[9] It is assumed that citrate is not complexed by tetramethylammonium ions.

Absence of Complex Formation between Tris and Citrate.—Figure 1 represents the titration curves for tris titrated with HCl and with citric acid, plotted according to Hofstee.[10] pK'_a values derived from these curves are 8.14 and 8.16, respectively, at 25° and $u = 0.16\ M$, tris concentration 0.02 *M*. These results indicate that tris is not complexed by citrate.

$K_{NaCit^{2-}}$ and $K_{KCit^{2-}}$.—Figure 2 represents partial titration curves of citrate in solutions containing (1) tetramethylammonium, (2) potassium or (3) sodium, respectively, as the predominant cation. The titration was continued until approximately one third of the citrate had been titrated, *i.e.*, until the concentration of the Cit^{3-} ion became very low. A consistent *p*H difference is noted, which becomes smaller as the titration progressed. Although these curves are not subject to complete analysis, the

(1) Supported by U. S. Public Health Service Grant (A-2306).

(2) A. B. Hastings, F. C. McLean, L. Eichelberger, J. L. Hall and E. DaCosta, *J. Biol. Chem.*, **107**, 351 (1934).

(3) J. Muus and H. Lebel, *Kgl. Danske. Videnskab. Selskab Mat.-fys. Medd.*, **13**, No. 19 (1936).

(4) R. Nordbö, *Skand. Arch. Physicl.*, **80**, 341 (1938).

(5) N. R. Joseph, *J. Biol. Chem.*, **164**, 529 (1946).

(6) E. Heinz, *Biochem. Z.*, **321**, 314 (1951).

(7) J. Schubert and A. Lindenbaum, *J. Am. Chem. Soc.*, **74**, 3529 (1952).

(8) O. Jardetzky and J. E. Wertz, *Arch. Biochem. Biophys.*, **65**, 569 (1956).

(9) M. Walser, *Anal. Chem.* **32**, 711 (1960).

(10) B. H. J. Hofstee, *Science*, **131**, 39 (1960).

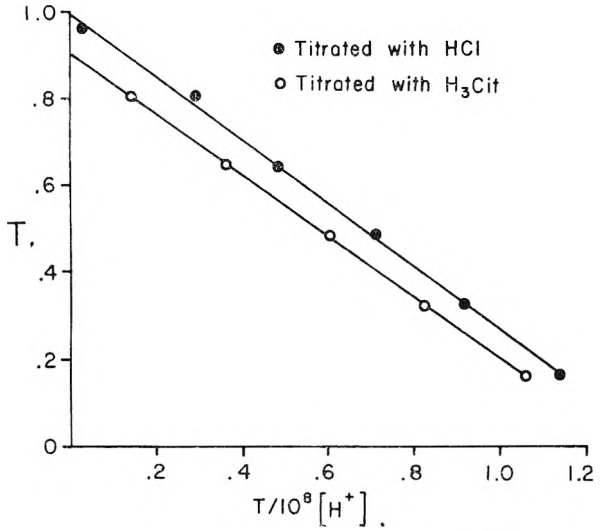

Fig. 1.—Titration of tris-(hydroxymethyl)-aminomethane with HCl and with citric acid: T, meq. acid per meq. base, plotted against $T/10^8[H^+]$. The slopes of the lines yield pK'_a.

TABLE I

COMPLEXING OF CALCIUM IONS BY CITRATE

I. IN SOLUTIONS OF TETRAMETHYLAMMONIUM CHLORIDE

[Cit], mM	[Ca], mM	pH	$A - A_0$	[Ca^{2+}], mM	[Ca-Cit$^-$], mM	[Cit^{3-}], mM	K_{CaCit^-}, M
Tris buffer, 0.05 M; 25°, μ = 0.16 M; A_0 = 0.418; A_1 = 1.122; K_D = 0.00314 M							
0.00	0.00	7.56	0.000				
.00	0.67		.125				
.00	1.34		.211				
.00	2.68		.329				
.00	5.36	7.56	.455				
.83	0.67	7.56	.067	0.33	0.34	0.49	0.00048
.83	1.34	7.56	.147	.83	0.51	0.32	.00052
2.78	1.34	7.53	.062	.30	1.04	1.74	.00050
2.78	2.68	7.53	.161	.93	1.75	1.03	.00055
8.34	2.68	7.55	.076	.38	2.30	6.04	.00099
8.34	5.36	7.51	.160	.92	4.44	3.90	.00081
							0.00064

II. IN SOLUTIONS OF SODIUM CHLORIDE

[Cit], mM	[Ca], mM	[Na], mM	[Ca^{2+}], mM	[Ca-Cit$^-$], mM	[Na-Cit^{2-}], mM	[Cit^{3-}], mM	K_{CaCit^-}, M
A. Tris buffer, 0.05 M; pH 7.58; 25°; μ = 0.16 M; A_0 = 0.452; A_1 = 1.161; K_D = 0.00485 M							
0.83	0.67	104	0.44	0.23	0.21	0.39	0.00075
2.78	1.34	102	0.46	0.88	.64	1.26	.00066
2.78	2.68	89	1.33	1.35	.44	0.99	.00098
8.34	2.68	102	0.46	2.22	2.07	4.05	.00084
							0.00081
B. Diethyl barbiturate buffer, 0.006 M, pH 7.57; 25°; μ = 0.14–0.16 M; A_0 = 0.462; A_1 = 1.187; K_D = 0.00457 M							
0.56	0.67	136	0.51	0.16	0.16	0.24	0.00076
0.56	1.34	133	1.05	0.29	0.11	0.16	.00058
5.00	1.34	114	0.29	1.05	1.43	2.52	.00069
5.00	2.68	107	0.69	1.99	1.05	1.96	.00068
5.00	5.36	100	2.03	3.33	0.56	1.11	.00068
							0.00068

only reasonable interpretation of the differences is complex formation between citrate, and sodium or potassium. Addition of tris buffer to these solutions at the same molar concentration as citrate yielded identical pH values (7.31).

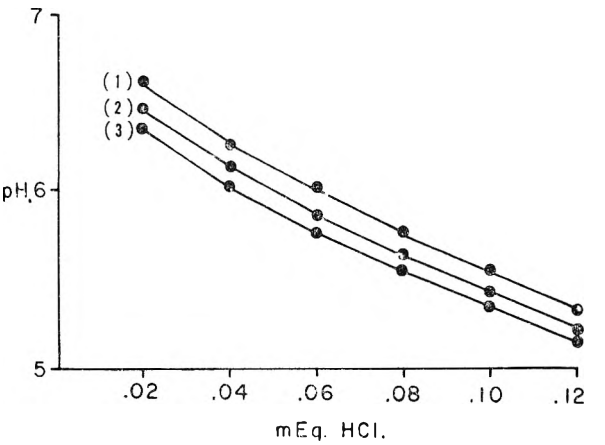

Fig. 2.—Partial titration curves of 0.013 mmole of sodium citrate in the presence of (1) tetramethylammonium chloride, 0.16 M (2) KCl, 0.16 M (3) NaCl, 0.16 M, as supporting electrolytes.

For the purposes of the present study, the desired dissociation constants are those of the complexes $NaCit^{2-}$ and $KCit^{2-}$. The data in Fig. 2 also point to the existence of the complexes $NaHCit^-$ and $KHCit^-$. The smaller pH differences observed near pH 5 indicate that these complexes are weaker (as expected on theoretical grounds). These interactions therefore cannot account for

TABLE II

COMPLEXING OF MAGNESIUM IONS BY CITRATE

I. IN SOLUTIONS OF TETRAMETHYLAMMONIUM CHLORIDE

[Cit], mM	[Mg], mM	pH	$A - A_0$	[Mg^{2+}], mM	[Mg-Cit$^-$], mM	[Cit^{3-}], mM	K_{MgCit^-}, M
Tris buffer, 0.05 M; 25°; μ = 0.16 M; A_0 = 0.415; A_1 = 0.920; K_D = 0.00152 M							
0.00	0.00	7.58	0.000				
.00	0.67		.159				
.00	1.34		.237				
.00	2.68		.318				
.00	5.36	7.58	.401				
.83	0.67	7.59	.078	0.27	0.47	0.36	0.00021
.83	1.34	7.59	.160	.69	0.65	0.18	.00020
2.78	1.34		.065	.22	1.12	1.66	.00033
2.78	2.68	7.58	.146	.62	2.06	0.72	.00022
8.34	2.68		.036	.12	0.56	5.78	.00027
8.34	5.36	7.58	.113	.44	4.92	3.42	.00030
							0.00026

II. IN SOLUTIONS OF SODIUM CHLORIDE

[Cit], mM	[Mg], mM	[Na], mM	[Mg^{2+}], mM	[Mg-Cit$^-$], mM	[Na-Cit^{2-}], mM	[Cit^{3-}], mM	K_{MgCit^-}, M
Tris buffer, 0.05 M; pH 7.58; 25°; μ = 0.16 M; A_0 = 0.408; A_1 = 1.010; K_D = 0.00215 M							
0.56	0.67	104	0.40	0.27	0.10	0.19	0.00028
0.56	1.34	97	.93	.41	.05	.10	.00023
1.67	0.67	108	.18	.49	.41	.77	.00028
1.67	1.34	102	.46	.88	.27	.52	.00027
1.67	2.68	97	1.47	1.21	.14	.32	.00039
5.00	2.68	102	0.35	2.33	.90	1.77	.00027
5.00	5.36	77	1.63	3.73	.35	0.92	.00040
							0.00030

the pH differences observed at the beginning of the titration, or in solutions at higher pH. Assuming that no citrate is complexed in the tetramethylammonium solution (sodium concentration being only 0.0075 M) and that pK_3 of citrate differs in these three solutions by the same amount as the pH differences observed during the beginning of the titration, values for $K_{NaCit^{2-}}$ and $K_{KCit^{2-}}$ may be calculated[11] to be 0.20 and 0.37 M, respectively, at 25° and $u = 0.16\ M$.

Complex Formation by Citrate in the Presence of Both Sodium and Alkaline Earth Cations.—In solutions containing sodium chloride in place of tetramethylammonium chloride, complexing of calcium and magnesium ions was measured spectrophotometrically. After correction for the complex $NaCit^{2-}$, calculated values for K_{CaCit^-} and k_{MgCit^-} are not significantly different from those obtained in the virtual absence of sodium (Tables I and II). The mean values obtained in both series are

$$K_{CaCit^-} = [Ca^{2+}][Cit^{3-}]/[CaCit^-] = 0.00070\ M$$
$$K_{MgCit^-} = [Mg^{2+}][Cit^{3-}]/[MgCit^-] = 0.00028\ M$$

both at $\mu = 0.16\ M$ and 25°.

Discussion

In Table III values obtained by several authors have been recalculated. The results of Heinz[6] have been omitted for the reasons given by Davies and Hoyle.[12,13] The latter authors did not determine $K_{CaCit^{2-}}$.

All of these authors employed pM methods and calculated Cit^{3-} as (total Cit- $MCit^-$). $[Na^+]$ can be taken as equal to total [Na]. Therefore

$$[NaCit^{2-}] = [Cit^{3-}]\frac{[Na]}{K_{NaCit^{2-}}}$$

The reported value, k_{MCit^-} is

$$k_{MCit^-} = \frac{[M^{2+}]}{[MCit^-]} \times ([Cit^{3-}] + [NaCit^{2-}]) = \frac{[M^{2+}][Cit^{3-}]}{[MCit^-]} \times (1 + [Na]/K_{NaCit^{2-}})$$

The corrected value, K_{MCit^-}, is therefore obtained as

$$K_{MCit^-} = k_{MCit^-}/(1 + [Na]/K_{NaCit^{2-}})$$

The values for pK_{CaCit} obtained in this work are smaller than those previously reported. The values obtained for pK_{MgCit^-} are similar to the two prior estimates, after correction for $NaCit^{2-}$.

TABLE III

SUMMARY OF REPORTED VALUES FOR pK_{CaCit^-} AND pK_{MgCit^-}, BEFORE AND AFTER CORRECTION FOR THE COMPLEX $NaCit^{2-}$

Authors	Complex	Av. [Na], M	Obsd.[a] pK range	Cor. pK mean
Hastings, *et al.*[2]	$CaCit^-$	0 147	3.17–3.25	3.46
Joseph[5]	$CaCit^-$	13	3.00–3.29	3.44
Schubert and Lindenbaum[7]	$CaCit^-$	16	Av. = 3.15	3.46
Muus and Lebel[3]	$CaCit^-$	16	Av. = 3.22	3.33
This work	$CaCit^-$	11	2.85–3.04[a]	3.14
This work	$CaCit^-$	003	3.01–3.32	3.19
Hastings, *et al.*[2]	$MgCit^-$	147	2.90–3.50	3.46
Nordbö[4]	$MgCit^-$	15	3.16–3.34	3.46
This work	$MgCit^-$	098	3.26–3.47[a]	3.52
This work	$MgCit^-$	003	3.52–3.70	3.58

[a] Neglecting the complex $NaCit^{2-}$. All determinations at 25°, $\mu = 0.14$–$0.16\ M$.

(11) R. M. Smith and R. A. Alberty, THIS JOURNAL, **60**, 180 (1956).
(12) C. W. Davis and B. E. J. Hoyle, *J. Chem. Soc.*, 4134 (1953).
(13) C. W. Davies and B. E. J. Hoyle, *ibid.*, 1038 (1955).

THERMODYNAMIC PROPERTIES OF TiC AT HIGH TEMPERATURES

BY S. FUJISHIRO AND N. A. GOKCEN

University of Pennsylvania, Philadelphia, Pa.

Received July 27, 1960

Equilibrium pressure of gaseous titanium in the reaction TiC(s) = C(graph) + Ti(g) has been determined in the range of 2383–2593°K. by means of graphite Knudsen cells. Results are expressed by $\log P_{Ti}$ (atm.) $= -(30.830/T) + 7.65$ and the related thermodynamic properties of TiC are calculated.

The transition metal carbides of Group IV, V and VI in the periodic chart have useful properties such as high melting points, great hardness and chemical stability. Their thermodynamic properties, however, are not adequately known. Available data on a number of carbides have been summarized by Brewer and his associates[1,2] and others.[3–5] Brantley and Beckman[6] investigated the equilibrium in $TiO_2 + 3C = TiC + 2CO$ in the range of 1278–1428°K., but in view of the fact that oxygen and carbon are simultaneously soluble in TiC, and further, the proportions in TiO_2 and TiC vary with temperature and pressure of CO, the compositions of reactants and products are uncertain.[7,8] Recently, Chupka, *et al.*,[9] measured the vapor pressure of Ti(g) over TiC, by using a Knudsen cell and determined the relative amounts of the gaseous species by means of a mass spectrometer. They found that Ti in TiC vaporizes mainly as Ti(g) and that

(1) L. Brewer, L. A. Bromley, P. W. Gilles and N. L. Lofgren, "Thermodynamic and Physical Properties of Nitrides, Carbides, Sulfides, Silicides and Phosphides" Paper No. 4 in "Chemistry and Metallurgy of Miscellaneous Materials" edited by L. L. Quill, McGraw-Hill Book Co., Inc., New York, N. Y., 1950.
(2) L. Brewer and A. W. Searcy, *Ann. Rev. Phys. Chem.*, **7**, 259 (1956).
(3) F. D. Richardson, *J. Iron and Steel Inst.*, **175**, 33 (1953).
(4) J. F. Elliott and M. Gleiser, "Thermochemistry for Steelmaking," Vol. 1, Addison-Wesley Publishing Co., Inc., Boston, Mass., 1960.
(5) O. H. Krikorian, Univ. of California Radiation Lab. No. 2888, 1955.
(6) L. R. Brantley and A. O. Beckman, *J. Am. Chem. Soc.*, **52**, 3956 (1930).
(7) H. Nowotny and G. Glenk, *Z. Metallkunde*, **38**, 265 (1947).
(8) W. Dawihl and W. Rix, *Z. anorg. allgem. Chem.*, **244**, 191 (1940).
(9) W. A. Chupka, J. Berkowitz C. G. Giese and M. G. Inghram, THIS JOURNAL, **62**, 611 (1958).

TiC(g), was not detectable in the gas phase. The main purpose of their investigation, however, was to determine the relative amounts of various gas species over TiC and other carbides.

The purpose of this investigation was to measure the equilibrium pressure of gaseous titanium over TiC by using a graphite Knudsen effusion cell, *i.e.*, to investigate equilibrium in the reaction

$$\mathrm{TiC(s)} = \mathrm{C(graph.)} + \mathrm{Ti(g)} \qquad (1)$$

from the equilibrium constant $K = P_{\mathrm{Ti}}$ for this reaction at various temperatures, the related thermodynamic properties of TiC have been obtained.

Experimental Method and Results

The experimental method for the determination of vapor pressure by means of a Knudsen cell has been presented elsewhere in detail[10-12]; a brief summary here is therefore sufficient.

A graphite Knudsen cell, 1 inch o.d., $^3/_{16}$ inch wall, 1.5 inches high and with a tightly-fitting threaded plug in the bottom, was made of the densest and the most impervious grade graphite rods supplied by the National Carbon Company. A $^3/_4$ inch drill bit with a a tip angle of 140° was used to thin the top of the cell. After the determination of weight loss of the cell without orifice but containing TiC, as will be described later, a small cylindrical hole was drilled in the center. The cell was placed into a graphite crucible with 3 baffles, each having a $^1/_2$ inch hole in the center. The crucible was then packed into a clear silica tube with 0.7 mm. granular graphite. The silica tube was cemented to a Pyrex glass head at a tapered ground joint. The system was kept under a vacuum of 5×10^{-6} mm. by means of a diffusion pump having a speed of 55 liters per second. The graphite assembly was then heated by an induction coil connected to a 20-kilocycle, mercury-gap type converter. Temperature was measured with a calibrated optical pyrometer through a shielded window on the Pyrex head. Transmissivity of the window had been determined for correcting the observed temperature readings. The accuracy of temperature measurements was well within ± 10°. Attainment of uniform cell temperatures, as observed through various apertures in the crucible, was made possible by the baffles in graphite crucible, and by the adjustment of the position of induction coil.

The experimental runs were made as follows. The cell without orifice was charged with approximately 5 g. of pure iodide grade Ti which readily forms TiC at 2000°. It was observed that when titanium was melted, it wet the entire inner surface of the cell and then formed a shell of TiC. The cell was placed in the furnace and degassed at 2300° for 4 hr. The furnace was cooled and pure argon was admitted to break the vacuum. The cell was removed and weighed accurately, placed in the furnace again, brought quickly to the desired temperature under vacuum, and the temperature was maintained constant within ± 5° for a period of 5–8 hr. After the cell was cooled as rapidly as possible down to room temperature, it was reweighed to determine the resulting weight loss which represented vaporization of graphite and of Ti after Ti diffused out of the cell wall mostly through the pores. Diffusion of Ti was unavoidable because even the densest graphite available is not free from porosity. Resulting data are listed in Table I. The loss of graphite by the evolution of oxides or other compounds of carbon was negligibly small because an empty cell (without TiC) heated to a lower temperature of 2000°K., where the vapor pressure of carbon is very small, lost less than 0.5 mg. of carbon in 4 hr.

The cell was then drilled to the desired orifice size and reweighed; dirt and manual contact with the cell was avoided. It was then replaced into the graphite crucible and the foregoing procedure was followed. The resulting weight loss, shown in Table II, represented the loss through the orifice and that shown in Table I. The difference between the weight loss for a run in Table II and the corresponding run in Table I gave the amount of Ti(g) which had effused out of the orifice. The pressure P of Ti(g) in dynes/cm.^{2} was then obtained from[10]

$$p = \left(W/kat\right)\sqrt{\frac{2\pi RT}{M}} \qquad (2)$$

where W is the weight of effused Ti(g) in grams; a, the area of orifice in Cm.^{2} as determined with shadowgraphs before and after an experiment; t, time in seconds; M, the molecular weight of the effusing gas; T, absolute temperature in °K.; R, the ideal gas constant; k, a correction factor due to the thickness of orifice. "k" is known as the "Clausing factor"[13] which is expressed by $k = 1/(1 + 0.5\,h/r)$ where h is the thickness, and r, the radius of orifice. The pressures computed from eq. 2 are listed in Table II after the appropriate conversion of units.

TABLE I

EXPERIMENTAL RESULTS; CELLS WITHOUT ORIFICE AND CONTAINING TiC

Temp., °K.	Time, sec. × 10^{-4}	Wt. loss, mg.
2383	2.58	5.0
2435[a]	2.68	16.1
2435	2.16	9.8
2467	2.36	12.8
2488	2.10	12.3
2519	1.70	22.0
2541	1.73	28.3
2593	1.44	49.0

[a] Refers to a cell made of a different batch of graphite.

TABLE II

EXPERIMENTAL RESULTS; CELLS WITH ORIFICE AND CONTAINING TiC

Temp., °K.	Time, sec. × 10^{-4}	Orifice[a] area, mm.^{2}	Wt. loss, mg.	Wt. loss from orifice, mg.	P (atm.) × 10^6	ΔH_0^0
2383	2.52	0.502	8.0	3.1	3.9	145,150
2435	2.49	.502	21.9	6.9[b]	10.6	143,420
2435	2.37	.502	15.0	4.3	6.8	145,574
2467	2.36	.502	22.0	9.2	14.7	143,656
2488	2.38	.502	26.3	13.0	21.7	142,925
2519	2.52	.500	49.8	17.2	26.4	143,689
2519	2.88	.290	50.2	12.9	31.4	142,825
2519	2.88	.215	46.4	9.1	29.9	143,607
2541	1.80	.502	44.5	15.0	32.0	143,963
2593	1.44	.502	73.2	24.2	65.3	143,194
					Av.	143,800

[a] k, the Clausing factor is 0.85 for all runs except 0.8 for the last two runs at 2519°K. [b] *Cf.*-first run at 2435°K. in Table I.

The stoichiometric composition of TiC was determined by analyzing two samples prepared at 2200 and 2300°. Each sample was prepared by melting 10 grams of pure Ti in a graphite crucible and holding it at the desired temperature for 7 hours under vacuum. The results showed that the stoichiometric ratio of Ti to C was unity well within analytical errors, and in agreement with the Ti–C phase diagram summarized by Hansen and Anderko.[14] Hence, reaction 1 represents the correct dissociation process.

The loss of weight by vaporization of graphite was determined as follows. Four experimental runs, made at 2298, 2383, 2488 and 2593°K. yielded 0.20, 0.60, 1.74 and 8.25 mg./hr. of weight loss, respectively, from an empty cell. Results showed that the loss of graphite represented approximately half of the total loss in Table I. A plot of the logarithm of weight loss *versus* the inverse of absolute temperature followed very closely a straight line, and showed that

(10) M. Knudsen, "Kinetic Theory of Gases," Methuen, Ltd., 1934.

(11) R. Speiser and J. W. Spretnak, "Vacuum Metallurgy," Am. Electrochem. Soc., 1955.

(12) J. L. Margrave, Chapter 10 in "Physico-chemical Measurements at High Temperatures," Edited by J. O. Bockris, J. L. White and J. D. Mackenzie, Butterworth Sci. Publications, 1959.

(13) P. Clausing, *Ann. Physik*, **12**, 961 (1932).

(14) M. Hansen and K. Anderko, "Constitution of Binary Alloys," McGraw-Hill Book Co., New York, N. Y., 1958, p. 383.

vaporization of graphite increased quite rapidly above 2600° K.; hence above this temperature it was difficult to obtain satisfactory results.

Additional runs with various orifice sizes are represented in Fig. 1 which shows the effect of orifice area on the observed vapor pressure. This effect has been discussed in detail by Whitman[15] and by Motzfeldt.[16] Briefly it may be summarized by using Motzfeldt's equation in the form

$$1/P_{obs} = 1/P_{eq} + ka/\alpha AP_{eq} \qquad (3)$$

In this equation P_{obs} and $P_{eq.}$ are the observed and the equilibrium pressures, respectively; k and a, the same quantities as before; α is the accommodation coefficient; and A, the surface area of TiC in cm.^{2}. When $1/P_{obs.}$ is plotted *versus* ka as shown in Fig. 1, extrapolation to zero orifice area gives $1/P_{eq.}$. The relationships in Fig. 1 are linear in the range of a = 0-0.7 mm.^{2}. The slopes of the lines in this range represent $1/\alpha AP_{eq.}$ which should be as small as possible for obtaining vapor pressures close to the equilibrium values. Figure 1 shows that when the orifice area is less than 0.7 mm.^{2}, the slope is small enough so that the observed pressure is the equilibrium pressure within experimental errors. When the orifice area is too large Ti is depleted from the surface of TiC and, therefore, Motzfeldt's equation is not followed. The data in Table II with a < 0.502 mm.^{2} are, therefore, very close to the equilibrium values.

The standard free energy change for each run is obtained from

$$\Delta F^0 = -RT \ln P_{Ti}$$

and then ΔH_0^0 is computed from

$$\Delta\left(\frac{F^0 - H^0}{T}\right) \equiv \frac{\Delta F^0}{T} - \frac{\Delta H_0^0}{T}$$

by using the free energy functions for Ti(g) and C(graph) listed by Stull and Sinke.[17] and for TiC(s) in the Bureau of Standards Report[18] No. 6645. The results are listed in the last column of Table II. From the average value of ΔH_0^0 = 143,800 ± 2000 cal. herein and the foregoing tabular data.[17,18] $\Delta H^0_{298.15}$ = 144,758 cal., ΔH^0_{2500} = 141.064, and ΔS^0_{2500} = 35.00 are obtained for reaction 1. Assuming that in the range of 2500 ± 200°K. ΔH^0 and ΔS^0 may be taken as constants, ΔF^0 may be expressed adequately in two terms, *i.e.*, by ΔF^0 = 141,064 − 35.00T. This equation may then be rewritten in the following form to represent the data in Table II at high temperatures

$$\log P_{Ti}(\text{atm.}) = -\frac{30{,}830}{T} + 7.65 \qquad (4)$$

Correlation with Other Data.—For Ti(s) + C(graph) = TiC(s) calorimetric measurements of Humphrey[19] yield $\Delta H^0_{298.15}$ = −43,800 ± 2000 cal. The data of Edwards, Johnston and Ditmars[20] for Ti(s) = Ti(g) by the Langmuir method yield $\Delta H^0_{298.15}$ = 113,415 cal. Combination of these heat effects gives $\Delta H^0_{298.15}$ = 157,215 cal. for reaction 1 which is 12,467 cal. higher than the average result of this investigation. Extrapolation of this quantity to 2500°K., and using[17,18] ΔS^0_{2500} = 35.00 yields

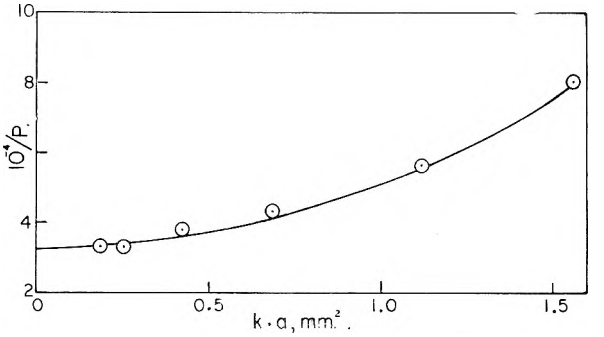

Fig. 1.—Variation of the observed pressure of Ti(g) over TiC + C(graph) with the orifice area.

$\log P_{Ti}(\text{atm.}) = -(33{,}550/T) + 7.65$ for reaction 1. The pressure of Ti(g) from this equation is about 12 times lower than that from eq. 4. The standard heat of formation of TiC computed from the present data is $\Delta H^0_{298.15}$ = −31,333, which is lower than Humphrey's result again by 12,467 cal. The discrepancy is rather difficult to account for. The authors have checked their method[21] with Cr_3C_2 and found excellent agreement with similarly computed results from published data. Most of the possible sources of error[16] in the effusion experiments would make the observed pressure low except simultaneously vaporizing substances. Vaporization of TiO (g) as a source giving higher weight losses is ruled out by thermodynamic calculations since any oxide of Ti would be reduced by graphite under high vacuum and at high temperatures. A small part of the discrepancy can be attributed to the uncertainties in and the long extrapolation of the heat capacity of TiC which is based on Naylor's original data[22] in the range of 373–1735°K. It is felt that additional data on the sublimation of titanium and the heat capacity of TiC are needed to account for the greater part of the discrepancy.

A single value of P_{Ti} = 8.6 × 10^{-7} atm. over TiC at about 2500°K. reported by Chupka, *et al.*,[9] is subject to a probable error of 100° in temperature fluctuations and measurements[23] and therefore no additional comparison will be made with their result.

Acknowledgment.—The authors are indebted to Mr. A. I. Kemppinen for carrying out the preliminary experiments. They also wish to express their appreciation for the constructive criticisms and discussions by Drs. R. J. Thorn, W. A. Chupka and O. C. Simpson of the Argonne National Laboratories. This research was sponsored by the U. S. Atomic Energy Commission, Contract AT(30-1) 1976.

(15) C. I. Whitman, *J. Chem. Phys.*, **20**, 161 (1952).

(16) K. Motzfeldt, THIS JOURNAL, **59**, 139 (1955).

(17) D. R. Stull and G. C. Sinke, "Thermodynamic Properties of the Elements," Am. Chem. Soc., Washington, D. C., 1956.

(18) National Bureau of Standards Report 6645, Table 2-38, 1960.

(19) G. L. Humphrey, *J. Am. Chem. Soc.*, **73**, 2261 (1951); for the uncertainty (±) see reference 18, p. 6.

(20) J. W. Edwards, H. L. Johnston and W. E. Ditmars, *ibid.*, **75**, 2467 (1953).

(21) S. Fujishiro and N. A. Gokcen, *Trans. Am. Inst. of Min. and Met. Eng.*, to be published.

(22) B. F. Naylor, *J. Am. Chem. Soc.*, **68**, 370 (1946). See also ref. 18.

(23) W. A. Chupka, private communication.

THERMODYNAMIC STUDIES OF HYDROBROMIC ACID IN ANHYDROUS ETHANOL[1]

BY LOYS J. NUNEZ AND M. C. DAY

Coates Chemical Laboratories, Louisiana State University, Baton Rouge, La.

Received August 4, 1960

Electromotive force measurements were made at 25° on the cell without liquid junction Pt, H_2(1 atm.) |HBr(m) ethanol| AgBr, Ag. The standard electrode potential of the silver, silver bromide electrode in anhydrous ethanol was determined to be −0.1939 v. on the molar concentration scale and −0.1816 v. on the molal concentration scale. Mean molal activity coefficients are tabulated and the $\mathring{a}$ value for hydrobromic acid in ethanol is determined. A new method for the preparation of silver–silver bromide electrodes is reported.

Introduction

Although there have been several determinations of the standard electrode potential of the silver–silver chloride electrode in anhydrous ethanol[2] and the standard potentials of both the silver–silver chloride and silver–silver bromide electrodes in anhydrous methanol,[3,4] there have been no comparable studies of the silver–silver bromide electrode in ethanol. From both a practical and a theoretical point of view the potential of the silver–silver bromide electrode in ethanol should be of interest. The greater solubility of the bromide salts of the alkali metals in ethanol compared to the corresponding chloride salts would indicate the possibility of a broader range of concentration studies. And in terms of simple solution concepts, a knowledge of the standard potential might lead to some general correlations.

For this study the cell without liquid junction

Pt, H_2(1 atm.) |HBr(m), ethanol| AgBr, Ag

was used to determine the standard potential of the silver–silver bromide electrode and to evaluate the activity coefficients of hydrobromic acid.

Experimental

Chemicals.—The anhydrous ethanol was prepared using a modification of the Bjerrum Method.[5] In order to remove trace quantities of benzene, 2% water by volume was added to U.S.I. absolute ethanol, U. S. P. grade, and the mixture was fractionally distilled. When the benzene had been removed as the benzene–water–ethanol azeotrope, magnesium alcoholate prepared from dry ethanol and magnesium was added in the ratio of 1 g. of magnesium alcoholate to 6.5 ml. of benzene-free ethanol. This solution was refluxed until free of water and was then immediately fractionally distilled. The middle fraction was taken as the pure anhydrous ethanol. All joints in the distillation apparatus were glass to glass with no stopcock grease being used. Both distillations were monitored by means of the Beckman Model D.K. Spectrophotometer. Using this method of detection, the maximum weight per cent. of benzene present should be less than 0.008 and that of water should be less than 0.02.

The anhydrous HBr was obtained from the Matheson Co., Inc., and all HBr solutions were prepared immediately before their use to minimize reaction between the ethanol and the HBr.

All ethanol and ethanol solutions were kept in a nitrogen dry box with P_2O_5 used as a desiccant.

Electrodes.—The silver–silver bromide electrodes were prepared by sealing a silver wire of 1 mm. diameter in one end of a section of glass tubing having a slightly larger diameter than the silver wire. Approximately one centimeter of silver wire was allowed to protrude from the glass tube at both ends, one end serving as a means of electrical contact to the external circuit and the other end serving as the surface of the electrode. One end was then heated in a flame until molten, and a spherical droplet was allowed to form. After cooling, a paste of silver oxide was applied, and this was heated until a spongy surface of metallic silver had covered the spherical surface. The electrode was then anodized in a dilute KBr solution as usual until a layer of AgBr had covered the surface of the electrode. All silver–silver bromide electrodes used in this investigation were prepared in this manner. Within the limitations of our experimental methods, they gave results identical to those prepared by the usual thermal electrolytic method.[6] However, they showed greater stability in the ethanol solvent.

The hydrogen electrode was a commercially available one of the Hildebrand type. The electrode was replatinized every two or three runs or whenever the system showed signs of instability. All electrodes were stored in anhydrous ethanol.

Procedure.—The cell was constructed so as to permit the use of two silver–silver bromide electrodes and one hydrogen electrode. For all measurements, the cell was placed in a water-bath thermostated at 25.25 ± 0.05°. The criterion for equilibrium was a stable reading for a period of one hour. This usually required several hours after the initiation of hydrogen bubbling. Before introduction into the cell, the electrodes were soaked for approximately one hour in an ethanol solution of the same HBr molality as that used for the given run. Prepurified hydrogen, sold by the Matheson Co., Inc., was passed first through a hydrogen catalytic purifier. It then went through a silica gel column and into a bubbling tower filled with a solution of identical composition as that present in the cell. Measurements were made at random choices of the concentration. After completion of a run, aliquots of the ethanol–HBr solution were withdrawn from the cell and titrated with a standardized solution of NaOH using phenolphthalein as an indicator. All concentrations should be accurate to within 0.02%.

Standard Electrode Potential.—Assuming the existence of extensive ionic association, we chose to use the extrapolation procedure[7] based on the equation

$$(E^{0\prime} - E_a) = E + 2k \log \alpha y_\alpha C = E^0 \qquad (1)$$

Here α is the degree of dissociation of HBr in ethanol and y_α is the molar activity coefficient for an ionic concentration of αC. The relation between α and y_α is given by

$$\alpha = 1/2\left[-\frac{K}{y_\alpha^2 C} \pm \left(\frac{K^2}{y_\alpha^4 C^2} + \frac{4K}{y_\alpha^2 C}\right)^{1/2}\right] \qquad (2)$$

where K is the ionization constant for HBr in ethanol. The determination of E^0 involves, then,

(1) Taken from a portion of the thesis submitted to the Louisiana State University by Loys J. Nunez in partial fulfillment of the requirements for the degree of Doctor of Philosophy.

(2) H. Taniguchi and G. J. Janz, *J. Phys. Chem.*, **61**, 688 (1957).

(3) R. A. Robinson and R. H. Stokes, "Electrolyte Solutions," Butterworths Scientific Publications, London, 1955, p. 457.

(4) E. W. Kanning and A. W. Campbell, *J. Am. Chem. Soc.*, **64**, 517 (1942).

(5) H. Lund and J. Bjerrum *Ber.*, **64B**, 210 (1931).

(6) H. Taniguchi and G. J. Janz, *J. Electrochem. Soc.*, **104**, 123 (1957).

(7) H. S. Harned and B. B. Owen, "The Physical Chemistry of Electrolytic Solutions," 2nd Ed., Reinhold Publ. Corp., New York, N. Y., 1950.

the evaluation of α and y_α at various concentrations and the extrapolation of a plot of $(E^{0\prime} - E_\alpha)$ *vs.* HBr concentration to infinite dilution. In the region where this approach is valid, a straight line of zero slope should be obtained that intersects the axis at E^0.

In order to obtain α and y_α, a first-order approximation of y_α is obtained by calculating $y_\pm$ from the Gronwall, La Mer and Sandved extended terms of the Debye–Hückel theory using a particular value of the ion size parameter $\mathring{a}$. Once a y_α has been approximated, an α may be determined from eq. 2. This α is now used to recalculate y_α by again determining $y_\pm$ from the extended terms expression at a new concentration of α C. This method of successive approximations is continued until a final α and y_α are obtained.

The observed potentials for the cell, corrected to a hydrogen pressure of 1 atm. are presented in Table I and are summarized in Fig. 1, where they are plotted as a function of the log of the HBr molality.

TABLE I

CORRECTED ELECTROMOTIVE FORCE DATA OF THE CELL

Pt, H_2(1 atm.) |HBr(m)Ethanol| AgBr, Ag

Molal concn.	Molar concn.	E, v.
0.00291	0.00229	0.1363
.00325	.00255	.1330
.0103	.00807	.0824
.01510	.0119	.0630
.02300	.01804	.0454
.0290	.0228	.0351
.0364	.0286	.0211
.0440	.0346	.0137
.0530	.0416	.0097
.0631	.0496	.0010
.0682	.0536	− .0011
.0881	.0692	− .0134

The empirical equation for the curve within the concentration range studied may be expressed as

$$E = -0.1021 \log m - 0.1221 \qquad (3)$$

where m represents molal concentration. The determination of the molalities was based upon the following expression for the density in g./ml. of the solutions as a function of HBr normality

$$D = 0.07993N + 0.7855 \qquad (4)$$

Extrapolations based on $\mathring{a}$ values of 4.0, 5.0, 6.5 and 8.0 Å. were made. These are given in Fig. 2, and the pertinent calculations for the extrapolation based on an ion size of 5.0 Å. are given in Table II using selected points based on eq. 3. Of these four choices, a value of 5.0 Å. for the ion size parameter gave the only curve approaching a zero slope, and it approached this slope only at concentrations less than 0.003 M. Using this extrapolation, the E^0 value for the Ag, AgBr electrode has been taken as −0.1939 v. on the molar concentration scale and −0.1816 v. on the molal concentration scale. The reliability may be estimated to be ±0.5 mv.

Dissociation Constant of Hydrogen Bromide.— In order to use the extrapolation procedure chosen for this work, it is necessary to know the thermodynamic dissociation constant of HBr in ethanol. For this purpose, we have used the conductivity

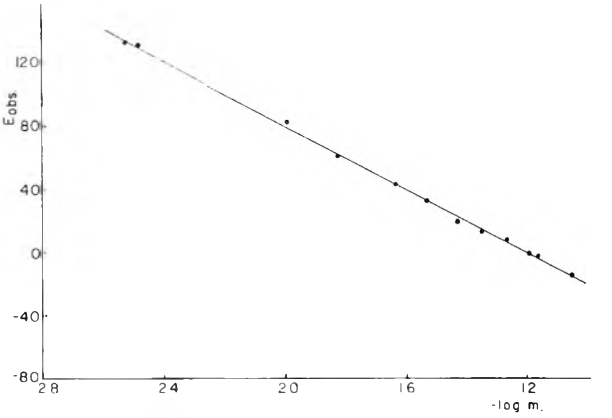

Fig. 1.—Corrected e.m.f. of the cell as a function of $-\log m_{HBr}$.

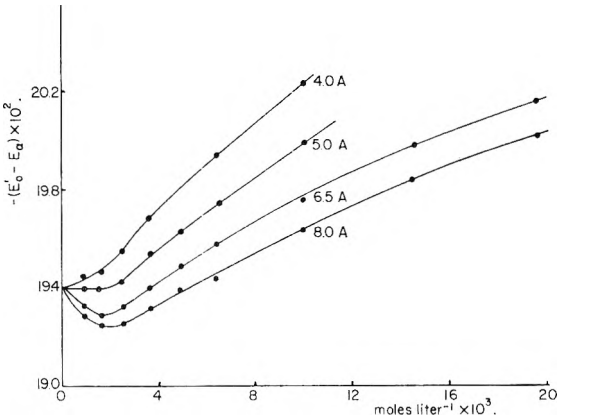

Fig. 2.—Extrapolation of $(E^{0\prime} - E_\alpha)$ in terms of molar concentration.

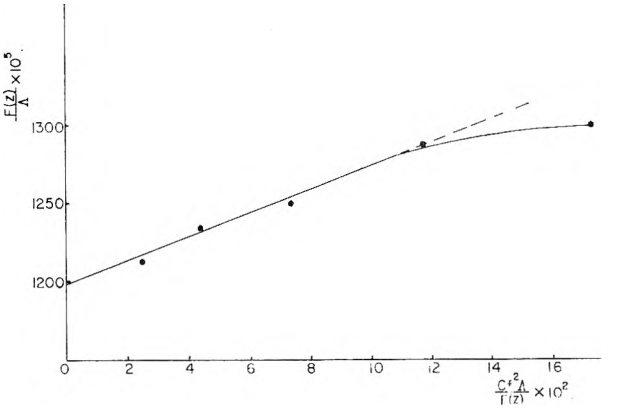

Fig. 3.—Evaluation of the dissociation constant of HBr in ethanol from the data of Goldschmidt and Dahll.

TABLE II

DETERMINATION OF $(E^{0\prime} - E_\alpha)$ ON THE MOLAR CONCENTRATION SCALE FOR $\mathring{a}$ = 5.0 Å.

C (mole/l.)	$E_{calc.}$ (v.)	α	y_α	$-(E^{0\prime} - E_\alpha)$ (v.)
0.0009	0.1783	0.970	0.818	0.1939
.0016	.1528	.950	.772	.1939
.0025	.1330	.940	.730	.1942
.0036	.1168	.920	.694	.1953
.0049	.1031	.910	.661	.1963
.0064	.0913	.895	.633	.1974
.0100	.0715	.870	.584	.1999

data of Goldschmidt and Dahll[8] along with the method of calculation proposed by Fuoss and Kraus.[9] This method should be valid as long as ionic interactions greater than pairwise are negligible. The relation between the conductance and the dissociation constant can be expressed as

$$\frac{F(Z)}{\Lambda} = \frac{1}{K\Lambda_0^2}\left[\frac{y_\alpha^2 C\Lambda}{F(Z)}\right] + \frac{1}{\Lambda_0} \qquad (5)$$

where Λ and Λ_0 are the equivalent conductance and equivalent conductance at infinite dilution, respectively, and $F(Z)$ is a function defined and tabulated by Fuoss. If $F(Z)/\Lambda$ is plotted against $y_\alpha^2 C\Lambda/F(Z)$, a straight line of slope $1/K\Lambda_0^2$ and intercept $1/\Lambda_0$ should be obtained. The results of these calculations on the data of Goldschmidt and Dahll are given in Table III, and the corresponding plot is seen in Fig. 3. These lead to a value for the dissociation constant of 0.0187 mole/l. for HBr in ethanol at 25°. This is a quite reasonable result in the light of the accepted value for the dissociation constant for HCl in ethanol[10] of 0.0113 mole/l.

Activity Coefficients of Hydrobromic Acid.—

(8) H. Goldschmidt and P. Dahll, *Z. physik. Chem., Leipsig*, **114**, 1 (1925).

(9) R. M. Fuoss, *J. Am. Chem. Soc.*, **57**, 488 (1935); R. M. Fuoss and C. A. Kraus, *ibid.*, **55**, 476 (1933).

(10) I. I. Bezman and F. H. Verhoek, *ibid.*, **67**, 1330 (1945).

TABLE III

DETERMINATION OF THE IONIZATION CONSTANT OF HBr IN ETHANOL

C (mole/l.)	Z	$F(Z)$	α	$y\alpha^2$	$F(Z)/\Lambda$	$C\Lambda^2/F(Z)$
0.00625	0.1624	0.82073	0.911	0.359	0.01301	0.1723
.00312	.1194	.87214	.923	.483	.01284	.1174
.00156	.0870	.90873	.947	.593	.01250	.0737
.000781	.0629	.93495	.959	.690	.01235	.0436
.000391	.0453	.95362	.976	.767	.01213	.0247

The molal activity coefficients were determined from the equation

$$\log \gamma_\pm = \frac{E_m^0 - E_m}{0.11832} - \log m \qquad (6)$$

in which $\gamma_\pm$ is defined such as to approach unity at infinite dilution in ethanol. Values of $\gamma_\pm$ are listed in Table IV, for convenient choices of the concentration.

TABLE IV

MEAN MOLAL ACTIVITY COEFFICIENT OF HYDROBROMIC ACID IN ETHANOL

Molal concn.	$\gamma_\pm$	Molal concn.	$\gamma_\pm$
0.005	0.649	0.04	0.488
.01	.590	.05	.474
.02	.537	.07	.452
.03	.507	.10	.431

DIALYSIS STUDIES. III. MODIFICATION OF PORE SIZE AND SHAPE IN CELLOPHANE MEMBRANES

BY L. C. CRAIG AND WM. KONIGSBERG

Rockefeller Institute Laboratories, New York, N. Y.

Received August 5, 1960

A search has been made for various ways of modifying the porosities of cellophane dialysis membranes. Mechanical stretching, acetylation and zinc chloride treatment have been found effective. Optimum porosities for studying solutes of molecular weights varying from the size of dipeptides to proteins of molecular weight over 100,000 can be made at will.

Introduction

Previous membrane diffusion studies from this Laboratory[1-3] have shown considerable promise in the use of this approach as a tool for separation and characterization of solutes with respect to their shape and size. Many factors, such as porosity of the membrane, temperature, *p*H, solvent, ionic strength, etc., were found to influence more or less the rate of diffusion of a particular solute through a membrane but perhaps even more interesting, the relative rate of diffusion of one solute as compared to another. The various factors showed considerable interdependence but the role of each factor could be revealed largely by comparative studies with solutes of known size and shape under standardized conditions.

It soon became evident in our studies[4] that the greatest selectivity in distinguishing one solute from another or of the effect of change of one of the factors, such as temperature, was achieved when the solute of interest was barely able to diffuse through the membrane. It, therefore, became highly desirable to learn how to change the porosity of the membrane without altering appreciably its properties in any other way.

Mechanical stretching seems to offer one possibility. When a wet cellophane casing is slowly stretched to near the bursting point by hydrostatic pressure, it will only partially return to its original size on release of the pressure. Such an enlarged casing will have a thinner wall but more important will permit those solutes which would barely diffuse through before treatment now to pass through at a much accelerated rate.

On the other hand, when a wet inflated casing with no hydrostatic pressure inside is stretched longitudinally to near the breaking point and then released, the tubing will return again only partly to its original size. It will have a permanently decreased diameter and those solutes which diffused through the unstretched membrane at a reasonable

(1) L. C. Craig and T. P. King, *J. Am. Chem. Soc.*, **77**, 6620 (1955).

(2) L. C. Craig, T. P. King and A. Stracher, *ibid.*, **79**, 3729 (1957).

(3) L. C. Craig, Wm. Konigsberg, A. Stracher and T. P. King, in Symposium on Protein Structure, p. 104, A. Neuberger, Ed., IUPAC Symposium July 1957, John Wiley and Sons, Inc., New York.

(4) This investigation was supported in part by a research grant, A-2493 B.B.C., from the National Institute of Arthritis and Metabolic Diseases of the National Institutes of Health, Public Health Service.

but retarded rate will now scarcely pass the longitudinally stretched casing.

Such mechanical treatment, from a theoretical viewpoint, offers a particularly interesting way of modifying pore sizes but can be accomplished only within certain limits. More drastic enlargement of pore size can be brought about by partial digestion of the casing with hydrolytic enzymes and by swelling the membrane with concentrated $ZnCl_2$.[5] Reduction of pore size has been accomplished by acetylation with acetic anhydride in pyridine and by this treatment subsequent to longitudinal stretching.

This paper will describe some of the experiments carried out thus far in connection with the modification of pore size and the behavior of these modified membranes in diffusion experiments.

Experimental

The experiments described here were all made with cellophane tubing purchased from time to time from the Visking Co., Chicago, Ill. Several different sizes were studied. Once received, a given roll was stored in the cold room in the plastic bag in which it had been sent in order that the porosity would not change with time.

The Stretching Trough.—The apparatus for the stretching experiments is shown in Fig. 1. A shallow trough of stainless steel was provided with two C clamps at either end. A suitable length of casing was cut, wetted and each end slipped over a glass collar whose outside diameter was near that of the inflated casing. The tubing was held on the glass collars by wrapping with a number of rubber bands sufficient to prevent slippage. Each glass collar was attached to the extended C clamp with a loop of string and the latter hooked over the ends of the trough A. One of the glass collars was closed with a solid rubber stopper. The other was closed with a rubber stopper through which passed a short piece of glass tubing. A rubber tube a few feet in length was attached to the glass tube at one end and to a levelling bulb at the other. The levelling bulb was filled with water. The upper opening of the bulb was closed by a rubber stopper and tube leading to a reducing valve for the application of controlled air pressure.

Air bubbles were expelled from the inflated casing into the levelling bulb by squeezing the casing. When hydrostatic pressure was not applied, longitudinal stretching was accomplished by tightening the clamps. The diameter of the tubing then decreased, sometimes as much as 30–40% at near the breaking point of the tubing. The original diameter and considerably more could be restored by applying hydrostatic pressure.

Since both the length and diameter could be measured at all times, the stretching could be done in such a way that the per cent. of increase longitudinally would be the same as that in the diameter. This gave the maximum increase in porosity.

Some lengths of tubing were not sufficiently uniform to stretch to a uniform diameter under hydrostatic pressure. This difficulty could be overcome by placing the tubing in a glass tube of the maximum inside diameter expected. The weakest part of the tubing would then reach this diameter under the hydrostatic pressure but stretch no further. Further pressure then would press all the tubing against the inside wall and give a more uniform size.

Different rolls of the Visking tubing showed somewhat different stretching characteristics. Certain rolls required up to 280 mm.

The Diffusion Cells.—Two slightly different types of cells have been effective. Schematic drawings of these are shown in Figs. 2 and 3. Both cells present the thinnest possible film of the dialyzing solution (about 0.1 to 0.2 mm. in depth) to the membrane. A different type of membrane diffusion cell has been proposed by Hoch and Turner.[6] It has certain advantages from the quantitative standpoint,

(5) J. W. McBain and R. F. Suewer, *J. Phys. Chem.*, **40**, 1157 (1936).

(6) H. Hoch and M. E. Turner, *Biochem. Biophys. Acta*, **38**, 410 (1960).

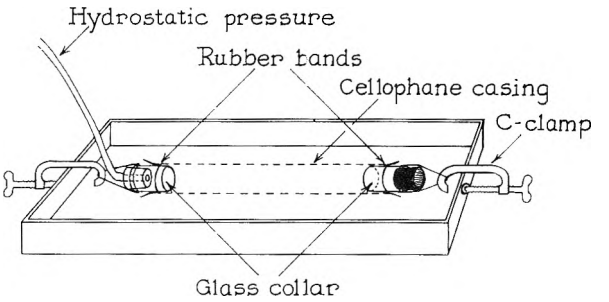

Fig. 1.—Assembly for controlled stretching of membranes.

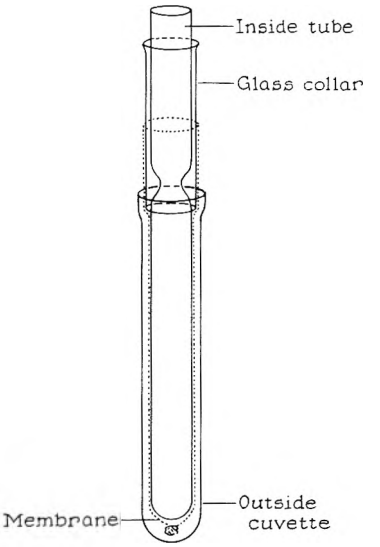

Fig. 2.—Cell for membrane diffusion.

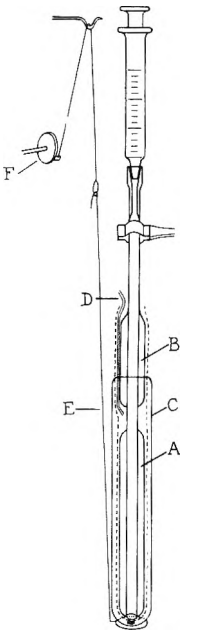

Fig. 3.—Alternate cell for longitudinally stretched membranes.

but the approach differs in other respects from the one in this Laboratory.

The cell in Fig. 2 differs only slightly from that earlier described[2] and will not be described in detail here. Instead of a hole at the top of the membrane to avoid pressure, a short length of fine polyethylene tubing, D of Fig. 2, served as the vent. The membrane was best tied off at the bottom with a silk thread.

With stretched membranes of different diameters, different sized cells were required. It is important to have the membrane fit the part A not too tightly nor yet too loosely. It should be adjusted so that without the cuvette C about twice the volume to be used inside should just begin to rise into the free space above A when the water is all in the annular space. If the membrane should be slightly too small, it can be stretched a little more by pinching off D and applying hydrostatic pressure from a larger syringe in place of the one customarily used. This also serves to check for leaks in the membrane. A rubber band around B can hold the membrane in place during this operation. Stretched membranes have a tendency to contract slightly over several days. The above procedure is convenient for readjusting them.

The cell shown in Fig. 2 can be used for membranes made less porous as well as for those made more porous. However, the one shown in Fig. 3 has certain advantages for the membranes made less porous. Here following the longitudinal stretching the glass collar used in the stretching operation was left on the membrane. Since the membrane was now of smaller diameter than the glass collar, an inside tube of the correct size for the membrane could be selected and easily passed through the collar. A constricted place on the inside tube just at the bottom of the glass collar provided

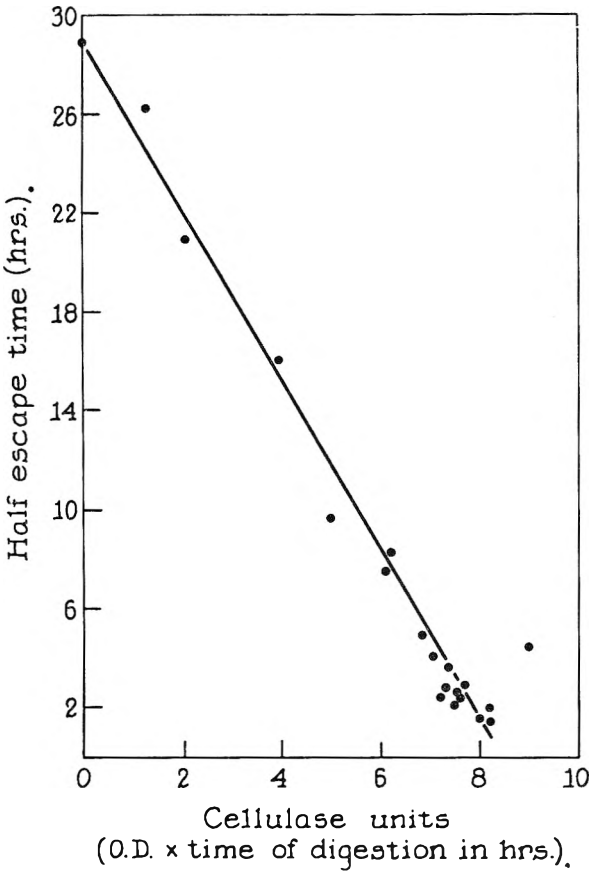

Fig. 4.—Curve for standardization of cellulose treatment of membranes.

the corresponding free space at the top of the membrane in case of expansion of the solution due to osmotic flow. The outside cuvette was flared sufficiently to permit it to pass over the glass collar and membrane a short distance as shown. The design permitted easy access to the inside solution by removal of the inside tube.

In both cases effective stirring could be accomplished in a very simple way. The inside part of the cell was held stationary by a clamp attached below the syringe joint in Fig. 2 or to the glass collar in Fig. 3. The outside cuvette in either case then could be made to move slowly up and down a distance of about a cm. by hooking a wire loop, E, a little smaller than the cuvette, over its lower end. The upper end of the wire was attached to a string which passed over a glass rod support to a motor-driven eccentric, F. The eccentric turned at a speed of about 13 r.p.m. Because of the flexibility of the membrane, this pumping action stirred the inside solution as well as the outside.

Acetylation of the Membrane.—A length of the tubing was wetted, the lower end tied off with silk thread and the upper opening slipped over a suitable glass collar. This formed an arrangement similar to that shown in Fig. 3 without the inside tube. The water in the membrane was then replaced by washing with dry pyridine. The cell, both the cuvette and inside were filled with a 10% solution of acetic anhydride in pyridine. After standing the required time, usually about 15 hr. at 25°, the solution was replaced with water and the membrane was washed with 0.01 *N* acetic acid until all the pyridine had been removed, *i.e.*, no further reduction of 260 mμ absorption in successive washes. This required several hours. On acetylation the membrane contracted somewhat and became less flexible. The membrane could be transferred to a cell of the type shown in Fig. 2 if desired but that shown in Fig. 3 was somewhat more convenient particularly when the membrane had been longitudinally stretched before acetylation.

Treatment of Membrane with $ZnCl_2$.—A solution containing 64 g. of anhydrous zinc chloride to 36 ml. of water was prepared.[5] A wet membrane of length somewhat longer than that needed for the cell was tied off at the bottom with the usual knot and a second knot to form a small loop. The upper end was put on a glass collar as in Fig. 3. A glass rod somewhat longer than the sac and bent at the lower end to hook into the second knot of the sac served to hold the sac stretched out but without strain. The rod could be held against the glass collar.

The $ZnCl_2$ solution at 25° was poured into the sac suspended in a 100-ml. graduate cylinder and the solution also poured into the graduate cylinder so that the membrane was in contact with the $ZnCl_2$ solution on both sides at the same time. Soon the membrane became very plastic and in order for the diameter of the tubing to remain as near uniform as possible the height of solution inside and outside must not differ greatly. A slight head of not more than a cm. was maintained inside during the treatment by adding more $ZnCl_2$ solution from time to time.

After the treatment period, usually from 1 to 15 min. depending on the porosity desired, the $ZnCl_2$ solution was carefully decanted and replaced by 0.01 *N* HCl. Here a little practice was required in order to avoid causing distortion while the membrane was in the plastic state. After several washes, the membrane was attached to a cell of the appropriate size preferably of the type shown in Fig. 2.

Treatment of Membranes with Cellulase.—A commercially obtained preparation of crude cellulase (Nutritional Biochemicals) from Aspergillus Oryzae was ground to a fine powder and dispersed in distilled water. After standing for 30 min., the suspension was centrifuged. The residue was re-extracted with water and centrifuged again. The brown supernatant solutions were combined. Optical density readings were taken at 280 mμ and the values obtained were used in making rough comparisons of enzyme concentrations of different samples of the enzyme. The solutions were stored at 4° and diluted as desired. The enzyme activity appeared to be relatively constant for periods up to one week.

Dialysis cells of the type shown in Fig. 2 were prepared as described above with 20/32 Visking. An arbitrary dilution of the enzyme in terms of O.D. units at 280 mμ in distilled water was placed both inside and outside the membrane at 25°. After an arbitrary time ranging between 1 and 16 hr., the cell was emptied and rinsed with 0.01 acetic acid. It was placed in a boiling water-bath for 10 min. to remove the last traces of enzyme activity.

The porosity obtained was measured by determination of the 50% escape time in a standard diffusion experiment with ovalbumin. Figure 4 is a plot of 50% escape time against the product of optical density at 280 mμ times the length of the digestion time in hours.

Discussion

Two main considerations make the present study of interest. One stems from the practical objective of having membranes of various sizes available for the separation of solutes differing widely in their size. The other has even greater interest not only for a better understanding of the selective mechanism which may be inherent in restricted diffusion but for the use of this information in the study of the size and shape of molecules.

The latter objective is a much more complicated one to realize than the first since the rate of diffusion of a solute through a membrane obviously depends on many factors. These include the nature of the membrane, the nature of the solvent, the nature of the solute, the temperature, the area of the effective membrane with respect to the volume of the solution of higher concentration and the effective concentration gradient. The nature of the membrane includes its thickness, the amount of porous space, the size and shape of the pores, its adsorptive properties and its ion-exchange properties. The nature of the solvent includes the *p*H, the viscosity of the solution and its solvent properties. The nature of the solute includes its size, its state of

association, its shape in solution and its charge at the particular *p*H of the solution.

Earlier studies[2,3] have given sufficient information about most of these factors so that experiments can be set up to give a reasonably good correlation between the size and/or shape of a particular solute. A more direct and certain correlation, however, has been desirable and is forthcoming in the present study.

There is at present considerable evidence[7] to indicate that the globular proteins can behave in solution as uniform suspended particles approaching a sphere in shape. At least this shape would be expected to provide the most rapid diffusion for a given size. The smallest hole through which such a sphere could diffuse would be a round one slightly larger than $(4/3)\pi r^3$ where r is the radius of the sphere. In order to pass a second ideal solute twice this size, it follows from the above relation of r to volume that a hole 1.26 times the diameter of the original one would be required.

The shape, depth and tortuosity of the pores in our particular cellophane are not known, but it might be expected that they would resemble somewhat the porous space in a sponge. Indeed, electron micrograph studies[8] with cellophane have indicated this to be true. Statistically these pores could offer a type of restricted diffusion which might be offered also by a series of holes of random shape and size as shown in Fig. 5a. A large solute barely able to pass the membrane could only pass through the largest holes while smaller ones could pass through any of the holes. Thus in addition to a higher free diffusion rate due to their smaller size, a much greater cross-sectional area also is provided for their diffusion. This is a possible although simplified explanation of the selectivity of the method of membrane diffusion.

If this reasoning is true, the stretching experiments become interesting since the over-all increased cross-sectional area of a membrane can be measured and compared with the relative restriction to diffusion offered to a solute of known size. Thus a membrane passing ribonuclease at 25° in 0.01 *N* acetic acid with a half-life of 6.6 hr., Fig. 6, was found to pass it with a half-life of 0.9 hr. when the membrane had been stretched both longitudinally and circularly about 20% after release of the pressure. Here a proportionately shorter cell was used so that about the same membrane area was provided. Obviously in order to account for this large increase in rate, many more pores have been increased to above the critical size which will permit ribonuclease to pass. No doubt, part of the increased speed of diffusion stems from the fact that the membrane is thinner after stretching. This, however, could certainly not account for more than a fraction of the difference noted.

On the other hand, if the casing is stretched in a longitudinal or linear way about 20% without the use of hydrostatic pressure, its diameter had decreased about 18%. A cell with the same membrane area as above was found to pass ribonuclease

(7) C. Tanford, in Symposium on Protein Structure, p. 35, A. Neuberger, Ed., IUPAC Symposium July 1957, John Wiley and Sons, Inc., New York.

(8) H. Spandau, *Angew. Chem.*, **65**, 183 (1953).

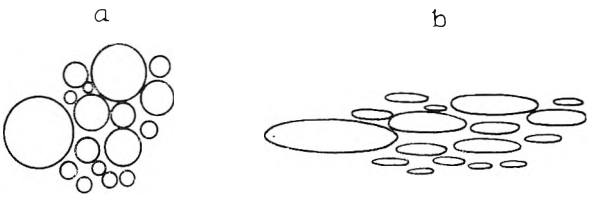

Fig. 5.—Schematic diagram of porous structures of membranes.

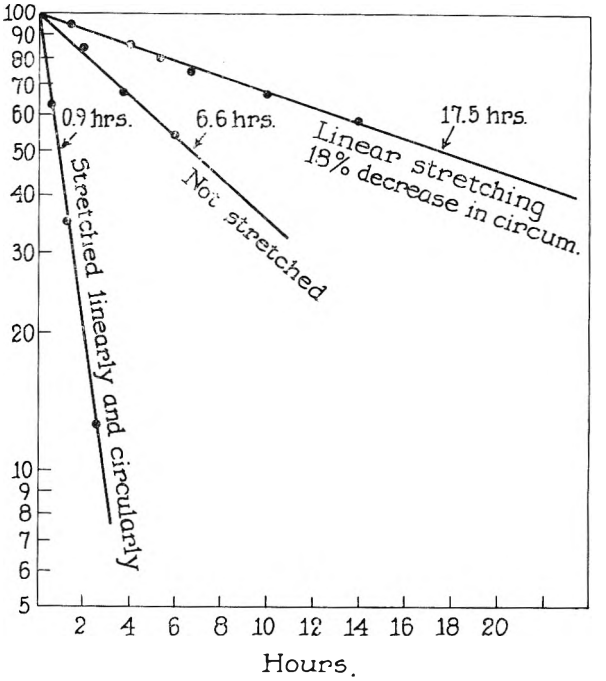

Fig. 6.—Escape curves of stretched membranes for ribonuclease.

at about 1/3 the rate, Fig. 6, as the unstretched membrane. In this case, many of the pores originally capable of passing the solute apparently could no longer do so.

An obvious explanation of this observation stems from the simplified concept of the pores shown in Fig. 5a. Stretching such a matrix in one direction only would be expected to provide holes of various sizes whose average shape would be elliptical rather than round as shown in Fig. 5b. Holes barely able to pass the sphere before this treatment would no longer permit passage after the alteration.

In an experiment with another somewhat more porous membrane, the half escape time of ribonuclease in 0.01 *N* acetic acid was 3.7 hr., Fig. 7. Another portion of the roll was stretched both longitudinally and circularly about 20% after release. A cell prepared from this casing was found to pass chymotrypsinogen with a half-life of 4.5 hr. as shown in Fig. 7. The unstretched membrane was found to pass chymotrypsinogen with a half-life of about 12 hr. Chymotrypsinogen, mol. wt. 25,000, is a little less than twice as large as ribonuclease, mol. wt. 13,600, assuming equal densities and shapes in this environment. The over-all stretching in cross-sectional area was about 1.45-fold. The somewhat faster than expected diffusion of chymotrypsinogen on this basis can be accounted for by the fact that the membrane also became

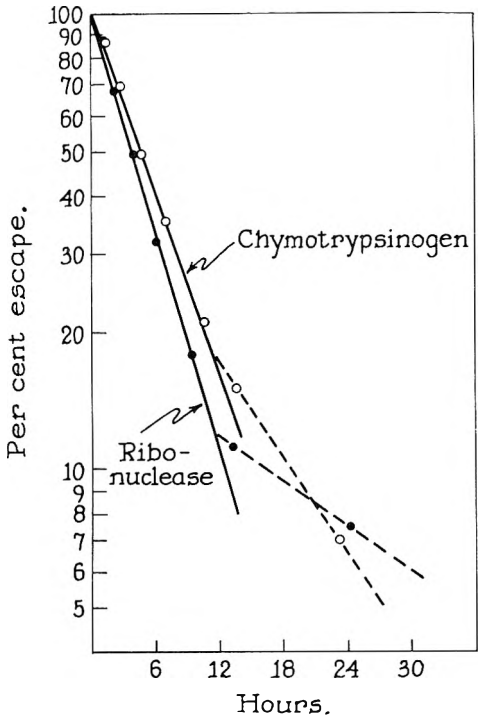

Fig. 7.—Comparative escape curves of ribonuclease and chymotrypsin.

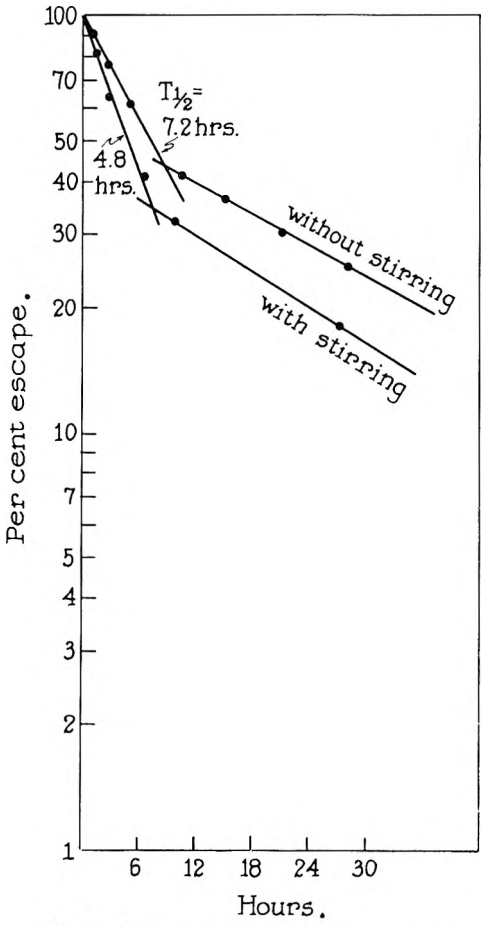

Fig. 8.—Effect of stirring on escape rate.

thinner on stretching. The pore channels would not be as long.

These rather simple experiments where the dimensions of the membrane are changed in a direct way offer strong proof that the method can be used in such a manner as to give a reliable measure of relative size and/or shape of various molecules in solution. The correlation noted could scarcely be due to factors other than size and shape. This conclusion has been reached with the understanding that other factors such as charge may play a decided role with these same solutes under other circumstances.

With this fundamental point disposed of, other considerations may be taken up in turn. One concerns stirring of the solutions. In the earlier work, no attempt was made to stir the solution because of the thin film nature of the solution of highest concentration. Recently, however, it has been found that efficient stirring easily can be achieved as described in the Experimental part. Stirring gives a faster over-all rate of diffusion as shown in Fig. 8 but seems to have no other effect. It does, however, permit the use of a membrane somewhat more loose on the holder which means the choice of the size of the cell for a particular membrane is not as critical as before. It will be noted that the break in the curve is higher than others previously reported. This seems to be characteristic of the particular bottle of ribonuclease as will be discussed elsewhere.

With the different sizes and different rolls within a size, a certain variation in stretching characteristics was noted. Certain rolls could be stretched further than others before breaking. Also certain rolls were less uniform in that pin holes were formed before final rupture. This was easily detected because of the hydrostatic pressure. However, with all the cellophane there was an upper limit to the amount of stretching feasible and attention was, therefore, directed toward chemical modification. Cellulase treatment and swelling with concentrated $ZnCl_2$ solution seemed to offer the most promise.

A commercially available crude cellulase preparation gave an aqueous solution which slowly attacked the membrane and made it more porous. The results were surprisingly reproducible as Fig. 4 indicates. However, digestion could be allowed to proceed only to a certain point as indicated in the figure before the membrane became mechanically too weak to use. The most porous membrane before digestion gave the most porous after digestion. This was also true after appropriate stretching to increase the pore size.

The data shown in Table I were obtained with one of the most porous, stretched and subsequently cellulase-treated membranes. The solvent was 0.01 *N* acetic acid. Obviously useful ranges of enlarged pore size can be obtained with cellulase but the membranes were always more fragile and were easily torn during the required manipulation. In fact with cellulase, it was not easy to get a stable membrane passing serum albumin at the rate shown. Many membranes passing ovalbumin in a range of 4–5 hr. half escape time would not pass serum albumin at all.

Treatment with $ZnCl_2$ solution offered a wider range of porosities and gave membranes with

TABLE I

COMPARATIVE ESCAPE RATES OF A SERIES OF PROTEINS THROUGH CELLULASE-TREATED CELLOPHANE

Protein	Mol. wt.	Half escape time, hr.
Trypsin	24,000	0.8
Pepsin	34,000	1.6
Hemoglobin	33,000[a]	1.5
Ovalbumin	45,000	2.0
Bovine albumin	67,000	14.5
Edestin	125,000	Does not escape

[a] Sub-unit.

stabilities not greatly different from untreated cellophane. The time required to reach a certain porosity in 64% $ZnCl_2$ seemed to vary with the particular cellophane. For example, a sample of 20/32 tubing treated for 15 min. was found to give a membrane which readily passed the dimer of human serum albumin,[9] mol. wt. 134,000. With this membrane the half escape times in 0.01 *N* acetic acid for ribonuclease, bovine serum albumin (monomer) and human serum albumin dimer were 0.25, 1 and 3 hr., respectively. Obviously this was too porous a membrane to give good selectivities with molecules of the size of ribonuclease or even of the size of the monomer of serum albumin. A shorter treatment should give a more optimum porosity and was found to do so. After 10 min. in the $ZnCl_2$ solution, a membrane was obtained which repeatedly passed the monomer of human serum albumin at a half escape time of 3 hr. The dimer slowly diffused through with a half escape time of more than 60 hr. When tested with a sample of human γ-globulin (mol. wt. from literature, 150,000), nothing diffused through.

A Zn-Cl_2-treated membrane was found to pass transfer RNA[10] in sodium chloride solution. Maximal stretching permitted only very slow diffusion.

A membrane from 23/32 Visking, originally much less porous and somewhat thicker than that from 20/32, could be treated for 16 min. before its strength was too greatly impaired. This membrane before treatment had a half escape time for subtilin, mol. wt. 3100, of several hours. After treatment it passed β-lactoglobulin, mol. wt. 35,000, to give a satisfactory escape curve with a half escape time of 3 hr. However, with the monomer of human serum albumin only very slow diffusion was permitted with a half escape time well beyond 60 hr. The $ZnCl_2$-treated membranes have shown the same characteristics as the untreated membranes as far as can be ascertained except that larger molecules must be used for their calibration and study. In some cases, membranes so treated have given persistent ultraviolet absorption from unknown substances shed into the solvents used for their calibration. This has been traced to a very fine turbidity which could be removed by filtration through a fine filter. Other ways of treating cellophane with $ZnCl_2$ to change the porosity[11] include varying the temperature or the concentration of the $ZnCl_2$.

For reduction of pore size, longitudinal stretching could not be made to close the pores beyond a certain range. After this treatment, acetylation was required to go further. Acetylation alone could be done in such a way that the membrane would not pass solutes larger than 1000, but further acetylation at higher temperatures gave a rather stiff membrane. On the other hand, when a membrane of low porosity such as 18/32 was stretched longitudinally to near the maximum and then acetylated, a more flexible membrane with the required low porosity was obtained.

A membrane from 18/32 Visking stretched approximately 30% longitudinally and then acetylated at 25° overnight in 27% acetic anhydride and pyridine gave the data shown in Table II. One treated similarly, except that it was acetylated for 3 hr. at 65°, gave the data in the last column. The higher selectivity of the slower membrane is very apparent. Comparison of these results with those obtained with molecules 10 and 100 times larger but with membranes of proportionately larger pore size is consistent with a selectivity based almost exclusively on size. A molecule 50% larger than another can be distinguished with about the same selectivity regardless of its size. For such comparisons, a membrane adjusted to a half escape time of 3 to 6 hr. for the solute of interest is experimentally a convenient range yet one offering reasonably high selectivity. With this rate a complete escape curve can be determined in about a day.

TABLE II

COMPARATIVE ESCAPE RATES OF A SERIES OF PEPTIDES THROUGH STRETCHED ACEYLATED CELLOPHANE

	Solute	Mol. wt.	25° acetylation Half time	65° acetylation Half time
1	$(NH_4)_2SO_4$	134	....	36 min.
2	Tryptophan	204	12 min.	48 min.
3	Gly·Tyr	238	20 min.	1.9 hr.
4	His·His	292	....	4.1 hr.
5	Gly·Gly·Gly	189	....	2 hr.
6	Val·Tyr·Val·His	516	36 min.	9.9 hr.
7	Ala·Ala·Try·Gly·Lys	508	....	14 hr.
8	Val·Phe·Val·His·Pro·Phe	744	45 min.	23 hr.
9	$AspNH_2$·Arg·Val·Phe·Val·His·Pro·Phe	1015	84 min.	....
10	Hypertensin I (a decapeptide)	1249	4 hr.	....
11	Bacitracin A[a] (a dodecapeptide)	1422	7.6 hr.	....
	Bacitracin A[a] (a dodecapeptide)		26 hr.	....

[a] In this experiment the solvent contained 1.0 *M* KCl in addition to 0.01 *N* acetic acid.

Some interesting structural correlations are possible from data such as those in Table II. For instance, peptide no. 7 is easily distinguished from 6 although it is a pentapeptide with a molecular weight slightly less than no. 6, a tetrapeptide. Again no. 8, a hexapeptide, can be distinguished easily from 7. Here the proline may be of especial interest from the standpoint of conformation.

The experiment with bacitracin is particularly interesting from a structural standpoint. In contrast to our experience with proteins and the effect of salt on the escape rate, an accelerated rate was noted as compared to salt-free 0.01 *N* acetic acid. In the analytical Spinco ultracentrifuge, Dr. D.

(9) T. P. King, D. Yphantis and L. C. Craig, *J. Am. Chem. Soc.*, **82**, 3355 (1960).

(10) J. Goldstein and L. C. Craig, *ibid.*, **82**, 1833 (1960).

(11) W. B. Seymour, *J. Biol. Chem.*, **134**, 701 (1940).

Yphantis found a molecular weight approximating 1400, a value in agreement with the monomer for bacitracin A in the salt-acetic acid solution. The possibility of dimerization in the salt-free acetic acid solution is not excluded, but it seems more likely that a shift in conformation is involved. This would be interesting in the light of the known labile structure[12] of bacitracin. Because of charge effects, the molecular weight could not be studied with reliability by centrifugation in salt-free acetic acid. However, in 0.1 *N* KCl–0.01 *N* acetic acid the same value of 1400 was obtained by sedimentation rate, but the half escape time here was also the higher value of 26 hr.

The more subtle structural interpretations of data such as those presented in Table II must be left until much more data with synthetic well-characterized peptides are at hand. However, a very interesting and important field of study is indicated.

From the reasoning suggested by Fig. 5, the distribution of pore sizes probably is important in achieving high selectivity. This is strongly suggested by the observation that selectivity improves so much when only the larger pores are able to pass the solute. However, little is known about the distribution actually present and whether or not stretching changes this distribution. It might be expected that longitudinal stretching would tend to make the effective diameters more uniform since the larger holes would tend to collapse relatively more. A more narrow range of pore size should give greater selectivity.

It would not be surprising to find that part of the high selectivity of many column processes, particularly those requiring porous supports, can result from the type of effect shown here. The newer "Sephadex"[13] chromatography is particularly interesting in its connection. In our experience, it has proven a very effective separation tool but does not separate solutes only on the basis of size as had originally been hoped. The adsorption effects have also been noted by others.[14]

We wish to thank Dr. Schwyzer and Dr. Wettstein of the Ciba Co. for a gift of most of the peptides used for the data given in Table II.

(12) Wm. Konigsberg and L. C. Craig, *J. Am. Chem. Soc.*, **81**, 3452 (1959).

(13) J. Porath and P. Flodin, *Nature*, **183**, 1657 (1959).

(14) B. Gellotte, *J. Chromatography*, **3**, 330 (1960).

THE B_5H_{11}–H_2–B_2H_6–B_4H_{10} GAS PHASE EQUILIBRIUM

BY ROBERT G. ADLER AND ROBERT D. STEWART

American Potash & Chemical Corporation, Whittier Research Laboratory, 201 West Washington Boulevard, Whittier, California

Received August 15, 1960

Equilibrium constants for the reaction $2B_5H_{11}(g) + 2H_2(g) \leftrightarrows 2B_4H_{10}(g) + B_2H_6(g)$ have been measured at 100.0, 112.4, 126.1 and 140.0°. The enthalpy change of the reaction has been calculated to be −7.56 kcal./mole and the entropy change to be −19.5 e.u./mole in the temperature range 100–140°.

Introduction

The equilibrium $2B_5H_{11}(g) + 2H_2(g) \leftrightarrows 2B_4H_{10}(g) + B_2H_6(g)$ was first observed by Burg and Schlesinger[1] in a study of the preparation of B_5H_{11}, its thermal decomposition and reaction with hydrogen, but no values for the equilibrium constants were reported. The present authors reported some preliminary equilibrium constants for the system calculated from values obtained for these species in a study of diborane pyrolysis.[2] The work reported here is an extension of these preliminary studies. The equilibrium was approached from both directions and was also determined in the copyrolysis of diborane and both pentaboranes to determine whether equilibrium was attained in the presence of these compounds. Equilibrium constants were determined at four temperatures from 100 to 140° and the entropy and enthalpy of the reaction were calculated from the constants.

Experimental

Diborane was prepared by the reaction of boron trifluoride etherate with lithium aluminum hydride in ethyl ether.[3] Pentaborane-11 was prepared by the pyrolysis of diborane in a flow system at 112° and a residence time of three minutes. This material had a vapor pressure of 52.1 mm., at 0° (literature value 52.8 mm.).[1] Analysis of the infrared spectrum failed to detect other boron hydride species.

Tetraborane was prepared by the reaction of pentaborane-11 with water,[4] and purified by distillation from −78° to a −150° trap.

Pyrolyses were carried out in sealed glass bulbs. The bulbs were immersed in an oil-bath in which the temperature was held constant within ± 0.1°. Timing was started upon immersion of the bulb. At 0.1 min. before the predetermined pyrolysis time the bulb was removed from the bath and allowed to drain for 0.1 min. It was then quenched in carbon tetrachloride at 0°, wiped quickly and the tip immersed in liquid nitrogen to freeze out the condensables. The bulb was then attached to a vacuum line through an opening device and the hydrogen transferred to a gas buret by a Sprengel pump. The volatile hydrides were transferred out of the bulb and the tetraborane and pentaboranes were separated from the diborane. The separation was accomplished by fractional condensation at −150 and −196°, at pressures on the order of 1 mm. Two such fractionations gave separations which were reproducible within 2–3%. The fraction passing the trap at −150° was measured as diborane. The −150° condensate also was measured as a vapor, and analyzed by the method of McCarty, *et al.*,[5] using equations developed from reference spectra made in this Laboratory.

Results

Equilibrium constants calculated for the reaction

(1) A. B. Burg and H. I. Schlesinger, *J. Am. Chem. Soc.*, **55**, 4009 (1933).

(2) R. D. Stewart and R. G. Adler, Paper presented before the Division of Physical Chemistry, 134th A. C. S. Meeting, Chicago, September 1958.

(3) I. Shapiro, H. G. Weiss, M. Schmich, S. Skolnik and G. B. L. Smith, *J. Am. Chem. Soc.*, **74**, 901 (1952).

(4) J. L. Boone and A. B. Burg, *ibid.*, **80**, 1519 (1958).

(5) L. V. McCarty, G. C. Smith and R. S. McDonald, *Anal. Chem.*, **26**, 1027 (1954).

$$2B_5H_{11}(g) + 2H_2(g) \rightleftharpoons 2B_4H_{10}(g) + B_2H_6(g)$$

are shown in Table I. From a plot of ln k_p *versus* $1/T$, the enthalpy and entropy changes for the reaction were determined as -7.56 kcal./mole and -19.5 e.u./mole by the method of least squares. These values appear valid for the range 100–140°. The linearity of the plot (within experimental error) appears to indicate that ΔC_p for the reaction over the temperature range studied is small, of the order of 1 cal./mole/°K. or less.

TABLE I

EQUILIBRIUM CONSTANTS FOR THE REACTION

$2B_5H_{11}(g) + 2H_2(g) = 2B_4H_{10}(g) + B_2H_6(g)$

Reactants	K_p (atm.$^{-1}$)
100.0°	
B_2H_6 760 mm.	1.52
B_2H_6 760 mm., B_4H_{10} 50 mm.	1.50
B_5H_{11} 60 mm., H_2 250 mm.	1.37
Av.	1.46
112.4°	
B_2H_6 760 mm.	1.06
B_2H_6 760 mm., B_4H_{10} 50 mm.	1.02
B_2H_6 760 mm., B_5H_{11} 50 mm.	0.99
B_2H_6 760 mm., B_5H_9 125 mm.	1.01
B_5H_{11} 50 mm., H_2 500 mm.	1.03
Av.	1.02
126.1°	
B_2H_6 760 mm.	0.77
140.0°	
B_2H_6 760 mm.	0.54

The time required to reach equilibrium varied with the temperature. The approach of the equilibrium constants to steady values in the pyrolysis of diborane is shown in Fig. 1. At each temperature equilibrium was attained in all of the systems studied at approximately the same rate with the exception of the diborane–pentaborane-9 system in which the rate was slightly slower. It is interesting, however, that the value of this equilibrium constant was in good agreement with that of the other systems even though it is known that pentaborane-9 reacts with diborane to form decaborane.[6]

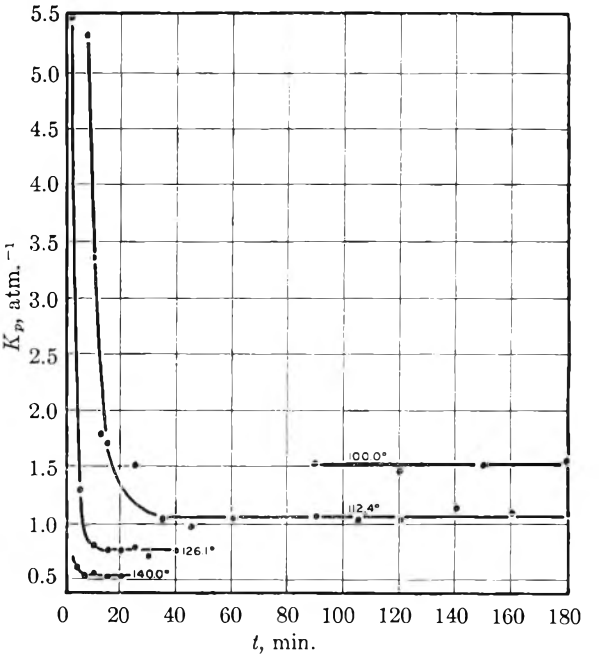

Fig. 1.—Approach to equilibrium at four temperatures in pyrolysis of diborane.

Acknowledgment.—The authors wish to acknowledge the support of this work by Wright Air Development Center under Contract AF 33(616)-488, 1956 Extension.

(6) M. Hillman, D. J. Mangold and I. H. Norman, Abstracts of 133rd A. C. S. Meeting, San Francisco, April, 1958, p. 18L.

THE HEAT CAPACITY OF AND A TRANSITION IN IRON(II) IODIDE ABOVE ROOM TEMPERATURE

BY FRANKLIN L. OETTING AND N. W. GREGORY

Department of Chemistry, University of Washington, Seattle, Washington

Received August 15, 1960

The heat capacity of FeI_2 has been measured between 70 and 500°. An anomaly suggestive of a second-order transition is observed between 360 and 385°. Powder patterns fail to show structural change associated with the anomaly.

The structural and thermodynamic properties of the iron(II) halides have been under study in this Laboratory for some time. In crystals of $FeCl_2$, $FeBr_2$ and FeI_2 grown from the vapors the metal ions are surrounded octahedrally by halogen ions and the layers of halogen ions are in a close-packed arrangement, CCP for $FeCl_2$ ($CdCl_2$ type structure) and HCP for $FeBr_2$ and FeI_2 ($Cd(OH)_2$ type structure). $FeCl_2$ and $FeBr_2$, when prepared by dehydration of their monohydrates, form crystals with the same general arrangement except that the halogen layers are stacked randomly[1]; powder samples of $FeCl_2$ have also been prepared in which both CCP and HCP arrangements have been detected.[1] Similar variations of structure have not been observed for FeI_2.

The heat capacity *vs.* temperature curve for $FeBr_2$ above room temperature shows an anomaly, beginning at about 360° and extending over a 45° temperature interval, with a shape suggestive of a second-order transition.[2] X-Ray powder patterns

(1) R. O. MacLaren and N. W. Gregory, *J. Am. Chem. Soc.*, **76**, 5874 (1954).

(2) N. W. Gregory and H. E. O'Neal, *ibid.*, **81**, 2649 (1959).

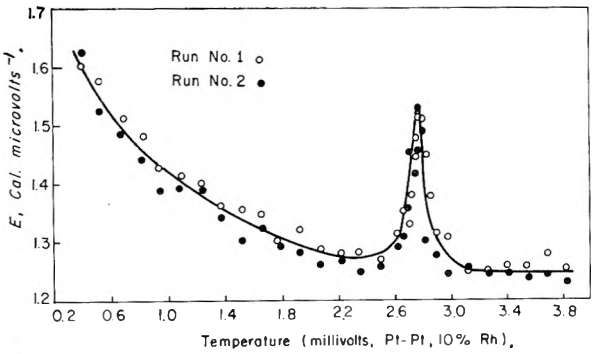

Fig. 1.—Energy per microvolt *vs.* temperature for cell filled with iron(II) iodide—sample A.

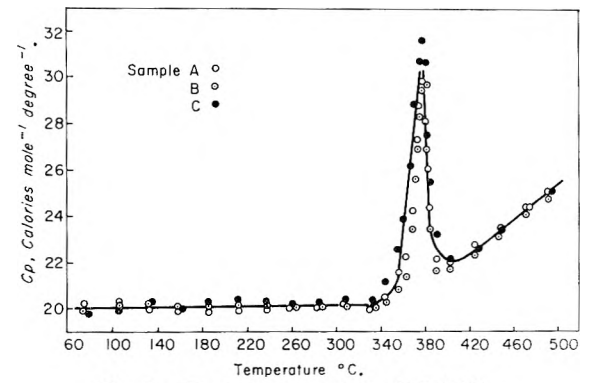

Fig. 2.—Heat capacity of iron(II) iodide.

indicated a structural change associated with this transition, although they did not provide sufficient evidence to establish the structure of the high temperature form. Both HCP and RP forms of $FeBr_2$ were observed to undergo the transition, HCP reversibly but RP irreversibly, the latter reverting to the HCP structure when cooled below the transition temperature.

The heat capacities of both the RP and CCP forms of iron (II) chloride have been measured between 60 and 500°.[3] An anomaly of the kind observed in $FeBr_2$ was not detected. After cooling a sample originally in the RP form (heated in the calorimeter to 500°), it was observed (by X-ray powder analysis) to have changed to the CCP form; however no anomaly in the heat capacity curve was detected and no measurable difference (*i.e.*, more than ± 1%) in the heat capacities of the material initially in RP and CCP forms was observed. Hence it appears that no significant energy effect is associated with the change of $FeCl_2$ from a random packed to a cubic close-packed form.

In the present work we have measured the heat capacity of FeI_2 between 70 and 500°. An anomaly similar to the one observed in $FeBr_2$ and at virtually the same temperature is found in the heat capacity curve; however, unlike $FeBr_2$, no change in structure of FeI_2 could be detected in powder patterns taken above and below the transition region. Analytical results indicate that FeI_2, when prepared by sublimation *in vacuo*, is slightly deficient in iodine.

(3) F. L. Oetting and N. W. Gregory, THIS JOURNAL, **65**, 138 (1961).

Experimental

Heat capacities were measured in the calorimeter described previously,[4] with only slight modifications.[3,5] FeI_2 was prepared by reaction of iodine vapor (source, Mallinckrodt, Analytical Reagent) and iron powder (Eimer and Amend, Electrolytic, Pure). The product sublimed away from the reaction zone (at 530°) and was baked out *in vacuo* at 150° to remove excess iodine and resublimed for further purification. FeI_3 has not been prepared in the solid state and does not appear to cause an impurity problem. FeI_2 appears stable over the temperature range for which heat capacity measurements were made. However when samples were resublimed in a high vacuum system (heated to *ca.* 500°) release of a small amount of iodine was observed. The loss of iodine appeared limited; its characteristic glow in a spark discharge in the vacuum system disappeared after a short period of heating. This observation as well as the fact that only traces of iron have been detected in the residual matter after sublimation suggests that the release of iodine is not associated with the simple heterogeneous decomposition of FeI_2 to the elements. Analyses of sublimates consistently gave ratios of I:Fe of the order of 1.95. Results and the treatment given the three samples used for the heat capacity measurements are summarized below.

Sample A (wt. 80.970 g.): prepared by sublimation of the iodine–iron reaction product in a stream of iodine vapor (pressure of I_2 *ca.* 1 mm.) from 530° to a region held at about 200°.

Sample B (wt. 88.776 g.): initial reaction product resublimed in high vacuum; then heated for six hours in a sealed tube at 450° with the pressure of iodine in the system at *ca.* 700 mm. (liquid iodine was held just below its boiling point in a side arm connected to the system).

Sample C (wt. 83.524 g.): initial reaction product simply resublimed in high vacuum system with continuous pumping.

In all cases after the treatment indicated the samples were transferred from the sublimation tubes to the calorimeter cell in a dry box, the cell removed and attached to a vacuum line, evacuated and pumped on at 150° for from six to eight hours to remove adsorbed gases; after cooling, 200 mm. pressure of argon was added and the cell sealed. Following heat capacity measurements, three representative samples of each of A, B and C were taken; each sample was divided into two portions analyzed independently for iron (dichromate method after removal of iodine) and iodine (precipitated as silver iodide). The variation indicated in the table shows the maximum deviation of individual values from the given average.

Theor. (FeI_2)	A	B	C
% Iron	18.03	18.24 ± 0.07	18.60 ± 0.02	18.36 ± 0.02
% Iodine	81.97	81.83 ± .09	81.31 ± .10	81.46 ± .11
Total	100.00	100.07	99.91	99.82
Fe:I ratio	1:2	1:1.97	1:1.93	1:1.95

The analytical results and behavior on sublimation suggest that the sublimate is slightly deficient in iodine (relative to the formula FeI_2). A small number of iodine vacancies might be associated with the presence of a small number of Fe^+ ions or Fe atoms in Fe^{++} sites, or possibly occupied by electrons. That sample B has the smallest Fe:I ratio is difficult to explain; the result for B and C should perhaps be considered the same within experimental error. If the apparent iodine deficiency in these samples is real (*i.e.* not a result of analytical error), one must conclude that under the conditions of the treatment given B, iodine does not react with the condensed crystals in such a way as to fill the vacancies. Sample A was actually sublimed in iodine vapor and appears nearer the stoichiometric compound; sublimation in a still higher pressure of iodine may yield a product with an Fe:I ratio of 2 (or higher). The evidence suggesting that FeI_2, prepared under the conditions described, is a non-stoichiometric phase, is not conclusive. Further study of this aspect of the problem is planned.

The heat capacities of the various samples A, B and C were identical within our experimental error at temperatures out-

(4) H. E. O'Neal and N. W. Gregory, *Rev. Sci. Instr.*, **30**, 434 (1959).

(5) For details see the Ph.D. thesis of Franklin L. Oetting, "The Heat Capacities of Iron(II) Chloride and Iron(II) Iodide," The University of Washington, 1960.

side the transition zone; hence the slight differences in composition are not important in this respect. The heat capacity of each sample was measured twice in consecutive continuous runs from 70 to 500°. Results were plotted for the two runs on a separate graph for each sample (results for sample A are representative and are shown on Fig. 1)[5] and smooth curves drawn through the data served as a basis for calculation of the heat capacity.

Results and Discussion

Results from the three samples are plotted together on Fig. 2. The maximum deviation of any point from the line drawn between 70 and 360° is 1.5% and the average deviation of 0.46%. The heat capacity is nearly constant in this temperature interval and may be represented by the equation

$$C_p = 19.83 + 5.8 \times 10^{-4}\, T\ (°\mathrm{K.})$$

Starting at 360°, however, an apparent second-order transition, extending over a 25 degree temperature range, was observed with all samples. In the constant heating method a temperature gradient is generated across the sample. In the vicinity of the transition this gradient was about four degrees and was kept nearly constant throughout the transition interval. Since the interval materially exceeds the gradient across the sample, the change is assumed to be second-order in character. The anomaly was reproduced in consecutive runs with each sample, demonstrating that the change responsible reversed itself on cooling. The extra energy absorbed in the region of the anomaly, evaluated by graphical integration, was found to be 144, 130 and 203 cal. mole^{-1} for samples A, B and C, respectively. The difference between the first two values is easily within experimental error; the value for C deviates by more than seems reasonable to attribute to experimental error and may possibly be associated with the difference in treatment of the samples, *e.g.*, C was not heated or sublimed in an iodine atmosphere although by analysis it appears similar to B.

Further work will be necessary to establish the nature of the phenomenon causing the heat capacity anomaly. One might expect it to be similar to that occurring in $FeBr_2$ although several differences in the behavior of the two substances have been noted. In the present work, high temperature powder patterns were taken using the apparatus described earlier[2] but with molybdenum radiation, which gave a larger number of diffraction lines within the limited angle of reflection permitted by the furnace. Powder patterns of FeI_2 taken between 400 and 500° could not be distinguished from those taken below the transition temperature. A similar comparison for $FeBr_2$ was repeated and the change in structure noted previously was confirmed.[2] The larger number of lines observed with Mo radiation now makes it possible to suggest that the high temperature form of $FeBr_2$ is the $CdCl_2$ type structure, *i.e.*, the halogens change to a cubic close-packed arrangement. However, as noted above, the iodide does not undergo a similar change and if the HCP (or RP) to CCP transition is the only thing responsible for the anomaly in $FeBr_2$, then the change in FeI_2 must be due to an entirely different phenomenon. It may also be noted that, unlike $FeCl_2$ and $FeBr_2$, dehydration of $FeI_2 \cdot H_2O$, conducted in the present study, did not lead to formation of a random-packed structure for the anhydrous iodide. Several attempts were made to prepare an RP form in this way, but only the usual HCP structure was obtained (all powder patterns of FeI_2 obtained in this work were in essential agreement with results published by Ferrari and Giorgi[6]). However, the existence of RP forms of $FeBr_2$ and $FeCl_2$ does not seem of direct importance relative to an anomaly in the heat capacity curves. Analysis of the bromide and the chloride did not indicate a halogen deficiency as in the case of the iodide. Possibly the anomaly observed in FeI_2 is associated with the presence defects in the lattice.

The heat capacity of FeI_2 between 400 and 500° lies above values below the transition and increases more rapidly with temperature than normally expected. Differential cooling experiments were conducted between 600° and room temperature; no evidence of any transition other than the melting point (*ca.* 590°) and the one detected in heat capacity measurements was found. No evidence of premelting (or sintering) was noted when the sample (heated only to 500°) was removed from the calorimeter cell. The vapor pressure of FeI_2 is so small that the heat of vaporization does not contribute materially to the apparent heat capacity between 400 and 500° (only *ca.* 30 ml. vapor space available).[7]

A previous study of the heat capacity of FeI_2 at room temperature and above has not been found in the literature. Milyutin and Pardenova[8] have measured C_P from 11.5 to 129°K.; the heat capacity has already reached 17.7 cal. mole^{-1} deg.$^{-1}$ at 129°K. FeI_2 is paramagnetic at room temperature.[9]

Financial support for this research was received from the Office of Ordnance Research, U.S. Army.

(6) A. Ferrari and F. Giorgi, *Rend. Accad. Lincei*, [6] **10**, 522 (1929).

(7) R. J. Sime and N. W. Gregory, THIS JOURNAL, **64**, 84 (1960).

(8) G. A. Milyutin and E. A. Pardenova, *Phys. Trans. Ukrain. Acad. Sci.*, **9**, 75 (1950).

(9) S. S. Shalyt, *Zh. Exp. Theor. Fiz.*, **9**, 1073 (1939).

NOTES

INORGANIC COMPLEX COMPOUNDS CONTAINING POLYDENTATE GROUPS. XIX. REACTION OF COMPLEXES OF MANGANESE(II) AND TETRAETHYLENEPENTAMINE WITH HYDROXIDE IONS[1]

By Hans B. Jonassen and V. V. Ramanujam[2]

Richardson Chemical Laboratories, Tulane University, New Orleans, Louisiana

Received December 17, 1959

The complex compounds formed between tetraethylenepentamine (abbrev. tetren) and manganese (II) ions have been investigated in these laboratories.[3]

The purpose of this study was to determine the types of complexes formed between tetren and manganese(II) ions in the presence of hydroxide ions.

Experimental

A. Reagents.—Tetren·5HCl was prepared by the method developed in these laboratories. Carbonate-free solutions of sodium hydroxide were prepared and standardized against potassium acid phthalate. Manganese(II) perchlorate was prepared from C.P. manganese sulfate and barium perchlorate. The solution was standardized by estimation of the manganese as pyrophosphate.

B. Apparatus.—The conductometric, potentiometric and magnetic titrations were made with assemblies described in an earlier paper.[4,5]

Results

1. Conductometric and Potentiometric Titrations.—When an equimolar mixture of manganese (II) perchlorate and tetren·5HCl is titrated conductometrically against hydroxide ions in the absence of oxygen[5] breaks are observed at 1, 2 and 4.5 equivalents of hydroxide ions. No breaks are observed at 5 or 5.5 equivalents, but a brown precipitate begins to appear when about 6 equivalents had been added.

Similar results were obtained when the change in *p*H was followed for the above system under the same conditions.

2. Magnetic Titration.—A plot of the Δw's due to change in magnetic susceptibility of the system when the same titration was followed with a Gouy magnetic balance showed breaks when 2 and 4.5 equivalents of alkali had been added. There is a decrease in the paramagnetic susceptibility of the system and this reaches a minimum at 4.5 equivalents of alkali. The moment calculated for this point by the application of Wiedemann's law[6] corresponded to about two unpaired electrons per manganese(II) ion.

Discussion

The break at one equivalent of hydroxide ions in the conductometric and potentiometric titrations has been interpreted to indicate that the first step in the reaction is the neutralization of the first hydrogen of the cation of the pentahydrochloride. The second break is due to the formation of the hydrogen complex,[7] $[MnH_3\ tetren]^{5+}$. Further addition of hydroxide ions leads to the formation of a new species on the addition of 4.5 equivalents of alkali.

By analogy with systems investigated and already reported[5,8] this ion seems to be a hydroxo-bridged binuclear complex. The reaction taking place between the addition of 2 and 4.5 equivalents of hydroxide would then be

$$2[MnH_3\ tetren]^{5+} + 5OH^- \longrightarrow [Mn_2(Htetren)_2OH]^{6+} + 4H_2O$$

The sixth octahedral coördination positions unfilled by the amine nitrogens and the bridging OH^- group would be filled by water giving then the ion $[Mn_2(Htetren)_2(H_2O)_2OH]^{5+}$. The structure postulated for this complex ion is given in Fig. 1.

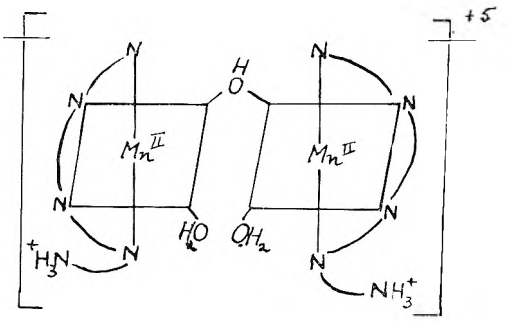

Fig. 1.

The absence of breaks in the titration curves when 5 and 5.5 equivalents of base had been added seems to indicate that the hydrogen of the Htetren has not been neutralized allowing only four of the aminonitrogens of the ligand to coördinate leaving the fifth nitrogen as an ammonium nitrogen.

The change of slope at 4.5 equivalents of the base in the potentiometric and conductometric titrations and the minimum at the same point in the magnetic titration seem to support the postulate of a hydroxo bridged binuclear complex ion.

Work on the structure of the corresponding iron (II) complex is under way. The corresponding complexes of iron and manganese in oxidation states higher than two seem to be absent in aqueous solutions since only the hydroxides of the metals were

(1) Abstracted in part from the Ph.D. Dissertation submitted by V. V. Ramanujam to the Tulane University, 1958. This research was supported in part by a grant from the National Institutes of Health.

(2) University of Madras, Guindy, Madras 25, India.

(3) L. Westerman, Dissertation, Tulane University, 1958.

(4) H. B. Jonassen, J. A. Bertrand, F. R. Groves, Jr., and R. J. Stearns, *J. Am. Chem. Soc.*, **79**, 4279 (1957).

(5) H. B. Jonassen and V. V. Ramanujam, This Journal, **63**, 411 (1959).

(6) P. W. Selwood, "Magnetochemistry," Interscience Publishers, Inc., New York, N. Y., 1956, p. 107.

(7) G. Schwarzenbach, *Helv. Chim. Acta*, **33**, 947 (1950).

(8) H. B. Jonassen and G. T. Strickland, This Journal, **80**, 312 (1958).

formed under similar experimental conditions. The Fe(II) complex shows unusual catalytic activity which is also under investigation in these laboratories.

RADIOLYSIS OF METHANE IN THE PRESENCE OF OXYGEN. THE FORMATION OF METHYL HYDROPEROXIDE

BY G. R. A. JOHNSON[1] AND G. A. SALMON

United Kingdom Atomic Energy Authority, Isotope Research Division, Technological Irradiation Group, Wantage Research Laboratories, Grove, Wantage, Berks.

Received May 16, 1960

Lind and Bardwell[2] showed that an over-all pressure change occurred when methane–oxygen mixtures were irradiated with radon α-rays. The end-products of the reaction were reported to be carbon dioxide and water, but no attempt was made to identify any intermediate products nor to establish the reaction mechanism. More recently, Mikhailov, *et al.*[3] studied the irradiation of methane–oxygen mixtures using a beam of electrons produced at 112 kv. The products identified were: hydrogen, carbon monoxide, carbon dioxide, ethane, ethylene, propane, butane and water. The presence of peroxides, aldehydes, acids and alcohols was shown by group reactions, but these products were not characterized. Relatively large total radiation doses ($>10^{19}$ e.v. ml.$^{-1}$) were used and, under these conditions, it is unlikely that the observed products would all be primary products of the radiolysis.

In the present work, the peroxide formed when methane–oxygen mixtures are irradiated with relatively low radiation doses ($<4 \times 10^{16}$ e.v. ml.$^{-1}$.) has been identified as methyl hydroperoxide and the dependence of the *initial* yield of methyl hydroperoxide on oxygen concentration has been investigated.

Experimental

Materials.—Two sources of methane were used (National Coal Board and Matheson, C.P.), identical results being obtained with each when they were compared. In each case, the gas was purified by trap-to-trap distillation, the middle fraction being used. Oxygen was used from a British Oxygen Gases cylinder without further purification.

Irradiation Procedure.—Irradiations were carried out using a ^{60}Co-γ-ray source (approximately 500 curies). The gases were irradiated at room temperature in a cylindrical annular "Pyrex" vessel, which surrounded the source. The vessel was evacuated and filled with gas to a known pressure by means of a conventional high-vacuum system. After irradiation, a known proportion of the gas was trapped over a suitable solvent (25 ml.) in a flask (500 ml.) connected to the irradiation vessel and the products taken up in the solvent. For the analysis of methyl hydroperoxide, water was used as solvent; for total peroxide, methanol was used, since dimethyl peroxide is only sparingly soluble in water.

Dosimetry.—The energy absorbed in the gas was measured using a nitrous oxide dosimeter (*cf.* Harteck and Dondes[4]). The vessel was filled with nitrous oxide (1 atmosphere and room temperature) and, after irradiation, a known volume of the irradiated gas trapped over a deaerated solution of sodium hydroxide (0.1 *N*). Nitrite, formed in the solution, was determined spectrophotometrically using 1-naphthylamine–sulfanilic acid reagent.[5] The yield of nitrite was directly proportional to the total irradiation-dose and the dose-rate was calculated taking $G(NO_2^-) = 2.3^6$ (G = number of molecules formed per 100 electron volts). The dose-rate in methane at N.T.P. in the same irradiation vessel was 1.9×10^{14} e.v. ml.$^{-1}$. min^{-1}; this was calculated from the dose-rate found in N_2O, assuming the energy absorbed to be directly proportional to the electron density of the gas.

Analytical.—The oxidation of iodide by peroxides, in the presence of excess iodide, is first order and the rate depends upon the peroxide used.[7,8] Use may be made of a measurement of the reaction rate to characterize organic peroxides.[9] Iodide reagent[10] was added to the aqueous solution of the radiation products. The formation of I_3^- was followed spectrophotometrically by measuring the absorption at 350 mμ. The rate was identical with that found using an authentic sample of methyl hydroperoxide under the same conditions. Hydrogen peroxide oxidizes iodide very much more rapidly than methyl hydroperoxide under the conditions used. Thus hydrogen peroxide can be determined by measuring the I_3^- immediately after adding the iodide reagent, at which time very little of the methyl hydroperoxide has reacted. For determination of methyl hydroperoxide, the solution was allowed to stand for about 15 hours after adding the iodide reagent before measuring the absorption at 350 mμ.

Dimethyl peroxide does not oxidize iodide under the conditions used. Total peroxide may be determined by means of ferrous thiocyanate[11] and the yield of dimethyl peroxide found from the difference in values given by this method and the iodide method. Total peroxide was measured in a solution of the irradiation products in methanol by the following procedure: ferrous thiocyanate reagent was prepared by mixing equal volumes of solutions of ferrous sulfate (20 g. in 100 ml. water containing 2 ml. of concentrated sulfuric acid) and ammonium thiocyanate (20 g. in 100 ml. of water) and diluting 1 ml. of the resulting solution to 50 ml. with methanol. Two ml. of the freshly prepared reagent was added to 10 ml. of the methanolic peroxide solution. The optical density at 430 mμ was measured 5 minutes after adding the reagent and the amount of peroxide in the sample found by comparison with a known hydrogen peroxide solution analyzed simultaneously by an identical procedure.

Results

Methyl hydroperoxide was detected as a product in irradiated methane–oxygen mixtures. Neither hydrogen peroxide nor any organic hydroperoxide other than methyl hydroperoxide was found in any of the experiments carried out.

The yields of methyl hydroperoxide at different total doses and different oxygen concentrations are given in Table I. Low total doses ($<4 \times 10^{16}$ e.v. ml.$^{-1}$) were employed so that the values measured would correspond to initial yields. This meant that the total amounts of methyl hydroperoxide produced were close to the lower limit of the analytical method and the accuracy of measurement was not high. However, within experimental error, the yield was directly proportional to total radiation-

(1) Attached from the Power-Gas Corporation, Ltd., Stockton-on-Tees, England. Department of Chemistry, University of Durham, King's College, Newcastle Upon Tyne 1, England.

(2) S. C. Lind and D. C. Bardwell, *J. Am. Chem. Soc.*, **48**, 2347 (1926).

(3) B. M. Mikhailov, M. E. Kyimcra and V. C. Bogdonov, "Trans. 1st All-Union Conference on Radiation Chemistry," 1958, p. 234.

(4) P. Harteck and S. Dondes, *Nucleonics*, **14**, 66 (1956).

(5) T. Rigg, G. Scholes and J. Weiss, *J. Chem. Soc.*, 3034 (1952).

(6) G. R. A. Johnson, to be published.

(7) R. L. Kooijman and W. L. Ghijsen, *Rec. trav. chim.*, **66**, 205 (1947).

(8) J. H. Knox and R. G. W. Norrish, *Proc. Roy. Soc.* (*London*), **221A**, 155 (1954).

(9) G. R. A. Johnson and J. Weiss, *Chemistry and Industry*, 358 (1955).

(10) A. O. Allen, C. J. Hochanadel, J. A. Ghormley and J. W. Davis, THIS JOURNAL, **56**, 575 (1952).

(11) A. C. Egerton, A. J. Everett, G. J. Minkoff, S. Rudrakanchana and K. C. Salooja, *Anal. chim. Acta*, **10**, 422 (1954).

dose and independent of oxygen concentration within the range studied (0.1 to 10.0 mole %).

TABLE I

FORMATION OF PEROXIDES FROM METHANE–OXYGEN MIXTURES (TOTAL PRESSURE ~760 MM.) IN PYREX GLASS VESSELS (VOL. = 130 ML.), IRRADIATED WITH Co-60 γ-RAYS Dose rate in the gas at N.T.P. = 1.9×10^{-14} e.v. ml.$^{-1}$ min.$^{-1}$

O_2 in gas mixture (mole %)	Total dose (e.v./ml.) $\times 10^{-16}$	MeOOH (measured by iodide method) Yield (moles/ml.) $\times 10^{9}$	MeOOH (measured by iodide method) G (molecules/100 e.v.)	Total peroxide (measured by ferrous thiocyanate) Yield (moles/ml.) $\times 10^{9}$	Total peroxide (measured by ferrous thiocyanate) G
0.1	0.92	0.44	2.9	..	..
	1.43	0.72	3.0	..	..
	1.92	1.05	3.3	..	..
1.0	0.63	0.37	3.5	..	..
	0.96	0.50	3.1	..	..
	1.24	1.00	4.2	..	..
	1.36	..	..	1.00	4.2
	1.46	..	..	0.80	3.3
	1.79	1.10	3.7	1.00	3.3
	1.95			1.20	3.7
	2.61	1.40	3.2	..	..
10.0	0.63	0.35	3.3	..	..
	0.96	0.48	3.0	..	..
	1.62	1.03	3.8	1.01	3.7
	1.95	..	..	1.08	3.3
	3.78	2.18	3.5	2.14	3.4

The yields of total peroxide are also given in Table I. Within experimental error, G (total peroxide) was found to be equal to G (methyl hydroperoxide) showing that dimethyl peroxide was not formed.

Discussion

Radiolysis of methane may lead to the formation of free-radicals as a result of excitation, of ion–molecule reactions, and of ion-neutralization. The formation of hydrogen atoms and of methyl and ethyl radicals in pure methane during irradiation has been postulated.[12,13] Oxygen, when present at small concentrations in irradiated methane, may be expected to act as a free-radical scavenger. It is probable that the methyl hydroperoxide formed in methane–oxygen mixtures on irradiation arises from methyl radicals *via* methyl peroxy radicals, which are generated in the reaction

$$CH_3\cdot + O_2 (+ M) = CH_3OO (+ M) \qquad (1)$$

Formation of methyl hydroperoxide and ethyl hydroperoxide in the mercury photosensitized oxidation of methane and ethane, respectively[14,15] and formation of methyl hydroperoxide in the radiolysis of aqueous solutions of methane and oxygen[9] has been interpreted in terms of interactions of the alkyl hydroperoxy radicals.

The value found for $G(CH_3OOH)$ ($\sim$ 3.5) in the present work indicates that a chain-oxidation does not occur in the radiolysis of methane–oxygen mixtures suggesting, in agreement with Watson and Darwent,[15] that the reaction

$$CH_3OO + CH_4 = CH_3OOH + CH_3 \qquad (2)$$

does not occur at room temperature.

If oxygen acts merely as a radical scavenger in the irradiated methane, the observation that the yield of methyl hydroperoxide is independent of the concentration of oxygen over the range 0.1 to 10.0 mole % implies that 0.1 mole % of oxygen is sufficient to scavenge all of the available radicals at the total pressures employed in these experiments (~760 mm.). It is of some interest that methyl hydroperoxide was the only peroxide found, and it must be assumed that H and C_2H_5, if formed, do not give peroxides under these conditions.

Methyl hydroperoxide formation in the radiolysis has been attributed to reactions of methyl radicals but an alternative mode of formation cannot, at present, be excluded. Thus, in addition to the scavenging of radicals by oxygen, it is possible that electron capture by oxygen may take place.[16] Even at oxygen concentrations below 0.1 mole %, the processes

$$O_2 + e^- = O_2^- \qquad (3)$$

$$O_2 + e^- = O^- + O \qquad (4)$$

may be important and capable of competing with electron capture by positive ions. Neutralization of positive ions by the negative ions O_2^- and O^-, which would occur as three-body recombinations at the pressures considered here,[17] may lead directly to stable oxygen-containing radicals.

(12) F. W. Lampe, *J. Am. Chem. Soc.*, **79**, 1055 (1957).

(13) G. G. Meisels, W. H. Hamill and R. R. Williams, THIS JOURNAL, **61**, 1456 (1957).

(14) J. A. Gray, *J. Am. Chem. Soc.*, **74**, 3150 (1952).

(15) J. S. Watson and B. de B. Darwent, THIS JOURNAL, **61**, 577 (1957).

(16) G. S. Hurst and T. E. Bortner, *Radiation Research*, Suppl. 1, 547 (1959).

(17) H. S. W. Massey and E. H. S. Burhop, "Electronic and Ionic Impact Phenomena," Oxford Univ. Press, 1956, p. 630.

THE HEAT OF CHLORINATION OF DIBORON TETRAFLUORIDE[1]

BY STUART R. GUNN AND LEROY G. GREEN

Lawrence Radiation Laboratory, University of California, Livermore, California

Received June 20, 1960

The preparation and properties of B_2F_4 have been described by Finch and Schlesinger[2] who noted that its chemical properties were similar to those of B_2Cl_4. It thus appeared probable that the compound would add chlorine nearly quantitatively and that this reaction could be performed calorimetrically, as was done with B_2Cl_4,[3] to determine the heat of formation of the compound and hence an additional value for the boron–boron single-bond energy.

The thermal stability of B_2F_4 is greater than that of B_2Cl_4; however, when the chlorination was performed under conditions similar to those used with B_2Cl_4, similar amounts of solid products were formed. It was then found that addition of a small amount of helium to the reaction tube

(1) This work was performed under the auspices of the U. S. Atomic Energy Commission.

(2) A. Finch and H. I. Schlesinger, *J. Am. Chem. Soc.*, **80**, 3573 (1958).

(3) S. R. Gunn, L. G. Green and A. I. von Egidy, THIS JOURNAL, **63**, 1787 (1959).

reduced this solid formation to a negligible amount, presumably due to the more rapid transfer of heat from the reaction zone.

Materials.—B_2F_4 was prepared by the method of Finch and Schlesinger in a vacuum line equipped with mercury float valves. The samples, ranging from 1.2 to 1.5 mmoles, were measured in a volume of 270 ml. and condensed in glass ampoules of about 7 ml. Chlorine was purified by fractional bulb-to-bulb distillation.

Experimental Procedure.—The reaction vessel, calorimeter and performance of the runs were as previously described. Following a run, the gas in the reaction vessel was sealed in a tube with mercury, shaken overnight to remove chlorine, and measured in the same calibrated bulb used for the sample measurement.

Results.—Results of the measurements are given in Table I.

TABLE I

HEAT OF REACTION OF B_2F_4 WITH Cl_2

Run	Temp., °C.	Helium, cm.	Mol. wt.	Moles product / Moles sample	$-\Delta H$, kcal. mole^{-1}
1	5	0	98.1	1.969	78.9
2	5	10	< 99.0	...	81.2
3	25	10	<100.2	2.012	81.9
4	25	8	98.5	2.003	82.8
5	25	10	98.2	2.012	82.3

Observed heats were corrected for the PV heat effect associated with admission of chlorine to the reaction vessel. The ΔC_p correction for runs at 5° is negligible. An error occurred in the determination of the sample weight in runs 2 and 3 in that the ampoule after breaking was left filled with an unknown mixture of helium and air; otherwise the sample weight, sample volume and product volume should all be accurate within a few tenths of a per cent. No gas imperfection corrections were applied to the volume measurements, but this error would be small at the pressures involved. The somewhat high values of the molecular weight doubtless indicate the presence of small amounts of unconverted B_2Cl_4 in the sample; but since the heat of chlorination of gaseous B_2Cl_4 is nearly the same as that of B_2F_4 and the heat of reaction is referred to the sample volume, this should introduce no error. Since the ratio of product volume to sample volume is close to the theoretical value of 2 except for the first run, amounts of other impurities must be small. A considerable amount of solid material was formed in the first run, but only traces in the others. We shall take -82.0 ± 1.0 kcal mole^{-1} for ΔH.

A mixture of BF_3 and BCl_3 reacts to give an equilibrium amount of the mixed halides; this process has been investigated by Higgins, *et al.*,[4] and by Gunn and Sanborn.[5] It may be estimated that in the present work the net reaction is approximately

$$B_2F_4 + Cl_2 \longrightarrow 0.92BF_3 + 0.46BF_2Cl + 0.32BFCl_2 + 0.30BCl_3$$

Using the standard heats of formation BF_3, -270.0,[6] BF_2Cl, -211.5[5]; $BFCl_2$, -153.9[5]; and BCl_3, -97.1[7], ΔH_f^0 (B_2F_4) is calculated to be -342.0 kcal. mole^{-1}.

Using $+18.3$ for ΔH_f^0(F, g)[8] and $+135.2 \pm 4$ for ΔH_f^0 (B, g)[6] the thermochemical B–F bond energy in BF_3 is 153.3; assuming this to be unchanged in B_2F_4, E(B–B) is 72.4. This is to be compared with a value of 79.0 derived for E(B–B) in B_2Cl_4 by the same method. This calculation is probably less valid for B_2F_4 than for B_2Cl_4; in B_2Cl_4 the B–Cl distance is nearly the same as in BCl_3 whereas the B–F distance in B_2F_4 is roughly 0.03 Å. longer than in BF_3.[9] Also the B–B distance in B_2F_4 is roughly 0.08 Å. shorter in B_2F_4 than in B_2Cl_4.

(4) T. H. S. Higgins, E. C. Leisegang, C. J. G. Raw and A. J. Rossouw, *J. Chem. Phys.*, **23**, 1544 (1955).

(5) S. R. Gunn and R. H. Sanborn, *ibid.*, **33**, 955 (1960).

(6) W. H. Evans, E. J. Prosen and D. D. Wagman, "Thermodynamic and Transport Properties of Gases, Liquids, and Solids," American Society of Mechanical Engineers, McGraw–Hill Book Co., New York, N. Y., 1959, p. 226.

(7) W. H. Johnson, R. G. Miller and E. J. Prosen, *J. Research NBS*, **62**, 213 (1959).

(8) F. D. Rossini, *et al.*, Circular of the National Bureau of Standards 500, 1952.

(9) L. Trefonas and W. N. Lipscomb, *J. Chem. Phys.*, **28**, 54 (1958).

AN EXPLANATION OF THE FACT THAT ELECTROSTATIC CONSIDERATIONS ALONE QUALITATIVELY CORRELATE THE VARIATION OF RATES OF CHEMICAL REACTIONS WITH SOLVENT

BY N. C. DENO

College of Chemistry and Physics, Pennsylvania State University, University Park, Pa.

Received June 20, 1960

The Brönsted eq., $k/k_0 = f_Af_B/f^*$, has been the usual point of departure for discussing the effect of solvent on the rates of chemical reactions.[1-3] The terms are defined as follows: k and k_0 are the rate constants in solvent and reference solvent, f_A and f_B are the molar activity coefficients (f = activity/molarity) of the reactants A and B, and f^* is the molar activity coefficient of the transition state. The terms involving f in the reference solvent need not appear by the device of assigning them the value unity as the standard state assignment.

Combining the Brönsted eq. with equations derived from purely electrostatic considerations, such as the Born or Debye–Hückel, has led to qualitative and sometimes quantitative relations between rates and solvent.[2,3] An equivalent qualitative theory has developed in organic chemistry.[4]

The striking fact that has not been emphasized is that although such electrostatic considerations predict k/k_0 and thus f_Af_B/f^*, they completely fail to predict f_A and f_B. This failure is most clearly seen with inert uncharged molecules. One of the bases for deriving the McGowan eq., $\log f = k_MP$, was that electrostatic interactions between solute and two different solvents were nearly equal and cancelled.[5,6] The success of this eq. in correlating a wide variety of distribution coefficient

(1) L. P. Hammett, "Physical Organic Chemistry," McGraw–Hill Book Co., New York, N. Y., 1940, pp. 127–129.

(2) K. J. Laidler, "Chemical Kinetics," McGraw–Hill Book Co., New York, N. Y., 1950, Chapter 5.

(3) E. S. Amis, "Kinetics of Chemical Change in Solution," The Macmillan Co., New York, N. Y., 1949, Chapters 4, 8, and 9.

(4) C. K. Ingold, "Structure and Mechanism in Organic Chemistry," Cornell Univ. Press, Ithaca, N. Y., 1953, pp. 345–371 and 453–460.

(5) J. C. McGowan, *J. Appl. Chem.*, **4**, 41 (1954); **2**, 323 (1952).

(6) N. Deno and H. E. Berkheimer, *J. Chem. Eng. Data*, **5**, 1 (1960).

and solubility data[5,6] demonstrates that for activity coefficients of inert uncharged molecules, electrostatic interactions between solute and solvent are second-order effects in most cases. Even with ions, electrostatic effects are only part of the story. In a forthcoming paper on the activity coefficients of ions, it will be shown that it is only with the smallest of ions that electrostatic effects predominantly govern the activity coefficients.

In the eq., $\log f = k_M P$, k_M is a measure of the difference in internal pressure between solvent and reference solvent and P is the parachor. From the derivation of this eq., P is used solely as a measure of the molecular volume of solute and is computed from the available atomic and structural increments.[7]

For a reaction in which reactants and transition state are all non-polar, such as many free radical reactions, the Brönsted eq. combined with the McGowan eq. leads to the eq. $\log k/k_0 = k_M \cdot (P_A + P_B - P^*)$. From studies on the variation of rates with external pressure, it has been found that the volume of activation, ΔV^*, is nearly zero for non-polar reactions.[8,9] Thus $P_A + P_B = P^*$ and $\log k/k_0 = 0$.

Electrostatic effects and $k_M P$ terms are independent variables so that when electrostatic effects are present

$$\log k/k_0 = k_M P \text{ terms} + \text{electrostatic terms}$$

It is thus the approximate cancelling of the $k_M P$ terms that explains why log k/k_0 depends primarily on electrostatic effects. However, it is in these cases where electrostatic effects are important that ΔV^* differs significantly from zero,[8,9] and the cancelling of the $k_M P$ terms is not exact. Values of ΔV^* have about ± 30 ml./mole as an upper limit. For water–hydrocarbons, $k_M = 0.0130$, and this is the largest k_M value yet found ($k_M = 0.0120$ for water-ethanol). Thus an upper limit to the contribution of $k_M P$ terms to $\log k/k_0$ is $k_M \Delta V^* = (2.0)(0.0130)(30) = 0.8$.[10]

The eq. $\log k/k_0 = mY$ has been found to correlate the rates of solvolysis reactions with solvent.[11] The term Y depended on the solvent and was called the "ionizing power" of the solvent. This interpretation seemed anomalous because in the many examples studied, $\log k/k_0$ was as much dependent on changes in $\log f$ of the non-ionic reactant as on changes in $\log f$ of the ionic or polar transition state. By calculating the contribution of the $k_M P$ terms to $\log k/k_0$, the contribution of the electrostatic effect can be determined by difference. One example will demonstrate the approach.

For the solvolysis of *t*-butyl chloride, $\log k_{H_2O}/k_{EtOH} = 5.5$. In 80% ethanol, $\Delta V^* = -23$ ml./mole and the values in water and ethanol must be similar. The $k_M P$ term would be $(2.0)(0.0120)(23) = 0.55$. This represents 10% of the total $\log k_{H_2O}/k_{EtOH}$ and so to a first approximation it is proper to interpret Y values as due to electrostatic interactions between solvent and solutes.

(7) O. R. Quayle, *Chem. Revs.*, **53**, 484 (1953).

(8) J. Buchanan and S. D. Hamann, *Trans. Faraday Soc.*, **49**, 1425 (1953); H. G. David and S. D. Hamann, *ibid.*, **50**, 1188 (1954).

(9) K. J. Laidler and C. Chen, *ibid.*, **54**, 1026 (1958); K. J. Laidler, *Faraday Soc. Disc.*, **22**, 88 (1956).

(10) The factor of about 2.0 arises because $V_b = 0.49P$ and $V_m = 0.42P$ where V_b and V_m are the molecular volumes at the b.p. and m.p. (J. C. McGowan, *Rec. trav. chim.*, **75**, 199 (1956)).

(11) E. Grunwald and S. Winstein, *J. Am. Chem. Soc.*, **70**, 846 (1948); S. Winstein, E. Grunwald and H. W. Jones, *ibid.*, **73**, 2700 (1951); A. H. Fainberg and S. Winstein, *ibid.*, **78**, 2770 (1956), and **79**, 5937 (1957); S. Winstein, A. H. Fainberg and E. Grunwald, *ibid.*, **79**, 4146 (1957).

THE DECARBOXYLATION OF OXAMIC ACID IN ANILINE AND IN *o*-TOLUIDINE

BY LOUIS WATTS CLARK[1]

Department of Chemistry, Saint Mary of the Plains College, Dodge City, Kansas

Received July 5, 1960

In the decarboxylation of malonic acid in non-ionizing, polar solvents, the rate-determining step appears to be the formation of a transition complex involving coördination between the electrophilic, polarized carbonyl carbon atom of the un-ionized diacid and an unshared pair of electrons on a nucleophilic atom of the solvent molecule.[2] In kinetic studies of this reaction in more than fifty non-aqueous solvents inductive and steric effects in harmony with this proposed mechanism invariably were observed.[3] It appears highly probable, also, that the decarboxylation of oxalic acid in polar solvents involves the same sort of mechanism as does that of malonic acid.[4]

Although oxamic acid, apparently, never has been the subject of any kind of kinetic study, the analogy between it and oxalic acid suggested that it, too, should be capable of undergoing decarboxylation in polar solvents by essentially the same mechanism as that of oxalic acid and malonic acid. Preliminary experiments in this Laboratory revealed that smooth decarboxylation of oxamic acid does take place at moderate temperatures in polar solvents. In order to ascertain whether or not this decarboxylation follows the same mechanism as that of oxalic acid and malonic acid kinetic studies of the reaction were carried out in two aromatic amines, aniline and *o*-toluidine. Results of this investigation are reported herein.

Experimental

Reagents.—(1) The oxamic acid used in this investigation was analytical reagent grade, 100.0% assay. Two methods of assay were employed: volumetric and gasometric. In the volumetric analysis a weighed sample was digested for three hours with excess standard sodium hydroxide until all ammonia was driven off, the solution cooled and the excess base determined by titration with standard hydrochloric acid. In the gasometric analysis, each decarboxylation experiment, when properly carried out, yielded the theoretical volume of carbon dioxide at STP. (2) The solvents were reagent grade chemicals. Before the beginning of each decarboxylation experiment each sample of each solvent was distilled at atmospheric pressure directly into the dried reaction flask.

Apparatus and Technique.—The kinetic experiments were conducted in a constant-temperature oil-bath by measuring the volume of CO_2 evolved at constant pressure, as described

(1) Western Carolina College, Cullowhee, N. C.

(2) G. Fraenkel, R. L. Belford and P. E. Yankwich, *J. Am. Chem. Soc.* **76**, 15 (1954).

(3) L. W. Clark, THIS JOURNAL, **64**, 917 (1960), and previous papers in this series.

(4) L. W. Clark, *ibid.*, **61**, 699 (1957).

in a previous paper.[5] In each experiment a 0.1585-g. sample of oxamic acid (the amount required to produce 40.0 ml. of CO_2 at STP on complete reaction) was introduced in the usual manner into the reaction flask containing a weighed sample of solvent saturated with dry CO_2 gas.

Results

In some experiments at the beginning of this study some peculiar experimental difficulties were experienced: (1) the experiment would halt before the entire amount of CO_2 was collected, and (2) the evolved CO_2 would then start to be resorbed, the entraining liquid rising up into the buret, finally coming to complete rest at zero volume.

In seeking for an explanation of this behavior some white crystals were observed adhering to the inside walls of the condenser. These crystals were collected and analyzed and found to be oxamic acid. Apparently the formamide produced concomitantly with the CO_2 in the decarboxylation experiment tended to combine with the CO_2 by a reverse reaction to give the original compound. It was found that, by employing a rather large volume of solvent and using a gentle stirring action instead of a more vigorous one, this reverse reaction could be circumvented almost completely until practically all the original oxamic acid sample had decomposed. (Upon standing, however, resorption of the evolved CO_2 would begin to take place, and after several hours the entraining liquid would again rise to the zero line in the buret. Crystals of oxamic acid, corresponding to the stoichiometric weight used originally, would then be found adhering to the condenser walls.)

Inasmuch as oxamic acid apparently had not been investigated previously from a standpoint of kinetics a careful study was made of the effect of concentration on the reaction velocity constant. In this study seven decarboxylation experiments were carried out in aniline at 160.54° corr., using, respectively, 50, 71, 75, 90, 120, 130 and 135 g. of solvent. The results of this study indicated that there was no detectable change in the specific reaction velocity constant at this temperature with change in concentration. However, inasmuch as better results were obtained when larger volumes of solvent were used, the practice was adopted of running future experiments in 110–135 g. of solvent.

The rate of decarboxylation of oxamic acid in aniline and in *o*-toluidine was then measured at four different temperatures over a range of about 20°. The plot of log $(V_\infty - V_t)$ was linear over nearly the entire course of the experiment indicating that the reaction is first order. The average rate constants calculated in the usual manner from the slopes of the experimental logarithmic plots are brought together in Table I. The parameters of the Eyring equation, based upon the data in Table I, are shown in Table II.

Discussion

The effective positive charges on the two carbonyl carbon atoms of oxalic acid are partially neutralized by a shift of electrons (a + E effect) from the two hydroxyl oxygen atoms. In oxamic acid these charges are partially neutralized by a + E effect of one hydroxyl oxygen atom and one amide nitrogen atom. Since nitrogen is less electronegative than oxygen, the nitrogen will release electrons more readily than will the oxygen. This means that the carbonyl carbon atom of oxalic acid will have a higher effective positive charge than will that of oxamic acid. If, as analogy suggests, the decarboxylation of oxamic acid proceeds in polar solvents by the same mechanism as that which has been established for oxalic acid—an electrophilic carbonyl carbon atom of the acid coördinating with an unshared pair of electrons on a nucleophilic atom of the solvent molecule to form a transition complex—then, in a given solvent, it would be expected that the ΔH^* of the reaction would be lower for the acid whose carbonyl carbon atom has the higher effective positive charge—namely, oxalic acid.[6]

Table I

Apparent First-order Rate Constants for the Decarboxylation of Oxamic Acid in Aniline and in *o*-Toluidine

Solvent	Temp., °C. cor.	No. of runs	$k \times 10^4$, sec.$^{-1}$	Av. deviation
Aniline	142.73	3	0.859	±0.003
	146.31	2	1.66	± .02
	151.90	3	4.55	± .02
	160.50	7	20.00	± .04
o-Toluidine	137.36	2	1.26	± .005
	142.44	3	2.86	± .02
	149.30	3	8.25	± .02
	156.22	2	23.73	± .03

Table II

Kinetic Data for the Decarboxylation of Oxamic Acid in Aniline and in *o*-Toluidine

Solvent	ΔH^*, kcal.	ΔS^*, e.u.	$k_{150°} \times 10^4$ sec.$^{-1}$
Aniline	59.7	+68.0	3.17
o-Toluidine	53.7	+57.1	8.66

In Table III are shown the values of the Eyring parameters for the decarboxylation of oxalic acid, oxamic acid, and malonic acid in aniline solution. It will be observed (lines 1 and 2 of Table III) that, in aniline, the ΔH^* for the decarboxylation of oxalic acid is actually 19 kcal. less than that for the decarboxylation of oxamic acid. These data are strong evidence for the validity of the postulated mechanism.

Table III

Kinetic Data for the Decarboxylation of Oxalic Acid, Oxamic Acid and Malonic Acid in Aniline Solution

Reactant	ΔH^*, kcal.	ΔS^*, e.u.	$k_{140°} \times 10^4$, sec.$^{-1}$
Oxalic acid[4]	40.3	+16.2	1.45
Oxamic acid	59.7	+68.0	0.52
Malonic acid[7]	26.9	− 4.5	50.0

Further confirmation for the proposal may be obtained by a study of the data in Table II. If oxamic acid coördinates with a pair of unshared electrons on the nitrogen atom of aniline in a manner similar to that of oxalic acid and malonic acid, then the presence of a methyl group *ortho* to the amino

(5) L. W. Clark *ibid.*, **60**, 1150 (1956).

(6) K. J. Laidler, "Chemical Kinetics," McGraw-Hill Book Co., Inc., New York, N. Y., 1950, p. 138.

(7) L. W. Clark, This Journal, **62**, 79 (1958).

group would be expected to have two effects: (1) it would release electrons due to a positive inductive effect, thus increasing the effective negative charge on the nitrogen atom and giving rise to a decrease in ΔH^*, and, (2) it would sterically hinder the approach of oxamic acid to the nitrogen atom, resulting in a decrease in ΔS^*. In Table II (lines 1 and 2) it will be observed, in fact, that both ΔH^* and ΔS^* for the decarboxylation of oxamic acid decrease on going from aniline to *o*-toluidine. At 150° the decarboxylation of oxamic acid takes place about three times as fast in *o*-toluidine as in aniline in spite of the increased steric hindrance, due to the compensating effect of the lowered activation energy.

In view of the fact that all the experimental results obtained are in complete accord with the theoretical predictions, there remains little doubt but that the original assumption is correct, namely, that oxamic acid decomposes in polar solvents by the same mechanism as do oxalic acid and malonic acid.

In Table III it will be noticed that the ΔS^* for the decarboxylation of oxamic acid in aniline is considerably larger than that for oxalic acid. This indicates that, in all probability, discrete molecules of oxamic acid are involved in the rate-determining, coördinating step, whereas, in the case of oxalic acid, an association cluster or so-called "supermolecule" composed of perhaps three single molecules is involved.[8]

If, as appears to be the case, the mechanism of the decomposition of oxalic acid is similar to that of malonic acid, the fact that, in aniline, ΔH^* for the malonic acid reaction is lower than that for oxalic acid (see Table III, lines 1 and 3) indicates that the effective positive charge on the polarized carbonyl carbon atom of malonic acid is greater than it is on that of oxalic acid. This difference in charge between the two acids is probably attributable in great measure to the presence of the methylene group in the malonic acid molecule which tends to prevent the transmission of inductive effects between the two terminal carboxyl groups.[9]

Oxalic acid and oxamic acid may be regarded as types of α-keto acids, whereas malonic acid may be regarded as an example of a β-keto acid. On the basis of these results it may be presumed that, in general, other α-keto and β-keto acids will undergo decarboxylation in polar solvents by the same mechanism as that which has been proposed for oxalic acid, oxamic acid and malonic acid. If this is correct, it would be anticipated that, in view of the large difference in activation energies, β-keto acids will be more unstable than α-keto acids, that is, they will suffer decarboxylation more easily under similar conditions. As a matter of fact this anticipation is found to be correct. For example, in the decarboxylation of oxalacetic acid in the presence of nucleophilic catalysts, pyruvic acid and carbon dioxide, not formylacetic acid and carbon dioxide, are obtained.[10] Oxalacetic acid may be regarded both as an α-keto acid and a β-keto acid. In the decarboxylation reaction it is the β-keto moiety which suffers cleavage first, the α-keto portion proving to be the more stable.

Acknowledgments.—(1) Valuable assistance was rendered by Donald McCoy in carrying out the analyses. (2) This research was supported by the National Science Foundation, Washington, D. C.

(8) W. Hückel, "Theoretical Principles of Organic Chemistry," Vol. II, Elsevier Publishing Co., New York, N. Y., 1958, p. 329 *et seq.*

(9) R. Q. Brewster, "Organic Chemistry," Second Edition, Prentice-Hall, Inc., New York, N. Y., 1953, p. 581.

(10) F. Haurowitz, "Biochemistry," John Wiley and Sons, Inc., New York, N. Y., 1955, p. 54.

CRYSTAL STRUCTURE OF POTASSIUM SILYL

BY M. A. RING AND D. M. RITTER

Department of Chemistry, University of Washington, Seattle 5, Washington

Received July 5, 1960

Potassium silyl, $KSiH_3$, recently prepared,[1] has been examined by X-ray powder diffraction, the first such measurement on a metal derivative of a Group IV hydride. Eight reflections were observed using Cu Kα radiation (λ 1.5418 Å.) on a Philips powder camera of 56.78 mm. effective radius, determined using six NaCl reflections with correction for absorption error. The calibration was necessary because insufficient back reflection was obtained to apply the Straumanis technique. The structure is cubic of the NaCl type with the K positions at 000, $\frac{1}{2}\frac{1}{2}0$, $0\frac{1}{2}\frac{1}{2}$, $\frac{1}{2}0\frac{1}{2}$, the silicon positions at $00\frac{1}{2}$, $\frac{1}{2}00$, $0\frac{1}{2}0$, $\frac{1}{2}\frac{1}{2}\frac{1}{2}$ and $a_0 = 7.15 \pm 0.02$ Å. giving an X-ray density of 1.29 g. cm.$^{-3}$. No effort was made to locate the hydrogen atoms, owing to the use of so few reflections and the probability that the silyl anions rotate. The observed intensities (listed in Table I) were obtained by graphical integration of the microphotometer curve. The scattering factors of Viervoll and Ögrim[2] for silicon, and for potassium those of Berghuis[3] were used to obtain the calculated intensities.

TABLE I

RELATIVE INTENSITIES

$$R = \frac{\Sigma\,||F_o| - |F_c||}{\Sigma\,|F_o|} = 0.07$$

hkl	Calculated	Observed
111	0.07	0.02
200	1.00	1.00
220	0.73	0.78
311	.03	.02
222	.26	.30
400	.12	.09
420	.32	.33
422	.24	.16

We are indebted to Mr. Henry Montgomery and to Professor E. C. Lingafelter for their assistance and advice. This research was supported by the United States Air Force through the Air Force Office of Scientific Research of the Air Research and Development Command under contract No. AF

(1) M. A. Ring and D. M. Ritter, *J. Am. Chem. Soc.*, **83**, in press.

(2) H. Viervoll and O. Ögrim, *Acta Cryst.*, **2**, 277 (1949).

(3) J. Berghuis, Ij. M. Haanappel, M. Potters, B. O. Loopstra, C. H. MacGillavry and A. L. Veenendaal, *Acta Cryst.*, **8**, 478 (1955).

COMPRESSIBILITIES AND ISOCHORES OF $(C_3F_7COOCH_2)_4C$, c-$Si_4O_4(CH_3)_8$, n-C_5H_{12}, n-C_8H_{18}, 2,2,4-$C_5H_9(CH_3)_3$, c-C_5H_{10}, c-C_6H_{12}, c-$C_6H_{11}CH_3$, $C_6H_5CH_3$, p-$C_6H_4(CH_3)_2$, s-$C_6H_3(CH_3)_3$, CH_2Cl_2

By Kōzō Shinoda[1] and J. H. Hildebrand

Department of Chemistry, University of California, Berkeley, California

Received July 5, 1960

The measurements herein reported were made primarily in order to have data for evaluating the contribution of expansion to the entropy of solution, the magnitude of which has been emphasized in recent studies.[2]

The apparatus used is shown in Fig. 1. The bulb had a capacity of 35.33 cc. The volume of the capillary stem was 0.00399 cc. per cm.

A liquid was cooled, well degassed, and introduced into the evacuated bulb. A small amount of mercury was introduced to confine the liquid. A series of three or more pressures ranging from 0.3 to 2.2 atm., was applied to the capillary and the jacket. The temperature was controlled to within 0.001°; 2 to 4 hours were allowed to attain equilibrium. Correction was made for the compressibility of Pyrex.

In this range, ΔV *vs.* ΔP was strictly linear within the limits of error, therefore our figures for compressibility are essentially $\beta = -(\partial \ln V/\partial P)_T$. The liquids were all carefully purified. We estimate an accuracy within 1 per cent.

The results are given in Table I together with, for

Table I

Units: Atmos., Cc., Mole, 25°

	$10^4\beta$	Vol. per mole	$(\partial P/\partial T)_v$
$(C_3F_7COOCH_2)_4C$	1.06	541.5	9.28
c-$Si_4O_4(CH_3)_8$	1.56	312.2	7.96
n-C_5H_{12}	2.17	116.1	7.65
n-C_8H_{18}	1.35	163.5	8.52
2,2,4-$C_5H_9(CH_3)_3$	1.58	166.1	7.63
c-C_5H_{10}	1.37	94.7	9.71
c-C_6H_{12}	1.15	108.7	10.5
c-$C_6H_{11}CH_3$	1.18	128.3	9.6
$C_6H_5CH_3$	0.93	106.9	11.5
p-$C_6H_4(CH_3)_2$	0.92	123.9	11.1
s-$C_6H_3(CH_3)_3$	0.88	139.6	10.7
CH_2Cl_2	1.09	64.5	12.4

convenience, molal volumes, and liquid isochores calculated by the relation:

$$(\partial P/\partial T)_V = -(\partial \ln V/\partial T)_P/(\partial \ln V/\partial P)_T$$

These figures serve to calculate other important thermodynamic functions, *e.g.*, $(\partial E/\partial V)_T$ and $(\partial S/\partial V)_T$.

The only liquid in the table for which we find references for β is $C_6H_5CH_3$, for which Freyer, Hubbard and Andrews[3] found 0.93_4 and Tyrer[4] found 0.94_1, both from adiabatic compressibility. Our figure is in excellent agreement.

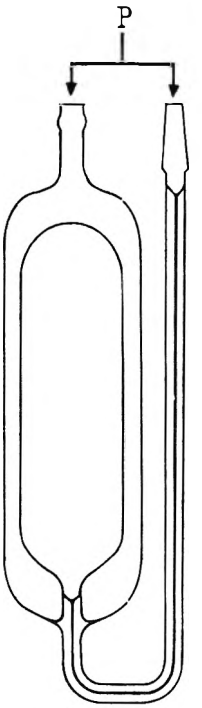

Fig. 1.

This work has been supported by the Atomic Energy Commission.

(1) Department of Chemistry, Faculty of Engineering, Yokohama National University, Ohka-Machi, Minami Ku, Yokohama, Japan.

(2) J. H. Hildebrand, This Journal, **64**, 370 (1960); K. Shinoda and J. H. Hildebrand, *ibid.*, **61**, 789 (1957).

(3) E. B. Freyer, J. C. Hubbard and D. H. Andrews, *J. Am. Chem. Soc.*, **51**, 759 (1929).

(4) D. Tyrer, *J. Chem. Soc.*, **103**, 1675 (1913).

MASS DEPENDENT ION COLLECTION EFFICIENCIES IN A MASS SPECTROMETER[1]

By Don A. Kubose and William H. Hamill

Department of Chemistry, The University of Notre Dame, Notre Dame Indiana

Received July 11, 1960

Calculations of gaseous ion–molecule reaction cross sections Q from mass spectrometric measurements require a knowledge of the primary and secondary ion currents, I_P and I_S, the length of primary ion path, l, through the reacting gas M and the concentration n_M. These are related by equation 1[2,3]

$$Q = I_S(I_P l n_M) - 1 \qquad (1)$$

The validity of this equation depends upon equal collection efficiencies for the primary and secondary ions. Differences arising from mass dependent discrimination in the slit systems are negligible in the present context except at lower masses and can be calculated.[4] This still leaves unsettled the

(1) Contribution from the Radiation Project of the University of Notre Dame, supported in part under AEC Contract AT(11-1)-38.

(2) D. P. Stevenson and D. O. Schissler, *J. Chem. Phys.*, **23**, 1353 (1955).

(3) F. H. Field, J. L. Franklin and F. W. Lampe, *J. Am. Chem. Soc.*, **74**, 2419 (1957).

(4) N. Coggeshall, *J. Chem. Phys.*, **12**, 19 (1944).

TABLE I

RATIO OF ANALYZED ION CURRENT I_a TO TOTAL ION CURRENT I_t AT VARIOUS m/e, NORMALIZED TO UNITY FOR XENON

m/e / E_r(v./cm.)	2	4	15.5	18.9	20.2	25.7	33.4	40	83.7	131.3
12	1.18	1.16	0.98	0.96	1.06	0.97	1.06	0.99	1.04	1.00
20	1.14	1.13	.94	.95	1.02	.96	1.03	.96	1.02	1.00
28	1.11	1.11	.95	.93	1.00	.94	1.01	.95	1.02	1.00
40	1.11	1.09	.95	.94	1.00	.94	1.02	.95	1.00	1.00
60	1.11	1.09	.96	.95	1.00	.94	1.01	.95	1.00	1.00
80	1.05	1.04	.97	.96	1.00	.95	1.02	.94	0.99	1.00

question whether any other effects contribute to discrimination among ions at different m/e, and between primary and secondary ions which originate in different regions of the ionization chamber.

In previous studies of ion–molecule reactions this possible source of error has not been adequately accounted for, although Stevenson and Schissler[5] used H_2^+, HD^+ and D_2^+ to establish an empirical correction for mass dependent discrimination in the corresponding interval of m/e.

This report describes an experimental approach to the problem which only requires comparing the ratio of the analyzed ion current, I_a, measured conventionally at given m/e to the total saturation current, I_t, measured on the negatively biased repeller electrodes. If ions appear over an appreciable range of m/e, then it is evidently required that for some one ion species k, $I_{ak} >> \Sigma I_{ai}$. The noble gases meet this requirement best and some molecular gases are also acceptable.

Experimental

These experiments were performed with a CEC model 21–103A mass spectrometer with a model 31–402 ion source. The repeller to exit slit electrode spacing is 0.25 cm. with the electron beam nearly midway between them. The electron ionizing current was 10.5 μa., the ionizing voltage was 60 v. and the reservoir pressure was 300 μ throughout. The ion accelerating voltage was 1230 v. $\pm$ 5% for all m/e. The m/e interval of interest was scanned electrostatically. Measurements of I_a were made at several repeller voltages.

Total positive ion current in the ionization chamber of the mass spectrometer was always measured by connecting both repeller electrodes to ground through the input resistance of a vibrating reed electrometer, using a 22.5 v. bias, corresponding to a field of 90 v./cm.

Gases used were H_2, D_2, CH_4, CD_4, Ne, C_2H_2, H_2S, Ar, Kr and Xe. They contained only negligible impurities. For noble gases the I_a/I_t ratios are taken at the average m/e (weighted by abundances) for the singly charged isotopic ions. For methane, the weighted average of the m/e 13, 14, 15 and 16 ions was used. For methane-d_4, the weighted average of m/e 14, 16, 18 and 20 was used. For C_2H_2 and H_2S, m/e 24, 25, 26, 27 and m/e 32, 33, 34, 35, 36, respectively, were used.

Ion abundance curves were determined for Ar^+, Ar^{++}, Kr^+, Kr^{++} and Xe^+, Xe^{++} at E_r = 12 v./cm. repeller field strength.

Results

The total ion current measured for the noble gases was corrected for the appreciable contributions from doubly charged ions of argon, krypton and xenon.[6,7] In each instance the effect of repeller field upon electron energy was allowed for. The corrected total ion current was taken as $I_a^+ I_t/(I_a^+ + I_a^{++})$. Analogously for CH_4, CD_4, C_2H_2 and H_2S the corrected total current becomes $I_a I_t/\Sigma I_{ai}$ where the summation applies to all ionic species.

The results, which appear in Table I, cover the useful range of repeller fields. In the m/e region investigated there is little discrimination (in the instrument used) for any repeller field except for a small increase at low m/e. Our concern with this problem is primarily to establish conditions for distinguishing among various possible ion–molecule force laws and reaction rate expressions.

(5) D. P. Stevenson and D. O. Schissler, *ibid.*, **29**, 282 (1958).
(6) W. Bleakney, *Phys. Rev.*, **36**, 1303 (1930).
(7) J. T. Tate and P. T. Smith, *ibid.*, **46**, 773 (1934).

A COMPARISON OF THE MEASUREMENT OF HEATS OF ADSORPTION BY CALORIMETRIC AND CHROMATOGRAPHIC METHODS ON THE SYSTEM NITROGEN–BONE MINERAL

BY R. A. BEEBE[1] AND P. H. EMMETT

Departments of Chemistry, Amherst College, Amherst, Massachusetts and Johns Hopkins University, Baltimore, Maryland

Received July 18, 1960

Several investigations[2–4] reported in the literature have been concerned with the determination of heats of adsorption from the retention times obtained in gas–solid chromatography. However, in none of this work has it been possible to make a direct comparison between the heat values derived from chromatography and the heats measured calorimetrically for the same adsorption system.

As a part of a program of adsorption studies on bone mineral in the Amherst laboratory, calorimetric data are available for the differential heats of adsorption of nitrogen at $-195°$ on this adsorbent. These data will be submitted in the near future for publication in detailed form. In the Johns Hopkins laboratory we have determined the retention times for nitrogen pulses in helium carrier gas over a column of the bone mineral. Thus we are in a position to compare the heat values determined by the two methods.

The bovine bone mineral supplied by the Armour Research Laboratories, designated as OSSAR, consisted of granules of 20–40 mesh which proved to be a convenient form for use in both the calorimetric and the chromatographic work. A considerable amount of information on the adsorption characteristics of water, methanol and nitrogen on this material are given in a recent paper.[5] The OSSAR was

(1) One of us (R.A.B.) expresses appreciation to the Petroleum Research Foundation for fellowship aid which made it possible to spend the academic year 1959–1960 in the laboratories of Johns Hopkins University and the University of Bristol.

(2) E. Cremer and F. Prior, *Z. Elektrochem.*, **55**, 66 (1951).
(3) S. A. Greene and H. Pust, THIS JOURNAL, **62**, 55 (1958).
(4) H. W. Habgood and J. F. Hanlan, *Can. J. Chem.*, **87**, 843 (1959).
(5) M. E. Dry and R. A. Beebe, THIS JOURNAL, **64**, 1300 (1960).

packed into a 220 cm. column of Pyrex glass tubing of 0.45 cm. internal diameter which was wound into a helix 4.0 cm. in diameter and 20 cm. high. This form of the column was convenient for high temperature treatment and for immersion in suitable cryostatic baths used in the retention time measurements. The OSSAR sample weighed 16.5 g. and its specific surface area was 100 $m.^2/g.$

In the most definitive measurements of the present research, the column was dried overnight in a stream of dry helium at 480°. This treatment presumably removed substantially all the adsorbed water without destruction of the hydroxyapatite structure. The nitrogen pulses effluent from the column were observed by means of a Gow-Mac katharometer and were traced on a standard type of recorder. The flow rate employed was 35 $cm.^3$ per minute. The input pressure of the helium stream was maintained constant by a simple device described by James and Martin.[6] The volume of the nitrogen pulses contained between two four-way stopcocks was 2.3 $cm.^3$. The pulses used were either pure nitrogen or a mixture of 1% nitrogen with 99% helium. The observed retention time measured at the peak of the recorded effluent nitrogen pulse was corrected to allow for the time that would have been required for passage through a non-adsorbing column. The magnitude of this correction at each temperature employed was determined by substituting hydrogen for nitrogen in the pulses, making the reasonable assumption that hydrogen was not being appreciably adsorbed on the column at these temperatures.

The corrected retention times for the pure nitrogen pulses on the 480° dried column measured at 0, −31 and −78° were 17.1, 54.0 and 783 seconds, respectively. Similar measurements with 1% nitrogen to 99% helium in the pulses at the above three temperatures resulted in corrected retention times of 34.6, 109 and 1820 seconds, respectively. Following the method of Habgood and Hanlan[3] we have calculated heats of adsorption from the chromatographic data. The values obtained for the pure nitrogen and the one per cent. nitrogen pulses are 5.6 and 5.8 kcal./mole, respectively.

The calorimetrically determined differential heats of adsorption for successive increments of nitrogen on the bone mineral at −195° fall off more or less linearly from 5.4 kcal. for an initial increment covering 3% of the monolayer to approximately 2.2 kcal. for the monolayer. In view of the low coverage obtained in the chromatographic work it seems reasonable to compare the results of the present work with the calorimetric data at the lowest coverage. More exact agreement than that obtained is probably not to be expected because of small differences in the state of the OSSAR surface as well as the difference in the temperature of measurement by the two methods.

In some preliminary experiments conducted under less carefully controlled conditions we have determined retention times for nitrogen on OSSAR which was partially dried by treating it at room temperature with a stream of helium as taken directly from the tank. This drying procedure presumably left a monolayer or more of adsorbed water on the sample. For four separate nitrogen pulse runs in the temperature range −78 to −145° we obtained retention times yielding heat of adsorption values in the range 2.5 to 3.0 kcal. in qualitative agreement with calorimetric heats ranging from 3.3 kcal. for 8% coverage down to 2.0 kcal. for a monolayer. It is probable that the surface was less completely dehydrated in the chromatographic work than in the calorimetry. Thus we might expect a lower binding energy for nitrogen at low coverage as determined in the chromatographic experiments.

(6) D. H. James and A. J. P. Martin, *Biochem. J.*, **50**, 682 (1952).

It is noteworthy that the retention time is greatly increased by dilution of the nitrogen pulse passing through the OSSAR column. In fact, it was approximately doubled by a hundred-fold dilution of the pulse at each of the temperatures cited above. We believe this effect is due to a slight non-linearity in the adsorption isotherm over the range of partial pressures of nitrogen covered in the present experiments. However, regardless of the cause, it is apparent that this change in retention time with partial pressure must be guarded against in the operation of a gas-solid chromatographic column for gas analysis.

Acknowledgment.—The authors are grateful to Dr. Frank S. Stone for helpful discussion and especially for his pertinent suggestions in interpreting the chromatographic data, and to Dr. James M. Holmes who made the calorimetric measurements cited here.

One of us (R.A.B.) is also grateful to W. A. Van Hook for his expert assistance and advice in reducing the time required to put the chromatographic system into operation.

STABILIZATION ENERGIES IN NON-AROMATIC CONJUGATED POLYENES

BY WM. F. YATES

Research Department, Monsanto Chemical Company, Texas City Texas

Received July 15, 1960

The earliest evidence for extra "stabilization energy" in certain conjugated polyenes was noted in the thermodynamic properties of those compounds. Their heats of combustion and heats of hydrogenation differed appreciably from the values they may have been expected to have from an examination of similar non-stabilized models. The term "stabilization energy" in fact implies reference to a model, as pointed out by Kistiakowsky and others.[1] It has also been pointed out by Turner[2] that the stabilization energies of compounds include electron delocalization energies, terms for bond length changes, bond hybridization changes, steric effects, and other factors. Dewar and Schmeising[3] have attempted to show that simple conjugated dienes, such as butadiene, have no bond delocalization energy, and all of the so-called "resonance energy" of such molecules can be explained by taking into account the type of bond hybridization. In support of this hypothesis they have calculated the single bond energies for various types of C hybridization using molecular orbital methods and have shown that the single bonds between C_{sp^3}-C_{sp^3}, C_{sp^3}-C_{sp^2}, C_{sp^2}-C_{sp^2}, C_{sp^2}-H, and C_{sp^3}-H are indeed quite different. Any stabilization energies based on heats of hydrogenation must take into account the corresponding changes in hybridization.

There remains an area of Dewar's hypothesis

(1) (a) G. B. Kistiakowsky, J. R. Ruhoff, H. A. Smith and W. E. Vaughan, *J. Am. Chem. Soc.*, **58**, 146 (1936); (b) J. B. Conant and G. B. Kistiakowsky, *Chem. News.*, **20**, 181 (1937).

(2) R. B. Turner, Proceedings of the Eighth Rice Institute Research Conference, April 24, 1959.

(3) M. J. S. Dewar and H. N. Schmeising, *Tetrahedron*, **5**, 166 (1959).

which must face a test of old fashioned thermodynamic consistency: that all of the stabilization energy of butadiene can be accounted for in the C_{sp^2}-C_{sp^2} hybridization in the central single bond. Mulliken[4] has shown that even in very simple molecules, such as ethylene, the C bonds are not pure sp^2 hybrids, and one cannot expect to calculate the bond energies in a classical butadiene molecule with sufficient accuracy to make the necessary hybridization corrections to account for the heat of hydrogenation.

In this paper we shall attempt to find the average bond energies by the usual methods using the standard heats of formation of the compounds involved. The purpose of the work will be to see whether changes in conformation between C atoms with sp^2 hybridizations have any effect on the bond energies, thereby throwing some light on the problem of bond delocalization.

The C–C Bond Energy in Conjugated Polyenes.—From the hydrogenolysis of butadiene

$$CH_2{=}CH{-}CH{=}CH_2 + H_2 \longrightarrow 2C_2H_4$$

the heat of reaction, Q_B, from standard heats of formation[5] is -1.75 kcal./mole.

$$Q_B = E'_{CC}{}^{B} + E_{HH} - 2E'_{CH} \qquad (1)$$

where $E_{CC}{}'^{B}$ is the central bond energy in butadiene, E_{HH} is the bond energy in the H_2 molecule, and E'_{CH} is the bond energy for the CH bond in ethylene. The value of E'_{CH} can be computed by the usual procedure from the standard heat of formation of ethylene, graphite and atomic hydrogen

$$C_2H_4 \longrightarrow 2C\ (\text{graphite}) + 4H$$

$$Q = 4E'_{CH} - \frac{4}{3}L_C$$

in which Q is the heat of reaction shown and L_C is the latent heat of vaporization of graphite. E'_{CH} is then found to have the value of 106.20 kcal./mole.

The value of $E'_{CC}{}^{B}$ in equation 1 is then 106.47 kcal./mole. It should be noted here that if Dewar's value of 100.9 kcal. for E'_{CH} is used the value of $E'_{CC}{}^{B}$ is 95.87 against the value of 100.4 which he calculates by the molecular orbital treatment. The difference probably arises largely from the fact that the C bonds involved are not pure sp^2-sp^2 bonds, and there may be extra delocalization energy (the very point we are examining).

Cyclooctatetraene provides an interesting model for examination because here again all of the single bonds are formed from C_{sp^2}-C_{sp^2} overlap, but the double bonds have been rotated through 90°,[6] thus greatly diminishing the possibility of bond delocalization between adjacent double bonds. There still exists, however, the possibility for some *trans*-annular π-bond interaction, and, as Mulliken[4] points out, secondary hyperconjugation can be introduced.

By the previous method used with butadiene, the complete hydrogenolysis of cyclooctatetraene to ethylene has a heat of reaction, $Q_{C'}$, of -17.90 kcal./mole. In this calculation a value of $\Delta H_f{}^0$ for cyclooctatetraene of 67.90 was used and was calculated from the heat of hydrogenation (determined by Turner[7a] and co-workers), and the heat of formation of cyclooctane.[8] Turner's heat of hydrogenation was determined in solution, so its use to determine a gas phase heat of formation may introduce an error. In the equation

$$Q_{C'} = 4E'_{CC}{}^{C8} + 4E_{HH} - 8E'_{CH}.$$

$E'_{CC}{}^{C8}$ is found to be 103.73 kcal./mole, or 2.74 ± 0.3 kcal. less than the value in butadiene. An alternate value for the heat of formation of cyclooctatetraene vapor (71.0 kcal.) is available from combustion data[7b] and the heat of vaporization.[7c] If this alternate value is used $E'_{CC}{}^{C8}$ is found to be 103.0 kcal./mole.

Cyclooctatriene provides still another model for examination in which the conjugated double bonds are rotated through approximately 90°. Here the problem is not quite so simple, however, in that two of the bonds broken in hydrogenolysis are formed by sp^2-sp^3 overlap. In the reaction

$$\text{Cyclooctatriene} + 4H_2 \longrightarrow C_2H_6 + 3C_2H_4$$

$$Q_{C''} = -25.04$$

Here again Turner's[6] heat of hydrogenation was used to calculate $\Delta H_f{}^0 = 42.30$ for cyclooctatriene and the same possible error is included. We then have

$$Q_{C''} = 2E''_{CC}{}^{C8} + 2E'_{CC}{}^{C8} + 4E_{HH} - 6E'_{CH} - 2E_{CH} \qquad (2)$$

in which $E''_{CC}{}^{C8}$ is the C_{sp^2}-C_{sp^3} bond energy in cyclooctatriene and E_{CH} is the CH bond energy in ethane. E_{CH} is found to be 98.54 kcal./mole from the reaction[5]

$$C_2H_6 \longrightarrow 2C\ (\text{diamond}) + 6H$$

$E''_{CC}{}^{C8}$ was calculated from the hydrogenolysis of *cis*-cyclooctene to $3C_2H_6 + C_2H_4$ and the value of $E_{CC}{}^{C8}$, the C_{sp^2}-C_{sp^3} bond in the hydrogenolysis of cyclooctene was determined from the hydrogenolysis of cyclooctane. In this way compensation for bond weakening due to strain characteristic of the C_8 saturated ring is taken into account.

We have for these values

$E_{CC}{}^{C8}$ ($C_{sp^3} - C_{sp^3}$) in cyclooctane, 80.17 kcal./mole
$E''_{CC}{}^{C8}$, ($C_{sp^2} - C_{sp^3}$) in *cis*-cyclooctene, 92.72 kcal./mole

Using these values then in equation 2 we get 103.54 kcal./mole for $E'_{CC}{}^{C8}$, the bond energy for C_{sp^2}-C_{sp^2} single bonds in cyclooctatriene. This is in excellent agreement with the value of 103.73 in cyclooctatetraene.

For still another model for study we have chosen cycloheptatriene. In this compound the three conjugated double bonds have been assumed to be near planar[9] and the value of $E'_{CC}{}^{C7}$ should lie somewhere between the 106.47 value in butadiene and the 103.6 value in the 8-member ring polyenes.

(4) R. S. Mulliken, *Tetrahedron*, **6**, 68 (1959).

(5) "Selected Values of the Properties of Hydrocarbons," API Project 44, at the Carnegie Institute of Technology, April 30, 1959.

(6) (a) W. B. Person, G. C. Pimentel and K. S. Pitzer, *J. Am. Chem. Soc.*, **74**, 3437 (1952); (b) I. L. Karle, *J. Chem. Phys.*, **20**, 65 (1952).

(7) (a) R. B. Turner, W. R. Meador, W. von E. Doering, J. R. Mayer and D. W. Wiley, *J. Am. Chem. Soc.*, **79**, 4127 (1957); (b) E. J. Prosen, W. H. Johnson and F. D. Rossini, *ibid.*, **72**, 626 (1950); (c) D. W. Scott, M. E. Gross, G. D. Oliver and H. M. Huffman, *ibid.*, **71**, 1634 (1949).

(8) H. L. Finke, D. W. Scott, M. E. Gross, J. F. Messerly and G. Waddington, *ibid.*, **78**, 5469 (1956).

(9) W. von E. Doering, G. Labor, R. Vonderwahl, N. F. Chamberlain and R. B. Williams, *ibid.*, **78**, 5448 (1956).

Using methods identical in all respects to the cases above a value of 105.87 for $E'_{CC}{}^{C7}$ is found. The calculations necessitate the use of 99.50 kcal./mole for E_{CH} in methane, 80.88 kcal./mole for $E''_{CC}{}^{C7}$ in cycloheptatriene and *cis*-cycloheptene, and the standard heats of formation reported in the literature or computed from heats of hydrogenation.[7,10,11]

Conclusions

To summarize then, we have these bond energies for C_{sp^2}–C_{sp^2} single bonds

in butadiene	106.47 kcal./mole
in cycloheptatriene	105.87 kcal./mole
in cyclooctatetraene	103.73 kcal./mole
in cyclooctatriene	103.54 kcal./mole

It is still impossible to attribute all of the difference in energy of *ca.* 2.8 kcal./mole between the single bond in butadiene and the C8 cyclopolyenes to resonance or any other single phenomenon. The difference in bond energy is, however, in good agreement with the rotational barrier in butadiene as calculated by Mulliken and Parr[12] and later refined by Mulliken.[4] Turner has derived a value of 2.4 kcal./mole for the stabilization energy of cyclooctatetraene as referred to a cyclohexene–cyclooctatriene model.[7a] If this 2.4 kcal./mole is due mostly to *trans*-annular π-bond interaction, then half of it must be added to the 2.8 kcal. difference in bond energy between the coplanar and 90° rotated model to get 4.0 ± 0.3 kcal./mole for the rotational barrier in butadiene, in excellent agreement with Mulliken.

The conclusion we then draw is that there is significant stabilization energy in butadiene which cannot be attributed to a pure C_{sp^2}–C_{sp^2} bond alone. Even if the use of average bond energies does not subsequently prove to be exact (*i.e.*, if E'_{CH} in cyclooctatetraene is different from E'_{CH} in ethylene), we would see an error in the E'_{CC} calculated in the models used but probably very little error reflected in the differences between the E'_{CC} values.

(10) R. B. Turner and W. R. Meador, *ibid.*, **79**, 4133 (1957).
(11) J. B. Conn, G. B. Kistiakowsky and E. A. Smith, *ibid.*, **61**, 1868 (1939).
(12) R. S. Mulliken and R. G. Parr, *J. Chem. Phys.*, **19**, 1271 (1951).

NUCLEAR MAGNETIC RESONANCE SPECTRUM OF N-BENZYLTHIENO[3,2-b]-PYRROLE[1]

BY R. J. TUITE, H. R. SNYDER, A. L. PORTE AND H. S. GUTOWSKY

Noyes Chemical Laboratory, University of Illinois, Urbana, Illinois

Received July 26, 1960

We have found that the position of nuclear substitution in thieno[3,2-b]pyrroles[2,3] usually can be deduced directly from n.m.r. spectral data. An unexpected spin-spin coupling of the protons in the α-positions of the two heterocyclic rings proved to be the key to the interpretation of the spectra; although these protons are separated by six bonds, the coupling constant amounts to about 1 c.p.s. On the basis of the spectra of representative compounds in the series, we wish to report here the interpretation of the spectrum of N-benzylthieno-[3,2-b]pyrrole (I), the synthesis of which is reported elsewhere.[4] The relative magnitudes of the cross-ring couplings in this compound can be explained in terms of a π-electron mechanism.

The α-proton of a 5-membered aromatic heterocycle generally absorbs at a lower magnetic field than a corresponding β-proton.[5,6] In the spectra of thieno[3,2-b]pyrroles the peak assigned to the 5-proton occurs between −3.19 and −2.18 p.p.m. (relative to water) and that to the 6-proton between −1.84 and −1.31 p.p.m., all spectra showing good peak separation at both 40 and 60 Mc.[7] In the spectra of several 2,3-disubstituted pyrroles (II) and 2,3-disubstituted (III) and 2,3,4-trisubstituted (IV) thienopyrroles the value of the coupling constant[3,5] $J_{\alpha\beta}$ (J_{56} in the thienopyrroles) is in the range 3.0 ± 0.5 c.p.s. (In the NH series, there is further splitting of the α and β protons by the NH proton, and, since $J_{45} \cong J_{46} \cong J_{56}$, a pair of triplets is observed[3].) The J_{56} values of several 2,3,4-trisubstituted thienopyrroles are included in Table I.

TABLE I

PROTON-PROTON COUPLING CONSTANTS IN C.P.S. OBSERVED IN THE N.M.R. SPECTRA OF SUBSTITUTED THIENO[3,2-b]-PYRROLES (IV)

Substituents				Coupling constants[a]	
R_2	R_3	R_4	R_6	J_{56}	J_{26}
CO_2Et	OH	CO_2Et	H	3.7	..
CO_2Et	OH	Et	H	2.7	..
CO_2Et	OCH_3	CO_2Et	H	3.2	..
CO_2Et	OCH_3	Et	H	3.0	..
CO_2Et	OAc	CO_2Et	H	3.5	..
H	OAc	$COCH_3$	H	3.5	1.2
$COCH_3$	OAc	$COCH_3$	H	3.5	..
H	OAc	$COCH_3$	$CH_2C_6H_5$	..	1.3

[a] The values given are the average splittings observed at 60 Mc. with moderate resolution, uncorrected for second-order effects.

With the knowledge of the approximate line positions of the 5 and 6 protons and of the value for J_{56}, the spectrum of 3-acetoxy-4-acetylthieno-[3,2-b]pyrrole (V) can be explained. In addition to the expected coupling of the 5-proton at −2.36 p.p.m. with the 6-proton at −1.70 p.p.m. ($J_{56} \cong$ 3.5 c.p.s.), there is a further splitting of the −2.36 p.p.m. peak by the 2-proton, which appears at −2.00 p.p.m. ($J_{25} \cong$ 1.2 c.p.s.). The latter cross-ring splitting is also observed in the spectrum of VI ($J_{25} \cong$ 1.3 c.p.s.).[4]

(1) This investigation was supported in part by the Office of Naval Research and in part by a grant [C3969(C1)Bio] from the National Cancer Institute, Public Health Service. Also, grateful acknowledgment is made to the donors of the Petroleum Research Fund, administered by the American Chemical Society, for support of part of the work.
(2) D. S. Matteson and H. R. Snyder, *J. Am. Chem. Soc.*, **79**, 3610 (1957).
(3) W. R. Carpenter and H. R. Snyder, *ibid.*, **82**, 2592 (1960).
(4) A. D. Josey, R. J. Tuite and H. R. Snyder, *ibid.*, **82**, 1597 (1960).
(5) R. Abraham and H. Bernstein, *Canad. J. Chem.*, **37**, 1056 (1959).
(6) E. J. Corey, G. Slomp, S. Dev, S. Tobinaga and E. R. Glazier, *J. Am. Chem. Soc.*, **80**, 1204 (1958).
(7) The spectra were determined with a Varian Associates V-4300-B high resolution n.m.r. spectrophotometer on 20% solutions in deuteriochloroform with methylene chloride as an external standard.

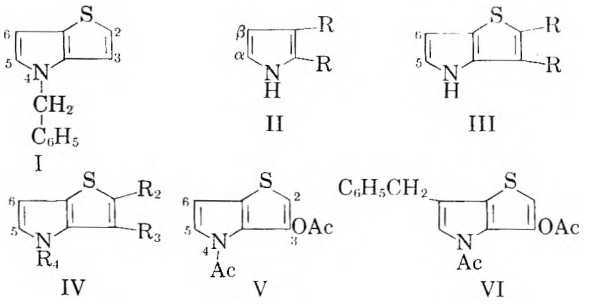

The values of J_{56} and J_{25} now can be used in interpreting the spectrum of I. In addition to the partially resolved benzenoid multiplet, the aromatic region contains a series of two quartets and two doublets, under conditions of moderate resolution. Each component of the two doublets is further resolvable into a close doublet, giving the series of four quartets shown in part A of Fig. 1. From

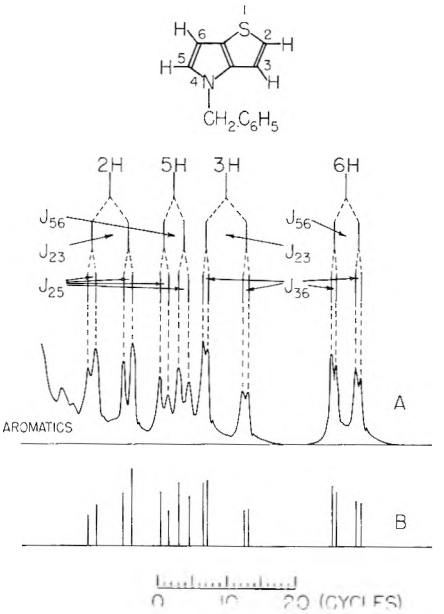

Fig. 1.—The spectrum of the heterocyclic ring protons in N-benzylthieno[3,2-b]pyrrole, observed at 60 Mc. with the magnetic field increasing from left to right (A). The line spectrum (B) was computed with an electronic digital computer (Illiac) using exact expressions for the four-spin system and the parameters, all in c.p.s.: $\nu_2 = 0$; $\nu_3 = 16.3$; $\nu_5 = 8.9$; $\nu_6 = 33.8$; $J_{23} = 4.9$; $J_{25} = 1.3$; $J_{26} = 0$; $J_{35} = 0$; $J_{36} = 0.5$; and $J_{56} = 2.9$.

their positions and coupling constants, these quartets are assigned (from lower to higher field) to the 2-, 5-, 3- and 6-protons, respectively. We have made a full analysis of the spectrum of the heterocyclic ring protons, the results of which are summarized in Fig. 1, part B. The value of 4.9 c.p.s. found for J_{23} agrees well with that reported for $J_{\alpha\beta}$ in mononuclear thiophenes.[8,9] The absence of further resolved splittings indicates that J_{26} and J_{35} are less than *ca.* 0.3 c.p.s., which is the approximate limit of resolution of the instrument at 60 Mc.

(8) S. Gronowitz and R. A. Hoffman, *Arkiv. Kemi*, **13**, 279 (1958).

(9) R. Abraham and H. Bernstein, *Canad. J. Chem.*, **37**, 2095 (1959).

The values cited for J_{25} and J_{36} are surprisingly large when one considers that six bonds separate the nuclei which are coupled. To our knowledge, there are no previously reported cases of spin–spin interaction of appreciable magnitude between two protons which are separated by more than five bonds. However, coupling *via* five bonds has been reported in several cases, including 1 c.p.s. between the aldehydic proton and the 5-proton in 2-thiophene carboxaldehyde,[10] 0.9 c.p.s. between the corresponding protons in furfural,[11] and 0.15 to 0.45 c.p.s. between the *para* protons in derivatives of benzene.[12,13]

The observed long-range cross-ring couplings in I must be transmitted through the π-electronic system, for they are too large to be accounted for by transmission through the σ-framework. There must, therefore, be significant interaction between the σ- and the π-electronic systems in these five-membered rings. The relative magnitudes of couplings can be accounted for, qualitatively, by electronic interactions shown schematically in Ia and Ib.

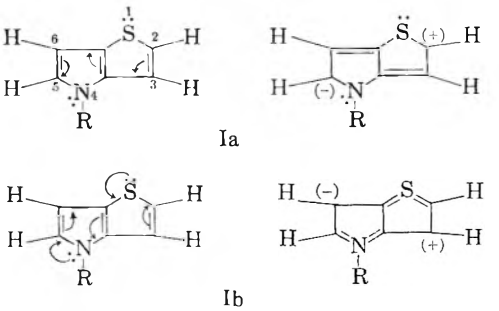

σ-π Interaction at carbon-2 couples the spin of proton-2 to the π-electronic system, and the mesomeric effect then transmits this coupling to the remaining protons of the system *via* σ-π interactions at other sites in the molecule. However, as shown in (Ia), the mesomeric effect couples electronic perturbations at carbon-2 preferentially with carbon-5 rather than with carbon-6, *i.e.*, J_{25} is greater than J_{26}. Similarly, in (Ib), the mesomeric effect couples proton-3 with proton-6 rather than with proton-5, *i.e.*, J_{36} is greater than J_{35}. Furthermore, the contribution of structure Ib to the total π-electron wave function for the molecule is less than that of Ia,[14] and so J_{25} is greater than J_{36}.

It is to be expected that mutual interactions between substituents will be transmitted across the ring system in a manner similar to the coupling between protons. For example, chemical effects between substituents in the 2- and 5- positions will be greater than those between the same substituents in the 2- and 6-positions.

(10) S. Gronowitz and R. A. Hoffman, *Acta Chem. Scand.*, **13**, 1687 (1959).

(11) J. B. Leane and R. E. Richards, *Trans. Faraday Soc.*, **55**, 518 (1959).

(12) J. P. Heeschen and H. S. Gutowsky, unpublished work.

(13) Coupling constants *via* five bonds have been reported and reviewed by F. A. L. Anet, *J. Chem. Phys.*, **32**, 1274 (1960), who reports cross-ring coupling of 0.8 c.p.s. between the 4- and 8-hydrogens, which are separated by five bonds, in two substituted quinolines.

(14) V. Schomaker and L. Pauling, *J. Am. Chem. Soc.*, **61**, 1779 (1939).

FORMATION OF METHYL HYDROPEROXIDE IN THE PHOTOOXIDATION OF AZOMETHANE[1]

By M. Shanin[2] and K. O. Kutschke

Division of Pure Chemistry, National Research Council, Ottawa 2, Canada

Received July 22, 1960

Various radicals have been suggested as precursors of the secondary products which are commonly investigated in the reaction of methyl radicals with oxygen. The "third-body" nature of reaction 1 was demonstrated by Hoare and Walsh[3]

$$CH_3\cdot + O_2 + M \longrightarrow CH_3OO\cdot + M \qquad (1)$$

Sleppy and Calvert[4] and Christie,[5] but little is known of the subsequent reactions of methylperoxy radicals so formed. It is anticipated that reaction 1 will be exothermic (between 20–30 kcal./mole) and thus will result in a vibrationally excited species which could be stabilized by collision with a third-body (M). Subsequent to this process, methylperoxy radical is expected to undergo familiar abstraction reactions which are observed with other alkylperoxy radicals. Gray[6] studied the mercury photosensitized oxidation of methane below 50° in a fast flow system (*ca.* 1 l./min.), and reported that methyl hydroperoxide, which was determined iodometrically, was the major product. The mechanism suggested was

$$CH_3\cdot + O_2 \longrightarrow CH_3O_2\cdot \qquad (2)$$

$$CH_3O_2\cdot + CH_4 \longrightarrow CH_3OOH + CH_3\cdot \qquad (3)$$

and also

$$CH_3O_2\cdot + CH_4 \longrightarrow CH_3OOCH_3 + H \qquad (4)$$

Methyl hydroperoxide, however, has not been identified unambiguously in the azomethane and acetone photooxidation systems. The products chiefly observed[7–9] were methanol, formaldehyde and formic acid. To account for the production of methanol, the predominant radical in the system has been assumed to be the methoxy radical and several suggestions have been made whereby the conversion of methylperoxy radical to methoxy radical is accomplished.

In order to clarify these contradictory conclusions and also to obtain further insight into the reactions in azomethane photooxidation, a flow system was set up in which the contents of the reaction cell (azomethane, 6.6 mm.; oxygen 11 mm.; carbon dioxide 48 cm.) were circulated by means of an all-glass piston pump through a multiple trap attached to the system by ground glass joints and kept at −77°. The pump operated at about 3 l./min., and the time taken to circulate gases from the reaction cell to the cold trap was about 3–4 seconds. In order to maintain this rate no stopcocks were used in the circulating system. The upper part of the trap was warmed by a small electric fan to avoid mist formation. No metal valves were used. After long periods of irradiation (corresponding to the decomposition of about 60 μmole of azomethane, whose partial pressure was maintained constant by excess liquid in the cold trap[10] while the trap was held at −77°, the gases were expanded slowly into larger volumes and pumped until the pressure in the system reached 10^{-1} mm. Air was admitted to the system and the trap removed. Stopcocks were attached to the trap at the joints and, after removing the air, the contents were analyzed mass spectrometrically. It was hoped that *m/e* 48 (CH_3OOH) would be prominent if methyl hydroperoxide were present in quantity; the contribution by any residual azomethane to this mass number is negligible. Initial experiments showed no trace of a peak at *m/e* 47, 48 or 49. However, on a sudden and direct introduction of the gases from the multiple trap to the ionization chamber, very large peaks at *m/e* 47 and 48 were recorded. The heights of these peaks were found to decrease sharply and they disappeared after a few minutes with a half-life of approximately 25 seconds. It was thought that metal valves and connecting tubing (brass and stainless steel at room temperature) in the inlet system of the mass spectrometer might have caused surface catalyzed decomposition of the methyl hydroperoxide. The observation was repeated many times by pumping out the gases already in the mass spectrometer and introducing a fresh supply of the vapor from the multiple trap into the ionization chamber. Two other mass spectrometers, each with different lengths of metal tubing in the inlet system, were employed. The rate of decrease in the peak heights of *m/e* 48 and 47, and hence the decomposition of the hydroperoxide, was found to vary depending on the surface area exposed. A synthetic sample of methyl hydroperoxide prepared by Dr. L. C. Leitch of these laboratories was then examined similarly and found to behave in an exactly identical fashion; the peak height of *m/e* 48 exhibited an identical half-life.

To observe the possible products of the decomposition of methyl hydroperoxide, observations were made on two other mass numbers, 30 (formaldehyde) and 32 (methanol). The peak height at *m/e* 32 was found to remain unaffected, while that at *m/e* 30 (formaldehyde) was observed to increase at a rate, almost equal to the decrease in the peak height of *m/e* 48. It is concluded, therefore, that reaction 5 takes place very rapidly on the surface of the metal.

$$CH_3OOH \longrightarrow HCHO + H_2O \qquad (5)$$

Following these results, the observation of the mass number of the hydroperoxide, together with its rapid decomposition, was taken as a criterion to identify the presence of methyl hydroperoxide in subsequent experiments. The results summarized in Table I, indicate three important features.

(i) Methyl hydroperoxide is formed by reaction 6 at temperatures as high as 158°

(1) Issued as N.R.C. No. 6107.

(2) National Research Council Post-doctorate, 1958–1960.

(3) D. E. Hoare and A. D. Walsh, *Trans. Faraday Soc.*, **53**, 1102 (1957).

(4) W. C. Sleppy and J. G. Calvert, *J. Am. Chem. Soc.*, **81**, 769 (1959).

(5) M. I. Christie, *Proc. Roy. Soc.* (*London*), **A244**, 411 (1958).

(6) J. A. Gray, *J. Chem. Soc.*, 3105 (1952).

(7) P. L. Hanst and J. G. Calvert, This Journal, **63**, 71 (1959).

(8) R. L. Strong and K. O. Kutschke, *Can. J. Chem.*, **37**, 1456 (1959).

(9) F. Wenger and K. O. Kutschke, *ibid.*, **37**, 1546 (1959).

(10) G. R. Hoey and K. O. Kutschke, *Can. J. Chem.*, **33**, 496 (1955).

$$CH_3OO\cdot + RH \longrightarrow CH_3OOH + R\cdot \quad (6)$$

RH might be azomethane although it might also be formaldehyde, since the experiments were carried to a high conversion at constant azomethane concentration.

(ii) Experiment 7 was done under conditions similar to those reported by Hanst and Calvert,[7] except for lower intensity. While they did not find methyl hydroperoxide among their reaction products, under our conditions, this substance was readily detected.

(iii) Abstraction of a deuterium atom from CD_4 by $CH_3O_2\cdot$, even at temperatures as high as 158° is not rapid.

The results of Gray[6] and Nalbandyan[11] on methane, might then be reinterpreted in terms of the mechanism suggested by Watson and Darwent[12] for ethane oxidation.

A preliminary estimate of the quantum yield of the hydroperoxide (iodometric titration), indicated that it lay between 0.5 and unity for conditions as in experiments 4 and 5, but with CH_4 and at 100°. Thus it was an important product of the reaction. More quantitative work on the formation of methyl hydroperoxide is now in progress.

TABLE I

CONSTANT PRESSURE OF AZOMETHANE = 6.6 MM. PRESSURE OF OXYGEN (AT ROOM TEMPERATURE) = 11 MM.

Expt. no.	Other gases present in cm.	Temp., °C.	CH_3OOH *m/e* 48	CH_3OOD, *m/e* 49 CD_3OOH, *m/e* 51 CD_3OOD, *m/e* 52
1	CO_2; 48	27	Present	
2	CO_2; 48	105	Present	
3	CO_2; 48	158	Present	
4	CD_4; 48	27	Present	Absent
5	CD_4; 48	158	Present	Absent
6	Propylene; 12	27	Present	
7	Oxygen; 70	27	Present	

The authors wish to acknowledge the generous assistance of Dr. F. P. Lossing and his associates for the mass spectrometric analyses.

(11) A. B. Nalbandyan, *Zhur. Fiz. Khim.*, **32**, 1443 (1948).

(12) J. S. Watson and B. deB. Darwent, THIS JOURNAL, **61**, 577 (1957).

COMMUNICATIONS TO THE EDITOR

GAS CHROMATOGRAPHY OF PARA-HYDROGEN, ORTHOHYDROGEN, HYDROGEN DEUTERIDE AND DEUTERIUM

Sir:

The gas chromatographic separation of hydrogen isotopes HD and D_2[1] and nuclear spin isomers para-H_2 and ortho-H_2[2] on suitable adsorbents kept at −195° was demonstrated in 1958. Since then it has become of interest to suppress the separation of para–ortho isomers and hence to give three peaks corresponding to H_2, HD, D_2 on a single chromatogram. Smith and Hunt[3] used chromia–alumina columns and Moore and Ward[4] used alumina packings coated with ferric oxide, both making rapid para–ortho interconversion and thereby giving a unified peak for these isomers. In the absence of such paramagnetic substances on the columns, ortho-H_2 and HD overlap and the three apparent peaks are para-H_2, ortho-H_2 plus HD and D_2, respectively, as already reported by Van Hook and Emmett[5] and by Kwan.[6]

While the lack of a H_2 peak[1] or the overlapping of ortho-H_2 and HD is not disadvantageous for the analyses of these hydrogen isotopes[6,7] it would be worthwhile to separate ortho-H_2 and HD or to obtain four separate peaks, para-H_2, ortho-H_2, HD and D_2, on a single chromatogram. In this communication we wish to present such a method and analytical data found with it.

The separation of this kind would be realized if one employs two sorts of columns in series; the first contains alumina or Molecular Sieves and the second paramagnetic substances in addition. Para-H_2, eluted out of the first column, would undergo rapid para–ortho conversion during passage through the second column presenting a peak. Ortho-H_2, with a certain time delay, will follow a similar behavior. Now, if the second column be efficient enough also for the separation of three isotopic forms, ortho-H_2 and HD ought to be separated on this column. Consequently, we may expect the four peaks mentioned above.

Experiments were made with the apparatus and procedure reported previously.[6] An active alumina column 200 × 0.4 cm. was employed as the first column. The second one was filled with active alumina coated with ferric oxide after Moore and Ward,[4] its length being 50 cm. Hydrogen components, passed through the columns, were burned on a combustion tube kept at 450° before entering the thermal conductivity gauge. The column temperature was −195°. Helium was used as the carrier gas, its flow rate being 65–69 cc./min.

The chromatogram obtained for hydrogen isotope samples of 0.3–0.9 cc. gave rise to, as expected, four peaks with retention times ranging from 6 to 10 minutes. An approximate evaluation of the peak area was made by dropping vertical lines from the minimum between the peaks to the base line and

(1) S. Ohkoshi, Y. Fujita and T. Kwan, *Bull. Chem. Soc. Japan*, **31**, 770 (1958).

(2) W. R. Moore and H. R. Ward, *J. Am. Chem. Soc.*, **80**, 2909 (1958).

(3) H. A. Smith and P. P. Hunt, *J. Phys. Chem.*, **64**, 383 (1960).

(4) W. R. Moore and H. R. Ward, *ibid.*, **64**, 832 (1960).

(5) W. A. Van Hook and P. H. Emmett, *ibid.*, **64**, 673 (1960).

(6) T. Kwan, *J. Res. Inst. Catalysis, Japan*, **8**, 18 (1960).

(7) S. Ohkoshi, S. Tenma, Y. Fujita and T. Kwan, *Bull. Chem. Soc. Japan*, **31**, 772 (1958).

then weighing each portion. The area thus determined was assumed to be proportional to the amount present. Such analysis data, obtained for hydrogen samples of different isotopic compositions, are shown in Table I. The result seems to be satisfactory, if one considers the approximations involved.

TABLE I

GAS CHROMATOGRAPHIC ANALYSES OF HYDROGEN I AND ISOMERS (VOLUME %)

Sample		Para-H_2	Ortho-H_2	HD	D_2
I	Calcd.	9.3	27.9	48.0	14.8
	Found	9.0	24.6	48.9	17.2
II	Calcd.	18.5	32.7	37.5	11.5
	Found	15.1	36.3	37.5	11.7

DEPARTMENT OF CHEMISTRY
FACULTY OF SCIENCE
HOKKAIDO UNIVERSITY — SHOZO FURUYAMA
SAPPORO, JAPAN
CHEMICAL LABORATORY
FACULTY OF PHARMACEUTICAL SCIENCES
UNIVERSITY OF TOKYO — TAKAO KWAN
TOKYO, JAPAN

RECEIVED NOVEMBER 7, 1960

POLAROGRAPHY OF TANTALUM–ETHYLENEDIAMINETETRAACETATE COMPLEX

Sir:

In the course of a study of complexing agents for niobium and tantalum, we have found a hitherto unreported complex of tantalum(V) and EDTA. Milligram quantities of tantalum may be held in solution in the *p*H range from 3 to 6 with EDTA of at least 0.01 *M* concentration. Furthermore, these solutions exhibit reduction of Ta(V) to Ta(IV) at the dropping mercury electrode. The only previously reported examples of the existence of tantalum(IV) in aqueous media, by Zeltzer[1] in HCl solutions and by Elson[2] in acid tartrate solutions are somewhat doubtful inasmuch as the phenomena could not be reproduced either by Ferrett and Milner[3] or by ourselves.

The polarographic investigation of the tantalum complex indicates that a one electron reversible reduction takes place at the dropping mercury electrode. This is similar to the behavior of the Nb(V)–EDTA complex reported by Ferrett and Milner[3] and studied in greater detail by us.[4] The half-wave potential is independent of EDTA concentration, but it is *p*H dependent. In the *p*H region of 3.3 to 5.6 the half-wave potential varies linearly from −1.23 v. to −1.36 v. *vs.* the S.C.E., indicating that one hydrogen ion takes part in the reduction of the Ta(V)–EDTA complex. The temperature coefficient of the half-wave potential is negative and less than 1 mv. per degree which is characteristic of a diffusion controlled process.

The diffusion current of the Ta-EDTA complex, in solutions of given *p*H values, is proportional to the concentration of tantalum in solution in the range studied from 10 to 100 μg. Ta/ml. with an average deviation of 5%. From *p*H 3.3 to 4.0 the diffusion current is reasonably constant, then it decreases for a given concentration of tantalum as the *p*H of the solution increases.

The wave obtained by the conventional polarographic method is difficult to analyze because solvent reduction occurs before a well-defined plateau is formed on the Ta–EDTA wave. (For this reason, and because the reduction wave of Nb(IV)–Nb(III) occurs in this region,[3,4] the method is not recommended as an analytical procedure for tantalum.) However, the above results are reproducible if proper precautions are observed.

Stock solutions were prepared for this investigation by fusing Ta_2O_5 (Electro Metallurgical Co., Division of Union Carbide Corp., 99.6% Ta_2O_5 min.) in K_2CO_3–KOH in a nickel crucible. The melt was leached in water, filtered and made up to volume. Final solutions were prepared by taking aliquots of the stock solution and adding, dropwise with constant swirling, to acidified solutions of EDTA (usually sufficient EDTA to make the final solution 0.1 *M* in this reagent). Adjustments in *p*H were also made gradually and with constant swirling of the solution. This procedure insured getting stable tantalum solutions. Final solutions were stable for at least one week. Nickel does not interfere in this procedure.

Platinum crucibles cannot be used because the small amount of platinum taken into solution during the fusion process with K_2CO_3 gives a large catalytic wave in the presence of EDTA (not previously reported in the literature) at about −1.1 v. which makes analysis of the Ta–EDTA wave even more difficult.

Acknowledgment.—Financial assistance from Wright Air Development Division is gratefully acknowledged.

DEPARTMENT OF CHEMISTRY
UNIVERSITY OF ARIZONA — ROBERT E. KIRBY
TUCSON, ARIZONA — HENRY FREISER

RECEIVED NOVEMBER 7, 1960

SURFACE RECOMBINATIONS OF CHLORINE AND BROMINE ATOMS

Sir:

In 1933 Rodebush and Klingelhoefer[1] and Schwab and Friess[2] independently reported the production of chlorine atoms in a flow system (with an electrical discharge). Though their results on the rate of surface recombination of these atoms disagree markedly, their conclusions apparently have discouraged anyone else from attempting to produce halogen atoms in a flow system. Schwab, who reported on both bromine and chlorine atoms in greater detail in 1934,[3,4] concluded that: (1)

(1) S. Zeltzer, *Collection Czech. Chem. Communications*, **4**, 319 (1932).
(2) R. E. Elson, *J. Am. Chem. Soc.*, **75**, 4193 (1953).
(3) D. J. Ferrett and G. W. C. Milner, *J. Chem. Soc.*, 1186 (1956).
(4) R. E. Kirby and H. Freiser, to be published.

(1) W. H. Rodebush and W. C. Klingelhoefer, *J. Am. Chem. Soc.*, **55**, 130 (1933).
(2) G. M. Schwab and H. Friess, *Naturwissenschaften*, **21**, 222 (1933).
(3) G. M. Schwab and H. Friess, *Z. Elektrochem.*, **39**, 586 (1933).
(4) G. M. Schwab, *Z. physik. Chem.*, **327**, 452 (1934).

glass and quartz surfaces remove bromine atoms on almost every collision, and remove chlorine atoms on about one collision in 20; (2) most other surfaces are even more efficient at removing atoms; (3) no effective "poison" could be found to prevent recombination.

In an attempt to study the low pressure recombination of halogen atoms in the gas phase, we have reinvestigated the problem of surface recombination of halogen atoms. The atoms were prepared with a 2450 megacycle microwave discharge. They were detected with a silver mirror, a Wrede gauge, and an isothermal calorimetric detector previously used to study oxygen atoms.[5]

No atoms could be measured 10^{-3} second after the discharge in a Pyrex or quartz tube, or when it was coated with platinum, cobalt, silver, polyethylene, Teflon, NaCl, AgCl, NaOH, or $Al(OH)_3$. However 15 to 50% of the halogen molecules were found to be dissociated when the tube was coated with H_3PO_4, H_3AsO_4, H_2SO_4 and H_3BO_3. The recombination coefficient (γ) on these surfaces is of the order of 10^{-4} at 25° with both chlorine and bromine atoms, though the H_3PO_4 and H_2SO_4 coatings yield initial atom concentrations several times larger than H_3BO_3 and H_3AsO_4. The latter effect may be due to some change in poisoning efficiency at the high discharge temperatures.

The significance of these preliminary results may be summarized as follows: (1) Chlorine and bromine atoms cannot be prepared in significant concentrations in clean Pyrex and quartz tubes with a microwave discharge. Rough calculations from our results suggest that the chlorine and bromine atoms survive fewer than ten collisions with the glass walls immediately after the discharge. This agrees with some indirect results obtained by Ashmore and Spencer.[6] In view of these observations it is possible that workers[7] have not observed the e.s.r. absorption of chlorine atoms in the discharge products of Cl_2 because of the absence of atoms rather than the lack of a sharp absorption spectrum.

(2) A number of surface "poisons" exist which are capable of reducing chlorine and bromine atom surface-recombination to a rate comparable to that obtained for O, N and H atoms. Since these poisons can be used at temperatures over 200°, they can be used in photochemical and thermal decomposition studies which involve halogen atoms. In the past, surface reactions with glass often have complicated such studies.[6]

(3) It is notable that the poisons which are effective with O, N and H atoms are also effective with halogen atoms. These "poisons" are all oxy-acids of non metals (electronegatively ≥ 2). Selenic and telluric acids were not tried but may also be effective. Silicic acid does not seem to exist as the ortho-acid, and the remaining acids are too volatile for use as surface poisons.

A detailed study of the recombination coefficient (γ) for each surface and its temperature coefficient is being made in this laboratory. It is hoped that this may throw some light on the nature of the association which leads to surface recombination.

CHEMISTRY DEPARTMENT E. A. OGRYZLO
UNIVERSITY OF BRITISH COLUMBIA
VANCOUVER 8, B. C., CANADA

RECEIVED DECEMBER 12, 1960

(5) L. Elias, E. A. Ogryzlo and H. I. Schiff, *Can. J. Chem.*, **37**, 1680 (1959).

(6) P. G. Ashmore and M. S. Spencer, *Trans. Faraday Soc.*, **55**, 1868 (1959).

(7) C. K. Jen, S. N. Foner, E. L. Cochran and V. A. Bowers, *Phys. Rev.*, **112**, 1169 (1958).

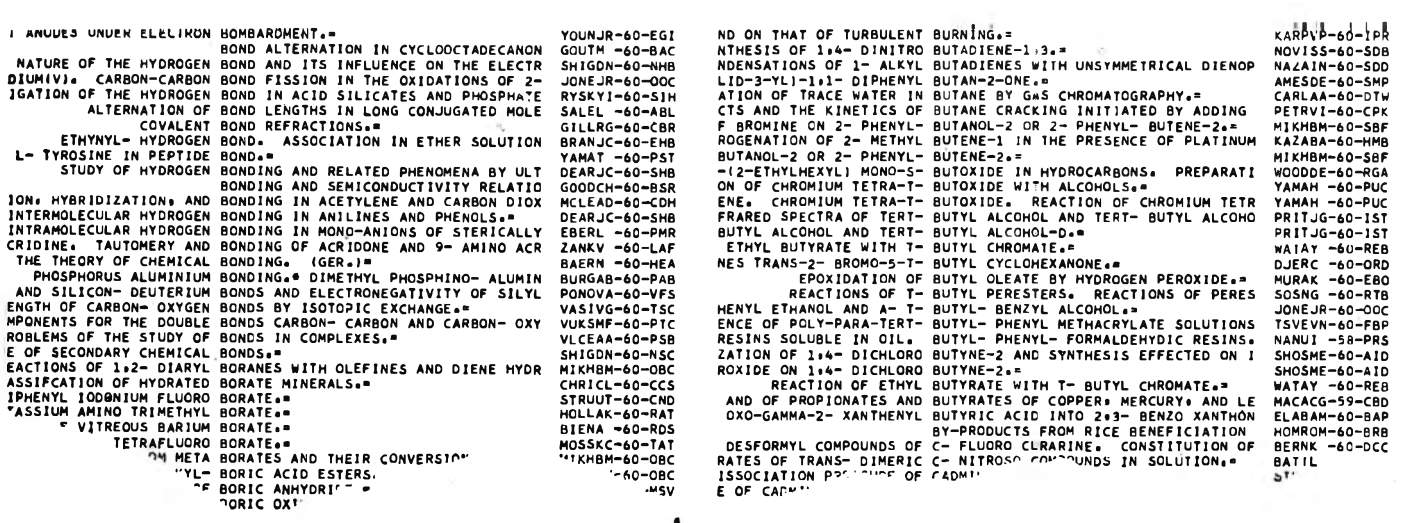

SAMPLE OF KEYWORD INDEX

announcing a new publication

CHEMICAL TITLES

the express service for increasing "current awareness" of new chemical research

● Starting in January 1961, CHEMICAL TITLES will be issued twice each month with each issue reporting approximately 3000 titles from the most recent chemical research. This service provides a current author and keyword index to selected chemical journals and is intended to fill the void between primary publication and the appearance of abstracts.

Taken from 575 journals—110 Russian—of pure and applied chemistry, these titles are listed for maximum convenience of use. The first part is a permuted title index in which keywords from each title are arranged alphabetically with each keyword in full or partial context. The second part is an alphabetical index of authors together with full titles of papers and journals in which they appear. You can find a source in a minute.

Timeliness matches ease of use. All titles are found in the listing *within two weeks of the time they are received* in the offices of The Chemical Abstracts Service, the publisher. No other index or alerting service provides such prompt and complete coverage.

Prices and discounts follow:

	Base Rate	Rate per Volume College and University	ACS Member
1st–10th subscriptions (each)	$65	$50	$50*
Additional 11th–25th subscriptions (each)	45	45	...
26th and each succeeding subscription	30	30	...

*** Single subscription only**

ORDER FROM: CIRCULATION DEPARTMENT • AMERICAN CHEMICAL SOCIETY
1155 SIXTEENTH STREET, N.W. • WASHINGTON 6, D.C.